ISSN 1007-9327 (print)
ISSN 2219-2840 (online)

World Journal of *Gastroenterology*

Weekly Volume 31 Number 15 April 21, 2025

Published by Baishideng Publishing Group Inc

World Journal of Gastroenterology

Contents

Weekly Volume 31 Number 15 April 21, 2025

EDITORIAL

Yao YQ, Cao QY, Li Z. Delaying liver aging: Analysis of structural and functional alterations. *World J Gastroenterol* 2025; 31(15): 103773 [DOI: 10.3748/wjg.v31.i15.103773]

REVIEW

Li Y, Wu YT, Wu H. Management of hepatic encephalopathy following transjugular intrahepatic portosystemic shunts: Current strategies and future directions. *World J Gastroenterol* 2025; 31(15): 103512 [DOI: 10.3748/wjg.v31.i15.103512]

Liu JJ, Zhou M, Yuan T, Huang ZY, Zhang ZY. Conversion treatment for advanced intrahepatic cholangiocarcinoma: Opportunities and challenges. *World J Gastroenterol* 2025; 31(15): 104901 [DOI: 10.3748/wjg.v31.i15.104901]

ORIGINAL ARTICLE

Case Control Study

Han L, Peng QY, Yu J, Liu YW, Li W, Ping F, Zhang HB, Li YX, Xu LL. Early detection of gastroparesis with diabetic ketoacidosis as initial manifestation: A case-control study. *World J Gastroenterol* 2025; 31(15): 101695 [DOI: 10.3748/wjg.v31.i15.101695]

Clinical Trials Study

Shi PN, Song ZZ, He XN, Hong JM. Evaluation of scoring systems and hematological parameters in the severity stratification of early-phase acute pancreatitis. *World J Gastroenterol* 2025; 31(15): 105236 [DOI: 10.3748/wjg.v31.i15.105236]

Prospective Study

Wu ZP, Wang YF, Shi FW, Cao WH, Sun J, Yang L, Ding FP, Hu CX, Kang WW, Han J, Yang RH, Song QK, Jin JW, Shi HB, Ma YM. Predictive models and clinical manifestations of intrapulmonary vascular dilatation and hepatopulmonary syndrome in patients with cirrhosis: Prospective comparative study. *World J Gastroenterol* 2025; 31(15): 105720 [DOI: 10.3748/wjg.v31.i15.105720]

Basic Study

Wang B, Li Y, Ouyang Q, Xu MT, Wang YY, Fu SJ, Liu WQ, Liu XT, Ling H, Zhang X, Xiu RJ, Liu MM. Strain- and sex-dependent variability in hepatic microcirculation and liver function in mice. *World J Gastroenterol* 2025; 31(15): 101058 [DOI: 10.3748/wjg.v31.i15.101058]

Wang XY, Liu F, Wang QT, Li SZ, Ye YZ, Chen T, Cai BC. Rhapontin activates nuclear factor erythroid 2-related factor 2 to ameliorate 1-methyl-4-phenyl-1,2,3,6-tetrahydropyridine-induced gastrointestinal dysfunction in Parkinson's disease mice. *World J Gastroenterol* 2025; 31(15): 104875 [DOI: 10.3748/wjg.v31.i15.104875]

Feng J, Wang JP, Hu JR, Li P, Lv P, He HC, Cheng XW, Cao Z, Han JJ, Wang Q, Su Q, Liu LX. Multi-omics reveals the associations among the fecal metabolome, intestinal bacteria, and serum indicators in patients with hepatocellular carcinoma. *World J Gastroenterol* 2025; 31(15): 104996 [DOI: 10.3748/wjg.v31.i15.104996]

LETTER TO THE EDITOR

Kirkik D, Kalkanli Tas S. Arachidonate 15-lipoxygenase: A promising therapeutic target for alleviating inflammation in acute pancreatitis. *World J Gastroenterol* 2025; 31(15): 102752 [DOI: 10.3748/wjg.v31.i15.102752]

Cai H, Yang CH, Gao P. Rethinking carnitine palmitoyltransferase II and liver stem cells in metabolic dysfunction-associated fatty liver disease-related hepatocellular carcinoma. *World J Gastroenterol* 2025; 31(15): 104528 [DOI: 10.3748/wjg.v31.i15.104528]

Meng HJ, Mao Y, Zhao DQ, Shi SG. Prognostic value of the triglyceride-glucose index in advanced gastric cancer: A call for further exploration. *World J Gastroenterol* 2025; 31(15): 104574 [DOI: 10.3748/wjg.v31.i15.104574]

ABOUT COVER

Peer Review of *World Journal of Gastroenterology*, Iyad A Issa, MD, Department of Gastroenterology & Hepatology, Harley Street Medical Center, Marina Village, P.O.Box 41475 Abu Dhabi, United Arab Emirates. iyadissa71@gmail.com

AIMS AND SCOPE

The primary aim of *World Journal of Gastroenterology* (*WJG*, *World J Gastroenterol*) is to provide scholars and readers from various fields of gastroenterology and hepatology with a platform to publish high-quality basic and clinical research articles and communicate their research findings online. *WJG* mainly publishes articles reporting research results and findings obtained in the field of gastroenterology and hepatology and covering a wide range of topics including gastroenterology, hepatology, gastrointestinal endoscopy, gastrointestinal surgery, gastrointestinal oncology, and pediatric gastroenterology.

INDEXING/ABSTRACTING

The *WJG* is now abstracted and indexed in Science Citation Index Expanded (SCIE), MEDLINE, PubMed, PubMed Central, Scopus, Reference Citation Analysis, China Science and Technology Journal Database, and Superstar Journals Database. The 2024 edition of Journal Citation Reports® cites the 2023 journal impact factor (JIF) for *WJG* as 4.3; Quartile: Q1. The *WJG*'s CiteScore for 2023 is 7.8.

RESPONSIBLE EDITORS FOR THIS ISSUE

Production Editor: *Si Zhao*; **Production Department Director:** *Xu Guo*; **Cover Editor:** *Jia-Ru Fan*.

NAME OF JOURNAL
World Journal of Gastroenterology

ISSN
ISSN 1007-9327 (print) ISSN 2219-2840 (online)

LAUNCH DATE
October 1, 1995

FREQUENCY
Weekly

PUBLICATION DATE
April 21, 2025

PUBLISHING PARTNER
Shanghai Pancreatic Cancer Institute and Pancreatic Cancer Institute, Fudan University
Biliary Tract Disease Institute, Fudan University

INSTRUCTIONS TO AUTHORS
https://www.wjgnet.com/bpg/gerinfo/204

GUIDELINES FOR ETHICS DOCUMENTS
https://www.wjgnet.com/bpg/GerInfo/287

GUIDELINES FOR NON-NATIVE SPEAKERS OF ENGLISH
https://www.wjgnet.com/bpg/gerinfo/240

PUBLICATION ETHICS
https://www.wjgnet.com/bpg/GerInfo/288

PUBLICATION MISCONDUCT
https://www.wjgnet.com/bpg/gerinfo/208

POLICY OF CO-AUTHORS
https://www.wjgnet.com/bpg/GerInfo/310

ARTICLE PROCESSING CHARGE
https://www.wjgnet.com/bpg/gerinfo/242

STEPS FOR SUBMITTING MANUSCRIPTS
https://www.wjgnet.com/bpg/GerInfo/239

ONLINE SUBMISSION
https://www.f6publishing.com

PUBLISHING PARTNER's OFFICIAL WEBSITE
https://www.shca.org.cn
https://www.zs-hospital.sh.cn

World Journal of Gastroenterology

Submit a Manuscript: https://www.f6publishing.com

World J Gastroenterol 2025 April 21; 31(15): 103773

DOI: 10.3748/wjg.v31.i15.103773

ISSN 1007-9327 (print) ISSN 2219-2840 (online)

EDITORIAL

Delaying liver aging: Analysis of structural and functional alterations

Yu-Qin Yao, Qiong-Yue Cao, Zheng Li

Specialty type: Gastroenterology and hepatology

Provenance and peer review: Invited article; Externally peer reviewed.

Peer-review model: Single blind

Peer-review report's classification

Scientific Quality: Grade B, Grade B, Grade C, Grade C

Novelty: Grade B, Grade B, Grade C, Grade C

Creativity or Innovation: Grade B, Grade B, Grade B, Grade C

Scientific Significance: Grade B, Grade B, Grade C, Grade C

P-Reviewer: Horkaew P; Martinez-Molina C; Wang L

Received: December 3, 2024

Revised: February 23, 2025

Accepted: April 7, 2025

Published online: April 21, 2025

Processing time: 139 Days and 21 Hours

Yu-Qin Yao, Qiong-Yue Cao, Zheng Li, College of Health Sciences, School of Life Sciences, Jiangsu Normal University, Xuzhou 221000, Jiangsu Province, China

Corresponding author: Zheng Li, PhD, College of Health Sciences, School of Life Sciences, Jiangsu Normal University, No. 101 Shanghai Road, Xuzhou 221000, Jiangsu Province, China. lizhengcpu@163.com

Abstract

This article is based on a recent bibliometric analysis of research progress on liver aging. The liver is notable for its extraordinary ability to rejuvenate, thereby safeguarding and maintaining the organism's integrity. With advancing age, there is a noteworthy reduction in both the liver's size and blood circulation. Furthermore, the wide range of physiological alterations driven on by aging may foster the development of illnesses. Previous studies indicate that liver aging is linked to impaired lipid metabolism and abnormal gene expression associated with chronic inflammation. Factors such as mitochondrial dysfunction and telomere shortening accumulate, which may result in increased hepatic steatosis, which impacts liver regeneration, metabolism, and other functions. Knowing the structural and functional changes could help elderly adults delay liver aging. Increasing public awareness of anti-aging interventions is essential. Besides the use of dietary supplements, alterations in lifestyle, including changes in dietary habits and physical exercise routines, are the most efficacious means to decelerate the aging process of the liver. This article highlights recent advances in the mechanism research of liver aging and summarizes the promising intervention options to delay liver aging for preventing related diseases.

Key Words: Liver aging; Telomere; Hepatocytes; Caloric restriction; Physical exercise; Regeneration

Core Tip: The natural aging process can impair liver functions, including regeneration and metabolism, disrupting hepatic balance and increasing the risk of liver diseases. Cellular and morphological changes are attributable to altered molecular mechanisms. Comprehending the processes of hepatocyte senescence is essential for delaying liver aging through appropriate lifestyle modifications, pinpointing triggers, devising therapeutic strategies, and assessing the effectiveness of interventions against liver diseases. Consequently, it is imperative to conduct further research on the molecular pathways involved.

Citation: Yao YQ, Cao QY, Li Z. Delaying liver aging: Analysis of structural and functional alterations. *World J Gastroenterol* 2025; 31(15): 103773
URL: https://www.wjgnet.com/1007-9327/full/v31/i15/103773.htm
DOI: https://dx.doi.org/10.3748/wjg.v31.i15.103773

INTRODUCTION

The liver, a complex organ with multifaceted functions, operates under rigorous physiological regulation. As individuals age, the liver experiences substantial alterations in its composition, functionality, and vulnerability to diseases[1,2]. Currently, hepatic disorders contribute significantly to global morbidity and mortality. Previous research indicates that the buildup of age-related damage activates compensatory pathways in liver cells, such as cellular senescence and altered nutrient sensing. Excessive activation of these pathways can hinder liver regeneration and exacerbate liver disease progression[3]. For instance, aging can lead to reduced liver perfusion, impaired hepatocyte function, and altered microcirculation within the liver sinusoids. These alterations have a significant negative impact on liver function, increasing the risk of liver diseases and complications in the elderly[4]. Lifestyle modifications have demonstrated efficacy in treating certain prevalent liver diseases, highlighting the crucial role of lifestyle in disease outcomes[5]. These interventions primarily encompass caloric restriction (CR) and physical exercise. CR is recognized as an effective dietary strategy that enhances health and prolongs the lifespan of species[6-8]. Exercise stimulates the release of beneficial substances from muscles, contributing to overall health and preventing metabolic disorders[9,10]. Given its pivotal regulatory functions, the aging liver exhibits heightened susceptibility to disease and disrupts overall metabolic homeostasis. A bibliometric analysis has revealed an exponential surge in the number of publications concerning hepatic aging over the past four decades[11]. The objective of this article is to delineate the critical facets of liver aging, synthesize the latest research on lifestyle interventions, and underscore their potential to improve the quality of life for individuals entering and progressing through middle age and beyond[12,13].

BASIC FUNCTIONS OF THE LIVER

The liver plays a critical role in various physiological functions. Following food consumption, it metabolizes nutrients through various biochemical reactions. For instance, the body's decision to store glucose as glycogen or produce it through gluconeogenesis is determined by the level of energy intake. Moreover, the liver metabolizes proteins, fats, vitamins, hormones, and other chemicals. Beyond its metabolic functions, it also regulates blood volume, supports immune responses, decomposes xenobiotics, and modulates endocrine activities. These processes are essential for maintaining the organism's stability and homeostasis[1].

CHANGES IN THE LIVER WITH AGING

Aging is associated with numerous structural and functional modifications in the liver. Notable alterations include a decline in liver volume and blood flow, an accumulation of lipofuscin in hepatocytes, a decrease in the density of smooth endoplasmic reticulum, compromised bile acid secretion, and reduced capacity for liver regeneration[14,15]. These age-related physiological modifications might amplify liver damage and inflammation, thereby heightening the risk of chronic liver disease and mortality[16]. For instance, analysis of multiple external datasets has uncovered a significant overexpression of 40 genes from the HepG2 senescence signature in various conditions, including chronic liver disease. This finding offers compelling evidence for the occurrence of hepatocyte senescence in chronic liver disease and suggests that these genes may serve as potential biomarkers for the disease's progression[17].

MOLECULAR MECHANISMS OF LIVER AGING

Liver aging encompasses intricate processes resulting in the accumulation of senescent cells within the hepatic tissue. This accumulation is influenced by both intrinsic aging processes and extrinsic elements, including habits, environmental

exposures, and chronic liver pathologies. Hepatocyte senescence is a complex phenomenon involving interwoven signaling pathways. The hedgehog signaling system is an important biochemical route that coordinates many developmental processes while maintaining tissue homeostasis. It is essential in regulating cell survival, proliferation, and differentiation. This pathway is critical for developing and maintaining hepatocytes and bile ducts within the liver. The hedgehog signaling pathway initiates the activation of yes-associated protein 1 (Yap1) in hepatic stem cells, thereby promoting their differentiation into myofibroblasts. Simultaneously, myofibroblasts facilitate Yap1 activation in hepatocytes through paracrine signaling, which in turn stimulates hepatocyte proliferation and dedifferentiation, thereby contributing to liver regeneration. The interplay between the hedgehog pathway and Yap1 in liver regeneration presents promising therapeutic targets for the treatment of cirrhosis and hepatocellular carcinoma[18]. This regulator, which plays a crucial role in controlling mitosis and morphogenesis, is inhibited in senescent hepatocytes, which reduces cellular proliferation and impairs the liver's ability to regenerate following injury. Additionally, disruption of this pathway in young hepatocytes recapitulates the aging process, thereby underscoring its essential role in maintaining hepatocyte viability[19].

Furthermore, mitochondria, essential organelles within cells, are primary producers of intracellular reactive oxygen species (ROS) and are particularly prone to oxidative stress. ROS, unstable oxygen derivatives, can harm cells and tissues when present in large quantities. Oxidative damage to mitochondria can impair their functionality, leading to cell death *via* apoptosis and necrosis. Mitochondrial dysfunction often intensifies ROS production, creating a harmful cycle[20]. Studies have demonstrated that senescent cells manifest distinct characteristics, including cell cycle arrest, DNA damage, elevated production of ROS, and the secretion of a senescence-associated secretory phenotype (SASP). Pro-inflammatory cytokines, chemokines, growth factors, and proteases are released by senescent cells in SASP. SASP includes a range of secreted factors and signaling molecules released by senescent cells. These substances can alter the microenvironment and impact nearby cells. In response to oxidative stress or chronic DNA damage, SASP first aids in tissue healing and encourages the immune system to eliminate damaged cells[21]. However, long-term SASP activation causes chronic inflammation, throws off tissue homeostasis, spreads senescence to nearby cells, and fuels aging-related diseases like cancer, fibrosis, and neurodegeneration. These attributes can perturb hepatic function and facilitate the advancement of liver disease[22-24].

Differentially methylated regions denote specific genomic sites where methylation of DNA takes place. These regions are critical for the regulation of gene expression, as the methylation status of these sites modifies chromatin structure, thereby influencing the accessibility of transcription factors to the DNA. Epigenetic alterations observed in aging and regenerating livers exhibit unique DNA methylation profiles in most differentially methylated regions located within gene structures and repetitive sequences[25]. Telomere attrition is a contributing factor to the aging process. During each cell division cycle, telomeres progressively shorten due to DNA polymerase's inability to replicate the terminal segments of chromosomes fully[26]. When telomeres reach a critically reduced length, they lose their capacity to preserve cellular integrity, leading to cellular senescence or genomic instability. The gradual build-up of senescent cells throughout life is linked to the secretion of pro-inflammatory cytokines, which initiate age-related diseases and degenerative conditions[26-29]. The molecular mechanisms involved in the aging process of the liver are summarized in Figure 1.

Nevertheless, these molecular mechanisms are not independent entities; rather, they are interrelated and exhibit mutual influence. For instance, the p53 and DNA damage response pathways are activated in response to telomere dysfunction-induced DNA damage. This activation leads to the suppression of peroxisome proliferator-activated receptor-gamma coactivator-1α and peroxisome proliferator-activated receptor-gamma coactivator-1β, culminating in mitochondrial dysfunction[30]. The hedgehog signaling pathway regulates the expression and activity of telomerase reverse transcriptase (hTERT) *via* its critical transcription factors, GLI1 and GLI2. These factors directly interact with the hTERT promoter region, thereby enhancing telomerase activity and promoting hTERT transcription. Telomerase replenishes telomeric repeats to prevent shortening and maintain telomere length[31].

INTERVENTIONS OF LIFESTYLE

One of the most fascinating and challenging areas of scientific study is anti-aging treatments. Presently, mitigating liver aging encompasses CR, moderate physical exercise, and using botanical compounds for therapeutic purposes[32]. CR induces metabolic stress, eliciting adaptive cellular responses that augment repair mechanisms, diminish inflammation, and enhance insulin sensitivity. These alterations are conducive to the prevention of age-related pathologies, as CR has been linked to improvements in mitochondrial function, maintenance of telomere integrity, and suppression of the SASP, potentially mitigating age-related cellular damage and promoting hepatic health. Notably, the dietary composition is instrumental in this context. Diets abundant in fruits, vegetables, whole grains, lean proteins, and healthful lipids, such as the Mediterranean diet, confer additional health advantages by supplying antioxidants, phytochemicals, and anti-inflammatory agents. The synergistic application of CR with a nutrient-rich dietary regimen shows significant potential in fostering longevity and promoting healthy aging processes[7,8,33]. A study implemented a 30% CR in excision repair cross-complementation group 1-deficient mice to evaluate its effects on lifespan and liver aging. Histological examination indicated that CR diminished hepatocyte nuclear anomalies, such as polyploidy, and decreased H2AX levels. The findings suggest that CR alleviates age-related liver pathologies and may serve as a potential therapeutic approach for mitigating age-associated liver deterioration[34]. Long-term CR was shown to decelerate the pace of aging in healthy adults, as measured by the DunedinPACE[35] DNA methylation algorithm. Participants in the CR group exhibited a significant reduction in DunedinPACE values by 0.29 units (95% confidence interval: -0.45, -0.13) at 12 months and 0.25 units (95% confidence interval: -0.41, -0.09) at 24 months compared to the control group. These reductions correspond to a

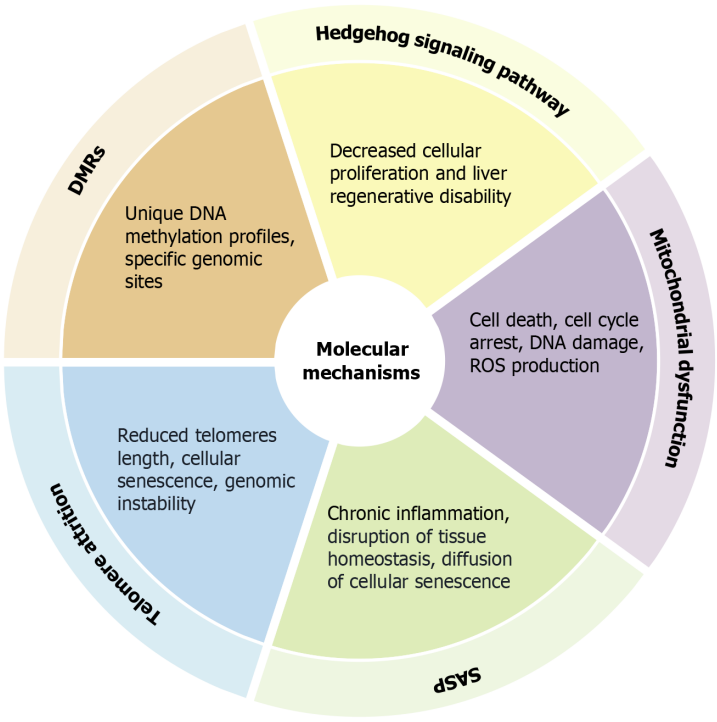

Figure 1 Summary of molecular mechanisms in liver aging. Cellular senescence is linked to changes and effects at the molecular level. These include the role of the Hedgehog signaling pathway in inhibiting liver regeneration and cellular proliferation, the effects of mitochondrial dysfunction, such as reactive oxygen species production and apoptosis, the link between senescence-associated secretory phenotype and the spread of senescence and chronic inflammation, the traits of telomere attrition that cause genomic instability, and the distinct DNA methylation profiles in differentially methylated regions. DMRs: Differentially methylated regions; ROS: Reactive oxygen species; SASP: Senescence-associated secretory phenotype.

2-3% slower pace of aging, highlighting the potential of CR as a promising intervention to enhance health and promote longevity[36].

Physical exercise is acknowledged as a fundamental component of a healthy lifestyle, capable of preventing chronic diseases such as cardiovascular and metabolic disorders, as well as cognitive deterioration. Research suggests that myokines, secreted by the activated skeletal muscles during physical activity, likely act as mediators that impart these health advantages. They enhance metabolic functions, increase glucose absorption, stimulate fat combustion, and modulate the regeneration of skeletal muscle tissue[10,37]. Resistance exercise has been demonstrated to enhance muscle strength among older adults significantly. A recent study implemented a long-term treadmill exercise regimen in transgenic mice. Histopathological evaluation through hematoxylin and eosin staining and CD68 immunofluorescence revealed significant changes in liver tissue. Notably, exercise led to a more organized arrangement of hepatocytes, the normalization of hepatic sinusoids, and a marked reduction in Kupffer cell aggregation. These enhancements indicate that exercise has a notable protective effect against liver aging, underlining its potential as a therapeutic intervention for age-related liver disease[38]. Moreover, the synergistic effect of exercise combined with dietary interventions has been demonstrated to be more efficacious in retarding liver aging than either intervention administered independently.

Diets abundant in health-beneficial botanical compounds, such as anthocyanidins, flavones, and isoflavones, have been implicated in the postponement of liver aging[39]. Anthocyanins are renowned for their potent antioxidant properties. Individuals with a higher intake of dietary anthocyanins exhibit a slower progression of aging-related characteristics[40,41]. Paeonol effectively neutralizes free radicals and modulates the activity of antioxidant enzymes. It significantly improves cognitive impairments and attenuates neuropathological changes in mouse models[42]. Similarly, silymarin is efficacious in mitigating D-galactose-induced mitochondrial dysfunction and demonstrates a protective role in liver health[43,44]. Artificial intelligence (AI) and machine learning (ML) are being used more and more in medicine in the digital age, especially in the treatment of liver illnesses. Computer imaging driven by AI and ML improves diagnostic precision, automates segmentation, and makes minimally invasive surgery and preoperative planning easier[45]. However, precisely defining tumor borders in intricate situations continues to be difficult. Despite this, the continuous development of technology gives hope that AI and ML will continue to make important strides, benefiting patients even more and enhancing the effectiveness of healthcare services[46]. Aging is an inevitable aspect of life that demands scientific scrutiny. Despite its complexity, recent advancements in algorithmic development have significantly propelled aging research forward. The field stands to benefit immensely from advanced data analytical techniques and accelerated drug discovery processes, particularly within personalized medicine frameworks. Quantum algorithms, such as the quantum approximate optimization algorithm, demonstrate the potential to outperform classical methods in solving complex optimization problems. This could revolutionize our understanding of aging mechanisms and pave the way for innovative therapeutic strategies[47].

CONCLUSION

Aging is a complex process involving various changes that increase susceptibility to chronic illnesses. Advancing age is not only a risk factor for the initiation of chronic liver conditions but also a primary driver of disease progression and the transition to end-stage liver disease. Understanding the molecular mechanisms underlying aging could facilitate the identification of therapeutic targets for age-related diseases and decelerate the aging process. Interleukin-6 (IL-6) and IL-8, key components of SASP, are implicated in aging, chronic inflammation, and age-related pathologies. These cytokines represent well-established therapeutic targets, with rapid clinical trial progression. Tocilizumab, an IL-6 receptor antagonist, inhibits signaling pathways critical for triple-negative breast cancer growth and angiogenesis. This mechanism positions Tocilizumab as a potential therapeutic strategy for triple-negative breast cancer, particularly in suppressing tumor-associated angiogenesis[48]. Therapeutic strategies targeting these cytokines may open new avenues for anti-aging interventions. Further research is essential to delineate their mechanisms of action in specific diseases and to facilitate the development of targeted therapeutic approaches. The diverse DNA methylation phenotypes resulting from CR can be measured through data, which in turn can provide some guidance for the implementation and evaluation of CR. However, this requires a comprehensive consideration of individual differences and other health indicators, and long-term follow-up studies are needed to verify its effects and safety[49]. Although lifestyle modifications can provide some temporary relief in delaying the progression of liver aging, their impact is constrained. Addressing age-related liver diseases necessitates targeting pivotal factors, including cellular senescence, the SASP, mitochondrial dysfunction, and other relevant mechanisms. An integrated therapeutic strategy is likely the most effective way to combat these diseases. It is hoped that more in-depth research on the detailed mechanisms of liver aging will be published in the future.

FOOTNOTES

Author contributions: Yao YQ and Cao QY contributed to analysis of data, drafting the article, and final approval; Li Z contributed to design of the study, revising the article, and final approval.

Supported by the National Natural Science Foundation of China, No. 82104525; and Open Foundation of Key Laboratory of Tropical Plant Resource Chemistry of Hainan Province, No. rdzw2024s01.

Conflict-of-interest statement: All the authors report no relevant conflicts of interest for this article.

Country of origin: China

ORCID number: Zheng Li 0000-0002-2882-6600.

S-Editor: Wei YF
L-Editor: A
P-Editor: Zhao S

REFERENCES

1 **Trefts E**, Gannon M, Wasserman DH. The liver. *Curr Biol* 2017; **27**: R1147-R1151 [PMID: 29112863 DOI: 10.1016/j.cub.2017.09.019]
2 **Asrani SK**, Devarbhavi H, Eaton J, Kamath PS. Burden of liver diseases in the world. *J Hepatol* 2019; **70**: 151-171 [PMID: 30266282 DOI: 10.1016/j.jhep.2018.09.014]
3 **Pinto C**, Ninfole E, Gaggiano L, Benedetti A, Marzioni M, Maroni L. Aging and the Biological Response to Liver Injury. *Semin Liver Dis* 2020; **40**: 225-232 [PMID: 31887774 DOI: 10.1055/s-0039-3402033]
4 **Maeso-Díaz R**, Ortega-Ribera M, Fernández-Iglesias A, Hide D, Muñoz L, Hessheimer AJ, Vila S, Francés R, Fondevila C, Albillos A, Peralta C, Bosch J, Tacke F, Cogger VC, Gracia-Sancho J. Effects of aging on liver microcirculatory function and sinusoidal phenotype. *Aging Cell* 2018; **17**: e12829 [PMID: 30260562 DOI: 10.1111/acel.12829]
5 **Ezzat WM**. Impact of lifestyle interventions on pathogenesis of nonalcoholic fatty liver disease. *World J Gastroenterol* 2024; **30**: 2633-2637 [PMID: 38855152 DOI: 10.3748/wjg.v30.i20.2633]
6 **Cava E**, Fontana L. Will calorie restriction work in humans? *Aging (Albany NY)* 2013; **5**: 507-514 [PMID: 23924667 DOI: 10.18632/aging.100581]
7 **Kennedy BK**, Steffen KK, Kaeberlein M. Ruminations on dietary restriction and aging. *Cell Mol Life Sci* 2007; **64**: 1323-1328 [PMID: 17396225 DOI: 10.1007/s00018-007-6470-y]
8 **Masoro EJ**. Overview of caloric restriction and ageing. *Mech Ageing Dev* 2005; **126**: 913-922 [PMID: 15885745 DOI: 10.1016/j.mad.2005.03.012]
9 **Gao Y**, Zhang W, Zeng LQ, Bai H, Li J, Zhou J, Zhou GY, Fang CW, Wang F, Qin XJ. Exercise and dietary intervention ameliorate high-fat diet-induced NAFLD and liver aging by inducing lipophagy. *Redox Biol* 2020; **36**: 101635 [PMID: 32863214 DOI:

10.1016/j.redox.2020.101635]
10 **So B**, Kim HJ, Kim J, Song W. Exercise-induced myokines in health and metabolic diseases. *Integr Med Res* 2014; **3**: 172-179 [PMID: 28664094 DOI: 10.1016/j.imr.2014.09.007]
11 **Han QH**, Huang SM, Wu SS, Luo SS, Lou ZY, Li H, Yang YM, Zhang Q, Shao JM, Zhu LJ. Mapping the evolution of liver aging research: A bibliometric analysis. *World J Gastroenterol* 2024; **30**: 4461-4480 [PMID: 39534417 DOI: 10.3748/wjg.v30.i41.4461]
12 **Sanfeliu-Redondo D**, Gibert-Ramos A, Gracia-Sancho J. Cell senescence in liver diseases: pathological mechanism and theranostic opportunity. *Nat Rev Gastroenterol Hepatol* 2024; **21**: 477-492 [PMID: 38485755 DOI: 10.1038/s41575-024-00913-4]
13 **Hu SJ**, Jiang SS, Zhang J, Luo D, Yu B, Yang LY, Zhong HH, Yang MW, Liu LY, Hong FF, Yang SL. Effects of apoptosis on liver aging. *World J Clin Cases* 2019; **7**: 691-704 [PMID: 30968034 DOI: 10.12998/wjcc.v7.i6.691]
14 **Schmucker DL**. Age-related changes in liver structure and function: Implications for disease ? *Exp Gerontol* 2005; **40**: 650-659 [PMID: 16102930 DOI: 10.1016/j.exger.2005.06.009]
15 **Tajiri K**, Shimizu Y. Liver physiology and liver diseases in the elderly. *World J Gastroenterol* 2013; **19**: 8459-8467 [PMID: 24379563 DOI: 10.3748/wjg.v19.i46.8459]
16 **Fontana L**, Zhao E, Amir M, Dong H, Tanaka K, Czaja MJ. Aging promotes the development of diet-induced murine steatohepatitis but not steatosis. *Hepatology* 2013; **57**: 995-1004 [PMID: 23081825 DOI: 10.1002/hep.26099]
17 **Aravinthan A**, Shannon N, Heaney J, Hoare M, Marshall A, Alexander GJ. The senescent hepatocyte gene signature in chronic liver disease. *Exp Gerontol* 2014; **60**: 37-45 [PMID: 25240687 DOI: 10.1016/j.exger.2014.09.011]
18 **Swiderska-Syn M**, Xie G, Michelotti GA, Jewell ML, Premont RT, Syn WK, Diehl AM. Hedgehog regulates yes-associated protein 1 in regenerating mouse liver. *Hepatology* 2016; **64**: 232-244 [PMID: 26970079 DOI: 10.1002/hep.28542]
19 **Maeso-Díaz R**, Dalton GD, Oh S, Du K, Tang L, Chen T, Dutta RK, Hartman JH, Meyer JN, Diehl AM. Aging reduces liver resiliency by dysregulating Hedgehog signaling. *Aging Cell* 2022; **21**: e13530 [PMID: 34984806 DOI: 10.1111/acel.13530]
20 **Szeto HH**. Mitochondria-targeted peptide antioxidants: novel neuroprotective agents. *AAPS J* 2006; **8**: E521-E531 [PMID: 17025271 DOI: 10.1208/aapsj080362]
21 **Watanabe S**, Kawamoto S, Ohtani N, Hara E. Impact of senescence-associated secretory phenotype and its potential as a therapeutic target for senescence-associated diseases. *Cancer Sci* 2017; **108**: 563-569 [PMID: 28165648 DOI: 10.1111/cas.13184]
22 **Azman KF**, Safdar A, Zakaria R. D-galactose-induced liver aging model: Its underlying mechanisms and potential therapeutic interventions. *Exp Gerontol* 2021; **150**: 111372 [PMID: 33905879 DOI: 10.1016/j.exger.2021.111372]
23 **Di Micco R**, Krizhanovsky V, Baker D, d'Adda di Fagagna F. Cellular senescence in ageing: from mechanisms to therapeutic opportunities. *Nat Rev Mol Cell Biol* 2021; **22**: 75-95 [PMID: 33328614 DOI: 10.1038/s41580-020-00314-w]
24 **Huda N**, Liu G, Hong H, Yan S, Khambu B, Yin XM. Hepatic senescence, the good and the bad. *World J Gastroenterol* 2019; **25**: 5069-5081 [PMID: 31558857 DOI: 10.3748/wjg.v25.i34.5069]
25 **Wang J**, Zhang W, Liu X, Kim M, Zhang K, Tsai RYL. Epigenome-wide analysis of aging effects on liver regeneration. *BMC Biol* 2023; **21**: 30 [PMID: 36782243 DOI: 10.1186/s12915-023-01533-1]
26 **Penrice DD**, Jalan-Sakrikar N, Jurk D, Passos JF, Simonetto DA. Telomere dysfunction in chronic liver disease: The link from aging. *Hepatology* 2024; **80**: 951-964 [PMID: 37102475 DOI: 10.1097/HEP.0000000000000426]
27 **Chakravarti D**, Hu B, Mao X, Rashid A, Li J, Li J, Liao WT, Whitley EM, Dey P, Hou P, LaBella KA, Chang A, Wang G, Spring DJ, Deng P, Zhao D, Liang X, Lan Z, Lin Y, Sarkar S, Terranova C, Deribe YL, Blutt SE, Okhuysen P, Zhang J, Vilar E, Nielsen OH, Dupont A, Younes M, Patel KR, Shroyer NF, Rai K, Estes MK, Wang YA, Bertuch AA, DePinho RA. Telomere dysfunction activates YAP1 to drive tissue inflammation. *Nat Commun* 2020; **11**: 4766 [PMID: 32958778 DOI: 10.1038/s41467-020-18420-w]
28 **Aikata H**, Takaishi H, Kawakami Y, Takahashi S, Kitamoto M, Nakanishi T, Nakamura Y, Shimamoto F, Kajiyama G, Ide T. Telomere reduction in human liver tissues with age and chronic inflammation. *Exp Cell Res* 2000; **256**: 578-582 [PMID: 10772830 DOI: 10.1006/excr.2000.4862]
29 **Barnes RP**, Fouquerel E, Opresko PL. The impact of oxidative DNA damage and stress on telomere homeostasis. *Mech Ageing Dev* 2019; **177**: 37-45 [PMID: 29604323 DOI: 10.1016/j.mad.2018.03.013]
30 **Zhu Y**, Liu X, Ding X, Wang F, Geng X. Telomere and its role in the aging pathways: telomere shortening, cell senescence and mitochondria dysfunction. *Biogerontology* 2019; **20**: 1-16 [PMID: 30229407 DOI: 10.1007/s10522-018-9769-1]
31 **Mazumdar T**, Sandhu R, Qadan M, DeVecchio J, Magloire V, Agyeman A, Li B, Houghton JA. Hedgehog signaling regulates telomerase reverse transcriptase in human cancer cells. *PLoS One* 2013; **8**: e75253 [PMID: 24086482 DOI: 10.1371/journal.pone.0075253]
32 **Wang W**, Xu K, Shang M, Li X, Tong X, Liu Z, Zhou L, Zheng S. The biological mechanism and emerging therapeutic interventions of liver aging. *Int J Biol Sci* 2024; **20**: 280-295 [PMID: 38164175 DOI: 10.7150/ijbs.87679]
33 **Mair W**, Dillin A. Aging and survival: the genetics of life span extension by dietary restriction. *Annu Rev Biochem* 2008; **77**: 727-754 [PMID: 18373439 DOI: 10.1146/annurev.biochem.77.061206.171059]
34 **Vermeij WP**, Dollé ME, Reiling E, Jaarsma D, Payan-Gomez C, Bombardieri CR, Wu H, Roks AJ, Botter SM, van der Eerden BC, Youssef SA, Kuiper RV, Nagarajah B, van Oostrom CT, Brandt RM, Barnhoorn S, Imholz S, Pennings JL, de Bruin A, Gyenis Á, Pothof J, Vijg J, van Steeg H, Hoeijmakers JH. Restricted diet delays accelerated ageing and genomic stress in DNA-repair-deficient mice. *Nature* 2016; **537**: 427-431 [PMID: 27556946 DOI: 10.1038/nature19329]
35 **Belsky DW**, Caspi A, Corcoran DL, Sugden K, Poulton R, Arseneault L, Baccarelli A, Chamarti K, Gao X, Hannon E, Harrington HL, Houts R, Kothari M, Kwon D, Mill J, Schwartz J, Vokonas P, Wang C, Williams BS, Moffitt TE. DunedinPACE, a DNA methylation biomarker of the pace of aging. *Elife* 2022; **11**: e73420 [PMID: 35029144 DOI: 10.7554/eLife.73420]
36 **Waziry R**, Ryan CP, Corcoran DL, Huffman KM, Kobor MS, Kothari M, Graf GH, Kraus VB, Kraus WE, Lin DTS, Pieper CF, Ramaker ME, Bhapkar M, Das SK, Ferrucci L, Hastings WJ, Kebbe M, Parker DC, Racette SB, Shalev I, Schilling B, Belsky DW. Effect of long-term caloric restriction on DNA methylation measures of biological aging in healthy adults from the CALERIE trial. *Nat Aging* 2023; **3**: 248-257 [PMID: 37118425 DOI: 10.1038/s43587-022-00357-y]
37 **Leal LG**, Lopes MA, Batista ML Jr. Physical Exercise-Induced Myokines and Muscle-Adipose Tissue Crosstalk: A Review of Current Knowledge and the Implications for Health and Metabolic Diseases. *Front Physiol* 2018; **9**: 1307 [PMID: 30319436 DOI: 10.3389/fphys.2018.01307]
38 **Yuan S**, Wang Y, Yang J, Tang Y, Wu W, Meng X, Jian Y, Lei Y, Liu Y, Tang C, Zhao Z, Zhao F, Liu W. Treadmill exercise can regulate the redox balance in the livers of APP/PS1 mice and reduce LPS accumulation in their brains through the gut-liver-kupffer cell axis. *Aging (Albany*

NY) 2024; **16**: 1374-1389 [PMID: 38295303 DOI: 10.18632/aging.205432]

39 **Xing W**, Gao W, Zhao Z, Xu X, Bu H, Su H, Mao G, Chen J. Dietary flavonoids intake contributes to delay biological aging process: analysis from NHANES dataset. *J Transl Med* 2023; **21**: 492 [PMID: 37480074 DOI: 10.1186/s12967-023-04321-1]

40 **Esposito S**, Gialluisi A, Costanzo S, Di Castelnuovo A, Ruggiero E, De Curtis A, Persichillo M, Cerletti C, Donati MB, de Gaetano G, Iacoviello L, Bonaccio M; On Behalf Of The Investigators For The Moli-Sani Study. Dietary Polyphenol Intake Is Associated with Biological Aging, a Novel Predictor of Cardiovascular Disease: Cross-Sectional Findings from the Moli-Sani Study. *Nutrients* 2021; **13**: 1701 [PMID: 34067821 DOI: 10.3390/nu13051701]

41 **Elisia I**, Hu C, Popovich DG, Kitts DD. Antioxidant assessment of an anthocyanin-enriched blackberry extract. *Food Chem* 2007; **101**: 1052-1058 [DOI: 10.1016/j.foodchem.2006.02.060]

42 **Zhong SZ**, Ge QH, Qu R, Li Q, Ma SP. Paeonol attenuates neurotoxicity and ameliorates cognitive impairment induced by d-galactose in ICR mice. *J Neurol Sci* 2009; **277**: 58-64 [PMID: 19007942 DOI: 10.1016/j.jns.2008.10.008]

43 **Wadhwa K**, Pahwa R, Kumar M, Kumar S, Sharma PC, Singh G, Verma R, Mittal V, Singh I, Kaushik D, Jeandet P. Mechanistic Insights into the Pharmacological Significance of Silymarin. *Molecules* 2022; **27**: 5327 [PMID: 36014565 DOI: 10.3390/molecules27165327]

44 **Zhu SY**, Dong Y, Tu J, Zhou Y, Zhou XH, Xu B. Silybum marianum oil attenuates oxidative stress and ameliorates mitochondrial dysfunction in mice treated with D-galactose. *Pharmacogn Mag* 2014; **10**: S92-S99 [PMID: 24914315 DOI: 10.4103/0973-1296.127353]

45 **Horkaew P**, Chansangrat J, Keeratibharat N, Le DC. Recent advances in computerized imaging and its vital roles in liver disease diagnosis, preoperative planning, and interventional liver surgery: A review. *World J Gastrointest Surg* 2023; **15**: 2382-2397 [PMID: 38111769 DOI: 10.4240/wjgs.v15.i11.2382]

46 **Wei Y**, Yang M, Zhang M, Gao F, Zhang N, Hu F, Zhang X, Zhang S, Huang Z, Xu L, Zhang F, Liu M, Deng J, Cheng X, Xie T, Wang X, Liu N, Gong H, Zhu S, Song B, Liu M. Focal liver lesion diagnosis with deep learning and multistage CT imaging. *Nat Commun* 2024; **15**: 7040 [PMID: 39147767 DOI: 10.1038/s41467-024-51260-6]

47 **Wilczok D**. Deep learning and generative artificial intelligence in aging research and healthy longevity medicine. *Aging (Albany NY)* 2025; **17**: 251-275 [PMID: 39836094 DOI: 10.18632/aging.206190]

48 **Alraouji NN**, Aboussekhra A. Tocilizumab inhibits IL-8 and the proangiogenic potential of triple negative breast cancer cells. *Mol Carcinog* 2021; **60**: 51-59 [PMID: 33264466 DOI: 10.1002/mc.23270]

49 **Taha BA**, Abdulrahm ZM, Addie AJ, Haider AJ, Alkawaz AN, Yaqoob IAM, Arsad N. Advancing optical nanosensors with artificial intelligence: A powerful tool to identify disease-specific biomarkers in multi-omics profiling. *Talanta* 2025; **287**: 127693 [PMID: 39919475 DOI: 10.1016/j.talanta.2025.127693]

World Journal of Gastroenterology

Submit a Manuscript: https://www.f6publishing.com

World J Gastroenterol 2025 April 21; 31(15): 103512

DOI: 10.3748/wjg.v31.i15.103512

ISSN 1007-9327 (print) ISSN 2219-2840 (online)

REVIEW

Management of hepatic encephalopathy following transjugular intrahepatic portosystemic shunts: Current strategies and future directions

Ying Li, Yu-Tong Wu, Hao Wu

Specialty type: Gastroenterology and hepatology

Provenance and peer review: Invited article; Externally peer reviewed.

Peer-review model: Single blind

Peer-review report's classification

Scientific Quality: Grade A, Grade A

Novelty: Grade A, Grade B

Creativity or Innovation: Grade B, Grade B

Scientific Significance: Grade A, Grade A

P-Reviewer: Chen YL; Gau SY

Received: November 22, 2024

Revised: March 4, 2025

Accepted: April 2, 2025

Published online: April 21, 2025

Processing time: 148 Days and 0.2 Hours

Ying Li, Hao Wu, Department of Gastroenterology and Hepatology, West China Hospital, Sichuan University, Chengdu 610041, Sichuan Province, China

Yu-Tong Wu, Chongqing Medical University-University of Leicester Joint Institute, Chongqing Medical University, Chongqing 400016, China

Co-first authors: Ying Li and Yu-Tong Wu.

Corresponding author: Hao Wu, Department of Gastroenterology and Hepatology, West China Hospital, Sichuan University, No. 37 Guoxue Xiang, Chengdu 610041, Sichuan Province, China. 594264513@qq.com

Abstract

Transjugular intrahepatic portosystemic shunts (TIPSs) are generally used for the management of complications of portal hypertension in patients with decompensated cirrhosis. However, hepatic encephalopathy (HE), which impairs neuropsychiatric function and motor control, remains the primary adverse effect of TIPS, limiting its utility. Prompt prevention and treatment of post-TIPS HE are critical, as they are strongly associated with readmission rates and poor quality of life. This review focuses on the main pathophysiological mechanisms underlying post-TIPS HE, explores advanced biomarkers and predictive tools, and discusses current management strategies and future directions to prevent or reverse HE following TIPS. These strategies include preoperative patient assessment, individualized shunt diameter optimization, spontaneous portosystemic shunt embolization during the TIPS procedure, postoperative preventive and therapeutic measures such as nutrition management, medical therapy, fecal microbiota transplantation, and stent reduction.

Key Words: Cirrhosis; Portal hypertension; Transjugular intrahepatic portosystemic shunt; Hepatic encephalopathy; Pathophysiological mechanisms; Management strategies

Core Tip: Hepatic encephalopathy (HE) is the main complication following transjugular intrahepatic portosystemic shunt (TIPS), significantly impairs patients' quality of life. Preoperative evaluation is crucial to mitigate the risk of post-TIPS HE. The shunt diameter and embolization of spontaneous portosystemic shunts should be considered according to the portal pressure gradient. Rifaximin is effective for preventing post-TIPS HE. Endovascular shunt reduction is a potential intervention for refractory HE post-TIPS. Sarcopenia is associated with post-TIPS HE, and the impact of nutritional management on HE following TIPS warrants further investigation. The efficacy of fecal microbiota transplantation in post-TIPS HE requires further validation.

Citation: Li Y, Wu YT, Wu H. Management of hepatic encephalopathy following transjugular intrahepatic portosystemic shunts: Current strategies and future directions. *World J Gastroenterol* 2025; 31(15): 103512
URL: https://www.wjgnet.com/1007-9327/full/v31/i15/103512.htm
DOI: https://dx.doi.org/10.3748/wjg.v31.i15.103512

INTRODUCTION

Transjugular intrahepatic portosystemic shunt (TIPS) placement is a standard procedure for treating portal hypertension-related complications, which mainly include recurrent ascites and variceal rebleeding. The major drawbacks of TIPS have been shunt dysfunction and the development of hepatic encephalopathy (HE)[1]. With technical progress and the use of polytetrafluoroethylene-covered stents, the rate of shunt dysfunction has dramatically decreased[2]. However, HE, which is induced and exacerbated by TIPS placement, continues to pose a significant clinical challenge in patients with decompensated cirrhosis[3]. The incidence of post-TIPS HE ranges from 35% to 50%, seriously affects the quality of life of patients and their families, increases readmission and is a major cause of health care expenses[4-7].

The diagnosis of overt HE (OHE) is usually straightforward in clinical practice once other known brain diseases are excluded. However, minimal HE (MHE) is characterized by subtle signs and symptoms that can be detected only through specialized psychometric tests. HE can be classified into three types according to its pathogenesis: Type A is found in patients with acute liver failure, type B is found in those with portosystemic shunts, and type C is found in those with cirrhosis[8]. This review focuses mainly on patients with type C HE. HE is classified into two main categories based on severity: Covert HE, including MHE and West Haven grades 0-1; and OHE, which includes grades 2-4. Furthermore, in terms of its temporal evolution, OHE can be classified as episodic, recurrent (more than one episode within a 6-month period) or persistent (no return to normal or baseline neuropsychiatric function between episodes)[8].

Post-TIPS HE is closely associated with patient baseline characteristics, portosystemic shunt diameter, status of spontaneous portosystemic shunt (SPSS) embolization, and postoperative management. It is imperative for clinicians to understand the pathophysiological mechanisms of post-TIPS HE to effectively prevent and manage this complication. Therefore, this review outlines comprehensive strategies for the prevention and treatment of post-TIPS HE based on its underlying mechanisms, encompassing preoperative, intraoperative, and postoperative approaches (Figure 1). We aim to offer practical recommendations for minimizing HE occurrence and improving patient outcomes after TIPS.

PATHOPHYSIOLOGY OF POST-TIPS HE

The pathogenesis of HE in cirrhotic patients primarily involves hyperammonemia, systemic and neuroinflammation, oxidative stress, and dysfunction of the gut-liver-brain axis[9]. Additionally, genetic and epigenetic factors have been implicated in the development of HE[10]. Among these, hyperammonemia is regarded as the central driver of HE[11].

Hyperammonamia

In healthy individuals, ammonia production primarily occurs in the colon due to the activity of the gut microbiota, which converts glutamine into ammonia *via* enterocytic glutaminase[12]. Ammonia from the gut undergoes the urea cycle within hepatocytes to form urea, which is then excreted by the kidneys. Indeed, muscles also provide alternative pathways for ammonia removal by synthesizing glutamine from glutamate[13] (Figure 2A). In liver cirrhosis, the ability of hepatocytes to remove ammonia before it reaches the systemic circulation is severely impaired, which leads to hyperammonamia[14]. Elevated blood ammonia levels and increased permeability of the blood-brain barrier (BBB) contribute to increased blood ammonia levels in central nervous system, leading to astroglial swelling and the development of HE[15, 16]. In addition, 50% to 70% of cirrhotic patients develop sarcopenia, which substantially reduces the capacity of skeletal muscle for ammonia detoxification and increases the incidence of HE[17] in Figure 2B. TIPS is performed by creating an intrahepatic portosystemic shunt that connects the right or main portal vein to the hepatic vein to alleviate portal pressure [18]. Stent placement causes significant changes in hepatic hemodynamics, leading to a further reduction in first-pass hepatic clearance of neurotoxins that originate from the intestine. This reduction allows for greater amounts of unprocessed ammonia to enter the systemic circulation compared with patients with liver cirrhosis who have not undergone TIPS placement. Although one study showed that TIPS may improve sarcopenia, the improvement might not be sufficient to clear ammonia caused by portosystemic shunting and may not significantly reduce the occurrence of HE

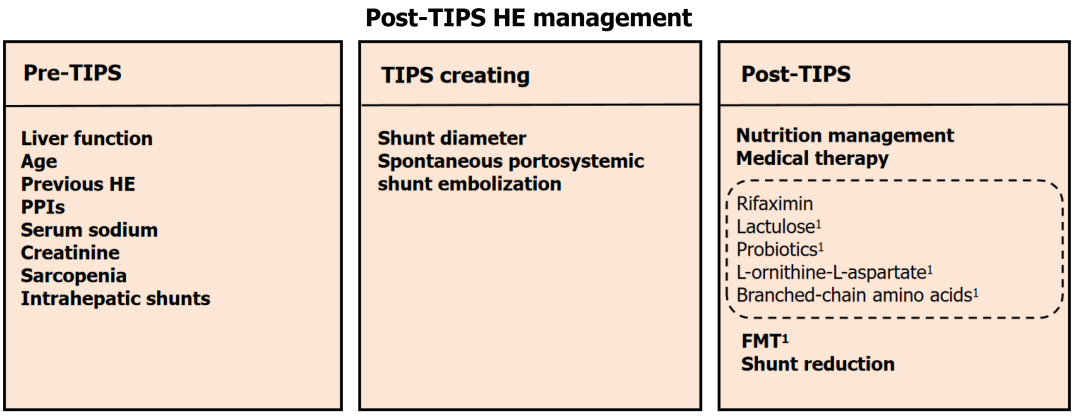

Figure 1 Management of hepatic encephalopathy following transjugular intrahepatic portosystemic shunt requires a comprehensive approach, encompassing preoperative, intraoperative, and postoperative interventions. [1]Further studies are needed to confirm these findings. TIPS: Transjugular intrahepatic portosystemic shunt; HE: Hepatic encephalopathy; PPIs: Proton pump inhibitors; FMT: Fecal microbiota transplantation.

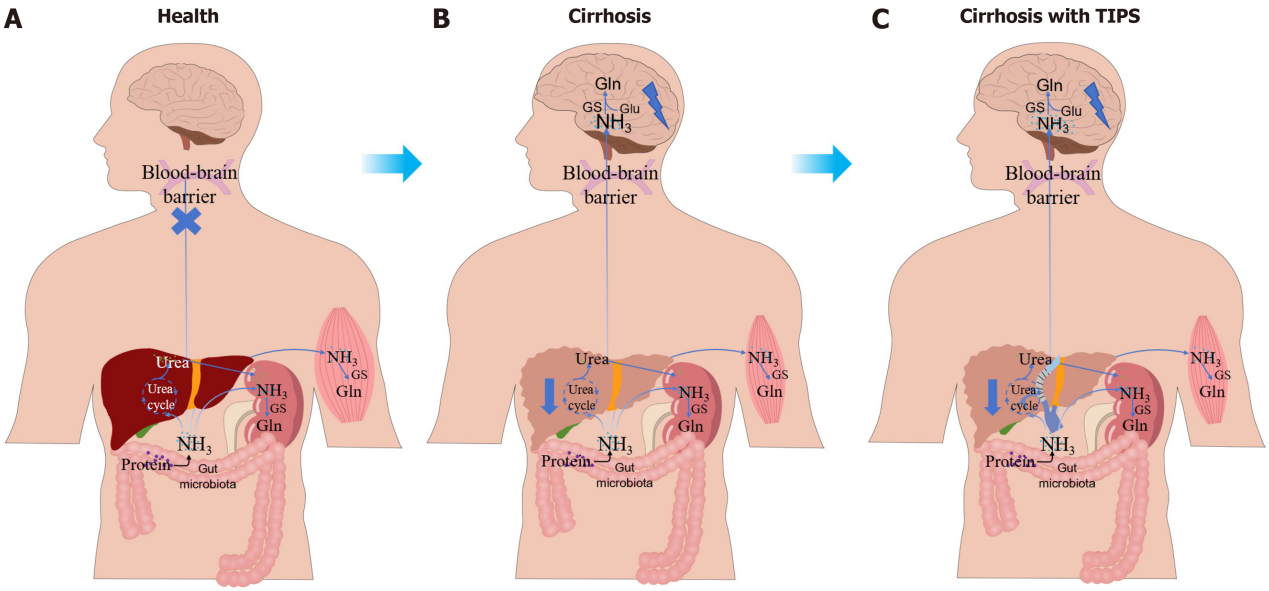

Figure 2 Metabolic profiles of blood ammonia in different populations. A: In the health, gut-derived ammonia is primarily metabolized in the liver *via* the urea cycle and excreted by the kidneys, maintaining blood ammonia as $NH4^+$ and preventing its passage across the blood-brain barrier (BBB); B: In cirrhotic patients, impaired liver function disrupts the urea cycle, reducing ammonia conversion to urea. Combined with sarcopenia, which diminishes muscle ammonia metabolism, excess ammonia crosses the BBB, leading to astrocyte glutamine accumulation, swelling, and hepatic encephalopathy; C: In patients who undergo transjugular intrahepatic portosystemic shunt, sarcopenia may improve compared with non-transjugular intrahepatic portosystemic shunt patients; however, significant hepatic bypass of blood ammonia through the shunt leads to systemic circulation. This elevated ammonia can cross the BBB, increasing the risk of hepatic encephalopathy. Gln: Glutamine; GS: Glutamine synthetase; Glu: Glutamic acid.

(Figure 2C)[19]. However, it should be noted that blood ammonia levels are not always proportional to post-TIPS HE, and a thorough clinical assessment is crucial to prevent misdiagnosis[20].

Systemic and neuroinflammatory effects

Systemic inflammation plays a pivotal role in the pathogenesis of HE in patients with cirrhosis, contributing to increased BBB permeability and eliciting a neuroinflammatory response *via* the activation of microglia and brain endothelial cells [21-23]. The abrupt hemodynamic changes induced by TIPS may facilitate the passage of inflammatory cytokines across the dysfunctional BBB, triggering neuroinflammation and increasing the risk of post-TIPS HE. Li *et al*[24] reported a significant association between preoperative serum interleukin-6 (IL-6) levels and the development of post-TIPS OHE in a prospective cohort study of 125 cirrhosis patients who underwent TIPS placement. Furthermore, toxic substances such as ammonia can activate microglia and cause the secretion of pro-inflammatory cytokines like IL-β and tumor necrosis factor-alpha (TNF-α), which promote the development of HE[25]. Further research is required to explore the role of inflammation in post-TIPS HE and to determine whether preoperative anti-inflammatory strategies can mitigate its occurrence.

Oxidative stress

Oxidative stress, frequently observed in cirrhosis, compromises BBB permeability through the reactivity of reactive oxygen and nitrogen species with lipids, proteins, and DNA, playing a crucial role in the pathogenesis of HE[26]. It induces the release of reactive oxygen species and mitochondrial dysfunction, leading to an increase in GABAergic tone in the central nervous system, thereby contributing to the development of HE[27]. Additionally, elevated ammonia and inflammation further direct oxidative stress in neurons, resulting in reactive oxygen species production and the development of HE[28]. Elevated blood ammonia levels following TIPS may promote the development of HE through this mechanism, and further investigations are needed in future studies to elucidate this relationship. Recent research suggests that antioxidant properties of vitamin D may alleviate oxidative stress in HE, but the role of vitamin D in patients undergoing TIPS procedures should be further explored[29].

Gut-liver-brain axis dysfunction

The functional integrity of the gut barrier and optimal hepatic function are essential for maintaining the homeostasis of the gut-liver-brain axis in a healthy state, effectively preventing the translocation of toxic metabolic products into the brain[30]. However, in patients with liver cirrhosis, the integrity of the gut barrier is compromised, and gut permeability is increased as a result of systemic and local inflammation, as well as bacterial translocation. This disruption facilitates the harmful metabolites into the bloodstream[31]. Compromised hepatic function leads to inadequate detoxification of gut-derived metabolites, facilitating their passage across the BBB and promoting the development of HE. Following TIPS, increased intestinal absorption facilitates the systemic circulation of toxic metabolites, which bypass hepatic detoxification and directly enter the brain, thereby increased the risk of HE. Additionally, in a prospective study of 106 TIPS-treated cirrhotic patients, the post-TIPS HE group presented increased autochthonous taxa and decreased pathogenic taxa relative to the non-HE group[32]. He *et al*[33] also identified that high baseline phenylethylamine levels, which are derived mainly from *Ruminococcus gnavus*, are correlated with a sevenfold higher risk of post-TIPS HE. A prospective study revealed no genus-level gut microbiota differences in hepatitis B-related portal hypertension patients with or without pre-TIPS HE, but post-TIPS HE was associated with increased *Morganella*, a urease-producing bacterium that elevates blood ammonia[34-36]. These findings indicate that post-TIPS HE may be closely associated with gut microbiota dysbiosis, highlighting its potential as a therapeutic and preventive target for HE following TIPS placement.

Genetic and epigenetic factors

HE is intricately linked to genetic and epigenetic mechanisms involving ammonia metabolism, neuroinflammation, and neurotransmitter regulatory pathways. Astrocytic glutamine synthetase (GS) converts glutamate and ammonia into glutamine, contributing to astrocyte swelling[37,38]. Activation of the intestinal GS gene has been linked to an increased risk of HE in cirrhotic patients[39]. Furthermore, the presence of two long alleles in the GS microsatellite promoter region was predominantly observed in HE patients[40]. Myocyte enhancer factor 2C, a key transcription factor in neuronal development and plasticity, is regulated by lnc240 through interaction with miR-1264-5p. In cirrhotic HE mice, lnc240 downregulation enhances the binding of miR-1264-5p binding to myocyte enhancer factor 2C, leading to neuronal dysfunction[41]. Gut barrier integrity is vital for gut-liver-brain axis homeostasis. In decompensated states, defensin and mucin sulfation genes were downregulated, whereas IL-1, IL-6, and TNF-related genes are upregulated in intestinal epithelial cells[42]. RNA sequencing analysis in a HE mouse model revealed that astrocytes upregulated corticoid receptor and oxidative stress signaling, while microglia displayed transcriptome changes associated with immune cell recruitment, highlighting the inflammation and hypoxia pathways in HE pathogenesis[43]. These findings provide critical insights into the pathophysiological mechanisms of HE and offer novel perspectives for precision medicine and targeted therapies. TIPS placement may further activate pathways associated with the development of HE on the aforementioned genetic basis, thereby increasing the incidence of HE, which warrants further validation in future studies.

ADVANCED BIOMARKERS AND PREDICTIVE TOOLS OF POST-TIPS HE

Advanced biomarkers

Specific biomarkers are crucial for pre-TIPS patient selection, significantly reducing the incidence of post-TIPS HE. Beyond traditional hepatic biochemical markers such as albumin, creatinine, and total bilirubin, an increasing number of biomarkers have been identified as associated with post-TIPS HE[44,45]. Elevated preoperative serum IL-6 levels are strongly linked to post-TIPS HE, indicating a higher risk of severe HE in cirrhotic patients[24]. In contrast, Tiede *et al*[46] reported no associations between systemic inflammatory markers (IL-6, TNF-α, and IL-β) and post-TIPS OHE in a two-year prospective study of 62 patients. Variations in preoperative liver function and patient characteristics likely contribute to these conflicting outcomes. The predictive role of systemic inflammation for post-TIPS HE may be limited due to the intricate and dynamic mechanisms underlying HE in cirrhosis. Furthermore, bile acid levels in the peripheral vein decrease after TIPS, and mass spectrometry analysis reveals an inverse correlation between the abundance of three specific conjugated di- and tri-hydroxylated bile acids and the severity of post-TIPS HE[47]. A prospective study of 106 cirrhotic patients receiving TIPS demonstrated a decrease in Lachnospiraceae abundance in the HE+ group, highlighting the potential of gut microbiota as a predictive target for post-TIPS HE[32]. Skeletal muscle plays a critical role in ammonia metabolism, and sarcopenia has been identified as a significant risk factor for the development of HE following TIPS placement[48].

Advanced predictive tools

Artificial intelligence (AI) algorithms are integral to fields such as biomics and healthcare analytics. In HE management, AI-based analysis of multidimensional data has revolutionized early detection, risk assessment, and tailored therapeutic interventions[49]. AI-based models, such as machine learning and deep learning algorithms, analyze biomarkers and imaging data to identify subtle patterns predictive of HE onset and progression. Yang *et al*[50] compared various classification methods for HE prediction in cirrhosis, demonstrating that the weighted random forest model is suitable for developing a risk assessment system for HE. Bajaj *et al*[51] established a 20-microbial species stool signature using machine learning, which was validated in a multicenter cohort, to distinguish HE from non-HE cases and correct misdiagnoses, thereby improving diagnostic precision and risk stratification for HE. Radiomics enhances these approaches by extracting high-dimensional quantitative features from medical imaging, such as magnetic resonance imaging and computed tomography, to identify biomarkers linked to disease severity and neurological outcomes. Chen *et al*[52] constructed a model (area under the curve = 0.719) to predict post-TIPS OHE *via* 3D liver and spleen evaluation, optimizing the TIPS candidacy assessment. Models utilizing clinical and hepatic vascular characteristics from computed tomography images (area under the curve = 0.814) showed robust performance in predicting OHE risk, with good calibration[53]. Collectively, these technologies enable more precise diagnosis, enhanced prediction of HE episodes, and personalized therapeutic strategies, ultimately improving patient outcomes. Future research should focus on refining the accuracy of post-TIPS HE prediction.

MANAGEMENT STRATEGIES

Assessment of patients before TIPS placement

Pre-TIPS liver function is significantly correlated with postoperative prognosis, and a Child-Pugh score > 13 or a model for end-stage liver disease score > 19 has been advocated as a contraindication for TIPS[54]. Common factors that affect HE after TIPS include age, a history of HE, the use of proton pump inhibitors (PPIs), serum sodium and creatinine levels, and the presence of sarcopenia[55,56]. Advanced age is a significant risk factor for post-TIPS HE. A meta-analysis revealed that patients over 70 years of age had a significantly greater incidence of HE after TIPS and a marked increase in readmission rates within 30 days[57,58]. This finding may be related to increased BBB permeability and decreased function of neural cells in elderly patients[59]. Moreover, a history of HE increases the incidence of HE following TIPS, and recurrent or persistent OHE has been advocated as a contraindication for TIPS[60]. PPIs are widely used in gastrointestinal diseases such as reflux esophagitis and peptic ulcers. A retrospective study revealed that the duration of preoperative PPI use was positively correlated with the incidence of postoperative HE, and the incidence of HE decreased after the discontinuation of PPIs[61]. This could be associated with PPIs modifying the pH of the gastrointestinal tract, which results in alterations in the gut microbiota that subsequently impact blood ammonia metabolism[62]. However, a study including 397 patients with liver cirrhosis who received TIPS revealed that 59.1% of patients treated with PPIs did not have a clear indication for PPI use[63]. Therefore, it is essential to adhere strictly to appropriate prescribing indications, especially for patients planned for the TIPS procedure. Additionally, preoperative serum sodium levels have also been identified as relevant to HE following TIPS. Merola *et al*[64] conducted a retrospective chart review and reported that a lower preoperative serum sodium concentration was associated with a greater risk of HE within the first week post-TIPS. Hyponatraemia exacerbates cerebral edema and combines with hyperammonamia to further impair brain cell function[65]. The serum creatinine level, which reflects renal function, is positively correlated with the incidence of HE after TIPS, as renal dysfunction can impede blood ammonia metabolism and affect the elimination of metabolic products[66]. Skeletal muscle is one of the sites of ammonia metabolism; however, most patients with liver cirrhosis have sarcopenia. Other studies have shown that the presence of sarcopenia before TIPS placement is a risk factor for post-TIPS HE, and improvements in sarcopenia reduce the occurrence of post-TIPS HE[48,67]. Furthermore, reduced muscle mass, such as that associated with myosteatosis, also increases the risk of HE occurring after TIPS[68]. The controlling nutritional status score, which consists of the serum albumin level, total cholesterol, and total peripheral lymphocyte count, has emerged as a reliable indicator for assessing the risk of OHE in patients with cirrhosis after the TIPS procedure [69]. Moreover, Liu *et al*[19] reported that sarcopenia can be improved in cirrhotic patients following TIPS placement. Although these factors increase the risk of post-TIPS HE, they are not absolute contraindications for TIPS placement. A full understanding of patient characteristics is essential to establish more accurate evaluations and effective treatment strategies.

Shunt diameter determination

The selection of the TIPS stent diameter is crucial for the occurrence of HE after TIPS. A stent diameter that is too small can result in insufficient shunting and ineffective reduction of portal pressure, whereas a stent diameter that is too large increases the incidence of postoperative HE. Currently, a uniform recommendation for the selection of the stent diameter is lacking. The use of the smallest possible stent that can effectively control the complications of portal hypertension is generally advised. The 2023 American Association for the Study of Liver Diseases guidelines recommend a stent diameter of 8 mm[70]. The European guidelines do not specify a particular stent diameter[71]. According to the Baveno VII guidelines, a hepatic venous pressure gradient of < 12 mmHg or a reduction in the portal pressure gradient (PPG) of more than 50% from baseline after stent placement can effectively reduce the risk of recurrent variceal bleeding[72].

Several studies have compared the impact of placing stents with different diameters on portal hypertension complications and the incidence of HE. Initially, patients who underwent TIPS were randomly assigned to either the 8-mm diameter stent group or the 10-mm diameter stent group by Riggio *et al*[73]. They reported that the incidence of portal

hypertension complications was greater in the 8-mm diameter stent group, whereas there was no significant difference in HE between the two groups. However, a meta-analysis including 5 studies and 489 patients indicated that, compared with a 10-mm stent, placing an 8-mm diameter stent did not significantly affect variceal rebleeding but did reduce the incidence of HE[74]. A randomized controlled trial (RCT) revealed that, compared with a 10-mm diameter stent, an 8-mm diameter stent not only reduced liver impairment but also halved the risk of HE, with no significant difference in rebleeding rates[75]. Furthermore, Trebicka *et al*[76] reported that covered stents with an 8 mm diameter may improve survival compared with 10 mm stents. The above studies suggest that an 8-mm diameter stent may be recommended for use in patients to prevent variceal bleeding because it does not increase the risk of rebleeding or liver impairment. However, the most critical factor in selecting the stent diameter is the patient's baseline characteristics and treatment goals rather than the specific size of the stent. A retrospective study revealed that a 6-mm shunt significantly reduced the incidence of OHE, protected perioperative liver function, and did not affect the rebleeding rate in patients with a small liver volume[77]. For patients with cirrhosis and refractory ascites who are at high risk for postoperative HE, a stent diameter smaller than 8 mm may be more appropriate[18].

Adjustable stents provide a balanced approach for managing post-TIPS HE and complications related to portal hypertension. Monnin-Bares *et al*[78] introduced a technique using a balloon-expandable stent-graft and a lasso catheter for adjustable shunt diameter reduction, permitting reversible titration *via* stent-graft dilation or lasso tightening. The use of adjustable stents requires further validation in large-scale studies to confirm their efficacy and safety.

SPSS embolization

SPSS was identified in 71% of patients with medically refractory HE[79]. These shunts develop as a compensatory mechanism to alleviate portal hypertension, allowing blood to flow from the portal vein directly into the systemic circulation *via* collateral vessels[33]. Spontaneous splenorenal shunts and spontaneous gastrorenal shunts are relatively common types of SPSSs in patients with cirrhosis[80]. The presence of spontaneous shunts allows some of the portal venous blood to bypass the liver and directly enter the systemic circulation, including gut-derived toxins such as ammonia. These toxins can cross the BBB and interfere with the function of neuroglial cells[37]. Once formed, SPSSs tend to persist and do not easily regress. One-third of SPSSs remain even after TIPS normalizes portal pressure, which may be one of the reasons for persistent HE after TIPS[81]. A multicenter study revealed that the total area of the SPSS can independently predict the incidence of HE and mortality in patients with cirrhosis[82]. An RCT revealed that in patients with variceal bleeding, the combination of TIPS and embolization of a large SPSS decreased the incidence of post-TIPS HE without significantly increasing the risk of other complications[83]. Additionally, a meta-analysis conducted by Yang *et al* [84] involving a total of 4 studies and 1243 patients demonstrated that the prevalence of SPSS is associated with an increased risk of OHE after TIPS and that embolization of the SPSS during TIPS placement reduces the risk of OHE. The North American practice guidelines recommend considering embolization for SPSSs > 6 mm to reduce the risk of HE after TIPS[85]. Commonly used methods for SPSS embolization include balloon-occluded retrograde transvenous obliteration, plug-assisted retrograde transvenous obliteration, and coil-assisted retrograde transvenous obliteration[86]. However, the above studies have certain limitations, such as small sample sizes and the inclusion of patients with cirrhosis, primarily due to hepatitis B virus infection.

HE prophylaxis and treatment after TIPS operation

Nutrition management: Malnutrition is a prevalent issue in patients with liver cirrhosis, affects 20%-50% of this patient population, and poses a risk for the development of post-TIPS HE[48,87]. Although restricted protein intake was previously recommended for patients with HE, more recent research has suggested that protein restriction in patients with HE should be based on the severity of HE and the patient's current nutritional status[88,89]. The European Association for the Study of the Liver (EASL) clinical practice guidelines also recommend that daily protein and caloric intake for patients with HE should not fall below the general recommendations for cirrhotic patients, with a minimum daily caloric intake of 35 kcal/kg and a minimum daily protein intake of 1.2-1.5 g/kg[90]. The use of vegetables and dairy protein over animal protein is encouraged[91]. An RCT of 120 cirrhotic patients demonstrated that nutritional therapy (30-35 kcal/kg and 1.0-1.5 g of vegetable protein/kg of ideal body weight/day) effectively treats MHE and improves health-related quality of life[92]. Kato *et al*[93] also reported that 8 weeks of nutritional support improved MHE in 68.4% of patients. A recent retrospective cohort study revealed that nutritional counseling effectively improved mortality and prevented OHE in patients with alcohol-associated liver disease[94].

However, to date, protein intake management has focused primarily on the prevention and treatment of HE in patients with liver cirrhosis. Only one retrospective prospective study reported that early dietary intervention can reduce the incidence of HE after TIPS in patients with cirrhosis[95]. Therefore, guidelines that recommend dietary management for the prevention of HE after TIPS placement are currently lacking. In clinical practice, both nutritional interventions and dietary counseling are essential and cost-effective measures. However, their efficacy is often constrained by patient compliance and variations in dietary habits.

Medical therapy: Lactulose, a nonabsorbable disaccharide metabolized by the colonic microbiota into short-chain organic acids, creates an acidic environment that inhibits NH_3-producing bacteria, promotes beneficial microorganisms, and converts NH_3 to nonabsorbable $NH4^+$ to reduce ammonia levels[96]. Wang *et al*[97] demonstrated that lactulose is a safe and effective treatment for MHE because it decreases the abundance of *Pediococcus*, *Clostridium*, and *Pseudomonas* and increases the abundance of *Anaerosinus* and *Akkermansia*. The EASL guidelines recommend lactulose as the first-line treatment for HE, and it is effective for treating covert HE, preventing HE, and providing secondary prophylaxis after the first episode of OHE[90]. A recent clinical trial demonstrated that lactulose plus rifaximin decreased ammonia production in patients with cirrhosis, as quantified by the constant ammonia infusion technique, which measures whole-body

ammonia metabolism[98]. In addition, lactulose promotes the elimination of accumulated blood in the gastrointestinal tract of patients with concurrent esophageal variceal bleeding and suppresses the production and absorption of ammonia to prevent HE. However, some studies have also shown that lactulose can lead to complications such as bloating, flatulence, and severe and unpredictable diarrhea, which may result in dehydration[99]. Current studies on the use of lactulose for the treatment and prevention of HE after TIPS are limited. An RCT from 2005 by Riggio *et al*[100] suggested that lactulose is not effective in the prophylaxis of HE after TIPS compared with no treatment. However, this study only compared the incidence of HE within 1 month after TIPS, so factors including insufficient medication duration cannot be completely excluded. Furthermore, Seifert *et al*[101] reported that the combination of lactulose and rifaximin is more effective in patients with HE prior to TIPS than in those with no history of HE. Lactulose is effective in the treatment and prevention of HE in patients with cirrhosis who have not received a TIPS. However, most current treatments and preventive measures for HE after TIPS are not significantly different from those used in the control group. This lack of efficacy may be due to insufficient medication time for patients and the impact of preoperative HE episodes. Alternatively, the preventive effect of lactulose through the aforementioned mechanisms may be insufficient to prevent HE in patients with a high risk of HE compared with patients who have not received a TIPS. Further large-scale RCTs are needed to explore the effects of lactulose alone on HE in patients who have undergone TIPS.

Rifaximin, a nonsystemic antibiotic based on rifamycin, has low gastrointestinal absorption and broad-spectrum antibacterial action without ototoxicity or nephrotoxicity[102]. Owing to its minimal absorption, it has high bioavailability within the gastrointestinal tract[99]. Rifaximin can be used to treat HE by improving bacterial translocation and systemic endotoxemia, reducing systemic inflammation, and repairing the intestinal barrier[103,104]. Rifaximin selectively increases the abundance of *Bifidobacterium*, *Faecalibacterium prausnitzii*, and *Lactobacillus* while reducing the abundance of Veillonellaceae without significantly altering the overall composition of the gut microbiota[105]. Furthermore, recent research utilizing human small intestinal organoids has demonstrated that rifaximin exerts direct effects on ammonia clearance within the small intestinal epithelium by enhancing intracellular nitrogen detoxification through mechanisms independent of the pregnane X receptor[106]. Bass *et al*[99] reported that rifaximin was more effective than placebo in maintaining remission from HE and reducing the risk of hospitalization related to HE over a six-month follow-up period. Furthermore, Wang *et al*[97] reported that rifaximin is efficacious in the treatment of MHE and can improve the composition of the gut microbiota. A multicenter RCT suggested that rifaximin is efficacious in preventing HE following TIPS by comparing patients who received rifaximin in conjunction with lactulose therapy post-TIPS to those who did not[107]. However, most of the studies evaluating the treatment of HE after TIPS were based on the combination of lactulose and rifaximin. Thus, the therapeutic effect of rifaximin alone on post-TIPS HE could not be comprehensively assessed. To date, only one prospective RCT has evaluated the therapeutic and prophylactic effects of rifaximin alone for OHE within 6 months after TIPS and revealed that rifaximin can prevent the development of post-TIPS OHE. Nonetheless, this study focused mainly on patients with alcoholic cirrhosis and recurrent ascites. As a result, the preventive efficacy of rifaximin in patients with other etiologies and variceal rebleeding remains undetermined[108]. The 2022 EASL guidelines and 2023 American Association for the Study of Liver Diseases practice guidelines suggest that rifaximin can be considered to prevent HE in cirrhotic patients with a history of OHE before TIPS placement[70,71]. However, in clinical practice, several studies have noted that the increasing incidence of *Clostridium difficile* infection and its relatively high cost limit its widespread use[109,110]. Therefore, the efficacy, safety, and optimal duration of rifaximin treatment for managing post-TIPS HE should be further evaluated in future multicenter RCTs.

Probiotics: HE is linked to an imbalance of in intestinal homeostasis[111]. Probiotics primarily affect the intestine, treating HE by regulating intestinal flora dysbiosis, enhancing intestinal mucosal barrier function, and modulating intestinal immunity and inflammation-related factors[112]. Various probiotics contain different combinations of bacterial species and play different roles in the treatment and prevention of HE. Bajaj *et al*[113] demonstrated that *Lactobacillus GG* is associated with reduced endotoxemia and microecological imbalance, whereas Stadlbauer *et al*[114] reported that *Lactobacillus casei* Shirota restored neutrophil phagocytic capacity. Yang *et al*[115] found that ProBiotic-4 (*Bifidobacterium lactis*, *Lactobacillus casei*, *Bifidobacterium bifidum*, and *Lactobacillus acidophilus*) alleviated cognitive impairment in aged mice *via* the suppression of Toll-like receptor 4- and RIG-I-induced nuclear factor-kappa B signaling and inflammation. Most current studies on probiotic treatment for HE include *Bifidobacterium longum*, *Lactobacillus bulgaricus*, and *Streptococcus thermophilus* which are key components of their probiotic formulations[116,117]. Probiotics are as effective as lactulose and rifaximin in reversing MHE and preventing OHE, with the added advantage of having fewer side effects[118]. Xia *et al*[119] demonstrated the efficacy of probiotics in treating MHE in patients with hepatitis B virus-induced cirrhosis by comparing changes in cognitive function, the gut microbiota, and venous blood ammonia levels after three months of probiotic treatment *vs* no treatment. Another RCT reported that taking probiotics for three months is effective in preventing the occurrence of HE in patients with liver cirrhosis[120]. Dhiman *et al*[121] conducted a double-blind RCT and revealed that the oral administration of probiotics for six months can prevent the recurrence of HE and reduce hospitalization rates. Notably, while the aforementioned studies indicate the effectiveness of probiotics in the treatment or prevention of HE, these studies have included populations from different regions, with inconsistent probiotic administration times and varying types of probiotics. Therefore, the optimal duration for probiotic treatment and the generalizability of these probiotics in HE patients are unclear.

However, the role of probiotics in the prevention and treatment of post-TIPS HE remains uncertain. Probiotics reduce ammonia production by modulating the composition of the intestinal flora, thereby reducing the amount of ammonia that enters the BBB and lowering the incidence of HE. Theoretically, although the use of portal-systemic shunts is increased after TIPS, the incidence of post-TIPS HE is reduced if less ammonia is absorbed from the intestine into the blood. This has been demonstrated in our preliminary study on the prophylaxis of HE after TIPS with probiotics

(ChiCTR2200062996). Multicenter prospective RCTs are needed to confirm the role of probiotics in the treatment and prevention of HE following TIPS.

L-ornithine-L-aspartate: The main metabolic pathway for ammonia is the synthesis of urea in the liver through the urea cycle, and ornithine and aspartate are essential substrates in the urea cycle. Moreover, in extrahepatic tissues such as the brain and muscles, ammonia is converted into glutamine, a nontoxic transport form, through the action of GS, which is activated by ornithine and aspartate[122]. L-ornithine-L-aspartate (LOLA) is a combination of ornithine and aspartate that plays an important role in reducing blood ammonia levels both within and outside the liver[123].

A double-blind RCT conducted by Jain *et al*[124], which focused primarily on patients with grade 3 to 4 OHE, revealed that the continuous intravenous infusion of LOLA for 5 days, in addition to lactulose and rifaximin treatment, was more effective in improving HE grades and reducing the time to recovery from HE than lactulose and rifaximin alone were and decreased 28-day mortality. Other studies have shown that, compared with lactulose and probiotics, LOLA has an equivalent therapeutic effect on HE[125]. Whether the effect of LOLA treatment on HE is associated with the different types of HE (acute HE, chronic HE, or MHE) and the route of LOLA administration (oral or intravenous) remains controversial a review of the treatment and prevention of HE in patients with liver cirrhosis indicated that the efficacy of LOLA is not related to different types of HE or the route of administration[126]. Jiang *et al*[127] reported that the LOLA is effective in the treatment of acute HE and chronic HE but ineffective in the treatment of MHE. A meta-analysis revealed that oral administration of LOLA is more effective than intravenous infusion in the treatment of MHE[128]. Bai *et al*[113] compared the venous blood ammonia levels of patients who did and did not receive a LOLA infusion and reported a decrease in venous blood ammonia levels in the group that received a LOLA infusion 7 days post-TIPS. Furthermore, the levels of transaminases and bilirubin were significantly lower in the LOLA-treated group than in the control group, indicating that LOLA can improve liver function after TIPS[113]. However, Seifert *et al*[101] found no significant difference in the prevention of HE after TIPS between patients with previous HE who received LOLA in addition to rifaximin and lactulose treatment and those who did not. Rees *et al*[129] enrolled 7 patients who received a TIPS and 8 patients who did not undergo TIPS, challenged them with a glutamine load and administered either LOLA or placebo intravenously, finding that the LOLA improved psychometric testing performance in the non-TIPS group, but no significant improvement was observed in the TIPS group. This may be related to the higher baseline blood ammonia levels in patients who underwent TIPS. However, the study included only 15 patients, so it is difficult to exclude selective bias and other nonintervention factors leading to this conclusion. In summary, we can preliminarily conclude that the LOLA can reduce blood ammonia levels after TIPS and improve cognitive function in patients. However, this effect seems to be insignificant in patients with previous HE.

Branched-chain amino acids: The occurrence of HE is related to an imbalance in the ratio of branched-chain amino acids (BCAAs) (valine, leucine, and isoleucine) to aromatic amino acids (AAAs) (phenylalanine, tyrosine, and tryptophan) in the blood[130]. In healthy individuals, BCAAs and AAAs provide energy for the body and participate in protein synthesis and the regulation of various physiological functions through a series of complex biochemical reactions. In patients with cirrhosis, liver function is impaired, which reduces the synthesis of BCAAs and decreases the breakdown of AAAs to ultimately increase the BCAA/AAA ratio. Excess AAAs can cross the BBB and be converted into neurotransmitters within the brain. The abnormal accumulation of these neurotransmitters can lead to neurological dysfunction and interfere with neural signal transmission.

Supplementation with BCAAs can increase the ratio of BCAAs in the blood, restoring amino acid balance and thereby inhibiting the production and release of false neurotransmitters, thus treating HE[131]. In addition, BCAAs decrease the occurrence of HE by regulating the gut microbiota and improving gut barrier function[132]. An RCT revealed that patients with alcoholic cirrhosis and HE who received a combination of antibiotics and BCAAs had faster and more complete recoveries than did those who received antibiotics alone[133]. Additionally, Vidot *et al*[134] found that the combination of BCAAs and prebiotics was more effective in treating HE than prebiotics alone. However, in an RCT that included 116 patients with cirrhosis and a previous episode of HE, supplementation with BCAAs in the diet did not reduce the recurrence rate of HE but did improve MHE and skeletal muscle mass[135]. Furthermore, an early study suggested that BCAAs reduce the concentration of AAAs in the blood of HE patients but do not improve brain function [136]. Therefore, the EASL clinical practice guidelines state that while BCAAs are beneficial for HE patients, their role in preventing HE recurrence still needs to be further validated by high-quality RCTs[71]. Regarding the treatment and prevention of HE after TIPS placement, further research on the role of BCAAs is still needed.

Fecal microbiota transplantation: The intestinal microbiome, which consists of various bacteria, fungi, viruses, and other organisms, has proinflammatory or anti-inflammatory effects[137]. In healthy individuals, the intestinal microbiota remains in a balanced state. In patients with liver cirrhosis combined with HE, the reduced production of bile acids disrupts this balance, leading to an increase in harmful bacteria and a decrease in beneficial bacteria[111]. The reduced production of short-chain fatty acids leads to an increase in the intestinal pH, allowing urease-producing bacteria to continue to grow and produce ammonia and endotoxins, which results in hyperammonamia, systemic inflammation, and impaired intestinal barrier function[138].

Fecal microbiota transplantation (FMT) involves transferring fecal materials from healthy donors to patients with dysregulated intestinal environments to restore the gut microbiota balance. Administration methods include colonoscopy, enema, nasogastric, or nasojejunal routes[139,140]. The mechanism by which FMT exerts its effects may involve increasing the colonization of beneficial gut bacteria in patients with liver cirrhosis and HE, thereby reducing intestinal edema, mucosal injury, and inflammatory infiltration[141]. Additionally, FMT reduces blood ammonia levels and improves HE by downregulating the expression of proinflammatory cytokines[142]. An RCT divided patients with recurrent HE into a standard treatment (SOC) group and an SOC plus 5 days of broad-spectrum antibiotic treatment

followed by the FMT group. This study revealed that FMT did not increase the incidence of serious adverse events in patients. Additionally, the SOC plus 5 days of broad-spectrum antibiotic treatment followed by FMT group presented improved psychometric hepatic encephalopathy scores and increased gut microbiota diversity[143]. However, in this study, the specific SOC regimen was not detailed, and it is unclear whether patients continued to receiving rifaximin treatment after FMT is unclear. Furthermore, patients received 5 days of broad-spectrum antibiotic treatment prior to FMT, which hindered the evaluation of the impact of FMT on changes in the gut microbiota separately. Bajaj *et al*[144] reported that decompensated cirrhotic patients, including those with HE, presented increased levels of virulence factors (VFs). Compared with the control and pre-FMT methods, FMT was able to reduce VF. The efficacy of FMT is closely related to the selection of both the recipient and the donor. Bloom *et al*[141] conducted an open-label study based on fecal metagenomic testing before and after FMT. They reported that FMT improved cognitive function in HE patients and that its efficacy varied with changes in donors and recipients. Additionally, the authors noted that FMT did not completely reshape the faecal microbiome; instead, subtle or proximal gut changes may underlie its therapeutic mechanism. A meta-analysis that included twenty-one studies indicated that microbiome therapies, including probiotics, symbiotics, and FMT, were more effective at improving MHE and preventing progression to OHE[145]. However, none of these studies specified the dose of fecal material, dosing frequency, or ideal donor and delivery modality. Additionally, most of the studies included a limited number of patients.

Although changes in the gut microbiota are associated with the occurrence of HE after TIPS, no studies have yet been conducted on the use of FMT for the treatment of HE following TIPS placement has not yet been studied. Li *et al*[32] conducted a prospective longitudinal study of 106 patients with cirrhosis who had undergone TIPS and reported that gut microbiota dysbiosis was associated with the occurrence of post-TIPS HE. These findings suggest that the gut microbiome is a target for the treatment of post-TIPS HE. Additionally, in the open-label study by Bloom *et al*[141] mentioned above, four patients (40%) had received a TIPS prior to FMT, and TIPS did not significantly affect the treatment of HE with FMT.

Post-TIPS HE is correlated with gut microbiota shifts. In a study by Li *et al*[146], two cirrhotic patients with recurrent grade 2-3 HE experienced improved liver function and a significant decline in HE attacks following three FMT treatments. Bloom *et al*[147] reported in their open-label study that 40% of patients (n = 4) had a history of TIPS before receiving FMT, and TIPS placement did not significantly impact the therapeutic outcomes of FMT for HE. These findings suggest that the gut microbiome could be a potential therapeutic target for post-TIPS HE and that the role of FMT needs further validation through RCTs.

Endovascular techniques for shunt reduction: An episode of OHE occurs in 35% to 50% of patients after TIPS, whereas refractory HE, including recurrent or persistent HE that cannot be controlled by dietary and pharmacological interventions, occurs in approximately 8% of patients[7,148]. For such patients, stent occlusion or diameter reduction represents a potential therapeutic strategy. However, stent occlusion is associated with a marked increase in the incidence of portal hypertension-related complications and is generally not recommended. To date, the primary techniques for stent reduction include the parallel stent method, the hourglass configuration method, and the tapered stent-graft method. Among these methods, the parallel stent method is more widely applied. Moreover, research has indicated that the hourglass configuration method can be utilized to alter the stent graft, efficiently diminishing shunt flow and improving OHE[149]. In an observational study of 12 patients who developed refractory HE after TIPS, shunt reduction was performed *via* an hourglass-shaped balloon-expandable expanded polytetrafluoroethylene stent-graft inserted into the original shunt. A follow-up at approximately 1 year revealed no recurrence of HE, but there was no improvement in liver dysfunction[150]. Additionally, Rowley *et al*[151] employed the parallel reduction technique to reduce the stent in 10 patients who developed refractory HE after TIPS. Among them, recurrent HE improved in 8 out of 10 patients, but the survival rate at 1 year without liver transplantation was only 10%. These findings suggest that stent reduction can effectively alleviate refractory HE after TIPS, but it may not improve liver function or the survival rate. Furthermore, the recurrence of portal hypertension-related complications such as ascites and variceal bleeding after stent reduction is also a major issue. Shah *et al*[152] studied 33 patients who required stent reduction, 14% of whom experienced a recurrence of ascites after the stent reduction procedure. A review highlighted that following TIPS stent reduction, which involves an increase in the PPG from 8 mmHg to 12 mmHg, the recurrence rate of portal hypertension-related symptoms is 29%[153].

Notably, while the abovementioned studies offer insights into managing post-TIPS refractory HE, their small sample sizes and absence of control groups indicate that the observed improvements in HE could be due to factors unrelated to stent reduction. Moreover, comparing the differences in symptoms related to portal hypertension, liver function, and patient survival rates between those who have undergone stent reduction and those who have not is essential to assess the efficacy of stent reduction precisely for patients with refractory HE following TIPS placement.

FUTURE DIRECTIONS

First, early detection and identification of MHE following TIPS is crucial for the timely removal of precipitating factors, thereby preventing the occurrence of OHE. The creation of an efficient predictive model for MHE based on serum biochemical indicators, cognitive assessment systems, and radiomics warrants further investigation. Second, when sarcopenia is targeted as a therapeutic endpoint, comprehensive preoperative and postoperative nutritional assessments for patients who receive a TIPS, along with dietary guidance provided by nutritionists, may represent a nonpharmacological approach to prevent HE after TIPS placement. Third, the optimal size of the shunt channel that should be embolized to increase the prevention efficiency of HE after TIPS creation needs further investigation. Fourth, future research should focus on developing adjustable stents based on PPG and post-TIPS HE. Finally, the efficacy and safety of FMT as a treatment for HE following TIPS placement need to be investigated in the future.

CONCLUSION

This review is based on physiopathology and provides a detailed exposition about the assessment of patients before TIPS placement, the determination of stent diameter during the procedure, the combination of SPSS embolization, and patient diet, medication, FMT and stent reduction management after TIPS placement. Although TIPS increases the risk of HE in patients, most cases of HE can be effectively controlled by dietary intervention and drug management, and only a small number of recurrent or persistent HE cases require stent reduction. An increasing number of management strategies have been shown to be effective in the treatment of post-TIPS HE. A recent study confirmed that post-TIPS HE does not affect patient survival rates[154]. TIPS also decreases the further decompensation rates of complications other than HE[155]. Therefore, we believe that HE should not be a major barrier to the performance of TIPS. Multicenter RCTs are needed to further validate the effectiveness of the aforementioned HE management strategies after TIPS and to explore new therapeutic options in the future.

FOOTNOTES

Author contributions: Li Y and Wu YT reviewed literature and produced the initial draft; Wu H reviewed and edited the manuscript. All authors have read and approved the final manuscript. Li Y and Wu YT contributed equally to this work as co-first authors.

Supported by the National Natural Science Foundation of China, No. 82270649.

Conflict-of-interest statement: All the authors report no relevant conflicts of interest for this article.

Country of origin: China

ORCID number: Ying Li 0009-0009-0895-5913; Yu-Tong Wu 0009-0000-0933-8380; Hao Wu 0000-0002-4573-7968.

S-Editor: Wang JJ
L-Editor: A
P-Editor: Xu ZH

REFERENCES

1 **European Association for the Study of the Liver**. EASL Clinical Practice Guidelines for the management of patients with decompensated cirrhosis. *J Hepatol* 2018; **69**: 406-460 [PMID: 29653741 DOI: 10.1016/j.jhep.2018.03.024]
2 **Bureau C**, Garcia-Pagan JC, Otal P, Pomier-Layrargues G, Chabbert V, Cortez C, Perreault P, Péron JM, Abraldes JG, Bouchard L, Bilbao JI, Bosch J, Rousseau H, Vinel JP. Improved clinical outcome using polytetrafluoroethylene-coated stents for TIPS: results of a randomized study. *Gastroenterology* 2004; **126**: 469-475 [PMID: 14762784 DOI: 10.1053/j.gastro.2003.11.016]
3 **Fonio P**, Discalzi A, Calandri M, Doriguzzi Breatta A, Bergamasco L, Martini S, Ottobrelli A, Righi D, Gandini G. Incidence of hepatic encephalopathy after transjugular intrahepatic portosystemic shunt (TIPS) according to its severity and temporal grading classification. *Radiol Med* 2017; **122**: 713-721 [PMID: 28510807 DOI: 10.1007/s11547-017-0770-6]
4 **Bai M**, Qi XS, Yang ZP, Yang M, Fan DM, Han GH. TIPS improves liver transplantation-free survival in cirrhotic patients with refractory ascites: an updated meta-analysis. *World J Gastroenterol* 2014; **20**: 2704-2714 [PMID: 24627607 DOI: 10.3748/wjg.v20.i10.2704]
5 **Hudson M**, Schuchmann M. Long-term management of hepatic encephalopathy with lactulose and/or rifaximin: a review of the evidence. *Eur J Gastroenterol Hepatol* 2019; **31**: 434-450 [PMID: 30444745 DOI: 10.1097/MEG.0000000000001311]
6 **Montagnese S**, Bajaj JS. Impact of Hepatic Encephalopathy in Cirrhosis on Quality-of-Life Issues. *Drugs* 2019; **79**: 11-16 [PMID: 30706419 DOI: 10.1007/s40265-018-1019-y]
7 **Zuo L**, Lv Y, Wang Q, Yin Z, Wang Z, He C, Guo W, Niu J, Bai W, Li K, Yu T, Yuan X, Chen H, Liu H, Xia D, Wang E, Luo B, Li X, Yuan J, Han N, Nie Y, Fan D, Han G. Early-Recurrent Overt Hepatic Encephalopathy Is Associated with Reduced Survival in Cirrhotic Patients after Transjugular Intrahepatic Portosystemic Shunt Creation. *J Vasc Interv Radiol* 2019; **30**: 148-153.e2 [PMID: 30638778 DOI: 10.1016/j.jvir.2018.08.023]
8 **American Association for the Study of Liver Diseases**; European Association for the Study of the Liver. Hepatic encephalopathy in chronic liver disease: 2014 practice guideline by the European Association for the Study of the Liver and the American Association for the Study of Liver Diseases. *J Hepatol* 2014; **61**: 642-659 [PMID: 25015420 DOI: 10.1016/j.jhep.2014.05.042]
9 **Arjunan A**, Sah DK, Jung YD, Song J. Hepatic Encephalopathy and Melatonin. *Antioxidants (Basel)* 2022; **11**: 837 [PMID: 35624703 DOI: 10.3390/antiox11050837]
10 **Warskulat U**, Kreuels S, Müller HW, Häussinger D. Identification of osmosensitive and ammonia-regulated genes in rat astrocytes by Northern blotting and differential display reverse transcriptase-polymerase chain reaction. *J Hepatol* 2001; **35**: 358-366 [PMID: 11592597 DOI: 10.1016/s0168-8278(01)00149-0]
11 **Jaffe A**, Lim JK, Jakab SS. Pathophysiology of Hepatic Encephalopathy. *Clin Liver Dis* 2020; **24**: 175-188 [PMID: 32245525 DOI:

10.1016/j.cld.2020.01.002]
12 **Frieg B**, Görg B, Gohlke H, Häussinger D. Glutamine synthetase as a central element in hepatic glutamine and ammonia metabolism: novel aspects. *Biol Chem* 2021; **402**: 1063-1072 [PMID: 33962502 DOI: 10.1515/hsz-2021-0166]
13 **Sheasgreen C**, Lu L, Patel A. Pathophysiology, diagnosis, and management of hepatic encephalopathy. *Inflammopharmacology* 2014; **22**: 319-326 [PMID: 25300964 DOI: 10.1007/s10787-014-0217-9]
14 **Butterworth RF**, Giguère JF, Michaud J, Lavoie J, Layrargues GP. Ammonia: key factor in the pathogenesis of hepatic encephalopathy. *Neurochem Pathol* 1987; **6**: 1-12 [PMID: 3306479 DOI: 10.1007/BF02833598]
15 **Wijdicks EF**. Hepatic Encephalopathy. *N Engl J Med* 2016; **375**: 1660-1670 [PMID: 27783916 DOI: 10.1056/NEJMra1600561]
16 **Zhang LJ**, Zhong J, Lu GM. Multimodality MR imaging findings of low-grade brain edema in hepatic encephalopathy. *AJNR Am J Neuroradiol* 2013; **34**: 707-715 [PMID: 22383235 DOI: 10.3174/ajnr.A2968]
17 **Jindal A**, Jagdish RK. Sarcopenia: Ammonia metabolism and hepatic encephalopathy. *Clin Mol Hepatol* 2019; **25**: 270-279 [PMID: 31006226 DOI: 10.3350/cmh.2019.0015]
18 **Deltenre P**, Zanetto A, Saltini D, Moreno C, Schepis F. The role of transjugular intrahepatic portosystemic shunt in patients with cirrhosis and ascites: Recent evolution and open questions. *Hepatology* 2023; **77**: 640-658 [PMID: 35665949 DOI: 10.1002/hep.32596]
19 **Liu J**, Ma J, Yang C, Chen M, Shi Q, Zhou C, Huang S, Chen Y, Wang Y, Li T, Xiong B. Sarcopenia in Patients with Cirrhosis after Transjugular Intrahepatic Portosystemic Shunt Placement. *Radiology* 2022; **303**: 711-719 [PMID: 35289658 DOI: 10.1148/radiol.211172]
20 **Bajaj JS**, Pyrsopoulos NT, Rahimi RS, Heimanson Z, Allen C, Rockey DC. Serum Ammonia Levels Do Not Correlate With Overt Hepatic Encephalopathy Severity in Hospitalized Patients With Cirrhosis. *Clin Gastroenterol Hepatol* 2024; **22**: 1950-1952.e1 [PMID: 38423347 DOI: 10.1016/j.cgh.2024.02.015]
21 **Rose CF**, Amodio P, Bajaj JS, Dhiman RK, Montagnese S, Taylor-Robinson SD, Vilstrup H, Jalan R. Hepatic encephalopathy: Novel insights into classification, pathophysiology and therapy. *J Hepatol* 2020; **73**: 1526-1547 [PMID: 33097308 DOI: 10.1016/j.jhep.2020.07.013]
22 **Maharshi S**, Sharma BC. Prophylaxis of hepatic encephalopathy: current and future drug targets. *Hepatol Int* 2024; **18**: 1096-1109 [PMID: 38492132 DOI: 10.1007/s12072-024-10647-9]
23 **Jayakumar AR**, Rama Rao KV, Norenberg MD. Neuroinflammation in hepatic encephalopathy: mechanistic aspects. *J Clin Exp Hepatol* 2015; **5**: S21-S28 [PMID: 26041953 DOI: 10.1016/j.jceh.2014.07.006]
24 **Li J**, Liu Y, Li M, Rong X, Yuan Z, Ren C, Liu S, Li L, Zhao C, Gao L, Feng D. Association of preoperative IL-6 levels with overt HE in patients with cirrhosis after TIPS. *Hepatol Commun* 2023; **7**: e0128 [PMID: 37026755 DOI: 10.1097/HC9.0000000000000128]
25 **Cui W**, Sun CM, Liu P. Alterations of blood-brain barrier and associated factors in acute liver failure. *Gastroenterol Res Pract* 2013; **2013**: 841707 [PMID: 23762040 DOI: 10.1155/2013/841707]
26 **Dröge W**. Free radicals in the physiological control of cell function. *Physiol Rev* 2002; **82**: 47-95 [PMID: 11773609 DOI: 10.1152/physrev.00018.2001]
27 **Bai Y**, Li K, Li X, Chen X, Zheng J, Wu F, Chen J, Li Z, Zhang S, Wu K, Chen Y, Wang Y, Yang Y. Effects of oxidative stress on hepatic encephalopathy pathogenesis in mice. *Nat Commun* 2023; **14**: 4456 [PMID: 37488119 DOI: 10.1038/s41467-023-40081-8]
28 **Bobermin LD**, Wartchow KM, Flores MP, Leite MC, Quincozes-Santos A, Gonçalves CA. Ammonia-induced oxidative damage in neurons is prevented by resveratrol and lipoic acid with participation of heme oxygenase 1. *Neurotoxicology* 2015; **49**: 28-35 [PMID: 26003724 DOI: 10.1016/j.neuro.2015.05.005]
29 **Johnson CD**, Stevens CM, Bennett MR, Litch AB, Rodrigue EM, Quintanilla MD, Wallace E, Allahyari M. The Role of Vitamin D Deficiency in Hepatic Encephalopathy: A Review of Pathophysiology, Clinical Outcomes, and Therapeutic Potential. *Nutrients* 2024; **16**: 4007 [PMID: 39683402 DOI: 10.3390/nu16234007]
30 **Mancini A**, Campagna F, Amodio P, Tuohy KM. Gut : liver : brain axis: the microbial challenge in the hepatic encephalopathy. *Food Funct* 2018; **9**: 1373-1388 [PMID: 29485654 DOI: 10.1039/c7fo01528c]
31 **Aguirre Valadez JM**, Rivera-Espinosa L, Méndez-Guerrero O, Chávez-Pacheco JL, García Juárez I, Torre A. Intestinal permeability in a patient with liver cirrhosis. *Ther Clin Risk Manag* 2016; **12**: 1729-1748 [PMID: 27920543 DOI: 10.2147/TCRM.S115902]
32 **Li M**, Li K, Tang S, Lv Y, Wang Q, Wang Z, Luo B, Niu J, Zhu Y, Guo W, Bai W, Wang E, Xia D, Wang Z, Li X, Yuan J, Yin Z, Trebicka J, Han G. Restoration of the gut microbiota is associated with a decreased risk of hepatic encephalopathy after TIPS. *JHEP Rep* 2022; **4**: 100448 [PMID: 35313729 DOI: 10.1016/j.jhepr.2022.100448]
33 **He X**, Hu M, Xu Y, Xia F, Tan Y, Wang Y, Xiang H, Wu H, Ji T, Xu Q, Wang L, Huang Z, Sun M, Wan Y, Cui P, Liang S, Pan Y, Xiao S, He Y, Song R, Yan J, Quan X, Wei Y, Hong C, Liao W, Li F, El-Omar E, Chen J, Qi X, Gao J, Zhou H. The gut-brain axis underlying hepatic encephalopathy in liver cirrhosis. *Nat Med* 2025; **31**: 627-638 [PMID: 39779925 DOI: 10.1038/s41591-024-03405-9]
34 **Zhao HW**, Zhang JL, Liu FQ, Yue ZD, Wang L, Zhang Y, Dong CB, Wang ZC. Alterations in the gut microbiome after transjugular intrahepatic portosystemic shunt in patients with hepatitis B virus-related portal hypertension. *World J Gastroenterol* 2024; **30**: 3668-3679 [PMID: 39193001 DOI: 10.3748/wjg.v30.i31.3668]
35 **Minnullina L**, Pudova D, Shagimardanova E, Shigapova L, Sharipova M, Mardanova A. Comparative Genome Analysis of Uropathogenic Morganella morganii Strains. *Front Cell Infect Microbiol* 2019; **9**: 167 [PMID: 31231616 DOI: 10.3389/fcimb.2019.00167]
36 **Wang Q**, Wang B, Saxena V, Miles L, Tiao J, Mortensen JE, Nathan JD. The gut-liver axis: impact of a mouse model of small-bowel bacterial overgrowth. *J Surg Res* 2018; **221**: 246-256 [PMID: 29229136 DOI: 10.1016/j.jss.2017.08.049]
37 **Häussinger D**, Kircheis G, Fischer R, Schliess F, vom Dahl S. Hepatic encephalopathy in chronic liver disease: a clinical manifestation of astrocyte swelling and low-grade cerebral edema? *J Hepatol* 2000; **32**: 1035-1038 [PMID: 10898326 DOI: 10.1016/s0168-8278(00)80110-5]
38 **Olde Damink SW**, Jalan R, Dejong CH. Interorgan ammonia trafficking in liver disease. *Metab Brain Dis* 2009; **24**: 169-181 [PMID: 19067143 DOI: 10.1007/s11011-008-9122-5]
39 **Romero-Gómez M**, Jover M, Del Campo JA, Royo JL, Hoyas E, Galán JJ, Montoliu C, Baccaro E, Guevara M, Córdoba J, Soriano G, Navarro JM, Martínez-Sierra C, Grande L, Galindo A, Mira E, Mañes S, Ruiz A. Variations in the promoter region of the glutaminase gene and the development of hepatic encephalopathy in patients with cirrhosis: a cohort study. *Ann Intern Med* 2010; **153**: 281-288 [PMID: 20820037 DOI: 10.7326/0003-4819-153-5-201009070-00002]
40 **Mayer LB**, Krawczyk M, Grünhage F, Lammert F, Stokes CS. A genetic variant in the promoter of phosphate-activated glutaminase is associated with hepatic encephalopathy. *J Intern Med* 2015; **278**: 313-322 [PMID: 25880019 DOI: 10.1111/joim.12374]
41 **Zhang H**, Yu G, Li J, Tu C, Hui Y, Liu D, Chen M, Zhang J, Gong X, Guo G. Overexpressing lnc240 Rescues Learning and Memory Dysfunction in Hepatic Encephalopathy Through miR-1264-5p/MEF2C Axis. *Mol Neurobiol* 2023; **60**: 2277-2294 [PMID: 36645630 DOI:

10.1007/s12035-023-03205-1]
42 **Jiang X**, Xu Y, Fagan A, Patel B, Zhou H, Bajaj JS. Single nuclear RNA sequencing of terminal ileum in patients with cirrhosis demonstrates multi-faceted alterations in the intestinal barrier. *Cell Biosci* 2024; **14**: 25 [PMID: 38369527 DOI: 10.1186/s13578-024-01209-5]
43 **Claeys W**, Van Hoecke L, Lernout H, De Nolf C, Van Imschoot G, Van Wonterghem E, Verhaege D, Castelein J, Geerts A, Van Steenkiste C, Vandenbroucke RE. Experimental hepatic encephalopathy causes early but sustained glial transcriptional changes. *J Neuroinflammation* 2023; **20**: 130 [PMID: 37248507 DOI: 10.1186/s12974-023-02814-w]
44 **Yao C**, Huang L, Wang M, Mao D, Wang M, Zheng J, Long F, Huang J, Liu X, Zhang R, Xie J, Cheng C, Yao F, Huang G. Establishment and validation of a nomogram model for riskprediction of hepatic encephalopathy: a retrospective analysis. *Sci Rep* 2023; **13**: 19544 [PMID: 37945916 DOI: 10.1038/s41598-023-47012-z]
45 **Peng Y**, Wei Q, Liu Y, Wu Z, Zhang H, Wu H, Chai J. Prediction and Risk Factors for Prognosis of Cirrhotic Patients with Hepatic Encephalopathy. *Gastroenterol Res Pract* 2021; **2021**: 5623601 [PMID: 34712321 DOI: 10.1155/2021/5623601]
46 **Tiede A**, Stockhoff L, Ehrenbauer AF, Rieland H, Cornberg M, Meyer BC, Gabriel MM, Wedemeyer H, Hinrichs JB, Weissenborn K, Falk CS, Maasoumy B. Value of systemic inflammation markers for the detection of minimal and prediction of overt hepatic encephalopathy after TIPS insertion. *Metab Brain Dis* 2024; **40**: 58 [PMID: 39656322 DOI: 10.1007/s11011-024-01436-2]
47 **Dantas Machado AC**, Ramos SF, Gauglitz JM, Fassler AM, Petras D, Aksenov AA, Kim UB, Lazarowicz M, Barnard Giustini A, Aryafar H, Vodkin I, Warren C, Dorrestein PC, Zarrinpar A, Zarrinpar A. Portosystemic shunt placement reveals blood signatures for the development of hepatic encephalopathy through mass spectrometry. *Nat Commun* 2023; **14**: 5303 [PMID: 37652904 DOI: 10.1038/s41467-023-40741-9]
48 **Nardelli S**, Lattanzi B, Torrisi S, Greco F, Farcomeni A, Gioia S, Merli M, Riggio O. Sarcopenia Is Risk Factor for Development of Hepatic Encephalopathy After Transjugular Intrahepatic Portosystemic Shunt Placement. *Clin Gastroenterol Hepatol* 2017; **15**: 934-936 [PMID: 27816756 DOI: 10.1016/j.cgh.2016.10.028]
49 **Xu X**, Yang Y, Tan X, Zhang Z, Wang B, Yang X, Weng C, Yu R, Zhao Q, Quan S. Hepatic encephalopathy post-TIPS: Current status and prospects in predictive assessment. *Comput Struct Biotechnol J* 2024; **24**: 493-506 [PMID: 39076168 DOI: 10.1016/j.csbj.2024.07.008]
50 **Yang H**, Li X, Cao H, Cui Y, Luo Y, Liu J, Zhang Y. Using machine learning methods to predict hepatic encephalopathy in cirrhotic patients with unbalanced data. *Comput Methods Programs Biomed* 2021; **211**: 106420 [PMID: 34555589 DOI: 10.1016/j.cmpb.2021.106420]
51 **Bajaj JS**, O'Leary JG, Jakab SS, Fagan A, Sikaroodi M, Gillevet PM. Gut microbiome profiles to exclude the diagnosis of hepatic encephalopathy in patients with cirrhosis. *Gut Microbes* 2024; **16**: 2392880 [PMID: 39189586 DOI: 10.1080/19490976.2024.2392880]
52 **Chen X**, Wang T, Ji Z, Luo J, Lv W, Wang H, Zhao Y, Duan C, Yu X, Li Q, Zhang J, Chen J, Zhang X, Huang M, Zhou S, Lu L, Huang M, Fu S. 3D automatic liver and spleen assessment in predicting overt hepatic encephalopathy before TIPS: a multi-center study. *Hepatol Int* 2023; **17**: 1545-1556 [PMID: 37531069 DOI: 10.1007/s12072-023-10570-5]
53 **Chen X**, Huang M, Yu X, Chen J, Xu C, Jiang Y, Li Y, Zhao Y, Duan C, Luo Y, Zhang J, Lv W, Li Q, Luo J, Dong D, An T, Lu L, Fu S. Hepatic-associated vascular morphological assessment to predict overt hepatic encephalopathy before TIPS: a multicenter study. *Hepatol Int* 2024; **18**: 1238-1248 [PMID: 38833138 DOI: 10.1007/s12072-024-10686-2]
54 **García-Pagán JC**, Saffo S, Mandorfer M, Garcia-Tsao G. Where does TIPS fit in the management of patients with cirrhosis? *JHEP Rep* 2020; **2**: 100122 [PMID: 32671331 DOI: 10.1016/j.jhepr.2020.100122]
55 **Ehrenbauer AF**, Schneider H, Stockhoff L, Tiede A, Lorenz C, Dirks M, Witt J, Gabriel MM, Wedemeyer H, Hinrichs JB, Weissenborn K, Maasoumy B. Predicting overt hepatic encephalopathy after TIPS: Value of three minimal hepatic encephalopathy tests. *JHEP Rep* 2023; **5**: 100829 [PMID: 37600959 DOI: 10.1016/j.jhepr.2023.100829]
56 **Fagiuoli S**, Bruno R, Debernardi Venon W, Schepis F, Vizzutti F, Toniutto P, Senzolo M, Caraceni P, Salerno F, Angeli P, Cioni R, Vitale A, Grosso M, De Gasperi A, D'Amico G, Marzano A; AISF TIPS Special Conference. Consensus conference on TIPS management: Techniques, indications, contraindications. *Dig Liver Dis* 2017; **49**: 121-137 [PMID: 27884494 DOI: 10.1016/j.dld.2016.10.011]
57 **Ahmed Z**, Farooq U, Faiza Arif S, Aziz M, Iqbal U, Nawaz A, Lee-Smith W, Badal J, Mahmood A, Kobeissy A, Nawras A, Hassan M, Saab S. Transjugular Intrahepatic Portosystemic Shunt Outcomes in the Elderly Population: A Systematic Review and Meta-Analysis. *Gastroenterology Res* 2022; **15**: 325-333 [PMID: 36660467 DOI: 10.14740/gr1571]
58 **Pan JJ**, Chen C, Caridi JG, Geller B, Firpi R, Machicao VI, Hawkins IF Jr, Soldevila-Pico C, Nelson DR, Morelli G. Factors predicting survival after transjugular intrahepatic portosystemic shunt creation: 15 years' experience from a single tertiary medical center. *J Vasc Interv Radiol* 2008; **19**: 1576-1581 [PMID: 18789725 DOI: 10.1016/j.jvir.2008.07.021]
59 **Hassoun Z**, Deschênes M, Lafortune M, Dufresne MP, Perreault P, Lepanto L, Gianfelice D, Bui B, Pomier-Layrargues G. Relationship between pre-TIPS liver perfusion by the portal vein and the incidence of post-TIPS chronic hepatic encephalopathy. *Am J Gastroenterol* 2001; **96**: 1205-1209 [PMID: 11316171 DOI: 10.1111/j.1572-0241.2001.03704.x]
60 **Bai M**, Qi X, Yang Z, Yin Z, Nie Y, Yuan S, Wu K, Han G, Fan D. Predictors of hepatic encephalopathy after transjugular intrahepatic portosystemic shunt in cirrhotic patients: a systematic review. *J Gastroenterol Hepatol* 2011; **26**: 943-951 [PMID: 21251067 DOI: 10.1111/j.1440-1746.2011.06663.x]
61 **Dai R**, Sag AA, Martin JG, Befera NT, Pabon-Ramos WM, Suhocki PV, Smith TP, Kim CY, Muir AJ, Ronald J. Proton pump inhibitor use is associated with increased rates of post-TIPS hepatic encephalopathy: Replication in an independent patient cohort. *Clin Imaging* 2021; **77**: 187-192 [PMID: 33940357 DOI: 10.1016/j.clinimag.2021.04.034]
62 **Tsai CF**, Chen MH, Wang YP, Chu CJ, Huang YH, Lin HC, Hou MC, Lee FY, Su TP, Lu CL. Proton Pump Inhibitors Increase Risk for Hepatic Encephalopathy in Patients With Cirrhosis in A Population Study. *Gastroenterology* 2017; **152**: 134-141 [PMID: 27639806 DOI: 10.1053/j.gastro.2016.09.007]
63 **Sturm L**, Bettinger D, Giesler M, Boettler T, Schmidt A, Buettner N, Thimme R, Schultheiss M. Treatment with proton pump inhibitors increases the risk for development of hepatic encephalopathy after implantation of transjugular intrahepatic portosystemic shunt (TIPS). *United European Gastroenterol J* 2018; **6**: 1380-1390 [PMID: 30386611 DOI: 10.1177/2050640618795928]
64 **Merola J**, Chaudhary N, Qian M, Jow A, Barboza K, Charles H, Teperman L, Sigal S. Hyponatremia: A Risk Factor for Early Overt Encephalopathy after Transjugular Intrahepatic Portosystemic Shunt Creation. *J Clin Med* 2014; **3**: 359-372 [PMID: 26237379 DOI: 10.3390/jcm3020359]
65 **Guevara M**, Baccaro ME, Torre A, Gómez-Ansón B, Ríos J, Torres F, Rami L, Monté-Rubio GC, Martín-Llahí M, Arroyo V, Ginès P. Hyponatremia is a risk factor of hepatic encephalopathy in patients with cirrhosis: a prospective study with time-dependent analysis. *Am J Gastroenterol* 2009; **104**: 1382-1389 [PMID: 19455124 DOI: 10.1038/ajg.2009.293]
66 **Liao Y**, Zhang L, Wang JT, Yue ZD, Fan ZH, Wu YF, Zhang Y, Dong CB, Wang XQ, Cui T, Meng MM, Bao L, Chen SB, Liu FQ, Wang L. A novel nomogram predicting overt hepatic encephalopathy after transjugular intrahepatic portosystemic shunt in portal hypertension patients.

Sci Rep 2023; **13**: 15244 [PMID: 37709823 DOI: 10.1038/s41598-023-42061-w]

67 **Liu J**, Yang C, Yao J, Bai Y, Li T, Wang Y, Shi Q, Wu X, Ma J, Zhou C, Huang S, Xiong B. Improvement of sarcopenia is beneficial for prognosis in cirrhotic patients after TIPS placement. *Dig Liver Dis* 2023; **55**: 918-925 [PMID: 36682922 DOI: 10.1016/j.dld.2023.01.001]

68 **Shi W**, Yin H, Yu Z, Li Y, Bai X, Fu S, Duan C, Xu W, Yang Y. Myosteatosis is an independent risk factor for overt hepatic encephalopathy after transjugular intrahepatic portosystemic shunting. *Eur J Gastroenterol Hepatol* 2024; **36**: 897-903 [PMID: 38477843 DOI: 10.1097/MEG.0000000000002729]

69 **Li J**, Feng D, Pang N, Zhao C, Gao L, Liu S, Li L. Controlling nutritional status score as a new indicator of overt hepatic encephalopathy in cirrhotic patients following transjugular intrahepatic portosystemic shunt. *Clin Nutr* 2022; **41**: 560-566 [PMID: 35032860 DOI: 10.1016/j.clnu.2021.12.036]

70 **Lee EW**, Eghtesad B, Garcia-Tsao G, Haskal ZJ, Hernandez-Gea V, Jalaeian H, Kalva SP, Mohanty A, Thabut D, Abraldes JG. AASLD Practice Guidance on the use of TIPS, variceal embolization, and retrograde transvenous obliteration in the management of variceal hemorrhage. *Hepatology* 2024; **79**: 224-250 [PMID: 37390489 DOI: 10.1097/HEP.0000000000000530]

71 **European Association for the Study of the Liver**. EASL Clinical Practice Guidelines on the management of hepatic encephalopathy. *J Hepatol* 2022; **77**: 807-824 [PMID: 35724930 DOI: 10.1016/j.jhep.2022.06.001]

72 **de Franchis R**, Bosch J, Garcia-Tsao G, Reiberger T, Ripoll C; Baveno VII Faculty. Baveno VII - Renewing consensus in portal hypertension. *J Hepatol* 2022; **76**: 959-974 [PMID: 35120736 DOI: 10.1016/j.jhep.2021.12.022]

73 **Riggio O**, Ridola L, Angeloni S, Cerini F, Pasquale C, Attili AF, Fanelli F, Merli M, Salvatori FM. Clinical efficacy of transjugular intrahepatic portosystemic shunt created with covered stents with different diameters: results of a randomized controlled trial. *J Hepatol* 2010; **53**: 267-272 [PMID: 20537753 DOI: 10.1016/j.jhep.2010.02.033]

74 **Huang Z**, Yao Q, Zhu J, He Y, Chen Y, Wu F, Hua T. Efficacy and safety of transjugular intrahepatic portosystemic shunt (TIPS) created using covered stents of different diameters: A systematic review and meta-analysis. *Diagn Interv Imaging* 2021; **102**: 279-285 [PMID: 33303394 DOI: 10.1016/j.diii.2020.11.004]

75 **Wang Q**, Lv Y, Bai M, Wang Z, Liu H, He C, Niu J, Guo W, Luo B, Yin Z, Bai W, Chen H, Wang E, Xia D, Li X, Yuan J, Han N, Cai H, Li T, Xie H, Xia J, Wang J, Zhang H, Wu K, Fan D, Han G. Eight millimetre covered TIPS does not compromise shunt function but reduces hepatic encephalopathy in preventing variceal rebleeding. *J Hepatol* 2017; **67**: 508-516 [PMID: 28506905 DOI: 10.1016/j.jhep.2017.05.006]

76 **Trebicka J**, Bastgen D, Byrtus J, Praktiknjo M, Terstiegen S, Meyer C, Thomas D, Fimmers R, Treitl M, Euringer W, Sauerbruch T, Rössle M. Smaller-Diameter Covered Transjugular Intrahepatic Portosystemic Shunt Stents Are Associated With Increased Survival. *Clin Gastroenterol Hepatol* 2019; **17**: 2793-2799.e1 [PMID: 30940552 DOI: 10.1016/j.cgh.2019.03.042]

77 **Yan H**, Xiang Z, Zhao C, Luo S, Liu H, Li M, Huang M. 6-mm shunt transjugular intrahepatic portosystemic shunt in patients with severe liver atrophy and variceal bleeding. *Eur Radiol* 2024; **34**: 4697-4707 [PMID: 38006453 DOI: 10.1007/s00330-023-10346-3]

78 **Monnin-Bares V**, Thony F, Sengel C, Bricault I, Leroy V, Ferretti G. Stent-graft narrowed with a lasso catheter: an adjustable TIPS reduction technique. *J Vasc Interv Radiol* 2010; **21**: 275-280 [PMID: 20123211 DOI: 10.1016/j.jvir.2009.10.019]

79 **Riggio O**, Efrati C, Catalano C, Pediconi F, Mecarelli O, Accornero N, Nicolao F, Angeloni S, Masini A, Ridola L, Attili AF, Merli M. High prevalence of spontaneous portal-systemic shunts in persistent hepatic encephalopathy: a case-control study. *Hepatology* 2005; **42**: 1158-1165 [PMID: 16250033 DOI: 10.1002/hep.20905]

80 **Nardelli S**, Riggio O, Gioia S, Puzzono M, Pelle G, Ridola L. Spontaneous porto-systemic shunts in liver cirrhosis: Clinical and therapeutical aspects. *World J Gastroenterol* 2020; **26**: 1726-1732 [PMID: 32351289 DOI: 10.3748/wjg.v26.i15.1726]

81 **Vidal-González J**, Simón-Talero M, Genescà J. Should prophylactic embolization of spontaneous portosystemic shunts be routinely performed during transjugular intrahepatic portosystemic shunt placement? *Dig Liver Dis* 2018; **50**: 1324-1326 [PMID: 30005961 DOI: 10.1016/j.dld.2018.06.013]

82 **Praktiknjo M**, Simón-Talero M, Römer J, Roccarina D, Martínez J, Lampichler K, Baiges A, Low G, Llop E, Maurer MH, Zipprich A, Triolo M, Maleux G, Fialla AD, Dam C, Vidal-González J, Majumdar A, Picón C, Toth D, Darnell A, Abraldes JG, López M, Jansen C, Chang J, Schierwagen R, Uschner F, Kukuk G, Meyer C, Thomas D, Wolter K, Strassburg CP, Laleman W, La Mura V, Ripoll C, Berzigotti A, Calleja JL, Tandon P, Hernandez-Gea V, Reiberger T, Albillos A, Tsochatzis EA, Krag A, Genescà J, Trebicka J; Baveno VI-SPSS group of the Baveno Cooperation. Total area of spontaneous portosystemic shunts independently predicts hepatic encephalopathy and mortality in liver cirrhosis. *J Hepatol* 2020; **72**: 1140-1150 [PMID: 31954206 DOI: 10.1016/j.jhep.2019.12.021]

83 **Lv Y**, Chen H, Luo B, Bai W, Li K, Wang Z, Xia D, Guo W, Wang Q, Li X, Yuan J, Cai H, Xia J, Yin Z, Fan D, Han G. Concurrent large spontaneous portosystemic shunt embolization for the prevention of overt hepatic encephalopathy after TIPS: A randomized controlled trial. *Hepatology* 2022; **76**: 676-688 [PMID: 35266571 DOI: 10.1002/hep.32453]

84 **Yang M**, Qiu Y, Wang W. Concurrent spontaneous portosystemic shunt embolization for the prevention of overt hepatic encephalopathy after TIPS: A systematic review and meta-analysis. *Dig Liver Dis* 2024; **56**: 978-985 [PMID: 37926635 DOI: 10.1016/j.dld.2023.10.013]

85 **Boike JR**, Thornburg BG, Asrani SK, Fallon MB, Fortune BE, Izzy MJ, Verna EC, Abraldes JG, Allegretti AS, Bajaj JS, Biggins SW, Darcy MD, Farr MA, Farsad K, Garcia-Tsao G, Hall SA, Jadlowiec CC, Krowka MJ, Laberge J, Lee EW, Mulligan DC, Nadim MK, Northup PG, Salem R, Shatzel JJ, Shaw CJ, Simonetto DA, Susman J, Kolli KP, VanWagner LB; Advancing Liver Therapeutic Approaches (ALTA) Consortium. North American Practice-Based Recommendations for Transjugular Intrahepatic Portosystemic Shunts in Portal Hypertension. *Clin Gastroenterol Hepatol* 2022; **20**: 1636-1662.e36 [PMID: 34274511 DOI: 10.1016/j.cgh.2021.07.018]

86 **Lee EW**, Lee AE, Saab S, Kee ST. Retrograde Transvenous Obliteration (RTO): A New Treatment Option for Hepatic Encephalopathy. *Dig Dis Sci* 2020; **65**: 2483-2491 [PMID: 32002756 DOI: 10.1007/s10620-020-06050-7]

87 Nutritional status in cirrhosis. Italian Multicentre Cooperative Project on Nutrition in Liver Cirrhosis. *J Hepatol* 1994; **21**: 317-325 [PMID: 7836699]

88 **Nguyen DL**, Morgan T. Protein restriction in hepatic encephalopathy is appropriate for selected patients: a point of view. *Hepatol Int* 2014; **8**: 447-451 [PMID: 25525477 DOI: 10.1007/s12072-013-9497-1]

89 **Daftari G**, Tehrani AN, Pashayee-Khamene F, Karimi S, Ahmadzadeh S, Hekmatdoost A, Salehpour A, Saber-Firoozi M, Hatami B, Yari Z. Dietary protein intake and mortality among survivors of liver cirrhosis: a prospective cohort study. *BMC Gastroenterol* 2023; **23**: 227 [PMID: 37400778 DOI: 10.1186/s12876-023-02832-1]

90 **European Association for the Study of the Liver**. EASL Clinical Practice Guidelines on nutrition in chronic liver disease. *J Hepatol* 2019; **70**: 172-193 [PMID: 30144956 DOI: 10.1016/j.jhep.2018.06.024]

91 **Iqbal U**, Jadeja RN, Khara HS, Khurana S. A Comprehensive Review Evaluating the Impact of Protein Source (Vegetarian vs. Meat Based) in Hepatic Encephalopathy. *Nutrients* 2021; **13**: 370 [PMID: 33530344 DOI: 10.3390/nu13020370]

92 **Maharshi S**, Sharma BC, Sachdeva S, Srivastava S, Sharma P. Efficacy of Nutritional Therapy for Patients With Cirrhosis and Minimal Hepatic Encephalopathy in a Randomized Trial. *Clin Gastroenterol Hepatol* 2016; **14**: 454-460.e3; quiz e33 [PMID: 26453952 DOI: 10.1016/j.cgh.2015.09.028]

93 **Kato A**, Tanaka H, Kawaguchi T, Kanazawa H, Iwasa M, Sakaida I, Moriwaki H, Murawaki Y, Suzuki K, Okita K. Nutritional management contributes to improvement in minimal hepatic encephalopathy and quality of life in patients with liver cirrhosis: A preliminary, prospective, open-label study. *Hepatol Res* 2013; **43**: 452-458 [PMID: 22994429 DOI: 10.1111/j.1872-034X.2012.01092.x]

94 **Hanai T**, Nishimura K, Unome S, Miwa T, Nakahata Y, Imai K, Suetsugu A, Takai K, Shimizu M. Nutritional counseling improves mortality and prevents hepatic encephalopathy in patients with alcohol-associated liver disease. *Hepatol Res* 2024; **54**: 1089-1098 [PMID: 38683882 DOI: 10.1111/hepr.14053]

95 **Luo L**, Fu S, Zhang Y, Wang J. Early diet intervention to reduce the incidence of hepatic encephalopathy in cirrhosis patients: post-Transjugular Intrahepatic Portosystemic Shunt (TIPS) findings. *Asia Pac J Clin Nutr* 2016; **25**: 497-503 [PMID: 27440683 DOI: 10.6133/apjcn.092015.14]

96 **Gerber T**, Schomerus H. Hepatic encephalopathy in liver cirrhosis: pathogenesis, diagnosis and management. *Drugs* 2000; **60**: 1353-1370 [PMID: 11152016 DOI: 10.2165/00003495-200060060-00008]

97 **Wang MW**, Ma WJ, Wang Y, Ma XH, Xue YF, Guan J, Chen X. Comparison of the effects of probiotics, rifaximin, and lactulose in the treatment of minimal hepatic encephalopathy and gut microbiota. *Front Microbiol* 2023; **14**: 1091167 [PMID: 37032856 DOI: 10.3389/fmicb.2023.1091167]

98 **Eriksen PL**, Djernes L, Vilstrup H, Ott P. Clearance and production of ammonia quantified in humans by constant ammonia infusion - the effects of cirrhosis and ammonia-targeting treatments. *J Hepatol* 2023; **79**: 340-348 [PMID: 37061198 DOI: 10.1016/j.jhep.2023.03.042]

99 **Bass NM**, Mullen KD, Sanyal A, Poordad F, Neff G, Leevy CB, Sigal S, Sheikh MY, Beavers K, Frederick T, Teperman L, Hillebrand D, Huang S, Merchant K, Shaw A, Bortey E, Forbes WP. Rifaximin treatment in hepatic encephalopathy. *N Engl J Med* 2010; **362**: 1071-1081 [PMID: 20335583 DOI: 10.1056/NEJMoa0907893]

100 **Riggio O**, Masini A, Efrati C, Nicolao F, Angeloni S, Salvatori FM, Bezzi M, Attili AF, Merli M. Pharmacological prophylaxis of hepatic encephalopathy after transjugular intrahepatic portosystemic shunt: a randomized controlled study. *J Hepatol* 2005; **42**: 674-679 [PMID: 15826716 DOI: 10.1016/j.jhep.2004.12.028]

101 **Seifert LL**, Schindler P, Schoster M, Weller JF, Wilms C, Schmidt HH, Maschmeier M, Masthoff M, Köhler M, Heinzow H, Wildgruber M. Recurrence of Hepatic Encephalopathy after TIPS: Effective Prophylaxis with Combination of Lactulose and Rifaximin. *J Clin Med* 2021; **10**: 4763 [PMID: 34682886 DOI: 10.3390/jcm10204763]

102 **Scarpignato C**, Pelosini I. Rifaximin, a poorly absorbed antibiotic: pharmacology and clinical potential. *Chemotherapy* 2005; **51** Suppl 1: 36-66 [PMID: 15855748 DOI: 10.1159/000081990]

103 **Patel VC**, Lee S, McPhail MJW, Da Silva K, Guilly S, Zamalloa A, Witherden E, Støy S, Manakkat Vijay GK, Pons N, Galleron N, Huang X, Gencer S, Coen M, Tranah TH, Wendon JA, Bruce KD, Le Chatelier E, Ehrlich SD, Edwards LA, Shoaie S, Shawcross DL. Rifaximin-α reduces gut-derived inflammation and mucin degradation in cirrhosis and encephalopathy: RIFSYS randomised controlled trial. *J Hepatol* 2022; **76**: 332-342 [PMID: 34571050 DOI: 10.1016/j.jhep.2021.09.010]

104 **Bajaj JS**, Heuman DM, Sanyal AJ, Hylemon PB, Sterling RK, Stravitz RT, Fuchs M, Ridlon JM, Daita K, Monteith P, Noble NA, White MB, Fisher A, Sikaroodi M, Rangwala H, Gillevet PM. Modulation of the metabiome by rifaximin in patients with cirrhosis and minimal hepatic encephalopathy. *PLoS One* 2013; **8**: e60042 [PMID: 23565181 DOI: 10.1371/journal.pone.0060042]

105 **Kimer N**, Pedersen JS, Tavenier J, Christensen JE, Busk TM, Hobolth L, Krag A, Al-Soud WA, Mortensen MS, Sørensen SJ, Møller S, Bendtsen F; members of the CoRif study group. Rifaximin has minor effects on bacterial composition, inflammation, and bacterial translocation in cirrhosis: A randomized trial. *J Gastroenterol Hepatol* 2018; **33**: 307-314 [PMID: 28671712 DOI: 10.1111/jgh.13852]

106 **de Wit K**, Beuers U, Mukha A, Stigter ECA, Gulersonmez MC, Ramos Pittol JM, Middendorp S, Takkenberg RB, van Mil SWC. Rifaximin stimulates nitrogen detoxification by PXR-independent mechanisms in human small intestinal organoids. *Liver Int* 2023; **43**: 649-659 [PMID: 36463417 DOI: 10.1111/liv.15491]

107 **de Wit K**, Schaapman JJ, Nevens F, Verbeek J, Coenen S, Cuperus FJC, Kramer M, Tjwa ETTL, Mostafavi N, Dijkgraaf MGW, van Delden OM, Beuers UHW, Coenraad MJ, Takkenberg RB. Prevention of hepatic encephalopathy by administration of rifaximin and lactulose in patients with liver cirrhosis undergoing placement of a transjugular intrahepatic portosystemic shunt (TIPS): a multicentre randomised, double blind, placebo controlled trial (PEARL trial). *BMJ Open Gastroenterol* 2020; **7**: e000531 [PMID: 33372103 DOI: 10.1136/bmjgast-2020-000531]

108 **Bureau C**, Thabut D, Jezequel C, Archambeaud I, D'Alteroche L, Dharancy S, Borentain P, Oberti F, Plessier A, De Ledinghen V, Ganne-Carrié N, Carbonell N, Rousseau V, Sommet A, Péron JM, Vinel JP. The Use of Rifaximin in the Prevention of Overt Hepatic Encephalopathy After Transjugular Intrahepatic Portosystemic Shunt : A Randomized Controlled Trial. *Ann Intern Med* 2021; **174**: 633-640 [PMID: 33524293 DOI: 10.7326/M20-0202]

109 **Bouza E**, Alcalá L, Marín M, Valerio M, Reigadas E, Muñoz P, González-Del Vecchio M, de Egea V. An outbreak of Clostridium difficile PCR ribotype 027 in Spain: risk factors for recurrence and a novel treatment strategy. *Eur J Clin Microbiol Infect Dis* 2017; **36**: 1777-1786 [PMID: 28501926 DOI: 10.1007/s10096-017-2991-y]

110 **Zullo A**, Hassan C, Ridola L, Lorenzetti R, Campo SM, Riggio O. Rifaximin therapy and hepatic encephalopathy: Pros and cons. *World J Gastrointest Pharmacol Ther* 2012; **3**: 62-67 [PMID: 22966484 DOI: 10.4292/wjgpt.v3.i4.62]

111 **Bajaj JS**. The role of microbiota in hepatic encephalopathy. *Gut Microbes* 2014; **5**: 397-403 [PMID: 24690956 DOI: 10.4161/gmic.28684]

112 **Patel R**, DuPont HL. New approaches for bacteriotherapy: prebiotics, new-generation probiotics, and synbiotics. *Clin Infect Dis* 2015; **60** Suppl 2: S108-S121 [PMID: 25922396 DOI: 10.1093/cid/civ177]

113 **Bajaj JS**, Heuman DM, Hylemon PB, Sanyal AJ, Puri P, Sterling RK, Luketic V, Stravitz RT, Siddiqui MS, Fuchs M, Thacker LR, Wade JB, Daita K, Sistrun S, White MB, Noble NA, Thorpe C, Kakiyama G, Pandak WM, Sikaroodi M, Gillevet PM. Randomised clinical trial: Lactobacillus GG modulates gut microbiome, metabolome and endotoxemia in patients with cirrhosis. *Aliment Pharmacol Ther* 2014; **39**: 1113-1125 [PMID: 24628464 DOI: 10.1111/apt.12695]

114 **Stadlbauer V**, Mookerjee RP, Hodges S, Wright GA, Davies NA, Jalan R. Effect of probiotic treatment on deranged neutrophil function and cytokine responses in patients with compensated alcoholic cirrhosis. *J Hepatol* 2008; **48**: 945-951 [PMID: 18433921 DOI: 10.1016/j.jhep.2008.02.015]

115 **Yang X**, Yu D, Xue L, Li H, Du J. Probiotics modulate the microbiota-gut-brain axis and improve memory deficits in aged SAMP8 mice. *Acta Pharm Sin B* 2020; **10**: 475-487 [PMID: 32140393 DOI: 10.1016/j.apsb.2019.07.001]

116 **Pratap Mouli V**, Benjamin J, Bhushan Singh M, Mani K, Garg SK, Saraya A, Joshi YK. Effect of probiotic VSL#3 in the treatment of minimal hepatic encephalopathy: A non-inferiority randomized controlled trial. *Hepatol Res* 2015; **45**: 880-889 [PMID: 25266207 DOI: 10.1111/hepr.12429]

117 **Pereg D**, Kotliroff A, Gadoth N, Hadary R, Lishner M, Kitay-Cohen Y. Probiotics for patients with compensated liver cirrhosis: a double-blind placebo-controlled study. *Nutrition* 2011; **27**: 177-181 [PMID: 20452184 DOI: 10.1016/j.nut.2010.01.006]

118 **Viramontes Hörner D**, Avery A, Stow R. The Effects of Probiotics and Symbiotics on Risk Factors for Hepatic Encephalopathy: A Systematic Review. *J Clin Gastroenterol* 2017; **51**: 312-323 [PMID: 28059938 DOI: 10.1097/MCG.0000000000000789]

119 **Xia X**, Chen J, Xia J, Wang B, Liu H, Yang L, Wang Y, Ling Z. Role of probiotics in the treatment of minimal hepatic encephalopathy in patients with HBV-induced liver cirrhosis. *J Int Med Res* 2018; **46**: 3596-3604 [PMID: 29806520 DOI: 10.1177/0300060518776064]

120 **Lunia MK**, Sharma BC, Sharma P, Sachdeva S, Srivastava S. Probiotics prevent hepatic encephalopathy in patients with cirrhosis: a randomized controlled trial. *Clin Gastroenterol Hepatol* 2014; **12**: 1003-8.e1 [PMID: 24246768 DOI: 10.1016/j.cgh.2013.11.006]

121 **Dhiman RK**, Rana B, Agrawal S, Garg A, Chopra M, Thumburu KK, Khattri A, Malhotra S, Duseja A, Chawla YK. Probiotic VSL#3 reduces liver disease severity and hospitalization in patients with cirrhosis: a randomized, controlled trial. *Gastroenterology* 2014; **147**: 1327-37.e3 [PMID: 25450083 DOI: 10.1053/j.gastro.2014.08.031]

122 **Abraldes JG**, Caraceni P, Ghabril M, Garcia-Tsao G. Update in the Treatment of the Complications of Cirrhosis. *Clin Gastroenterol Hepatol* 2023; **21**: 2100-2109 [PMID: 36972759 DOI: 10.1016/j.cgh.2023.03.019]

123 **Stauch S**, Kircheis G, Adler G, Beckh K, Ditschuneit H, Görtelmeyer R, Hendricks R, Heuser A, Karoff C, Malfertheiner P, Mayer D, Rösch W, Steffens J. Oral L-ornithine-L-aspartate therapy of chronic hepatic encephalopathy: results of a placebo-controlled double-blind study. *J Hepatol* 1998; **28**: 856-864 [PMID: 9625322 DOI: 10.1016/s0168-8278(98)80237-7]

124 **Jain A**, Sharma BC, Mahajan B, Srivastava S, Kumar A, Sachdeva S, Sonika U, Dalal A. L-ornithine L-aspartate in acute treatment of severe hepatic encephalopathy: A double-blind randomized controlled trial. *Hepatology* 2022; **75**: 1194-1203 [PMID: 34822189 DOI: 10.1002/hep.32255]

125 **Bai M**, Yang Z, Qi X, Fan D, Han G. l-ornithine-l-aspartate for hepatic encephalopathy in patients with cirrhosis: a meta-analysis of randomized controlled trials. *J Gastroenterol Hepatol* 2013; **28**: 783-792 [PMID: 23425108 DOI: 10.1111/jgh.12142]

126 **Goh ET**, Stokes CS, Sidhu SS, Vilstrup H, Gluud LL, Morgan MY. L-ornithine L-aspartate for prevention and treatment of hepatic encephalopathy in people with cirrhosis. *Cochrane Database Syst Rev* 2018; **5**: CD012410 [PMID: 29762873 DOI: 10.1002/14651858.CD012410.pub2]

127 **Jiang Q**, Jiang XH, Zheng MH, Chen YP. L-Ornithine-l-aspartate in the management of hepatic encephalopathy: a meta-analysis. *J Gastroenterol Hepatol* 2009; **24**: 9-14 [PMID: 18823442 DOI: 10.1111/j.1440-1746.2008.05582.x]

128 **Butterworth RF**, McPhail MJW. L-Ornithine L-Aspartate (LOLA) for Hepatic Encephalopathy in Cirrhosis: Results of Randomized Controlled Trials and Meta-Analyses. *Drugs* 2019; **79**: 31-37 [PMID: 30706425 DOI: 10.1007/s40265-018-1024-1]

129 **Rees CJ**, Oppong K, Al Mardini H, Hudson M, Record CO. Effect of L-ornithine-L-aspartate on patients with and without TIPS undergoing glutamine challenge: a double blind, placebo controlled trial. *Gut* 2000; **47**: 571-574 [PMID: 10986219 DOI: 10.1136/gut.47.4.571]

130 **Gluud LL**, Dam G, Les I, Marchesini G, Borre M, Aagaard NK, Vilstrup H. Branched-chain amino acids for people with hepatic encephalopathy. *Cochrane Database Syst Rev* 2017; **5**: CD001939 [PMID: 28518283 DOI: 10.1002/14651858.CD001939.pub4]

131 **Soeters PB**, Fischer JE. Insulin, glucagon, aminoacid imbalance, and hepatic encephalopathy. *Lancet* 1976; **2**: 880-882 [PMID: 62115 DOI: 10.1016/s0140-6736(76)90541-9]

132 **Badal BD**, Fagan A, Tate V, Mousel T, Gallagher ML, Puri P, Davis B, Miller J, Sikaroodi M, Gillevet P, Gedguadas R, Kupcinkas J, Thacker L, Bajaj JS. Substitution of One Meat-Based Meal With Vegetarian and Vegan Alternatives Generates Lower Ammonia and Alters Metabolites in Cirrhosis: A Randomized Clinical Trial. *Clin Transl Gastroenterol* 2024; **15**: e1 [PMID: 38696431 DOI: 10.14309/ctg.0000000000000707]

133 **Cerra FB**, Cheung NK, Fischer JE, Kaplowitz N, Schiff ER, Dienstag JL, Bower RH, Mabry CD, Leevy CM, Kiernan T. Disease-specific amino acid infusion (F080) in hepatic encephalopathy: a prospective, randomized, double-blind, controlled trial. *JPEN J Parenter Enteral Nutr* 1985; **9**: 288-295 [PMID: 3892073 DOI: 10.1177/0148607185009003288]

134 **Vidot H**, Cvejic E, Finegan LJ, Shores EA, Bowen DG, Strasser SI, McCaughan GW, Carey S, Allman-Farinelli M, Shackel NA. Supplementation with Synbiotics and/or Branched Chain Amino Acids in Hepatic Encephalopathy: A Pilot Randomised Placebo-Controlled Clinical Study. *Nutrients* 2019; **11**: 1810 [PMID: 31390762 DOI: 10.3390/nu11081810]

135 **Les I**, Doval E, García-Martínez R, Planas M, Cárdenas G, Gómez P, Flavià M, Jacas C, Mínguez B, Vergara M, Soriano G, Vila C, Esteban R, Córdoba J. Effects of branched-chain amino acids supplementation in patients with cirrhosis and a previous episode of hepatic encephalopathy: a randomized study. *Am J Gastroenterol* 2011; **106**: 1081-1088 [PMID: 21326220 DOI: 10.1038/ajg.2011.9]

136 **Wahren J**, Denis J, Desurmont P, Eriksson LS, Escoffier JM, Gauthier AP, Hagenfeldt L, Michel H, Opolon P, Paris JC, Veyrac M. Is intravenous administration of branched chain amino acids effective in the treatment of hepatic encephalopathy? A multicenter study. *Hepatology* 1983; **3**: 475-480 [PMID: 6345330 DOI: 10.1002/hep.1840030402]

137 **Basson AR**, Zhou Y, Seo B, Rodriguez-Palacios A, Cominelli F. Autologous fecal microbiota transplantation for the treatment of inflammatory bowel disease. *Transl Res* 2020; **226**: 1-11 [PMID: 32585148 DOI: 10.1016/j.trsl.2020.05.008]

138 **Cong J**, Zhou P, Zhang R. Intestinal Microbiota-Derived Short Chain Fatty Acids in Host Health and Disease. *Nutrients* 2022; **14**: 1977 [PMID: 35565943 DOI: 10.3390/nu14091977]

139 **Ramai D**, Zakhia K, Ofosu A, Ofori E, Reddy M. Fecal microbiota transplantation: donor relation, fresh or frozen, delivery methods, cost-effectiveness. *Ann Gastroenterol* 2019; **32**: 30-38 [PMID: 30598589 DOI: 10.20524/aog.2018.0328]

140 **Youngster I**, Mahabamunuge J, Systrom HK, Sauk J, Khalili H, Levin J, Kaplan JL, Hohmann EL. Oral, frozen fecal microbiota transplant (FMT) capsules for recurrent Clostridium difficile infection. *BMC Med* 2016; **14**: 134 [PMID: 27609178 DOI: 10.1186/s12916-016-0680-9]

141 **Bloom PP**, Donlan J, Torres Soto M, Daidone M, Hohmann E, Chung RT. Fecal microbiota transplant improves cognition in hepatic encephalopathy and its effect varies by donor and recipient. *Hepatol Commun* 2022; **6**: 2079-2089 [PMID: 35384391 DOI: 10.1002/hep4.1950]

142 **Li Y**, Lv L, Ye J, Fang D, Shi D, Wu W, Wang Q, Wu J, Yang L, Bian X, Jiang X, Jiang H, Yan R, Peng C, Li L. Bifidobacterium adolescentis CGMCC 15058 alleviates liver injury, enhances the intestinal barrier and modifies the gut microbiota in D-galactosamine-treated rats. *Appl Microbiol Biotechnol* 2019; **103**: 375-393 [PMID: 30345482 DOI: 10.1007/s00253-018-9454-y]

143 **Bajaj JS**, Kassam Z, Fagan A, Gavis EA, Liu E, Cox IJ, Kheradman R, Heuman D, Wang J, Gurry T, Williams R, Sikaroodi M, Fuchs M, Alm E, John B, Thacker LR, Riva A, Smith M, Taylor-Robinson SD, Gillevet PM. Fecal microbiota transplant from a rational stool donor improves hepatic encephalopathy: A randomized clinical trial. *Hepatology* 2017; **66**: 1727-1738 [PMID: 28586116 DOI: 10.1002/hep.29306]

144 **Bajaj JS**, Shamsaddini A, Acharya C, Fagan A, Sikaroodi M, Gavis E, McGeorge S, Khoruts A, Fuchs M, Sterling RK, Lee H, Gillevet PM. Multiple bacterial virulence factors focused on adherence and biofilm formation associate with outcomes in cirrhosis. *Gut Microbes* 2021; **13**: 1993584 [PMID: 34743650 DOI: 10.1080/19490976.2021.1993584]

145 **Gao J**, Nie R, Chang H, Yang W, Ren Q. A meta-analysis of microbiome therapies for hepatic encephalopathy. *Eur J Gastroenterol Hepatol* 2023; **35**: 927-937 [PMID: 37505972 DOI: 10.1097/MEG.0000000000002596]

146 **Li J**, Wang D, Sun J. Application of fecal microbial transplantation in hepatic encephalopathy after transjugular intrahepatic portosystemic shunt. *Medicine (Baltimore)* 2022; **101**: e28584 [PMID: 35060521 DOI: 10.1097/MD.0000000000028584]

147 **Bloom PP**, Tapper EB, Young VB, Lok AS. Microbiome therapeutics for hepatic encephalopathy. *J Hepatol* 2021; **75**: 1452-1464 [PMID: 34453966 DOI: 10.1016/j.jhep.2021.08.004]

148 **Riggio O**, Angeloni S, Salvatori FM, De Santis A, Cerini F, Farcomeni A, Attili AF, Merli M. Incidence, natural history, and risk factors of hepatic encephalopathy after transjugular intrahepatic portosystemic shunt with polytetrafluoroethylene-covered stent grafts. *Am J Gastroenterol* 2008; **103**: 2738-2746 [PMID: 18775022 DOI: 10.1111/j.1572-0241.2008.02102.x]

149 **Maleux G**, Verslype C, Heye S, Wilms G, Marchal G, Nevens F. Endovascular shunt reduction in the management of transjugular portosystemic shunt-induced hepatic encephalopathy: preliminary experience with reduction stents and stent-grafts. *AJR Am J Roentgenol* 2007; **188**: 659-664 [PMID: 17312051 DOI: 10.2214/AJR.05.1250]

150 **Fanelli F**, Salvatori FM, Rabuffi P, Boatta E, Riggio O, Lucatelli P, Passariello R. Management of refractory hepatic encephalopathy after insertion of TIPS: long-term results of shunt reduction with hourglass-shaped balloon-expandable stent-graft. *AJR Am J Roentgenol* 2009; **193**: 1696-1702 [PMID: 19933667 DOI: 10.2214/AJR.09.2968]

151 **Rowley MW**, Choi M, Chen S, Hirsch K, Seetharam AB. Refractory Hepatic Encephalopathy After Elective Transjugular Intrahepatic Portosystemic Shunt: Risk Factors and Outcomes with Revision. *Cardiovasc Intervent Radiol* 2018; **41**: 1765-1772 [PMID: 29872892 DOI: 10.1007/s00270-018-1992-2]

152 **Shah RJ**, Alqadi MM, Duvvuri M, Kim YJ, Tyagi R, Lokken RP, Gaba RC. Clinical Outcomes and Patency after Transjugular Intrahepatic Portosystemic Shunt Reduction for Overshunting Adverse Events. *J Vasc Interv Radiol* 2022; **33**: 1507-1512 [PMID: 35964879 DOI: 10.1016/j.jvir.2022.08.007]

153 **Li X**, Partovi S, Coronado WM, Gadani S, Martin C, Thompson D, Levitin A, Kapoor B. Hepatic Encephalopathy After TIPS Placement: Predictive Factors, Prevention Strategies, and Management. *Cardiovasc Intervent Radiol* 2022; **45**: 570-577 [PMID: 34981195 DOI: 10.1007/s00270-021-03045-3]

154 **Nardelli S**, Riggio O, Marra F, Gioia S, Saltini D, Bellafante D, Adotti V, Guasconi T, Ridola L, Rosi M, Caporali C, Fanelli F, Roccarina D, Bianchini M, Indulti F, Spagnoli A, Merli M, Vizzutti F, Schepis F. Episodic overt hepatic encephalopathy after transjugular intrahepatic portosystemic shunt does not increase mortality in patients with cirrhosis. *J Hepatol* 2024; **80**: 596-602 [PMID: 38097113 DOI: 10.1016/j.jhep.2023.11.033]

155 **Larrue H**, D'Amico G, Olivas P, Lv Y, Bucsics T, Rudler M, Sauerbruch T, Hernandez-Gea V, Han G, Reiberger T, Thabut D, Vinel JP, Péron JM, García-Pagán JC, Bureau C. TIPS prevents further decompensation and improves survival in patients with cirrhosis and portal hypertension in an individual patient data meta-analysis. *J Hepatol* 2023; **79**: 692-703 [PMID: 37141993 DOI: 10.1016/j.jhep.2023.04.028]

World Journal of Gastroenterology

Submit a Manuscript: https://www.f6publishing.com

World J Gastroenterol 2025 April 21; 31(15): 104901

DOI: 10.3748/wjg.v31.i15.104901

ISSN 1007-9327 (print) ISSN 2219-2840 (online)

REVIEW

Conversion treatment for advanced intrahepatic cholangiocarcinoma: Opportunities and challenges

Jun-Jie Liu, Mi Zhou, Tong Yuan, Zhi-Yong Huang, Zun-Yi Zhang

Specialty type: Gastroenterology and hepatology

Provenance and peer review: Unsolicited article; Externally peer reviewed.

Peer-review model: Single blind

Peer-review report's classification

Scientific Quality: Grade A, Grade B, Grade C

Novelty: Grade B, Grade B, Grade B

Creativity or Innovation: Grade B, Grade B, Grade B

Scientific Significance: Grade B, Grade B, Grade B

P-Reviewer: Wei R; Zhao K

Received: January 5, 2025

Revised: February 22, 2025

Accepted: March 26, 2025

Published online: April 21, 2025

Processing time: 102 Days and 20.7 Hours

Jun-Jie Liu, Mi Zhou, Tong Yuan, Zhi-Yong Huang, Zun-Yi Zhang, Hepatic Surgery Center, Tongji Hospital, Tongji Medical College, Huazhong University of Science and Technology, Wuhan 430030, Hubei Province, China

Co-corresponding authors: Zhi-Yong Huang and Zun-Yi Zhang.

Corresponding author: Zun-Yi Zhang, MD, Associate Professor, Hepatic Surgery Center, Tongji Hospital, Tongji Medical College, Huazhong University of Science and Technology, No. 1095 Jiefang Avenue, Wuhan 430030, Hubei Province, China. zunyizhangtjmu@163.com

Abstract

The prevalence of intrahepatic cholangiocarcinoma (ICC) is increasing globally. Despite advancements in comprehending this intricate malignancy and formulating novel therapeutic approaches over the past few decades, the prognosis for ICC remains poor. Owing to the high degree of malignancy and insidious onset of ICC, numerous cases are detected at intermediate or advanced stages of the disease, hence eliminating the chance for surgical intervention. Moreover, because of the highly invasive characteristics of ICC, recurrence and metastasis postresection are prevalent, leading to a 5-year survival rate of only 20%-35% following surgery. In the past decade, different methods of treatment have been investigated, including transarterial chemoembolization, transarterial radioembolization, radiotherapy, systemic therapy, and combination therapies. For certain patients with advanced ICC, conversion treatment may be utilized to facilitate surgical resection and manage disease progression. This review summarizes the definition of downstaging conversion treatment and presents the clinical experience and evidence concerning conversion treatment for advanced ICC.

Key Words: Intrahepatic cholangiocarcinoma; Conversion treatment; Downstaging; Combination therapy; Chemotherapy; Immunotherapy; Locoregional therapies

Core Tip: The conversion treatment for unresectable intrahepatic cholangiocarcinoma (ICC) can reduce tumor burden and enhance the likelihood of surgical resection. Chemotherapy is still the base treatment for advanced ICC. However, locoregional therapies and systemic therapies are promising treatment strategies for advanced ICC, aiming to enhance tumor response and improve patient outcomes. Achieving an adequate future liver remnant is crucial to prevent posthepatectomy liver failure; techniques are being investigated to enhance future liver remnant and improve outcomes in patients with advanced ICC.

Citation: Liu JJ, Zhou M, Yuan T, Huang ZY, Zhang ZY. Conversion treatment for advanced intrahepatic cholangiocarcinoma: Opportunities and challenges. *World J Gastroenterol* 2025; 31(15): 104901
URL: https://www.wjgnet.com/1007-9327/full/v31/i15/104901.htm
DOI: https://dx.doi.org/10.3748/wjg.v31.i15.104901

INTRODUCTION

Intrahepatic cholangiocarcinoma (ICC) ranks as the second most prevalent primary liver cancer after hepatocellular carcinoma (HCC), constituting approximately 10%-15% of primary liver cancers[1]. Chronic inflammation typically occurs when ICC develops, leading to cholestasis and subsequent cholangiocyte injury[2]. The numerous risk factors for ICC include bile duct cysts, cholangitis, Caroli's disease, hepatolithiasis, cirrhosis, viral hepatitis, parasitic infection, digestive diseases, and metabolic and endocrine disorders, among others[3]. As the main risk factors for ICC have become more common over the past few decades, mortality from this disease has tended to grow in a number of areas across the world[4].

Surgical treatment is the most effective approach for achieving long-term survival in patients with cholangiocarcinoma. The patient should undergo surgery if radical resection of cholangiocarcinoma is feasible and if there are no distant metastases or other surgical contraindications[5]. However, cholangiocarcinoma is typically asymptomatic in the initial stages, leading to a diagnosis only when the disease has progressed significantly, severely limiting therapy options and resulting in a poor outcome[6,7]. Only 20%-30% of patients have resectable disease[8]. Even in cases where surgical resection is performed with the goal of curing the disease, the 5-year overall survival (OS) rate is only 20%-35%[2].

Nonsurgical therapy for ICC has advanced significantly in recent years. Chemotherapy, targeted therapy, immunotherapy, and their combination might yield favorable outcomes in the management of advanced or unresectable ICC; furthermore, localized interventions such as transarterial chemoembolization (TACE), hepatic arterial infusion (HAI) chemotherapy (HAIC), transarterial radioembolization (TARE), and radiotherapy are frequently utilized. Advancements in technology and pharmaceuticals, coupled with systemic therapies, not only yield superior outcomes in terms of tumor reduction but also increase patient survival. Conversion treatment is the process of transforming an unresectable ICC into a resectable ICC and then surgically excising the tumor. Several studies have shown that conversion treatment, which involves the use of systemic or local therapies, can increase the percentage of patients suitable for curative resection, hence considerably improving their long-term survival rates[9-13].

As methods of treatment improve, future research will focus mostly on identifying the most efficient conversion treatment procedures for advanced ICC, particularly to determine which patients are most likely to benefit from this strategy. A unified definition of conversion treatment and explicit criteria for patient selection are essential for the advancement of this therapeutic technique and the assurance of consistent clinical outcomes.

CONCEPT AND SIGNIFICANCE OF CONVERSION TREATMENT

The conversion treatment method is a novel approach for unresectable malignancies that was originally suggested for HCC patients and aims to reduce the tumor burden by applying combination therapy, thereby making patients appropriate for surgical resection[14,15]. In recent years, conversion treatment has received increasing interest in the field of ICC, as increasing amounts of data indicate that multimodal strategies for treatment can enhance resectability and patient outcomes. In contrast to HCC, where conversion treatment is well established, ICC has historically exhibited low conversion rates; however, advancements in systemic and locoregional therapies are progressively altering this approach. A study showed that patients with advanced ICC who undergo surgical resection following successful conversion treatment have a two-year survival rate of 88%, with a median survival of 46 months[16].

In certain instances, radical excision may be unfeasible because of the advanced stage of the tumor and its infiltration into hepatic blood vessels[13]. Nonetheless, some patients may have the chance to undergo radical resection *via* conversion treatment to achieve tumor downstaging. Given the rapid development of antitumor therapies, a combination therapy approach may lead to tumor downstaging in patients with unresectable ICC, increase the likelihood of radical surgical resection, and prolong patient survival. The optimal conversion treatment results in a high objective response rate (ORR), minimal harmful effects on patients, and the ability to achieve conversion as rapidly as possible. In addition to improving survival, conversion treatment can also offer symptomatic relief by diminishing the tumor burden, potentially alleviating biliary obstruction, discomfort, and other symptoms related to ICC. Thus, this may result in an increase in quality of life, even when complete resection is not possible.

Conversion treatment typically involves the application of active treatment modalities (such as targeted therapy, immunotherapy, *etc.*) to manage or reverse tumor proliferation, which has significant potential for a cure or prolonged response. In contrast, palliative care primarily aims to alleviate symptoms and enhance quality of life[17]. It includes interventions such as percutaneous transhepatic biliary drainage and biliary stenting. It is typically employed for individuals with advanced ICC and has poor treatment efficacy on the tumor itself.

There are currently no clear criteria for the indications for conversion treatment in ICC. Some patients with advanced ICC who are unsuitable for surgical resection due to inadequate residual liver volume, impaired liver function, and other factors might be included in conversion treatment. The following section outlines the significant breakthroughs in locoregional and systemic as well as combination therapies for the conversion treatment of ICC.

OPTIONS FOR ICC CONVERSION TREATMENT

Chemotherapy

In 2010, the ABC-02 study recommended the gemcitabine + cisplatin (GC) regimen as a first-line treatment option for advanced cholangiocarcinoma and reported an ORR of 26.1%[18]. In another phase III clinical study (KHBO1401-MITSUBA), the ORR for the GC regimen group in patients with advanced cholangiocarcinoma was 15%, with no instances of successful conversion treatment reported. In the GC + S-1 regimen, the ORR was 41.5%, with three patients successfully converted to surgical resection[19]. In addition to the GC regimen, the combination of gemcitabine and oxaliplatin (Gemox) is another therapy recommended by the National Comprehensive Cancer Network guidelines for advanced cholangiocarcinoma[20]. Despite the absence of a randomized trial evaluating the efficacy of the Gemox regimen against the GC regimen, Gemox was favored as a standard regimen in certain areas and was utilized as a reference regimen in multiple clinical trials for cholangiocarcinoma[21].

A retrospective study assessed the efficacy of neoadjuvant chemotherapy in managing initially unresectable ICC. Among the 74 advanced ICC patients, 39 (53%) successfully converted and underwent further resection following a median of six cycles of treatment[22]. The results revealed that individuals with locally advanced ICC who underwent surgical intervention after neoadjuvant chemotherapy presented comparable outcomes to those with initially resectable ICC who received surgery only[22]. A GC regimen combined with nab-paclitaxel was studied in a clinical trial. The survival results were encouraging, with a median OS of 19.2 months[23]. Twelve patients (20%) were successfully converted from unresectable to resectable and subsequently underwent surgery[23].

Radiotherapy

Owing to the different radiosensitivities of hepatic tissue and the limitations of radiotherapy technology, radiotherapy is infrequently utilized for the management of liver cancer. Nonetheless, advancements in imaging and radiation technologies, together with an enhanced comprehension of the radiation tolerance of normal liver tissue, have prompted an increasing number of researchers to use radiotherapy for the treatment of liver cancer[24,25]. The treatment effects observed in contemporary research exhibit considerable variability[26-28], potentially attributable to disparities in radiotherapy methods and study cohorts.

A retrospective analysis involved 79 patients with unresectable ICC, 70 of whom underwent systemic chemotherapy prior to radiation. The overall 3-year survival rate for the total group was 44%. Patients receiving a biologically equivalent radiation dose exceeding 80.5 Gy had a superior survival rate of 73% compared with 38%, and the local control (LC) rates were 78% and 45%, respectively[29]. Another phase II study evaluated the application of proton radiation in 92 patients with localized, unresectable ICC or HCC. Patients underwent 15 portions of proton treatment, culminating in a maximum cumulative dosage of 67.5 Gy equivalent. The ICC patients had a median tumor size of 6 cm, with 25% having more than one tumor and 30% having vascular thrombosis. The two-year LC and OS rates in the ICC group were 94% and 47%, respectively[30]. Data from preclinical and clinical studies have shown that radiation therapy enhances T cell infiltration, increases the quantity of lymphocytes that infiltrate tumors, and broadens the repertoire of T cell receptors[31]. This could serve as a potential method to augment the efficacy of immunotherapy, offering a combination therapy alternative for the conversion treatment of unresectable ICC.

TACE

TACE is a therapeutic approach for people with locally advanced malignancies that aims to administer locally high concentrations of chemotherapy to induce tumor ischemia[32,33]. TACE has been utilized in multiple liver malignancies, including ICC. In this method, the hepatic artery supplying blood to the tumor is accessible, typically through femoral artery access, and identified *via* conventional angiography[34]. TACE is performed by administering an emulsion containing chemotherapy drugs and an oily contrast medium such as lipiodol conventional TACE or special particles combined with chemotherapy drugs (drug-eluting bead-TACE). The chemotherapy drugs mixed with the oil-based contrast agent are injected into the hepatic artery during conventional TACE. The artery is subsequently embolized with embolic material, cutting off the tumor's blood supply[35]. Common chemotherapy medications include cisplatin, mitomycin C, and doxorubicin[36]. However, the high liquidity of lipiodol leads to systemic toxicity. Consequently, alternative interventional embolic materials, including drug-eluting beads, have been studied to increase drug loading and release in TACE therapy, referred to as drug-eluting bead-TACE[37].

Compared with HCC, ICC has a limited arterial blood supply, making it challenging for TACE to achieve optimal embolization efficacy. The OS following TACE is limited, with considerable variation in patient selection, sample size, and research methodology across different studies. Overall, the median OS reported in various studies ranged from 6 to

21 months[37-43]. It has been reported that when combined with the GC regimen, the ORR of D-TACE can reach 68%, enabling the effective conversion of 25% of patients into operable patients. The median OS of the combined treatment group was 33.7 months[44].

TARE

The technique used in TARE parallels that utilized in TACE. This method uses microspheres tagged with the β-emitter yttrium-90 (Y-90) to direct radiation onto inoperable primary or metastatic liver cancers[45]. Owing to the preferential entrapment of Y-90 microspheres in tumor blood vessels, substantial doses of radiation can be delivered to the tumor while presenting acceptable radiation levels for adjacent normal liver tissue[46].

Mouli *et al*[47] reported that Y-90 radioembolization for unresectable ICC resulted in an overall objective tumor response in 98% of patients; the mean tumor shrinkage rate was 35%. According to the World Health Organization standards, 11 patients (25%) achieved a partial response, 33 patients (73%) demonstrated stable disease, and 1 patient (2%) experienced increasing disease. Five patients (11%) were downstaged to a resectable condition following treatment and successfully underwent R0 resection[47]. Similarly, in another study combining GC chemotherapy and Y-90 microspheres, 9 patients (22%) were able to be downstaged to surgery, and 8 of them (20%) successfully underwent R0 surgical resection, with a median OS of 46 months after surgery[16].

In previous studies on TARE, tumor size or load has typically not been regarded as an exclusion criterion. Several studies have included patients with tumors larger than 5 cm or exhibiting multifocal intrahepatic disease[48,49]. The inclusion of patients with significant tumor burdens indicates that TARE may serve as a feasible therapeutic alternative for conversion treatment in ICC. TARE may effectively reduce tumor size and enhance resectability, serving as a bridge to curative surgery for patients with originally unresectable ICC. Further research on TARE for the treatment of ICC can elucidate more patient tumor characteristics and identify more suitable treatment populations to improve treatment outcomes.

HAIC

Compared with systemic chemotherapy, HAIC aims to provide substantial quantities of chemotherapeutic agents into the hepatic circulation, resulting in a more prominent local cytotoxic effect[50]. In HAIC, frequently utilized chemotherapeutic agents include floxuridine, gemcitabine, oxaliplatin, cisplatin, and their combinations[51-54]. Tumor size is not a contraindication for HAIC treatment, and certain trials have incorporated patients with tumors exceeding 10 cm in diameter[53,55].

A phase II clinical trial assessed the efficacy of HAI of floxuridine in conjunction with systemic chemotherapy for the treatment of 38 patients with unresectable ICC. The 6-month progression free survival (PFS) rate was 84.1%, 22 patients (58%) achieved a partial response, 32 patients (84%) achieved disease control, and 4 patients were successfully converted to surgical resection, with one achieving complete response[53]. In another study of HAI with gemcitabine in conjunction with oxaliplatin for the treatment of locally advanced ICC, 2 out of 12 patients achieved a partial response and underwent R0 resection surgery[56]. A study evaluated the therapeutic efficacy of HAIC *vs* first-line systemic chemotherapy for ICC, revealing superior outcomes for patients in the HAIC cohort compared with those receiving systemic chemotherapy[57]. In the subgroup analysis, patients with single tumors appeared to benefit from the consideration of HAIC for OS and PFS. These findings indicate that HAIC may exhibit superior efficacy in patients with early unresectable ICC. Nonetheless, additional prospective and randomized investigations are needed to validate this conclusion.

Targeted therapy

Targeted therapy is a treatment approach that has developed dramatically over the past decade. The mechanism of action involves inhibiting the signal transduction pathway during tumor proliferation by binding to the specific targets *via* chemical compounds, thereby inducing apoptosis in tumor cells, ultimately facilitating tumor stage reduction, and increasing the likelihood of surgical resection. In targeted therapy, key oncogenic targets in ICC tumor cells have been identified, and drugs to inhibit these targets have been developed. Mutations in genetic targets can be detected in nearly 40% of cholangiocarcinoma patients[58]. Common mutations may vary depending on where the tumor occurs. Mutations in isocitrate dehydrogenase-1 (IDH1) and rearrangements of fibroblast growth factor receptor 2 (FGFR2) are predominantly associated with ICC, whereas mutations in TP53 and KRAS, together with ERBB2 amplifications, are more frequently observed in extrahepatic cholangiocarcinoma (ECC)[21,59]. Mutations in the BAP1 and neurotropic tyrosine kinase receptor (*NTRK*) genes are commonly observed in ICC, whereas ECC typically shows abnormalities in the *ELF3* and *ARID1B* genes, along with fusions of PRKACA and PRKACB[60-62].

FGFR abnormalities (fusion, mutation, and amplification) are crucial in the development of ICC; however, the mutation rate is low in ECC and gallbladder carcinoma[63]. Mutations in FGFR can result in dysregulated FGFR signaling, which may promote cancer by increasing cell proliferation, invasion, and angiogenesis[64]. Therapeutics targeting FGFR2 and its gene family have demonstrated significant potential in the treatment of ICC[65]. Pemigatinib, an inhibitor of FGFR1-3, has obtained Food and Drug Administration approval for the management of advanced cholangiocarcinoma[66]. Among patients with advanced cholangiocarcinoma who had FGFR2 rearrangements and fusion mutations, pemigatinib had an ORR of 35.5% in the FIGHT-202 study; 98% of these patients had ICC. Furthermore, among 107 advanced cholangiocarcinoma patients, two individuals who experienced tumor downstaging underwent effective surgical intervention, with a conversion rate of 1.8% and an average survival duration of 17.8 months[67].

IDH1 mutations are prevalent in cholangiocarcinoma, and occur more commonly in ICC than in ECC[68]. IDH1 is a member of the IDH protein family. Mutant IDH enzymes exhibit neomorphic activity, catalyzing the conversion of the physiological metabolite α-ketoglutarate to 2-hydroxyglutarate. 2-hydroxyglutarate functions as an oncometabolite, and

its accumulation induces multiple epigenetic alterations[69]. Ivosidenib, a targeted agent for IDH1 mutations, prolongs OS among patients with advanced cholangiocarcinoma with IDH1 mutations[70]. In the ClarIDHy trial, patients with advanced cholangiocarcinoma who received ivosidenib exhibited a median OS of 10.3 months[71]. The findings of the trial supported the approval of this drug for clinical use[71].

The overexpression of human epidermal growth factor receptor 2 (HER2) is more prevalent in ECC (19.9%) than in ICC (4.8%)[72]. The overexpression of HER2 proteins promotes the formation of homodimers or heterodimers. Consequently, development and proliferation are predominantly facilitated by the mitogen-activated protein kinase and phosphatidylinositol 3-kinase pathways[73]. A phase II clinical trial (KCSG-HB19-14) demonstrated that trastuzumab in combination with oxaliplatin, leucovorin, and 5-fluorouracil (FOLFOX) chemotherapy resulted in an ORR of 29.4% in patients with HER2-positive advanced cholangiocarcinoma who had previously failed GC chemotherapy, with a median OS of 10.7 months and no reported cases of successful conversion[74].

The incidence of *NTRK* gene fusion in cholangiocarcinoma is less than 1%, and it is not commonly used as a regular screening marker[75]. However, some clinical trials have shown positive outcomes. Entrectinib and larotrectinib are NTRK inhibitors that have demonstrated success in treating patients with advanced malignancies that are NTRK fusion positive. Among patients with systemic treatment-treated NTRK fusion-positive advanced malignancies, those treated with entrectinib had an ORR of 57%[76]. Another clinical trial of larotrectinib for the treatment of NTRK fusion-positive malignancies reported an ORR of 75%[77].

In addition to single-target inhibitors, multitarget inhibitors have also shown efficacy in the treatment of ICC. Lenvatinib is a multitarget inhibitor of tyrosine kinase receptors that targets FGFR1-4, vascular endothelial growth factor receptor 1-3, and platelet-derived growth factors receptor-α, among others[78]. A phase II clinical trial demonstrated that lenvatinib monotherapy as a second-line treatment for advanced cholangiocarcinoma can achieve an ORR of 11.5% and a median survival duration of 7.35 months[79]. In 2021, the American Society of Clinical Oncology Annual Meeting reported a phase II clinical trial (NCT03951597) assessing the treatment of advanced ICC with lenvatinib combined with toripalimab and Gemox chemotherapy. In patients who completed the follow-up, the ORR was 80%, and the disease control rate (DCR) was 93.3%. Three patients were successfully converted and received surgical therapy[80]. Given the high ORR of 80%, it is important to interpret these results with caution. The limitations of this investigation, including sample size, bias in patient selection, treatment regimen variability, and study design, should be noted. In summary, while the high ORR is encouraging, it is crucial to emphasize that further studies are needed to confirm these findings in a broader patient population and with more standardized treatment protocols. For patients with ICC, the use of targeted therapies has new potential for conversion treatment. Many targeted therapies are in basic or clinical research, with several demonstrating promising antitumor efficacy; however, additional multicenter clinical trials are necessary to provide more reliable clinical evidence.

Immunotherapy

Immunotherapy has been investigated for ICC as a significant treatment option, and positive outcomes have been reported. As research on tumor immunity has advanced, an increasing number of studies have focused on programmed cell death 1 (PD-1), its ligand (PD-L1) inhibitors, and adoptive cell therapy (ACT). Research indicates that PD-L1 expression is increased in ICC tumor tissues, suggesting that PD-1/PD-L1 inhibitors could function as effective immunotherapies for ICC patients.

A clinical study of nivolumab performed a subgroup analysis of PD-L1 expression levels to evaluate its impact on median PFS. The findings indicated that patients exhibiting PD-L1 positivity (characterized by ≥ 1% of tumor cells exhibiting PD-L1 expression) experienced prolonged PFS[81]. Compared with chemotherapy alone, the findings of the TOPAZ-1 study indicated that the combination of durvalumab with GC enhanced OS, PFS, and the ORR in patients with unresectable advanced cholangiocarcinoma. The median OS for patients receiving combination therapy was 12.9 months, whereas it was 11.3 months for those receiving chemotherapy[82]. In another clinical trial, KEYNOTE-966, which had a median follow-up duration of 36.6 months, the median OS for the pembrolizumab cohort was 12.7 months, whereas it was 10.9 months for the placebo cohort[83]. The TOPAZ-1 and KEYNOTE-966 clinical trials confirmed the efficacy of immune checkpoint inhibitors targeting PD-1 and PD-L1 when combined with chemotherapy for advanced cholangiocarcinoma treatment. However, the variability in treatment protocols across studies, including differences in drug doses, treatment durations, and combination regimens, can impact the comparability and reliability of these results.

Early clinical results have been encouraging for ACT, a treatment based on the engineering and isolation of living T cells along with other immune cells[84]. This form of therapy has been extensively utilized in melanoma[85]. Kverneland *et al*[86] utilized ACT to treat three patients with advanced cholangiocarcinoma; one of the patients achieved a partial response. Furthermore, several reports exist regarding chimeric antigen receptor-modified T cell therapy for cholangiocarcinoma. A study targeting epidermal growth factor receptor (EGFR) in advanced cholangiocarcinoma included 19 patients with unresectable biliary system malignancies exhibiting high EGFR positivity (> 50% of cancer cells expressed EGFR). The findings indicated that one patient achieved a complete response, whereas the disease remained stable in 10 patients, yielding a median PFS of 4 months[87]. In recent years, ACT has demonstrated efficacy in various tumor treatments through optimization and improvement. However, its potential pivotal role in ICC conversion treatment requires further fundamental and clinical investigation.

Conversion treatment for future liver remnant volume

Posthepatectomy liver failure (PHLF) following major liver resection is linked to a high mortality rate. An adequate future liver remnant (FLR) is a critical element in reducing the risk of PHLF[88]. The method of promoting an FLR increase prior to tumor resection is a prevalent approach for facilitating conversion treatment in patients with FLR deficiency. A study revealed that an FLR less than 25% triples the likelihood of postoperative hepatic dysfunction and

serves as a predictor of morbidity and duration of hospitalization. Ninety percent of patients who underwent trisectionectomy with an FLR of 25% or less exhibited postoperative hepatic dysfunction, while none of those with an FLR over 25% did[89].

By encouraging FLR hypertrophy, causing shrinkage of the liver volume intended for resection, and refining patient selection, portal vein embolization (PVE) lowers the risk of major hepatectomy[90]. The duration necessary for the remnant liver to regenerate post-PVE is typically prolonged (approximately 4 to 6 weeks), and more than 20% of patients ultimately forfeit the opportunity to have surgery because of tumor advancement or inadequate FLR proliferation during the interim period[91,92]. Current treatment techniques for these patients include combined TACE, hepatic vein embolization, and other methods to increase FLR growth and control tumor development[93,94]. Presently, PVE is infrequently used in the management of cholangiocarcinoma[95,96], and additional clinical trials are needed to investigate its value in conversion treatment. Some experts suggest that PVE is particularly crucial when the FLR is projected to be less than 25% of the whole hepatic volume in a healthy liver, less than 30% in cases of chemotherapy-induced liver damage, or less than 40% in a liver weakened by underlying cirrhosis. However, PVE must be administered cautiously to patients with severe liver cirrhosis, older patients, and rapidly progressing tumors.

To prevent PHLF, associating liver partition and portal vein ligation for staged hepatectomy (ALPPS) have been implemented to promote hypertrophy of the FLR[97,98]. This novel approach was swiftly embraced by hepatobiliary surgery for managing advanced liver tumors owing to its extremely high R0 resection rate[99,100]. A propensity score matching analysis demonstrated a significantly greater OS for patients with locally advanced ICC in the ALPPS group than for those receiving palliative chemotherapy[101]. Similarly, to validate the use of ALLPS in conversion treatment, further research with a greater degree of evidence is necessary.

Other treatments

The immunogenic subtype of ICC is correlated with increased sensitivity to immune checkpoint inhibitors, indicating that antigen-presenting cells may play a role in T cell priming and activation[102]. A recent preclinical study revealed that CD40-mediated activation of antigen-presenting cells in ICC markedly improved the efficacy of anti-PD-1 therapy, offering a novel approach for combination immunotherapy[103]. Photodynamic therapy is an advanced treatment that involves the intravenous delivery of a photosensitizing chemical, which is then activated by light exposure at a certain wavelength, leading to ischemic necrosis[104]. Many researchers have investigated its ability to reshape the tumor environment and efficiently stimulate antitumor immunity[105,106]. Thymosin alpha 1 is endogenously present in the thymus and is essential for T cell maturation and differentiation[107]. Recent research has indicated that thymosin alpha 1 could markedly increase OS in HCC patients[108]. Its potential involvement in the conversion treatment of ICC warrants further investigation by researchers.

Endoluminal radiofrequency ablation (RFA) has emerged as a novel therapeutic in the past decade. A radiofrequency catheter is inserted into the bile duct during endoscopy. RFA can diminish the tumor burden by inducing localized tumor damage and may also contribute to the modulation of tumor immunity, hence offering survival advantages for patients who are ineligible for radical surgery[109]. Nonetheless, the impact of RFA on survival remains contentious[110]. In addition, studies have explored the role of microwave ablation in the treatment of advanced ICC[111,112]. To standardize therapy options and improve patient selection, more prospective trials are needed.

COMBINATION THERAPY: OPPORTUNITIES AND CHALLENGES

Combination therapy is an excellent approach that enhances efficacy, significantly surpassing that of monotherapy. The combination of many therapies can augment the immunogenicity of tumor cells and modify the tumor environment, yielding more promising outcomes. Researchers have recently assessed the safety and clinical efficacy of lenvatinib combined with durvalumab and FOLFOX-HAIC among individuals with unresectable ICC. The findings indicated that the ORR according to the mRECIST criteria was 65.2%, the median PFS was 11.9 months, and 3 patients (13%) demonstrated tumor reduction or downstaging posttreatment, ultimately undergoing radical tumor resection[113]. A retrospective real-world study demonstrated that a triple regimen of chemotherapy, lenvatinib, and an anti-PD-1 antibody yielded favorable outcomes. The PFS was 4.6 months for the chemotherapy-only group, 11.9 months for the chemotherapy combined with anti-PD-1 antibody dual-regimen group, and 23.4 months for the triple-regimen group. In the triple-regimen cohort, two patients had substantial posttreatment outcomes, allowing them to proceed with radical surgical operations[114]. More clinical studies on combination conversion treatment for advanced ICC are listed in Table 1.

Advancements in different methods of treatment have increased hope in the management of ICC (Figure 1). Nonetheless, the optimal timing for surgical intervention following effective conversion treatment remains uncertain. Furthermore, considerations must include the duration required for the medicine to exhibit efficacy, potential adverse reactions, and the necessity for prior discontinuation of the medication. Some clinicians endorse prompt curative resection subsequent to successful conversion treatment. The degree of urgency is predicated on the potential risk of forfeiting surgical options should tumor reprogression occur. Nevertheless, in practical settings, many patients who achieve effective tumor control *via* conversion treatment are often reluctant to undergo surgery, preferring to sustain their current condition. This hesitance predominantly stems from apprehensions regarding surgical intervention and the possible disruption of the tumor microenvironment postoperatively, which may heighten the risk of tumor recurrence. The timing of surgery is predominantly contingent upon the physician's experience. For patients with ICC, multidisciplinary teams (MDTs) may be helpful in determining the best time for surgery and conversion treatment. Owing to the

Table 1 Summary of clinical studies on conversion treatment for advanced intrahepatic cholangiocarcinoma

Study design	Intervention	Patients, *n*	Conversion treatment rate (%)	Key findings	Ref.
Retrospective study	Lenvatinib + durvalumab + FOLFOX-HAIC	23	13	Lenvatinib + durvalumab + FOLFOX-HAIC showed high ORR (65.2% mRECIST, 39.1% RECIST 11), with a median OS of 17.9 months and PFS of 11.9 months, supporting its potential as a first-line option for unresectable ICC	Zhao *et al*[113], 2024
Retrospective study	GC chemotherapy *vs* GC chemotherapy + PD-1 inhibitors *vs* GC chemotherapy + lenvatinib + PD-1 inhibitors	22 *vs* 20 *vs* 53	0 *vs* 0 *vs* 3.8	The triple-regimen group had the longest OS (39.6 months), significantly exceeding the dual-regimen (OS = 20.8 months) and chemo-only groups (OS = 13.1 months). ORR was 18.2% (chemo), 55.5% (dual), and 54.7% (triple), indicating superior efficacy of combination therapy for advanced ICC	Dong *et al*[114], 2024
Retrospective study	Gemox-HAIC + Gem-SYS combined with lenvatinib and PD-1 inhibitor	21	19	Gemox-HAIC plus Gem-SYS with lenvatinib + PD-1 inhibitor achieved a median OS of 19.5 months in large unresectable ICC. ORR was 52.3%. The regimen was well tolerated, with no grade 5 AEs	Ni *et all*[128], 2024
Retrospective study	Systemic chemotherapy *vs* systemic chemotherapy + PD-L1 inhibitors *vs* HAIC + lenvatinib + PD-L1 inhibitors	50 *vs* 49 *vs* 42	0 *vs* 2 *vs* 9.5	ORR (50.0%) and DCR (88.1%) were highest in the HAIC + lenvatinib + PD-L1 inhibitor group, surpassing systemic chemotherapy alone (ORR = 6.0%, DCR = 52.0%) and systemic chemotherapy + PD-L1 inhibitor (ORR = 18.4%, DCR = 73.5%). Fewer grade 3-4 AEs were reported in the HAIC + lenvatinib + PD-L1 inhibitor group, supporting its superiority over systemic chemotherapy alone for unresectable ICC	Lin *et al*[129], 2024
Retrospective study	Chemotherapy *vs* chemotherapy + PD-1/L1	30 *vs* 51	0 *vs* 5.9	The chemotherapy + anti-PD-1/PD-L1 group had significantly longer OS (11 months *vs* 8 months) than chemotherapy alone. ORR (29.4%) and DCR (78.4%) were also higher compared to chemotherapy alone (ORR = 13.3%, DCR = 73.3%), supporting its superior efficacy	Madzikatire *et al*[130], 2024
Retrospective study	Radiotherapy *vs* EQD2 < 60 Gy + GC chemotherapy *vs* EQD2 ≥ 60 Gy + GC chemotherapy	21 *vs* 70 *vs* 25	0 *vs* 8.6 *vs* 28	Patients receiving EQD2 ≥ 60 Gy + chemotherapy had the highest curative resection rate (28%) and significantly better OS than those receiving lower-dose radiotherapy or radiotherapy alone. These findings suggest that high-dose radiotherapy combined with chemotherapy improves outcomes in locally advanced unresectable ICC	Im *et al*[131], 2024
Retrospective study	SIRT using yttrium-90	28	34.5	SIRT for localized and locally advanced ICCA achieved a radiologic response rate of 57.1%, with a median OS of 22.9 months. 34.5% of patients were successfully downstaged to surgery or transplant, leading to significantly longer OS, supporting SIRT as an effective treatment option for advanced ICC	Yu *et al*[48], 2024
Retrospective study	GC chemotherapy *vs* HAIP chemotherapy	76 *vs* 192	1.3 *vs* 6.8	HAIP chemotherapy significantly improved survival in liver-confined unresectable ICCA compared to systemic chemotherapy. Median OS was 27.7 months with HAIP *vs* 11.8 months with GC chemotherapy	Franssen *et al*[132], 2024
Retrospective study	PD-1 inhibitors + lenvatinib + Gemox chemotherapy	53	11.3	PD-1 inhibitor + lenvatinib + Gemox chemotherapy showed a median OS of 14.3 months in advanced ICC. ORR was 52.8% and DCR was 94.3%, demonstrating high anti-tumor activity. Tumor burden score, TNM stage, and PD-L1 expression were identified as independent prognostic factors for survival	Zhu *et al*[133], 2023
Phase 2 clinical trial	Toripalimab + lenvatinib + Gemox chemotherapy	30	10	Toripalimab + lenvatinib + Gemox achieved an ORR of 80% and a DCR of 93.3% in advanced ICC. Median OS was 22.5 months, and PFS was 10.2 months. Patients with PD-L1 positivity (≥ 1%) showed a trend toward improved response	Shi *et al*[134], 2023
Retrospective study	Yttrium-90 + gemcitabine, cisplatin, and capecitabine	13	53.8	Yttrium-90 TARE combined with gemcitabine, cisplatin, and capecitabine achieved a median OS of 29 months and PFS of 13 months in locally	Ahmed *et al*[135], 2023

				advanced ICC. 53.8% of patients were downstaged to surgery, leading to significantly improved OS. Complete and partial responses were observed in 38.5% and 46.2% of patients, respectively	
Retrospective study	TACE + TKIs + anti-PD-1 *vs* HAIC + TKIs + anti-PD-1	19 *vs* 39	0 *vs* 15.4	The HAIC + TKIs + anti-PD-1 group achieved significantly higher ORR (RECIST: 48.7% *vs* 15.8%; mRECIST: 61.5% *vs* 21.1%) and DCR (82.1% *vs* 36.8%) compared to TACE + TKIs + anti-PD-1 in unresectable ICC	Zhang *et al* [136], 2022
Retrospective study	TACE + lenvatinib	44	63.6	TACE combined with lenvatinib successfully downstaged 63.6% of patients with initially unresectable ICC to surgical resection. Among them, 82.1% achieved R0 resection. Patients who underwent successful downstaging had significantly better OS	Yuan *et al*[137], 2022
Phase 2 clinical trial	Gem/Cis *vs* Gem/Cis-DEBIRI	22 *vs* 24	8 *vs* 25 (downsizing to resection/ablation)	The Gem/Cis + DEBIRI group had significantly higher ORR at 2, 4, and 6 months compared to Gem/Cis alone. Downsizing to resection/ablation was more frequent (25% *vs* 8%). Median OS (33.7 months *vs* 12.6 months) were significantly improved, supporting Gem/Cis + DEBIRI as a safe and effective treatment option for unresectable ICC	Martin *et al*[44], 2022
Retrospective study	Yttrium-90	136	8.1	Yttrium-90 radioembolization achieved a median OS of 14.2 months in unresectable ICC. 8.1% of patients were downstaged to resection, with 72.7% achieving R0 resection. Post-resection median OS was 39.9 months, supporting Y90 as an effective treatment with potential for downstaging and long-term survival benefits	Gupta *et al* [138], 2022
Retrospective study	Yttrium-90	81	3.7	Yttrium-90 transarterial radioembolization achieved a median OS of 14.5 months in unresectable ICC, with objective response and DCRs of 41.8% and 83.6%, respectively	Bargellini *et al* [139], 2020
Retrospective study	Yttrium-90	115	4	Yttrium-90 radioembolization in unresectable ICC resulted in a median OS of 29 months from diagnosis. 4% of patients were downstaged to curative-intent resection, supporting yttrium-90 as a potential option for tumor control and downstaging	Buettner *et al* [140], 2020
Phase 2 clinical trial	HAI floxuridine + systemic Gemox	38	11	HAI plus systemic Gemox achieved a median OS of 25.0 months and a median PFS of 11.8 months in unresectable ICC. 58% of patients achieved a partial response, and 4 patients (11%) were downstaged to resection, with 1 complete pathologic response. Patients with IDH1/2 mutations had significantly better two-year OS	Cercek *et al*[53], 2020
Phase 2 clinical trial	SIRT + chemotherapy	41	22	SIRT combined with cisplatin and gemcitabine achieved a 39% response rate (RECIST) and a 98% DCR in unresectable ICC. Median PFS was 14 months, and median OS was 22 months. 22% of patients were downstaged to surgery, with 20% achieving R0 resection. These findings support SIRT plus chemotherapy as an effective treatment with potential for surgical downstaging	Edeline *et al* [16], 2020
Retrospective study	HAI of gemcitabine plus oxaliplatin	12	16.7	HAI of gemcitabine + oxaliplatin for unresectable locally advanced ICC achieved a DCR of 91%. Median OS was 9.1 months, and time to progression was 20.3 months. Partial responses enabled R0 resection in 2 patients, supporting HAI as a promising and tolerable therapy for locally advanced ICC	Ghiringhelli *et al*[56], 2013
Retrospective study	Drug eluting bead-TACE	26	3.8	Drug-eluting bead transarterial chemoembolization achieved a median OS of 11.7 months and PFS of 3.9 months. Local tumor control was achieved in 66% of DEB-TACE patients, with one patient successfully downstaged to resection. These findings suggest DEB-TACE is a safe and effective alternative for ICC	Kuhlmann *et al* [141], 2012
Prospective	Drug-eluting bead	24	12.5	Drug-eluting bead therapy achieved a median	Schiffman *et al*

multicenter study	therapy loaded with irinotecan	OS of 17.5 months, significantly longer than chemotherapy alone in unresectable ICC. One patient was successfully downstaged to resection. These findings suggest that drug-eluting bead therapy is a safe and effective adjunctive treatment for ICC, providing a survival advantage over chemotherapy alone	[142], 2011

FOLFOX: Oxaliplatin, leucovorin, and 5-fluorouracil; HAIC: Hepatic arterial infusion chemotherapy; RECIST: Response evaluation criteria in solid tumors; ORR: Objective response rate; OS: Overall survival; PFS: Progression-free survival; ICC: Intrahepatic cholangiocarcinoma; GC: Gemcitabine plus cisplatin; PD-1: Programmed cell death protein 1; AEs: Adverse events; PD-L1: Programmed cell death-ligand 1; DCR: Disease control rate; Gemox: Gemcitabine and oxaliplatin; Gem-SYS: Systemic gemcitabine chemotherapy; EQD2: Equivalent radiotherapy dose in 2 Gy fractions; SIRT: Selective internal radiation therapy; ICCA: Intrahepatic cholangiocarcinoma; TNM: Tumor-node-metastasis; HAIP: Hepatic arterial infusion pump; TKIs: Tyrosine kinase inhibitors; TACE: Transarterial chemoembolization; DEBIRI: Irinotecan drug-eluting beads; HAI: Hepatic arterial infusion; IDH: Isocitrate dehydrogenase.

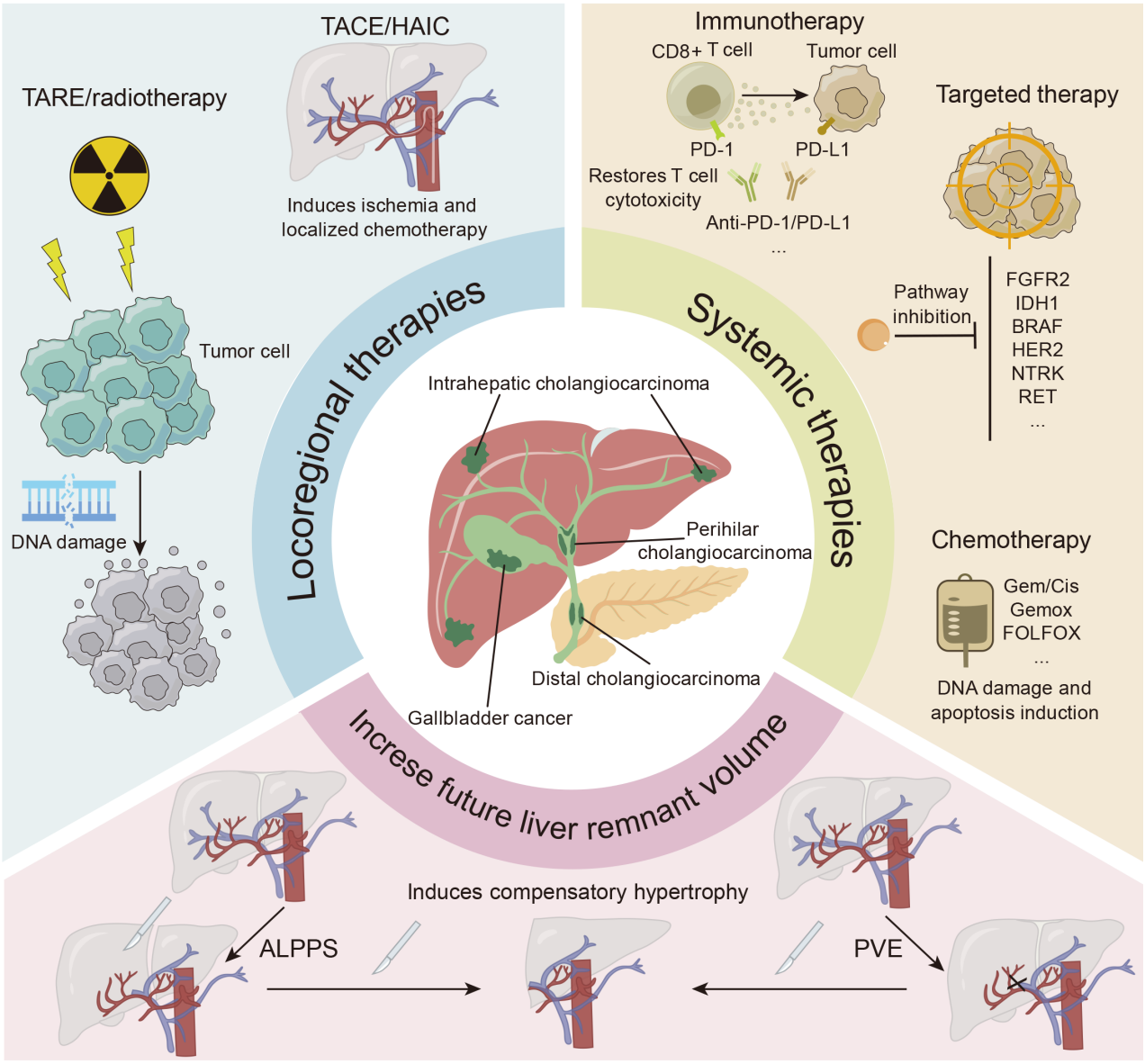

Figure 1 Schematic presentation of multiple conversion treatment options for intrahepatic cholangiocarcinoma. TACE: Transarterial chemoembolization; HAIC: Hepatic arterial infusion chemotherapy; TARE: Transarterial radioembolization; PD-1: Programmed cell death 1; PD-L1: Programmed cell death-ligand 1; FGFR2: Fibroblast growth factor receptor 2; IDH1: Isocitrate dehydrogenase-1; HER2: Human epidermal growth factor receptor 2; NTRK: Neurotropic tyrosine kinase receptor; RET: Rearranged during transfection; Gem: Gemcitabine; Cis: Cisplatin; Gemox: Gemcitabine and oxaliplatin; FOLFOX: Oxaliplatin, leucovorin, and 5-fluorouracil; ALPPS: Associating liver partition and portal vein ligation for staged hepatectomy; PVE: Portal vein embolization.

essential contribution of MDTs in enhancing patient outcomes, the National Comprehensive Cancer Network and other authorities advocate the use of MDTs in the management of cholangiocarcinoma[20,115-117]. Future studies are needed to ascertain the optimal period for effective conversion treatment and to identify suitable biological markers for predicting treatment efficacy (Table 2).

Table 2 Ongoing clinical trials of combination therapy for advanced intrahepatic cholangiocarcinoma

ClinicalTrials.gov reference	Study phase	Interventions	Primary endpoint	Status
NCT05400902	Phase 2	HAIC combined with tislelizumab and apatinib	ORR	Recruiting
NCT05535647	Phase 2	Regorafenib and HAIC	ORR	Not yet recruiting
		FOLFOX		
NCT06239532	Phase 2	TAE + HAIC + tislelizumab + surufatinib	ORR	Recruiting
NCT05010668	Phase 2	Cryoablation combined with sintilimab plus lenvatinib	ORR	Recruiting
NCT04954781	Phase 2	TACE in combination with tislelizumab	ORR	Recruiting
NCT06298968	Phase 2	Combined therapy using GC, lenvatinib and adebrelimab	ORR	Recruiting
NCT04961970	Phase 3	HAIC with FOLFOX	OS	Recruiting
		Systemic chemotherapy with GP		
NCT06335927	Phase 2	HAIC-Gemox + cadonilimab + regorafenib	ORR	Recruiting
NCT04238637	Phase 2	Y-90 SIRT + durvalumab	ORR	Recruiting
		Y-90 SIRT + durvalumab + tremelimumab		
NCT05342194	Phase 3	Toripalimab, lenvatinib, and gemcitabine-based chemotherapy	OS	Not yet recruiting
		Toripalimab, oral placebo, and gemcitabine-based chemotherapy		
		Intravenous placebo, oral placebo, and gemcitabine-based chemotherapy		
NCT04299581	Phase 2	Cryoablation combined with anti-PD-1 antibody	ORR	Recruiting
NCT05781958	Phase 2	Cadonilimab combined with gemcitabine and cisplatin	ORR	Active, not recruiting
NCT05174650	Phase 2	Combined treatment with atezolizumab and derazantinib	ORR	Active, not recruiting
NCT05422690	Phase 2	Gemcitabine, cisplatin and durvalumab chemotherapy treatments with Y-90	ORR	Recruiting
NCT04454905	Phase 2	Camrelizumab in combination with apatinib	PFS	Recruiting
NCT06648525	Phase 2	Adebrelimab + irinotecan liposomes + 5-fluorouracil + calcium folinate + lenvatinib	PFS	Not yet recruiting
		Adebrelimab + irinotecan liposomes + 5-fluorouracil + calcium folinate		
NCT05738057	Phase 2	Combined therapy using D-TACE, gemcitabine and cisplatin, and camrelizumab	Conversion rate	Recruiting
NCT05835245	Phase 2	Cryoablation combined with sintilimab plus lenvatinib	ORR	Recruiting
NCT06058663	Phase 1	Radioembolization with tremelimumab and durvalumab	Incidence of treatment-emergent adverse events	Recruiting
NCT05655949	Phase 2	Gemcitabine + cisplatin + durvalumab + Y-90 selective internal radiation therapy	PFS	Recruiting
			Incidence of grade 3 or higher treatment-related toxicity	

NCT06567600	Phase 2	Low-dose gemcitabine and cisplatin and PD-1/PD-L1 antibody	ORR	Not yet recruiting
NCT04634058	Phase 2	PD-L1 antibody combined with CTLA-4 antibody	ORR	Recruiting
NCT01862315	Phase 2	Hepatic arterial infusion with floxuridine and dexamethasone combined with systemic Gemox	PFS	Active, not recruiting
NCT05348811	Phase 2	HAIC combined with donafenib and sintilimab	ORR	Recruiting
NCT06192797	Phase 2	Combined HAIC, lenvatinib and pucotenlimab	Number of patients amendable to curative surgical interventions	Recruiting
NCT06192784	Phase 2	Combined DEB-TACE, lenvatinib and pucotenlimab	Number of patients amendable to curative surgical interventions	Recruiting
NCT04834674	Phase 2	DEB-TACE combined with apatinib and PD-1 antibody	ORR PFS	Recruiting
NCT05913661	Phase 2	Pemigatinib combined with PD-1 inhibitor	ORR	Recruiting

HAIC: Hepatic arterial infusion chemotherapy; ORR: Objective response rate; FOLFOX: Oxaliplatin, leucovorin, and 5-fluorouracil; TAE: Transcatheter arterial embolization; GC: Gemcitabine plus cisplatin; GP: Gemcitabine and cisplatin; Gemox: Gemcitabine and oxaliplatin; Y-90: Yttrium-90; SIRT: Selective internal radiation therapy; OS: Overall survival; PD-1: Programmed cell death 1; PFS: Progression free survival; PD-L1: Programmed cell death-ligand 1; CTLA-4: Cytotoxic T-lymphocyte antigen-4; DEB-TACE: Drug-eluting bead transarterial chemoembolization.

BIOMARKERS FOR TREATMENT GUIDANCE AND RESPONSE PREDICTION

On the basis of extensive research on the pathogenesis of ICC, personalized precision therapy based on immune and targeted therapy has emerged as a new treatment approach that has transformed clinical practice in recent years. Additionally, a number of studies have investigated biomarkers in order to better achieve the goal of precision treatment. It is becoming increasingly recognized that biomarkers, as potent tools for predicting treatment effects and patient prognosis, can be used to guide clinical practice and optimize the benefits of patient conversion treatment.

As mentioned above, the identification of sensitive biomarkers, such as FGFR2 fusions and IDH1 mutations, has become an important step in selecting ICC patients for targeted therapy. Furthermore, more genes are under investigation as biomarkers. In a previous study, researchers discovered that ARID1A is downregulated in ICC, which was correlated with unfavorable clinicopathological characteristics and poor prognosis, indicating that ARID1A may function as a prognosis indicator for ICC patients[118]. BAP1 is also regarded as a putative tumor suppressor in ICC and may function as a significant prognostic indicator and potential therapeutic target. Reduced BAP1 expression is strongly associated with OS and recurrence-free survival after surgery[119].

PD-1/PD-L1 expression is frequently utilized as a biomarker for immune checkpoint inhibitors. In the setting of ICC, PD-L1 expression is strongly linked with tumor invasion, tumor-node-metastasis stage, and other markers[120,121]. The immune system may successfully resume its attack on tumor cells by blocking the interaction between PD-1/PD-L1, and this therapeutic approach has emerged as a significant advancement in cancer treatment today[122].

Microsatellite instability has been investigated as a biomarker for the treatment of ICC[123], but the infrequency of microsatellite instability in ICC has hindered the ability to draw definitive conclusions about its occurrence and prognostic significance[124]. Furthermore, research has demonstrated that tumor mutation burden is an independent marker for the prognosis of ICC patients[125]. In addition to the biomarkers mentioned above, other factors that are being investigated include circulating tumor DNA and interleukin-6[126,127]. The identification of ICC biomarkers offers a basis for the development of clinical treatment strategies. Consequently, it is crucial to focus on the identification and investigation of ICC molecular targets and immune checkpoints to facilitate conversion treatment for patients with advanced ICC.

CONCLUSION

ICC remains an aggressive cancer that is almost always fatal and is becoming more common. Liver resection is one treatment that can improve long-term survival for people with ICC; however, the overall prognosis for these patients remains poor. Through ongoing advancements in tumor therapy, the stage of ICC can be reduced *via* systemic or local treatments in conjunction with techniques such as PVE and ALPPS, hence improving the resectability of ICC.

Conversion treatment has emerged as a viable option for patients with initially unresectable ICC, aiming to reduce the tumor burden and increase the likelihood of successful surgical resection. Although this approach has potential, there are

still several challenges. The interventions used for ICC differ markedly among studies regarding combinations of medicines, dosing protocols, and patient criteria, resulting in diversity in clinical outcomes. The purpose of most related clinical trials is to explore the efficacy of new treatment options, and a small number of patients have unexpected conversion resections obtained during palliative treatment. Consequently, the treatment methods that yielded favorable outcomes in the trial have limited applicability for ICC conversion treatment. In conclusion, while conversion treatment may serve as a revolutionary treatment approach for patients with locally advanced ICC, considerable efforts are needed to produce more solid data. Reliable recommendations for the clinical implementation of conversion treatment in ICC can be established only through these procedures.

FOOTNOTES

Author contributions: Huang ZY and Zhang ZY conceived the overall concept and framework of the manuscript; Liu JJ contributed to writing, editing, illustrating, and reviewing the literature; Zhou M and Yuan T participated in the discussion and design of the manuscript. All authors have read and approved the final version. Huang ZY and Zhang ZY contributed equally to this study and are recognized as co-corresponding authors.

Conflict-of-interest statement: All the authors report no relevant conflicts of interest for this article.

Country of origin: China

ORCID number: Jun-Jie Liu 0000-0001-8768-3868; Tong Yuan 0009-0005-2585-4154; Zhi-Yong Huang 0000-0002-5208-3149; Zun-Yi Zhang 0000-0002-0370-1596.

S-Editor: Wang JJ
L-Editor: A
P-Editor: Zhao S

REFERENCES

1 **Bray F**, Laversanne M, Sung H, Ferlay J, Siegel RL, Soerjomataram I, Jemal A. Global cancer statistics 2022: GLOBOCAN estimates of incidence and mortality worldwide for 36 cancers in 185 countries. *CA Cancer J Clin* 2024; **74**: 229-263 [PMID: 38572751 DOI: 10.3322/caac.21834]

2 **Moris D**, Palta M, Kim C, Allen PJ, Morse MA, Lidsky ME. Advances in the treatment of intrahepatic cholangiocarcinoma: An overview of the current and future therapeutic landscape for clinicians. *CA Cancer J Clin* 2023; **73**: 198-222 [PMID: 36260350 DOI: 10.3322/caac.21759]

3 **Khan SA**, Tavolari S, Brandi G. Cholangiocarcinoma: Epidemiology and risk factors. *Liver Int* 2019; **39** Suppl 1: 19-31 [PMID: 30851228 DOI: 10.1111/liv.14095]

4 **Bertuccio P**, Malvezzi M, Carioli G, Hashim D, Boffetta P, El-Serag HB, La Vecchia C, Negri E. Global trends in mortality from intrahepatic and extrahepatic cholangiocarcinoma. *J Hepatol* 2019; **71**: 104-114 [PMID: 30910538 DOI: 10.1016/j.jhep.2019.03.013]

5 **Razumilava N**, Gores GJ. Cholangiocarcinoma. *Lancet* 2014; **383**: 2168-2179 [PMID: 24581682 DOI: 10.1016/S0140-6736(13)61903-0]

6 **Banales JM**, Cardinale V, Carpino G, Marzioni M, Andersen JB, Invernizzi P, Lind GE, Folseraas T, Forbes SJ, Fouassier L, Geier A, Calvisi DF, Mertens JC, Trauner M, Benedetti A, Maroni L, Vaquero J, Macias RI, Raggi C, Perugorria MJ, Gaudio E, Boberg KM, Marin JJ, Alvaro D. Expert consensus document: Cholangiocarcinoma: current knowledge and future perspectives consensus statement from the European Network for the Study of Cholangiocarcinoma (ENS-CCA). *Nat Rev Gastroenterol Hepatol* 2016; **13**: 261-280 [PMID: 27095655 DOI: 10.1038/nrgastro.2016.51]

7 **Andersen JB**, Spee B, Blechacz BR, Avital I, Komuta M, Barbour A, Conner EA, Gillen MC, Roskams T, Roberts LR, Factor VM, Thorgeirsson SS. Genomic and genetic characterization of cholangiocarcinoma identifies therapeutic targets for tyrosine kinase inhibitors. *Gastroenterology* 2012; **142**: 1021-1031.e15 [PMID: 22178589 DOI: 10.1053/j.gastro.2011.12.005]

8 **Akateh C**, Ejaz AM, Pawlik TM, Cloyd JM. Neoadjuvant treatment strategies for intrahepatic cholangiocarcinoma. *World J Hepatol* 2020; **12**: 693-708 [PMID: 33200010 DOI: 10.4254/wjh.v12.i10.693]

9 **Adamus N**, Edeline J, Henriques J, Fares N, Lecomte T, Turpin A, Vernerey D, Vincens M, Chanez B, Tougeron D, Tournigand C, Assenat E, Delaye M, Manfredi S, Bouché O, Williet N, Vienot A, Blaise L, Mas L, Neuzillet C, Boilève A, Roth GS. First-line chemotherapy with selective internal radiation therapy for intrahepatic cholangiocarcinoma: The French ACABi GERCOR PRONOBIL cohort. *JHEP Rep* 2025; **7**: 101279 [PMID: 39897613 DOI: 10.1016/j.jhepr.2024.101279]

10 **Igata Y**, Kudo M, Kojima M, Kami S, Aoki K, Satake T, Kobayashi T, Sugimoto M, Kobayashi S, Konishi M, Gotohda N. Conversion surgery after gemcitabine and cisplatin plus durvalumab for advanced intrahepatic cholangiocarcinoma: A case report. *World J Clin Cases* 2024; **12**: 6721-6727 [PMID: 39650816 DOI: 10.12998/wjcc.v12.i34.6721]

11 **Zhao S**, Zhang X, Luo J, Yan H, Zhang J, Lin R, Zhu K. Conversion therapy for unresectable intrahepatic cholangiocarcinoma using gemcitabine plus S-1 combined with PD-1 inhibitors: a case report. *Front Oncol* 2024; **14**: 1476593 [PMID: 39882451 DOI: 10.3389/fonc.2024.1476593]

12 **Zhang HW**, Yu HB. Case report: Translational treatment of unresectable intrahepatic cholangiocarcinoma: Tislelizumab, Lenvatinib, and

GEMOX in one case. *Front Oncol* 2024; **14**: 1428370 [PMID: 39077469 DOI: 10.3389/fonc.2024.1428370]

13 **Zhang Z**, Wang X, Li H, Sun H, Chen J, Lin H. Case Report: Camrelizumab combined with gemcitabine and oxaliplatin in the treatment of advanced intrahepatic cholangiocarcinoma: a case report and literature review. *Front Immunol* 2023; **14**: 1230261 [PMID: 37671157 DOI: 10.3389/fimmu.2023.1230261]

14 **Sun HC**, Zhu XD. Downstaging Conversion Therapy in Patients With Initially Unresectable Advanced Hepatocellular Carcinoma: An Overview. *Front Oncol* 2021; **11**: 772195 [PMID: 34869008 DOI: 10.3389/fonc.2021.772195]

15 **Wang MD**, Xu XJ, Wang KC, Diao YK, Xu JH, Gu LH, Yao LQ, Li C, Lv GY, Yang T. Conversion therapy for advanced hepatocellular carcinoma in the era of precision medicine: Current status, challenges and opportunities. *Cancer Sci* 2024; **115**: 2159-2169 [PMID: 38695305 DOI: 10.1111/cas.16194]

16 **Edeline J**, Touchefeu Y, Guiu B, Farge O, Tougeron D, Baumgaertner I, Ayav A, Campillo-Gimenez B, Beuzit L, Pracht M, Lièvre A, Le Sourd S, Boudjema K, Rolland Y, Boucher E, Garin E. Radioembolization Plus Chemotherapy for First-line Treatment of Locally Advanced Intrahepatic Cholangiocarcinoma: A Phase 2 Clinical Trial. *JAMA Oncol* 2020; **6**: 51-59 [PMID: 31670746 DOI: 10.1001/jamaoncol.2019.3702]

17 **Makki M**, Bentaleb M, Abdulrahman M, Suhool AA, Al Harthi S, Ribeiro MA Jr. Current interventional options for palliative care for patients with advanced-stage cholangiocarcinoma. *World J Clin Oncol* 2024; **15**: 381-390 [PMID: 38576598 DOI: 10.5306/wjco.v15.i3.381]

18 **Valle J**, Wasan H, Palmer DH, Cunningham D, Anthoney A, Maraveyas A, Madhusudan S, Iveson T, Hughes S, Pereira SP, Roughton M, Bridgewater J; ABC-02 Trial Investigators. Cisplatin plus gemcitabine versus gemcitabine for biliary tract cancer. *N Engl J Med* 2010; **362**: 1273-1281 [PMID: 20375404 DOI: 10.1056/NEJMoa0908721]

19 **Ioka T**, Kanai M, Kobayashi S, Sakai D, Eguchi H, Baba H, Seo S, Taketomi A, Takayama T, Yamaue H, Takahashi M, Sho M, Kamei K, Fujimoto J, Toyoda M, Shimizu J, Goto T, Shindo Y, Yoshimura K, Hatano E, Nagano H; Kansai Hepatobiliary Oncology Group (KHBO). Randomized phase III study of gemcitabine, cisplatin plus S-1 versus gemcitabine, cisplatin for advanced biliary tract cancer (KHBO1401-MITSUBA). *J Hepatobiliary Pancreat Sci* 2023; **30**: 102-110 [PMID: 35900311 DOI: 10.1002/jhbp.1219]

20 **Benson AB**, D'Angelica MI, Abrams T, Abbott DE, Ahmed A, Anaya DA, Anders R, Are C, Bachini M, Binder D, Borad M, Bowlus C, Brown D, Burgoyne A, Castellanos J, Chahal P, Cloyd J, Covey AM, Glazer ES, Hawkins WG, Iyer R, Jacob R, Jennings L, Kelley RK, Kim R, Levine M, Palta M, Park JO, Raman S, Reddy S, Ronnekleiv-Kelly S, Sahai V, Singh G, Stein S, Turk A, Vauthey JN, Venook AP, Yopp A, McMillian N, Schonfeld R, Hochstetler C. NCCN Guidelines® Insights: Biliary Tract Cancers, Version 2.2023. *J Natl Compr Canc Netw* 2023; **21**: 694-704 [PMID: 37433432 DOI: 10.6004/jnccn.2023.0035]

21 **Yoo C**, Hyung J, Chan SL. Recent Advances in Systemic Therapy for Advanced Intrahepatic Cholangiocarcinoma. *Liver Cancer* 2024; **13**: 119-135 [PMID: 38638168 DOI: 10.1159/000531458]

22 **Le Roy B**, Gelli M, Pittau G, Allard MA, Pereira B, Serji B, Vibert E, Castaing D, Adam R, Cherqui D, Sa Cunha A. Neoadjuvant chemotherapy for initially unresectable intrahepatic cholangiocarcinoma. *Br J Surg* 2018; **105**: 839-847 [PMID: 28858392 DOI: 10.1002/bjs.10641]

23 **Shroff RT**, Javle MM, Xiao L, Kaseb AO, Varadhachary GR, Wolff RA, Raghav KPS, Iwasaki M, Masci P, Ramanathan RK, Ahn DH, Bekaii-Saab TS, Borad MJ. Gemcitabine, Cisplatin, and nab-Paclitaxel for the Treatment of Advanced Biliary Tract Cancers: A Phase 2 Clinical Trial. *JAMA Oncol* 2019; **5**: 824-830 [PMID: 30998813 DOI: 10.1001/jamaoncol.2019.0270]

24 **Apisarnthanarax S**, Barry A, Cao M, Czito B, DeMatteo R, Drinane M, Hallemeier CL, Koay EJ, Lasley F, Meyer J, Owen D, Pursley J, Schaub SK, Smith G, Venepalli NK, Zibari G, Cardenes H. External Beam Radiation Therapy for Primary Liver Cancers: An ASTRO Clinical Practice Guideline. *Pract Radiat Oncol* 2022; **12**: 28-51 [PMID: 34688956 DOI: 10.1016/j.prro.2021.09.004]

25 **Li Y**, Shimizu S, Mizumoto M, Iizumi T, Numajiri H, Makishima H, Li G, Sakurai H. Proton Beam Therapy for Multifocal Hepatocellular Carcinoma (HCC) Showing Complete Response in Pathological Anatomy After Liver Transplantation. *Cureus* 2022; **14**: e25744 [PMID: 35812555 DOI: 10.7759/cureus.25744]

26 **Smart AC**, Goyal L, Horick N, Petkovska N, Zhu AX, Ferrone CR, Tanabe KK, Allen JN, Drapek LC, Qadan M, Murphy JE, Eyler CE, Ryan DP, Hong TS, Wo JY. Hypofractionated Radiation Therapy for Unresectable/Locally Recurrent Intrahepatic Cholangiocarcinoma. *Ann Surg Oncol* 2020; **27**: 1122-1129 [PMID: 31873931 DOI: 10.1245/s10434-019-08142-9]

27 **Jackson MW**, Amini A, Jones BL, Rusthoven CG, Schefter TE, Goodman KA. Treatment Selection and Survival Outcomes With and Without Radiation for Unresectable, Localized Intrahepatic Cholangiocarcinoma. *Cancer J* 2016; **22**: 237-242 [PMID: 27441741 DOI: 10.1097/PPO.0000000000000213]

28 **Jiang W**, Zeng ZC, Tang ZY, Fan J, Zhou J, Zeng MS, Zhang JY, Chen YX, Tan YS. Benefit of radiotherapy for 90 patients with resected intrahepatic cholangiocarcinoma and concurrent lymph node metastases. *J Cancer Res Clin Oncol* 2010; **136**: 1323-1331 [PMID: 20130909 DOI: 10.1007/s00432-010-0783-1]

29 **Tao R**, Krishnan S, Bhosale PR, Javle MM, Aloia TA, Shroff RT, Kaseb AO, Bishop AJ, Swanick CW, Koay EJ, Thames HD, Hong TS, Das P, Crane CH. Ablative Radiotherapy Doses Lead to a Substantial Prolongation of Survival in Patients With Inoperable Intrahepatic Cholangiocarcinoma: A Retrospective Dose Response Analysis. *J Clin Oncol* 2016; **34**: 219-226 [PMID: 26503201 DOI: 10.1200/JCO.2015.61.3778]

30 **Hong TS**, Wo JY, Yeap BY, Ben-Josef E, McDonnell EI, Blaszkowsky LS, Kwak EL, Allen JN, Clark JW, Goyal L, Murphy JE, Javle MM, Wolfgang JA, Drapek LC, Arellano RS, Mamon HJ, Mullen JT, Yoon SS, Tanabe KK, Ferrone CR, Ryan DP, DeLaney TF, Crane CH, Zhu AX. Multi-Institutional Phase II Study of High-Dose Hypofractionated Proton Beam Therapy in Patients With Localized, Unresectable Hepatocellular Carcinoma and Intrahepatic Cholangiocarcinoma. *J Clin Oncol* 2016; **34**: 460-468 [PMID: 26668346 DOI: 10.1200/JCO.2015.64.2710]

31 **Zhu M**, Jin M, Zhao X, Shen S, Chen Y, Xiao H, Wei G, He Q, Li B, Peng Z. Anti-PD-1 antibody in combination with radiotherapy as first-line therapy for unresectable intrahepatic cholangiocarcinoma. *BMC Med* 2024; **22**: 165 [PMID: 38637772 DOI: 10.1186/s12916-024-03381-4]

32 **Mosconi C**, Solaini L, Vara G, Brandi N, Cappelli A, Modestino F, Cucchetti A, Golfieri R. Transarterial Chemoembolization and Radioembolization for Unresectable Intrahepatic Cholangiocarcinoma-a Systemic Review and Meta-Analysis. *Cardiovasc Intervent Radiol* 2021; **44**: 728-738 [PMID: 33709272 DOI: 10.1007/s00270-021-02800-w]

33 **Owen M**, Makary MS, Beal EW. Locoregional Therapy for Intrahepatic Cholangiocarcinoma. *Cancers (Basel)* 2023; **15**: 2384 [PMID: 37190311 DOI: 10.3390/cancers15082384]

34 **Gorji L**, Aoun H, Critchfield J, Al Hallak N, Beal EW. Locoregional Therapy for Intrahepatic Cholangiocarcinoma: The Role of Intra-Arterial Therapies. *Cancers (Basel)* 2023; **15**: 4727 [PMID: 37835420 DOI: 10.3390/cancers15194727]

35 **Savic LJ**, Chapiro J, Geschwind JH. Intra-arterial embolotherapy for intrahepatic cholangiocarcinoma: update and future prospects.

Hepatobiliary Surg Nutr 2017; **6**: 7-21 [PMID: 28261591 DOI: 10.21037/hbsn.2016.11.02]

36 **Currie BM**, Soulen MC. Decision Making: Intra-arterial Therapies for Cholangiocarcinoma-TACE and TARE. *Semin Intervent Radiol* 2017; **34**: 92-100 [PMID: 28579676 DOI: 10.1055/s-0037-1602591]

37 **Zhou TY**, Zhou GH, Zhang YL, Nie CH, Zhu TY, Wang HL, Chen SQ, Wang BQ, Yu ZN, Wu LM, Zheng SS, Sun JH. Drug-eluting beads transarterial chemoembolization with CalliSpheres microspheres for treatment of unresectable intrahepatic cholangiocarcinoma. *J Cancer* 2020; **11**: 4534-4541 [PMID: 32489470 DOI: 10.7150/jca.39410]

38 **Luo J**, Zheng J, Shi C, Fang J, Peng Z, Huang J, Sun J, Zhou G, Li T, Zhu D, Xu H, Hou Q, Ying S, Sun Z, Du H, Xie X, Cao G, Ji W, Han J, Gu W, Guo X, Shao G, Yu Z, Zhou J, Yu W, Zhang X, Li L, Hu H, Hu T, Wu X, Chen Y, Ji J, Hu W. Drug-eluting beads transarterial chemoembolization by CalliSpheres is effective and well tolerated in treating intrahepatic cholangiocarcinoma patients: A preliminary result from CTILC study. *Medicine (Baltimore)* 2020; **99**: e19276 [PMID: 32195932 DOI: 10.1097/MD.0000000000019276]

39 **Sun T**, Zhang W, Chen L, Ren Y, Liu Y, Zheng C. A comparative study of efficacy and safety of transarterial chemoembolization with CalliSpheres and conventional transarterial chemoembolization in treating unresectable intrahepatic cholangiocarcinoma patients. *J Cancer* 2022; **13**: 1282-1288 [PMID: 35281867 DOI: 10.7150/jca.67523]

40 **Vogl TJ**, Naguib NN, Nour-Eldin NE, Bechstein WO, Zeuzem S, Trojan J, Gruber-Rouh T. Transarterial chemoembolization in the treatment of patients with unresectable cholangiocarcinoma: Results and prognostic factors governing treatment success. *Int J Cancer* 2012; **131**: 733-740 [PMID: 21976289 DOI: 10.1002/ijc.26407]

41 **Liu D**, Wang J, Ma Z, Zhang N, Zhao Y, Yang X, Wen Z, Xie H. Treatment of unresectable intrahepatic cholangiocarcinoma using transarterial chemoembolisation with irinotecan-eluting beads: analysis of efficacy and safety. *Cardiovasc Intervent Radiol* 2022; **45**: 1092-1101 [PMID: 35588011 DOI: 10.1007/s00270-022-03108-z]

42 **Herber S**, Otto G, Schneider J, Manzl N, Kummer I, Kanzler S, Schuchmann A, Thies J, Düber C, Pitton M. Transarterial chemoembolization (TACE) for inoperable intrahepatic cholangiocarcinoma. *Cardiovasc Intervent Radiol* 2007; **30**: 1156-1165 [PMID: 17508242 DOI: 10.1007/s00270-007-9032-7]

43 **Park SY**, Kim JH, Yoon HJ, Lee IS, Yoon HK, Kim KP. Transarterial chemoembolization versus supportive therapy in the palliative treatment of unresectable intrahepatic cholangiocarcinoma. *Clin Radiol* 2011; **66**: 322-328 [PMID: 21356394 DOI: 10.1016/j.crad.2010.11.002]

44 **Martin RCG 2nd**, Simo KA, Hansen P, Rocha F, Philips P, McMasters KM, Tatum CM, Kelly LR, Driscoll M, Sharma VR, Crocenzi TS, Scoggins CR. Drug-Eluting Bead, Irinotecan Therapy of Unresectable Intrahepatic Cholangiocarcinoma (DELTIC) with Concomitant Systemic Gemcitabine and Cisplatin. *Ann Surg Oncol* 2022; **29**: 5462-5473 [PMID: 35657463 DOI: 10.1245/s10434-022-11932-3]

45 **Kennedy A**, Brown DB, Feilchenfeldt J, Marshall J, Wasan H, Fakih M, Gibbs P, Knuth A, Sangro B, Soulen MC, Pittari G, Sharma RA. Safety of selective internal radiation therapy (SIRT) with yttrium-90 microspheres combined with systemic anticancer agents: expert consensus. *J Gastrointest Oncol* 2017; **8**: 1079-1099 [PMID: 29299370 DOI: 10.21037/jgo.2017.09.10]

46 **Tong AK**, Kao YH, Too CW, Chin KF, Ng DC, Chow PK. Yttrium-90 hepatic radioembolization: clinical review and current techniques in interventional radiology and personalized dosimetry. *Br J Radiol* 2016; **89**: 20150943 [PMID: 26943239 DOI: 10.1259/bjr.20150943]

47 **Mouli S**, Memon K, Baker T, Benson AB 3rd, Mulcahy MF, Gupta R, Ryu RK, Salem R, Lewandowski RJ. Yttrium-90 radioembolization for intrahepatic cholangiocarcinoma: safety, response, and survival analysis. *J Vasc Interv Radiol* 2013; **24**: 1227-1234 [PMID: 23602420 DOI: 10.1016/j.jvir.2013.02.031]

48 **Yu Q**, Ungchusri E, Pillai A, Liao CY, Baker T, Fung J, DiSabato D, Zhang M, Liao C, Van Ha T, Ahmed O. Selective internal radiation therapy using yttrium-90 microspheres for treatment of localized and locally advanced intrahepatic cholangiocarcinoma. *Eur Radiol* 2024; **34**: 2374-2383 [PMID: 37812295 DOI: 10.1007/s00330-023-10203-3]

49 **Gangi A**, Shah J, Hatfield N, Smith J, Sweeney J, Choi J, El-Haddad G, Biebel B, Parikh N, Arslan B, Hoffe SE, Frakes JM, Springett GM, Anaya DA, Malafa M, Chen DT, Chen Y, Kim RD, Shridhar R, Kis B. Intrahepatic Cholangiocarcinoma Treated with Transarterial Yttrium-90 Glass Microsphere Radioembolization: Results of a Single Institution Retrospective Study. *J Vasc Interv Radiol* 2018; **29**: 1101-1108 [PMID: 30042074 DOI: 10.1016/j.jvir.2018.04.001]

50 **Massani M**, Bonariol L, Stecca T. Hepatic Arterial Infusion Chemotherapy for Unresectable Intrahepatic Cholangiocarcinoma, a Comprehensive Review. *J Clin Med* 2021; **10**: 2552 [PMID: 34207700 DOI: 10.3390/jcm10122552]

51 **Franssen S**, Soares KC, Jolissaint JS, Tsilimigras DI, Buettner S, Alexandrescu S, Marques H, Lamelas J, Aldrighetti L, Gamblin TC, Maithel SK, Pulitano C, Margonis GA, Weiss MJ, Bauer TW, Shen F, Poultsides GA, Marsh JW, Cercek A, Kemeny N, Kingham TP, D'Angelica M, Pawlik TM, Jarnagin WR, Koerkamp BG. Comparison of Hepatic Arterial Infusion Pump Chemotherapy vs Resection for Patients With Multifocal Intrahepatic Cholangiocarcinoma. *JAMA Surg* 2022; **157**: 590-596 [PMID: 35544131 DOI: 10.1001/jamasurg.2022.1298]

52 **Ishii M**, Itano O, Morinaga J, Shirakawa H, Itano S. Potential efficacy of hepatic arterial infusion chemotherapy using gemcitabine, cisplatin, and 5-fluorouracil for intrahepatic cholangiocarcinoma. *PLoS One* 2022; **17**: e0266707 [PMID: 35452492 DOI: 10.1371/journal.pone.0266707]

53 **Cercek A**, Boerner T, Tan BR, Chou JF, Gönen M, Boucher TM, Hauser HF, Do RKG, Lowery MA, Harding JJ, Varghese AM, Reidy-Lagunes D, Saltz L, Schultz N, Kingham TP, D'Angelica MI, DeMatteo RP, Drebin JA, Allen PJ, Balachandran VP, Lim KH, Sanchez-Vega F, Vachharajani N, Majella Doyle MB, Fields RC, Hawkins WG, Strasberg SM, Chapman WC, Diaz LA Jr, Kemeny NE, Jarnagin WR. Assessment of Hepatic Arterial Infusion of Floxuridine in Combination With Systemic Gemcitabine and Oxaliplatin in Patients With Unresectable Intrahepatic Cholangiocarcinoma: A Phase 2 Clinical Trial. *JAMA Oncol* 2020; **6**: 60-67 [PMID: 31670750 DOI: 10.1001/jamaoncol.2019.3718]

54 **Li S**, Deng M, Wang Q, Mei J, Zou J, Lin W, Shi M, Chen M, Wei W, Guo R. Transarterial Infusion Chemotherapy with FOLFOX Could be an Effective and Safe Treatment for Unresectable Intrahepatic Cholangiocarcinoma. *J Oncol* 2022; **2022**: 2724476 [PMID: 35342396 DOI: 10.1155/2022/2724476]

55 **Huang P**, Huang X, Zhou Y, Yang G, Sun Q, Shi G, Chen Y. The Efficacy and Safety of Hepatic Arterial Infusion Chemotherapy Based on FOLFIRI for Advanced Intrahepatic Cholangiocarcinoma as Second-Line and Successive Treatment: A Real-World Study. *Can J Gastroenterol Hepatol* 2022; **2022**: 9680933 [PMID: 36199981 DOI: 10.1155/2022/9680933]

56 **Ghiringhelli F**, Lorgis V, Vincent J, Ladoire S, Guiu B. Hepatic arterial infusion of gemcitabine plus oxaliplatin as second-line treatment for locally advanced intrahepatic cholangiocarcinoma: preliminary experience. *Chemotherapy* 2013; **59**: 354-360 [PMID: 24821200 DOI: 10.1159/000362223]

57 **Yang Z**, Fu Y, Wu W, Hu Z, Pan Y, Wang J, Chen J, Hu D, Zhou Z, Chen M, Zhang Y. Comparison of hepatic arterial infusion chemotherapy with mFOLFOX vs. first-line systemic chemotherapy in patients with unresectable intrahepatic cholangiocarcinoma. *Front Pharmacol* 2023; **14**: 1234342 [PMID: 37731737 DOI: 10.3389/fphar.2023.1234342]

58 **Mazzaferro V**, Gorgen A, Roayaie S, Droz Dit Busset M, Sapisochin G. Liver resection and transplantation for intrahepatic cholangiocarcinoma. *J Hepatol* 2020; **72**: 364-377 [PMID: 31954498 DOI: 10.1016/j.jhep.2019.11.020]

59 **Manne A**, Woods E, Tsung A, Mittra A. Biliary Tract Cancers: Treatment Updates and Future Directions in the Era of Precision Medicine and Immuno-Oncology. *Front Oncol* 2021; **11**: 768009 [PMID: 34868996 DOI: 10.3389/fonc.2021.768009]

60 **Banales JM**, Marin JJG, Lamarca A, Rodrigues PM, Khan SA, Roberts LR, Cardinale V, Carpino G, Andersen JB, Braconi C, Calvisi DF, Perugorria MJ, Fabris L, Boulter L, Macias RIR, Gaudio E, Alvaro D, Gradilone SA, Strazzabosco M, Marzioni M, Coulouarn C, Fouassier L, Raggi C, Invernizzi P, Mertens JC, Moncsek A, Ilyas SI, Heimbach J, Koerkamp BG, Bruix J, Forner A, Bridgewater J, Valle JW, Gores GJ. Cholangiocarcinoma 2020: the next horizon in mechanisms and management. *Nat Rev Gastroenterol Hepatol* 2020; **17**: 557-588 [PMID: 32606456 DOI: 10.1038/s41575-020-0310-z]

61 **Komuta M**. Intrahepatic cholangiocarcinoma: Tumour heterogeneity and its clinical relevance. *Clin Mol Hepatol* 2022; **28**: 396-407 [PMID: 35032970 DOI: 10.3350/cmh.2021.0287]

62 **Rodrigues PM**, Olaizola P, Paiva NA, Olaizola I, Agirre-Lizaso A, Landa A, Bujanda L, Perugorria MJ, Banales JM. Pathogenesis of Cholangiocarcinoma. *Annu Rev Pathol* 2021; **16**: 433-463 [PMID: 33264573 DOI: 10.1146/annurev-pathol-030220-020455]

63 **Aitcheson G**, Mahipal A, John BV. Targeting FGFR in intrahepatic cholangiocarcinoma [iCCA]: leading the way for precision medicine in biliary tract cancer [BTC]? *Expert Opin Investig Drugs* 2021; **30**: 463-477 [PMID: 33678096 DOI: 10.1080/13543784.2021.1900821]

64 **Babina IS**, Turner NC. Advances and challenges in targeting FGFR signalling in cancer. *Nat Rev Cancer* 2017; **17**: 318-332 [PMID: 28303906 DOI: 10.1038/nrc.2017.8]

65 **Nishida N**. The role of FGFR inhibitors in the treatment of intrahepatic cholangiocarcinoma-unveiling the future challenges in drug therapy. *Hepatobiliary Surg Nutr* 2023; **12**: 790-794 [PMID: 37886210 DOI: 10.21037/hbsn-23-411]

66 **Hoy SM**. Pemigatinib: First Approval. *Drugs* 2020; **80**: 923-929 [PMID: 32472305 DOI: 10.1007/s40265-020-01330-y]

67 **Abou-Alfa GK**, Sahai V, Hollebecque A, Vaccaro G, Melisi D, Al-Rajabi R, Paulson AS, Borad MJ, Gallinson D, Murphy AG, Oh DY, Dotan E, Catenacci DV, Van Cutsem E, Ji T, Lihou CF, Zhen H, Féliz L, Vogel A. Pemigatinib for previously treated, locally advanced or metastatic cholangiocarcinoma: a multicentre, open-label, phase 2 study. *Lancet Oncol* 2020; **21**: 671-684 [PMID: 32203698 DOI: 10.1016/S1470-2045(20)30109-1]

68 **Boscoe AN**, Rolland C, Kelley RK. Frequency and prognostic significance of isocitrate dehydrogenase 1 mutations in cholangiocarcinoma: a systematic literature review. *J Gastrointest Oncol* 2019; **10**: 751-765 [PMID: 31392056 DOI: 10.21037/jgo.2019.03.10]

69 **Lavacchi D**, Caliman E, Rossi G, Buttitta E, Botteri C, Fancelli S, Pellegrini E, Roviello G, Pillozzi S, Antonuzzo L. Ivosidenib in IDH1-mutated cholangiocarcinoma: Clinical evaluation and future directions. *Pharmacol Ther* 2022; **237**: 108170 [PMID: 35296436 DOI: 10.1016/j.pharmthera.2022.108170]

70 Ivosidenib Boosts OS in Cholangiocarcinoma. *Cancer Discov* 2021; **11**: 2953-2954 [PMID: 34635569 DOI: 10.1158/2159-8290.CD-NB2021-0389]

71 **Zhu AX**, Macarulla T, Javle MM, Kelley RK, Lubner SJ, Adeva J, Cleary JM, Catenacci DVT, Borad MJ, Bridgewater JA, Harris WP, Murphy AG, Oh DY, Whisenant JR, Lowery MA, Goyal L, Shroff RT, El-Khoueiry AB, Chamberlain CX, Aguado-Fraile E, Choe S, Wu B, Liu H, Gliser C, Pandya SS, Valle JW, Abou-Alfa GK. Final Overall Survival Efficacy Results of Ivosidenib for Patients With Advanced Cholangiocarcinoma With IDH1 Mutation: The Phase 3 Randomized Clinical ClarIDHy Trial. *JAMA Oncol* 2021; **7**: 1669-1677 [PMID: 34554208 DOI: 10.1001/jamaoncol.2021.3836]

72 **Galdy S**, Lamarca A, McNamara MG, Hubner RA, Cella CA, Fazio N, Valle JW. HER2/HER3 pathway in biliary tract malignancies; systematic review and meta-analysis: a potential therapeutic target? *Cancer Metastasis Rev* 2017; **36**: 141-157 [PMID: 27981460 DOI: 10.1007/s10555-016-9645-x]

73 **Zhu K**, Yang X, Tai H, Zhong X, Luo T, Zheng H. HER2-targeted therapies in cancer: a systematic review. *Biomark Res* 2024; **12**: 16 [PMID: 38308374 DOI: 10.1186/s40364-024-00565-1]

74 **Lee CK**, Chon HJ, Cheon J, Lee MA, Im HS, Jang JS, Kim MH, Park S, Kang B, Hong M, Kim JW, Park HS, Kang MJ, Park YN, Choi HJ. Trastuzumab plus FOLFOX for HER2-positive biliary tract cancer refractory to gemcitabine and cisplatin: a multi-institutional phase 2 trial of the Korean Cancer Study Group (KCSG-HB19-14). *Lancet Gastroenterol Hepatol* 2023; **8**: 56-65 [PMID: 36328033 DOI: 10.1016/S2468-1253(22)00335-1]

75 **Taghizadeh H**, Dong Y, Gruenberger T, Prager GW. Perioperative and palliative systemic treatments for biliary tract cancer. *Ther Adv Med Oncol* 2024; **16**: 17588359241230756 [PMID: 38559612 DOI: 10.1177/17588359241230756]

76 **Doebele RC**, Drilon A, Paz-Ares L, Siena S, Shaw AT, Farago AF, Blakely CM, Seto T, Cho BC, Tosi D, Besse B, Chawla SP, Bazhenova L, Krauss JC, Chae YK, Barve M, Garrido-Laguna I, Liu SV, Conkling P, John T, Fakih M, Sigal D, Loong HH, Buchschacher GL Jr, Garrido P, Nieva J, Steuer C, Overbeck TR, Bowles DW, Fox E, Riehl T, Chow-Maneval E, Simmons B, Cui N, Johnson A, Eng S, Wilson TR, Demetri GD; trial investigators. Entrectinib in patients with advanced or metastatic NTRK fusion-positive solid tumours: integrated analysis of three phase 1-2 trials. *Lancet Oncol* 2020; **21**: 271-282 [PMID: 31838007 DOI: 10.1016/S1470-2045(19)30691-6]

77 **Drilon A**, Laetsch TW, Kummar S, DuBois SG, Lassen UN, Demetri GD, Nathenson M, Doebele RC, Farago AF, Pappo AS, Turpin B, Dowlati A, Brose MS, Mascarenhas L, Federman N, Berlin J, El-Deiry WS, Baik C, Deeken J, Boni V, Nagasubramanian R, Taylor M, Rudzinski ER, Meric-Bernstam F, Sohal DPS, Ma PC, Raez LE, Hechtman JF, Benayed R, Ladanyi M, Tuch BB, Ebata K, Cruickshank S, Ku NC, Cox MC, Hawkins DS, Hong DS, Hyman DM. Efficacy of Larotrectinib in TRK Fusion-Positive Cancers in Adults and Children. *N Engl J Med* 2018; **378**: 731-739 [PMID: 29466156 DOI: 10.1056/NEJMoa1714448]

78 **Kudo M**, Finn RS, Qin S, Han KH, Ikeda K, Piscaglia F, Baron A, Park JW, Han G, Jassem J, Blanc JF, Vogel A, Komov D, Evans TRJ, Lopez C, Dutcus C, Guo M, Saito K, Kraljevic S, Tamai T, Ren M, Cheng AL. Lenvatinib versus sorafenib in first-line treatment of patients with unresectable hepatocellular carcinoma: a randomised phase 3 non-inferiority trial. *Lancet* 2018; **391**: 1163-1173 [PMID: 29433850 DOI: 10.1016/S0140-6736(18)30207-1]

79 **Ueno M**, Ikeda M, Sasaki T, Nagashima F, Mizuno N, Shimizu S, Ikezawa H, Hayata N, Nakajima R, Morizane C. Phase 2 study of lenvatinib monotherapy as second-line treatment in unresectable biliary tract cancer: primary analysis results. *BMC Cancer* 2020; **20**: 1105 [PMID: 33198671 DOI: 10.1186/s12885-020-07365-4]

80 **Jian Z**, Fan J, Shi GM, Huang XY, Wu D, Yang GH, Ji Y, Chen Y, Liang F, Lu JC, Ge NL, Sun HC, Huang XW, Qiu SJ, He YF, Yang XR, Xu Y, Gao Q, Sun J. Gemox chemotherapy in combination with anti-PD1 antibody toripalimab and lenvatinib as first-line treatment for advanced intrahepatic cholangiocarcinoma: A phase 2 clinical trial. *J Clin Oncol* 2021; **39**: 4094 [DOI: 10.1200/JCO.2021.39.15_suppl.4094]

81 **Kim RD**, Chung V, Alese OB, El-Rayes BF, Li D, Al-Toubah TE, Schell MJ, Zhou JM, Mahipal A, Kim BH, Kim DW. A Phase 2 Multi-institutional Study of Nivolumab for Patients With Advanced Refractory Biliary Tract Cancer. *JAMA Oncol* 2020; **6**: 888-894 [PMID:

32352498 DOI: 10.1001/jamaoncol.2020.0930]

82 **Oh DY**, He AR, Bouattour M, Okusaka T, Qin S, Chen LT, Kitano M, Lee CK, Kim JW, Chen MH, Suksomboon charoen T, Ikeda M, Lee MA, Chen JS, Potemski P, Burris HA 3rd, Ostwal V, Tanasanvimon S, Morizane C, Zaucha RE, McNamara MG, Avallone A, Cundom JE, Breder V, Tan B, Shimizu S, Tougeron D, Evesque L, Petrova M, Zhen DB, Gillmore R, Gupta VG, Dayyani F, Park JO, Buchschacher GL Jr, Rey F, Kim H, Wang J, Morgan C, Rokutanda N, Żotkiewicz M, Vogel A, Valle JW. Durvalumab or placebo plus gemcitabine and cisplatin in participants with advanced biliary tract cancer (TOPAZ-1): updated overall survival from a randomised phase 3 study. *Lancet Gastroenterol Hepatol* 2024; **9**: 694-704 [PMID: 38823398 DOI: 10.1016/S2468-1253(24)00095-5]

83 **Finn RS**, Ueno M, Yoo C, Ren Z, Furuse J, Kelley RK, Chan SL, Edeline J, Klümpen H, Yau T, Verslype C, Ozaka M, Bouattour M, Park JO, Vogel A, Valle JW, Starkopf L, Malhotra U, Siegel AB, Qin S. Three-year follow-up data from KEYNOTE-966: Pembrolizumab (pembro) plus gemcitabine and cisplatin (gem/cis) compared with gem/cis alone for patients (pts) with advanced biliary tract cancer (BTC). *J Clin Oncol* 2024; **42**: 4093 [DOI: 10.1200/JCO.2024.42.16_suppl.4093]

84 **Olson DJ**, Odunsi K. Adoptive Cell Therapy for Nonhematologic Solid Tumors. *J Clin Oncol* 2023; **41**: 3397-3407 [PMID: 37104722 DOI: 10.1200/JCO.22.01618]

85 **Martín-Lluesma S**, Svane IM, Dafni U, Vervita K, Karlis D, Dimopoulou G, Tsourti Z, Rohaan MW, Haanen JBAG, Coukos G. Efficacy of TIL therapy in advanced cutaneous melanoma in the current immuno-oncology era: updated systematic review and meta-analysis. *Ann Oncol* 2024; **35**: 860-872 [PMID: 39053767 DOI: 10.1016/j.annonc.2024.07.723]

86 **Kverneland AH**, Chamberlain CA, Borch TH, Nielsen M, Mørk SK, Kjeldsen JW, Lorentzen CL, Jørgensen LP, Riis LB, Yde CW, Met Ö, Donia M, Svane IM. Adoptive cell therapy with tumor-infiltrating lymphocytes supported by checkpoint inhibition across multiple solid cancer types. *J Immunother Cancer* 2021; **9**: e003499 [PMID: 34607899 DOI: 10.1136/jitc-2021-003499]

87 **Guo Y**, Feng K, Liu Y, Wu Z, Dai H, Yang Q, Wang Y, Jia H, Han W. Phase I Study of Chimeric Antigen Receptor-Modified T Cells in Patients with EGFR-Positive Advanced Biliary Tract Cancers. *Clin Cancer Res* 2018; **24**: 1277-1286 [PMID: 29138340 DOI: 10.1158/1078-0432.CCR-17-0432]

88 **Reese T**, Gilg S, Böcker J, Wagner KC, Vali M, Engstrand J, Kern A, Sturesson C, Oldhafer KJ, Sparrelid E. Impact of the future liver remnant volume before major hepatectomy. *Eur J Surg Oncol* 2024; **50**: 108660 [PMID: 39243696 DOI: 10.1016/j.ejso.2024.108660]

89 **Shoup M**, Gonen M, D'Angelica M, Jarnagin WR, DeMatteo RP, Schwartz LH, Tuorto S, Blumgart LH, Fong Y. Volumetric analysis predicts hepatic dysfunction in patients undergoing major liver resection. *J Gastrointest Surg* 2003; **7**: 325-330 [PMID: 12654556 DOI: 10.1016/s1091-255x(02)00370-0]

90 **Shindoh J**, D Tzeng CW, Vauthey JN. Portal vein embolization for hepatocellular carcinoma. *Liver Cancer* 2012; **1**: 159-167 [PMID: 24159580 DOI: 10.1159/000343829]

91 **Aloia TA**. Associating Liver Partition and Portal Vein Ligation for Staged Hepatectomy: Portal Vein Embolization Should Remain the Gold Standard. *JAMA Surg* 2015; **150**: 927-928 [PMID: 26308668 DOI: 10.1001/jamasurg.2015.1646]

92 **Piron L**, Deshayes E, Escal L, Souche R, Herrero A, Pierredon-Foulongne MA, Assenat E, le Lam N, Quenet F, Guiu B. [Portal vein embolization: Present and future]. *Bull Cancer* 2017; **104**: 407-416 [PMID: 28477870 DOI: 10.1016/j.bulcan.2017.03.009]

93 **Ogata S**, Belghiti J, Farges O, Varma D, Sibert A, Vilgrain V. Sequential arterial and portal vein embolizations before right hepatectomy in patients with cirrhosis and hepatocellular carcinoma. *Br J Surg* 2006; **93**: 1091-1098 [PMID: 16779884 DOI: 10.1002/bjs.5341]

94 **Hwang S**, Ha TY, Ko GY, Kwon DI, Song GW, Jung DH, Kim MH, Lee SK, Lee SG. Preoperative Sequential Portal and Hepatic Vein Embolization in Patients with Hepatobiliary Malignancy. *World J Surg* 2015; **39**: 2990-2998 [PMID: 26304608 DOI: 10.1007/s00268-015-3194-2]

95 **Nevermann N**, Bode J, Vischer M, Krenzien F, Lurje G, Pelzer U, Fehrenbach U, Auer TA, Schmelzle M, Pratschke J, Schöning W. Perioperative outcome and long-term survival for intrahepatic cholangiocarcinoma after portal vein embolization and subsequent resection: A propensity-matched study. *Eur J Surg Oncol* 2023; **49**: 107100 [PMID: 37918318 DOI: 10.1016/j.ejso.2023.107100]

96 **Olthof PB**, Aldrighetti L, Alikhanov R, Cescon M, Groot Koerkamp B, Jarnagin WR, Nadalin S, Pratschke J, Schmelze M, Sparrelid E, Lang H, Guglielmi A, van Gulik TM; Perihilar Cholangiocarcinoma Collaboration Group. Portal Vein Embolization is Associated with Reduced Liver Failure and Mortality in High-Risk Resections for Perihilar Cholangiocarcinoma. *Ann Surg Oncol* 2020; **27**: 2311-2318 [PMID: 32103419 DOI: 10.1245/s10434-020-08258-3]

97 **Vennarecci G**, Grazi GL, Sperduti I, Busi Rizzi E, Felli E, Antonini M, D'Offizi G, Ettorre GM. ALPPS for primary and secondary liver tumors. *Int J Surg* 2016; **30**: 38-44 [PMID: 27112834 DOI: 10.1016/j.ijsu.2016.04.031]

98 **Balci D**, Sakamoto Y, Li J, Di Benedetto F, Kirimker EO, Petrowsky H. Associating liver partition and portal vein ligation for staged hepatectomy (ALPPS) procedure for cholangiocarcinoma. *Int J Surg* 2020; **82S**: 97-102 [PMID: 32645441 DOI: 10.1016/j.ijsu.2020.06.045]

99 **Alvarez FA**, Ardiles V, de Santibañes M, Pekolj J, de Santibañes E. Associating liver partition and portal vein ligation for staged hepatectomy offers high oncological feasibility with adequate patient safety: a prospective study at a single center. *Ann Surg* 2015; **261**: 723-732 [PMID: 25493362 DOI: 10.1097/SLA.0000000000001046]

100 **Schadde E**, Malagó M, Hernandez-Alejandro R, Li J, Abdalla E, Ardiles V, Lurje G, Vyas S, Machado MA, de Santibañes E. Monosegment ALPPS hepatectomy: extending resectability by rapid hypertrophy. *Surgery* 2015; **157**: 676-689 [PMID: 25712199 DOI: 10.1016/j.surg.2014.11.015]

101 **Li J**, Moustafa M, Linecker M, Lurje G, Capobianco I, Baumgart J, Ratti F, Rauchfuss F, Balci D, Fernandes E, Montalti R, Robles-Campos R, Bjornsson B, Topp SA, Fronek J, Liu C, Wahba R, Bruns C, Brunner SM, Schlitt HJ, Heumann A, Stüben BO, Izbicki JR, Bednarsch J, Gringeri E, Fasolo E, Rolinger J, Kristek J, Hernandez-Alejandro R, Schnitzbauer A, Nuessler N, Schön MR, Voskanyan S, Petrou AS, Hahn O, Soejima Y, Vicente E, Castro-Benitez C, Adam R, Tomassini F, Troisi RI, Kantas A, Oldhafer KJ, Ardiles V, de Santibanes E, Malago M, Clavien PA, Vivarelli M, Settmacher U, Aldrighetti L, Neumann U, Petrowsky H, Cillo U, Lang H, Nadalin S. ALPPS for Locally Advanced Intrahepatic Cholangiocarcinoma: Did Aggressive Surgery Lead to the Oncological Benefit? An International Multi-center Study. *Ann Surg Oncol* 2020; **27**: 1372-1384 [PMID: 32002719 DOI: 10.1245/s10434-019-08192-z]

102 **Job S**, Rapoud D, Dos Santos A, Gonzalez P, Desterke C, Pascal G, Elarouci N, Ayadi M, Adam R, Azoulay D, Castaing D, Vibert E, Cherqui D, Samuel D, Sa Cuhna A, Marchio A, Pineau P, Guettier C, de Reyniès A, Faivre J. Identification of Four Immune Subtypes Characterized by Distinct Composition and Functions of Tumor Microenvironment in Intrahepatic Cholangiocarcinoma. *Hepatology* 2020; **72**: 965-981 [PMID: 31875970 DOI: 10.1002/hep.31092]

103 **Diggs LP**, Ruf B, Ma C, Heinrich B, Cui L, Zhang Q, McVey JC, Wabitsch S, Heinrich S, Rosato U, Lai W, Subramanyam V, Longerich T, Loosen SH, Luedde T, Neumann UP, Desar S, Kleiner D, Gores G, Wang XW, Greten TF. CD40-mediated immune cell activation enhances response to anti-PD-1 in murine intrahepatic cholangiocarcinoma. *J Hepatol* 2021; **74**: 1145-1154 [PMID: 33276030 DOI:

10.1016/j.jhep.2020.11.037]
104 **Kahaleh M**, Mishra R, Shami VM, Northup PG, Berg CL, Bashlor P, Jones P, Ellen K, Weiss GR, Brenin CM, Kurth BE, Rich TA, Adams RB, Yeaton P. Unresectable cholangiocarcinoma: comparison of survival in biliary stenting alone versus stenting with photodynamic therapy. *Clin Gastroenterol Hepatol* 2008; **6**: 290-297 [PMID: 18255347 DOI: 10.1016/j.cgh.2007.12.004]
105 **Wang W**, Gao Y, Xu J, Zou T, Yang B, Hu S, Cheng X, Xia Y, Zheng Q. A NRF2 Regulated and the Immunosuppressive Microenvironment Reversed Nanoplatform for Cholangiocarcinoma Photodynamic-Gas Therapy. *Adv Sci (Weinh)* 2024; **11**: e2307143 [PMID: 38308097 DOI: 10.1002/advs.202307143]
106 **Huang YP**, Wang YX, Zhou H, Liu ZT, Zhang ZJ, Xiong L, Zou H, Wen Y. Surufatinib combined with photodynamic therapy induces ferroptosis to inhibit cholangiocarcinoma in vitro and in tumor models. *Front Pharmacol* 2024; **15**: 1288255 [PMID: 38645554 DOI: 10.3389/fphar.2024.1288255]
107 **Mao L**. Thymosin alpha 1 - Reimagine its broader applications in the immuno-oncology era. *Int Immunopharmacol* 2023; **117**: 109952 [PMID: 36871535 DOI: 10.1016/j.intimp.2023.109952]
108 **Linye H**, Zijing X, Wei P, Chao H, Chuan L, Tianfu W. Thymosin alpha-1 therapy improves postoperative survival after curative resection for solitary hepatitis B virus-related hepatocellular carcinoma: A propensity score matching analysis. *Medicine (Baltimore)* 2021; **100**: e25749 [PMID: 34011034 DOI: 10.1097/MD.0000000000025749]
109 **Xia M**, Qin W, Hu B. Endobiliary radiofrequency ablation for unresectable malignant biliary strictures: Survival benefit perspective. *Dig Endosc* 2023; **35**: 584-591 [PMID: 36843564 DOI: 10.1111/den.14542]
110 **Jarosova J**, Zarivnijova L, Cibulkova I, Mares J, Macinga P, Hujova A, Falt P, Urban O, Hajer J, Spicak J, Hucl T. Endoluminal radiofrequency ablation in patients with malignant biliary obstruction: a randomised trial. *Gut* 2023; **72**: 2286-2293 [PMID: 37652677 DOI: 10.1136/gutjnl-2023-329700]
111 **Yang GW**, Zhao Q, Qian S, Zhu L, Qu XD, Zhang W, Yan ZP, Cheng JM, Liu QX, Liu R, Wang JH. Percutaneous microwave ablation combined with simultaneous transarterial chemoembolization for the treatment of advanced intrahepatic cholangiocarcinoma. *Onco Targets Ther* 2015; **8**: 1245-1250 [PMID: 26060410 DOI: 10.2147/OTT.S84764]
112 **Zhang A**, Liu B, Xu D, Sun Y. Advanced intrahepatic cholangiocarcinoma treated using anlotinib and microwave ablation: A case report. *Medicine (Baltimore)* 2019; **98**: e18435 [PMID: 31876723 DOI: 10.1097/MD.0000000000018435]
113 **Zhao R**, Zhou J, Miao Z, Xiong X, Wei W, Li S, Guo R. Efficacy and safety of lenvatinib plus durvalumab combined with hepatic arterial infusion chemotherapy for unresectable intrahepatic cholangiocarcinoma. *Front Immunol* 2024; **15**: 1397827 [PMID: 38799453 DOI: 10.3389/fimmu.2024.1397827]
114 **Dong Z**, Sui C, Lu J, Guo J, Duan K, Wang K, Geng L, Dai B, Yang J. Chemotherapy combined with lenvatinib and PD-1 may be a potential better alternative option for advanced unresectable intrahepatic cholangiocarcinoma: a retrospective real-world study. *Front Immunol* 2024; **15**: 1463574 [PMID: 39290704 DOI: 10.3389/fimmu.2024.1463574]
115 **Bourien H**, Lamarca A, McNamara MG, Hubner RA, Valle JW, Edeline J. Druggable molecular alterations in bile duct cancer: potential and current therapeutic applications in clinical trials. *Expert Opin Investig Drugs* 2021; **30**: 975-983 [PMID: 34420429 DOI: 10.1080/13543784.2021.1964470]
116 **Vogel A**, Bridgewater J, Edeline J, Kelley RK, Klümpen HJ, Malka D, Primrose JN, Rimassa L, Stenzinger A, Valle JW, Ducreux M; ESMO Guidelines Committee. Electronic address: clinicalguidelines@esmo.org. Biliary tract cancer: ESMO Clinical Practice Guideline for diagnosis, treatment and follow-up. *Ann Oncol* 2023; **34**: 127-140 [PMID: 36372281 DOI: 10.1016/j.annonc.2022.10.506]
117 **Cho MT**, Gholami S, Gui D, Tejaswi SL, Fananapazir G, Abi-Jaoudeh N, Jutric Z, Samarasena JB, Li X, Valerin JB, Mercer J, Dayyani F. Optimizing the Diagnosis and Biomarker Testing for Patients with Intrahepatic Cholangiocarcinoma: A Multidisciplinary Approach. *Cancers (Basel)* 2022; **14**: 392 [PMID: 35053557 DOI: 10.3390/cancers14020392]
118 **Yang SZ**, Wang AQ, Du J, Wang JT, Yu WW, Liu Q, Wu YF, Chen SG. Low expression of ARID1A correlates with poor prognosis in intrahepatic cholangiocarcinoma. *World J Gastroenterol* 2016; **22**: 5814-5821 [PMID: 27433094 DOI: 10.3748/wjg.v22.i25.5814]
119 **Chen XX**, Yin Y, Cheng JW, Huang A, Hu B, Zhang X, Sun YF, Wang J, Wang YP, Ji Y, Qiu SJ, Fan J, Zhou J, Yang XR. BAP1 acts as a tumor suppressor in intrahepatic cholangiocarcinoma by modulating the ERK1/2 and JNK/c-Jun pathways. *Cell Death Dis* 2018; **9**: 1036 [PMID: 30305612 DOI: 10.1038/s41419-018-1087-7]
120 **Dong Z**, Liao B, Shen W, Sui C, Yang J. Expression of Programmed Death Ligand 1 Is Associated with the Prognosis of Intrahepatic Cholangiocarcinoma. *Dig Dis Sci* 2020; **65**: 480-488 [PMID: 31410753 DOI: 10.1007/s10620-019-05787-0]
121 **Wu H**, Wei Y, Jian M, Lu H, Song Q, Hao L, Yue Y. Clinicopathological and Prognostic Significance of Immunoscore and PD-L1 in Intrahepatic Cholangiocarcinoma. *Onco Targets Ther* 2021; **14**: 39-51 [PMID: 33442265 DOI: 10.2147/OTT.S288982]
122 **Chen F**, Sheng J, Li X, Gao Z, Zhao S, Hu L, Chen M, Fei J, Song Z. Unveiling the promise of PD1/PD-L1: A new dawn in immunotherapy for cholangiocarcinoma. *Biomed Pharmacother* 2024; **175**: 116659 [PMID: 38692063 DOI: 10.1016/j.biopha.2024.116659]
123 **Marabelle A**, Le DT, Ascierto PA, Di Giacomo AM, De Jesus-Acosta A, Delord JP, Geva R, Gottfried M, Penel N, Hansen AR, Piha-Paul SA, Doi T, Gao B, Chung HC, Lopez-Martin J, Bang YJ, Frommer RS, Shah M, Ghori R, Joe AK, Pruitt SK, Diaz LA Jr. Efficacy of Pembrolizumab in Patients With Noncolorectal High Microsatellite Instability/Mismatch Repair-Deficient Cancer: Results From the Phase II KEYNOTE-158 Study. *J Clin Oncol* 2020; **38**: 1-10 [PMID: 31682550 DOI: 10.1200/JCO.19.02105]
124 **Goeppert B**, Roessler S, Renner M, Singer S, Mehrabi A, Vogel MN, Pathil A, Czink E, Köhler B, Springfeld C, Pfeiffenberger J, Rupp C, Weiss KH, Schirmacher P, von Knebel Doeberitz M, Kloor M. Mismatch repair deficiency is a rare but putative therapeutically relevant finding in non-liver fluke associated cholangiocarcinoma. *Br J Cancer* 2019; **120**: 109-114 [PMID: 30377340 DOI: 10.1038/s41416-018-0199-2]
125 **Song JP**, Liu XZ, Chen Q, Liu YF. High tumor mutation burden indicates a poor prognosis in patients with intrahepatic cholangiocarcinoma. *World J Clin Cases* 2022; **10**: 790-801 [PMID: 35127895 DOI: 10.12998/wjcc.v10.i3.790]
126 **Choi WJ**, Ivanics T, Gravely A, Gallinger S, Sapisochin G, O'Kane GM. Optimizing Circulating Tumour DNA Use in the Perioperative Setting for Intrahepatic Cholangiocarcinoma: Diagnosis, Screening, Minimal Residual Disease Detection and Treatment Response Monitoring. *Ann Surg Oncol* 2023; **30**: 3849-3863 [PMID: 36808320 DOI: 10.1245/s10434-023-13126-x]
127 **Saeheng T**, Karbwang J, Na-Bangchang K. Interleukin-6 and Lymphocyte-to-Monocyte Ratio Indices Identify Patients with Intrahepatic Cholangiocarcinoma. *Biomedicines* 2024; **12**: 844 [PMID: 38672199 DOI: 10.3390/biomedicines12040844]
128 **Ni JY**, Sun HL, Guo GF, Zhou X, Wei JX, Xu LF. Hepatic arterial infusion of GEMOX plus systemic gemcitabine chemotherapy combined with lenvatinib and PD-1 inhibitor in large unresectable intrahepatic cholangiocarcinoma. *Int Immunopharmacol* 2024; **140**: 112872 [PMID: 39121605 DOI: 10.1016/j.intimp.2024.112872]

129 **Lin YS**, Li S, Yang X, Guo RP, Huang YH, Bai KH, Weng J, Yun JP. First-line hepatic arterial infusion chemotherapy plus lenvatinib and PD-(L)1 inhibitors versus systemic chemotherapy alone or with PD-(L)1 inhibitors in unresectable intrahepatic cholangiocarcinoma. *J Cancer Res Clin Oncol* 2024; **150**: 309 [PMID: 38890157 DOI: 10.1007/s00432-024-05795-2]

130 **Madzikatire TB**, Heng S, Gu H, Shan Y, Lin E, Banda J, Debora A, Madziva BA, Bowa MJ, Mudhuri MG, Bwalya C. Real-world outcomes of chemotherapy plus immune checkpoint inhibitors versus chemotherapy alone in advanced, unresectable, and recurrent intrahepatic cholangiocarcinoma. *Front Immunol* 2024; **15**: 1390887 [PMID: 38846939 DOI: 10.3389/fimmu.2024.1390887]

131 **Im JH**, Yu JI, Kim TH, Kim TG, Kim JW, Seong J. Combined High-Dose Radiotherapy with Sequential Gemcitabine-Cisplatin Based Chemotherapy Increase the Resectability and Survival in Locally Advanced Unresectable Intrahepatic Cholangiocarcinoma: A Multi-institutional Cohort Study. *Cancer Res Treat* 2024; **56**: 838-846 [PMID: 38186240 DOI: 10.4143/crt.2023.886]

132 **Franssen S**, Holster JJ, Jolissaint JS, Nooijen LE, Cercek A, D'Angelica MI, Homs MYV, Wei AC, Balachandran VP, Drebin JA, Harding JJ, Kemeny NE, Kingham TP, Klümpen HJ, Mostert B, Swijnenburg RJ, Soares KC, Jarnagin WR, Groot Koerkamp B. Gemcitabine with Cisplatin Versus Hepatic Arterial Infusion Pump Chemotherapy for Liver-Confined Unresectable Intrahepatic Cholangiocarcinoma. *Ann Surg Oncol* 2024; **31**: 115-124 [PMID: 37814188 DOI: 10.1245/s10434-023-14409-z]

133 **Zhu C**, Li H, Yang X, Wang S, Wang Y, Zhang N, Wang Y, Xue J, Zhang L, Ning C, Yang X, Xun Z, Chao J, Long J, Sang X, Zhu Z, Zhao H. Efficacy, safety, and prognostic factors of PD-1 inhibitors combined with lenvatinib and Gemox chemotherapy as first-line treatment in advanced intrahepatic cholangiocarcinoma: a multicenter real-world study. *Cancer Immunol Immunother* 2023; **72**: 2949-2960 [PMID: 37247023 DOI: 10.1007/s00262-023-03466-8]

134 **Shi GM**, Huang XY, Wu D, Sun HC, Liang F, Ji Y, Chen Y, Yang GH, Lu JC, Meng XL, Wang XY, Sun L, Ge NL, Huang XW, Qiu SJ, Yang XR, Gao Q, He YF, Xu Y, Sun J, Ren ZG, Fan J, Zhou J. Toripalimab combined with lenvatinib and GEMOX is a promising regimen as first-line treatment for advanced intrahepatic cholangiocarcinoma: a single-center, single-arm, phase 2 study. *Signal Transduct Target Ther* 2023; **8**: 106 [PMID: 36928584 DOI: 10.1038/s41392-023-01317-7]

135 **Ahmed O**, Yu Q, Patel M, Hwang G, Pillai A, Liao CY, Fung J, Baker T. Yttrium-90 Radioembolization and Concomitant Systemic Gemcitabine, Cisplatin, and Capecitabine as the First-Line Therapy for Locally Advanced Intrahepatic Cholangiocarcinoma. *J Vasc Interv Radiol* 2023; **34**: 702-709 [PMID: 36521794 DOI: 10.1016/j.jvir.2022.12.017]

136 **Zhang N**, Yu BR, Wang YX, Zhao YM, Zhou JM, Wang M, Wang LR, Lin ZH, Zhang T, Wang L. Clinical outcomes of hepatic arterial infusion chemotherapy combined with tyrosine kinase inhibitors and anti-PD-1 immunotherapy for unresectable intrahepatic cholangiocarcinoma. *J Dig Dis* 2022; **23**: 535-545 [PMID: 36148493 DOI: 10.1111/1751-2980.13127]

137 **Yuan P**, Song J, Wang F, Zhu G, Chen B. Combination of TACE and Lenvatinib as a promising option for downstaging to surgery of initially unresectable intrahepatic cholangiocarcinoma. *Invest New Drugs* 2022; **40**: 1125-1132 [PMID: 35793038 DOI: 10.1007/s10637-022-01257-z]

138 **Gupta AN**, Gordon AC, Gabr A, Kalyan A, Kircher SM, Mahalingam D, Mulcahy MF, Merkow RP, Yang AD, Bentrem DJ, Caicedo-Ramirez JC, Riaz A, Thornburg B, Desai K, Sato KT, Hohlastos ES, Kulik L, Benson AB, Salem R, Lewandowski RJ. Yttrium-90 Radioembolization of Unresectable Intrahepatic Cholangiocarcinoma: Long-Term Follow-up for a 136-Patient Cohort. *Cardiovasc Intervent Radiol* 2022; **45**: 1117-1128 [PMID: 35732931 DOI: 10.1007/s00270-022-03183-2]

139 **Bargellini I**, Mosconi C, Pizzi G, Lorenzoni G, Vivaldi C, Cappelli A, Vallati GE, Boni G, Cappelli F, Paladini A, Sciuto R, Masi G, Golfieri R, Cioni R. Yttrium-90 Radioembolization in Unresectable Intrahepatic Cholangiocarcinoma: Results of a Multicenter Retrospective Study. *Cardiovasc Intervent Radiol* 2020; **43**: 1305-1314 [PMID: 32642986 DOI: 10.1007/s00270-020-02569-4]

140 **Buettner S**, Braat AJAT, Margonis GA, Brown DB, Taylor KB, Borgmann AJ, Kappadath SC, Mahvash A, IJzermans JNM, Weiss MJ, Lamarca A, Bell JK, Valle JW, Hagendoorn J, Koerkamp BG, Sze DY, Lam MGEH. Yttrium-90 Radioembolization in Intrahepatic Cholangiocarcinoma: A Multicenter Retrospective Analysis. *J Vasc Interv Radiol* 2020; **31**: 1035-1043.e2 [PMID: 32473757 DOI: 10.1016/j.jvir.2020.02.008]

141 **Kuhlmann JB**, Euringer W, Spangenberg HC, Breidert M, Blum HE, Harder J, Fischer R. Treatment of unresectable cholangiocarcinoma: conventional transarterial chemoembolization compared with drug eluting bead-transarterial chemoembolization and systemic chemotherapy. *Eur J Gastroenterol Hepatol* 2012; **24**: 437-443 [PMID: 22261548 DOI: 10.1097/MEG.0b013e3283502241]

142 **Schiffman SC**, Metzger T, Dubel G, Andrasina T, Kralj I, Tatum C, McMasters KM, Scoggins CR, Martin RC. Precision hepatic arterial irinotecan therapy in the treatment of unresectable intrahepatic cholangiocellular carcinoma: optimal tolerance and prolonged overall survival. *Ann Surg Oncol* 2011; **18**: 431-438 [PMID: 20862554 DOI: 10.1245/s10434-010-1333-4]

World Journal of Gastroenterology

Submit a Manuscript: https://www.f6publishing.com

World J Gastroenterol 2025 April 21; 31(15): 101695

DOI: 10.3748/wjg.v31.i15.101695

ISSN 1007-9327 (print) ISSN 2219-2840 (online)

ORIGINAL ARTICLE

Case Control Study

Early detection of gastroparesis with diabetic ketoacidosis as initial manifestation: A case-control study

Li Han, Qing-Yi Peng, Jie Yu, Yi-Wen Liu, Wei Li, Fan Ping, Hua-Bing Zhang, Yu-Xiu Li, Ling-Ling Xu

Specialty type: Gastroenterology and hepatology

Provenance and peer review: Unsolicited article; Externally peer reviewed.

Peer-review model: Single blind

Peer-review report's classification

Scientific Quality: Grade A, Grade B, Grade B, Grade C, Grade C

Novelty: Grade A, Grade A, Grade B, Grade B, Grade B

Creativity or Innovation: Grade B, Grade B, Grade B, Grade B, Grade C

Scientific Significance: Grade A, Grade B, Grade B, Grade B, Grade B

P-Reviewer: Ajith TA; Budaya TN; Haque MA; Huang ZP; Teli B

Received: September 23, 2024

Revised: January 21, 2025

Accepted: March 21, 2025

Published online: April 21, 2025

Processing time: 206 Days and 15.3 Hours

Li Han, Qing-Yi Peng, Jie Yu, Yi-Wen Liu, Wei Li, Fan Ping, Hua-Bing Zhang, Yu-Xiu Li, Ling-Ling Xu, Department of Endocrinology, Key Laboratory of Endocrinology of National Health Commission, Translation Medicine Center, Peking Union Medical College Hospital, Chinese Academy of Medical Sciences and Peking Union Medical College, Beijing 100730, China

Co-first authors: Li Han and Qing-Yi Peng.

Corresponding author: Ling-Ling Xu, PhD, Professor, Department of Endocrinology, Key Laboratory of Endocrinology of National Health Commission, Translation Medicine Center, Peking Union Medical College Hospital, Chinese Academy of Medical Sciences and Peking Union Medical College, Shuaifuyuan Street, Beijing 100730, China. llxuwsh@163.com

Abstract

BACKGROUND

Gastroparesis may repeatedly induce diabetic ketoacidosis (DKA), and the differential diagnosis of these diseases is challenging because of similar gastrointestinal symptoms. If DKA is accompanied by gastroparesis, patients present with persistent gastrointestinal symptoms without relief and may even experience recurrent DKA. Misdiagnosis results in poor treatment outcomes and prognosis. We hypothesized that biomarkers or screening tools can be identified by comparing the clinical data between DKA alone and DKA + gastroparesis to facilitate early screening.

AIM

To achieve early detection and diagnosis of DKA + gastroparesis to enable early treatment aimed at relieving gastrointestinal symptoms and preventing re-induction of DKA.

METHODS

We conducted a case-control study in which 15 patients hospitalized for DKA at the Endocrinology Department of Peking Union Medical College Hospital and diagnosed with DKA and gastroparesis between December 1999 and January 2023 (DKA + gastroparesis group) were included. Then, we selected 60 DKA patients without DKA as a control group (DKA alone group) based on gender, age, disease course, and diabetes subtype in a 1:4 matching ratio. Clinical manifestations and physical and laboratory examination results were statistically compared between the groups.

RESULTS
The DKA + gastroparesis group was composed of nine males and six females, with a mean age of 35 ± 11 years, while the DKA alone group included 34 males and 26 females, with a mean age of 34 ± 17 years. In the DKA + gastroparesis group, urine ketone levels normalized, while gastrointestinal symptoms persisted despite treatment, and the tests indicated lower glycosylated hemoglobin levels (HbA1c; 7.07% *vs* 11.51%, $P < 0.01$), largest amplitude of glycemic excursions (5.86 *vs* 17.41, $P < 0.01$), standard deviation of blood glucose (SDBG; 2.69 *vs* 5.83, $P < 0.01$), and coefficient of blood glucose variation (0.31 *vs* 0.55, $P = 0.014$) compared with the DKA alone group. Probable gastroparesis was considered at HbA1c < 8.55%. Besides, the patients in the DKA + gastroparesis group had lower body mass index (19.28 kg/m^2 *vs* 23.86 kg/m^2, $P = 0.02$) and higher high density lipoprotein cholesterol level (2.34 mmol/L *vs* 1.05 mmol/L, $P = 0.019$) compared to the DKA alone group, but no difference was observed in the remaining lipid profiles between the two groups.

CONCLUSION
Gastroparesis should be considered in DKA patients who fail to have improved gastrointestinal symptoms after ketone elimination and acidosis correction, particularly when the HbA1c level is < 8.55%.

Key Words: Diabetes mellitus; Diabetic ketoacidosis; Diabetic gastroparesis; Early detection; Diagnosis

Core Tip: Persistent gastroparesis can repeatedly trigger diabetic ketoacidosis (DKA) and is difficult to correct. We compared the clinical manifestations and biomarkers between patients with DKA alone and those with DKA + gastroparesis to help promptly detect and diagnose DKA with gastroparesis, relieve gastrointestinal symptoms, and prevent re-induction of DKA. Notably, we found that if patients with DKA present persistent gastrointestinal symptoms without relief, lower glycosylated hemoglobin (HbA1c) levels, lower body mass index, and higher high-density lipoprotein cholesterol levels after ketone elimination and acidosis correction, gastroparesis should be considered in clinical practice, particularly when the HbA1c level is < 8.55%. Furthermore, gastrointestinal examinations should be performed in a timely manner to facilitate diagnosis.

Citation: Han L, Peng QY, Yu J, Liu YW, Li W, Ping F, Zhang HB, Li YX, Xu LL. Early detection of gastroparesis with diabetic ketoacidosis as initial manifestation: A case-control study. *World J Gastroenterol* 2025; 31(15): 101695
URL: https://www.wjgnet.com/1007-9327/full/v31/i15/101695.htm
DOI: https://dx.doi.org/10.3748/wjg.v31.i15.101695

INTRODUCTION

Gastroparesis is a gastrointestinal disease with objective evidence of delayed gastric emptying of solid foods after excluding mechanical distal gastric obstruction. Clinical symptoms of gastric retention include nausea, vomiting, early satiety, and abdominal distension[1]. Diabetic gastroparesis is a serious complication in patients with diabetes during disease progression, and a gastroparesis risk of up to 50% exists in patients with types 1 and 2 diabetes and poor blood glucose control[2]. In addition to gastrointestinal symptoms, diabetic gastroparesis may manifest as hypoglycemia, which is induced by frequent glucose variation secondary to delayed postprandial plasma glucose elevation due to slowed gastrointestinal motility[3]; it may also manifest as hyperglycemic symptoms of diabetic ketoacidosis (DKA) or hypertonic hyperglycemia syndrome (HHS). The risk of DKA or HHS was 4-fold higher in patients with diabetic gastroparesis than in those without[4]. In gastroparesis patients, delayed gastric emptying leads to delayed peak blood glucose levels. Unchanged pre-meal insulin timing increases the risk of postprandial early hypoglycemia and pre-meal hyperglycemia. Therefore, delayed gastric emptying complicates blood glucose control in patients with diabetes, especially in those receiving insulin treatment[5]. Gastroparesis is a chronic condition, with an average symptom duration of 26.5 months[6]; however, a sharp rise in blood glucose can alter gastric emptying in the short term by influencing glucose-excited/inhibited neurons in gastric excitation/inhibition neural pathways[5]. For example, a rapid increase in blood glucose in DKA can induce acute gastroparesis, and they may occur simultaneously. DKA patients often present with similar gastrointestinal symptoms similar to gastroparesis patients, including nausea, vomiting, and abdominal pain. Thus, the differential diagnosis of DKA and gastroparesis is challenging based on clinical symptoms, and imaging examinations, such as gastric emptying scintigraphy, wireless motility capsule, and ^{13}C-urea breath test, are not routinely performed for DKA patients, which makes DKA + gastroparesis easily neglected. During the diagnosis and treatment of patients with DKA, DKA is caused by gastroparesis only in a small number of patients. Misdiagnosis by physicians may result in these patients enduring persistent gastrointestinal symptoms, poor blood glucose control, and recurrent DKA in a short period. Therefore, the early diagnosis of DKA + gastroparesis is necessary but challenging for clinicians. However, there is limited research on this topic, and the conclusions are inconsistent. Two case reports reported DKA with gastroparesis[6,7], while others reported that moderate DKA does not affect gastric emptying[8]. The small sample size, severity

of DKA, blood glucose levels, and regional factors may help explain these differences. Therefore, the present study statistically analyzed the differences in clinical manifestations and biochemical indices between patients with gastroparesis-induced DKA and those with DKA only, with an aim to provide a reference for clinical diagnosis and treatment of these conditions.

MATERIALS AND METHODS

This was a cross-sectional study. A total of 1176 patients who were hospitalized for DKA at the Endocrinology Department of Peking Union Medical College Hospital (PUMCH) between December 1999 and January 2023 were included. To compare the differences between DKA + gastroparesis and DKA alone patients, we reviewed the medical records of 15 patients diagnosed with DKA + gastroparesis between December 1999 and January 2023 (DKA + gastroparesis group). To select a control group, we adopted a matched design, typical of case-control studies. To optimize statistical power, we used a 1:4 matching ratio. Each patient was paired with four controls based on gender, age, disease course, and diabetes subtype in a 1:4 ratio. Finally, 60 DKA alone patients of similar gender, age, disease course, and diabetes subtype were selected as a control group.

The inclusion criteria for the 15 patients with DKA + gastroparesis were as follows: (1) Patients previously diagnosed as having type 1 or 2 diabetic mellitus; (2) DKA was diagnosed according to the following criteria: Arterial blood gas pH < 7.3 and/or $HCO3^-$ < 18 mmol/L, blood ketone > 3.0 mmol/L, or urine ketone body (++) or above, and blood glucose > 13.9 mmol/L; (3) Patients who met the diagnostic criteria for gastroparesis: Presence of clinical manifestations, such as nausea, vomiting, early satiety, abdominal distension, and other gastrointestinal symptoms; 5-hour gastric emptying < 50%; or 48-hour total gastrointestinal emptying < 90% after excluding mechanical gastrointestinal obstruction, ulceration, and gastrointestinal bleeding by gastrointestinal endoscopy, upper gastroenterography, or abdominal X-ray plain scan, or other imaging diagnosis evidence including gastric dysrhythmia and bradygastria confirmed by electrogastrogram; (4) Laboratory tests included routine blood examination, liver and kidney function, inflammatory markers, and routine stool testing to help exclude gastrointestinal infections; and (5) Patients with DKA whose urine ketone levels normalized, while gastrointestinal symptoms persisted despite treatment.

A total of 60 DKA alone patients of similar age, gender, disease course, and diabetes subtype to the DKA + gastroparesis group were retrieved using the PUMCH medical record query and analysis system as controls, and the inclusion criteria were as follows: (1) Diagnosis of type 1 or 2 diabetes mellitus but with no history of gastroparesis; (2) DKA was diagnosed according to the following criteria: Arterial blood gas pH < 7.3 and/or $HCO3^-$ < 18 mmol/L, blood ketone > 3.0 mmol/L, or urine ketone body (++) or above, and blood glucose > 13.9 mmol/L; and (3) patients who were hospitalized for DKA and achieved improvement in gastrointestinal symptoms after the treatment of ketone elimination and acidosis correction. The control group patients were regularly followed at our outpatient clinic, and to date, none have presented with unexplained gastrointestinal symptoms or received a diagnosis of gastroparesis upon gastrointestinal examination. The Gastroparesis Cardinal Symptom Index (GCSI), a screening questionnaire, was used to assess the severity of gastroparesis-related symptoms. It comprises nine items and measures important symptoms associated with gastroparesis, including nausea or vomiting, postprandial fullness or early satiety, and abdominal bloating. If no gastrointestinal symptoms exist, a GCSI score < 18 points does not meet the clinical suspicion criteria for gastroparesis[9]. Therefore, gastroparesis was ruled out clinically.

General data, clinical symptoms and manifestations, and laboratory examination data were collected from the medical records of patients in the two groups, and the clinical indices were statistically analyzed between the groups. Particularly, the largest amplitude of glycemic excursions (LAGE), standard deviation of blood glucose (SDBG), mean amplitude of glucose excursions (MAGE), coefficient of blood glucose variation (CV), and pre- and post-prandial blood glucose variations were calculated from daily multipoint blood glucose recordings during hospitalization in both DKA and DKA + gastroparesis patients.

Statistical analysis

Statistical analyses were performed using SPSS software (version 27.0; IBM Corp., Armonk, NY, United States). The normally distributed quantitative data are presented as the mean ± SD, while the qualitative data with a skewed distribution are expressed as median and quartiles (Q1, Q3). Laboratory examination results were comparatively analyzed between the DKA + gastroparesis and DKA groups. The sample size of the DKA + gastroparesis group was < 20, and the normality test lacked sufficient power. Intergroup comparisons of continuous variables with a skewed distribution, including age, body mass index (BMI), course of disease, total cholesterol (TC), triglycerides (TG), high-density lipoprotein cholesterol (HDL-C), low-density lipoprotein cholesterol (LDL-C), glycosylated hemoglobin (HbA1c), LAGE, SDBG, MAGE, CV, and preprandial and postprandial blood glucose variation, were performed using the Mann-Whitney *U* test. The significance level of $\alpha = 0.05$ was used, and $P < 0.05$ for two-tailed tests indicated that the difference between groups was statistically significant. R studio software (version 4.3.1) was employed to plot ROC curves and calculate the area under the curve (AUC). AUC > 0.5 and $P < 0.05$ indicated appreciated prediction and diagnostic value, with larger AUC values indicating higher diagnostic value. MedCalc software was used for validation and to calculate the cut-offs and corresponding sensitivity and specificity indices.

Table 1 Comparison between diabetic ketoacidosis with gastroparesis and diabetic ketoacidosis alone

	DKA + gastroparesis (*n* = 15)	DKA alone (*n* = 60)	*P* value[1]
Age (mean, ± SD) (years)	35.47 ± 10.97	33.60 ± 17.1	0.474
Female patients, *n* (%)	6.0 (40.0)	26.0 (43.3)	0.818
Type 2 DM, *n* (%)	7.0 (46.7)	28.0 (46.7)	0.495
Course of disease (years)	9.0 (5.0-13.0)	7.0 (0-14.0)	0.265
BMI (kg/m^2)	19.28 ± 3.16[b]	23.86 ± 5.90[b]	0.007
TC (mmol/L)	6.09 ± 2.64	5.26 ± 2.14	0.263
TG (mmol/L)	3.82 ± 4.39	2.85 ± 5.41	0.553
HDL-C (mmol/L)	2.34 ± 1.60[a]	1.05 ± 0.36[a]	0.019
LDL-C (mmol/L)	4.44 ± 2.61	3.08 ± 1.31	0.09
HbA1c (%)	7.07 ± 1.04[a]	11.51 ± 2.75[a]	0.01
SDBG (mmol/L)	2.69 ± 0.56[a]	5.83 ± 2.07[a]	0.01
LAGE (mmol/L)	5.86 ± 2.87[a]	17.41 ± 7.22[a]	0.01
MAGE (mmol/L)	4.50 ± 1.62	6.36 ± 3.41	0.125
CV (%)	0.31 ± 0.11[a]	0.55 ± 0.25[a]	0.014
Blood glucose variation before and after meals (mmol/L)	2.85 ± 1.79	3.44 ± 4.19	0.473
Fasting C-peptide (nmol/L)	0.44 ± 0.33	0.75 ± 0.75	0.353
Fasting insulin (μU/mL)	23.40 ± 27.86	20.40 ± 32.71	0.9
ACR (mg/g)	245.22 ± 320.06	125.12 ± 416.71	0.536

[1]Mann-Whitney *U* test.
[a]$P < 0.05$.
[b]$P < 0.01$.
DKA: Diabetic ketoacidosis; BMI: Body mass index; TC: Total cholesterol; TG: Triglycerides; HDL-C: High-density lipoprotein cholesterol; LDL-C: Low-density lipoprotein cholesterol; HbA1c: Glycosylated hemoglobin; SDBG: Standard deviation of blood glucose; LAGE: Largest amplitude of glycemic excursions; MAGE: Mean amplitude of glucose excursions; CV: Coefficient of blood glucose variation; ACR: Urinary albumin-creatinine ratio.

RESULTS

Sample disposition

A total of 75 patients were enrolled in the study, including 15 DKA + gastroparesis patients [9 (60%) males and 6 (40%) females; mean age: 35 ± 11 years; ratio of type 1/type 2/other special types diabetic patients: 7:7:1; mean course of diabetes mellitus: 7 (6, 11 years)] and 60 DKA alone patients [34 (56.7%) males and 26 (43.3%) females; mean age: 34 ± 17 years; ratio of type 1/type 2/unclear type diabetic patients: 19/28/13; mean course of diabetes mellitus: 7 (0, 14) years] (Table 1).

Clinical symptoms pre- and post-treatment

Clinical symptoms of polyuria, polydipsia, dehydration, respiratory compensation, and changes in cognitive state before therapy quickly improved after ketone elimination and acidosis correction in both groups. Patients in the DKA + gastroparesis group exhibited several types of gastrointestinal discomfort. Apart from nausea and vomiting, abdominal distension was particularly prominent and was characterized by early satiety, postprandial fullness, and prolonged duration. This sensation of fullness significantly affected their ability to eat. Other symptoms included reflux, heartburn, abdominal pain, and constipation. The gastrointestinal symptoms persisted even after the correction of ketonuria and acidosis. Prompt diagnosis and treatment using prokinetic agents led to significant improvement in gastrointestinal symptoms, with abdominal distension exhibiting the most remarkable improvement. In contrast, patients in the DKA alone group mainly experienced nausea and vomiting, with other gastrointestinal symptoms being less pronounced. Gastrointestinal symptoms rapidly disappeared after the resolution of ketonuria.

Laboratory examination

Lower HbA1c levels, LAGE, SDBG, and CV were observed in the DKA + gastroparesis group (7.07% *vs* 11.51%, $P < 0.01$; 5.86 *vs* 17.41, $P < 0.01$; 2.69 *vs* 5.83, $P < 0.01$; 0.31 *vs* 0.55, $P = 0.014$, respectively), but no significant difference was observed in MAGE between the two groups. BMI was lower and HDL-C level was higher in the DKA + gastroparesis

group than in the DKA group (19.28 *vs* 23.86 kg/m^2, P = 0.02; 2.34 *vs* 1.05 mmol/L, P = 0.019), and no significant differences were observed in TC, TG, or LDL-C between the two groups. Similarly, no remarkable differences were observed in the fasting C-peptide level, fasting insulin level, and urinary albumin creatinine ratio between the groups (Table 1).

For lower HbA1c levels in the DKA + gastroparesis group, we further investigated whether HbA1c could be used to predict gastroparesis in DKA patients. The AUC (Figure 1) was 0.918 (P < 0.0001, 95% confidence interval [CI]: 0.779-0.981), cutoff was 8.55% (sensitivity = 0.825, 95%CI: 0.663-0.958; specificity = 1, 95%CI: 0.715-1.0), and HbA1c < 8.55% indicated probable DKA + gastroparesis.

DISCUSSION

This study summarized the clinical manifestations and biochemical indices of DKA + gastroparesis, and the study results suggested that if patients with DKA have no improvement in gastrointestinal symptoms after urine ketone normalization and acidosis correction, gastroparesis should be considered. The patients with DKA as onset symptom who were finally diagnosed with gastroparesis had significant differences in blood glucose variation and lipid from DKA patients, specifically lower BMI and HbA1c level, higher HDL-C level, and smaller random blood glucose variation; HbA1c < 8.55% indicates a greater probability of gastroparesis in DKA patients.

Serum HbA1c level is not only an important factor influencing the gastric emptying time in patients with type 2 diabetes[10,11], but its increase is also a risk factor for gastrointestinal symptoms in these patients, as reported in a cross-sectional epidemiological study[12]. Poor blood glucose control and high blood glucose and HbA1c levels are regarded as early predictors of gastroparesis in type 2 diabetes mellitus and risk factors for its progression[13,14]. Notably, this study demonstrated that patients diagnosed with DKA + gastroparesis had lower HbA1c levels, suggesting good blood glucose control in the short term; at HbA1c < 8.55%, probable gastroparesis was considered for DKA patients, which may be inconsistent with previous research findings. This can be attributed to several factors. Due to varying disease durations among patients, hyperglycemia is indeed a key factor in the development of gastroparesis, with significantly elevated HbA1c levels observed in early and mid-stage cases. However, in our study, in patients with gastroparesis, the condition persisted for a long time before admission, leading to reduced food intake, early satiety, weight loss, lower blood glucose levels, and smaller random blood glucose variations. However, because hyperglycemia is a known risk factor for gastroparesis, clinicians may easily overlook the diagnosis of gastroparesis when the HbA1c level is only mildly elevated. Currently, there is a lack of relevant foundational and clinical research, so the other potential pathophysiological mechanisms remain unclear. Further prospective studies are needed to gain a deeper understanding of these findings. Our study results proved that for DKA patients with HbA1c < 8.55%, close attention must be paid to changes in gastrointestinal symptoms, and if these symptoms persist after urine ketone levels normalize, relevant examinations should be performed to identify gastroparesis.

None of previous studies have indicated that lipid dysmetabolism is associated with gastroparesis[15], but the later can delay the arrival time of nutrients to the small intestine and thus result in continuous lipid absorption and elevation of blood lipids, especially TG, and the affected patients have a poor response to conventional lipid-lowering treatment[16]. In a rat experiment of diabetic gastroparesis, postprandial hypertriglyceridemia was observed and significantly improved after treatment with gastro-kinetic agents[17]. In this study, both the DKA alone and DKA + gastroparesis groups exhibited lipid abnormalities based on the average levels of each lipid component. Lipid abnormalities may not be recognized as diagnostic factors. However, patients with DKA + gastroparesis had a lower BMI but higher HDL-C levels though there were no significant differences in TC, TG, or LDL-C levels between the groups, which is not consistent with results from previous studies. The underlying causes and pathophysiological mechanisms may be considered as follows: (1) In gastroparesis patients with a chronic and prolonged disease, an underlying gastrointestinal neuropathy exists[18], which may be re-induced or worsened by acute hyperglycemia in DKA, and previous long-term gastrointestinal discomfort can lead to a decrease in food intake, body weight, and BMI. Weight loss can also increase HDL-C levels. For every 1 kg of weight loss, HDL-C levels can reportedly rise by 0.35-0.46 mg/dL[19]; and (2) HDL-C is primarily synthesized in the liver and small intestine. Diet and nutrition reportedly influence cholesterol homeostasis, affecting lipid metabolism and progression of atherosclerosis[20]. Plasma HDL concentrations correlate directly with plasma sterol markers of intestinal cholesterol absorption and reciprocally with cholesterol synthesis[21]. Gastroparesis affects normal gastric emptying and disrupts food digestion and absorption, leading to intestinal lipid absorption and metabolism disorders. Abnormal intestinal lipid absorption and metabolism may explain the increased HDL-C levels. However, whether BMI and HDL-C levels affect gastroparesis progression and treatment outcomes remains unclear. Future prospective studies are needed to validate these findings and establish a more causal relationship.

Based on previous case reports, patients with DKA + gastroparesis presented with persistent vomiting without relief, nausea, abdominal pain, and other gastrointestinal symptoms, which did not improve after simple hydration and insulin treatment; the imaging examination indicated gastric retention, and the aforementioned symptoms were relieved after gastrointestinal decompression and drainage using a nasogastric tube[6]. Meanwhile, a case study showed that gastroparesis could repeatedly induce DKA; thus, it was regarded as one of the factors that aggravates or induces DKA[7]. If DKA patients present with persistent gastrointestinal symptoms without relief, lower HbA1c levels and BMI, and higher HDL-C levels after ketone elimination and acidosis correction, gastroparesis should be considered, and gastrointestinal examinations such as gastric emptying scintigraphy, wireless motility capsule, and ^{13}C-urea breath test should be performed promptly[22]. Moreover, decompression and gastrointestinal prokinetic therapy, such as metoclopramide, erythromycin, domperidone, and mosapride, should be initiated as soon as possible to prevent the re-induction of DKA.

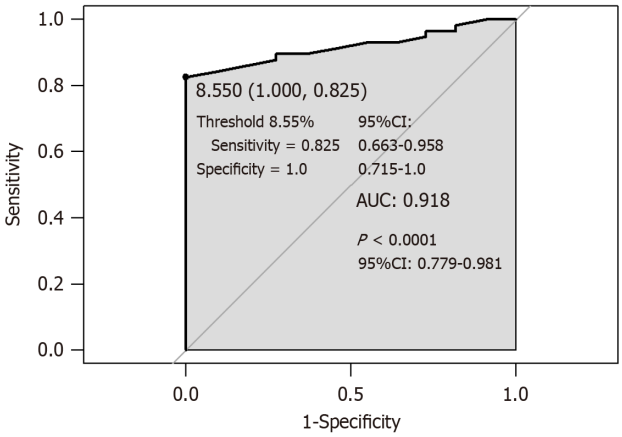

Figure 1 Receiver operating characteristic curve of glycosylated hemoglobin-based prediction of gastroparesis in diabetic ketoacidosis patients. Receiver operating characteristic curve analysis of the relationship between glycosylated hemoglobin (HbA1c) and diabetic ketoacidosis + gastroparesis exhibited an area under the curve of 0.918 (P < 0.001). The HbA1c threshold with the best sensitivity (82.5%) and specificity (100%) was 8.55%. HbA1c: Glycosylated hemoglobin; AUC: Area under the curve.

This study has several strengths. First, few previous studies on DKA + gastroparesis exist; specifically, only two case reports have reported it. Limited literature exists on the incidence and clinical characteristics of DKA + gastroparesis patients. This is the first clinical study to retrospectively analyze the differences in clinical manifestations and biochemical indices between DKA + gastroparesis patients and those with DKA alone. Although only 15 patients with DKA + gastroparesis were included, the sample size was relatively large, which has considerable reference value for clinical applications. Second, many indices, besides HbA1c level, were used in this study to evaluate daily blood glucose variations, such as CV, SDBG, LAGE, and MAGE. The findings of lower CV, LAGE, and SDBG levels in the DKA + gastroparesis group reflected a smaller daily blood glucose variation, which assessed blood glucose control and variation from a different perspective.

This study also has some limitations. First, this was a single-center study with a small sample size, and the generalization of the statistical analysis results is limited. Advancements in primary-tier diabetes management have made the early detection of gastroparesis and DKA in community hospitals possible, enabling timely intervention without hospitalization. In contrast, some patients with DKA complicated by gastroparesis may be initially discharged after resolution of ketoacidosis, with the diagnosis of coexisting gastroparesis becoming evident only after multiple DKA-related hospital admissions. Consequently, the number of hospitalized patients with DKA and coexisting gastroparesis remains limited. Although our study involved a relatively small sample size, it offers certain advantages over previous studies, particularly in terms of sample size. Future studies with larger sample sizes and multicenter design are necessary to validate our conclusions. Second, inherent limitations associated with retrospective studies exist: (1) Our study may have been subject to unmeasured or unaccounted-for biases and confounding factors. To address this, we employed matched controls in the selection of the control group to minimize selection bias and mitigate the influence of confounders. However, owing to the nature of retrospective studies, eliminating these potential biases and confounders remains challenging; and (2) Clinical data were incomplete and difficult to trace. For example, when calculating the daily blood glucose variation, the blood glucose data at seven time points within a day were required[23] to compute the CV, but only the blood glucose data at five time points were collected by reviewing the medical records of the patients in this study, resulting in a bias in the computed blood glucose variation value. Future large-scale prospective studies are needed to validate these findings and explore the underlying causal relationships and potential mechanisms.

CONCLUSION

In summary, gastroparesis should be considered in clinical practice if patients with DKA experience persistent gastrointestinal symptoms without relief. For DKA patients with HbA1c < 8.55%, smaller random blood glucose variation, lower BMI, and higher HDL-C levels, probable gastroparesis should be considered. Imaging examinations must be performed to establish a definitive diagnosis (Figure 2). After diagnosis, gastro-kinetic agents should be administrated promptly to not only improve gastric retention and relieve gastrointestinal symptoms but also strengthen blood glucose control, reduce blood glucose variation, and avoid re-induction of DKA.

Continuous gastroparesis can repeatedly trigger DKA, which is challenging to address. The risk of recurrent DKA can be fundamentally reduced by promptly identifying and treating triggers. Prospective studies with larger sample sizes and multicenter design are required to enhance the depth of the research and provide more valuable insights for clinical practice.

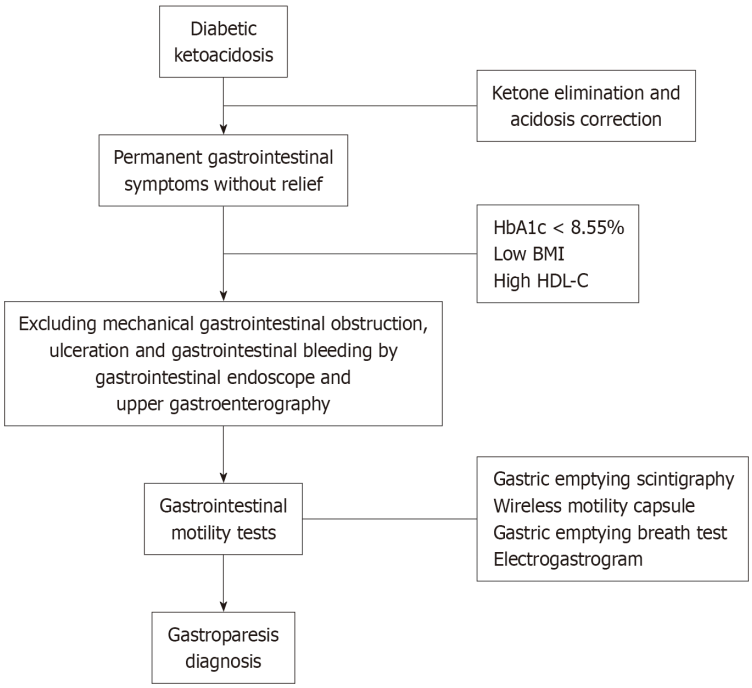

Figure 2 Flow for early detection of gastroparesis in patients with diabetic ketoacidosis. HbA1c: Glycosylated hemoglobin; BMI: Body mass index; HDL-C: High density lipoprotein cholesterol.

ACKNOWLEDGEMENTS

We express our sincere gratitude to Ling-Ling Xu, who made great contributions to manuscript revision.

FOOTNOTES

Author contributions: Han L and Peng QY contributed equally to this work as co-first authors. Han L and Xu LL selected the topic and designed this study; Han L, Yu J, Liu YW, Ping F, Li W, Zhang HB, and Li YX reviewed the medical records, chose patients who met the inclusion criteria, and collected the data; Han L analyzed the data and drew an interesting conclusion; Han L and Peng QY made joint efforts to write the main manuscript text; Xu LL revised the manuscript. All authors read and approved the final manuscript.

Supported by National High Level Hospital Clinical Research Funding, No. 2022-PUMCH-B-015; and the Chinese Academy of Medical Sciences (CAMS) Innovation Fund for Medical Sciences, No. 2021-I2M-C&T-B-003.

Institutional review board statement: This study was reviewed and approved by the Medical Ethics Review Committee of Peking Union Medical College Hospital (No. K4854).

Informed consent statement: Since this was a retrospective study and the data were anonymous, informed consent was waived by the Ethics Committee of Peking Union Medical College Hospital.

Conflict-of-interest statement: The authors declare that they have no competing interests to disclose.

Data sharing statement: The dataset generated and/or analyzed during the current study are not publicly available to protect the privacy of the respondents.

STROBE statement: The authors have read the STROBE Statement—checklist of items, and the manuscript was prepared and revised according to the STROBE Statement—checklist of items.

Country of origin: China

ORCID number: Wei Li 0000-0002-3332-1287; Fan Ping 0000-0001-7650-6612; Hua-Bing Zhang 0000-0001-6259-7584; Ling-Ling Xu 0000-0003-1341-4141.

S-Editor: Qu XL
L-Editor: Wang TQ
P-Editor: Zheng XM

REFERENCES

1 **Shin AS**, Camilleri M. Diagnostic assessment of diabetic gastroparesis. *Diabetes* 2013; **62**: 2667-2673 [PMID: 23881199 DOI: 10.2337/db12-1706]
2 **Aswath GS**, Foris LA, Ashwath AK, Patel K. Diabetic Gastroparesis. 2023 Mar 27. In: StatPearls [Internet]. Treasure Island (FL): StatPearls Publishing; 2025 Jan- [PMID: 28613545]
3 **Sang MM**, Wu TZ, Sun ZL. [Advances in the pathogenesis and clinical management of diabetes-related gastrointestinal symptoms]. *Zhonghua Tangniaobing Zazhi* 2021; **13**: 513-516 [DOI: 10.3760/cma.j.cn115791-20200730-00471]
4 **Butalia S**, Johnson JA, Ghali WA, Rabi DM. Clinical and socio-demographic factors associated with diabetic ketoacidosis hospitalization in adults with Type 1 diabetes. *Diabet Med* 2013; **30**: 567-573 [PMID: 23323955 DOI: 10.1111/dme.12127]
5 **Goyal RK**. Gastric Emptying Abnormalities in Diabetes Mellitus. *N Engl J Med* 2021; **384**: 1742-1751 [PMID: 33951363 DOI: 10.1056/NEJMra2020927]
6 **Sharayah AM**, Hajjaj N, Osman R, Livornese D. Gastroparesis in a patient with diabetic ketoacidosis. *Cleve Clin J Med* 2019; **86**: 238-239 [PMID: 30951455 DOI: 10.3949/ccjm.86a.18116]
7 **Pape A**, Nguyen HV, Flack JR. Recurrent diabetic ketoalkalosis in a patient with Type 1 diabetes mellitus and severe gastroparesis. *Diabet Med* 2010; **27**: 607-608 [PMID: 20536961 DOI: 10.1111/j.1464-5491.2010.02988.x]
8 **Jalleh RJ**, Phillips L, Umapathysivam MM, Jones KL, Marathe CS, Watson LE, Bound M, Rayner CK, Horowitz M. Gastric emptying during and following resolution of moderate diabetic ketoacidosis in type 1 diabetes: a case series. *BMJ Open Diabetes Res Care* 2024; **12** [PMID: 38575155 DOI: 10.1136/bmjdrc-2023-003854]
9 **Brown LK**, Xu J, Freedman BI, Hsu FC, Bowden DW, Koch KL. Symptoms Suggestive of Gastroparesis in a Community-Based Cohort of European Americans and African Americans with Type 2 Diabetes Mellitus. *Dig Dis Sci* 2020; **65**: 2321-2330 [PMID: 31820181 DOI: 10.1007/s10620-019-05974-z]
10 **Javadi H**, Bayani H, Mogharrabi M, Pashazadeh AM, Semnani S, Semnani S, Nabipour I, Assadi M. Relation between clinical features and gastric emptying time in diabetic patients. *Nucl Med Rev Cent East Eur* 2015; **18**: 3-6 [PMID: 25633509 DOI: 10.5603/NMR.2015.0002]
11 **Izzy M**, Lee M, Johns-Keating K, Kargoli F, Beckoff S, Chun K, Tokayer A. Glycosylated hemoglobin level may predict the severity of gastroparesis in diabetic patients. *Diabetes Res Clin Pract* 2018; **135**: 45-49 [PMID: 29111279 DOI: 10.1016/j.diabres.2017.10.016]
12 **Bytzer P**, Talley NJ, Hammer J, Young LJ, Jones MP, Horowitz M. GI symptoms in diabetes mellitus are associated with both poor glycemic control and diabetic complications. *Am J Gastroenterol* 2002; **97**: 604-611 [PMID: 11922554 DOI: 10.1111/j.1572-0241.2002.05537.x]
13 **Asghar S**, Asghar S, Shahid S, Sajjad H, Abdul Nasir J, Usman M. Gastroparesis-Related Symptoms in Patients With Type 2 Diabetes Mellitus: Early Detection, Risk Factors, and Prevalence. *Cureus* 2023; **15**: e35787 [PMID: 37025723 DOI: 10.7759/cureus.35787]
14 **Bharucha AE**, Kudva Y, Basu A, Camilleri M, Low PA, Vella A, Zinsmeister AR. Relationship between glycemic control and gastric emptying in poorly controlled type 2 diabetes. *Clin Gastroenterol Hepatol* 2015; **13**: 466-476.e1 [PMID: 25041866 DOI: 10.1016/j.cgh.2014.06.034]
15 **Bharucha AE**, Kudva YC, Prichard DO. Diabetic Gastroparesis. *Endocr Rev* 2019; **40**: 1318-1352 [PMID: 31081877 DOI: 10.1210/er.2018-00161]
16 **Adar T**, Lysy J. Pseudodyslipidemia: are we over-treating dyslipidemia in diabetic patients with undiagnosed gastroparesis? *Endocrine* 2014; **45**: 26-27 [PMID: 24197805 DOI: 10.1007/s12020-013-0064-2]
17 **Xie W**, Xing D, Zhao Y, Su H, Meng Z, Chen Y, Du L. A new tactic to treat postprandial hyperlipidemia in diabetic rats with gastroparesis by improving gastrointestinal transit. *Eur J Pharmacol* 2005; **510**: 113-120 [PMID: 15740731 DOI: 10.1016/j.ejphar.2005.01.019]
18 **Tseng PH**, Chao CC, Cheng YY, Chen CC, Yang PH, Yang WK, Wu SW, Wu YW, Cheng MF, Yang WS, Wu MS, Hsieh ST. Diabetic visceral neuropathy of gastroparesis: Gastric mucosal innervation and clinical significance. *Eur J Neurol* 2022; **29**: 2097-2108 [PMID: 35322505 DOI: 10.1111/ene.15333]
19 **Bays HE**, Kirkpatrick CF, Maki KC, Toth PP, Morgan RT, Tondt J, Christensen SM, Dixon DL, Jacobson TA. Obesity, dyslipidemia, and cardiovascular disease: A joint expert review from the Obesity Medicine Association and the National Lipid Association 2024. *J Clin Lipidol* 2024; **18**: e320-e350 [PMID: 38664184 DOI: 10.1016/j.jacl.2024.04.001]
20 **Endo Y**, Fujita M, Ikewaki K. HDL Functions-Current Status and Future Perspectives. *Biomolecules* 2023; **13** [PMID: 36671490 DOI: 10.3390/biom13010105]
21 **Nunes VS**, Leança CC, Panzoldo NB, Parra E, Cazita PM, Nakandakare ER, de Faria EC, Quintão EC. HDL-C concentration is related to markers of absorption and of cholesterol synthesis: Study in subjects with low vs. high HDL-C. *Clin Chim Acta* 2011; **412**: 176-180 [PMID: 20932966 DOI: 10.1016/j.cca.2010.09.039]
22 **Camilleri M**, Kuo B, Nguyen L, Vaughn VM, Petrey J, Greer K, Yadlapati R, Abell TL. ACG Clinical Guideline: Gastroparesis. *Am J Gastroenterol* 2022; **117**: 1197-1220 [PMID: 35926490 DOI: 10.14309/ajg.0000000000001874]
23 **Sieber J**, Flacke F, Link M, Haug C, Freckmann G. Improved Glycemic Control in a Patient Group Performing 7-Point Profile Self-Monitoring of Blood Glucose and Intensive Data Documentation: An Open-Label, Multicenter, Observational Study. *Diabetes Ther* 2017; **8**: 1079-1085 [PMID: 28913822 DOI: 10.1007/s13300-017-0306-z]

World Journal of Gastroenterology

Submit a Manuscript: https://www.f6publishing.com

World J Gastroenterol 2025 April 21; 31(15): 105236

DOI: 10.3748/wjg.v31.i15.105236

ISSN 1007-9327 (print) ISSN 2219-2840 (online)

ORIGINAL ARTICLE

Clinical Trials Study

Evaluation of scoring systems and hematological parameters in the severity stratification of early-phase acute pancreatitis

Pei-Na Shi, Zhang-Zhang Song, Xu-Ni He, Jie-Ming Hong

Specialty type: Gastroenterology and hepatology

Provenance and peer review: Unsolicited article; Externally peer reviewed.

Peer-review model: Single blind

Peer-review report's classification

Scientific Quality: Grade A, Grade B, Grade B, Grade B

Novelty: Grade A, Grade B, Grade B, Grade C

Creativity or Innovation: Grade A, Grade B, Grade B, Grade C

Scientific Significance: Grade A, Grade B, Grade B, Grade B

P-Reviewer: Wu YM; Xu DH; Zhou X

Received: January 18, 2025

Revised: February 24, 2025

Accepted: March 25, 2025

Published online: April 21, 2025

Processing time: 91 Days and 19.1 Hours

Pei-Na Shi, Zhang-Zhang Song, Xu-Ni He, Jie-Ming Hong, Department of Gastroenterology, Ningbo Yinzhou No. 2 Hospital, Ningbo 315000, Zhejiang Province, China

Corresponding author: Jie-Ming Hong, MD, Chief Physician, Department of Gastroenterology, Ningbo Yinzhou No. 2 Hospital, No. 998 Qianhe North Road, Yinzhou District, Ningbo 315000, Zhejiang Province, China. jm_hong@126.com

Abstract

BACKGROUND

Acute pancreatitis (AP) is an emergency gastrointestinal disease that requires immediate diagnosis and urgent clinical treatment. An accurate assessment and precise staging of severity are essential in initial intensive therapy.

AIM

To explore the prognostic value of inflammatory markers and several scoring systems [Acute Physiology and Chronic Health Evaluation II, the bedside index of severity in AP (BISAP), Ranson's score, the computed tomography severity index (CTSI) and sequential organ failure assessment] in severity stratification of early-phase AP.

METHODS

A total of 463 patients with AP admitted to our hospital between 1 January 2021 and 30 June 2024 were retrospectively enrolled in this study. Inflammation marker and scoring system levels were calculated and compared between different severity groups. Relationships between severity and several predictors were evaluated using univariate and multivariate logistic regression models. Predictive ability was estimated using receiver operating characteristic curves.

RESULTS

Of the 463 patients, 50 (10.80%) were classified as having severe AP (SAP). The results revealed that the white cell count significantly increased, whereas the prognostic nutritional index measured within 48 hours (PNI_{48}) and calcium (Ca^{2+}) were decreased as the severity of AP increased ($P < 0.001$). According to multivariate logistic regression, C-reactive protein measured within 48 hours (CRP_{48}), Ca^{2+} levels, and PNI_{48} were independent risk factors for predicting SAP. The area under the curve (AUC) values for the CRP_{48}, Ca^{2+}, PNI_{48}, Acute Physiology and Chronic Health Evaluation II, sequential organ failure assessment, BISAP, CTSI, and Ranson scores for the prediction of SAP were 0.802, 0.736, 0.871, 0.799, 0.783,

0.895, 0.931 and 0.914, respectively. The AUC for the combined CRP_{48} + Ca^{2+} + PNI_{48} model was 0.892. The combination of PNI_{48} and Ranson achieved an AUC of 0.936.

CONCLUSION

Independent risk factors for developing SAP include CRP_{48}, Ca^{2+}, and PNI_{48}. CTSI, BISAP, and the combination of PNI_{48} and the Ranson score can act as reliable predictors of SAP.

Key Words: Acute pancreatitis; Scoring systems; Severity stratification; Prognostic nutritional index; Severity

Core Tip: Acute pancreatitis (AP) is an emergency gastrointestinal disease that requires immediate diagnosis and urgent clinical treatment. An accurate assessment and staging of severity are essential in initial intensive therapy. This study systematically explored the prognostic value of inflammatory markers and several scoring systems in severity stratification of early-phase AP. 463 patients with AP were enrolled in this study. The results revealed that C-reactive protein measured within 48 hours, calcium and prognostic nutritional index measured within 48 hours were independent risk factors for predicting severe AP. Computed tomography severity index, bedside index of severity in AP, and the combination of prognostic nutritional index measured within 48 hours and the Ranson score can act as reliable predictor of severity AP.

Citation: Shi PN, Song ZZ, He XN, Hong JM. Evaluation of scoring systems and hematological parameters in the severity stratification of early-phase acute pancreatitis. *World J Gastroenterol* 2025; 31(15): 105236
URL: https://www.wjgnet.com/1007-9327/full/v31/i15/105236.htm
DOI: https://dx.doi.org/10.3748/wjg.v31.i15.105236

INTRODUCTION

Acute pancreatitis (AP), a serious and rapidly developing inflammatory process of the pancreas, is one of the leading gastrointestinal diseases requiring immediate diagnosis and urgent clinical treatment[1-3]. Biliary sludge and/or gallstones, alcohol consumption, and hypertriglyceridemia, are the most common causes of AP, whereas drugs, obesity, diabetes, autoimmune disease, and infection are also potential causes[4,5]. AP can be classified into three categories based on severity: Mild AP (MAP), moderately severe AP (MSAP), and severe AP (SAP), according to the Atlanta's criteria in 2012. Most cases of AP are self-limited and resolve spontaneously with a favorable clinical recovery. However, the remaining approximately 20%-30% of patients may develop severe forms of AP and serious local and/or systemic complications with deterioration[6]. Severe cases may deteriorate rapidly for a brief period of time in the early stages of disease, resulting in systemic inflammatory response syndrome and even multiple organ dysfunction syndrome[7]. An accurate assessment and precise staging of severity are essential in the initial intensive therapy, thereby improving the prognosis.

Currently, numerous risk scoring systems have been proposed and applied to identify the severity of AP. Acute Physiology and Chronic Health Evaluation II (APACHE II), the bedside index of severity in AP (BISAP), Ranson's score, and the computed tomography (CT) severity index (CTSI) are commonly used scoring systems in the clinic[8]. The APACHE II score is helpful for intensive care unit outcome prediction; however, its use is complex and prone to mistakes [9]. CTSI can be used to evaluate pancreatic inflammation and necrosis to predict the severity of AP and is usually used after 48-72 hours post-presentation[10,11]. Other recent scores, such as the BISAP score, have been proposed as simple and accurate tools for the early identification of in-hospital mortality[12]. The sequential organ failure assessment (SOFA) score has also been applied to stratify risk and monitor responses to treatment in recent years[9]. However, these scoring systems have been criticized at times due to limitations such as low sensitivity, unnecessary complexity, an overly restrictive process, high cost, and too many parameters limiting widespread use[13]. Concurrently, a number of hematological and biochemical parameters have been used to predict the prognosis of AP at an early stage, such as C-reactive protein (CRP), blood urea nitrogen, and D-dimer[8]. However, most of these parameters cannot be used to comprehensively and systematically assess the severity of AP. Previous studies have suggested a potential clinical relationship between some combined hematological parameters and systemic inflammation, including the neutrophil-lymphocyte ratio (NLR), platelet-lymphocyte ratio (PLR), lymphocyte-monocyte ratio (LMR), and red cell distribution width[14,15]. The prognostic nutritional index (PNI), which is calculated by the ratio of the albumin concentration and lymphocyte count, has attracted attention as an easily accessible biomarker reflecting inflammation and nutritional status[16]. These inflammation-based laboratory markers have also been investigated to predict illness severity in AP[17-19]. However, although scoring systems and hematological parameters have been previously explored to identify the adverse outcomes associated with AP, previous studies have revealed inconsistencies in their predictive ability. Few systematic studies have focused on the combination of these values in AP. Thus, this study systematically explored the prognostic value of these inflammatory markers (NLR, LMR, PLR, PNI, and CRP) and several scoring systems (APACHE II, SOFA, BISAP, CTSI, and Ranson) in the severity stratification of AP in the early phase.

MATERIALS AND METHODS

Patient selection

This study consecutively analyzed patients with AP admitted to Ningbo Yinzhou No. 2 Hospital between January 1, 2021, and June 30, 2024. The study was approved by the Human Ethics Committee of the Yinzhou No. 2 Hospital (approval number: Y2024-50) and the study was conducted with the patients' informed consent. The diagnosis and severity stratification of AP were performed according to the 2012 revised Atlanta classification. The diagnosis of AP was based on two or more of the following features: (1) Abdominal pain characteristic of AP; (2) Threefold elevation of serum amylase and/or lipase levels above the upper limit of normal; and (3) Characteristic findings of AP on abdominal ultrasonography, magnetic resonance imaging or CT scan[1]. MAP was defined as an absence of organ failure and local complications; MSAP was defined as the presence of local or systemic complications and/or organ failure relieved within 48 hours; and SAP was defined as persistent organ failure for more than 48 hours[1]. The definition of organ failure included respiratory, renal, and cardiovascular failure, which was based on a score of 2 or more using the modified Marshall scoring system[20]. Biliary AP was defined as the existence of gallstones or biliary sludge on ultrasonography, CT, or magnetic resonance imaging. Hypertriglyceridemia-induced AP was defined as a serum triglyceride (TG) level reaching 11.3 mmol/L or TG levels between 5.65 and 11.3 mmol/L with chylous serum. Alcoholic AP was defined as a history of alcohol abuse within 48 hours before the onset of illness. Other possible causes of AP should be excluded when the above etiological diagnosis is made. Patients who met the following criteria were excluded: Age < 16 years, short hospital stay of less than 48 hours, pregnancy, chronic pancreatitis or pancreatic carcinoma, metastatic tumor, or severe infectious and immunosuppressive conditions.

Data collection

A detailed history and physical examinations of all enrolled patients, including age, gender, and body mass index (BMI), were conducted after admission. Laboratory parameters were collected upon arrival at the hospital, including complete blood counts, blood gas analyses, serum amylase, electrolytes, D dimer, and renal and hepatic function. The calcium (Ca^{2+}) level was measured within 48 hours after admission. The worst value of all the laboratory parameters and vital signs were selected during the collection period. Additional outcome measures included length of hospital stay, the interval between medical attention and symptom onset, the presence of organ failure, and local complications. Contrast-enhanced CT was performed in all patients on days 2-5 after admission. Two senior radiologists calculated the CTSI score after contrast-enhanced CT. The radiologists who participated were blinded to all the clinical data and the scoring results of the other evaluators. The APACHE II, BISAP, and SOFA scores in the first 24 hours and the Ranson score at 48 hours after admission were recorded. Markers of inflammation (NLR, LMR, and PLR) levels were calculated at admission. PNI and CRP levels were measured at admission (PNI_i; CRP_i) and within 48 hours (PNI_{48}; CRP_{48}). There were no missing data during the research process.

Statistical analysis

Statistical analysis was performed with Statistical Product and Service Solutions software 27.0 (SPSS, Chicago, IL, United States) and GraphPad Prism (GraphPad Software, La Jolla, CA, United States). Sample size calculation was performed using Power Analysis and Sample Size (PASS, Kaysville, UT, United States) at the study design stage. The calculation was based on a predefined type I error of 0.05 (α = 0.05) and a test power of 0.9 (β = 0.1). Categorical variables were statistically compared using the χ^2 test or Fisher's exact test and are presented as numbers and percentages. Continuous variables were verified by the Kolmogorov-Smirnov test for the normality test. Variables that were normally distributed are presented as the means with standard deviations and were compared by one-way analysis of variance (ANOVA). Variables with skewed distributions are presented as medians with interquartile ranges and were compared using Kruskal-Wallis *H* test. Multiple variables were further evaluated and adjusted using the Bonferroni method for multiple comparisons. All parameters were tested by univariate logistic regression and *P* values < 0.05 were considered potentially significant. The clinical significance of each parameter was also considered for selection. The potential independent predictive variables were subsequently evaluated using forward stepwise multivariate logistic regression analyses. Multivariate models were established after eliminating the factors with collinearity. Receiver operating characteristic (ROC) analysis was used, and the area under the curve (AUC) was compared to evaluate the predictive accuracy of each scoring system and the laboratory predictive variables. The sensitivity, specificity, positive predictive value, and negative predictive value were assessed for severity prediction. A *P* value < 0.05 was considered to indicate statistical significance.

RESULTS

A total of 463 patients with AP were enrolled and categorized into three groups: MAP (*n* = 319, 68.90%), MSAP (*n* = 94, 20.30%), and SAP (*n* = 50, 10.80%). Tables 1 and 2 show the clinical profiles and basic characteristics of the patients. There were 309 (66.7%) males and 154 (33.3%) females with a median age of 49.0 (37.0-63.0) years and a mean BMI of 25.27 ± 4.01 kg/m^2. There were no differences in respect to age (*P* = 0.057), gender (*P* = 0.683), or BMI (*P* = 0.700) among the three groups. The majority of etiologies included hypertriglyceridemia (*n* = 162, 35.0%) and gallstone (*n* = 156, 33.7%). With regard to comorbidities, 121 patients (26.1%) had diabetes mellitus, 154 patients (33.3%) had hypertension, 24 patients (5.2%) had coronary artery disease, 10 patients (2.2%) had chronic kidney disease, and 184 patients (39.7%) had biliary tract disease. As the disease worsened, the length of hospital stays significantly increased (*P* < 0.001). However, the duration of medical attention from symptom onset among the three groups was not significantly different (*P* = 0.182).

Table 1 Demographics and clinical profile in patients with acute pancreatitis, *n* (%)

Variables	MAP	MSAP	SAP	Total	*P* value
n	319	94	50	463	
Age (years)	48.0 (36.0-60.0)	50.5 (37.0-73.3)	52.0 (37.8-71.8)	49.0 (37.0-63.0)	0.057
Gender					
Male	209 (67.6)	66 (21.4)	34 (11.0)	309 (66.7)	0.683
Female	110 (71.4)	28 (18.2)	16 (10.4)	154 (33.3)	
Etiology of AP					
Gallstone	100 (21.6)	37 (8.0)	19 (4.1)	156 (33.7)	0.002[a]
Alcohol	26 (5.6)	5 (1.1)	7 (1.5)	38 (8.2)	
Hypertriglyceridemia	102 (22.0)	40 (8.6)	20 (4.3)	162 (35.0)	
Others	91 (19.7)	12 (2.6)	4 (0.9)	107 (23.1)	
BMI (kg/m^2), mean ± SD	25.16 ± 3.89	25.49 ± 4.36	25.54 ± 4.07	25.27 ± 4.01	0.700
Smoking	135 (42.3)	45 (47.8)	21 (42.0)	201 (43.4)	0.620
Comorbidities					
Diabetes mellitus	63 (19.7)	38 (40.4)	20 (40.0)	121 (26.1)	< 0.001[a]
Hypertension	97 (30.4)	43 (45.7)	14 (28.0)	154 (33.3)	0.015[a]
Coronary artery disease	11 (3.4)	8 (8.5)	5 (10.0)	24 (5.2)	0.027
Chronic kidney disease	6 (1.9)	3 (3.2)	1 (2.0)	10 (2.2)	0.684
Biliary tract disease	123 (38.6)	43 (45.7)	18 (36.0)	184 (39.7)	0.388
Healthy	104 (32.6)	18 (19.1)	10 (20.0)	132 (28.5)	0.015[a]
Medical attention from symptom onset (hours)	17.0 (10.0-27.0)	22.0 (10.0-38.5)	17.0 (8.8-24.0)	18.0 (10.0-30.0)	0.182
Hospital stay (days)	7.0 (6.0-9.0)	10.0 (8.0-13.0)	18.0 (15.0-26.0)	8.0 (6.0-11.0)	< 0.001[a]

[a]$P < 0.05$.

AP: Acute pancreatitis; MAP: Mild acute pancreatitis; MSAP: Moderately severe acute pancreatitis; SAP: Severe acute pancreatitis; BMI: Body mass index.

Compared with the MAP group, the MSAP group presented significantly higher levels of CRP_i, CRP_{48}, D dimer, lactate dehydrogenase (LDH), and glucose ($P < 0.001$). However, they did not differ between the MSAP and SAP groups. The Ca^{2+} level significantly decreased as the severity of AP increased ($P < 0.001$), whereas the white cell count increased ($P < 0.001$). The serum platelet and hematocrit levels did not differ significantly among the different severity groups. The NLR of the MSAP group was significantly greater than that of the MAP group ($P < 0.001$), whereas the LMR was lower ($P = 0.003$). However, the NLR and LMR did not differ between the MSAP and SAP groups ($P = 0.546$; $P = 1.000$). There was no statistically significant difference in PLR between the different severity groups. The PNI_{48} was lower in the SAP group than in the MAP group ($P < 0.001$). APACHE II, BISAP, CTSI, SOFA, and Ranson scores all were significantly higher in the SAP group than in the MSAP group than in the MAP group ($P < 0.001$).

Univariate logistic regression analyses were used to evaluate all the predictors. The results revealed that etiology, diabetes mellitus status, white cell count, CRP_i, CRP_{48}, red cell distribution width, Ca^{2+}, LDH, D dimer, TG, NLR, and PNI_{48} were potentially significant variables. Multivariate logistic regression revealed that CRP_{48} [adjusted odds ratio (OR) = 1.007, 95% confidence interval (CI): 1.002-1.011, $P = 0.010$], Ca^{2+} (adjusted OR = 0.125, 95%CI: 0.022-0.700, $P = 0.007$) and PNI_{48} (adjusted OR = 0.800, 95%CI: 0.720-0.880 $P < 0.001$) were independent risk factors for predicting SAP (Table 3). The combined CRP_{48} + Ca^{2+} + PNI_{48} model was constructed using the formula = 8.825 + 0.008 × CRP_{48} (mg/L) - 2.286 × Ca^{2+} (mmol/L) - 0.185 × PNI_{48}.

Table 4 and Figure 1 showed the comparisons of the ROC curves for SAP among CRP_{48}, Ca^{2+}, and PNI_{48}, the combined CRP_{48} + Ca^{2+} + PNI_{48} model, and all the scoring systems. The AUC values for CRP_{48}, Ca^{2+}, PNI_{48}, APACHE II, SOFA, BISAP, CTSI, and Ranson scores for the prediction of SAP were 0.802, 0.736, 0.871, 0.799, 0.783, 0.895, 0.931 and 0.914, respectively. The sensitivity, specificity, positive predictive value, and negative predictive value for the above parameters were determined with optimal cutoff values of 118.25, 2.045, 38.53, 7.50, 1.50, 1.50, 4.50, and 2.50, respectively. The AUC for the combined CRP_{48} + Ca^{2+} + PNI_{48} model was 0.892, which was superior to those obtained for CRP_{48} ($Z = 2.771$, $P = 0.006$) and Ca^{2+} ($Z = 4.625$, $P < 0.001$). However, a comparison between the PNI_{48} model and the combined CRP_{48} + Ca^{2+} + PNI_{48} model revealed no difference ($Z = 1.610$, $P = 0.107$). Among the single parameters, CTSI demonstrated the highest accuracy for predicting SAP. However, there was no significant difference between pairwise comparisons among CTSI, BISAP, and Ranson (CTSI *vs* BISAP, $Z = 1.640$, $P = 0.101$; CTSI *vs* Ranson, $Z = 0.793$, $P = 0.428$; Ranson *vs* BISAP, $Z = 0.836$,

Table 2 Basic characteristics in patients with acute pancreatitis

Variables	MAP	MSAP	SAP	*P* value		
				All group	1 *vs* 2	2 *vs* 3
WCC (× 10^9/L)	10.2 (7.90-12.70)	13.05 (9.80-16.25)	13.41 ± 4.51	< 0.001	< 0.001	< 0.001[a]
Platelet (× 10^9/L)	227.58 ± 67.77	215.50 (168.00-256.25)	213.72 ± 77.64	0.267	/	/
CRP_i (mg/L)	2.70 (0-19.30)	8.55 (1.70-75.95)	9.95 (0.83-73.35)	< 0.001	< 0.001	1.000
CRP_{48} (mg/L)	34.10 (4.60-91.40)	119.50 ± 70.00	166.33 ± 88.67	< 0.001	< 0.001	0.125
HCT (%)	42.77 ± 5.05	43.29 ± 5.47	43.42 ± 6.27	0.562	/	/
RDW	13.20 (12.80-13.80)	13.50 (12.90-14.20)	13.85 (13.20-14.65)	< 0.001	0.178	0.102
GLU (mmol/L)	6.66 (5.40-8.72)	8.45 (6.42-12.04)	10.28 (7.48-14.33)	< 0.001	< 0.001	0.326
BUN (mmol/L)	4.53 (3.55-5.59)	4.86 (3.63-6.32)	5.32 (4.18-6.29)	0.019	0.211	1.000
Ca^{2+} (mmol/L)	2.23 ± 0.15	2.14 ± 0.16	1.96 ± 0.34	< 0.001	< 0.001	< 0.001[a]
AST (IU/L)	25.00 (17.90-68.00)	34.65 (17.00-138.25)	41.00 (22.00-352.70)	0.067	/	/
Creatinine (mg/dL)	63.00 (52.20-78.00)	67.00 (55.75-87.00)	65.50 (54.25-84.25)	0.082	/	/
LDH	224.00 (189.00-277.00)	250.00 (198.50-426.75)	299.50 (228.25-414.25)	< 0.001	0.031	0.080
D dimer	195.00 (105.00-356.00)	358.50 (173.25-967.50)	467.00 (211.50-859.25)	< 0.001	< 0.001	0.782
Triglyceride	1.86 (1.05-8.44)	2.33 (1.06-17.50)	2.45 (1.21-20.99)	0.052	/	/
NLR	5.61 (3.40-9.89)	8.73 (5.21-14.20)	10.23 (6.71-16.49)	< 0.001	< 0.001	0.546
LMR	2.53 (1.60-3.69)	1.84 (1.01-3.22)	1.64 (0.98-3.01)	< 0.001	0.003	1.000
PLR	153.37 (113.33-230.19)	183.02 (115.48-262.88)	201.41 (131.94-297.87)	0.044	0.475	0.902
PNI_i	50.7 (46.45-54.55)	49.61 ± 8.65	48.83 (41.29-52.75)	0.035	0.299	1.000
PNI_{48}	43.37 ± 5.40	38.38 ± 5.68	34.43 ± 3.87	< 0.001	< 0.001	< 0.001[a]
APACHE II	5.00 (3.00-6.00)	7.50 (5.00-10.00)	9.00 (6.75-13.25)	< 0.001	< 0.001	0.046[a]
SOFA	0 (0-1.00)	1.00 (0-3.00)	2.00 (1.00-4.00)	< 0.001	< 0.001	0.011[a]
BISAP	0 (0-1.00)	2.00 (1.00-2.00)	2.00 (2.00-3.00)	< 0.001	< 0.001	0.014[a]
CTSI	2.00 (2.00-3.00)	4.00 (3.00-5.00)	6.00 (5.00-6.25)	< 0.001	< 0.001	0.004[a]
Ranson	1.00 (0-2.00)	3.00 (2.00-4.00)	4.50 (3.00-6.00)	< 0.001	< 0.001	0.001[a]

[a]$P < 0.05$.

MAP: Mild acute pancreatitis; MSAP: Moderately severe acute pancreatitis; SAP: Severe acute pancreatitis; WCC: White cell count; CRPi: C-reactive protein measured at admission; CRP_{48}: C-reactive protein measured within 48 hours; RDW: Red cell distribution width; HCT: Hematocrit; GLU: Glucose; BUN: Blood urea nitrogen; AST: Aspartate aminotransferase; LDH: Lactate dehydrogenase; NLR: Neutrophil-lymphocyte ratio; LMR: Lymphocyte-monocyte ratio; PLR: Platelet-lymphocyte ratio; PNI_i: Prognostic nutritional index measured at admission; PNI_{48}: Prognostic nutritional index measured within 48 hours; APACHE II: Acute Physiology and Chronic Health Evaluation II; SOFA: Sequential organ failure assessment; BISAP: Bedside index of severity in acute pancreatitis; CTSI: Computed tomography severity index.

$P = 0.403$). Among the scoring systems evaluated in the first 24 hours, the BISAP score was superior to the APACHE II score ($Z = 3.124$, $P = 0.002$) and the SOFA score ($Z = 3.084$, $P = 0.002$). When both PNI_{48} and Ranson were measured within 48 hours, the combination of PNI_{48} and Ranson achieved an AUC of 0.936.

DISCUSSION

AP is an inflammatory disease of the pancreas, with significant morbidity and mortality in severe cases. In this study, we compared the predictive value of hematological parameters and several scoring systems (APACHE II, SOFA, BISAP, CTSI, and Ranson) for the onset of AP. We identified three independent risk factors: CRP_{48}, Ca^{2+}, and PNI_{48}. Our data also suggested that, among the comorbidities, diabetes mellitus was significantly associated with MSAP and SAP.

Table 3 Results of univariate and multivariate logistic regression analysis for predicting severe acute pancreatitis

Variables	Univariate analysis		Multivariate analysis	
	OR (95%CI)	*P* value	OR (95%CI)	*P* value
Age (> 50 years)	1.271 (0.707-2.288)	0.423		
Gender	1.066 (0.569-1.999)	0.841		
Etiology of AP	0.780 (0.622-0.979)	0.032[a]	1.191 (0.850-1.668)	0.309
BMI (≥ 25 kg/m^2)	1.180 (0.655-2.125)	0.617		
Smoking	0.948 (0.724-1.243)	0.701		
Comorbidities				
Diabetes mellitus	2.059 (1.120-3.785)	0.020[a]	1.814 (0.807-4.074)	0.149
Hypertension	0.758 (0.396-1.453)	0.404		
Coronary artery disease	2.304 (0.821-6.469)	0.113		
Chronic kidney disease	0.916 (0.114-7.386)	0.934		
Biliary tract disease	0.837 (0.455-1.540)	0.567		
Medical attention from symptom onset (hours)	0.995 (0.981-1.010)	0.506		
WCC (× 10^9/L)	1.095 (1.030-1.163)	0.003[a]	1.071 (0.994-1.155)	0.072
Platelet (× 10^9/L)	0.997 (0.993-1.002)	0.237		
CRP_i (mg/L)	1.006 (1.002-1.010)	0.001[a]	/	/
CRP_{48} (mg/L)	1.013 (1.009-1.017)	< 0.001[a]	1.006 (1.001-1.011)	0.010[a]
HCT (%)	1.020 (0.964-1.079)	0.499		
RDW	1.083 (1.002-1.170)	0.044[a]	1.000 (0.857-1.167)	0.998
GLU (mmol/L)	1.003 (0.994-1.013)	0.521		
BUN (mmol/L)	0.999 (0.982-1.017)	0.943		
Ca (mmol/L)	0.004 (0.001-0.021)	< 0.001[a]	0.091 (0.016-0.512)	0.007[a]
AST (IU/L)	1.001 (1.000-1.002)	0.121		
Creatinine (mg/dL)	1.000 (0.997-1.003)	0.993		
LDH	1.003 (1.001-1.005)	< 0.001[a]	1.001 (0.999-1.004)	0.282
D dimer	1.000 (1.000-1.001)	0.002[a]	1.000 (1.000-1.000)	0.189
Triglyceride	1.030 (1.004-1.056)	0.022[a]	1.032 (0.996-1.070)	0.086
NLR	1.036 (1.013-1.059)	0.002[a]	0.992 (0.961-1.024)	0.625
LMR	1.026 (0.975-1.081)	0.321		
PLR	1.001 (1.000-1.003)	0.065		
PNI_i	1.003 (0.997-1.009)	0.277		
PNI_{48}	0.765 (0.711-0.823)	< 0.001[a]	0.822 (0.749-0.902)	< 0.001[a]

[a]$P < 0.05$.

OR: Odds ratio; CI: Confidence interval; AP: Acute pancreatitis; BMI: Body mass index; WCC: White cell count; CRPi: C-reactive protein measured at admission; CRP_{48}: C-reactive protein measured within 48 hours; HCT: Hematocrit; RDW: Red cell distribution width; GLU: Glucose; BUN: Blood urea nitrogen; AST: Aspartate aminotransferase; LDH: Lactate dehydrogenase; NLR: Neutrophil-lymphocyte ratio; LMR: Lymphocyte-monocyte ratio; PLR: Platelet-lymphocyte ratio; PNI_i: Prognostic nutritional index measured at admission; PNI_{48}: Prognostic nutritional index measured within 48 hours.

The mechanisms and progressions of SAP are still poorly understood and may be associated with many factors. Some simple hematological parameters in the clinic, such as CRP and Ca^{2+}, are widely used to evaluate the condition of AP patients. CRP is an essential indicator of inflammatory reactions. The localization and deposition of CRP appear to be key mediators of serious disease process, including AP[21]. CRP enhances the inflammatory cascade by stimulating the complement system and inducing the secretion of pro-inflammatory cytokines such as tumor necrosis factor-α and interleukin-1β, thereby aggravating pancreatic tissue damage[22,23]. Prior studies have shown the poor predictive value

Table 4 Statistical data of receiver-operating characteristics curve analysis for predicting severe acute pancreatitis by different parameters

Variables	AUC (95%CI)	*P* value	Cut-off value	Sensitivity, %	Specificity, %	PPV, %	NPV, %
CRP_{48}	0.802 (0.734-0.870)	< 0.001	118.25	76.00	76.51	28.15	96.34
Ca^{2+}	0.736 (0.643-0.828)	< 0.001	2.045	60.00	84.99	32.61	94.61
PNI_{48}	0.871 (0.826-0.916)	< 0.001	38.53	90.00	74.33	29.80	98.40
CRP_{48} + Ca^{2+} + PNI_{48}	0.892 (0.843-0.940)	< 0.001	0.15	78.00	86.68	40.86	96.76
APACHE II	0.799 (0.735-0.864)	< 0.001	7.50	72.00	77.97	28.35	95.83
SOFA	0.783 (0.711-0.856)	< 0.001	1.50	72.00	74.09	25.17	95.63
BISAP	0.895 (0.862-0.929)	< 0.001	1.50	94.00	79.18	35.34	99.09
CTSI	0.931 (0.900-0.962)	< 0.001	4.50	80.00	89.83	48.78	97.38
Ranson	0.914 (0.878-0.949)	< 0.001	2.50	88.00	77.97	32.59	98.17
PNI_{48} + Ranson	0.936 (0.909-0.962)	< 0.001	0.07	94.00	81.11	37.60	99.11

AUC: Area under the curve; CI: Confidence interval; PPV: Positive predictive value; NPV: Negative predictive value; CRP_{48}: C-reactive protein measured within 48 hours; PNI_{48}: Prognostic nutritional index measured within 48 hours; APACHE II: Acute Physiology and Chronic Health Evaluation II; SOFA: Sequential organ failure assessment; BISAP: Bedside index of severity in acute pancreatitis; CTSI: Computed tomography severity index.

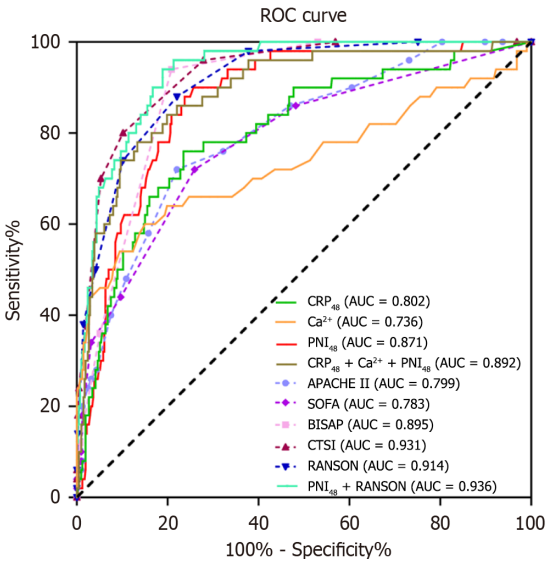

Figure 1 Receiver operating characteristic curve analysis for predicting severe acute pancreatitis by different parameters. ROC: Receiver operating characteristic; CRP_{48}: C-reactive protein measured within 48 hours; PNI_{48}: Prognostic nutritional index measured within 48 hours; APACHE II: Acute Physiology and Chronic Health Evaluation II; SOFA: Sequential organ failure assessment; BISAP: Bedside index of severity in acute pancreatitis; CTSI: Computed tomography severity index; AUC: Area under the curve.

of CRP levels at an early stage[24]. However, after 24-48 hours, the CRP level has good prognostic accuracy for SAP, mortality, and pancreatic necrosis[25,26]. Our studies revealed that CRP_i and CRP_{48} were significantly higher in MSAP compared with MAP, but no difference was detected between MSAP and SAP. CRP_{48} can be regarded as an independently predictive factor with the AUC value of 0.802. Therefore, continuous monitoring of CRP levels reliable for predicting severity.

Ca^{2+} is a versatile signal carrier that regulates various cellular functions[27]. Ca^{2+} overload and premature trypsinogen activation sabotage crucial cellular defense mechanisms, leading to pancreatic necrosis[28-30]. Previous studies have identified low Ca^{2+} levels as a risk factor for pancreatic necrosis, persistent organ failure, and SAP[31-33]. Similarly, in our study, the concentration of Ca^{2+} was negatively and significantly correlated with the severity of AP. PNI is regarded as a simple and effective parameter reflecting the nutritional and immunological status of the body. Prior studies confirmed the function of PNI as a predictive indicator for the prognosis of many cancers and inflammatory diseases[16,34]. Li *et al* [35] reported that PNI was independently associated with the development of SAP and mortality in AP patients. Despite this evidence, very few studies have reported a relationship between PNI and the severity of AP. In our study, we

estimated the prognostic value of PNI for predicting the severity of AP. Multivariate regression analyses indicated that PNI_{48} was independently associated with the occurrence of SAP. ROC curve analysis revealed that the ability of PNI_{48} to predict SAP was preferable, with an AUC value of 0.871. We found that the PNI_{48} level significantly decreased as the severity of AP increased, whereas the PNI_i level did not significantly change. The reason for this phenomenon may be inflammatory cascade and nutrient expenditure during the development of AP. Therefore, variations in the nutritional status of patients may be related to the severity of AP. As PNI may be affected by nutritional support, patients with a low PNI after nutritional treatment need more attention due to the possibility of AP aggravation.

Three inflammatory markers, CRP_{48}, Ca^{2+}, and PNI_{48}, were combined to construct a logistic regression model, including. Previous studies have also explored the use of combined indicators to predict AP. For instance, Li *et al*[36] utilized a combination of fatty liver, procalcitonin, and the CRP-to-lymphocyte ratio to diagnose SAP, achieving an AUC of 0.795, which also reflects a high level of diagnostic performance. Similarly, Kong *et al*[37] identified heparin-binding protein, procalcitonin, and CRP as risk factors for SAP and combined these three markers to predict the severity of AP. Yi *et al*[38] reported the independent predictive value of CRP, LDH, Ca^{2+}, and ascites in hypertriglyceridemia-induced AP. This combined diagnostic model demonstrated high accuracy, with an AUC of 0.960[38]. In our study, the AUC of the CRP_{48} + Ca^{2+} + PNI_{48} model reached 0.892, indicating strong predictive ability. To the best of our knowledge, we are the first to apply these three inflammatory markers to evaluate SAP. Our findings suggest that the combination of multiple hematological parameters can effectively predict SAP, highlighting the broader clinical practicability of integrated inflammatory parameters.

We found that the scores of several scoring systems (APACHE II, SOFA, BISAP, CTSI, and Ranson) significantly increased with the increasing severity of AP. The ROC curve indicated that CTSI achieved the highest AUC for the prediction of SAP among the single parameters, whereas the BISAP and Ranson scores presented similar results. The abilities of APACHE II and SOFA were fair, with AUC values of 0.799 and 0.783, respectively. The CTSI, a scoring system derived by Balthazar *et al*[39], has been widely used as a standard assessment to describe CT findings in AP[40]. Prior studies have confirmed that CTSI is significantly correlated with clinical outcome parameters, consistent with the revised Atlanta criteria grading of severity[11,41]. However, a CT scan is usually recommended after 48-72 hours to determine the exact extent of pancreatic necrosis[41]. Therefore, the CTSI obtained from CT scans in the early stage of the disease may not confirm the exact severity of AP. The evaluation of CTSI may emphasize local complications but not the systemic inflammatory response. Ranson and APACHE II have been used since the 1970s to assess the severity of AP. The main limitation of Ranson is the need for a 48-hour duration to complete the calculation. As PNI_{48} was also measured within 48 hours with good prognostic accuracy, we found that the combination of PNI_{48} and the Ranson score reached an AUC of 0.936, reflecting superior prognostic value. The BISAP was designed to construct a simple scoring system that provides an early estimation of AP risk based on five variables collected within 24 hours[12]. Our data showed BISAP performed better than APACHE II and SOFA in predicting SAP in patients during the first 24 hours. Therefore, BISAP is superior to other predictors in the prediction of SAP during the first 24 hours. As AP progresses to within 48 hours, the combination of PNI_{48} and the Ranson score could improve the prediction performance. CTSI can be a useful predictor of local complications.

There were several limitations in this study. Selection bias was inevitable since this was a retrospective single-center study with a limited sample size. Multicenter research with a large sample size could be conducted to confirm the value of the present analysis in further research. Second, laboratory parameters were collected upon arrival at the hospital and within 48 hours. Considering these variables change with time, they should be studied at additional time points. Using more detection methods and studying more relevant laboratory parameters may reveal other pertinent factors. Then, the common and classical scoring systems for AP were studied in this study. Some of the novel scoring systems are yet to be adopted and can be verified in future studies. Moreover, the mechanisms underlying the relationships between the predictors and severity of AP need to be investigated.

CONCLUSION

In conclusion, CRP_{48}, Ca^{2+}, and PNI_{48} were independent risk factors for AP in our study. The combination of CRP_{48}, Ca^{2+}, and PNI_{48} could be helpful tools as hematological parameters in evaluating SAP. CTSI was the best single parameter in predicting severity, but it had the shortcomings of assessing too later. BISAP can act as a simple and excellent predictor of SAP during the first 24 hours. As AP progresses to within 48 hours, the combination of PNI_{48} and the Ranson score could be a superior predictor of adverse outcomes in SAP.

FOOTNOTES

Author contributions: Shi PN and Hong JM designed the research; Song ZZ and He XN contributed to the data collection; Shi PN and He XN analyzed the data; Shi PN, Song ZZ, and Hong JM wrote the paper. All authors reviewed the manuscript.

Institutional review board statement: The study was approved by the Human Ethics Committee of the Yinzhou No. 2 Hospital (approval number: Y2024-50).

Clinical trial registration statement: This clinical trial was registered at ClinicalTrials.gov, No. ChiCTR2500098956.

Informed consent statement: Informed consent statement has been applied for exemption for this study.

Conflict-of-interest statement: All the authors report no relevant conflicts of interest for this article.

Data sharing statement: No additional data are available.

CONSORT 2010 statement: The authors have read the CONSORT 2010 Statement, and the manuscript was prepared and revised according to the CONSORT 2010 Statement.

Country of origin: China

ORCID number: Pei-Na Shi 0000-0003-1853-736X; Jie-Ming Hong 0009-0001-3392-6841.

S-Editor: Wang JJ
L-Editor: A
P-Editor: Zhao S

REFERENCES

1 **Banks PA**, Bollen TL, Dervenis C, Gooszen HG, Johnson CD, Sarr MG, Tsiotos GG, Vege SS; Acute Pancreatitis Classification Working Group. Classification of acute pancreatitis--2012: revision of the Atlanta classification and definitions by international consensus. *Gut* 2013; **62**: 102-111 [PMID: 23100216 DOI: 10.1136/gutjnl-2012-302779]

2 **Peery AF**, Crockett SD, Murphy CC, Jensen ET, Kim HP, Egberg MD, Lund JL, Moon AM, Pate V, Barnes EL, Schlusser CL, Baron TH, Shaheen NJ, Sandler RS. Burden and Cost of Gastrointestinal, Liver, and Pancreatic Diseases in the United States: Update 2021. *Gastroenterology* 2022; **162**: 621-644 [PMID: 34678215 DOI: 10.1053/j.gastro.2021.10.017]

3 **van Dijk SM**, Hallensleben NDL, van Santvoort HC, Fockens P, van Goor H, Bruno MJ, Besselink MG; Dutch Pancreatitis Study Group. Acute pancreatitis: recent advances through randomised trials. *Gut* 2017; **66**: 2024-2032 [PMID: 28838972 DOI: 10.1136/gutjnl-2016-313595]

4 **Boxhoorn L**, Voermans RP, Bouwense SA, Bruno MJ, Verdonk RC, Boermeester MA, van Santvoort HC, Besselink MG. Acute pancreatitis. *Lancet* 2020; **396**: 726-734 [PMID: 32891214 DOI: 10.1016/S0140-6736(20)31310-6]

5 **van Geenen EJ**, van der Peet DL, Bhagirath P, Mulder CJ, Bruno MJ. Etiology and diagnosis of acute biliary pancreatitis. *Nat Rev Gastroenterol Hepatol* 2010; **7**: 495-502 [PMID: 20703238 DOI: 10.1038/nrgastro.2010.114]

6 **Mederos MA**, Reber HA, Girgis MD. Acute Pancreatitis: A Review. *JAMA* 2021; **325**: 382-390 [PMID: 33496779 DOI: 10.1001/jama.2020.20317]

7 **Petrov MS**, Shanbhag S, Chakraborty M, Phillips AR, Windsor JA. Organ failure and infection of pancreatic necrosis as determinants of mortality in patients with acute pancreatitis. *Gastroenterology* 2010; **139**: 813-820 [PMID: 20540942 DOI: 10.1053/j.gastro.2010.06.010]

8 **Triester SL**, Kowdley KV. Prognostic factors in acute pancreatitis. *J Clin Gastroenterol* 2002; **34**: 167-176 [PMID: 11782614 DOI: 10.1097/00004836-200202000-00014]

9 **Quintairos A**, Pilcher D, Salluh JIF. ICU scoring systems. *Intensive Care Med* 2023; **49**: 223-225 [PMID: 36315260 DOI: 10.1007/s00134-022-06914-8]

10 **Bollen TL**, Singh VK, Maurer R, Repas K, van Es HW, Banks PA, Mortele KJ. A comparative evaluation of radiologic and clinical scoring systems in the early prediction of severity in acute pancreatitis. *Am J Gastroenterol* 2012; **107**: 612-619 [PMID: 22186977 DOI: 10.1038/ajg.2011.438]

11 **Alberti P**, Pando E, Mata R, Vidal L, Roson N, Mast R, Armario D, Merino X, Dopazo C, Blanco L, Caralt M, Gomez C, Balsells J, Charco R. Evaluation of the modified computed tomography severity index (MCTSI) and computed tomography severity index (CTSI) in predicting severity and clinical outcomes in acute pancreatitis. *J Dig Dis* 2021; **22**: 41-48 [PMID: 33184988 DOI: 10.1111/1751-2980.12961]

12 **Wu BU**, Johannes RS, Sun X, Tabak Y, Conwell DL, Banks PA. The early prediction of mortality in acute pancreatitis: a large population-based study. *Gut* 2008; **57**: 1698-1703 [PMID: 18519429 DOI: 10.1136/gut.2008.152702]

13 **Kiat TTJ**, Gunasekaran SK, Junnarkar SP, Low JK, Woon W, Shelat VG. Are traditional scoring systems for severity stratification of acute pancreatitis sufficient? *Ann Hepatobiliary Pancreat Surg* 2018; **22**: 105-115 [PMID: 29896571 DOI: 10.14701/ahbps.2018.22.2.105]

14 **Hunziker S**, Celi LA, Lee J, Howell MD. Red cell distribution width improves the simplified acute physiology score for risk prediction in unselected critically ill patients. *Crit Care* 2012; **16**: R89 [PMID: 22607685 DOI: 10.1186/cc11351]

15 **Ng WW**, Lam SM, Yan WW, Shum HP. NLR, MLR, PLR and RDW to predict outcome and differentiate between viral and bacterial pneumonia in the intensive care unit. *Sci Rep* 2022; **12**: 15974 [PMID: 36153405 DOI: 10.1038/s41598-022-20385-3]

16 **Sun K**, Chen S, Xu J, Li G, He Y. The prognostic significance of the prognostic nutritional index in cancer: a systematic review and meta-analysis. *J Cancer Res Clin Oncol* 2014; **140**: 1537-1549 [PMID: 24878931 DOI: 10.1007/s00432-014-1714-3]

17 **Jain V**, Nath P, Satpathy SK, Panda B, Patro S. Comparing Prognostic Scores and Inflammatory Markers in Predicting the Severity and Mortality of Acute Pancreatitis. *Cureus* 2023; **15**: e39515 [PMID: 37378221 DOI: 10.7759/cureus.39515]

18 **Zhou H**, Mei X, He X, Lan T, Guo S. Severity stratification and prognostic prediction of patients with acute pancreatitis at early phase: A retrospective study. *Medicine (Baltimore)* 2019; **98**: e15275 [PMID: 31008971 DOI: 10.1097/MD.0000000000015275]

19 **Guglielmini C**, Crisi PE, Tardo AM, Di Maggio R, Contiero B, Boari A, Fracassi F, Miglio A. Prognostic Role of Red Cell Distribution Width and Other Routine Clinico-Pathological Parameters in Dogs with Acute Pancreatitis. *Animals (Basel)* 2022; **12**: 3483 [PMID: 36552403 DOI:

10.3390/ani12243483]
20 **Marshall JC**, Cook DJ, Christou NV, Bernard GR, Sprung CL, Sibbald WJ. Multiple organ dysfunction score: a reliable descriptor of a complex clinical outcome. *Crit Care Med* 1995; **23**: 1638-1652 [PMID: 7587228 DOI: 10.1097/00003246-199510000-00007]
21 **McFadyen JD**, Kiefer J, Braig D, Loseff-Silver J, Potempa LA, Eisenhardt SU, Peter K. Dissociation of C-Reactive Protein Localizes and Amplifies Inflammation: Evidence for a Direct Biological Role of C-Reactive Protein and Its Conformational Changes. *Front Immunol* 2018; **9**: 1351 [PMID: 29946323 DOI: 10.3389/fimmu.2018.01351]
22 **Pepys MB**, Hirschfield GM. C-reactive protein: a critical update. *J Clin Invest* 2003; **111**: 1805-1812 [DOI: 10.1172/jci200318921]
23 **Szatmary P**, Grammatikopoulos T, Cai W, Huang W, Mukherjee R, Halloran C, Beyer G, Sutton R. Acute Pancreatitis: Diagnosis and Treatment. *Drugs* 2022; **82**: 1251-1276 [PMID: 36074322 DOI: 10.1007/s40265-022-01766-4]
24 **Tarján D**, Szalai E, Lipp M, Verbói M, Kói T, Erőss B, Teutsch B, Faluhelyi N, Hegyi P, Mikó A. Persistently High Procalcitonin and C-Reactive Protein Are Good Predictors of Infection in Acute Necrotizing Pancreatitis: A Systematic Review and Meta-Analysis. *Int J Mol Sci* 2024; **25**: 1273 [PMID: 38279274 DOI: 10.3390/ijms25021273]
25 **Cardoso FS**, Ricardo LB, Oliveira AM, Canena JM, Horta DV, Papoila AL, Deus JR. C-reactive protein prognostic accuracy in acute pancreatitis: timing of measurement and cutoff points. *Eur J Gastroenterol Hepatol* 2013; **25**: 784-789 [PMID: 23492986 DOI: 10.1097/MEG.0b013e32835fd3f0]
26 **Farkas N**, Hanák L, Mikó A, Bajor J, Sarlós P, Czimmer J, Vincze Á, Gódi S, Pécsi D, Varjú P, Márta K, Hegyi PJ, Erőss B, Szakács Z, Takács T, Czakó L, Németh B, Illés D, Kui B, Darvasi E, Izbéki F, Halász A, Dunás-Varga V, Gajdán L, Hamvas J, Papp M, Földi I, Fehér KE, Varga M, Csefkó K, Török I, Hunor-Pál F, Mickevicius A, Maldonado ER, Sallinen V, Novák J, Ince AT, Galeev S, Bod B, Sümegi J, Pencik P, Szepes A, Szentesi A, Párniczky A, Hegyi P. A Multicenter, International Cohort Analysis of 1435 Cases to Support Clinical Trial Design in Acute Pancreatitis. *Front Physiol* 2019; **10**: 1092 [PMID: 31551798 DOI: 10.3389/fphys.2019.01092]
27 **Li J**, Zhou R, Zhang J, Li ZF. Calcium signaling of pancreatic acinar cells in the pathogenesis of pancreatitis. *World J Gastroenterol* 2014; **20**: 16146-16152 [PMID: 25473167 DOI: 10.3748/wjg.v20.i43.16146]
28 **Frick TW**. The role of calcium in acute pancreatitis. *Surgery* 2012; **152**: S157-S163 [PMID: 22906890 DOI: 10.1016/j.surg.2012.05.013]
29 **Petersen OH**, Gerasimenko OV, Tepikin AV, Gerasimenko JV. Aberrant Ca(2+) signalling through acidic calcium stores in pancreatic acinar cells. *Cell Calcium* 2011; **50**: 193-199 [PMID: 21435718 DOI: 10.1016/j.ceca.2011.02.010]
30 **Zhang T**, Chen S, Li L, Jin Y, Liu S, Liu Z, Shi F, Xie L, Guo P, Cannon AC, Ergashev A, Yao H, Huang C, Zhang B, Wu L, Sun H, Chen S, Shan Y, Yu Z, Tolosa EJ, Liu J, Fernandez-Zapico ME, Ma F, Chen G. PFKFB3 controls acinar IP3R-mediated Ca2+ overload to regulate acute pancreatitis severity. *JCI Insight* 2024; **9**: e169481 [PMID: 38781030 DOI: 10.1172/jci.insight.169481]
31 **Yu S**, Wu D, Jin K, Yin L, Fu Y, Liu D, Zhang L, Yu X, Xu J. Low Serum Ionized Calcium, Elevated High-Sensitivity C-Reactive Protein, Neutrophil-Lymphocyte Ratio, and Body Mass Index (BMI) Are Risk Factors for Severe Acute Pancreatitis in Patients with Hypertriglyceridemia Pancreatitis. *Med Sci Monit* 2019; **25**: 6097-6103 [PMID: 31413252 DOI: 10.12659/MSM.915526]
32 **Xue E**, Shi Q, Guo S, Zhang X, Liu C, Qian B, Guo X, Hu N, Jiang F, Tao J, Wang W. Preexisting diabetes, serum calcium and D-dimer levels as predictable risk factors for pancreatic necrosis of patients with acute pancreatitis: a retrospective study. *Expert Rev Gastroenterol Hepatol* 2022; **16**: 913-921 [PMID: 36036225 DOI: 10.1080/17474124.2022.2116314]
33 **Peng T**, Peng X, Huang M, Cut J, Zhang Y, Wu H, Wang C. Corrigendum to "Serum calcium as an indicator of persistent organ failure in acute pancreatitis" [American Journal of Emergency Medicine (2017) 35:978-982]. *Am J Emerg Med* 2017; **35**: 1785 [PMID: 28751040 DOI: 10.1016/j.ajem.2017.06.056]
34 **Cakcak İE**, Kula O. Predictive evaluation of SIRI, SII, PNI, and GPS in cholecystostomy application in patients with acute cholecystitis. *Ulus Travma Acil Cerrahi Derg* 2022; **28**: 940-946 [PMID: 35775683 DOI: 10.14744/tjtes.2022.90249]
35 **Li Y**, Zhao Y, Feng L, Guo R. Comparison of the prognostic values of inflammation markers in patients with acute pancreatitis: a retrospective cohort study. *BMJ Open* 2017; **7**: e013206 [PMID: 28348184 DOI: 10.1136/bmjopen-2016-013206]
36 **Li X**, Zhang Y, Wang W, Meng Y, Chen H, Chu G, Li H, Qi X. An inflammation-based model for identifying severe acute pancreatitis: a single-center retrospective study. *BMC Gastroenterol* 2024; **24**: 63 [PMID: 38317108 DOI: 10.1186/s12876-024-03148-4]
37 **Kong D**, Lei Z, Wang Z, Yu M, Li J, Chai W, Zhao X. A novel HCP (heparin-binding protein-C reactive protein-procalcitonin) inflammatory composite model can predict severe acute pancreatitis. *Sci Rep* 2023; **13**: 9440 [PMID: 37296194 DOI: 10.1038/s41598-023-36552-z]
38 **Yi SL**, Zeng HL, Lin XT, Deng YF, Lin YF, Xie SS, Si LJ, Liu YP. Establishment and validation of early prediction model for hypertriglyceridemic severe acute pancreatitis. *Lipids Health Dis* 2023; **22**: 218 [PMID: 38066493 DOI: 10.1186/s12944-023-01984-z]
39 **Balthazar EJ**, Robinson DL, Megibow AJ, Ranson JH. Acute pancreatitis: value of CT in establishing prognosis. *Radiology* 1990; **174**: 331-336 [PMID: 2296641 DOI: 10.1148/radiology.174.2.2296641]
40 **Alhajeri A**, Erwin S. Acute pancreatitis: value and impact of CT severity index. *Abdom Imaging* 2008; **33**: 18-20 [PMID: 17846824 DOI: 10.1007/s00261-007-9315-0]
41 **Sahu B**, Abbey P, Anand R, Kumar A, Tomer S, Malik E. Severity assessment of acute pancreatitis using CT severity index and modified CT severity index: Correlation with clinical outcomes and severity grading as per the Revised Atlanta Classification. *Indian J Radiol Imaging* 2017; **27**: 152-160 [PMID: 28744075 DOI: 10.4103/ijri.IJRI_300_16]

World Journal of Gastroenterology

Submit a Manuscript: https://www.f6publishing.com

World J Gastroenterol 2025 April 21; 31(15): 105720

DOI: 10.3748/wjg.v31.i15.105720

ISSN 1007-9327 (print) ISSN 2219-2840 (online)

ORIGINAL ARTICLE

Prospective Study

Predictive models and clinical manifestations of intrapulmonary vascular dilatation and hepatopulmonary syndrome in patients with cirrhosis: Prospective comparative study

Zhi-Peng Wu, Ying-Fei Wang, Feng-Wei Shi, Wen-Hui Cao, Jie Sun, Liu Yang, Fang-Ping Ding, Cai-Xia Hu, Wei-Wei Kang, Jing Han, Rong-Hui Yang, Qing-Kun Song, Jia-Wei Jin, Hong-Bo Shi, Ying-Min Ma

Specialty type: Gastroenterology and hepatology

Provenance and peer review: Unsolicited article; Externally peer reviewed.

Peer-review model: Single blind

Peer-review report's classification

Scientific Quality: Grade B, Grade B

Novelty: Grade B, Grade B

Creativity or Innovation: Grade C, Grade C

Scientific Significance: Grade C, Grade C

P-Reviewer: Abdu S; Reese K

Received: February 12, 2025

Revised: March 13, 2025

Accepted: March 26, 2025

Published online: April 21, 2025

Processing time: 64 Days and 22.9 Hours

Zhi-Peng Wu, Ying-Fei Wang, Feng-Wei Shi, Wen-Hui Cao, Rong-Hui Yang, Hong-Bo Shi, Beijing Institute of Hepatology, Beijing Youan Hospital, Capital Medical University, Beijing 100069, China

Jie Sun, Department of Respiratory and Critical Care Medicine, Beijing Shijitan Hospital, Capital Medical University, Beijing 100038, China

Liu Yang, Fang-Ping Ding, Department of Respiratory and Critical Care Medicine, Beijing Youan Hospital, Capital Medical University, Beijing 100069, China

Cai-Xia Hu, Hepatic Disease and Tumor Interventional Treatment Center, Beijing Youan Hospital, Capital Medical University, Beijing 100069, China

Wei-Wei Kang, Fourth Department of Liver Disease, Beijing Youan Hospital, Capital Medical University, Beijing 100069, China

Jing Han, Ultrasound and Functional Diagnosis Center, Beijing Youan Hospital, Capital Medical University, Beijing 100069, China

Qing-Kun Song, Division of Clinical Epidemiology and Evidence-Based Medicine, Beijing Youan Hospital, Capital Medical University, Beijing 100069, China

Jia-Wei Jin, Department of Respiratory and Critical Care Medicine, Beijing Chaoyang Hospital, Capital Medical University, Beijing 100043, China

Ying-Min Ma, Beijing Institute of Hepatology, Department of Respiratory and Critical Care Medicine, Beijing Youan Hospital, Capital Medical University, Beijing 100069, Beijing, China

Co-first authors: Zhi-Peng Wu and Ying-Fei Wang.

Co-corresponding authors: Hong-Bo Shi and Ying-Min Ma.

Corresponding author: Ying-Min Ma, MD, Chief Physician, Full Professor, Beijing Institute of Hepatology, Department of Respiratory and Critical Care Medicine, Beijing Youan Hospital, Capital Medical University, No. 8 Xi Tou Tiao, Youanmenwai Street, Fengtai District, Beijing 100069, China. ma.yingmin@163.com

Abstract

BACKGROUND

Patients with cirrhosis with hepatopulmonary syndrome (HPS) have a poorer prognosis. The disease has a subtle onset, symptoms are easily masked, clinical attention is insufficient, and misdiagnosis rates are high.

AIM

To compare the clinical characteristics of patients with cirrhosis, cirrhosis combined with intrapulmonary vascular dilatation (IPVD), and HPS, and to establish predictive models for IPVD and HPS.

METHODS

Patients with cirrhosis were prospectively screened at a liver-specialized university teaching hospital. Clinical information and blood samples were collected, and biomarker levels in blood samples were measured. Patients with cirrhosis were divided into three groups: Those with pure cirrhosis, those with combined IPVD, and those with HPS based on contrast-enhanced transthoracic echocardiography results and the pulmonary alveolar-arterial oxygen gradient values. Univariate logistic regression and Least Absolute Shrinkage and Selection Operator (LASSO) regression methods were utilized to identify risk factors for IPVD and HPS, and nomograms were constructed to predict IPVD and HPS.

RESULTS

A total of 320 patients were analyzed, with 101 diagnosed with IPVD, of whom 54 were diagnosed with HPS. There were statistically significant differences in clinical parameters among these three groups of patients. Among the tested biomarkers, sphingosine 1 phosphate, angiopoietin-2, and platelet-derived growth factor BB were significantly associated with IPVD and HPS in patients with cirrhosis. Following LASSO logistic regression screening, prediction models for IPVD and HPS were established. The area under the receiver operating characteristic curve for IPVD prediction was 0.792 (95% confidence interval [CI]: 0.737-0.847), and for HPS prediction was 0.891 (95%CI: 0.848-0.934).

CONCLUSION

This study systematically compared the clinical characteristics of patients with cirrhosis, IPVD, and HPS, and constructed predictive models for IPVD and HPS based on clinical parameters and laboratory indicators. These models showed good predictive value for IPVD and HPS in patients with cirrhosis. They can assist clinicians in the early prognosis assessment of patients with cirrhosis, ultimately benefiting the patients.

Key Words: Liver cirrhosis; Hepatopulmonary syndrome; Prediction model; Clinical parameters; Biomarkers

Core Tip: This study included 320 patients with liver cirrhosis, among whom 101 were diagnosed with intrapulmonary vascular dilatation (IPVD), and of these, 54 were diagnosed with hepatopulmonary syndrome (HPS). Nine potential biomarkers possibly related to HPS were tested, and the clinical parameters and biomarker levels of three patient groups were compared. Predictive models for IPVD and HPS were built respectively based on patients' clinical information and three biomarkers: sphingosine 1 phosphate, angiopoietin-2, and platelet-derived growth factor BB.

Citation: Wu ZP, Wang YF, Shi FW, Cao WH, Sun J, Yang L, Ding FP, Hu CX, Kang WW, Han J, Yang RH, Song QK, Jin JW, Shi HB, Ma YM. Predictive models and clinical manifestations of intrapulmonary vascular dilatation and hepatopulmonary syndrome in patients with cirrhosis: Prospective comparative study. *World J Gastroenterol* 2025; 31(15): 105720

URL: https://www.wjgnet.com/1007-9327/full/v31/i15/105720.htm

DOI: https://dx.doi.org/10.3748/wjg.v31.i15.105720

INTRODUCTION

Hepatopulmonary syndrome (HPS) is characterized by hypoxemia and a constellation of pathophysiological alterations and clinical manifestations resulting from intrapulmonary vascular dilatation (IPVD) and impaired arterial oxygenation in the context of chronic liver disease and/or portal hypertension[1,2]. The prevalence of HPS among patients with cirrhosis varies considerably, ranging from 4% to 47%, with pulmonary vasodilation detectable in 13% to 80% of liver transplant candidates[3]. A prospective study found that patients with HPS had poorer quality of life in certain domains compared to those without HPS. Additionally, patients with HPS had a higher risk of death, even after adjusting for age, sex, and race/ethnicity[4].

Although the presence of HPS in patients with cirrhosis affects patient prognosis, clinical attention to HPS remains inadequate[2,5]. A diagnostic study of HPS in a large integrated healthcare system found that only a small fraction of patients with cirrhosis were diagnosed with HPS through International Classification of Diseases coding within the vast patient population. Following diagnosis, only a minority of patients met the diagnostic criteria[6]. The current gold standard for diagnosing HPS involves a combination of contrast-enhanced transthoracic echocardiography (CE-TTE) and assessment of the pulmonary alveolar-arterial oxygen gradient ($P(A\text{-}a)O_2$)[3,7]. However, the specificity of CE-TTE in diagnosing HPS is low. Many patients with cirrhosis may have some degree of intrapulmonary shunting, but they may not meet the diagnostic criteria for HPS due to the lack of hypoxemia[8]. Additionally, CE-TTE has drawbacks such as being invasive and costly, making it difficult to be widely used in clinical settings. While identifying patients with low oxygen levels based on arterial blood gas is straightforward, patients with cirrhosis may experience respiratory difficulties due to conditions like ascites, leading to hypoxemia. Furthermore, it has poor sensitivity. Therefore, research on biomarkers for IPVD and HPS is of significant importance[9,10].

Several molecular markers of endothelial dysfunction and angiogenesis, which correlate with IPVD in HPS, have emerged as potential discriminators between patients with cirrhosis with and without HPS. Basic scientific research has implicated various cytokines and growth factors as potential therapeutic targets in HPS[11]. Li *et al*[12] identified soluble vascular endothelial growth factor receptor 1 (VEGFR1) and the ratio of soluble VEGFR1 to placental growth factor as key variables for distinguishing between patients with and without HPS. Recent investigations have also suggested that serum levels of vascular cellular adhesion molecule 1 (VCAM1), von Willebrand factor (vWF), and bone morphogenetic protein-9 may serve as diagnostic markers for HPS in patients with cirrhosis[13-15].

In this study, we relied on a large cohort of patients with cirrhosis to analyze clinical parameters, common laboratory indices, and levels of nine potential biomarkers including sphingosine 1 phosphate (S1P), angiopoietin-2, and vWF, aiming to identify the clinical characteristics of patients with cirrhosis with IPVD and HPS. Ultimately, we constructed predictive models for IPVD and HPS in patients with cirrhosis through univariate logistic regression and Least Absolute Shrinkage and Selection Operator (LASSO) regression methods. By focusing on the predictive capabilities of specific biomarkers and integrating comprehensive patient data, we aim to provide valuable insights to guide clinical decision-making and improve patient outcomes.

MATERIALS AND METHODS

Participants

A total of 465 patients with liver cirrhosis admitted to Youan Hospital, Capital Medical University (Beijing, China) between April 2023 and May 2024 were included for screening. Demographic data, clinical information, and laboratory indices of the patients were collected from the electronic medical record system. Blood samples were retained from eligible patients for biomarker testing. Inclusion criteria were: (1) Patients with liver cirrhosis due to various reasons; (2) Age ≥ 18 years; 3) Availability of CE-TTE results and arterial blood gas analysis; and (4) Patient consent for participation in the study. Exclusion criteria were: (1) Concomitant primary lung diseases such as pneumonia, pulmonary vascular diseases, interstitial lung diseases, chronic obstructive pulmonary disease, bronchial asthma, and lung cancer; (2) Acute upper gastrointestinal bleeding; and (3) Refusal to participate in the study. The study was approved by the Hospital Ethics Committee (No. LL-2022-141-K) and registered in the ClinicalTrials.gov database under identifier number NCT05932927. All patients provided informed consent, and patient information was anonymized. Finally, 145 patients were excluded, primarily due to refusal to participate in the study and lack of CE-TTE results and arterial blood gas analysis. In the study, of 320 individuals, 101 were diagnosed with IPVD, and ultimately 54 individuals were diagnosed with HPS. Refer to Figure 1 for details.

Diagnostic methods

Diagnostic criteria for HPS: The gold standard for HPS diagnosis is the combination of CE-TTE and $P(A\text{-}a)O_2$. The diagnostic criteria proposed in the 2016 "International Liver Transplantation Society Practice Guidelines: Diagnosis and Treatment of Hepatopulmonary Syndrome and Portal Hypertension" are used for diagnosis[1]: (1) Presence of liver disease (typically cirrhosis with portal hypertension); (2) Positive CE-TTE results; and (3) Abnormal arterial blood gas results: $P(A\text{-}a)O_2 \geq 15$ mmHg when the patient is breathing room air in an upright position (1 mmHg = 0.133 kPa, if age > 64, then ≥ 20 mmHg). Patients diagnosed with HPS are classified based on severity using arterial oxygen pressure (PaO_2): mild if $PaO_2 \geq 80$ mmHg, moderate if $PaO_2 \geq 60$ mmHg and < 80 mmHg, severe if $PaO_2 \geq 50$ mmHg and < 60 mmHg, and very severe if $PaO_2 < 50$ mmHg.

Definition of $P(A\text{-}a)O_2$: $P(A\text{-}a)O_2$ is the most sensitive indicator for monitoring early lung ventilation abnormalities[16]. Patients are in an upright position, breathing room air, and undergo arterial blood gas testing. The formula for $P(A\text{-}a)O_2$ is: P (alveolar) O_2 - P (arterial) O_2 = [FiO_2 (Patm - PH_2O) - $PaCO_2$/0.8] - PaO_2, where FiO_2 represents the inspired oxygen concentration, Patm denotes atmospheric pressure, PH_2O indicates water vapor pressure, $PaCO_2$ stands for arterial carbon dioxide partial pressure, and PaO_2 represents arterial oxygen partial pressure.

Introduction to CE-TTE: CE-TTE is the preferred and cornerstone examination method for diagnosing IPVD[17,18]. A mixture of 10 mL of 0.5 g sodium bicarbonate injection and 300 mg of vitamin B6 injection is agitated in a syringe to form microbubbles with a diameter > 10 μm, which are then injected into a peripheral vein. In a normal human body, these bubbles are absorbed by the pulmonary capillary bed (diameter < 8-15 μm) when they return to the right heart *via* the

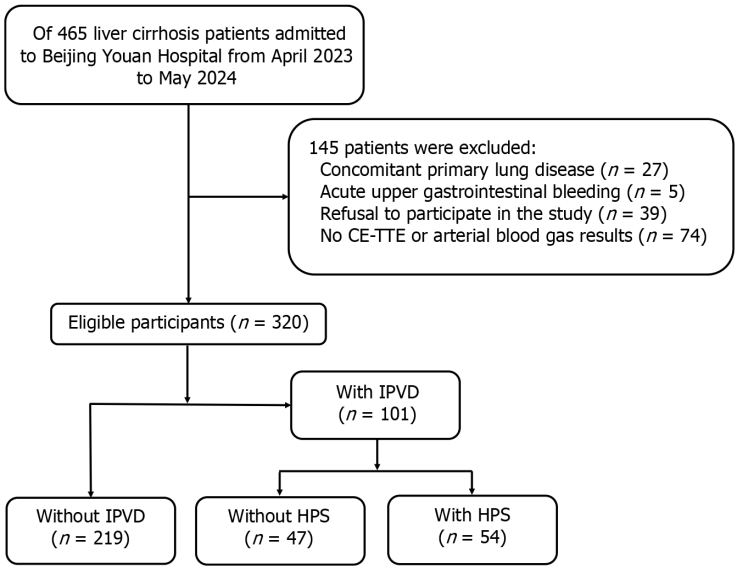

Figure 1 Flow diagram of patient enrollment. CE-TTE: Contrast-enhanced transthoracic echocardiography; HPS: Hepatopulmonary syndrome; IPVD: Intrapulmonary vascular dilatation.

systemic circulation and enter the pulmonary circulation, not reaching the left heart, thus only visible in the right heart. In patients with HPS, microbubbles flow back through dilated capillary beds or arteriovenous shunts and can appear in the left atrium after 3-6 cardiac cycles, showing a misty shadow on echocardiography. Appearance of microbubbles in the left atrium within three cardiac cycles suggests intracardiac shunting. If microbubbles are seen in the left atrium within 3-6 cardiac cycles after injection, the CE-TTE result is considered positive; the absence of microbubbles in the left atrium is considered a negative CE-TTE result.

Data collection

The following data were collected for all patients: Demographic information (*e.g.*, sex, age, height, weight), etiology of liver cirrhosis (*e.g.*, alcoholic hepatitis, hepatitis B virus, hepatitis C virus), comorbidities (*e.g.*, history of hypertension and diabetes), assessment of disease severity (Child-Pugh classification and Model for End-Stage Liver Disease [MELD] score), arterial blood gas results, laboratory indices (*e.g.*, complete blood count, liver function tests, renal function tests, coagulation function, infection markers), and the results of cardiac ultrasound examination. Refer to Table 1 for details.

Detection of biomarkers

A total of 10 mL of whole blood was drawn from patients who consented to participate in the study and placed into ethylene diamine tetraacetic acid-anticoagulated tubes. Plasma was separated by centrifugation at 2000 g for 10 minutes and stored at -80 °C in a freezer until uniform retrieval for the detection of plasma cytokine levels. Three biomarkers, S1P, angiopoietin-2, and vWF, were measured using enzyme-linked immunosorbent assay (ELISA) methods. Specifically, the following ELISA kits were used: Human S1P ELISA Kit (Catalog No. EKF58355), Angiopoietin-2 Human ELISA Kit (Catalog No. KHC1641), and Human vWF ELISA Kit (Catalog No. KHC1641). The levels of the additional six factors, sE-selectin, intercellular adhesion molecule-1 (ICAM-1), platelet-derived growth factor BB (PDGF-BB), tumor necrosis factor alpha (TNF-α), VCAM-1, and VEGF-A, were measured using the custom ProcartaPlex 6-Plex Assay (Thermo Fisher Scientific, Waltham, MA, United States), and the data were read on the Luminex 200 Instrument (Luminex Co., Austin, TX, United States). All procedures were strictly conducted following the manufacturers' instructions.

Statistical analyses

Statistical analyses were performed using SPSS 22.0 software and R language (version 4.0.3; IBM SPSS Statistics, Armonk, NY, United States). GraphPad Prism 9 (GraphPad Software, Inc., La Jolla, CA, United States) was used for graphing. Continuous variables are expressed as the median (mean) and interquartile range, while categorical variables are expressed as the number (n) and percentage (%). χ^2 test or Fisher's exact test was used for comparing categorical variables, t-test or Mann-Whitney U test was used for comparing continuous variables between two groups, and grouped F-test or the Kruskal-Wallis rank sum test was used for comparing continuous variables among multiple groups. Binary logistic regression models were used for univariate analysis of the association between variables and HPS, with results expressed as the odds ratio and 95% confidence interval (95%CI). LASSO regression was adopted to screen modeling factors, effectively avoiding overfitting, with 10-fold cross-validation set to select the appropriate parameter (λ). Receiver operating characteristic (ROC) curves were used to evaluate the classification and diagnostic efficacy of variables for HPS, with performance quantified by the area under the curve (AUC), and the optimal cut-off value determined by the Youden index. Cut-off value, sensitivity, specificity, accuracy, positive predictive value, and negative predictive value were also presented. Heatmaps were used to display correlation analysis between different clinical parameters and biomarkers. The

Table 1 Baseline characteristics and clinical data after hospitalization of patients with cirrhosis with and without intrapulmonary vascular dilatation, *n* (%)

Variables	Total (*n* = 320)	Without IPVD (*n* = 219)	With IPVD (*n* = 101)	*P* value
Demographic data				
Sex, male	246 (77)	178 (81)	68 (67)	0.006
Age, years	58 (52-65)	59 (53-66)	56.00 (49-62)	0.001
Weight, kg	69 (60-77)	70 (61-77)	65 (56-77)	0.024
Height, m	1.70 (1.64-1.74)	1.70 (1.65-1.75)	1.68 (1.60-1.73)	0.052
BMI, kg/m^2	24.03 (21.58-26.64)	24.47 (22.11-26.91)	23.24 (20.76-26.20)	0.046
Smoke	129 (40)	90 (41)	39 (39)	0.65
Drink	125 (39)	86 (39)	39 (39)	0.89
Cause[1]				
Alcoholic liver disease	65 (20)	43 (20)	22 (22)	0.66
Hepatitis B	189 (59)	142 (65)	47 (47)	0.002
Hepatitis C	44 (14)	31 (14)	13 (13)	0.76
NAFLD	5 (1.6)	3 (1.4)	2 (2.0)	0.65
Autoimmune hepatitis	26 (8.1)	12 (5.5)	14 (14)	0.011
Other	17 (5.3)	8 (3.7)	9 (8.9)	0.051
Co-morbidities				
Hypertension	93 (29)	77 (35)	16 (16)	< 0.001
Diabetes	91 (28)	73 (33)	18 (18)	0.004
Heart failure	25 (7.8)	18 (8.2)	7 (6.9)	0.69
Kidney failure	60 (19)	41 (19)	19 (19)	0.98
Liver cancer	193 (60)	143 (65)	50 (50)	0.007
Esophageal varices	201 (63)	137 (63)	64 (63)	0.97
Bleeding	89 (28)	59 (27)	30 (30)	0.61
Ascites	207 (65)	130 (59)	77 (76)	0.003
Hepatic encephalopathy	94 (29)	56 (26)	38 (38)	0.028
Clubbing of the fingers	3 (0.9)	2 (0.9)	1 (1.0)	0.99
Palmar erythema	61 (19)	35 (16)	26 (26)	0.039
Spider angioma	8 (2.5)	3 (1.4)	5 (5.0)	0.11
Disease severity				
MELD score	11.1 (5.9-17.8)	8.9 (5.5-14.3)	15.4 (10.0-25.8)	< 0.001
Child-Pugh classification				< 0.001
I	113 (35)	99 (45)	14 (14)	
II	147 (46)	91 (42)	56 (55)	
III	60 (19)	29 (13)	31 (31)	
Decompensated stage	238 (74)	151 (69)	87 (86)	0.001
Arterial blood gas				
PH	7.44 (7.42-7.46)	7.43 (7.41-7.45)	7.45 (7.42-7.47)	< 0.001
$P(A\text{-}a)O_2$, mmHg	16.7 (8.0-26.6)	14.4 (7.8-24.7)	23.6 (8.3-31.2)	0.014
PaO_2, mmHg	94.5 (84.6-105.1)	95.8 (85.6-105.9)	92.0 (81.5-102.5)	0.062
$PaCO_2$, mmHg	33.2 (29.9-36.9)	33.7 (30.7-37.3)	32.0 (28.7-35.4)	< 0.001

SpO_2, %	97.6 (96.8-98.3)	97.6 (96.9-98.3)	97.5 (96.6-98.2)	0.25
Laboratory parameters				
CRP, mg/L	7.27 (2.26-17.74)	5.70 (2.25-19.10)	8.73 (2.30-15.97)	0.92
PCT, ng/mL	0.11 (0.05-0.38)	0.10 (0.05-0.28)	0.11 (0.07-0.56)	0.063
WBC count, × 10^9/L	4.13 (2.91-6.15)	4.35 (3.16-6.42)	3.73 (2.58-5.02)	0.015
HGB, g/L	115 (95-131)	120 (99-135)	104 (84-117)	< 0.001
Platelet count, × 10^9/L	80 (55-125)	86 (63-133)	61 (41-93)	< 0.001
Neutrophil count, × 10^9/L	2.55 (1.67-4.34)	2.72 (1.82-4.57)	2.20 (1.42-3.81)	0.032
Lymphocyte count, × 10^9/L	0.84 (0.53-1.25)	0.90 (0.57-1.31)	0.68 (0.47-0.99)	0.002
NLR	2.97 (1.83-6.03)	2.72 (1.84-6.03)	3.31 (1.78-5.91)	0.41
PLR	93.7 (67.2-148.7)	95.9 (69.1-156.7)	88.0 (59.1-129.4)	0.074
LCR	0.11 (0.04-0.34)	0.11 (0.04-0.41)	0.11 (0.04-0.30)	0.62
SII	248 (132-509)	261 (145-534)	200 (93-454)	0.020
CAR	0.20 (0.07-0.58)	0.16 (0.07-0.56)	0.31 (0.08-0.61)	0.58
Albumin, g/L	33.1 (29.5-37.3)	34.7 (30.3-38.4)	31.0 (27.5-34.3)	< 0.001
Total protein, g/L	63.4 (57.8-69.0)	64.0 (58.6-69.4)	61.4 (57.4-67.5)	0.051
ALT, U/L	26 (18-47)	26 (18-51)	26 (19-35)	0.44
AST, U/L	43 (27-71)	41 (25-72)	47 (31-69)	0.11
TBIL, μmol/L	26.3 (16.6-50.2)	22.0 (14.9-38.5)	48.2 (26.8-87.4)	< 0.001
DBIL, μmol/L	11.6 (7.0-23.1)	9.1 (5.9-17.9)	20.6 (11.7-47.1)	< 0.001
BUN, mg/dL	5.59 (4.60-7.29)	5.58 (4.47-7.41)	5.59 (4.76-7.05)	0.94
Serum creatinine, mg/dL	62 (50-76)	62 (53-76)	62 (46-76)	0.40
Glucose, mg/dL	5.30 (4.71-6.44)	5.43 (4.84-6.82)	5.05 (4.56-5.79)	0.002
INR	1.19 (1.07-1.35)	1.14 (1.05-1.27)	1.30 (1.19-1.50)	< 0.001
D-dimer, mg/L	1.3 (0.4-4.2)	1.1 (0.4-4.2)	1.8 (0.8-4.1)	0.016
Prothrombin time, seconds	10.9 (9.7-12.5)	10.4 (9.5-11.8)	12.0 (11.0-13.9)	< 0.001
Prothrombin time activity, %	66 (55-80)	71 (60-83)	58 (47-67)	< 0.001
Sodium, mmol/L	140 (137-142)	140 (137-142)	140 (136-142)	0.39
Ultrasound				
Ejection fraction, %	69 (64-73)	69 (63-73)	69 (65-72)	0.671
Cardiac output, L/minute	5.4 (4.3-6.7)	5.0 (4.2-6.1)	6.1 (4.6-7.1)	0.011
E to e' ratio	9.0 (8.0-11.5)	9.0 (8.0-11.0)	10.0 (8.0-12.5)	0.017
Cardiac index, L/minute/m^2	3.05 (2.60-3.80)	2.90 (2.50-3.53)	3.40 (2.80-4.15)	0.003
Portal vein diameter, mm	13.0 (11.1-15.0)	13.0 (11.0-15.0)	13.0 (12.0-15.0)	0.443
Biomarkers				
S1P, pg/mL	46 (26-77)	51 (31-85)	33 (18-58)	< 0.001
Angiopoietin-2, pg/mL	3681 (2217-6473)	3110 (1975-5351)	5539 (3286-8805)	< 0.001
VWF, ng/mL	14.3 (7.4-30.5)	13.7 (7.2-29.7)	15.4 (8.9-30.9)	0.312
sE-selectin, ng/mL	18.7 (14.5-24.4)	19.3 (14.8-23.8)	17.1 (14.3-25.1)	0.912
ICAM-1, ng/mL	165 (95-304)	161 (92-280)	201 (104-410)	0.022
PDGF-BB, pg/mL	62 (34-112)	71 (38-123)	45 (25-76)	< 0.001
TNF alpha, pg/mL	42 (37-47)	42 (38-47)	41 (36-47)	0.412
VCAM-1, ng/mL	15.5 (10.0-22.3)	15.3 (10.1-21.2)	16.9 (10.0-23.4)	0.323

VEGF-A, pg/mL	121 (86-204)	117 (82-193)	124 (96-244)	0.062

[1]Cause: If a patient has multiple etiologies simultaneously, record them separately.

Normally distributed continuous variables are displayed as the mean ± standard deviation and were compared using the independent samples Student's *t* test. Non-normally distributed continuous variables are displayed as the median with interquartile range and were compared using the Mann-Whitney *U* test. Categorical variables are expressed as counts with percentages and were compared using Pearson's χ^2 or Fisher's exact test. ALT: Alanine aminotransferase; AST: Aspartate aminotransferase; BMI: Body mass index; BUN: Blood urea nitrogen; CAR: C-reactive protein-to-albumin ratio; CRP: C-reactive protein; DBIL: Direct bilirubin; HGB: Hemoglobin; ICAM-1: Intercellular adhesion molecule-1; INR: International normalized ratio; IPVD: Intrapulmonary vascular dilatation; LCR: Lymphocyte-to C-reactive protein ratio; MELD: Model for End-Stage Liver Disease; NAFLD: Non-alcoholic fatty liver disease; NLR: Neutrophil-to-lymphocyte ratio; P(A-a)O_2: Alveolar-arterial oxygen gradient; PaO_2: Partial pressure of oxygen in arterial blood; $PaCO_2$: Partial pressure of carbon dioxide in arterial blood; PCT: Procalcitonin; PDGF-BB: Platelet-derived growth factor BB; PH: Potential of hydrogen; PLR: Platelet-to-lymphocyte ratio; S1P: Sphingosine 1 phosphate; SII: Systemic inflammation index calculated as (neutrophil count × platelet count)/lymphocyte count; SpO_2: Peripheral oxygen saturation; TBIL: Total bilirubin; TNF: Tumor necrosis factor; VCAM-1: Vascular cell adhesion molecule-1; VEGF-A: Vascular endothelial growth factor A; vWF: Von Willebrand factor; WBC: White blood cell.

larger the absolute value of the correlation coefficient *r*, the higher the correlation; a positive *r* value indicates a positive correlation, while a negative value indicates a negative correlation. Nomograms are constructed by integrating the identified predictive factors. The accuracy of these predictive tools was assessed using the Hosmer-Lemeshow goodness-of-fit test and calibration plots. To evaluate their practical value in clinical settings, decision curve analysis was employed.

RESULTS

Clinical characteristics of patients with cirrhosis without IPVD, with IPVD, and with HPS showed statistically significant differences

After screening, a total of 320 patients were included in the analysis, with 101 patients meeting the diagnosis of IPVD, of whom 54 were diagnosed with HPS (Figure 1). The demographic data of these three patient groups, including age, sex, and weight, showed statistical differences. Differences were observed in etiology, including viral hepatitis B and autoimmune hepatitis. There were statistical differences in the proportions of comorbidities such as hypertension, diabetes, liver cancer, bleeding, and ascites. The severity of the diseases, as indicated by factors like MELD scores, and arterial blood gas analysis parameters such as oxygen partial pressure, also exhibited statistical differences. Laboratory markers such as procalcitonin, hemoglobin (HGB), and platelet count showed statistical variances. Additionally, significant statistical differences were observed in the levels of S1P, angiopoietin-2, ICAM-1, PDGF-BB, and VEGF-A measured in this study (Supplementary Table 1). Patients were further categorized into groups with and without IPVD (Table 1) and undiagnosed HPS and diagnosed HPS groups (Table 2).

Selection of variables to predict IPVD and HPS using univariate logistic regression and LASSO logistic regression

Univariate logistic regression was conducted on variables showing significant statistical differences between the IPVD and non-IPVD groups, revealing that the majority of variables with statistically significant differences among groups also displayed statistical differences in univariate regression analysis (Table 3). With the exception of body mass index, neutrophil count, systemic inflammation index, glucose, D-dimer, and ICAM-1, variables with statistically significant differences identified in univariate regression were included in the LASSO logistic regression, resulting in a final selection of seven factors: Age, hypertension, MELD score, P(A-a)O_2, S1P, angiopoietin-2, and PDGF-BB (Supplementary Figure 1). The results of univariate logistic regression predicting the relationship between variables and HPS are shown in Table 4, while the results of LASSO logistic regression are presented in Supplementary Figure 2. In the model, two clinical indicators, age and P(A-a)O_2, along with six laboratory markers, HGB, total bilirubin (TBIL), albumin, S1P, angiopoietin-2, and PDGF-BB, were included. Comparison of the levels of the three biomarkers such as S1P, angiopoietin-2, and PDGF-BB in individual patients among the three groups is shown in Figure 2. Areas under the ROC curves for predicting IPVD and HPS in patients with cirrhosis using these identified numerical factors are respectively illustrated in Figure 3. The predicted value information for different parameters is detailed in Table 5.

Heatmap of correlation analysis between different clinical parameters and biomarkers

Pairwise comparisons of correlations were performed for all variables that showed statistically significant differences in univariate logistic regression (Figure 4). Figure 4A shows the correlation coefficient *r* of Spearman's rank correlation between each pair of parameters, while Figure 4B shows the corresponding *P* value for each correlation coefficient *r*. We can see that many parameters have statistically significant correlations with each other. For example, age is correlated with international normalized ratio, prothrombin time, and prothrombin time activity (*r* values are -0.229, -0.231, and 0.231, respectively; all $P < 0.001$). We also observed that the correlations among the six numerical parameters included in the study were not statistically significant, suggesting that there is no collinearity among these parameters. This indicates that the combination of these parameters may better predict the presence of HPS in patients with cirrhosis. For instance, the *P* values of the correlation coefficients between age and the other five parameters are all greater than 0.05.

Table 2 Baseline characteristics and clinical data after hospitalization of patients with cirrhosis with and without hepatopulmonary syndrome, *n* (%)

Variables	Total (*n* = 320)	Without HPS (*n* = 266)	With HPS (*n* = 54)	*P* value
Demographic data				
Sex, male	246 (77)	208 (78)	38 (70)	0.21
Age, years	58 (52-65)	59 (53-66)	56 (49-59)	0.006
Weight, kg	69 (60-77)	70 (60-76)	67 (60-79)	0.57
Height, m	1.70 (1.64-1.74)	1.70 (1.64-1.74)	1.69 (1.60-1.75)	0.68
BMI, kg/m^2	24.03 (21.58-26.64)	24.17 (21.72-26.73)	23.42 (21.50-26.48)	0.54
Smoke	129 (40)	106 (40)	23 (43)	0.72
Drink	125 (39)	103 (39)	22 (41)	0.80
Cause[1]				
Alcoholic liver disease	65 (20)	52 (20)	13 (24)	0.45
Hepatitis B	189 (59)	167 (63)	22 (41)	0.003
Hepatitis C	44 (14)	37 (14)	7 (13)	0.85
NAFLD	5 (1.6)	4 (1.5)	1 (1.9)	0.99
Autoimmune hepatitis	26 (8.1)	17 (6.4)	9 (17)	0.024
Other	17 (5.3)	12 (4.5)	5 (9.3)	0.18
Co-morbidities				
Hypertension	93 (29)	82 (31)	11 (20)	0.12
Diabetes	91 (28)	81 (30)	10 (19)	0.076
Heart failure	25 (7.8)	19 (7.1)	6 (11)	0.40
Kidney failure	60 (19)	49 (18)	11 (20)	0.74
Liver cancer	193 (60)	169 (64)	24 (44)	0.009
Esophageal varices	201 (63)	137 (63)	34 (63)	0.91
Bleeding	89 (28)	79 (30)	10 (19)	0.095
Ascites	207 (65)	167 (63)	44 (81)	0.005
Hepatic encephalopathy	94 (29)	76 (29)	18 (33)	0.48
Clubbing of the fingers	3 (0.9)	3 (1.1)	0 (0.0)	0.99
Palmar erythema	61 (19)	48 (18)	13 (24)	0.30
Spider angioma	8 (2.5)	6 (2.3)	2 (3.7)	0.63
Disease severity				
MELD score	11.1 (5.9-17.8)	9.5 (5.8-15.7)	17.8 (10.6-35.0)	< 0.001
Child-Pugh classification				< 0.001
I	113 (35)	110 (41%)	3 (5.6)	
II	147 (46)	117 (44)	30 (56)	
III	60 (19)	39 (15)	21 (39)	
Decompensated stage	238 (74)	190 (71)	48 (89)	0.007
Arterial blood gas				
PH	7.44 (7.42-7.46)	7.43 (7.42-7.45)	7.45 (7.42-7.47)	0.005
P(A-a)O_2, mmHg	16.7 (8.0-26.6)	12.6 (6.6-23.4)	27.0 (24.4-38.0)	< 0.001
PaO_2, mmHg	94.5 (84.6-105.1)	97.9 (87.0-107.4)	83.4 (76.4-87.6)	< 0.001
$PaCO_2$, mmHg	33.2 (29.9-36.9)	33.8 (30.4-37.3)	31.0 (27.7-33.0)	< 0.001

SpO_2, %	97.6 (96.8-98.3)	97.9 (97.0-98.4)	96.8 (95.6-97.3)	< 0.001
Laboratory parameters				
CRP, mg/L	7.27 (2.26-17.74)	5.87 (2.25-17.40)	10.30 (2.30-17.58)	0.44
PCT, ng/mL	0.11 (0.05-0.38)	0.10 (0.05-0.28)	0.25 (0.08-0.90)	0.011
WBC count, × 10^9/L	4.13 (2.91-6.15)	4.25 (2.93-6.18)	3.91 (2.88-5.52)	0.72
HGB, g/L	115 (95-131)	118 (96-134)	103 (78-117)	< 0.001
Platelet count, × 10^9/L	80 (55-125)	82 (57-129)	64 (45-99)	0.035
Neutrophil count, × 10^9/L	2.55 (1.67-4.34)	2.55 (1.68-4.32)	2.52 (1.61-4.35)	0.99
Lymphocyte count, × 10^9/L	0.84 (0.53-1.25)	0.87 (0.53-1.26)	0.66 (0.42-1.13)	0.019
NLR	2.97 (1.83-6.03)	2.70 (1.78-5.85)	4.27 (2.77-6.99)	0.032
PLR	93.7 (67.2-148.7)	92.5 (67.7-148.7)	102.3 (61.4-148.2)	0.93
LCR	0.11 (0.04-0.34)	0.11 (0.04-0.41)	0.11 (0.04-0.18)	0.26
SII	248 (132-509)	242 (137-493)	280 (100-734)	0.99
CAR	0.20 (0.07-0.58)	0.18 (0.07-0.54)	0.38 (0.08-0.62)	0.21
Albumin, g/L	33.1 (29.5-37.3)	34.1 (30.2-38.0)	29.2 (26.3-33.2)	< 0.001
Total protein, g/L	63.4 (57.8-69.0)	63.7 (58.1-69.2)	61.4 (56.4-68.0)	0.12
ALT, U/L	26 (18-47)	26 (18-48)	24 (18-46)	0.64
AST, U/L	43 (27-71)	41 (26-69)	52 (35-115)	0.022
TBIL, μmol/L	26.3 (16.6-50.2)	23.2 (15.9-42.5)	53.9 (33.3-110.1)	< 0.001
DBIL, μmol/L	11.6 (7.0-23.1)	9.8 (6.5-19.6)	32.2(15.3-81.3)	< 0.001
BUN, mg/dL	5.59 (4.60-7.29)	5.55 (4.48-7.41)	5.70 (4.87-6.97)	0.56
Serum creatinine, mg/dL	62 (50-76)	62 (51-76)	64 (45-84)	0.85
Glucose, mg/dL	5.30 (4.71-6.44)	5.31 (4.76-6.59)	5.27 (4.66-6.08)	0.49
INR	1.19 (1.07-1.35)	1.17 (1.06-1.31)	1.31 (1.20-1.49)	< 0.001
D-dimer, mg/L	1.3 (0.4-4.2)	1.3 (0.4-4.2)	1.3 (0.5-4.5)	0.42
Prothrombin time, seconds	10.9 (9.7-12.5)	10.6 (9.6-12.1)	12.1 (11.2-13.8)	< 0.001
Prothrombin time activity, %	66 (55-80)	9 (57-82)	56 (50-64)	< 0.001
Sodium, mmol/L	140 (137-142)	140 (137-143)	138 (135-140)	< 0.001
Ultrasound				
Ejection fraction, %	69 (64-73)	69 (63-73)	68 (64-72)	0.83
Cardiac output, L/minute	5.4 (4.3-6.7)	5.1 (4.2-6.4)	6.6 (4.9-7.5)	0.002
E to e' ratio	9.0 (8.0-11.5)	9.0 (8.0-11.0)	10.0 (8.0-12.0)	0.45
Cardiac index, L/minute/m^2	3.05 (2.60-3.80)	3.00 (2.60-3.70)	3.75 (2.90-4.23)	0.005
Portal vein diameter, mm	13.0 (11.1-15.0)	13.0 (11.1-15.0)	13.0 (11.8-15.3)	0.34
Biomarkers				
S1P, pg/mL	46 (26-77)	49 (28-83)	32 (20-51)	0.002
Angiopoietin-2, pg/mL	3681 (2217-6473)	3457 (2074-5741)	6500 (3790-10892)	< 0.001
VWF, ng/mL	14.3 (7.4-30.5)	13.5 (7.3-26.8)	21.4 (8.9-30.9)	0.054
sE-selectin, ng/mL	18.7 (14.5-24.4)	18.7 (14.6-24.0)	19.0 (14.6-25.7)	0.53
ICAM-1, ng/mL	165 (95-304)	159 (90-284)	240 (121-392)	0.008
PDGF-BB, pg/mL	62 (34-112)	63 (35-118)	545 (25-77)	0.022
TNF alpha, pg/mL	42 (37-47)	42 (37-46)	41 (36-48)	0.68
VCAM-1, ng/mL	15.5 (10.0-22.3)	15.5 (10.0-21.4)	18.1 (10.5-24.5)	0.17

VEGF-A, pg/mL	121 (86-204)	117 (83-191)	140 (99-343)	0.008

[1]Cause: If a patient has multiple etiologies simultaneously, record them separately.

Normally distributed continuous variables are displayed as the mean ± standard deviation and were compared using the independent samples Student's *t* test. Non-normally distributed continuous variables are displayed as the median with interquartile range and were compared using the Mann-Whitney *U* test. Categorical variables are expressed as counts with percentages and were compared using Pearson's χ^2 or Fisher's exact test. ALT: Alanine aminotransferase; AST: Aspartate aminotransferase; BMI: Body mass index; BUN: Blood urea nitrogen; CAR: C-reactive protein-to-albumin ratio; CRP: C-reactive protein; DBIL: Direct bilirubin; HGB: Hemoglobin; HPS: Hepatopulmonary syndrome; ICAM-1: Intercellular adhesion molecule-1; INR: International normalized ratio; LCR: Lymphocyte-to C-reactive protein ratio; MELD: Model for End-Stage Liver Disease; NAFLD: Non-alcoholic fatty liver disease; NLR: Neutrophil-to-lymphocyte ratio; $P(A\text{-}a)O_2$: Alveolar-arterial oxygen gradient; PaO_2: Partial pressure of oxygen in arterial blood; $PaCO_2$: Partial pressure of carbon dioxide in arterial blood; PCT: Procalcitonin; PDGF-BB: Platelet-derived growth factor BB; PH: Potential of hydrogen; PLR: Platelet-to-lymphocyte ratio; S1P: Sphingosine 1 phosphate; SII: Systemic inflammation index calculated as (neutrophil count × platelet count)/lymphocyte count; SpO_2: Peripheral oxygen saturation; TBIL: Total bilirubin; TNF: Tumor necrosis factor; VCAM-1: Vascular cell adhesion molecule-1; VEGF-A: Vascular endothelial growth factor A; vWF: Von Willebrand factor; WBC: White blood cell.

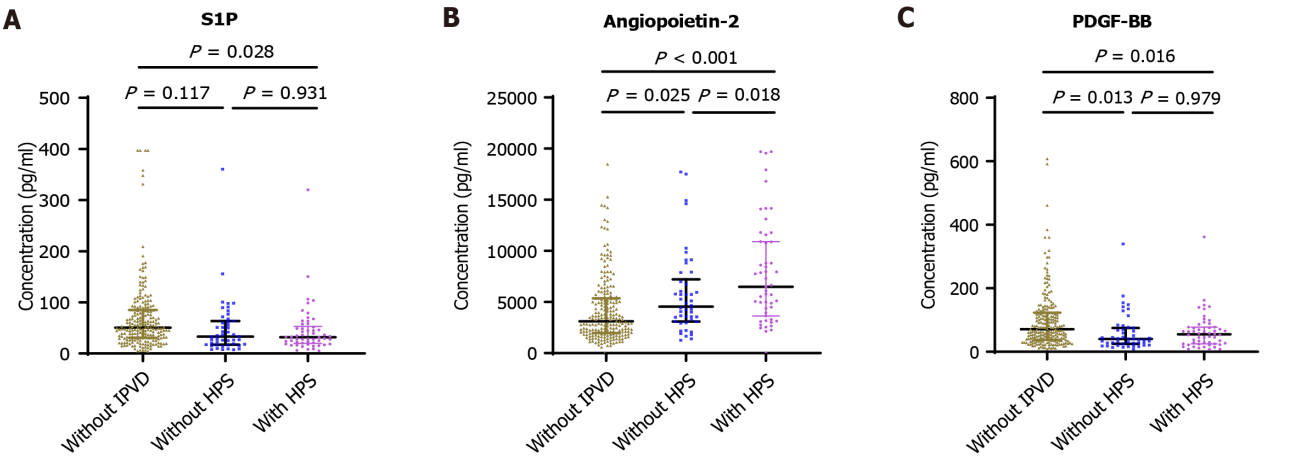

Figure 2 Novel biomarkers for intrapulmonary vascular dilatation and hepatopulmonary syndrome in patients with cirrhosis. Comparisons among multiple groups were performed using the Kruskal-Wallis rank sum test. A: Serum sphingosine 1 phosphate concentration; B: Serum angiopoietin-2 concentration; C: Serum platelet-derived growth factor BB concentration. HPS: Hepatopulmonary syndrome; IPVD: Intrapulmonary vascular dilatation; PDGF-BB: Platelet-derived growth factor BB; S1P: Sphingosine 1 phosphate.

Establishment of prediction models to predict IPVD and HPS in patients with cirrhosis

Based on LASSO regression, we developed a prediction model for IPVD in patients with cirrhosis using seven parameters (Figure 5A). The ROC curve (Figure 5B) for this model's predictions showed an AUC of 0.792 (95%CI: 0.737-0.847). The calibration curves of the model (Figure 5C) suggested that the constructed model has good simulation performance (P = 0.153). The decision curve also indicates that this clinical prediction model will effectively assist clinicians in identifying patients with cirrhosis with HPS (Figure 5D). The model for predicting HPS is presented in Figure 6A, with the area under the ROC curve of this model being 0.891 (95%CI: 0.848-0.934) (Figure 6B). The calibration curves depicted in Figure 6C indicate the well-performing simulation of the constructed model (P = 0.548). Furthermore, the decision curve in Figure 6D suggests that this clinical prediction model will effectively aid clinicians in identifying patients with cirrhosis with HPS.

DISCUSSION

HPS is a serious complication associated with liver cirrhosis, characterized by the triad of liver disease, pulmonary gas exchange abnormalities, and IPVD. This syndrome significantly impacts patients' respiratory function and overall quality of life, leading to increased morbidity and mortality among those with cirrhosis. The underlying pathophysiological mechanisms of HPS involve alterations in pulmonary vascular tone and architecture, which can result in hypoxemia due to significant shunting and ventilation-perfusion mismatch[19,20]. Currently, there is insufficient attention to HPS in clinical practice, and the diagnostic rate is not high. Many patients with cirrhosis may have HPS but remain undiagnosed. The proportion of patients undergoing CE-TTE examination is not sufficiently high, and relying solely on low arterial blood gas analysis of oxygen partial pressure is also insufficient for diagnosing HPS, as some of these patients may not have IPVD.

This study classified patients with cirrhosis into three groups: Those without IPVD, those with isolated IPVD, and those with both IPVD and hypoxemia (HPS group). A comparison of the clinical characteristics and common laboratory indices among these three groups revealed statistically significant differences. The study also found significant statistical

Table 3 Univariable logistic regression analysis for the predictors of intrapulmonary vascular dilatation in patients with cirrhosis

Variables	Univariate analysis	
	OR (95%CI)	*P* value
Sex, male	0.475 (0.277-0.812)	0.007
Age, years	0.957 (0.934-0.981)	< 0.001
Weight, kg	0.979 (0.961-0.998)	0.027
BMI, kg/m^2	0.946 (0.893-1.003)	0.064
Hepatitis B	0.472 (0.292-0.762)	0.002
Autoimmune hepatitis	2.776 (1.234-6.244)	0.014
Hypertension	0.347 (0.190-0.634)	< 0.001
Diabetes	0.434 (0.242-0.776)	0.005
Liver cancer	0.532 (0.329-0.858)	0.010
Ascites	2.196 (1.291-3.738)	0.004
Hepatic encephalopathy	1.756 (1.060-2.907)	0.029
Palmar erythema	1.822 (1.026-3.236)	0.040
MELD score	1.018 (1.007-1.028)	< 0.001
Child-Pugh classification		
I		
II	4.352 (2.269-8.345)	< 0.001
III	7.559 (3.554-16.078)	< 0.001
Decompensated stage	2.798 (1.486-5.269)	0.001
PH	12245 (13-11971501)	0.007
P(A-a)O_2	1.028 (1.008-1.048)	0.006
$PaCO_2$	0.915 (0.870-0.962)	< 0.001
HGB, g/L	0.974 (0.964-0.983)	< 0.001
Platelet count, × 10^9/L	0.991 (0.986-0.996)	< 0.001
Neutrophil count, × 10^9/L	0.942 (0.855-1.038)	0.228
Lymphocyte count, × 10^9/L	0.472 (0.291-0.766)	0.002
SII	1.000 (0.999-1.000)	0.136
Albumin, g/L	0.880 (0.838-0.923)	< 0.001
DBIL, μmol/L	1.004 (1.001-1.007)	0.006
Glucose, mg/dL	0.870 (0.754-1.003)	0.055
INR	6.529 (2.710-15.729)	< 0.001
D-dimer, mg/L	1.000 (1.000-1.001)	0.346
Prothrombin time, seconds	1.164 (1.074-1.261)	< 0.001
Prothrombin time activity, %	0.953 (0.938-0.968)	< 0.001
Cardiac output, L/minute	1.251 (1.059-1.478)	0.009
Effective ejection fraction, %	1.140 (1.028-1.264)	0.013
Cardiac index, L/minute/m^2	1.525 (1.128-2.061)	0.006
S1P, pg/mL	0.992 (0.986-0.997)	0.005
Angiopoietin-2, pg/mL	1.000 (1.000-1.000)	< 0.001
VWF, ng/mL	1.000 (1.000-1.000)	0.556
sE-selectin, ng/mL	1.000 (1.000-1.000)	0.909

ICAM-1, ng/mL	1.000 (1.000-1.000)	0.089
PDGF-BB, pg/mL	0.992 (0.988-0.997)	< 0.001
TNF alpha, pg/mL	0.996 (0.982-1.011)	0.600
VCAM-1, ng/mL	1.000 (1.000-1.000)	0.257
VEGF-A, pg/mL	1.001 (1.000-1.001)	0.195

CI: Confidence interval; DBIL: Direct bilirubin; HGB: Hemoglobin; ICAM-1: Intercellular adhesion molecule-1; INR: International normalized ratio; MELD: Model for End-Stage Liver Disease; OR: Odds ratio; P(A-a)O_2: Alveolar-arterial oxygen gradient; $PaCO_2$: Partial pressure of carbon dioxide in arterial blood; PDGF-BB: Platelet-derived growth factor BB; PH: Potential of hydrogen; S1P: Sphingosine 1 phosphate; SII: Systemic inflammation index calculated as (neutrophil count × platelet count)/lymphocyte count; TNF: Tumor necrosis factor; VCAM-1: Vascular cell adhesion molecule-1; VEGF-A: Vascular endothelial growth factor A; vWF: Von Willebrand factor.

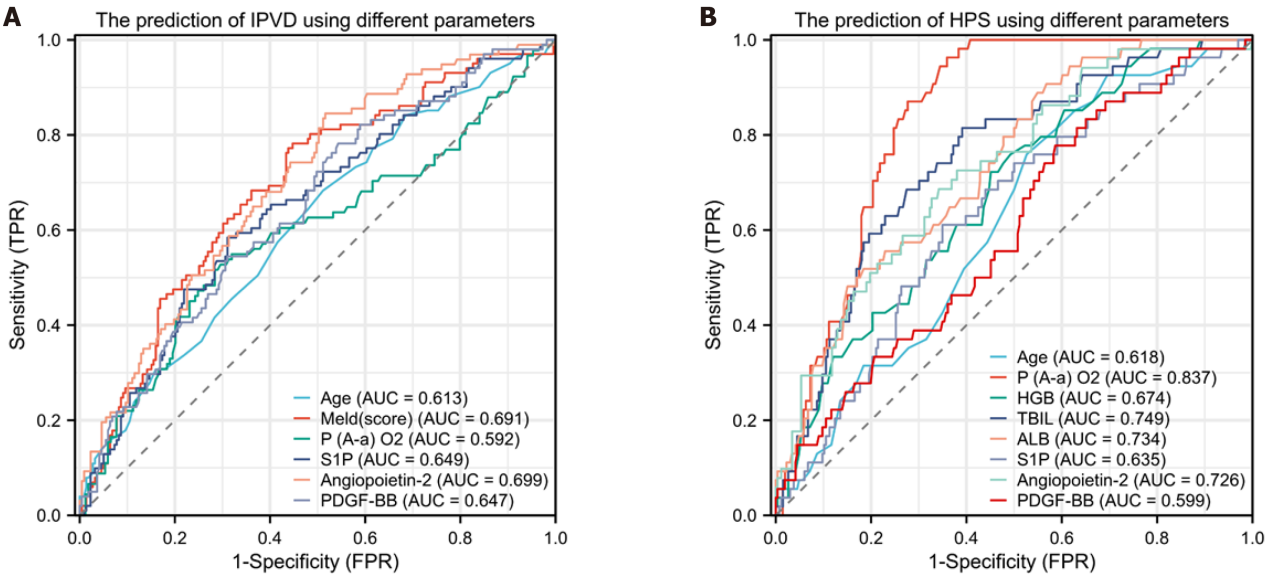

Figure 3 Receiver operating characteristic curves for predicting intrapulmonary vascular dilatation and hepatopulmonary syndrome by different parameters. A: Predicting intrapulmonary vascular dilatation (IPVD) in patients with cirrhosis. Area under the curve (AUC) for: Age was 0.613 (95% confidence interval [CI]: 0.546-0.679), Model for End-Stage Liver Disease (MELD) (score) 0.691 (95%CI: 0.629-0.753), arterial oxygen pressure 0.565 (95%CI: 0.496-0.633), reticulocalbin 3 0.587 (95%CI: 0.518-0.656), sphingosine 1 phosphate (S1P) 0.649 (95%CI: 0.584-0.714), angiopoietin-2 0.699 (95%CI: 0.638-0.760), and platelet-derived growth factor BB (PDGF-BB) 0.647 (95%CI: 0.583-0.711); B: Predicting hepatopulmonary syndrome (HPS) in patients with cirrhosis. AUC for age was 0.618 (95%CI: 0.542-0.693), pulmonary alveolar-arterial oxygen gradient (P(A-a)O_2) 0.837 (95%CI: 0.790-0.885), hemoglobin (HGB) 0.674 (95%CI: 0.600-0.749), total bilirubin (TBIL) 0.749 (95%CI: 0.681-0.818), albumin (ALB) 0.734 (95%CI: 0.667-0.801), S1P 0.635 (95%CI: 0.556-0.713); angiopoietin-2 0.726 (95%CI: 0.652-0.800), and PDGF-BB 0.599 (95%CI: 0.519-0.679). FPR: False-positive rate; TPR: True-positive rat.

differences in the levels of S1P, angiopoietin-2, and PDGF-BB among these groups. By combining these three biomarkers with clinical parameters, a clinical prediction model effectively predicted IPVD and HPS in patients with cirrhosis. The AUC for predicting IPVD was 0.792 (95%CI: 0.737-0.847), while for predicting HPS, the AUC was 0.891 (95%CI: 0.848-0.934).

Our research found that there were significant differences in clinical characteristics between patients with IPVD or HPS. For example, there were noticeable distinctions in factors such as bleeding, ascites, and the severity of the patients' conditions. Studies have shown that patients with HPS may not exhibit obvious respiratory symptoms in the early stages, only showing manifestations related to liver damage. As the disease progresses into the intermediate stage, patients may display varying degrees of hypoxia symptoms such as difficulty breathing, cyanosis, and clubbed fingers[2,21]. Regarding the severity of the disease, there is still debate on the relationship between the presence or severity of HPS and the severity of the patients' liver disease. Prospective studies have indicated that the occurrence of HPS is related to the severity of liver disease, but the conclusions of these studies have not been consistent. Some studies suggest that HPS may be associated with either the MELD score or the Child-Pugh score but not both[22,23], while others indicate correlations with both the MELD score and the Child-Pugh score[24-26]. However, previous studies have not consistently demonstrated differences in the severity of liver function between patients with and without HPS[4,18,27].

The pathogenesis of HPS remains incompletely elucidated. Current understanding posits that portal hypertension and hepatic dysfunction impair the liver's capacity to clear circulating pulmonary vasodilators (*e.g.*, nitric oxide) and modulate cytokine release (*e.g.*, TNF-α), leading to pulmonary vascular dilation and angiogenesis, ultimately culminating in HPS[28-30]. Guided by this pathophysiological framework, we collected comprehensive clinical data, with particular

Table 4 Univariable logistic regression analysis for the predictors of hepatopulmonary syndrome in patients with cirrhosis

Variables	Univariate analysis	
	OR (95%CI)	*P* value
Age, years	0.959 (0.931-0.988)	0.006
Hepatitis B	0.408 (0.224-0.740)	0.003
Autoimmune hepatitis	2.929 (1.230-6.979)	0.015
Liver cancer	0.459 (0.254-0.830)	0.010
Ascites	2.780 (1.340-5.767)	0.006
MELD score	1.019 (1.008-1.029)	< 0.001
Child-Pugh classification		
I		
II	9.402 (2.790-31.687)	< 0.001
III	19.744 (5.580-69.859)	< 0.001
Decompensated stage	3.200 (1.315-7.788)	0.010
PH	2123 (0.517-8719201)	0.071
$P(A\text{-}a)O_2$, mmHg	1.095 (1.065-1.126)	< 0.001
PaO_2, mmHg	0.921 (0.897-0.945)	< 0.001
$PaCO_2$, mmHg	0.864 (0.808-0.923)	< 0.001
SpO_2, %	0.726 (0.612-0.862)	< 0.001
PCT, ng/mL	1.133 (0.979-1.312)	0.094
HGB, g/L	0.975 (0.964-0.987)	< 0.001
Platelet count, $\times 10^9$/L	0.995 (0.989-1.001)	0.105
NLR	1.052 (1.001-1.106)	0.044
Albumin, g/L	0.847 (0.797-0.901)	< 0.001
AST, U/L	1.003 (0.999-1.007)	0.127
TBIL, μmol/L	1.004 (1.002-1.007)	< 0.001
DBIL, μmol/L	1.005 (1.002-1.009)	< 0.001
INR	3.457 (1.694-7.055)	< 0.001
Prothrombin time, seconds	1.098 (1.028-1.172)	0.005
Prothrombin time activity, %	0.960 (0.943-0.978)	< 0.001
Sodium, mmol/L	0.894 (0.840-0.952)	< 0.001
Cardiac output, L/minute	1.346 (1.108-1.635)	0.003
Cardiac index, L/minute/m^2	1.118 (0.929-1.347)	0.238
S1P	0.991 (0.983-0.999)	0.029
Angiopoietin-2	1.000 (1.000-1.000)	< 0.001
vWF	1.000 (1.000-1.000)	0.762
sE-selectin, pg/mL	1.000 (1.000-1.000)	0.546
ICAM-1, pg/mL	1.000 (1.000-1.000)	0.225
PDGF-BB, pg/mL	0.994 (0.988-0.999)	0.027
TNF alpha, pg/mL	1.000 (0.988-1.012)	0.951
VCAM-1, pg/mL	1.000 (1.000-1.000)	0.133
VEGF-A, pg/mL	1.001 (1.000-1.002)	0.051

AST: Aspartate aminotransferase; CI: Confidence interval; DBIL: Direct bilirubin; HGB: Hemoglobin; ICAM-1: Intercellular adhesion molecule-1; INR: International normalized ratio; MELD: Model for End-Stage Liver Disease; NLR: Neutrophil-to-lymphocyte ratio; OR: Odds ratio; P(A-a)O_2: Alveolar-arterial oxygen gradient; PaO_2: Partial pressure of oxygen in arterial blood; $PaCO_2$: Partial pressure of carbon dioxide in arterial blood; PCT: Procalcitonin; PDGF-BB: Platelet-derived growth factor BB; PH: Potential of hydrogen; S1P: Sphingosine 1 phosphate; SpO_2: Peripheral oxygen saturation; TBIL: Total bilirubin; TNF: Tumor necrosis factor; VCAM-1: Vascular cell adhesion molecule-1; VEGF-A: Vascular endothelial growth factor A; vWF: Von Willebrand factor; SII: Systemic inflammation index calculated as (neutrophil count × platelet count)/lymphocyte count.

Table 5 Predicted value information of different parameters and the combined model for intrapulmonary vascular dilatation and hepatopulmonary syndrome in patients with cirrhosis

Variables	Cut off value	Sensitivity	Specificity	Accuracy	PPV	NPV	Youden index
Predicting IPVD							
Age, years	60	0.68	0.49	0.55	0.38	0.77	0.17
MELD score	9	0.78	0.55	0.63	0.45	0.85	0.33
P(A-a)O_2, mmHg	24	0.52	0.72	0.65	0.49	0.73	0.23
S1P, pg/mL	36	0.58	0.69	0.66	0.46	0.78	0.27
Angiopoietin-2, pg/mL	2922	0.85	0.48	0.60	0.42	0.88	0.33
PDGF-BB, pg/mL	79	0.78	0.46	0.56	0.40	0.82	0.24
The combined model	0.27	0.87	0.59	0.69	0.52	0.90	0.47
Predicting HPS							
Age, years	60	0.76	0.47	0.52	0.22	0.91	0.23
P(A-a)O_2, mmHg,	18	0.96	0.64	0.71	0.41	0.99	0.60
HGB, g/L	115	0.72	0.55	0.58	0.25	0.91	0.27
Albumin, g/L	35	0.89	0.45	0.53	0.25	0.95	0.34
TBIL, μmol/L	29	0.81	0.61	0.64	0.30	0.94	0.42
S1P, pg/mL	36	0.61	0.65	0.64	0.26	0.89	0.26
Angiopoietin-2, pg/mL	4373	0.73	0.62	0.64	0.27	0.92	0.35
PDGF-BB, pg/mL	79	0.78	0.41	0.48	0.21	0.90	0.19
Combined model	0.14	0.94	0.74	0.78	0.47	0.98	0.68

HGB; Hemoglobin; HPS: Hepatopulmonary syndrome; IPVD: Intrapulmonary vascular dilatation; MELD: Model for End-Stage Liver Disease; NPV: Negative predictive value; P(A-a)O_2: Alveolar-arterial oxygen gradient; PDGF-BB: Platelet-derived growth factor BB; PPV: Positive predictive value; S1P: Sphingosine 1 phosphate; TBIL: Total bilirubin.

emphasis on biomarkers associated with vascular dilation, angiogenesis, and inflammation (including S1P, angiopoietin-2, vWF, sE-selectin, ICAM-1, PDGF-BB, TNF-α, VCAM-1, and VEGF-A) to develop a model for differentiating between patients with cirrhosis with and without HPS.

Experimental models of HPS have consistently demonstrated increased pulmonary angiogenesis[31,32]. Elevated angiopoietin-2 levels have been correlated with enhanced pathological angiogenesis in various studies of patients with liver disease. Kawut *et al*[23] reported that patients with HPS exhibited higher circulating levels of angiopoietin-2, VCAM-1, and vWF, and lower E-selectin levels compared to patients without HPS, suggesting that HPS is characterized by elevated proangiogenic biomarkers. Baweja *et al*[33] observed significantly lower plasma S1P levels in patients with HPS compared to those without HPS, with decreased S1P correlating with higher mortality in patients with HPS, indicating its potential as a diagnostic and prognostic biomarker for HPS. Consistent with these findings, our study demonstrated increased angiopoietin-2 levels and decreased S1P and PDGF-BB levels in patients with HPS compared to those without HPS.

To distinguish between IPVD and non-IPVD, S1P, angiopoietin-2, and PDGF-BB exhibited AUCs of 0.649, 0.699, and 0.647, respectively. To distinguish between HPS and non-HPS, S1P, angiopoietin-2, and PDGF-BB exhibited AUCs of 0.635, 0.726, and 0.599, respectively. The inclusion of vascular-related indicators in our model underscores the central role of vascular abnormalities in HPS pathogenesis and diagnosis.

Our study aligns with previous research. For instance, a 2022 study demonstrated a notable difference in vWF levels between the HPS and non-HPS groups[23]. However, our investigation did not reveal a statistically significant distinction between these cohorts. Nevertheless, our findings indicated a discernible trend towards divergence, with a *P* value of

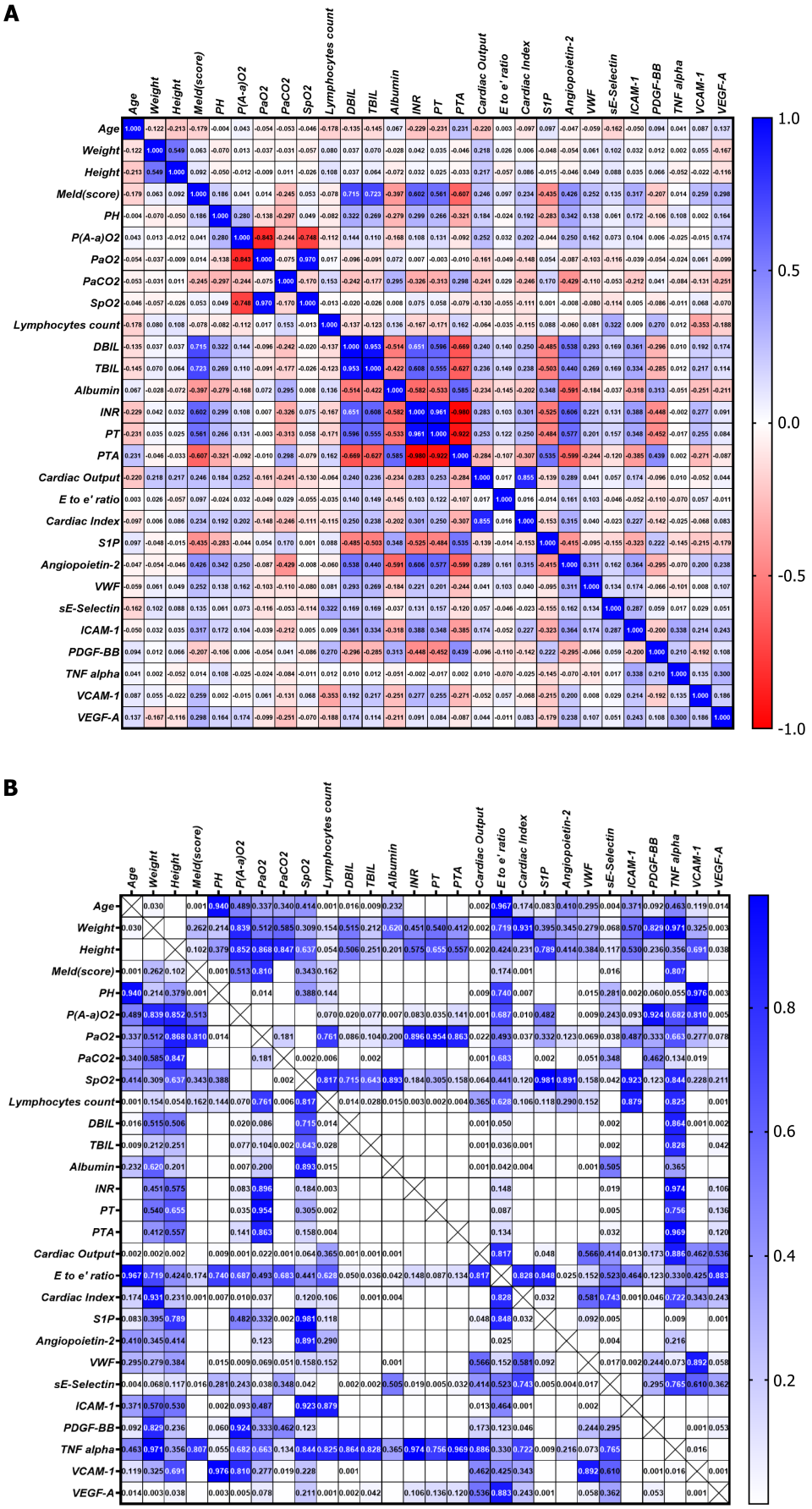

Figure 4 Heatmap depicting the correlation between clinical parameters and biomarkers. A: The values are presented as Spearman's correlation coefficient (*r*) for a sample of 320 runners. The colormap ranges from 1 to -1, with blue indicating the highest value and red indicating the lowest value; B: Heatmap of corresponding *P* values. The colormap ranges from 0 to 1, with blue representing the largest value and white representing the smallest value. White cells without

numerical values indicate that the *P* value is smaller than 0.001, indicating a highly significant correlation. DBIL: Direct bilirubin; ICAM-1: Intercellular adhesion molecule-1; INR: International normalized ratio; MELD: Model for End-Stage Liver Disease; P(A-a)O_2: Alveolar-arterial oxygen gradient; PaO_2: Partial pressure of oxygen in arterial blood; $PaCO_2$: Partial pressure of carbon dioxide in arterial blood; PDGF-BB: Platelet-derived growth factor BB; PH: Potential of hydrogen; PT: Prothrombin time; PTA: Prothrombin time activity; S1P: Sphingosine 1 phosphate; SpO_2: Peripheral oxygen saturation; TBIL: Total bilirubin; TNF: Tumor necrosis factor; VCAM-1: Vascular cell adhesion molecule-1; VEGF-A: Vascular endothelial growth factor A; vWF: Von Willebrand factor.

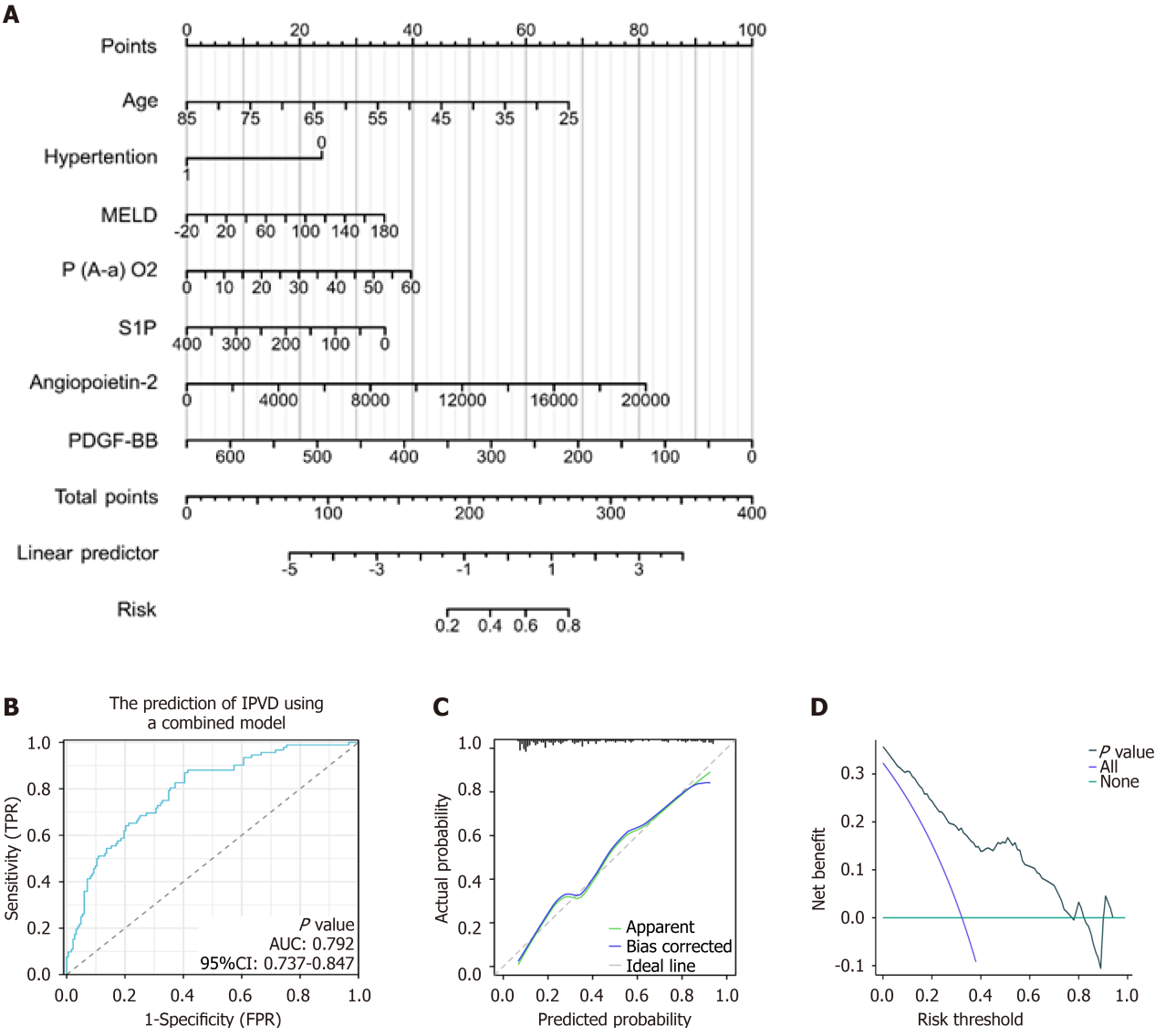

Figure 5 Predictive model for intrapulmonary vascular dilatation combining clinical parameters and biomarkers. A: Nomogram of the predictive model for intrapulmonary vascular dilatation (IPVD) in patients with cirrhosis. This model integrates four clinical parameters and three biomarkers; B: Receiver operating characteristic (ROC) curve predicting IPVD in patients with cirrhosis. Area under the curve (AUC) was 0.792 (95% confidence interval [CI]: 0.737-0.847); C: Calibration curves; D: Decision curve analysis of the nomogram for the prediction of IPVD. FPR: False-positive rate; MELD: Model for End-Stage Liver Disease; P(A-a)O_2: Alveolar-arterial oxygen gradient; PDGF-BB: Platelet-derived growth factor BB; S1P: Sphingosine 1 phosphate; TPR: True-positive rate.

0.054, marginally approaching the significance threshold of 0.05. Intriguingly, subgroup analysis indicated no significant disparity between IPVD and non-IPVD groups, with a *P* value of 0.312, suggesting that vWF may signal hypoxia more than vasodilation. Similarly, a previous study examined PDGF-BB, where although statistical significance was lacking, a trend was observed, with a *P* value of 0.08, nearing the 0.05 threshold[23]. By contrast, our study identified a statistical contrast in this marker between HPS and non-HPS groups, bolstering the credibility of our findings.

The innovative aspect of this study lies in the systematic comparison of the clinical characteristics of patients with cirrhosis, cirrhosis combined with IPVD, and HPS, and establishment of the development of comprehensive diagnostic models for IPVD and HPS incorporating age, hepatic function, respiratory function, and vascular function. This multifactorial approach, considering various pathogenic elements of HPS, may enhance diagnostic accuracy, potentially increasing HPS detection rates and reducing missed or misdiagnosed cases. Furthermore, the identification of PDGF-BB as a novel biomarker for distinguishing HPS in liver cirrhosis represents a significant contribution to the field, as it has not been previously reported in current literature[34,35]. A limitation of this study is the relatively small cohort of HPS

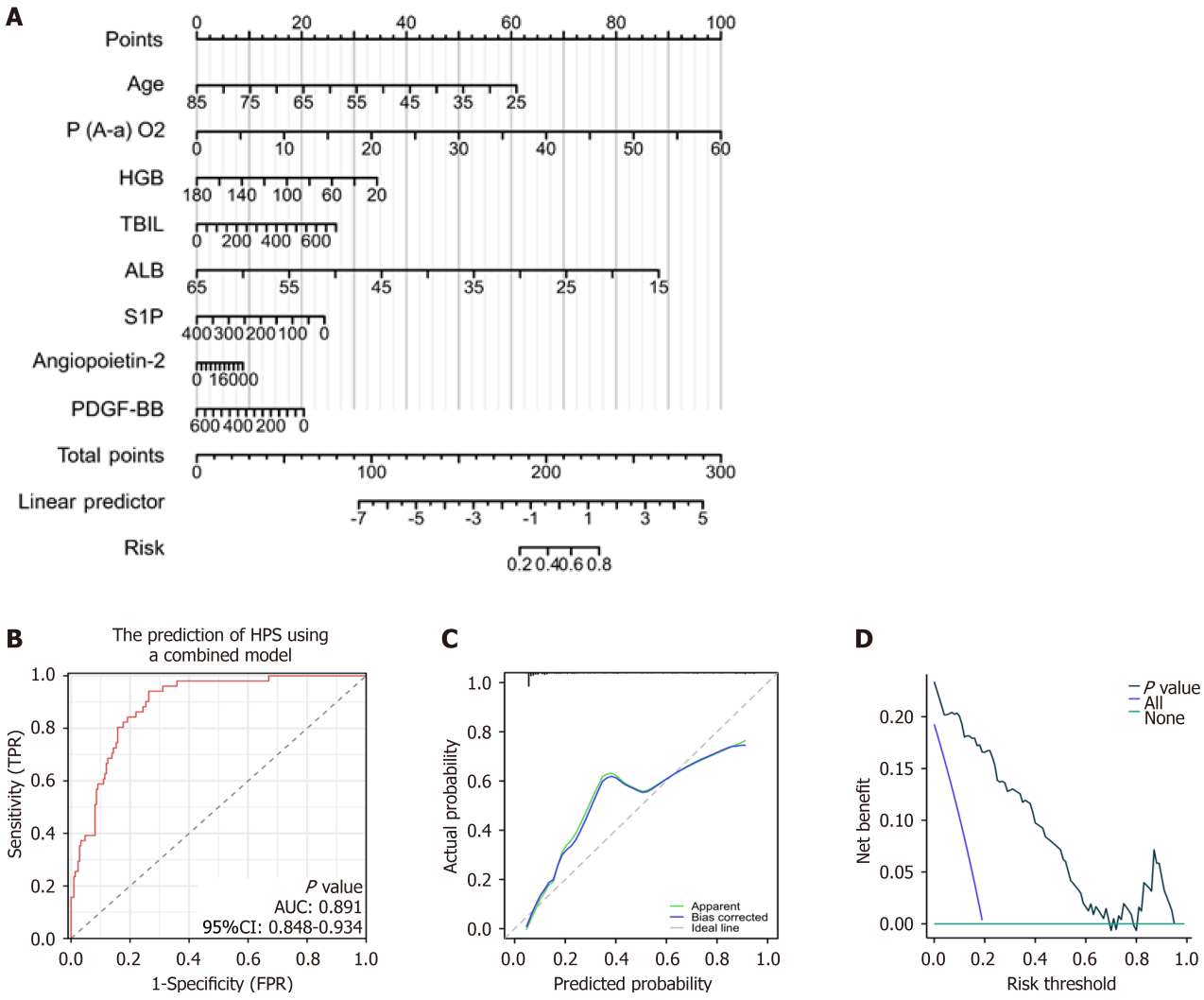

Figure 6 Predictive model for hepatopulmonary syndrome combining clinical parameters and biomarkers. A: Nomogram of the predictive model for hepatopulmonary syndrome (HPS) in patients with cirrhosis. This model integrates two clinical parameters and six biomarkers; B: Receiver operating characteristic (ROC) curve predicting HPS in patients with cirrhosis. Area under the curve (AUC) was 0.891 (95% confidence interval [CI]: 0.848-0.934); C: Calibration curves; D: Decision curve analysis of the nomogram for the prediction of HPS. ALB: Albumin; HGB: Hemoglobin; FPR: False-positive rate; P(A-a)O_2: Alveolar-arterial oxygen gradient; PDGF-BB: Platelet-derived growth factor BB; S1P: Sphingosine 1 phosphate; TBIL: Total bilirubin; TPR: True-positive rate.

cases, precluding detailed stratified analysis and external model validation. Future research will focus on expanding the case series to further validate our model and refine diagnostic methodologies for patients with HPS.

CONCLUSION

This study systematically compared the clinical characteristics of patients with cirrhosis, IPVD, and HPS, and constructed predictive models for IPVD and HPS based on clinical parameters and laboratory indicators. These models have shown good predictive value for IPVD and HPS in patients with cirrhosis. They can assist clinicians in the early prognosis assessment of patients with cirrhosis, ultimately benefiting the patients.

ACKNOWLEDGEMENTS

We would like to express our gratitude to Beijing Youan Hospital for granting access to the clinical data of the patients.

FOOTNOTES

Author contributions: Ma YM, Shi HB, Wu ZP, Wang YF, and Yang L contributed to the conceptualization of the study; Sun J, Shi FW, Cao WH, Hui CX, Kang WW, Han J, and Ding FP contributed to the data and blood sample collection; Wu ZP, Wang YF, Yang RH, and

Song QK contributed to the formal analyses; Ding FP, Wang YF, Yang L, and Cao WH contributed to ELISA testing; Ma YM, Shi HB, and Yang RH contributed to the funding acquisition; Ma YM, Shi HB, and Jin JW contributed to the investigation; Wu ZP, Wang YF, and Song QK contributed to the methodology; Ma YM, Shi HB, and Song QK contributed to the supervision and validation; Wu ZP, Wang YF, and Ding FP contributed to the visualization; Wu ZP, Wang YF, and Shi HB contributed to writing the original draft; Ma YM, Shi HB, and Jin JW contributed to revising the manuscript; All authors read and approved the final manuscript.

Supported by the National Key Research and Development Program of China, No. 2022YFC2305002; Beijing Natural Science Foundation, No. 7232079; Middle-aged and Young Talent Incubation Programs (Clinical Research) of Beijing Youan Hospital, No. BJYAYY-YN2022-12, No. BJYAYY-YN2022-13, and No. BJYAYY-YN2022-01; and the China Postdoctoral Science Foundation, No. 2023M732410 and No. 2024T170595.

Institutional review board statement: This study was reviewed and approved by the Ethical Committee of Beijing Youan Hospital (No. LL-2022-141-K).

Clinical trial registration statement: This study is registered at ClinicalTrials.gov under registration identification number NCT05932927.

Informed consent statement: All study participants, or their legal guardian, provided informed written consent prior to study enrollment, and patient information was anonymized.

Conflict-of-interest statement: Ma YM has received research funding from Beijing Natural Science Foundation, No. 7232079.

Data sharing statement: The datasets used and/or analyzed during the current study are available from the corresponding author on reasonable request.

CONSORT 2010 statement: The authors have read the CONSORT 2010 Statement, and the manuscript was prepared and revised according to the CONSORT 2010 Statement.

Country of origin: China

ORCID number: Zhi-Peng Wu 0009-0006-5675-3003; Ying-Fei Wang 0009-0003-1770-5824; Feng-Wei Shi 0009-0006-1240-3159; Wen-Hui Cao 0009-0004-6377-8140; Jie Sun 0009-0004-6326-7279; Liu Yang 0000-0002-2623-9410; Fang-Ping Ding 0009-0004-2987-3646; Cai-Xia Hu 0000-0002-9580-2799; Wei-Wei Kang 0000-0003-2071-0387; Jing Han 0000-0002-2986-2398; Rong-Hui Yang 0000-0002-9765-9666; Qing-Kun Song 0000-0002-1159-257X; Jia-Wei Jin 0000-0001-5598-6039; Hong-Bo Shi 0000-0002-3666-0196; Ying-Min Ma 0000-0002-2311-9712.

S-Editor: Fan M
L-Editor: Filipodia
P-Editor: Zhao S

REFERENCES

1 **Krowka MJ**, Fallon MB, Kawut SM, Fuhrmann V, Heimbach JK, Ramsay MA, Sitbon O, Sokol RJ. International Liver Transplant Society Practice Guidelines: Diagnosis and Management of Hepatopulmonary Syndrome and Portopulmonary Hypertension. *Transplantation* 2016; **100**: 1440-1452 [PMID: 27326810 DOI: 10.1097/TP.0000000000001229]

2 **Kumar P**, Rao PN. Hepatopulmonary Syndrome. *N Engl J Med* 2020; **382**: e14 [PMID: 32130817 DOI: 10.1056/NEJMicm1901205]

3 **Tapper EB**, Parikh ND. Diagnosis and Management of Cirrhosis and Its Complications: A Review. *JAMA* 2023; **329**: 1589-1602 [PMID: 37159031 DOI: 10.1001/jama.2023.5997]

4 **Fallon MB**, Krowka MJ, Brown RS, Trotter JF, Zacks S, Roberts KE, Shah VH, Kaplowitz N, Forman L, Wille K, Kawut SM; Pulmonary Vascular Complications of Liver Disease Study Group. Impact of hepatopulmonary syndrome on quality of life and survival in liver transplant candidates. *Gastroenterology* 2008; **135**: 1168-1175 [PMID: 18644373 DOI: 10.1053/j.gastro.2008.06.038]

5 **Sayadi A**, Duhaut L, Robert F, Savale L, Coilly A. [Hepatopulmonary syndrome]. *Rev Med Interne* 2024; **45**: 156-165 [PMID: 37005097 DOI: 10.1016/j.revmed.2023.03.008]

6 **Bommena S**, Gerkin RD, Agarwal S, Raevens S, Glassberg MK, Fallon MB. Diagnosis of Hepatopulmonary Syndrome in a Large Integrated Health System. *Clin Gastroenterol Hepatol* 2021; **19**: 2370-2378 [PMID: 33007510 DOI: 10.1016/j.cgh.2020.09.050]

7 **DuBrock HM**, Krowka MJ, Forde KA, Krok K, Patel M, Sharkoski T, Sprys M, Lin G, Oh JK, Mottram CD, Scanlon PD, Fallon MB, Kawut SM. Clinical Impact of Intrapulmonary Vascular Dilatation in Candidates for Liver Transplant. *Chest* 2018; **153**: 414-426 [PMID: 28987478 DOI: 10.1016/j.chest.2017.09.035]

8 **Warner S**, McKiernan PJ, Hartley J, Ong E, van Mourik ID, Gupte G, Abdel-Hady M, Muiesan P, Perera T, Mirza D, Sharif K, Kelly DA, Beath SV. Hepatopulmonary Syndrome in Children: A 20-Year Review of Presenting Symptoms, Clinical Progression, and Transplant Outcome. *Liver Transpl* 2018; **24**: 1271-1279 [PMID: 30066494 DOI: 10.1002/lt.25296]

9 **Mendizabal M**, Goldberg DS, Piñero F, Arufe DT, José de la Fuente M, Testa P, Coronel M, Baratta S, Podestá LG, Fallon MB, Silva MO. Isolated Intrapulmonary Vascular Dilatations and the Risk of Developing Hepatopulmonary Syndrome in Liver Transplant Candidates. *Ann*

Hepatol 2017; **16**: 548-554 [PMID: 28611257 DOI: 10.5604/01.3001.0010.0289]
10 **Raevens S**, Geerts A, Devisscher L, Van Vlierberghe H, Van Steenkiste C, Colle I. Recent advances in the approach to hepatopulmonary syndrome and portopulmonary hypertension. *Acta Gastroenterol Belg* 2021; **84**: 95-99 [PMID: 33639700 DOI: 10.51821/84.1.200]
11 **Certain MC**, Robert F, Baron A, Sitbon O, Humbert M, Guignabert C, Tu L, Savale L. [Hepatopulmonary syndrome: Prevalence, pathophysiology and clinical implications]. *Rev Mal Respir* 2022; **39**: 84-89 [PMID: 35219561 DOI: 10.1016/j.rmr.2022.02.055]
12 **Li YJ**, Wu XF, Wang DD, Li P, Liang H, Hu XY, Gan JQ, Sun YZ, Li JH, Li J, Shu X, Song AL, Yang CY, Yang ZY, Yu WF, Yang LQ, Wang XB, Belguise K, Xia ZY, Yi B. Serum Soluble Vascular Endothelial Growth Factor Receptor 1 as a Potential Biomarker of Hepatopulmonary Syndrome. *J Clin Transl Hepatol* 2023; **11**: 1150-1160 [PMID: 37577229 DOI: 10.14218/JCTH.2022.00421]
13 **Raevens S**, Coulon S, Van Steenkiste C, Colman R, Verhelst X, Van Vlierberghe H, Geerts A, Perkmann T, Horvatits T, Fuhrmann V, Colle I. Role of angiogenic factors/cell adhesion markers in serum of cirrhotic patients with hepatopulmonary syndrome. *Liver Int* 2015; **35**: 1499-1507 [PMID: 24766195 DOI: 10.1111/liv.12579]
14 **Horvatits T**, Drolz A, Roedl K, Herkner H, Ferlitsch A, Perkmann T, Müller C, Trauner M, Schenk P, Fuhrmann V. Von Willebrand factor antigen for detection of hepatopulmonary syndrome in patients with cirrhosis. *J Hepatol* 2014; **61**: 544-549 [PMID: 24798623 DOI: 10.1016/j.jhep.2014.04.025]
15 **Robert F**, Certain MC, Baron A, Thuillet R, Duhaut L, Ottaviani M, Chelgham MK, Normand C, Berrebeh N, Ricard N, Furlan V, Desroches-Castan A, Gonzales E, Jacquemin E, Sitbon O, Humbert M, Bailly S, Coilly A, Guignabert C, Tu L, Savale L. Disrupted BMP-9 Signaling Impairs Pulmonary Vascular Integrity in Hepatopulmonary Syndrome. *Am J Respir Crit Care Med* 2024; **210**: 648-661 [PMID: 38626313 DOI: 10.1164/rccm.202307-1289OC]
16 **Rodríguez-Roisin R**, Agustí AG, Roca J. The hepatopulmonary syndrome: new name, old complexities. *Thorax* 1992; **47**: 897-902 [PMID: 1465744 DOI: 10.1136/thx.47.11.897]
17 **Rodríquez-Roisin R**, Krowka MJ, Hervé P, Fallon MB; ERS (European Respiratory Society) Task Force-PHD Scientific Committee. Highlights of the ERS Task Force on pulmonary-hepatic vascular disorders (PHD). *J Hepatol* 2005; **42**: 924-927 [PMID: 15973780 DOI: 10.1016/j.jhep.2005.03.002]
18 **Abrams GA**, Jaffe CC, Hoffer PB, Binder HJ, Fallon MB. Diagnostic utility of contrast echocardiography and lung perfusion scan in patients with hepatopulmonary syndrome. *Gastroenterology* 1995; **109**: 1283-1288 [PMID: 7557096 DOI: 10.1016/0016-5085(95)90589-8]
19 **Ho V**. Current concepts in the management of hepatopulmonary syndrome. *Vasc Health Risk Manag* 2008; **4**: 1035-1041 [PMID: 19183751 DOI: 10.2147/vhrm.s3608]
20 **Umeda N**, Kamath PS. Hepatopulmonary syndrome and portopulmonary hypertension. *Hepatol Res* 2009; **39**: 1020-1022 [PMID: 19796040 DOI: 10.1111/j.1872-034X.2009.00552.x]
21 **Low ESL**, Patwala K, Apostolov R. Dyspnoea, clubbing, cirrhosis, and bubbles in both sides of the heart suggests hepatopulmonary syndrome. *Lancet* 2019; **394**: 510 [PMID: 31402029 DOI: 10.1016/S0140-6736(19)31720-9]
22 **Schenk P**, Fuhrmann V, Madl C, Funk G, Lehr S, Kandel O, Müller C. Hepatopulmonary syndrome: prevalence and predictive value of various cut offs for arterial oxygenation and their clinical consequences. *Gut* 2002; **51**: 853-859 [PMID: 12427789 DOI: 10.1136/gut.51.6.853]
23 **Kawut SM**, Krowka MJ, Forde KA, Al-Naamani N, Krok KL, Patel M, Bartoli CR, Doyle M, Moutchia J, Lin G, Oh JK, Mottram CD, Scanlon PD, Fallon MB; Pulmonary Vascular Complications of Liver Disease Study Group. Impact of hepatopulmonary syndrome in liver transplantation candidates and the role of angiogenesis. *Eur Respir J* 2022; **60** [PMID: 34949701 DOI: 10.1183/13993003.02304-2021]
24 **Pascasio JM**, Grilo I, López-Pardo FJ, Ortega-Ruiz F, Tirado JL, Sousa JM, Rodriguez-Puras MJ, Ferrer MT, Sayago M, Gómez-Bravo MA, Grilo A. Prevalence and severity of hepatopulmonary syndrome and its influence on survival in cirrhotic patients evaluated for liver transplantation. *Am J Transplant* 2014; **14**: 1391-1399 [PMID: 24730359 DOI: 10.1111/ajt.12713]
25 **Younis I**, Sarwar S, Butt Z, Tanveer S, Qaadir A, Jadoon NA. Clinical characteristics, predictors, and survival among patients with hepatopulmonary syndrome. *Ann Hepatol* 2015; **14**: 354-360 [PMID: 25864216 DOI: 10.1016/S1665-2681(19)31275-X]
26 **Schenk P**, Schöniger-Hekele M, Fuhrmann V, Madl C, Silberhumer G, Müller C. Prognostic significance of the hepatopulmonary syndrome in patients with cirrhosis. *Gastroenterology* 2003; **125**: 1042-1052 [PMID: 14517788 DOI: 10.1016/s0016-5085(03)01207-1]
27 **Krowka MJ**, Wiseman GA, Burnett OL, Spivey JR, Therneau T, Porayko MK, Wiesner RH. Hepatopulmonary syndrome: a prospective study of relationships between severity of liver disease, PaO(2) response to 100% oxygen, and brain uptake after (99m)Tc MAA lung scanning. *Chest* 2000; **118**: 615-624 [PMID: 10988181 DOI: 10.1378/chest.118.3.615]
28 **Raevens S**, Geerts A, Paridaens A, Lefere S, Verhelst X, Hoorens A, Van Dorpe J, Maes T, Bracke KR, Casteleyn C, Jonckx B, Horvatits T, Fuhrmann V, Van Vlierberghe H, Van Steenkiste C, Devisscher L, Colle I. Placental growth factor inhibition targets pulmonary angiogenesis and represents a therapy for hepatopulmonary syndrome in mice. *Hepatology* 2018; **68**: 634-651 [PMID: 29023811 DOI: 10.1002/hep.29579]
29 **Raevens S**, Fallon MB. Fingolimod as a sphingolipid modulator in hepatopulmonary syndrome: A critical review. *J Hepatol* 2023; **79**: e194-e195 [PMID: 37301264 DOI: 10.1016/j.jhep.2023.05.029]
30 **Zhang J**, Fallon MB. Hepatopulmonary syndrome: update on pathogenesis and clinical features. *Nat Rev Gastroenterol Hepatol* 2012; **9**: 539-549 [PMID: 22751459 DOI: 10.1038/nrgastro.2012.123]
31 **Yang C**, Sun M, Yang Y, Han Y, Wu X, Wu X, Cao H, Chen L, Lei Y, Hu X, Chen Y, Zeng Z, Li J, Shu X, Yang Z, Lu K, Li Y, Wang X, Yi B. Elevated circulating BMP9 aggravates pulmonary angiogenesis in hepatopulmonary syndrome rats through ALK1-Endoglin-Smad1/5/9 signalling. *Eur J Clin Invest* 2024; **54**: e14212 [PMID: 38591651 DOI: 10.1111/eci.14212]
32 **Mangoura SA**, Ahmed MA, Hamad N, Zaka AZ, Khalaf KA, Mahdy MA. Vildagliptin ameliorates intrapulmonary vasodilatation and angiogenesis in chronic common bile duct ligation-induced hepatopulmonary syndrome in rat. *Clin Res Hepatol Gastroenterol* 2024; **48**: 102408 [PMID: 38925324 DOI: 10.1016/j.clinre.2024.102408]
33 **Baweja S**, Kumari A, Negi P, Tomar A, Tripathi DM, Mourya AK, Rastogi A, Subudhi PD, Thangariyal S, Kumar G, Kumar J, Reddy GS, Sood AK, Vashistha C, Sarohi V, Bihari C, Maiwall R, Sarin SK. Hepatopulmonary syndrome is associated with low sphingosine-1-phosphate levels and can be ameliorated by the functional agonist fingolimod. *J Hepatol* 2023; **79**: 167-180 [PMID: 36996943 DOI: 10.1016/j.jhep.2023.03.018]
34 **Liao J**, Yang X, Yang J, Xiao J, Liu X, Zhuo Y, Yang J, Gu H. Fractalkine modulates pulmonary angiogenesis and tube formation by modulating CX3CR1 and growth factors in PVECs. *Open Life Sci* 2023; **18**: 20220670 [PMID: 38239497 DOI: 10.1515/biol-2022-0670]
35 **Raevens S**, Boret M, Fallon MB. Hepatopulmonary syndrome. *JHEP Rep* 2022; **4**: 100527 [PMID: 36035361 DOI: 10.1016/j.jhepr.2022.100527]

World Journal of Gastroenterology

Submit a Manuscript: https://www.f6publishing.com

World J Gastroenterol 2025 April 21; 31(15): 101058

DOI: 10.3748/wjg.v31.i15.101058

ISSN 1007-9327 (print) ISSN 2219-2840 (online)

ORIGINAL ARTICLE

Basic Study

Strain- and sex-dependent variability in hepatic microcirculation and liver function in mice

Bing Wang, Yuan Li, Qin Ouyang, Meng-Ting Xu, Ying-Yu Wang, Sun-Jing Fu, Wei-Qi Liu, Xue-Ting Liu, Hao Ling, Xu Zhang, Rui-Juan Xiu, Ming-Ming Liu

Specialty type: Gastroenterology and hepatology

Provenance and peer review: Unsolicited article; Externally peer reviewed.

Peer-review model: Single blind

Peer-review report's classification

Scientific Quality: Grade A, Grade A, Grade A, Grade B, Grade D

Novelty: Grade A, Grade A, Grade A, Grade B, Grade B

Creativity or Innovation: Grade A, Grade A, Grade A, Grade A, Grade B

Scientific Significance: Grade A, Grade A, Grade A, Grade A, Grade C

P-Reviewer: Fu SR; Sade R; Wang YQ

Received: September 4, 2024

Revised: February 2, 2025

Accepted: March 26, 2025

Published online: April 21, 2025

Processing time: 226 Days and 5.2 Hours

Bing Wang, Yuan Li, Meng-Ting Xu, Ying-Yu Wang, Wei-Qi Liu, Xue-Ting Liu, Rui-Juan Xiu, Ming-Ming Liu, Institute of Microcirculation, Chinese Academy of Medical Sciences and Peking Union Medical College, Beijing 100005, China

Bing Wang, Yuan Li, Meng-Ting Xu, Ying-Yu Wang, Wei-Qi Liu, Xue-Ting Liu, Rui-Juan Xiu, Ming-Ming Liu, International Center of Microvascular Medicine, Chinese Academy of Medical Sciences, Beijing 100005, China

Qin Ouyang, Department of Pathology, Wangjing Hospital, China Academy of Chinese Medical Science, Beijing 100102, China

Sun-Jing Fu, Department of Cardiology, Peking University China-Japan Friendship School of Clinical Medicine, Beijing 100029, China

Hao Ling, Department of Radiology, The Affiliated Changsha Central Hospital, Hengyang Medical School, University of South China, Changsha 410004, Hunan Province, China

Xu Zhang, Laboratory of Electron Microscopy, Ultrastructural Pathology Center, Peking University First Hospital, Beijing 100034, China

Ming-Ming Liu, Diabetes Research Center, Chinese Academy of Medical Sciences, Beijing 100005, China

Corresponding author: Ming-Ming Liu, PhD, Associate Professor, Institute of Microcirculation, Chinese Academy of Medical Sciences and Peking Union Medical College, No. 5 Dong Dan Third Alley, Dongcheng District, Beijing 100005, China. mingmingliu@imc.pumc.edu.cn

Abstract

BACKGROUND

The integrity and functionality of the hepatic microcirculation are essential for maintaining liver health, which is influenced by sex and genetic background. Understanding these variations is crucial for addressing disparities in liver disease outcomes.

AIM

To investigate the sexual dimorphism and genetic heterogeneity of liver microcirculatory function in mice.

METHODS
We assessed hepatic microhemodynamics in BALB/c, C57BL/6J, and KM mouse strains using laser Doppler flowmetry and wavelet analysis. We analyzed the serum levels of alanine transaminase, glutamic acid aminotransferase, total bile acid, total protein, alkaline phosphatase, and glucose. Histological and immunohistochemical staining were employed to quantify microvascular density and the expression levels of cluster of differentiation (CD) 31, and estrogen receptor α, and β. Statistical analyses, including the Mantel test and Pearson correlation, were conducted to determine the relationships among hepatic function, microcirculation, and marcocirculation between different sexes and across genetic backgrounds.

RESULTS
We identified sex-based disparities in hepatic microhemodynamics across all strains, with males exhibiting higher microvascular perfusion and erythrocyte concentration, but lower blood velocity. Strain-specific differences were evident, particularly in the endothelial oscillatory characteristics of the erythrocyte concentration. No sex-dependent differences in estrogen receptor expression were observed, while significant variations in CD31 expression and microvascular density were observed. The correlations highlighted relationships between hepatic microhemodynamics and liver function indicators.

CONCLUSION
Our findings indicate the influence of genetic and sex differences on hepatic microcirculation and liver function, highlighting the necessity of incorporating both genetic background and sex into hepatic physiology studies and potential liver disease management strategies.

Key Words: Hepatic microhemodynamics; Sex differences; Mouse strains; Biological oscillators; Hepatic microcirculation

Core Tip: This study reveals significant strain and sex-dependent variations in hepatic microcirculation among murine, highlighting the implications for liver health. Male mice exhibited higher microvascular perfusion and erythrocyte concentration, while sex-specific differences in endothelial function were indicated across strains. Cluster of differentiation 31 expression linked to microvascular density varied by sex, suggesting a role in hepatic microhemodynamics. These findings suggest the necessity of integrating genetic and sex factors into the understanding of liver physiology and pathology, potentially guiding personalized therapeutic strategies.

Citation: Wang B, Li Y, Ouyang Q, Xu MT, Wang YY, Fu SJ, Liu WQ, Liu XT, Ling H, Zhang X, Xiu RJ, Liu MM. Strain- and sex-dependent variability in hepatic microcirculation and liver function in mice. *World J Gastroenterol* 2025; 31(15): 101058
URL: https://www.wjgnet.com/1007-9327/full/v31/i15/101058.htm
DOI: https://dx.doi.org/10.3748/wjg.v31.i15.101058

INTRODUCTION

The liver, as the largest visceral organ in humans, accounts for approximately 2.5 % of the total body weight and receives approximately 25 % of cardiac output. This robust blood supply is predominantly sourced from two major vessels, with the portal vein contributing 70%-80% of the inflow by delivering nutrient-rich blood, while the hepatic arteries supply the remaining 20%-30% of oxygenated blood. These vessels undergo extensive bifurcation, culminating in terminal hepatic arterioles and portal venules, with diameters ranging from 15 μm-35 μm and lengths of 50 μm-70 μm[1]. This network ultimately feeds into the hepatic sinusoids, the critical components of the liver microvasculature. Sinusoids are characterized by a specialized fenestrated endothelium that not only increase permeability but also facilitates dynamic interactions between blood and hepatocytes[2], thereby playing a vital role in liver function and homeostasis.

The essential functions of the liver in biosynthesis, metabolism, detoxification, and immune surveillance are fundamentally reliant on the integrity of its microcirculation. This vascular system ensures the effective delivery of nutrients and oxygen to parenchymal tissues and plays a vital role in regulating vascular tone, facilitating leukocyte trafficking during hepatic inflammation, and enabling the clearance of toxins and pathogens from the bloodstream. Emerging evidence indicates that biological sex is a modifying factor of hepatic immune regulation, thereby contributing to hepatic immune outcomes in health and disease[3]. Additionally, genetic variations may alter the composition of liver-associated microbial DNA, further complicating the communication between host and microbial factors in liver function [4]. These lines of evidence represent potentially actionable mechanisms of disease biology. Disruptions in hepatic microvascular circulation emerge as critical factors in liver pathology, leading to organ injury or failure in ischemic and inflammatory diseases[5,6]. These disruptions are also associated with elevated mortality rates among affected individuals.

Moreover, the manifestation and progression of liver disease are significantly influenced by sex-based and genetic disparities. Research, including studies by Ruhl *et al*[7], has shown that men exhibit a higher prevalence of non-alcoholic fatty liver disease (NAFLD) and hepatocellular carcinoma (HCC) than women[8,9]. Women with NAFLD typically present a less atherogenic lipid profile and a more favorable cardiovascular risk[10]. Additionally, males are more susceptible to hepatic fibrosis, which correlates with an increased risk of inflammation-driven HCC[11,12]. Ethnic and racial differences further complicate the epidemiology of liver disease; for instance, the prevalence of NAFLD is highest in Europe (28.04%), followed by East Asia (19.24%) and the Middle East (12.95%)[13]. Genetic factors, particularly variants in the Patatin-like phospholipase domain-containing protein 3 (PNPLA3), add another layer of complexity, with varying frequencies of the rs738409 GG genotype observed across different populations[14].

Understanding the relationship between hepatic microhemodynamics and liver function is essential for unraveling the complex interplay of these physiological and pathological processes. Variations in microvascular structure and function, influenced by genetic and sex-based differences, can significantly impact hepatic perfusion, nutrient delivery, and metabolic regulation. These physiological disparities are crucial for maintaining liver homeostasis and may elucidate disparities in disease susceptibility and progression. The aim of our study was to investigate the relationship between hepatic microhemodynamics and liver function, with a particular focus on variations attributable to sex and genetic background.

MATERIALS AND METHODS

Animals

This study was conducted in strict accordance with the recommendations in the Guide for the Care and Use of Laboratory Animals of the National Institutes of Health. The protocol was approved by the Institutional Animal Care and Use Committee (IACUC) of the Institute of Microcirculation, Chinese Academy of Medical Sciences (CAMS) (Approval No. CAMS-IM-IACUC-2022-AE-0917). C57BL/6J mice are foundational in liver studies due to their well-defined genetics and reliable responses to models[15]. Details on liver fibrosis and inflammation can be obtained by studying BALB/c mice, which exhibit distinct metabolomic and immunological profiles[16]. KM mice, though less common, are valuable for research on oxidative stress and hepatotoxicity[17]. These strains facilitate the investigation of hepatic microhemodynamics across diverse genetic backgrounds. All mice aged 8 weeks (n = 6 each group), acquired from the Institute of Laboratory Animal Science, CAMS, Beijing, China, were housed under controlled conditions (temperature: 18-22 °C, humidity: 50%-65%, 12-hour/12-hour light/dark cycle) with ad libitum access to food and water. We employed a randomized block design to allocate the mice to experimental groups, controlling for baseline variations and ensuring balanced, comparable groups.

Monitoring of blood pressure

Blood pressure measurements were performed *via* a noninvasive tail-cuff method with the Intelligent Sphygmomanometer BP-2010A (Softron Biotechnology, Beijing, China). This method is established as equivalent to invasive techniques, showing strong correlations with intra-arterial measurements[18]. We chose this approach to avoid potential confounding effects on microhemodynamics associated with invasive methods. The mice were acclimatized for 5 minutes in a restraint device placed on a heated pad (37 °C) before systolic, diastolic, and mean arterial pressures were recorded over three consecutive trials. Blood glucose levels were determined *via* tail snip using the One Touch Ultra glucometer (LifeScan, Johnson and Johnson, Milpitas, CA, United States).

Determination of the integrated hepatic microcirculatory profile

To investigate hepatic microhemodynamics, we employed a laser Doppler blood perfusion monitoring system (Virtual machines, Moor Instruments, Ltd., Axminster, United Kingdom), which was calibrated with standard microspheres prior to the experiments. Following acclimatization for 10 minutes, the mice were initially anesthetized *via* inhalation of 2% isoflurane (R510-22; RWD Life Science Co., Shenzhen, China) in a 50% oxygen mixture through a small animal anesthesia machine (matrix VMR; Midmark Corporation, OH, United States). An incision was precisely made along the medioventral line to gently expose the entire liver, and the Versa-probe 4 (Moor Instruments) was stably positioned on the exposed hepatic tissue with the assistance of a probe holder (Moor Instruments). Three sites were selected, and measured for 1 minute each, and the backscattered light collected by the probe was processed by analog and digital signals to generate hepatic microhemodynamics. The microcirculatory blood distribution pattern was revealed in the scatter plot. The microvascular hemorheological parameters including microvascular blood flux, microvascular erythrocyte concentration, and microvascular blood velocity were analyzed quantitatively as functional evaluation of hepatic microhemodynamics.

Wavelet transform analysis

Wavelet transform analysis is superior to traditional Fourier analysis for blood flow signals due to its ability to handle non-stationary signals and provide detailed time frequency information. The microhemodynamic signals were subjected to oscillations ranging from 0.005 Hz-5.0 Hz, including nitric oxide (NO)-independent endothelial signals (0.005 Hz-0.0095 Hz), reflecting baseline endothelial function; NO-dependent endothelial signals (0.0095 Hz-0.04 Hz), representing responses regulated by NO; neurogenic signals (0.04 Hz-0.15 Hz), linked to neural influences on microhemodynamics; myogenic signals (0.15 Hz-0.4 Hz), representing smooth muscle responses to blood pressure changes; respiratory signals

(0.4 Hz-2.0 Hz), correlating with breathing patterns; and cardiac signals (2.0 Hz-5.0 Hz), which are associated with heart rate and rhythm[19,20]. Each of these signals is related to a specific physiological influence modulating the hepatic microcirculation response. Wavelet transformation was performed to create the representation of signals measured from hepatic microhemodynamics in the time frequency domain and estimate the contribution of rhythmical components in blood flow signal. Using the Morlet wavelet, a Gaussian window was scaled and shifted over time, while amplitudes were computed on the basis of average wavelet coefficients, thus the spectral attributes of the oscillators were derived. A spectral scalogram was then generated. Variables such as time (second), frequency (Hz), and spectral amplitude (AU) were situated within the coordinate system. Finally, the amplitudes of the six oscillators were compared across the different groups.

Liver function evaluation

Blood samples were collected from the inferior vena cava and then centrifuged at 3000 rpm for 20 minutes to obtain the serum. Subsequent biochemical analyses were conducted at the clinical laboratory of Peking Union Medical College Hospital, utilizing an automated biochemical analyzer (Beckman Coulter, United States) and an automatic protein analyzer (Siemens, Germany). The serum levels of alanine aminotransferase (ALT) (measured with the lactate dehydrogenase method), aspartate aminotransferase (AST) (measured with the malate dehydrogenase method), alkaline phosphatase (ALP) (measured with the nitrophenyl phosphate substrate-adenosine monophosphate buffer method), glucose (Glu) (measured with the hexokinase method), total protein (TP) (measured *via* biuret colorimetry) and total bile acid (TBA) (measured with an enzymatic cycling assay) were quantitatively determined. The selected markers were chosen because of their ability to reflect liver health and dysfunction. Each marker serves a distinct role in liver function, and tests to measure the levels of these markers are crucial for diagnosing liver diseases and monitoring their progression. ALT and AST are key indicators of hepatocellular injury, with elevated levels indicating liver cell damage. Elevated ALP levels indicate the potential for cholestasis or bile duct obstruction, while abnormal Glu levels indicate impaired metabolic function. TP levels, particularly albumin levels, are indicative of the synthetic capacity of the liver, with decreased levels indicating chronic disease. TBA levels reflect the ability of the liver to process bile acids; elevated levels suggest dysfunction. Reference intervals for the evaluated hepatic function parameters in mice were established on the basis of previous literature[21-23].

Histology and immunohistochemistry

For morphological studies, tissues were fixed with 4% paraformaldehyde, embedded in paraffin, and cut into 5 μm thick slices using a microtome (Leica Biosystems, Germany) for hematoxylin and eosin and immunohistochemical staining. For antigen retrieval, the slices were deparaffinized, rehydrated, and incubated in boiling 10 mmol/L citrate buffer (potential of hydrogen = 6.0; Zhongshan Golden Bridge Biotechnology, Beijing, China). The sections were subsequently incubated with 3% hydrogen peroxide to inhibit endogenous peroxidase activity, followed by blocking with 3% bovine serum albumin (TBD Science Technology, Tianjin, China) in phosphate-buffered saline. The sections were incubated in blocking buffer overnight at 4 °C, after incubating with primary mouse monoclonal antibodies against cluster of differentiation (CD) 31 (diluted 1:100; Santa Cruz Biotechnology), mouse estrogen receptor α (ERα) and estrogen receptor β (ERβ) monoclonal antibodies (diluted 1:25; Abcam). Horseradish peroxidase-conjugated secondary antibody (Zhongshan Golden Bridge Biotechnology, Beijing, China) and 3,3′-diaminobenzidine tetrahydrochloride solution (Zhongshan Golden Bridge Biotechnology, Beijing, China) were subsequently used for the incubation of sections, after which the section were dehydrated and mounted. An antibody mixture (Ambiping Medical Technology, Guangzhou, Guangdong Province, China) was used as an isotype control. Positive staining was detected using a Leica DFC450 microscope (Leica Microsystems, Leitz, Germany). For quantitative evaluation, ImageJ software (National Institutes of Health, Bethesda, MD, United States) was used to capture and analyze the digital images of the stained sections. In addition, the intensity of CD31, ERα and ERβ positive staining was quantified by calculating the integrated density. Microvascular density (MVD) was determined and quantified through manual counting of six random × 40 fields to obtain an average. In selecting these fields, we ensured optimal staining with vascular markers (CD31, ERα, and ERβ) for effective visualization, encompassing diverse tissue regions while excluding artifacts and avoiding overlapping fields.

Statistical analysis

All the measurements were performed in duplicate to ensure reliability. The statistical analysis was conducted with GraphPad Prism software (version 8.02; GraphPad Software, CA, United States). The data derived from laser Doppler signals and wavelet analysis were presented as the mean ± SEM. We employed two-factor analysis of variance (ANOVA) with interaction effects, incorporating sex and strain as independent variables. In cases of non-significant overall ANOVA results, we refrained from post-hoc comparisons to avoid misleading conclusions, and conducted further analyses only when significant main effects or interactions were observed, with Tukey's method applied for multiple comparisons to control the familywise error rate. Statistical significance was assessed using a predefined alpha threshold of 0.05. To elucidate the relationships between hepatic function and hepatic microhemodynamics in three murine strains, segregated by sex, both the Mantel test and Pearson correlation analysis were utilized. The Mantel test was used to assess relationships between distance matrices, especially those relevant to genetic divergence, while Pearson correlation was used to linear relationships. Pearson's correlation coefficients (r) were considered relevant for Pearson's $P < 0.05$ and values of $r > 0.4$ or $r < -0.4$.

RESULTS

Sexual dimorphism in hepatic microvascular perfusion across murine strains

Sex-specific differences in hepatic microvascular blood flux were evident, with males consistently demonstrating higher perfusion levels across all strains (all $P < 0.001$), suggesting a sex-determined influence on the variability of hepatic microvascular blood flux. Conversely, no significant sex differences in respiratory oscillations in hepatic microvascular blood flux were observed within each strain (Supplementary Table 1), although female KM mice exhibited greater oscillatory activity than their BALB/c and C57BL/6J counterparts did ($P < 0.01$) (Figure 1), suggesting strain-dependent modulation of hepatic microcirculation. Collectively, these findings illuminate the substantial heterogeneity in hepatic microvascular perfusion that may affect the responsiveness of the liver to physiological demands.

Disparities in hepatic microvascular erythrocyte concentration by sex and strain

Erythrocytes regulate endothelial and microvascular functions through the modulation of oxygen delivery. Significant sexual dimorphism of the erythrocyte concentration within the hepatic microvasculature was observed across all strains (all $P < 0.001$) (Supplementary Table 2). Compared with females, males of the C57BL/6J and KM strains presented increased erythrocyte concentrations, however, in BALB/c mice, where this trend was reversed (Figure 2A). Detailed analysis of endothelial oscillator amplitudes revealed that, compared with KM females, KM males had lower amplitudes in the endothelial frequency range (0.01 Hz-0.04 Hz), whereas C57BL/6J females presented the highest amplitudes (Figure 2B). KM males presented the lowest amplitudes relative to those of other strains (Figure 2C). Quantitative analysis of sex-related disparities in erythrocyte concentration oscillators at corresponding frequencies (Figure 2D) revealed that KM males presented increased enhanced endothelial oscillatory activity. Specifically, significant differences in both NO-independent ($P < 0.05$) and NO-dependent ($P < 0.05$) endothelial amplitudes were detected between KM females and males. Although no significant differences were revealed across other variables within the BALB/c and C57BL/6J strains, significant differences were identified in NO-independent endothelial oscillator amplitudes between C57BL/6J and KM males ($P < 0.05$). Collectively, these findings indicate heterogeneity in erythrocyte concentration, suggesting the multifaceted regulation of hepatic microcirculation by both sex and genetic determinants within these murine models.

Variation in hepatic microvascular blood velocity across mouse strains and between the sexes

The distribution of blood flow and erythrocyte fluxes within the hepatic microvascular network is critical for velocity. As shown in Figure 3A and Supplementary Table 3, significant variations in hepatic microvascular blood velocity were observed between the sexes and across the mouse strains. Compared with their male counterparts, female BALB/c mice presented higher microvascular velocities. Conversely, the C57BL/6J and KM strains demonstrated the opposite pattern, with males displaying lower velocities. Wavelet transform analysis revealed significant differences primarily in the amplitudes of cardiac and myogenic oscillators (Figure 3B and C). Compared with male C57BL/6J mice, female C57BL/6J mice presented greater variance in cardiac oscillator amplitudes. Figure 3D highlights the distinctive patterns in the myogenic oscillator of blood velocity, particularly in C57BL/6J and KM male mice. These findings suggest the role of sex and genetic strain in interpreting hepatic blood velocity, suggesting that both factors significantly influence associated physiological functions.

Histopathological analysis of sex-specific variations in the hepatic microvasculature

We subsequently performed hematoxylin and eosin staining to assess structural differences in the hepatic microvasculature. Additionally, we employed immunohistochemistry to evaluate the expression patterns of the endothelial cell marker CD31, ERα and ERβ, aiming to elucidate their potential roles in modulating these microhemodynamic variations. As shown in Figure 4A and B, Supplementary Figure 1 and Supplementary Table 4, contrary to expectations, no significant sex-based differences in the expression levels of ERα and ERβ were observed within the hepatic microvasculature. However, among the male mice, C57BL/6J mice presented significantly elevated expression levels of both ERα and ERβ compared with BALB/c and KM mice (all $P < 0.05$). In contrast, analysis of CD31 expression levels revealed significant sex differences across all strains. Compared with their male counterparts, female BALB/c and KM mice presented significantly greater CD31 expression levels, whereas C57BL/6J females presented a lower CD31 expression level ($P < 0.01$ for all comparisons). Additionally, MVD analysis indicated that males across all three strains presented greater MVD than females did (all $P < 0.05$, Figure 4C). Collectively, these findings suggest that CD31 plays a role in mediating sex differences in the observed microhemodynamic variations.

Correlation analysis of liver function indictors and hepatic microhemodynamics

To exclude the confounding effects of body weight heterogeneity on microhemodynamics, we employed a dual analytical approach comprising two-way ANOVA and correlation analysis. Two-way ANOVA revealed significant differences and interactions in body weight [F-ratio (2, 30) = 5.427; $P = 0.009$] (Supplementary Tables 5 and 6). Male C57BL/6 mice presented significantly greater body weights than females did ($P < 0.0001$), a trend not observed for the BALB/c and KM strains. KM mice consistently surpassed both C57BL/6 and BALB/c mice in terms of body mass, irrespective of sex (all $P < 0.0001$). These findings highlight the influence of genetic strain and sex on phenotypic diversity, however, these weight differences do not directly correlate with changes in hepatic microhemodynamics (Figure 5).

Liver function revealed sex differences in the serum ALP and TBA levels across the three mouse strains, as shown in Figure 5A and Supplementary Table 7. Females consistently presented higher TBA levels than males did, regardless of strain. Conversely, among KM mice, females presented significantly lower serum TP levels than males did. Strain-specific

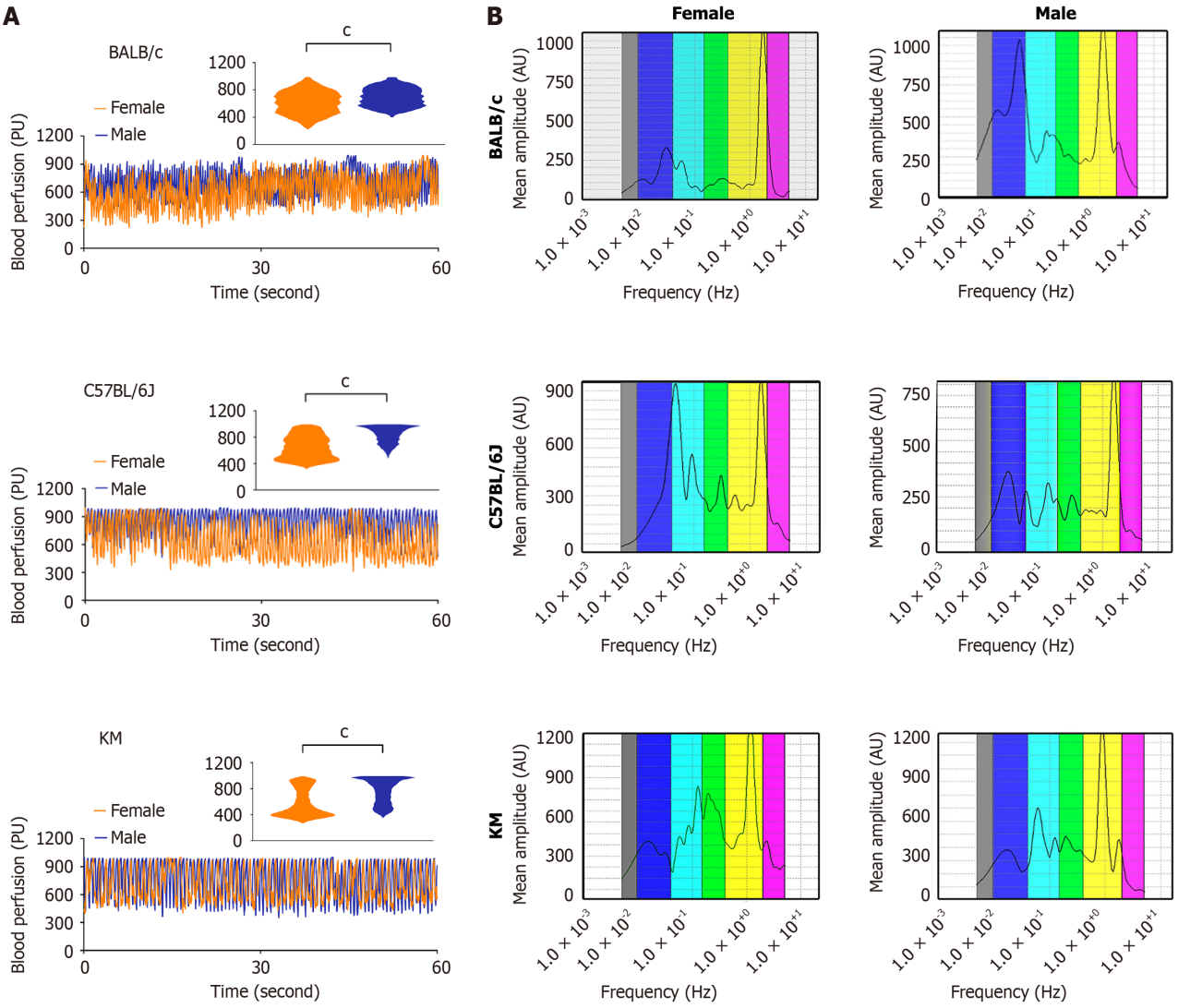
A
BALB/c
C57BL/6J
KM
Female
Male
Blood perfusion (PU)
Time (second)
B
Female
Male
BALB/c
C57BL/6J
KM
Mean amplitude (AU)
Frequency (Hz)
C
BALB/c
C57BL/6J
KM
Female
Male
Spectral amplitude
Frequency
Time (second)
High
Low

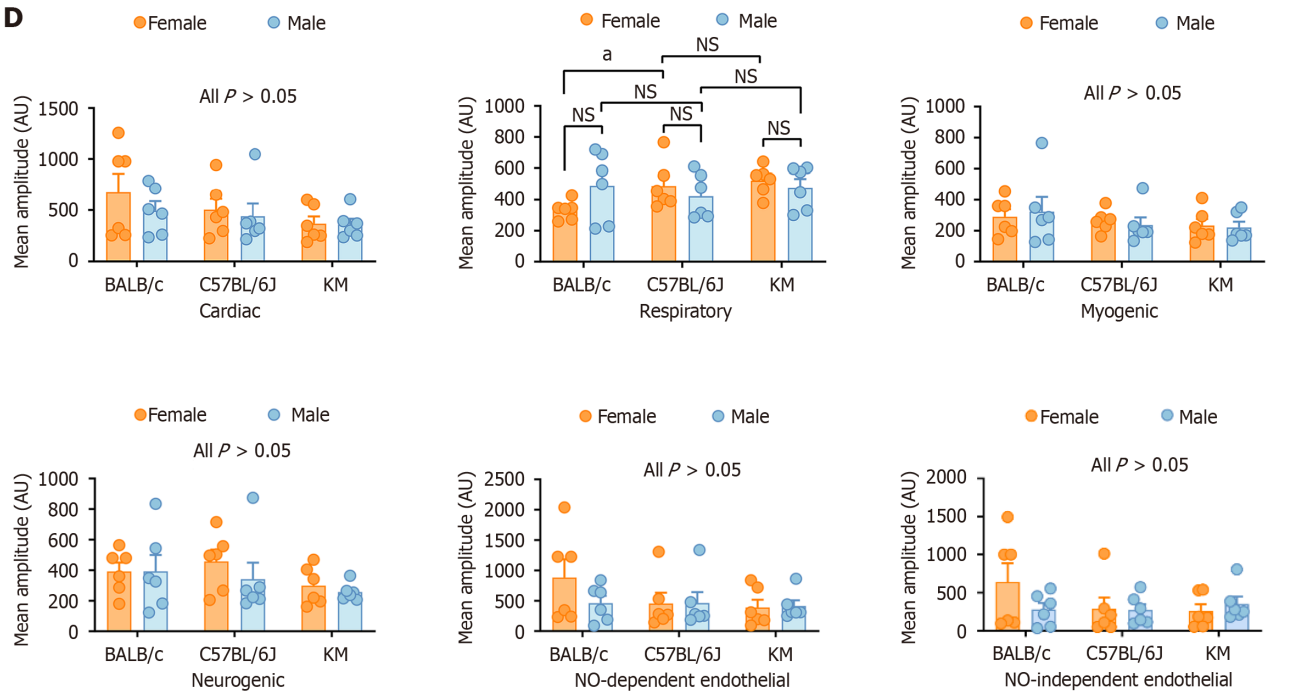

Figure 1 Comparative analysis of hepatic microcirculatory blood perfusion and characteristic oscillatory amplitudes between sexes and across three mouse strains. A: Hepatic microcirculatory blood perfusion patterns in the BALB/c, C57BL/6J, and KM mouse strains. The rectangular insert highlights the extracted pattern of microcirculatory blood distribution; B and C: Two-dimensional and three-dimensional spectral scalograms representing the characteristic amplitudes of hepatic microcirculation profiles; D: Quantitative analysis of characteristic oscillatory amplitudes in hepatic microcirculatory blood perfusion profiles. The data are presented as the mean ± SEM. n = 6 each group. $^{a}P < 0.05$. $^{c}P < 0.001$. AU: Amplitude; NO: Nitric oxide; NS: Not significant; PU: Perfusion unit.

differences were also identified: BALB/c females had significantly lower serum AST, TBA, and ALP levels than C57BL/6J females did (all $P < 0.0001$). Similarly, compared with C57BL/6J females, KM females presented lower serum TBA and ALP levels (all $P < 0.0001$). To investigate the potential influence of microhemodynamics on liver function, we analyzed the spectral components of microhemodynamics and their associations with hepatic parameters across sexes and strains. The significant correlations between the physiological amplitudes of hepatic microcirculation and liver function parameters are shown in Figure 5B and C and Supplementary Table 8. The ALT level was significantly positively correlated with the neurogenic amplitude of blood speed ($r = 0.342$, $P = 0.041$), and the AST level was similarly positively correlated with myogenic indicators of blood speed ($r = 0.333$, $P = 0.047$). Additionally, the TBA level was positively correlated with both the neurogenic amplitude of the erythrocyte concentration ($r = 0.384$, $P = 0.021$) and the blood speed ($r = 0.400$, $P = 0.016$). Conversely, the Glu level was negatively correlated with the respiratory amplitude of the erythrocyte concentration ($r = -0.342$, $P = 0.041$). Furthermore, similar correlations were observed between macrocirculatory microhemodynamics and liver function (Supplementary Table 9), with ALT and AST levels being correlated negatively with systolic blood pressure ($r = -0.428$, $P = 0.009$; $r = -0.464$, $P = 0.004$) and positively with diastolic blood pressure ($r = 0.449$, $P = 0.006$; $r = 0.491$, $P = 0.006$). These results suggest that the complex interplay between liver function and hepatic microhemodynamics is influenced by both sex and strain.

DISCUSSION

The liver has a complex microvascular network that is crucial for its diverse functions. The sex-based disparities in hepatic microcirculation indicate fundamental physiological adaptations and pathological vulnerabilities. Physiologically, increased microvascular perfusion and erythrocyte concentrations in male mice reflect an adaptive mechanism to meet heightened metabolic and anabolic demands[24], potentially mediated by androgen-driven modulation of endothelial function and erythropoiesis. This perfusion ensures efficient nutrient and oxygen delivery, supporting hepatocellular activity and resilience. In contrast, female mice exhibit lower perfusion rates coupled with higher blood velocity, suggesting a streamlined and efficient microvascular network possibly influenced by the vasodilatory and anti-inflammatory effects of estrogen[25,26]. Such configurations confer metabolic efficiency and increased clearance capacities, aligning with observed protective effects against metabolic liver diseases in females[27]. Pathologically, these sex-specific microcirculatory profiles have implications for liver disease susceptibility and progression. Elevated perfusion and erythrocyte load in males predispose them to increased shear stress and oxidative damage within the hepatic sinusoids, fostering an environment conducive to inflammatory cascades, fibrosis, and steatohepatitis[28-30]. The crosstalk between higher erythrocyte concentrations and reactive oxygen species (ROS) generation exacerbates hepatocellular injury,

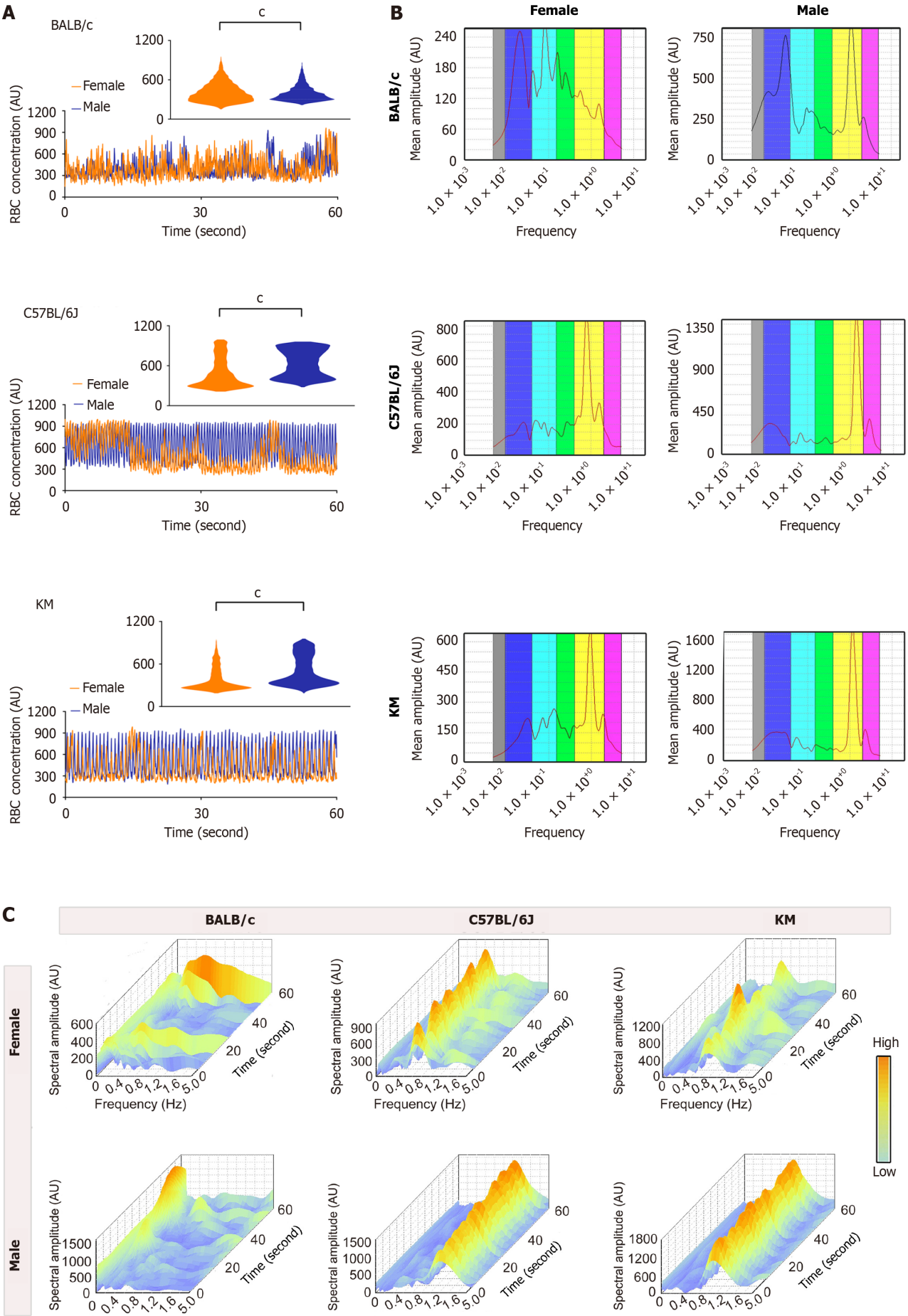
A
BALB/c
C57BL/6J
KM
Female
Male
RBC concentration (AU)
Time (second)
B
Female
Male
Mean amplitude (AU)
Frequency
C
BALB/c
C57BL/6J
KM
Female
Male
Spectral amplitude (AU)
Frequency (Hz)
Time (second)
High
Low

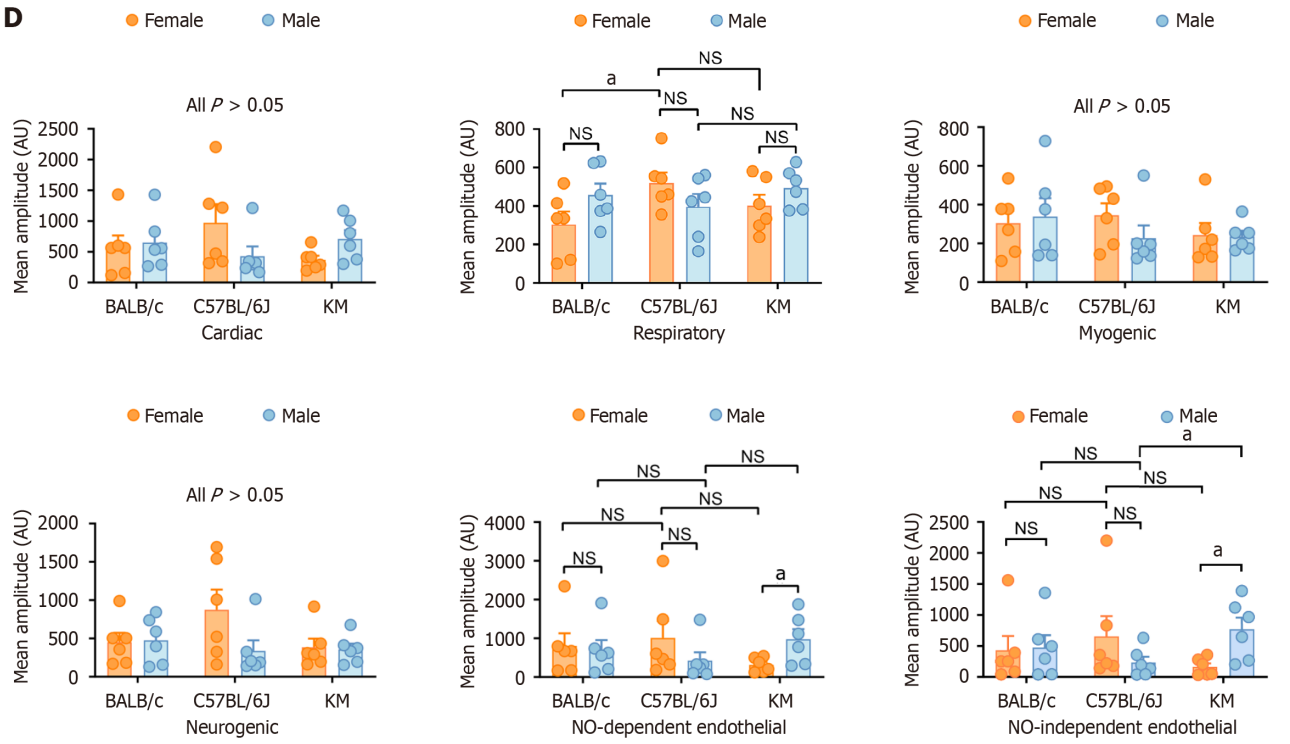

Figure 2 Comparative analysis of hepatic microcirculatory erythrocyte concentration between sexes and across three mouse strains. A: Microcirculatory erythrocyte concentration in BALB/c, C57BL/6J, and KM mice. The distribution pattern of erythrocyte concentration is presented in the rectangular insert; B and C: Two-dimensional and three-dimensional spectral scalograms illustrating the characteristic amplitude of the hepatic microcirculatory erythrocyte concentration; D: Quantitative assessment of the characteristic oscillatory amplitudes from the hepatic microcirculatory erythrocyte concentration profiles. The data are presented as the mean ± SEM. n = 6 each group. $^{a}P < 0.05$. $^{c}P < 0.001$. AU: Amplitude; NO: Nitric oxide; NS: Not significant; PU: Perfusion unit.

accelerating the transition from benign hepatic steatosis to severe fibrotic states. Conversely, the regulated blood flow and increased endothelial integrity in females mitigate excessive inflammatory responses and oxidative stress[31], thereby conferring resilience against progressive liver fibrosis and cirrhosis.

Our study also revealed strain-specific differences in microhemodynamics. These genetic determinants of hepatic microhemodynamics are rooted in divergent expression profiles of key regulatory proteins, including integrins, adhesion molecules[32], and intracellular signaling cascades that govern endothelial cell behavior and microvascular integrity. For example, polymorphisms in genes encoding for CD31 or estrogen receptors modulate endothelial function and responsiveness to hormonal cues, thereby influencing microvascular perfusion and erythrocyte dynamics. Additionally, strain-specific variations in mitochondrial efficiency and ROS handling could impact endothelial health and microcirculatory resilience, further diversifying hepatic responses to pathological stressors. Furthermore, genetic differences substantially influence microvascular structure and the expression of endothelial receptors and signaling pathways[33]. These findings emphasize the role of genetic determinants in shaping microvascular architecture and function, which in turn affect hepatic health. The variability in how different strains respond to similar physiological or pathological stimuli can be attributed to these genetic factors, which also correlate with the varying prevalence of hepatic conditions such as NAFLD and HCC in these models[34]. The differential expression of CD31 between sexes and across strains observed in our study indicates its role in maintaining endothelial integrity and regulating hepatic microcirculation. CD31 is essential for endothelial barrier function and leukocyte transmigration, while vascular endothelial growth factor receptor 1 (VEGFR1) orchestrates angiogenesis and macrophage recruitment during liver repair. The engagement of CD31 at sites of active vascular endothelial cell stimulation is essential for the maintenance of flow-driven physiological adjustments[35]. CD31 and VEGFR1 synergistically increase endothelial repair by modulating each other's signaling pathways. CD31 stabilizes VEGFR1 on the endothelial surface, thereby potentiating VEGFR1-mediated angiogenic responses essential for revascularization and tissue regeneration. Additionally, CD31-induced metabolic reprogramming toward glycolysis supports the energetic demands of VEGFR1-driven angiogenesis[36], particularly under the hypoxic conditions common in hepatic injury. Furthermore, the regulation of leukocyte transmigration by CD31 influences the local production of proangiogenic factors, creating a microenvironment that facilitates VEGFR1-mediated microvascular remodeling. Sex-specific hormonal differences modulate this processing, accounting for the observed disparities in microhemodynamics.

The sex-based disparities observed in hepatic microhemodynamics, especially the elevated microvascular perfusion and density in male mice alongside higher TBA levels in females, indicate differential susceptibility to liver diseases between the sexes. Elevated microvascular perfusion and increased MVD in males may facilitate a more extensive distribution of profibrotic and oncogenic factors within the liver, potentially exacerbating conditions such as hepatic fibrosis and HCC, which are more prevalent in males clinically. This increased perfusion could be driven by testosterone-mediated upregulation of angiogenic factors such as VEGF, promoting endothelial proliferation and microvascular expansion. Conversely, higher TBA levels in females reflect efficient bile acid metabolism and clearance, supporting

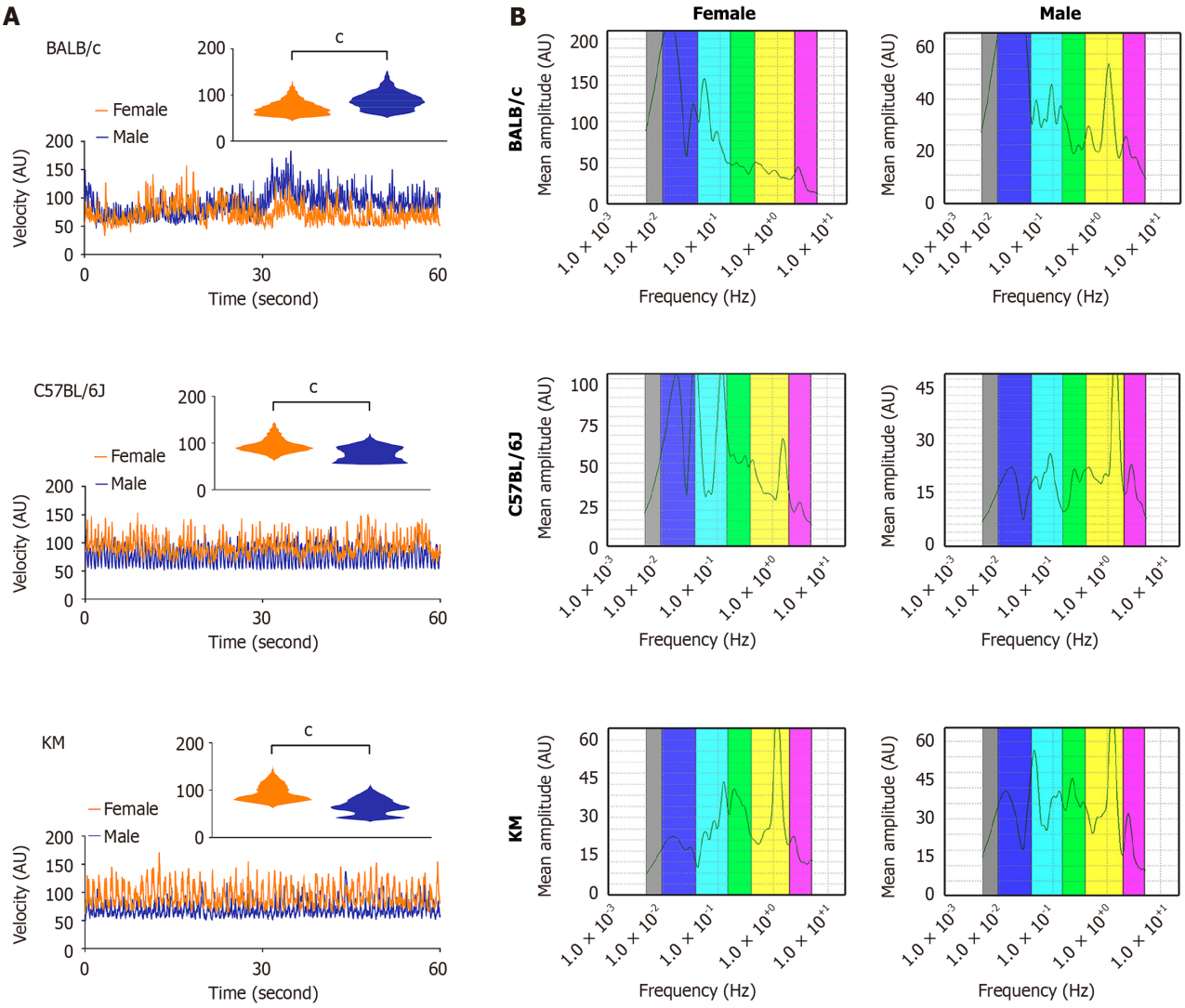
A
BALB/c
C57BL/6J
KM
Female
Male
Velocity (AU)
Time (second)
B
Female
Male
Mean amplitude (AU)
Frequency (Hz)

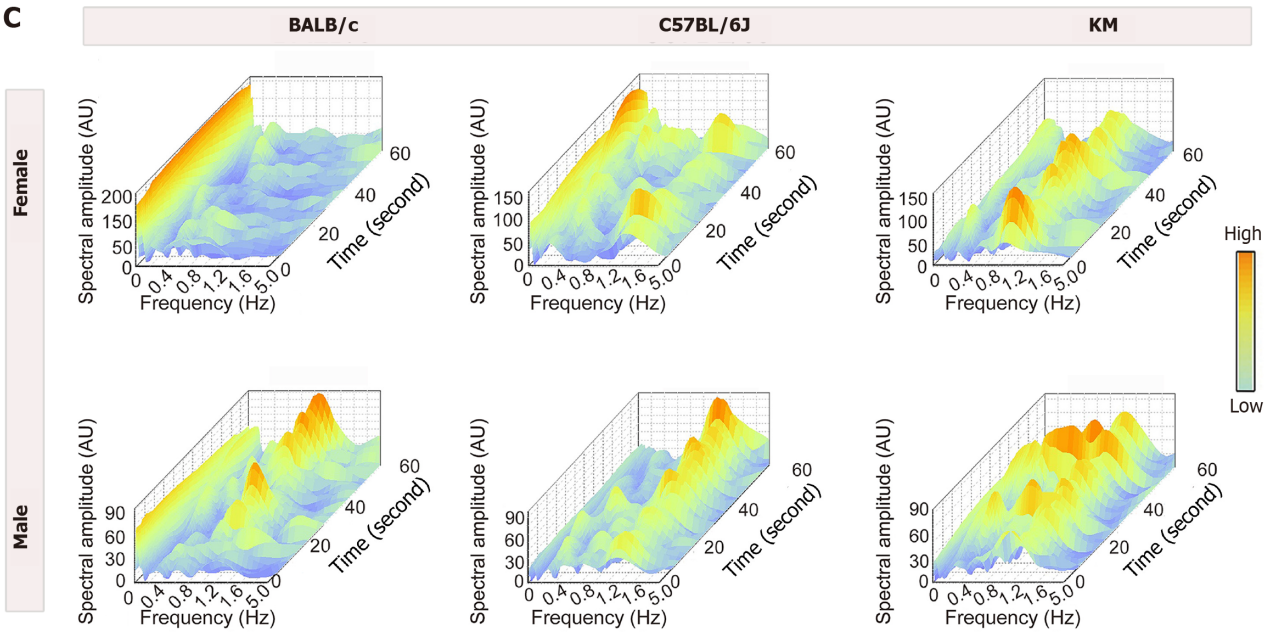
C
BALB/c
C57BL/6J
KM
Female
Male
Spectral amplitude (AU)
Frequency (Hz)
Time (second)
High
Low

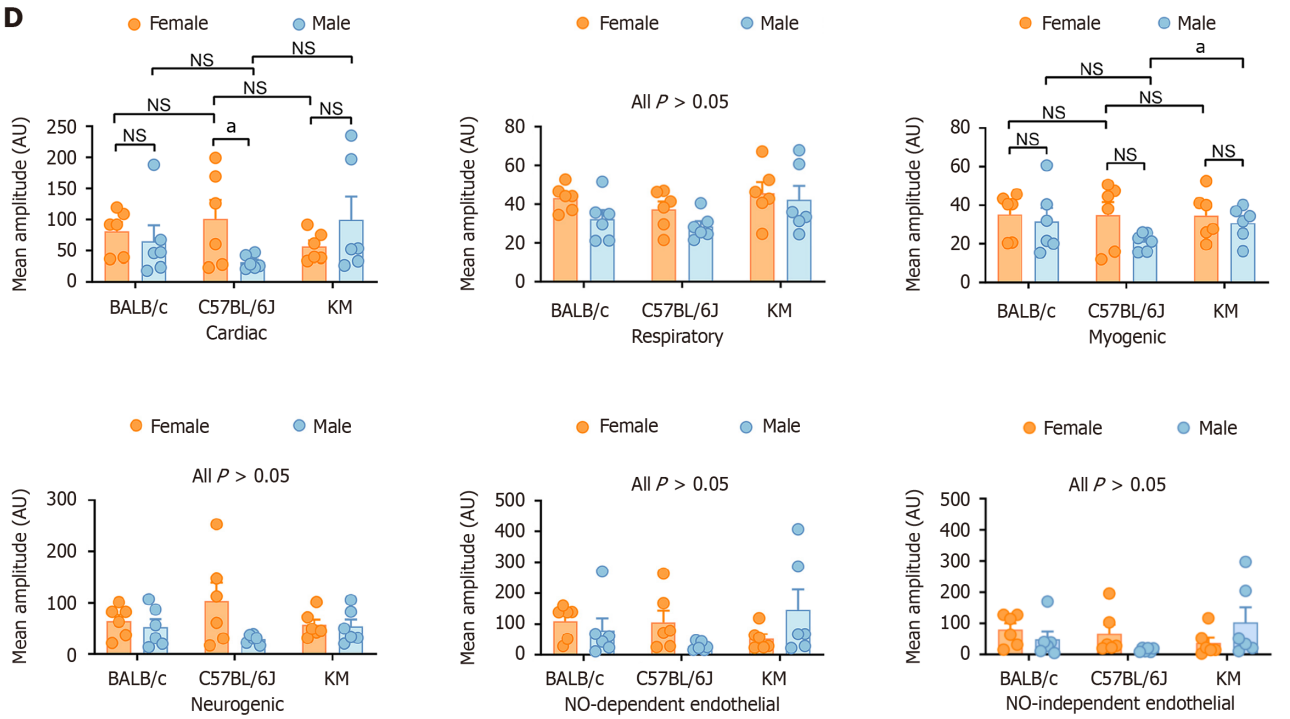

Figure 3 Comparative analysis of hepatic microcirculatory blood velocity between sexes and across three mouse strains. A: Hepatic microcirculatory blood velocity in BALB/c, C57BL/6J, and KM mice. The rectangular insert provides a detailed view of the hepatic microcirculatory blood velocity distribution pattern; B and C: Two-dimensional and three-dimensional spectral scalograms demonstrating the characteristic amplitudes of the hepatic microcirculatory blood velocity profiles; D: Quantitative analysis of the characteristic oscillatory amplitudes in the hepatic microcirculatory blood velocity profiles. The data are presented as the mean ± SEM. n = 6 each group. $^{a}P < 0.05$. $^{c}P < 0.001$. AU: Amplitude; NO: Nitric oxide; NS: Not significant; PU: Perfusion unit.

protective effects against lipid accumulation and insulin resistance, thereby reducing the risk of NAFLD and its progression to severe liver pathologies. Additionally, the vasoprotective and anti-inflammatory properties of estrogen may contribute to a regulated microvascular environment in females, mitigating excessive vascular remodeling and fibrosis. The lack of significant differences in estrogen receptor expression suggests that downstream signaling pathways, rather than receptor abundance, mediate these protective effects. Furthermore, the correlation between microhemodynamic data and levels of liver function markers such as ALT and AST suggest that microvascular dysfunction could serve as an early biomarker for hepatic injury[37], preceding overt biochemical disturbances[38]. This evidence provides support for sex- and genetic-specific diagnostic and therapeutic strategies, where modulating microcirculatory parameters could ameliorate disease trajectories. For example, increasing endothelial function and optimizing erythrocyte dynamics in males provide protective benefits, while leveraging estrogenic pathways in females could sustain vascular health and functional integrity. While the integration of microhemodynamic data with traditional biochemical markers holds promise for improving liver disease management[39], challenges remain. These findings suggests that microcirculatory assessments could significantly improve the early detection and monitoring of liver diseases[40], such as NAFLD and hepatic fibrosis. By integrating microhemodynamic data with traditional biochemical markers, clinicians could increase their accuracy of disease staging and progression tracking, potentially allowing timely implementation of interventions before substantial biochemical abnormalities arise.

Integrating our hepatic microhemodynamic findings with the findings of previous parallel studies on renal and intestinal microcirculation provides an overview of the systemic orchestration of microvascular function modulated by sex and genetic background[41,42]. Across the liver, kidneys, and intestine, male mice consistently exhibited elevated microvascular perfusion and erythrocyte concentrations but demonstrated lower blood velocities than females did, a phenomenon likely driven by sex hormones that influence endothelial responsiveness and vascular tone. Strain-specific differences, particularly in endothelial oscillatory characteristics, highlight the genetic predispositions that shape microvascular architecture and functionality. These organ-centric disparities reflect the interconnected nature of the systemic microcirculation, where hepatic, renal, and intestinal vessels collaboratively sustain overall physiological homeostasis, which informs the development of targeted therapeutic strategies that account for genetic and sex-related variability, thereby increasing the efficacy of interventions aimed at preserving or restoring microvascular function across multiple organ systems.

Building on our findings of sex- and strain-specific hepatic microcirculatory variations, targeted therapeutic strategies can be developed to modulate microvascular flow and improve endothelial function[43], particularly for conditions such as hepatic fibrosis and HCC[44,45]. Genetic and sex-specific profiles should be integrated in personalized medicine approaches to optimize treatments. For instance, utilizing vasodilators or NO promoting agents tailored to individual microcirculatory patterns could normalize blood flow and mitigate fibrosis progression[46]. Increasing endothelial integrity through antioxidants could prevent endothelial dysfunction and inhibit tumor angiogenesis in HCC. Addi-

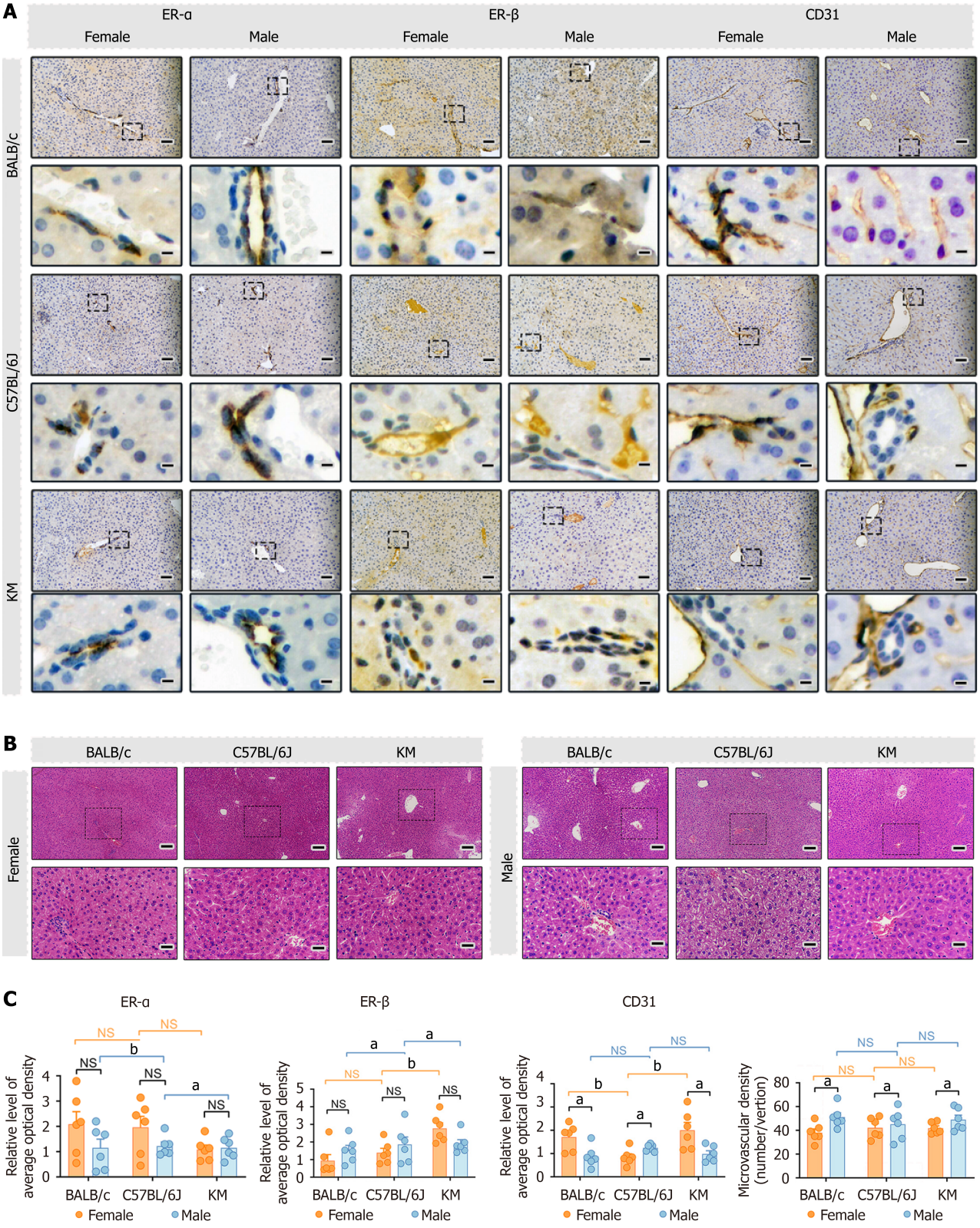

Figure 4 Hematoxylin and eosin staining and immunolabeling analysis of liver tissue from different sexes across BALB/c, C57BL/6J, and KM mice. A: Hematoxylin and eosin (HE) and immunohistochemical staining of estrogen receptor α (ERα), and estrogen receptor β (ERβ), and cluster of differentiation (CD) 31 in the liver. The scale bar represents 50 μm. The insert in the lower panel provides a detailed representation of liver tissues at a higher magnification. Scale bar = 10 μm; B: HE staining of liver tissue sections revealing morphological details. Scale bar = 200 μm. The insert in the lower panel provides a detailed representation of liver tissues at a higher magnification. Scale bar = 50 μm; C: Quantitative analysis of the protein expression levels of ERα, ERβ, and CD31 and the microvascular density in the livers of BALB/c, C57BL/6J, and KM mice. For each group, n = 6 samples, and six microscopic fields of view were selected for each sample. The data are presented as the mean ± SEM. n = 6 each group. $^{a}P < 0.05$. $^{b}P < 0.01$. NS: Not significant; Erα: Estrogen receptor α; Erβ: Estrogen receptor β; CD31: Cluster of differentiation 31.

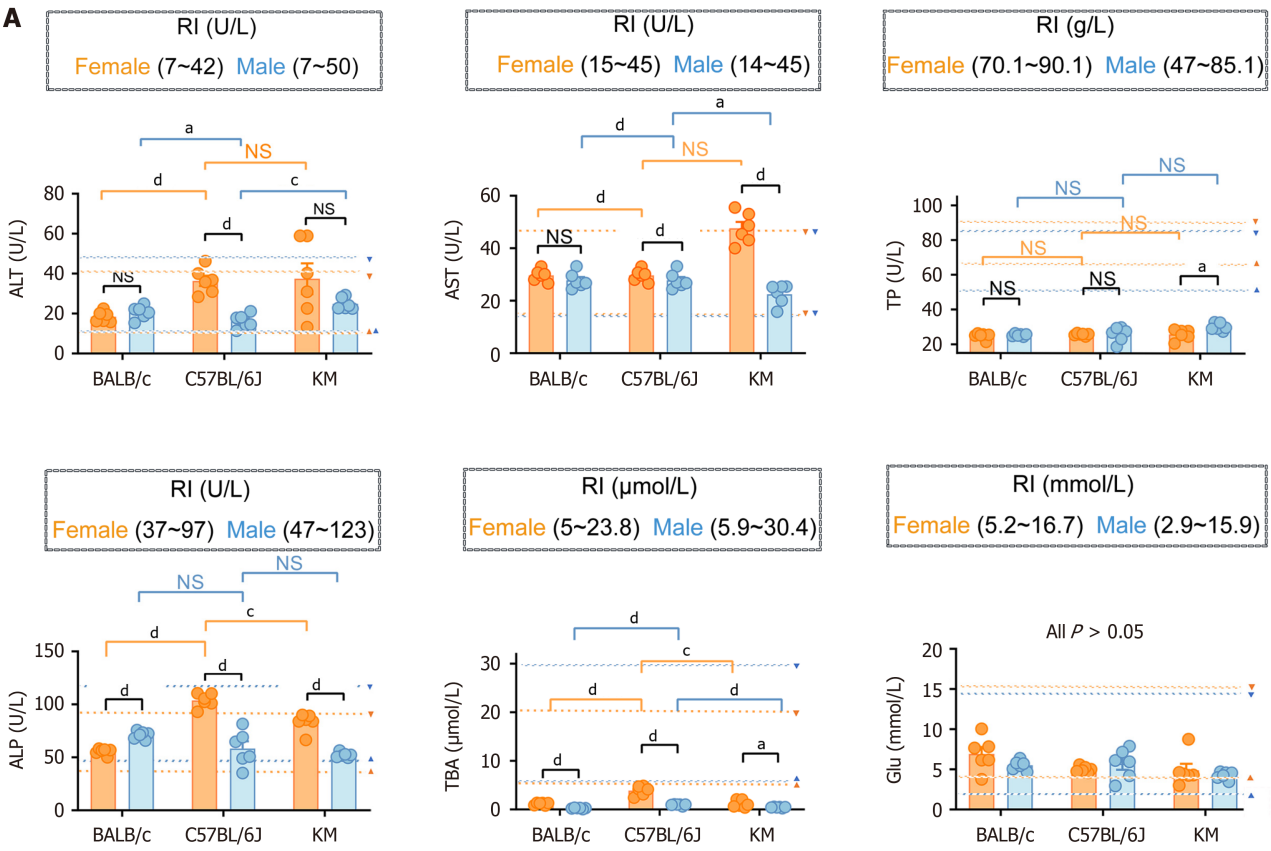
A
RI (U/L)
Female (7~42) Male (7~50)
ALT (U/L)
RI (U/L)
Female (15~45) Male (14~45)
AST (U/L)
RI (g/L)
Female (70.1~90.1) Male (47~85.1)
TP (U/L)
RI (U/L)
Female (37~97) Male (47~123)
ALP (U/L)
RI (μmol/L)
Female (5~23.8) Male (5.9~30.4)
TBA (μmol/L)
RI (mmol/L)
Female (5.2~16.7) Male (2.9~15.9)
All P > 0.05
Glu (mmol/L)
BALB/c
C57BL/6J
KM
NS

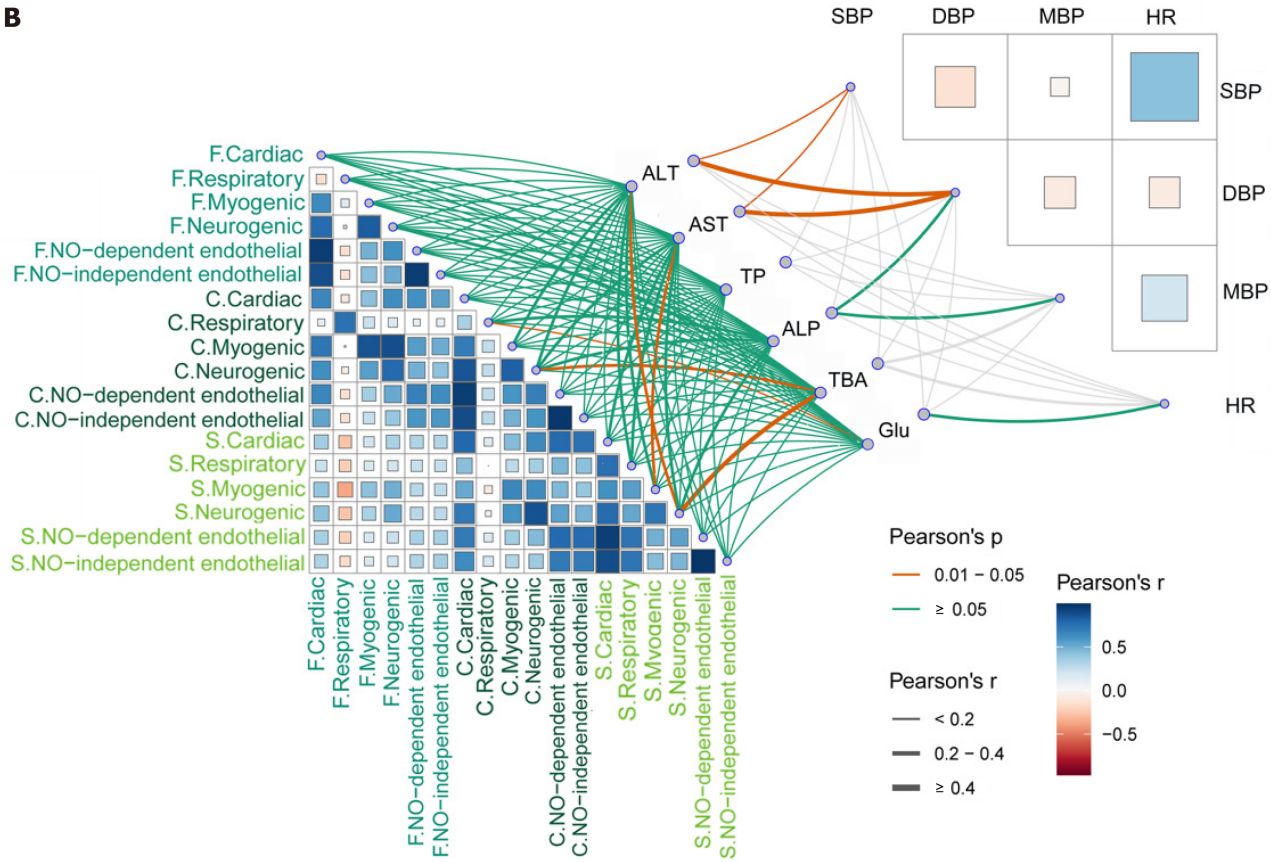
B
SBP
DBP
MBP
HR
F.Cardiac
F.Respiratory
F.Myogenic
F.Neurogenic
F.NO−dependent endothelial
F.NO−independent endothelial
C.Cardiac
C.Respiratory
C.Myogenic
C.Neurogenic
C.NO−dependent endothelial
C.NO−independent endothelial
S.Cardiac
S.Respiratory
S.Myogenic
S.Neurogenic
S.NO−dependent endothelial
S.NO−independent endothelial
ALT
AST
TP
ALP
TBA
Glu
Pearson's p
0.01 − 0.05
≥ 0.05
Pearson's r
< 0.2
0.2 − 0.4
≥ 0.4
Pearson's r
0.5
0.0
−0.5

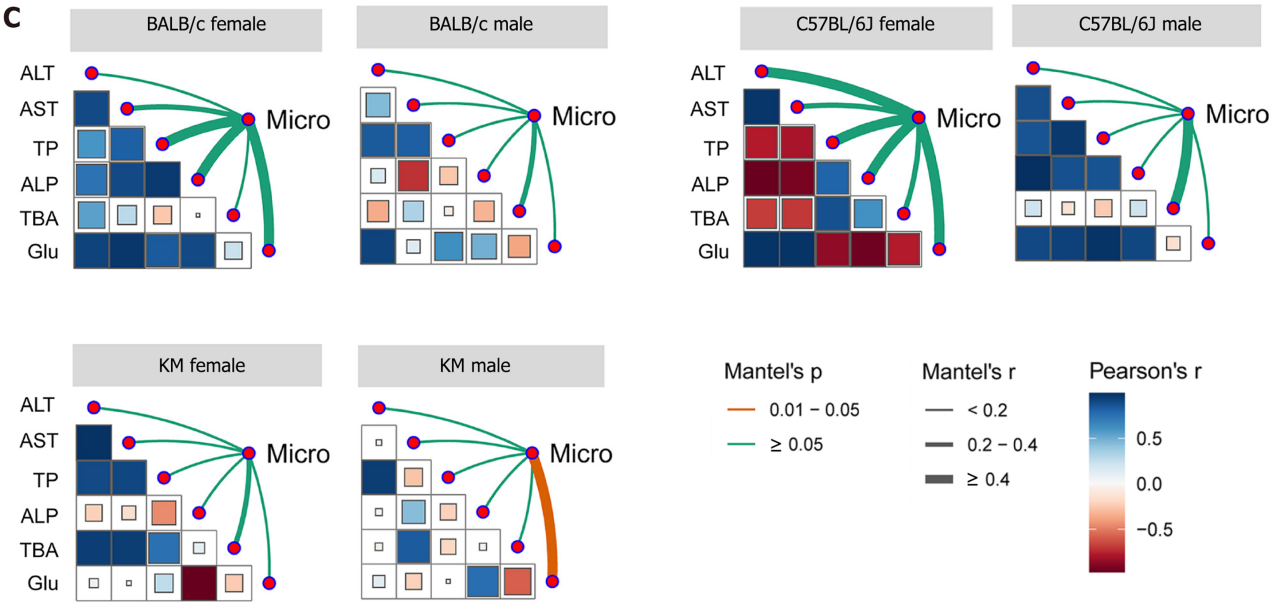

Figure 5 Relationship among hepatic microhemodynamics, liver function and macrohemodynamics. A: Cross-comparison of liver function between different mouse strains and sexes. The established reference values for each of the five indicators are marked with dashed lines, with triangles serving as indicating markers. Yellow represents females, whereas blue signifies males; B: Interrelationships among the mean amplitudes of the three microhemodynamic indicators and macrohemodynamic indicators were analyzed using Pearson correlation analysis. The correlations among liver function indicators, hepatic microhemodynamics, and blood pressure and heart rate were shown respectively with connecting lines indicating these relationships. Microhemodynamics indicators: Flux, concentration, and speed; Liver function indicators: Alanine aminotransferase, aspartate aminotransferase, total protein, alkaline phosphatase, total bile acid, and glucose; Macrohemodynamics indicators: Heart rate, systolic blood pressure, mean arterial pressure, and diastolic blood pressure. *P* values are represented by the color, and *r* values are represented by the line thickness; C: The relationships between microhemodynamics and liver function, across different mouse strains and between sexes, were independently analyzed using the Mantel test (n = 6 each group). The edge width signifies the correlation strength, while the edge color indicates statistical significance. "Micro" indicates the mean amplitude of the five characteristic frequencies of flux, concentration, and speed. The data are presented as the mean ± SEM. n = 6 each group. $^{a}P < 0.05$. $^{c}P < 0.001$. $^{d}P < 0.0001$. RI: Respiratory index; ALT: Alanine aminotransferase; AST: Aspartate aminotransferase; TP: Total protein; ALP: Alkaline phosphatase; TBA: Total bile acid; Glu: Glucose; SBP: Systolic blood pressure; HR: Heart rate; DBP: Diastolic blood pressure; MBP: Mean arterial pressure.

tionally, genetic screening for variants such as PNPLA3 could inform the selection of microcirculatory modulators[47], ensuring therapies are aligned with genetic predispositions. Incorporating hormone-based treatments, such as selective estrogen receptor modulators for females, could further refine efficacy and reduce adverse effects. Advanced drug delivery systems, such as nanoparticle carriers targeting endothelial cells[48], promise precise intervention within the hepatic microenvironment[49], maximizing therapeutic impact while minimizing systemic toxicity.

Strengths and limitations

Our study of hepatic microcirculation across different murine strains and between sexes has several limitations. Environmental factors such as stress, microbial exposure, and diet were not fully controlled, potentially confounding our observations of strain- and sex-related differences. The mechanisms underlying the sex- and strain-based differences observed remain unknown, particularly the roles of sex hormones. Additionally, the genetic diversity represented by the three murine strains does not capture the full spectrum. Moreover, our cross-sectional approach does not account for changes over time, necessitating longitudinal studies to fully understand the dynamics of hepatic microcirculation.

CONCLUSION

Our study highlights the heterogeneous nature of hepatic microhemodynamics, which is influenced by sex and genetic background. These findings improve our understanding of the contributions of the microcirculation to hepatic health and disease and highlight the importance of incorporating sex and genetic factors into future hepatic investigations, which could lead to personalized therapeutic strategies.

FOOTNOTES

Author contributions: Liu MM conceived and designed research; Wang B, Li Y, Ouyang Q, Xu MT, Fu SJ, Wang YY performed experiments; Xu MT, Liu WQ, Fu SJ, Wang YY analyzed data; Wang B, Xu MT interpreted results of experiments; Wang B prepared figures, drafted manuscript; Liu XT, Ling H, Zhang X, Xiu RJ, Liu MM edited and revised manuscript, approved final version of manuscript.

Supported by the Beijing Municipal Natural Science Foundation, No. 7212068; and the National Natural Science Foundation of China, No. 81900747.

Institutional review board statement: This study did not involve human participants, consequently, institutional review board statement and approval, and informed consent procedures were not applicable.

Institutional animal care and use committee statement: All procedures involving animals were reviewed and approved by the Institutional Animal Care and Use Committee of the Institute of Microcirculation, Chinese Academy of Medical Sciences and Peking Union Medical College (No. CAMS-IM-IACUC-2022-AE-09-17).

Conflict-of-interest statement: The authors declare that they have no conflict of interest.

Data sharing statement: Technical appendix, statistical code, and dataset available from the corresponding author at mingmingliu@imc.pumc.edu.cn.

ARRIVE guidelines statement: The authors have read the ARRIVE guidelines, and the manuscript was prepared and revised according to the ARRIVE guidelines.

Country of origin: China

ORCID number: Bing Wang 0000-0002-7287-0852; Yuan Li 0000-0002-0065-9038; Qin Ouyang 0009-0003-8813-4045; Meng-Ting Xu 0000-0002-4430-1302; Ying-Yu Wang 0009-0008-0206-7264; Sun-Jing Fu 0000-0002-2064-0537; Wei-Qi Liu 0009-0000-4022-0524; Xue-Ting Liu 0000-0002-4281-4462; Hao Ling 0000-0003-4786-6787; Xu Zhang 0000-0003-4499-2331; Rui-Juan Xiu 0000-0002-1446-2711; Ming-Ming Liu 0000-0002-6750-5068.

S-Editor: Fan M
L-Editor: A
P-Editor: Zhao S

REFERENCES

1 **McCuskey RS**. The hepatic microvascular system in health and its response to toxicants. *Anat Rec (Hoboken)* 2008; **291**: 661-671 [PMID: 18484612 DOI: 10.1002/ar.20663]
2 **McCuskey RS**. Morphological mechanisms for regulating blood flow through hepatic sinusoids. *Liver* 2000; **20**: 3-7 [PMID: 10726955 DOI: 10.1034/j.1600-0676.2000.020001003.x]
3 **Burra P**, Zanetto A, Schnabl B, Reiberger T, Montano-Loza AJ, Asselta R, Karlsen TH, Tacke F. Hepatic immune regulation and sex disparities. *Nat Rev Gastroenterol Hepatol* 2024; **21**: 869-884 [PMID: 39237606 DOI: 10.1038/s41575-024-00974-5]
4 **Pirola CJ**, Salatino A, Quintanilla MF, Castaño GO, Garaycoechea M, Sookoian S. The influence of host genetics on liver microbiome composition in patients with NAFLD. *EBioMedicine* 2022; **76**: 103858 [PMID: 35092912 DOI: 10.1016/j.ebiom.2022.103858]
5 **Ramalho FS**, Fernandez-Monteiro I, Rosello-Catafau J, Peralta C. Hepatic microcirculatory failure. *Acta Cir Bras* 2006; **21** Suppl 1: 48-53 [PMID: 17013514 DOI: 10.1590/s0102-86502006000700012]
6 **Farrell GC**, Teoh NC, McCuskey RS. Hepatic microcirculation in fatty liver disease. *Anat Rec (Hoboken)* 2008; **291**: 684-692 [PMID: 18484615 DOI: 10.1002/ar.20715]
7 **Ruhl CE**, Everhart JE. Determinants of the association of overweight with elevated serum alanine aminotransferase activity in the United States. *Gastroenterology* 2003; **124**: 71-79 [PMID: 12512031 DOI: 10.1053/gast.2003.50004]
8 **Clark JM**, Brancati FL, Diehl AM. The prevalence and etiology of elevated aminotransferase levels in the United States. *Am J Gastroenterol* 2003; **98**: 960-967 [PMID: 12809815 DOI: 10.1111/j.1572-0241.2003.07486.x]
9 **Riazi K**, Azhari H, Charette JH, Underwood FE, King JA, Afshar EE, Swain MG, Congly SE, Kaplan GG, Shaheen AA. The prevalence and incidence of NAFLD worldwide: a systematic review and meta-analysis. *Lancet Gastroenterol Hepatol* 2022; **7**: 851-861 [PMID: 35798021 DOI: 10.1016/S2468-1253(22)00165-0]
10 **Du T**, Sun X, Yuan G, Zhou X, Lu H, Lin X, Yu X. Sex differences in the impact of nonalcoholic fatty liver disease on cardiovascular risk factors. *Nutr Metab Cardiovasc Dis* 2017; **27**: 63-69 [PMID: 27956025 DOI: 10.1016/j.numecd.2016.10.004]
11 **Yang JD**, Abdelmalek MF, Guy CD, Gill RM, Lavine JE, Yates K, Klair J, Terrault NA, Clark JM, Unalp-Arida A, Diehl AM, Suzuki A; Nonalcoholic Steatohepatitis Clinical Research Network. Patient Sex, Reproductive Status, and Synthetic Hormone Use Associate With Histologic Severity of Nonalcoholic Steatohepatitis. *Clin Gastroenterol Hepatol* 2017; **15**: 127-131.e2 [PMID: 27523635 DOI: 10.1016/j.cgh.2016.07.034]
12 **Liu Y**, Zheng J, Hao J, Wang RR, Liu X, Gu P, Yu H, Yu Y, Wu C, Ou B, Peng Z. Global burden of primary liver cancer by five etiologies and global prediction by 2035 based on global burden of disease study 2019. *Cancer Med* 2022; **11**: 1310-1323 [PMID: 35118819 DOI: 10.1002/cam4.4551]
13 **Zhu JZ**, Dai YN, Wang YM, Zhou QY, Yu CH, Li YM. Prevalence of Nonalcoholic Fatty Liver Disease and Economy. *Dig Dis Sci* 2015; **60**:

3194-3202 [PMID: 26017679 DOI: 10.1007/s10620-015-3728-3]
14 **Zhao Y**, Zhao W, Ma J, Toshiyoshi M, Zhao Y. Patatin-like phospholipase domain-containing 3 gene (PNPLA3) polymorphic (rs738409) single nucleotide polymorphisms and susceptibility to nonalcoholic fatty liver disease: A meta-analysis of twenty studies. *Medicine (Baltimore)* 2023; **102**: e33110 [PMID: 36897668 DOI: 10.1097/MD.0000000000033110]
15 **Bacil GP**, Romualdo GR, Piagge PMFD, Cardoso DR, Vinken M, Cogliati B, Barbisan LF. Unraveling Hepatic Metabolomic Profiles and Morphological Outcomes in a Hybrid Model of NASH in Different Mouse Strains. *Antioxidants (Basel)* 2023; **12** [PMID: 36829849 DOI: 10.3390/antiox12020290]
16 **Rogers AB**. Stress of Strains: Inbred Mice in Liver Research. *Gene Expr* 2018; **19**: 61-67 [PMID: 30092856 DOI: 10.3727/105221618X15337408678723]
17 **Xu Z**, Kang Q, Yu Z, Tian L, Zhang J, Wang T. Research on the Species Difference of the Hepatotoxicity of Medicine Based on Transcriptome. *Front Pharmacol* 2021; **12**: 647084 [PMID: 33995060 DOI: 10.3389/fphar.2021.647084]
18 **Krege JH**, Hodgin JB, Hagaman JR, Smithies O. A noninvasive computerized tail-cuff system for measuring blood pressure in mice. *Hypertension* 1995; **25**: 1111-1115 [PMID: 7737724 DOI: 10.1161/01.hyp.25.5.1111]
19 **Aleksandrin VV**, Ivanov AV, Virus ED, Bulgakova PO, Kubatiev AA. Application of wavelet analysis to detect dysfunction in cerebral blood flow autoregulation during experimental hyperhomocysteinaemia. *Lasers Med Sci* 2018; **33**: 1327-1333 [PMID: 29611066 DOI: 10.1007/s10103-018-2485-x]
20 **Li Z**, Tam EW, Kwan MP, Mak AF, Lo SC, Leung MC. Effects of prolonged surface pressure on the skin blood flowmotions in anaesthetized rats--an assessment by spectral analysis of laser Doppler flowmetry signals. *Phys Med Biol* 2006; **51**: 2681-2694 [PMID: 16675876 DOI: 10.1088/0031-9155/51/10/020]
21 **Mazzaccara C**, Labruna G, Cito G, Scarfò M, De Felice M, Pastore L, Sacchetti L. Age-Related Reference Intervals of the Main Biochemical and Hematological Parameters in C57BL/6J, 129SV/EV and C3H/HeJ Mouse Strains. *PLoS One* 2008; **3**: e3772 [PMID: 19020657 DOI: 10.1371/journal.pone.0003772]
22 **Boehm O**, Zur B, Koch A, Tran N, Freyenhagen R, Hartmann M, Zacharowski K. Clinical chemistry reference database for Wistar rats and C57/BL6 mice. *Biol Chem* 2007; **388**: 547-554 [PMID: 17516851 DOI: 10.1515/BC.2007.061]
23 **He Q**, Su G, Liu K, Zhang F, Jiang Y, Gao J, Liu L, Jiang Z, Jin M, Xie H. Sex-specific reference intervals of hematologic and biochemical analytes in Sprague-Dawley rats using the nonparametric rank percentile method. *PLoS One* 2017; **12**: e0189837 [PMID: 29261747 DOI: 10.1371/journal.pone.0189837]
24 **Wu BN**, O'Sullivan AJ. Sex differences in energy metabolism need to be considered with lifestyle modifications in humans. *J Nutr Metab* 2011; **2011**: 391809 [PMID: 21773020 DOI: 10.1155/2011/391809]
25 **Stanhewicz AE**, Wenner MM, Stachenfeld NS. Sex differences in endothelial function important to vascular health and overall cardiovascular disease risk across the lifespan. *Am J Physiol Heart Circ Physiol* 2018; **315**: H1569-H1588 [PMID: 30216121 DOI: 10.1152/ajpheart.00396.2018]
26 **Shin J**, Hong J, Edwards-Glenn J, Krukovets I, Tkachenko S, Adelus ML, Romanoski CE, Rajagopalan S, Podrez E, Byzova TV, Stenina-Adongravi O, Cherepanova OA. Unraveling the Role of Sex in Endothelial Cell Dysfunction: Evidence From Lineage Tracing Mice and Cultured Cells. *Arterioscler Thromb Vasc Biol* 2024; **44**: 238-253 [PMID: 38031841 DOI: 10.1161/ATVBAHA.123.319833]
27 **Li Z**, Lu S, Qian B, Meng Z, Zhou Y, Chen D, Chen B, Yang G, Ma Y. Sex differences in hepatic ischemia–reperfusion injury: a cross-sectional study. *Sci Rep* 2023; **13**: 5724 [PMID: 37029182 DOI: 10.1038/s41598-023-32837-5]
28 **Reis SE**, Gloth ST, Blumenthal RS, Resar JR, Zacur HA, Gerstenblith G, Brinker JA. Ethinyl estradiol acutely attenuates abnormal coronary vasomotor responses to acetylcholine in postmenopausal women. *Circulation* 1994; **89**: 52-60 [PMID: 8281693 DOI: 10.1161/01.cir.89.1.52]
29 **Haynes MP**, Sinha D, Russell KS, Collinge M, Fulton D, Morales-Ruiz M, Sessa WC, Bender JR. Membrane estrogen receptor engagement activates endothelial nitric oxide synthase *via* the PI3-kinase-Akt pathway in human endothelial cells. *Circ Res* 2000; **87**: 677-682 [PMID: 11029403 DOI: 10.1161/01.res.87.8.677]
30 **Simoncini T**, Hafezi-Moghadam A, Brazil DP, Ley K, Chin WW, Liao JK. Interaction of oestrogen receptor with the regulatory subunit of phosphatidylinositol-3-OH kinase. *Nature* 2000; **407**: 538-541 [PMID: 11029009 DOI: 10.1038/35035131]
31 **Lazaro CM**, Victorio JA, Davel AP, Oliveira HCF. CETP expression ameliorates endothelial function in female mice through estrogen receptor-α and endothelial nitric oxide synthase pathway. *Am J Physiol Heart Circ Physiol* 2023; **325**: H592-H600 [PMID: 37539470 DOI: 10.1152/ajpheart.00365.2023]
32 **Theofilis P**, Sagris M, Oikonomou E, Antonopoulos AS, Siasos G, Tsioufis C, Tousoulis D. Inflammatory Mechanisms Contributing to Endothelial Dysfunction. *Biomedicines* 2021; **9** [PMID: 34356845 DOI: 10.3390/biomedicines9070781]
33 **Galley HF**, Webster NR. Physiology of the endothelium. *Br J Anaesth* 2004; **93**: 105-113 [PMID: 15121728 DOI: 10.1093/bja/aeh163]
34 **Younossi ZM**, Koenig AB, Abdelatif D, Fazel Y, Henry L, Wymer M. Global epidemiology of nonalcoholic fatty liver disease-Meta-analytic assessment of prevalence, incidence, and outcomes. *Hepatology* 2016; **64**: 73-84 [PMID: 26707365 DOI: 10.1002/hep.28431]
35 **Liu Y**, Bubolz AH, Shi Y, Newman PJ, Newman DK, Gutterman DD. Peroxynitrite reduces the endothelium-derived hyperpolarizing factor component of coronary flow-mediated dilation in PECAM-1-knockout mice. *Am J Physiol Regul Integr Comp Physiol* 2006; **290**: R57-R65 [PMID: 16166207 DOI: 10.1152/ajpregu.00424.2005]
36 **Cheung KCP**, Fanti S, Mauro C, Wang G, Nair AS, Fu H, Angeletti S, Spoto S, Fogolari M, Romano F, Aksentijevic D, Liu W, Li B, Cheng L, Jiang L, Vuononvirta J, Poobalasingam TR, Smith DM, Ciccozzi M, Solito E, Marelli-Berg FM. Preservation of microvascular barrier function requires CD31 receptor-induced metabolic reprogramming. *Nat Commun* 2020; **11**: 3595 [PMID: 32681081 DOI: 10.1038/s41467-020-17329-8]
37 **Mukhtar A**, Lotfy A, Hussein A, Fouad E. Splanchnic and systemic circulation cross talks: Implications for hemodynamic management of liver transplant recipients. *Best Pract Res Clin Anaesthesiol* 2020; **34**: 109-118 [PMID: 32334781 DOI: 10.1016/j.bpa.2019.12.003]
38 **Takahashi H**, Shigefuku R, Yoshida Y, Ikeda H, Matsunaga K, Matsumoto N, Okuse C, Sase S, Itoh F, Suzuki M. Correlation between hepatic blood flow and liver function in alcoholic liver cirrhosis. *World J Gastroenterol* 2014; **20**: 17065-17074 [PMID: 25493018 DOI: 10.3748/wjg.v20.i45.17065]
39 **Liu P**, Liang WL, Huang RT, Chen XX, Zou DH, Kurihara H, Li YF, Xu YH, Ouyang SH, He RR. Hepatic microcirculatory disturbance in liver diseases: intervention with traditional Chinese medicine. *Front Pharmacol* 2024; **15**: 1399598 [PMID: 39108760 DOI: 10.3389/fphar.2024.1399598]
40 **Kuwano A**, Kurokawa M, Kohjima M, Imoto K, Tashiro S, Suzuki H, Tanaka M, Okada S, Kato M, Ogawa Y. Microcirculatory disturbance in acute liver injury. *Exp Ther Med* 2021; **21**: 596 [PMID: 33884034 DOI: 10.3892/etm.2021.10028]

41 **Fu S**, Xu M, Wang B, Li B, Li Y, Wang Y, Liu X, Ling H, Wang Q, Zhang X, Li A, Zhang X, Liu M. Strain- and sex-specific differences in intestinal microhemodynamics and gut microbiota composition. *Gastroenterol Rep (Oxf)* 2024; **12**: goae087 [PMID: 39286773 DOI: 10.1093/gastro/goae087]

42 **Xu M**, Fu S, Wang B, Song X, Li B, Liu X, Li Y, Wang Y, Wang Q, Ling H, Li A, Liu M, Zhang X. Evaluation of Renal Microhemodynamics Heterogeneity in Different Strains and Sexes of Mice. *Lab Invest* 2024; **104**: 102087 [PMID: 38797344 DOI: 10.1016/j.labinv.2024.102087]

43 **Melia T**, Waxman DJ. Genetic factors contributing to extensive variability of sex-specific hepatic gene expression in Diversity Outbred mice. *PLoS One* 2020; **15**: e0242665 [PMID: 33264334 DOI: 10.1371/journal.pone.0242665]

44 **Airola C**, Pallozzi M, Cerrito L, Santopaolo F, Stella L, Gasbarrini A, Ponziani FR. Microvascular Thrombosis and Liver Fibrosis Progression: Mechanisms and Clinical Applications. *Cells* 2023; **12** [PMID: 37443746 DOI: 10.3390/cells12131712]

45 **Vairappan B**. Endothelial dysfunction in cirrhosis: Role of inflammation and oxidative stress. *World J Hepatol* 2015; **7**: 443-459 [PMID: 25848469 DOI: 10.4254/wjh.v7.i3.443]

46 **Skubic C**, Drakulić Ž, Rozman D. Personalized therapy when tackling nonalcoholic fatty liver disease: a focus on sex, genes, and drugs. *Expert Opin Drug Metab Toxicol* 2018; **14**: 831-841 [PMID: 29969922 DOI: 10.1080/17425255.2018.1492552]

47 **Liu M**, Park S. The Role of PNPLA3_rs738409 Gene Variant, Lifestyle Factors, and Bioactive Compounds in Nonalcoholic Fatty Liver Disease: A Population-Based and Molecular Approach towards Healthy Nutrition. *Nutrients* 2024; **16** [PMID: 38674929 DOI: 10.3390/nu16081239]

48 **Cristani M**, Citarella A, Carnamucio F, Micale N. Nano-Formulations of Natural Antioxidants for the Treatment of Liver Cancer. *Biomolecules* 2024; **14** [PMID: 39199418 DOI: 10.3390/biom14081031]

49 **O'Brien MH**, Pitot HC, Chung SH, Lambert PF, Drinkwater NR, Bilger A. Estrogen Receptor-α Suppresses Liver Carcinogenesis and Establishes Sex-Specific Gene Expression. *Cancers (Basel)* 2021; **13** [PMID: 34068249 DOI: 10.3390/cancers13102355]

World Journal of Gastroenterology

Submit a Manuscript: https://www.f6publishing.com

World J Gastroenterol 2025 April 21; 31(15): 104875

DOI: 10.3748/wjg.v31.i15.104875

ISSN 1007-9327 (print) ISSN 2219-2840 (online)

ORIGINAL ARTICLE

Basic Study

Rhapontin activates nuclear factor erythroid 2-related factor 2 to ameliorate 1-methyl-4-phenyl-1,2,3,6-tetrahydropyridine-induced gastrointestinal dysfunction in Parkinson's disease mice

Xin-Yu Wang, Fang Liu, Qi-Tong Wang, Shu-Zhu Li, Yu-Zhao Ye, Tao Chen, Ben-Chi Cai

Specialty type: Gastroenterology and hepatology

Provenance and peer review: Unsolicited article; Externally peer reviewed.

Peer-review model: Single blind

Peer-review report's classification

Scientific Quality: Grade A, Grade B, Grade C

Novelty: Grade A, Grade B, Grade B

Creativity or Innovation: Grade A, Grade B, Grade B

Scientific Significance: Grade A, Grade A, Grade B

P-Reviewer: Khedimi M; Wu J

Received: January 5, 2025

Revised: February 24, 2025

Accepted: March 24, 2025

Published online: April 21, 2025

Processing time: 103 Days and 18.8 Hours

Xin-Yu Wang, Fang Liu, Qi-Tong Wang, Shu-Zhu Li, Yu-Zhao Ye, Tao Chen, Ben-Chi Cai, Hainan General Hospital, Hainan Affiliated Hospital of Hainan Medical University, Hainan Medical University, Haikou 570100, Hainan Province, China

Co-first authors: Xin-Yu Wang and Fang Liu.

Co-corresponding authors: Tao Chen and Ben-Chi Cai.

Corresponding author: Ben-Chi Cai, Professor, Hainan General Hospital, Hainan Affiliated Hospital of Hainan Medical University, Hainan Medical University, No. 19 Xiuhua Road, Xiuying District, Haikou 570100, Hainan Province, China. caibenchi@hainmc.edu.cn

Abstract

BACKGROUND

Parkinson's disease (PD)-a progressive neurodegenerative disorder-is characterized by motor and gastrointestinal dysfunction. The exploration of novel therapeutic strategies for PD is vital.

AIM

To investigate the potential mechanism of action of rhapontin-a natural compound with known antioxidant and anti-inflammatory properties-in the context of PD.

METHODS

Network pharmacology was used to predict the targets and mechanisms of action of rhapontin in PD. Behavioral tests and tyrosine hydroxylase immunofluorescence analysis were used to assess the effect of rhapontin on symptoms and pathology in MPTP-induced mice. Interleukin (IL)-6, IL-1β, tumor necrosis factor (TNF)-α, and IL-10 levels in tissues were measured using an enzyme-linked immunosorbent assay (ELISA). Additionally, nuclear factor erythroid 2-related factor 2 (NRF2) activation was confirmed using western blotting.

RESULTS

NRF2 was predicted to be the key transcription factor underlying the therapeutic effects of rhapontin in PD, and its anti-PD action may be associated with its anti-inflammatory and antioxidant properties. Rhapontin ameliorated the loss of

dopaminergic neurons and gastrointestinal dysfunction in 1-methyl-4-phenyl-1,2,3,6-tetrahydropyridine (MPTP)-induced mice by activating NRF2. Additio-nally, rhapontin treatment significantly decreased pro-inflammatory cytokines (IL-6, TNF-α, IL-1β) in the substantia nigra, striatum, and colon, whereas it increased anti-inflammatory cytokine (IL-10) levels only in the colon, indicating the involvement of gut–brain axis in its neuroprotective potential. Finally, NRF2 was identified as a key transcription factor activated by rhapontin, particularly in the colon.

CONCLUSION

We elucidated the effects of rhapontin in MPTP-induced PD mouse models using a combination of network pharmacology analysis, behavioral assessments, immunofluorescence, ELISA, and Western blotting. Our findings revealed the multifaceted role of rhapontin in ameliorating PD through its anti-inflammatory and antioxidant properties, particularly by activating NRF2, paving the way for future research into targeted therapies for PD.

Key Words: Rhapontin; Gastrointestinal dysfunction; Parkinson's disease; Nuclear factor erythroid 2-related factor 2; Gut-Brain axis; Oxidative stress; Neuroinflammation

Core Tip: The specific objectives of this study are to identify key molecular targets of rhapontin, evaluate its impact on gastrointestinal symptoms in Parkinson's disease, and investigate its anti-inflammatory effects mediated by nuclear factor erythroid 2-related factor 2 activation.

Citation: Wang XY, Liu F, Wang QT, Li SZ, Ye YZ, Chen T, Cai BC. Rhapontin activates nuclear factor erythroid 2-related factor 2 to ameliorate 1-methyl-4-phenyl-1,2,3,6-tetrahydropyridine-induced gastrointestinal dysfunction in Parkinson's disease mice. *World J Gastroenterol* 2025; 31(15): 104875
URL: https://www.wjgnet.com/1007-9327/full/v31/i15/104875.htm
DOI: https://dx.doi.org/10.3748/wjg.v31.i15.104875

INTRODUCTION

Parkinson's disease (PD)-a progressive neurodegenerative disorder-is characterized by motor symptoms, such as tremors, rigidity, and bradykinesia, and non-motor symptoms, such as gastrointestinal (GI) dysfunction[1-4]. The rising prevalence of PD has driven a global search for effective therapeutic strategies. The gut-brain axis plays a critical role in the development and progression of PD[5-10], and impaired GI function has been implicated in the early stages of PD, preceding the onset of motor symptoms. Pathological substances such as alpha-synuclein produced in the gut can be retrogradely transported to the brain *via* the vagus nerve, accelerating the pathological process of PD[8]. In addition, the gut-brain axis influences the onset and progression of PD through the interaction between the gut microbiota and the host nervous system[9]. Dysbiosis of the gut microbiota can trigger inflammatory responses and neurotransmitter metabolic disorder. Meanwhile, intestinal barrier dysfunction worsens neuroinflammation in PD by allowing inflammatory factors and toxins to enter the bloodstream[10].

Although the exact mechanism underlying GI dysfunction in PD is not fully understood, inflammation and oxidative stress may be involved in both the gut-brain axis and GI dysfunction[11,12]. Current treatments focus primarily on symptomatic relief rather than addressing the underlying pathophysiology, including inflammation. Therefore, novel interventions that can mitigate these pathological processes are crucial, as existing therapies often exhibit limited efficacy and involve significant side effects.

The 1-methyl-4-phenyl-1,2,3,6-tetrahydropyridine (MPTP) is a well-established neurotoxin used to induce PD-like symptoms in animal models, mimicking the dopaminergic neuronal loss and motor deficits observed in human patients with PD[13-15]. MPTP exposure also results in significant GI dysfunction, including constipation and delayed gastric emptying, potentially mediated by inflammation[16,17]. Therefore, ameliorating inflammation in GI dysfunction could be a promising approach to ameliorate both motor and non-motor PD symptoms, providing new therapeutic avenues for the management of PD[18,19].

Rhapontin-a natural compound derived from *Rheum palmatum*-exhibits laxative effects and has been used in traditional Chinese medicine for centuries[20-23]. Rhapontin also exhibits potent antioxidant and anti-inflammatory properties[24]. Despite the promising pharmacological profile of rhapontin, a significant gap remains regarding its specific molecular mechanism of action in the context of PD. Rhapontin may reduce inflammation by activating the nuclear factor erythroid 2-related factor 2 (NRF2)[25,26]. NRF2 is a transcription factor that plays a pivotal role in regulating cellular responses to oxidative stress and inflammation[27,28]. The precise interactions between rhapontin and the NRF2 pathway in PD, as well as its effects on downstream signaling components, remain largely unexplored. This study aimed to bridge this gap by elucidating the mechanism through which rhapontin exerts its neuroprotective effects, particularly emphasizing its role in modulating oxidative stress, inflammation, and the gut-brain axis in MPTP-induced PD mouse models.

This study involved a multifaceted research approach, including bioinformatics analyses to identify potential rhapontin targets, construction of protein-protein interaction (PPI) networks to determine the signaling pathways involved, and behavioral assessments to assess the effects on motor and non-motor symptoms. By integrating network pharmacology and animal model experiments, this study achieves greater authenticity than pure bioinformatics analysis and higher credibility than approaches relying solely on animal models or molecular techniques. Additionally, we measured the levels of inflammatory markers and NRF2 expression and performed tyrosine hydroxylase-positive (TH^+) staining. The specific objectives of this study were to identify the key molecular targets of rhapontin, evaluate its effect on motor and GI symptoms in PD, and investigate its anti-inflammatory effects mediated by NRF2. Our findings contribute valuable insights into the therapeutic viability of rhapontin as a candidate for PD treatment, paving the way for future research and potential clinical applications.

MATERIALS AND METHODS

Network pharmacology analysis

A network pharmacology analysis was conducted to explore the potential mechanisms of action of rhapontin in PD. The Online Mendelian Inheritance in Man (OMIM) and Gene Expression Omnibus (GEO) databases were searched using the term "Parkinson's disease" to identify relevant genes. Subsequently, we also searched various databases, including the Traditional Chinese Medicine Systems Pharmacology Database (TCMSP; http://tcmspw.com/tcmsp.php), Search Tool for Interactions of Chemicals (STITCH; http://stitch.embl.de/), PharmMapper (http://pharmmapper.shsmu.edu.cn/), Evidence-Based TCM (ETCM; http://www.etcm.cn/), and PubChem (https://pubchem.ncbi.nlm.nih.gov/), to predict rhapontin targets. We used different keywords, such as rhapontin, rhaponitin, poniticin, and rhaponiticin, to enhance the accuracy of our target prediction. For gene selection, we set a threshold of P value < 0.05 and log2 (fold change) > 1 to ensure the identification of significantly associated genes. Only those consistently identified across multiple databases were included in our analysis. Venn diagrams were constructed to identify intersections between the compounds and disease targets. A PPI network was constructed using the STRING database. For PPI analysis, we used a confidence score threshold of 0.7 to filter high-confidence interactions. Kyoto Encyclopedia of Genes and Genomes (KEGG) pathway enrichment analysis was performed using the Metascape platform.

Animals and treatments

Forty male C57BL/6J mice, aged 8 weeks, were acquired from Hunan Slaughter Jingda Laboratory Animal Co., Ltd. The mice were acclimated to the laboratory conditions for 1 week, with a 12-hour light/dark cycle and ad libitum access to food and water, before the commencement of the experiment. All experimental procedures were approved by the Ethics Committee of Hainan Medical University and complied with the guidelines set forth by the National Institutes of Health for the humane treatment of laboratory animals. Carbon dioxide asphyxiation was used to euthanize all the mice. The mice were randomly divided into the MPTP (Sigma-Aldrich, United States) + rhapontin (Macklin, Shanghai, China) + ML385 (Targetmol, United States) group (n = 10), MPTP + rhapontin group (n = 10), MPTP group (n = 10), and control group (n = 10). Mice were intraperitoneally administered MPTP (20 mg/kg) daily for 4 consecutive days to induce PD, followed by a 3-day recovery period to allow for the manifestation of PD-like symptoms. Rhapontin (20 mg/kg/day) was gavaged to the mice starting 1 week prior to MPTP administration and continuing throughout the experimental period.

Behavioral tests

The open field test was conducted to assess general locomotor activity and exploratory behavior of the mice. Each mouse was placed in the center of a square arena (50 cm × 50 cm) with black walls, and the behavior was recorded for 10 min using a video-tracking system. After each trial, the apparatus was cleaned with 70% ethanol to eliminate olfactory cues. The total distance traveled was quantified to evaluate anxiety-like behaviors and motor function.

The pole-climbing test was used to assess forelimb asymmetry and motor coordination. The mouse was placed at the bottom, facing upward in a vertical wooden dowel (1 cm in diameter and 50 cm in height). The time required for the mouse to descend and reach the bottom was recorded. Each mouse was subjected to three trials, and the average time was calculated. This test is used to measure the asymmetry in forelimb use and the overall motor coordination ability of mice.

Fecal water content was used as an indicator of GI dysfunction. Fresh fecal pellets were collected from each mouse, weighed to obtain the wet weight, and then dry weight was obtained after drying them in an oven at 60 °C for 48 hours. The water content was calculated as the difference between the wet and dry weights and expressed as a percentage of the wet weight.

The number of fecal pellets produced within 15 minutes was used to assess GI motility. The mice were placed individually in clean cages with fresh bedding, and the number of fecal pellets excreted within a 15-minute period was counted. This test is used to quantitatively measure the bowel movement frequency, indicative of GI function.

All behavioral assays were conducted in a quiet, temperature-controlled room during the light phase of the circadian cycle to minimize external influences. The experimenters were blinded to the treatment groups. The data obtained from these tests were analyzed to evaluate the effects of MPTP-induced Parkinsonism and the potential ameliorative effects of rhapontin on motor and GI functions.

Immunofluorescence analysis

Brain sections containing the substantia nigra and striatum were subjected to immunofluorescence analysis to visualize TH^+ dopaminergic neurons. Sections were permeabilized with 0.3% Triton X-100, blocked with 5% normal donkey serum, and incubated with a primary antibody against TH (1:500, Servicebio, Wuhan, China) overnight at 4 °C. After washing with phosphate-buffered saline (PBS), the sections were incubated with a secondary antibody conjugated to Alexa Fluor 594 (1:200, Servicebio) for 1 hour at room temperature. Nuclei were counterstained with DAPI, images were captured using a confocal microscope, and the intensity of TH immunoreactivity in the striatum and substantia nigra was quantified using image analysis software.

Enzyme-linked immunosorbent assay

Interleukin (IL)-10, IL-6, IL-1β, and tumor necrosis factor (TNF) levels in the substantia nigra, striatum, and colon tissues were quantified using enzyme-linked immunosorbent assay (ELISA) kits (Thermo Fisher Scientific) following the manufacturer's instructions. Tissues were homogenized in PBS containing a protease inhibitor cocktail, and supernatants were collected after centrifugation. ELISA plates were coated with specific antibodies, blocked, and incubated with the tissue supernatants and standards. After incubation with horseradish peroxidase (HRP)-conjugated secondary antibodies and TMB substrate, absorbance was measured at 450 nm. The optical density values were plotted against the standard curve to determine cytokine concentrations in the samples, calculated in pg/mL and normalized to the total protein content of the tissue samples, which was determined using a BCA protein assay kit (Thermo Fisher Scientific).

Western blotting

NRF2 expression in the substantia nigra, striatum, and colon tissues was analyzed by western blotting. Briefly, tissues were homogenized in radioimmunoprecipitation assay buffer, and protein concentrations were measured using a BCA protein assay kit. Equal amounts of protein were resolved on sodium dodecyl sulfate-polyacrylamide gel electrophoresis gels, transferred onto polyvinylidene fluoride membranes, and incubated with primary antibodies against NRF2 (1:1000, Servicebio) and β-actin (1:5000, Servicebio) overnight at 4 °C. Membranes were then incubated with HRP-conjugated secondary antibodies (1:2000, Servicebio), and bands were visualized using an enhanced chemiluminescence detection system.

Statistical analysis

Data are presented as the mean ± SE. Statistical comparisons between the groups were performed using *t*-tests (our data met the assumptions of normality and equal variances). Statistical significance was set at $P < 0.05$. All statistical analyses were conducted using GraphPad Prism 8.0 software.

RESULTS

PPI network and key targets of rhapontin in PD

Figure 1A illustrates the chemical structure of rhapontin. We identified 83 genes from TCMSP, STITCH, PharmMapper, ETCM, and PubChem databases after integrating and deleting the reduplicated terms (Supplementary material). Furthermore, a total of 1468 genes were identified from OMIM and GEO databases after integrated deduplication (Supplementary material). The 22 overlapping genes from the two datasets were identified as potential rhapontin targets in PD (Figure 1B). Subsequently, the PPI network was constructed using the STRING database. The top 10 key targets were NFE2 L2, HMOX1, TNF, IL10, IL6, AKT1, BCL2, TP53, INS, and PTGS2 (Figure 1C). We then performed KEGG pathway enrichment analysis on potential therapeutic targets to gain insight into the key physiological mechanisms of rhapontin in PD. The response to oxidative stress and antioxidant activity were critical biological processes and molecular functions of rhapontin in the treatment of PD (Figure 1D).

Motor symptoms in the MPTP-induced mouse model were alleviated by rhapontin by activating NRF2

The above results suggested NRF2 as a key transcription factor underlying rhapontin mechanism of action in PD owing to its critical role in antioxidant and anti-inflammatory activities. Subsequently, we evaluated rhapontin effects on movement disorders and GI dysfunction in MPTP-induced mice using behavioral tests. Figure 2A presents the representative tracks from the open field test. Rhapontin restored the distance traveled by MPTP-induced mice ($P < 0.01$). The mice in the MPTP + rhapontin + ML385 group traveled shorter distances in the open field test than those in the MPTP + rhapontin group ($P < 0.01$; Figure 2B). Furthermore, MPTP-induced mice took more time to climb down the pole in the pole-climbing task than mice in the control ($P < 0.01$) and MPTP + rhapontin groups ($P < 0.01$). However, the NRF2 inhibitor, ML385, partly abolished the effect of rhapontin on the time taken to climb down the pole ($P < 0.05$) (Figure 2C).

Figure 3A and B shows dopaminergic neurons in each group based on the TH staining. We further analyzed the pathological changes. Notably, we observed the enhanced fluorescence intensity of TH^+ cells in the substantia nigra ($P < 0.01$) and striatum ($P < 0.01$) of the mice in the MPTP + rhapontin group compared with that in the mice in the MPTP group. However, ML385 treatment in the rhapontin + MPTP group decreased fluorescence intensity of TH^+ cells in the substantia nigra ($P < 0.05$) and striatum ($P < 0.01$; Figure 3C).

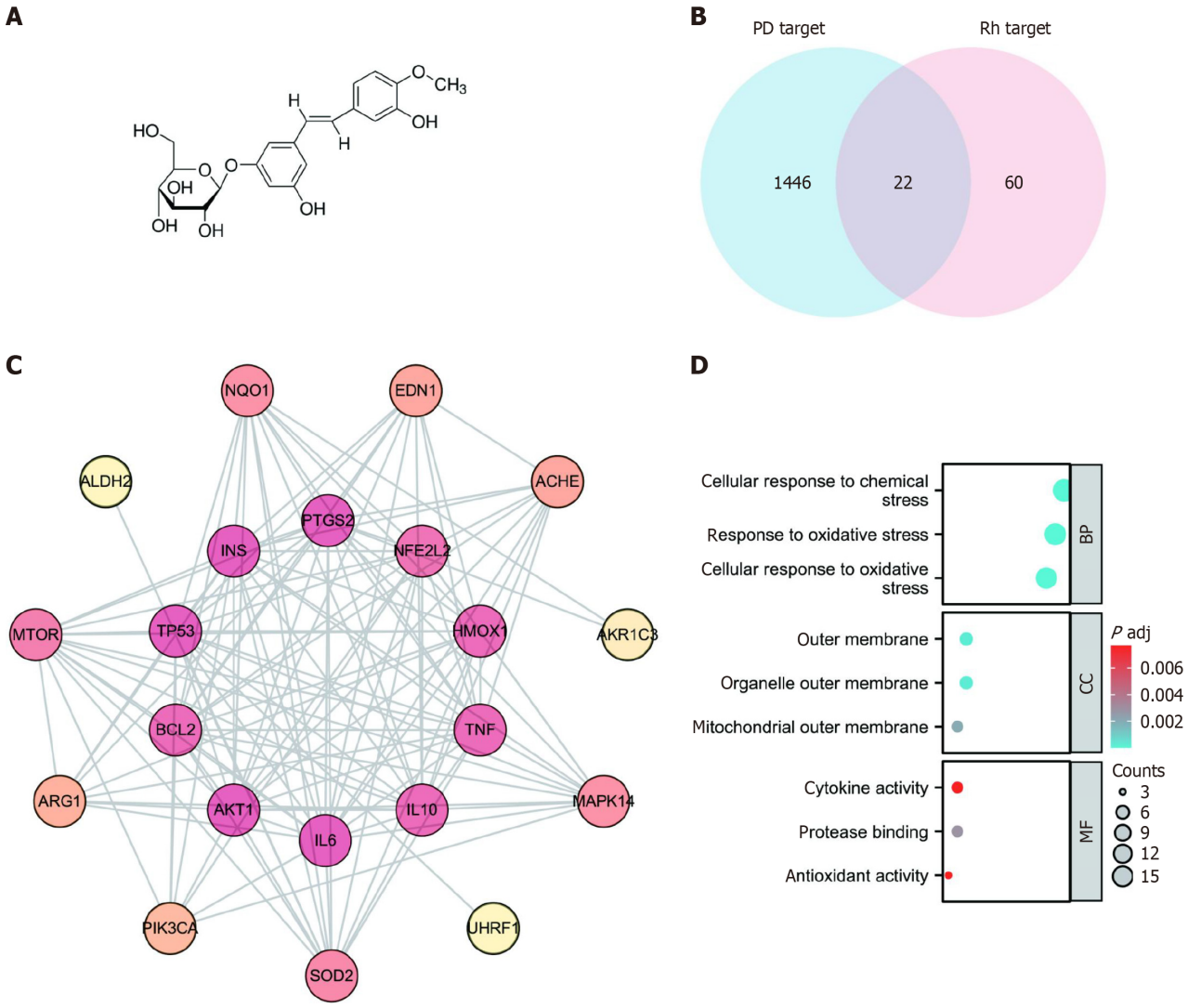

Figure 1 The network pharmacology analysis of rhapontin treatment of Parkinson's disease. A: The chemical structure of rhapontin; B: Venn diagram of overlapping targets associated with rhapontin in Parkinson's disease (PD); C: Protein-protein interaction of potential targets of rhapontin to treat PD. The deeper the color, the greater the degree. The line between two nodes represents the interaction; D: Gene ontology functional enrichment analysis. PD: Parkinson's disease; PPI: Protein-protein interaction; GO: Gene ontology; BP: Biological process; CC: Cell component; MF: Molecular function.

GI dysfunction in the MPTP-induced mouse model was ameliorated by rhapontin by activating NRF2

A series of experiments focusing on fecal pellets and fecal moisture were conducted to investigate rhapontin effects on GI dysfunction in the MPTP-induced PD mice (Figure 2D and E). MPTP-treated mice exhibited a significant reduction in the number of fecal pellets produced within 15 minutes compared with those in the control group ($P < 0.01$). Rhapontin treatment significantly increased the number of fecal pellets in the MPTP-induced PD mice ($P < 0.01$), indicating an improvement in GI motility. Additionally, fecal water content was significantly lower in the mice in the MPTP group than in the control group ($P < 0.01$). Rhapontin administration to MPTP-induced PD mice considerably increased their fecal water content, further supporting its beneficial effects on GI function ($P < 0.01$). Next, we co-administered ML385 and rhapontin to explore the underlying mechanisms. ML385 partially inhibited the beneficial effects of rhapontin, indicating that the improvement in GI function [fecal pellets ($P < 0.05$) and fecal moisture ($P < 0.01$)] by rhapontin may be mediated through a pathway involving NRF2 to some extent.

Rhapontin exerts its anti-inflammatory effects by activating NRF2, particularly in the colon

We quantified IL-6, IL-10, TNF-α, and IL-1β levels in the substantia nigra, striatum, and colon to investigate the anti-inflammatory effects of rhapontin in the MPTP-induced PD mouse model using ELISA. Additionally, we determined NRF2 expression in these regions using western blotting.

In the substantia nigra, MPTP treatment remarkably increased IL-6, TNF-α, and IL-1β levels compared with their levels in the substantia nigra of the mice in the control group ($P < 0.01$). However, rhapontin administration reduced the levels of these pro-inflammatory cytokines (Figure 4A), although the levels of IL-10, an anti-inflammatory cytokine, did not significantly change in the MPTP and MPTP + rhapontin groups (Figure 4A).

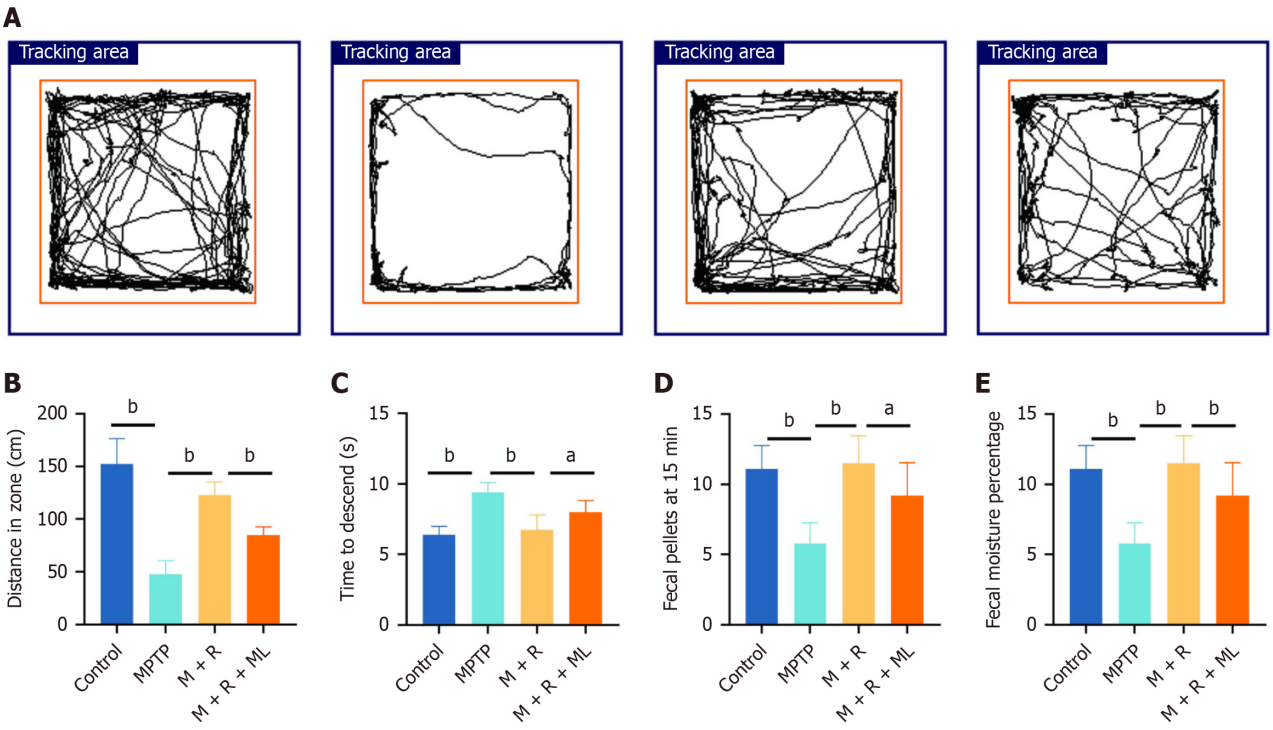

Figure 2 Rhapontin ameliorates 1-methyl-4-phenyl-1,2,3,6-tetrahydropyridine-induced motor and gastrointestinal dysfunction of Parkinson's disease mice. A: Representative traces of the open field test; B: Distance of the open field test; C: Time to descend of pole test; D: Fecal pellets of each group at 15 minutes; E: Fecal moisture percentage of each group; $n = 10$. $^{a}P < 0.05$; $^{b}P < 0.01$; MPTP: 1-methyl-4-phenyl-1,2,3,6-tetrahydropyridine; M: MPTP; R: Rhapontin; ML: ML385.

Similar trends were observed in the striatum. MPTP treatment significantly increased IL-6, TNF-α, and IL-1β levels ($P < 0.01$). However, rhapontin treatment attenuated these effects (Figure 3B), although IL-10 Levels did not significantly differ between the MPTP and MPTP + rhapontin groups (Figure 4B).

MPTP treatment increased IL-6, TNF-α, and IL-1β levels in the colon ($P < 0.01$). However, rhapontin treatment significantly reduced their levels compared with the MPTP group (Figure 4C). Unlike in the substantia nigra and striatum, IL-10 Levels were significantly elevated in the colon in the rhapontin-treated group compared with those in the MPTP group ($P < 0.01$; Figure 4C).

ML385 partially reversed the anti-inflammatory effects of rhapontin in all three regions, as indicated by increased IL-6, TNF-α, and IL-1β levels (Figure 4).

Western blotting revealed significantly increased NRF2 expression in the colon following rhapontin treatment ($P < 0.01$; Figure 5A). However, NRF2 expression in the substantia nigra and striatum did not significantly change in the MPTP and MPTP + rhapontin groups (Figure 5B and C).

These findings suggest that the gut-brain axis may play a crucial role in the protective effects of rhapontin against MPTP-induced inflammation in PD, and rhapontin exerts its anti-inflammatory effects by activating NRF2, particularly in the colon. We selected an appropriate sample size based on previous studies[29,30] and in accordance with the principle of minimizing the use of experimental animals. However, the modest sample size used in the experimental design may limit the statistical power and generalizability of the conclusions drawn. Future studies should address these limitations by incorporating larger cohorts and conducting clinical trials to verify the efficacy and safety of rhapontin in human populations, enhancing the robustness of our findings.

DISCUSSION

PD is a prevalent neurodegenerative disorder characterized by progressive loss of dopaminergic neurons in the substantia nigra, leading to debilitating motor and non-motor symptoms[31]. Clinical manifestations include tremors, rigidity, bradykinesia, and postural instability, which significantly affect the quality of life of affected individuals. Moreover, the increasing incidence of PD, particularly in the aging population, underscores the urgent need for effective therapeutic interventions to manage its symptoms and slow disease progression[32]. Current pharmacological strategies primarily focus on dopaminergic replacement therapy; however, they often fail to address the underlying pathophysiological processes, such as oxidative stress and neuroinflammation, which contribute to neuronal degeneration[32,33].

The earliest pathological changes in PD originate in the gut[34], as GI symptoms, such as constipation, often precede the onset of motor symptoms by several years[35]. The gut, which acts as a critical interface between the external environment and the internal milieu, is particularly susceptible to oxidative stress and inflammation, which are key

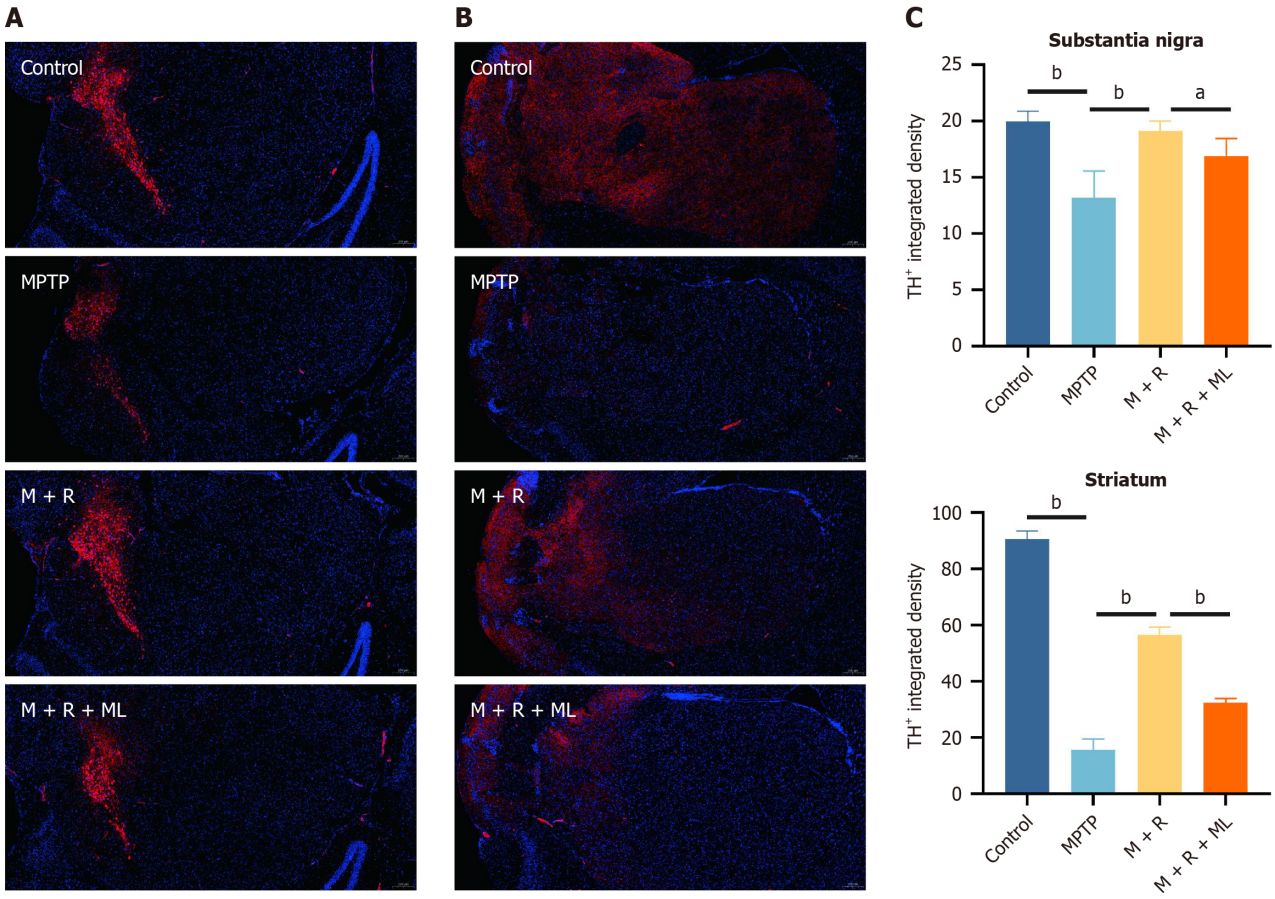

Figure 3 Rhapontin ameliorates dopaminergic neuronal damage of Parkinson's disease mice. A: Representative immunofluorescence images of TH-positive cells in the substantia nigra; B: Representative immunofluorescence images of TH-positive cells in the striatum; C: Quantification analysis of TH-positive cell number in Substantia nigra and Striatum. $n = 10$. $^{a}P < 0.05$; $^{b}P < 0.01$; MPTP: 1-methyl-4-phenyl-1,2,3,6-tetrahydropyridine; M: MPTP; R: Rhapontin; ML: ML385.

contributors to PD pathogenesis[36]. Inflammation in the gut may trigger neuroinflammation in PD[37]. The activation of enteric glial cells and the subsequent release of pro-inflammatory cytokines can lead to a cascade of events, including increased intestinal permeability, oxidative stress, and the propagation of neuroinflammatory signals to the central nervous system (CNS)[38]. This gut-brain axis is further reinforced by the role of the gut microbiota, which can modulate immune responses and oxidative stress, thereby influencing PD progression[39]. Moreover, the functional impairment of the gut in PD is intricately linked to oxidative stress and inflammation[40]. In PD, oxidative stress can exacerbate intestinal inflammation, leading to a vicious cycle of tissue damage and further oxidative stress[41]. The resulting inflammation propagates to the CNS, contributing to the degeneration of dopaminergic neurons in the substantia nigra pars compacta[42]. Collectively, the interplay among gut inflammation, oxidative stress, and neuroinflammation provides a comprehensive framework for understanding the early stages and progression of PD.

Rhapontin is increasingly recognized for its potential therapeutic benefits in GI disorders[29]. In this study, rhapontin effectively alleviated constipation symptoms in PD by modulating intestinal motility and improving fecal water content. This effect is likely mediated by its ability to inhibit GI inflammation and improve the overall gut environment. Specifically, rhapontin activated the NRF2 pathway in the colon, thereby suppressing the intestinal inflammation and improving GI function in mice with PD. Notably, NRF2 activation in the colon did not extend to the substantia nigra or striatum, suggesting a specific and localized effect on the GI tract. Furthermore, rhapontin may act *via* the gut-brain axis by activating NRF2 in the colon and reducing gut inflammation, thereby attenuating the systemic inflammatory response and oxidative stress that contribute to neuronal damage in PD. These insights provide a compelling rationale for further exploration of rhapontin as a novel therapeutic option for PD, potentially addressing both symptom management and disease progression.

NRF2, a transcription factor known for its role in antioxidant defense, plays a key role in maintaining the cellular redox balance and protecting against oxidative stress-induced damage[43]. In our study, rhapontin significantly increased NRF2 expression in the colon of mice with PD, which reduced oxidative stress and inflammation by upregulating downstream antioxidant genes. The localized activation of NRF2 in the colon rather than in the brain suggests that rhapontin primarily targets the GI tract to exert anti-inflammatory effects. NRF2 activation by rhapontin in the colon reduced the expression of pro-inflammatory cytokines, including TNF-α, IL-1β, and IL-6, which contribute to the development and progression of inflammatory bowel disease and other GI disorders[44]. Furthermore, rhapontin effectively alleviated intestinal inflammation by suppressing pro-inflammatory cytokines, which is a common feature of patients with PD[41]. This finding is consistent with those of previous studies highlighting the importance of NRF2 in the protection against intestinal inflam-

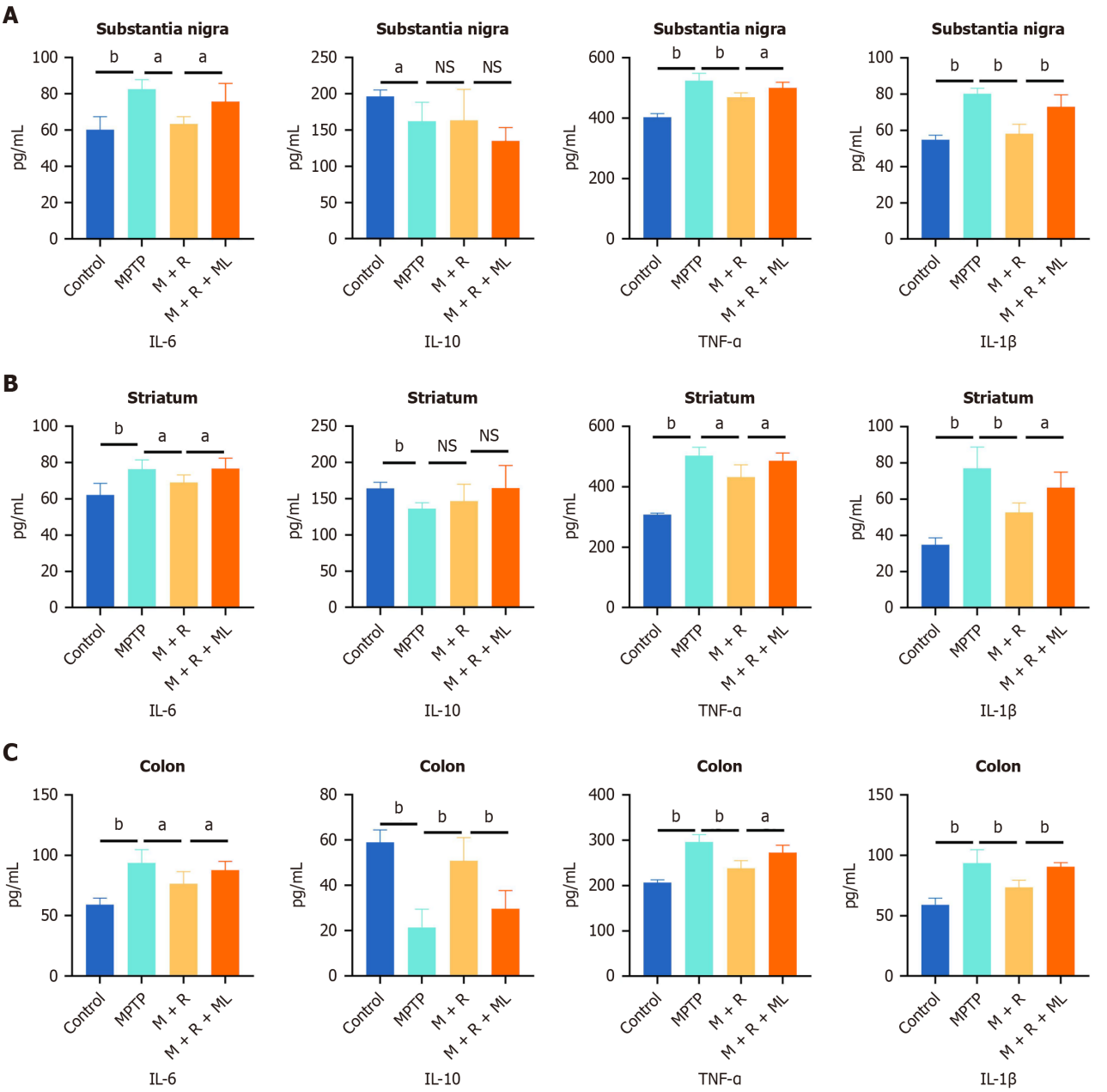

Figure 4 Rhapontin ameliorates inflammation of Parkinson's disease mice. A: Quantification analysis of pro-inflammatory cytokines [Interleukin (IL)-6, tumor necrosis factor-α, and IL-1β] and anti-inflammatory cytokines (IL-10) in the substantia nigra; B: Quantification analysis of pro-inflammatory cytokines and anti-inflammatory cytokines in the striatum; C: Quantification analysis of pro-inflammatory cytokines and anti-inflammatory cytokines in the colon; $n = 10$. $^{a}P < 0.05$; $^{b}P < 0.01$; NS: Not significant; MPTP: 1-methyl-4-phenyl-1,2,3,6-tetrahydropyridine; IL: Interleukin; TNF-α: Tumor necrosis factor-α; M: MPTP; R: Rhapontin; ML: ML385.

mation. Rhapontin also improved GI function in mice with PD, evident from the normalization of bowel movements and reduction in constipation symptoms. Improvement in GI function is likely mediated by the suppression of intestinal inflammation and NRF2 activation, which together help maintain the integrity of the intestinal barrier and promote normal bowel function.

Indeed, beyond the canonical antioxidant pathways, NRF2 activation influences several other molecular pathways that may contribute to the effects of rhapontin on PD. For example, NRF2 can inhibit the NF-κB signaling pathway, which is a pivotal mediator of inflammation[45]. By reducing the expression of pro-inflammatory cytokines and chemokines, NRF2 activation can shift the inflammatory response towards an anti-inflammatory phenotype, thereby mitigating inflammation. Additionally, NRF2 prevents the formation of the NLRP3 inflammasome, which is a key regulator of neuroinflammatory processes[46].

In addition to the molecular mechanisms, this study highlights the implications of rhapontin on the gut-brain axis. Unlike NRF2 activation in the colon, its activation was not observed in the substantia nigra and striatum following rhapontin treatment. However, rhapontin inhibited the expression of pro-inflammatory cytokines in these brain regions, indicating that its beneficial effects on the brain may be indirectly mediated by its action in the GI tract. The gut-brain axis-a bidirectional communication network between the gut and brain-plays a crucial role in the pathogenesis of PD[47]. By improving GI function and reducing intestinal inflammation, rhapontin may help reduce systemic inflammation,

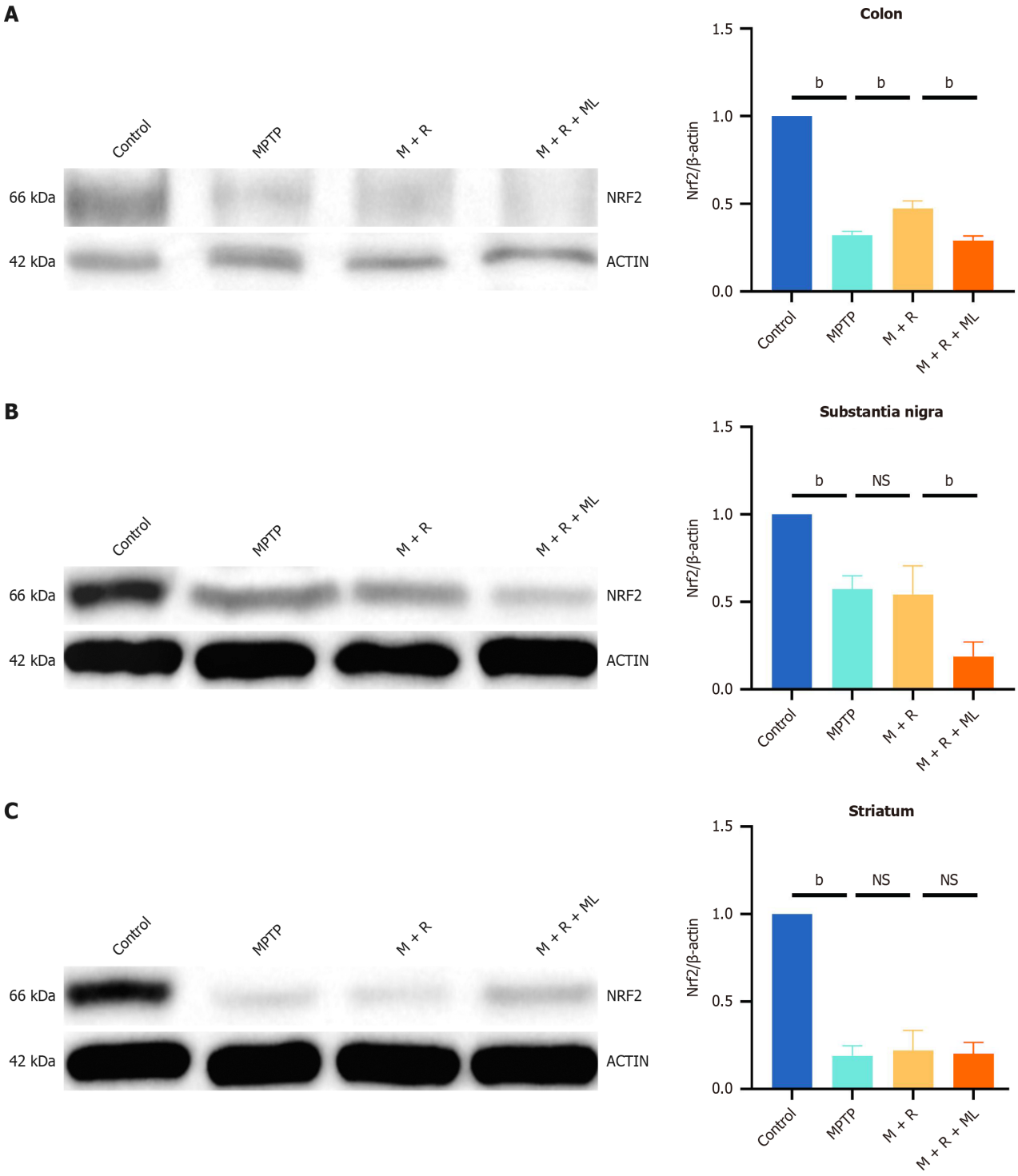

Figure 5 Rhapontin activates nuclear factor erythroid 2-related factor 2 in the colon. A: Western Blot image and analysis of nuclear factor erythroid 2-related factor 2 (NRF2) in colon; B: Western blot image and analysis of NRF2 in substantia nigra; C: Western blot image and analysis of NRF2 in striatum. $n = 10$. [a] $P < 0.05$; [b] $P < 0.01$; NS: Not significant; NRF2: Nuclear factor erythroid 2-related factor 2; MPTP: 1-methyl-4-phenyl-1,2,3,6-tetrahydropyridine; M: MPTP; R: Rhapontin; ML: ML385.

which contributes to PD progression.

The observation that IL-10 levels were significantly increased in the colon, but not in the brain, is intriguing. This localized effect in the colon may be attributed to the unique immunoregulatory environment of the gut, which is highly responsive to anti-inflammatory signaling. IL-10 is a key anti-inflammatory cytokine that limits immune cell activation and cytokine production in innate immune cell types[48]. The localized increase in IL-10 in the colon may contribute to the neuroprotective properties of rhapontin through several mechanisms. Its activation, specifically in the colon, is driven by the gut microbiota, which is known to modulate local immune responses through the production of short-chain fatty acids and other metabolites. These metabolites enhance IL-10 expression, thereby suppressing pro-inflammatory pathways and maintaining gut homeostasis[49]. In contrast, IL-10 can influence the gut microbiota composition, thus

promoting a more anti-inflammatory microbial profile that further supports the overall immune balance.

Furthermore, IL-10 promotes microglial phagocytic and clearance activities[50]. IL-10 expression did not significantly increase in the substantia nigra or striatum in our study, suggesting that IL-10 activation was primarily localized in the colon. This localized effect of rhapontin on IL-10 expression was consistent with that on NRF2. The observed reduction in pro-inflammatory cytokines in the substantia nigra and striatum, along with the elevation of anti-inflammatory cytokines such as IL-10 only in the colon, indicates that rhapontin mitigates neuroinflammation by affecting GI health, which is often compromised in patients with PD. Therefore, rhapontin plays a dual role in modulating both central and peripheral inflammatory responses, thereby improving overall patient outcomes. Understanding the relationship between gut health and neuroinflammation further emphasizes the need for a holistic approach in the management of PD, wherein the gut-brain axis could be a significant target for therapeutic interventions.

Recent studies have highlighted the critical role of the gut-brain axis in PD pathogenesis[41]. Rhapontin's effects on the colon, particularly its ability to reduce gut inflammation, may indirectly influence PD progression through this axis. Our study suggests that the anti-inflammatory properties of rhapontin in the gut can reduce inflammation in the CNS, which may be a key factor in delaying the progression of PD. Recent study indicate that α-synuclein pathology is induced by GI inflammation and then transfers to the brain by the gut-brain axis[51]. Rhapontin's impact on gut inflammation may reduce the accumulation of α-synuclein in the GI tract, which is known to spread to the brain and induce PD pathology. The relationship between intestinal inflammation and gut microbiota was close in PD[52]. Rhapontin may inhibit intestinal inflammation by modulating the gut microbiota, similar to many traditional Chinese medicine compounds[53]. Meanwhile, the inhibition of intestinal inflammation by rhapontin may also affect the gut microbiota. This crosstalk is worth further exploration. To further explore we will investigate the direct impact of rhapontin on α-synuclein pathology in both gut and brain models. Examine the role of rhapontin in modulating the gut microbiota and its downstream effects on neuroinflammation. We believe that further exploration of these mechanisms will provide valuable insights.

This study also has some limitations. First, the absence of clinical validation restricts the translational potential of the results to humans. Second, the integration of multiple datasets introduces variability, which could potentially skew the results and complicate data interpretation. Finally, this study has yet to fully elucidate the specific molecular mechanisms underlying rhapontin-mediated upregulation of the NRF2 pathway. While we have explored the role of the NRF2/IL-10 in the gut-brain axis of PD, the precise mechanism by which rhapontin activates NRF2 remains an area for further investigation in future studies.

We can speculate that rhapontin activates NRF2 in the colon, which subsequently promotes the increase of IL-10 and suppresses intestinal inflammation. This effect may alleviate neuroinflammation through the gut-brain axis, rather than by directly activating NRF2 in the brain. However, these conclusions lack clinical data support. For future clinical trials on rhapontin, we recommend a sample size of at least 100 participants, selected based on age (18-65 years), absence of chronic diseases, and normal lifestyle habits. The intervention should include an 8-12-week rhapontin administration with a placebo-controlled design. Outcome measures should focus on changes in gut microbiota composition (*via* metagenomic sequencing) and key physiological markers (*e.g.*, inflammatory and metabolic profiles). Long-term follow-up (1-2 years) is crucial for assessing safety and efficacy. Multi-center trials and individualized analyses are also advised to enhance study robustness and applicability. The detailed experimental design needs to be refined in future clinical studies. Furthermore, questions concerning the clinical dosage, bioavailability, and biosafety of rhapontin remain to be answered, and these explorations are vital for successful clinical translation.

CONCLUSION

In conclusion, our study demonstrated that rhapontin exerts therapeutic effects on GI dysfunction in PD by activating the NRF2 pathway in the colon. Subsequently, NRF2 activation suppresses intestinal inflammation and improves GI function, which may indirectly benefit the brain through the gut-brain axis. Activation of IL-10 in the colon further supports the anti-inflammatory effects of rhapontin. These findings provide valuable insights into the mechanisms through which rhapontin can be used to manage GI dysfunction in PD and highlight the potential of targeting the gut-brain axis for the treatment of neurodegenerative diseases. This study provides potential possibilities and a theoretical basis for the clinical application of rhapontin. Future studies should investigate the long-term effects of rhapontin and explore its potential as a therapeutic agent for PD.

FOOTNOTES

Author contributions: Chen T and Cai BC conceptualized and designed the research; Wan XY and Liu F screened patients and acquired clinical data; Wan XY and Liu F collected samples and performed laboratory analysis; Li SZ, Ye YZ, and Wang QT performed data analysis; Wan XY and Cai BC wrote the paper; All the authors have read and approved the final manuscript. Liu F was also responsible for patient screening, enrollment, collection of clinical data. Both authors have made crucial and indispensable contributions towards the completion of the project and thus qualified as the co-first authors of the paper. Both Chen T and Cai BC have played important and indispensable roles in the experimental design, data interpretation and manuscript preparation as the co-corresponding authors. Cai BC applied for and obtained the funds for this research project. Cai BC conceptualized, designed, and supervised the whole process of the project. He searched the literature, revised and submitted the early version of the manuscript. Chen T was instrumental and responsible for data re-analysis and re-interpretation, figure plotting, comprehensive literature search. This collaboration between Chen T and Cai BC is crucial for the publication of this manuscript and other manuscripts still in preparation.

Supported by the Hainan Provincial Natural Science Foundation of China, No. 823MS133 and No. 821QN0979.

Institutional animal care and use committee statement: The animal study protocol was reviewed and approved by the Animal Ethics Committee of Hainan Medical University, No. 2024[148]. All animal procedures were conducted in accordance with the guidelines for the care and use of laboratory animals.

Conflict-of-interest statement: The authors declare no conflicts of interest regarding this manuscript.

Data sharing statement: The data that support the findings of this study are available from the corresponding author upon reasonable request at caibenchi@hainmc.edu.cn.

ARRIVE guidelines statement: The authors have read the ARRIVE guidelines, and the manuscript was prepared and revised according to the ARRIVE guidelines.

Country of origin: China

ORCID number: Ben-Chi Cai 0000-0003-4235-1127.

S-Editor: Li L
L-Editor: A
P-Editor: Zheng XM

REFERENCES

1 **Del Tredici K**, Braak H. Lewy pathology and neurodegeneration in premotor Parkinson's disease. *Mov Disord* 2012; **27**: 597-607 [PMID: 22508278 DOI: 10.1002/mds.24921]
2 **Beitz JM**. Parkinson's disease: a review. *Front Biosci (Schol Ed)* 2014; **6**: 65-74 [PMID: 24389262 DOI: 10.2741/s415]
3 **Mitchell SD**, Sidiropoulos C. Therapeutic Applications of Botulinum Neurotoxin for Autonomic Symptoms in Parkinson's Disease: An Updated Review. *Toxins (Basel)* 2021; **13**: 226 [PMID: 33808714 DOI: 10.3390/toxins13030226]
4 **Morris HR**, Spillantini MG, Sue CM, Williams-Gray CH. The pathogenesis of Parkinson's disease. *Lancet* 2024; **403**: 293-304 [PMID: 38245249 DOI: 10.1016/S0140-6736(23)01478-2]
5 **Verugina NI**, Levin OS, Lyashenko EA. [The role of the gut microbiota in Parkinson's disease]. *Zh Nevrol Psikhiatr Im S S Korsakova* 2021; **121**: 86-91 [PMID: 34870920 DOI: 10.17116/jnevro202112110286]
6 **Chapelet G**, Leclair-Visonneau L, Clairembault T, Neunlist M, Derkinderen P. Can the gut be the missing piece in uncovering PD pathogenesis? *Parkinsonism Relat Disord* 2019; **59**: 26-31 [PMID: 30448099 DOI: 10.1016/j.parkreldis.2018.11.014]
7 **Jiao F**, Zhou L, Wu Z. The microbiota-gut-brain axis: a potential target in the small-molecule compounds and gene therapeutic strategies for Parkinson's disease. *Neurol Sci* 2025; **46**: 561-578 [PMID: 39546084 DOI: 10.1007/s10072-024-07878-x]
8 **Liang X**, Huang G, Wang Y, Andrikopoulos N, Tang H, Ding F, Li Y, Ke PC. Polystyrene Nanoplastics Hitch-Hike the Gut-Brain Axis to Exacerbate Parkinson's Pathology. *ACS Nano* 2025; **19**: 5475-5492 [PMID: 39883073 DOI: 10.1021/acsnano.4c13914]
9 **Zhang L**, Wei J, Liu X, Li D, Pang X, Chen F, Cao H, Lei P. Gut microbiota-astrocyte axis: new insights into age-related cognitive decline. *Neural Regen Res* 2025; **20**: 990-1008 [PMID: 38989933 DOI: 10.4103/NRR.NRR-D-23-01776]
10 **Rajkovaca Latic I**, Popovic Z, Mijatovic K, Sahinovic I, Pekic V, Vucic D, Cosic V, Miskic B, Tomic S. Association of intestinal inflammation and permeability markers with clinical manifestations of Parkinson's disease. *Parkinsonism Relat Disord* 2024; **123**: 106948 [PMID: 38554664 DOI: 10.1016/j.parkreldis.2024.106948]
11 **Raber J**, Sharpton TJ. Gastrointestinal Dysfunction in Neurological and Neurodegenerative Disorders. *Semin Neurol* 2023; **43**: 634-644 [PMID: 37607587 DOI: 10.1055/s-0043-1771459]
12 **Li Q**, Meng LB, Chen LJ, Shi X, Tu L, Zhou Q, Yu JL, Liao X, Zeng Y, Yuan QY. The role of the microbiota-gut-brain axis and intestinal microbiome dysregulation in Parkinson's disease. *Front Neurol* 2023; **14**: 1185375 [PMID: 37305758 DOI: 10.3389/fneur.2023.1185375]
13 **Lee E**, Hwang I, Park S, Hong S, Hwang B, Cho Y, Son J, Yu JW. MPTP-driven NLRP3 inflammasome activation in microglia plays a central role in dopaminergic neurodegeneration. *Cell Death Differ* 2019; **26**: 213-228 [PMID: 29786072 DOI: 10.1038/s41418-018-0124-5]
14 **Lee Y**, Park HR, Chun HJ, Lee J. Silibinin prevents dopaminergic neuronal loss in a mouse model of Parkinson's disease *via* mitochondrial stabilization. *J Neurosci Res* 2015; **93**: 755-765 [PMID: 25677261 DOI: 10.1002/jnr.23544]
15 **Meredith GE**, Rademacher DJ. MPTP mouse models of Parkinson's disease: an update. *J Parkinsons Dis* 2011; **1**: 19-33 [PMID: 23275799 DOI: 10.3233/JPD-2011-11023]
16 **Lai F**, Jiang R, Xie W, Liu X, Tang Y, Xiao H, Gao J, Jia Y, Bai Q. Intestinal Pathology and Gut Microbiota Alterations in a Methyl-4-phenyl-1,2,3,6-tetrahydropyridine (MPTP) Mouse Model of Parkinson's Disease. *Neurochem Res* 2018; **43**: 1986-1999 [PMID: 30171422 DOI: 10.1007/s11064-018-2620-x]
17 **Natale G**, Kastsiushenka O, Fulceri F, Ruggieri S, Paparelli A, Fornai F. MPTP-induced parkinsonism extends to a subclass of TH-positive neurons in the gut. *Brain Res* 2010; **1355**: 195-206 [PMID: 20691673 DOI: 10.1016/j.brainres.2010.07.076]
18 **Stavely R**, Ott LC, Rashidi N, Sakkal S, Nurgali K. The Oxidative Stress and Nervous Distress Connection in Gastrointestinal Disorders.

Biomolecules 2023; **13**: 1586 [PMID: 38002268 DOI: 10.3390/biom13111586]
19 **Yokoyama H**, Kuroiwa H, Yano R, Araki T. Targeting reactive oxygen species, reactive nitrogen species and inflammation in MPTP neurotoxicity and Parkinson's disease. *Neurol Sci* 2008; **29**: 293-301 [PMID: 18941931 DOI: 10.1007/s10072-008-0986-2]
20 **Tseng SH**, Lee HH, Chen LG, Wu CH, Wang CC. Effects of three purgative decoctions on inflammatory mediators. *J Ethnopharmacol* 2006; **105**: 118-124 [PMID: 16310993 DOI: 10.1016/j.jep.2005.10.003]
21 **Kong X**, Wan H, Su X, Zhang C, Yang Y, Li X, Yao L, Lin N. Rheum palmatum L. and Coptis chinensis Franch., exert antipyretic effect on yeast-induced pyrexia rats involving regulation of TRPV1 and TRPM8 expression. *J Ethnopharmacol* 2014; **153**: 160-168 [PMID: 24530855 DOI: 10.1016/j.jep.2014.02.007]
22 **Zhang Y**, Fan S, Hu N, Gu M, Chu C, Li Y, Lu X, Huang C. Rhein Reduces Fat Weight in db/db Mouse and Prevents Diet-Induced Obesity in C57Bl/6 Mouse through the Inhibition of PPARγ Signaling. *PPAR Res* 2012; **2012**: 374936 [PMID: 23049539 DOI: 10.1155/2012/374936]
23 **Chen D**, Liu JR, Cheng Y, Cheng H, He P, Sun Y. Metabolism of Rhaponticin and Activities of its Metabolite, Rhapontigenin: A Review. *Curr Med Chem* 2020; **27**: 3168-3186 [PMID: 30666906 DOI: 10.2174/0929867326666190121143252]
24 **Petrovici AR**, Anghel N, Dinu MV, Spiridon I. Dextran-Chitosan Composites: Antioxidant and Anti-Inflammatory Properties. *Polymers (Basel)* 2023; **15**: 1980 [PMID: 37177127 DOI: 10.3390/polym15091980]
25 **Shi Q**, Cheng Y, Dong X, Zhang M, Pei C, Zhang M. Effects of rhaponticin on retinal oxidative stress and inflammation in diabetes through NRF2/HO-1/NF-κB signalling. *J Biochem Mol Toxicol* 2020; **34**: e22568 [PMID: 32662907 DOI: 10.1002/jbt.22568]
26 **Zhang T**, Shi L, Li Y, Mu W, Zhang H, Li Y, Wang X, Zhao W, Qi Y, Liu L. Polysaccharides extracted from Rheum tanguticum ameliorate radiation-induced enteritis *via* activation of Nrf2/HO-1. *J Radiat Res* 2021; **62**: 46-57 [PMID: 33140083 DOI: 10.1093/jrr/rraa093]
27 **George M**, Reddy AP, Reddy PH, Kshirsagar S. Unraveling the NRF2 confusion: Distinguishing nuclear respiratory factor 2 from nuclear erythroid factor 2. *Ageing Res Rev* 2024; **98**: 102353 [PMID: 38815934 DOI: 10.1016/j.arr.2024.102353]
28 **Sies H**, Berndt C, Jones DP. Oxidative Stress. *Annu Rev Biochem* 2017; **86**: 715-748 [PMID: 28441057 DOI: 10.1146/annurev-biochem-061516-045037]
29 **Wei W**, Wang L, Zhou K, Xie H, Zhang M, Zhang C. Rhapontin ameliorates colonic epithelial dysfunction in experimental colitis through SIRT1 signaling. *Int Immunopharmacol* 2017; **42**: 185-194 [PMID: 27930969 DOI: 10.1016/j.intimp.2016.11.024]
30 **Liudvytska O**, Ponczek MB, Ciesielski O, Krzyżanowska-Kowalczyk J, Kowalczyk M, Balcerczyk A, Kolodziejczyk-Czepas J. Rheum rhaponticum and Rheum rhabarbarum Extracts as Modulators of Endothelial Cell Inflammatory Response. *Nutrients* 2023; **15**: 949 [PMID: 36839307 DOI: 10.3390/nu15040949]
31 **De Virgilio A**, Greco A, Fabbrini G, Inghilleri M, Rizzo MI, Gallo A, Conte M, Rosato C, Ciniglio Appiani M, de Vincentiis M. Parkinson's disease: Autoimmunity and neuroinflammation. *Autoimmun Rev* 2016; **15**: 1005-1011 [PMID: 27497913 DOI: 10.1016/j.autrev.2016.07.022]
32 **Langeskov-Christensen M**, Franzén E, Grøndahl Hvid L, Dalgas U. Exercise as medicine in Parkinson's disease. *J Neurol Neurosurg Psychiatry* 2024; **95**: 1077-1088 [PMID: 38418216 DOI: 10.1136/jnnp-2023-332974]
33 **Ben-Shlomo Y**, Darweesh S, Llibre-Guerra J, Marras C, San Luciano M, Tanner C. The epidemiology of Parkinson's disease. *Lancet* 2024; **403**: 283-292 [PMID: 38245248 DOI: 10.1016/S0140-6736(23)01419-8]
34 **Xiang J**, Tang J, Kang F, Ye J, Cui Y, Zhang Z, Wang J, Wu S, Ye K. Gut-induced alpha-Synuclein and Tau propagation initiate Parkinson's and Alzheimer's disease co-pathology and behavior impairments. *Neuron* 2024; **112**: 3585-3601.e5 [PMID: 39241780 DOI: 10.1016/j.neuron.2024.08.003]
35 **Elangovan A**, Dahiya B, Kirola L, Iyer M, Jeeth P, Maharaj S, Kumari N, Lakhanpal V, Michel TM, Rao KRSS, Cho SG, Yadav MK, Gopalakrishnan AV, Kadhirvel S, Kumar NS, Vellingiri B. Does gut brain axis has an impact on Parkinson's disease (PD)? *Ageing Res Rev* 2024; **94**: 102171 [PMID: 38141735 DOI: 10.1016/j.arr.2023.102171]
36 **Scuto M**, Rampulla F, Reali GM, Spanò SM, Trovato Salinaro A, Calabrese V. Hormetic Nutrition and Redox Regulation in Gut-Brain Axis Disorders. *Antioxidants (Basel)* 2024; **13**: 484 [PMID: 38671931 DOI: 10.3390/antiox13040484]
37 **Campos-Acuña J**, Elgueta D, Pacheco R. T-Cell-Driven Inflammation as a Mediator of the Gut-Brain Axis Involved in Parkinson's Disease. *Front Immunol* 2019; **10**: 239 [PMID: 30828335 DOI: 10.3389/fimmu.2019.00239]
38 **Heng Y**, Li YY, Wen L, Yan JQ, Chen NH, Yuan YH. Gastric Enteric Glial Cells: A New Contributor to the Synucleinopathies in the MPTP-Induced Parkinsonism Mouse. *Molecules* 2022; **27**: 7414 [PMID: 36364248 DOI: 10.3390/molecules27217414]
39 **Zhang X**, Tang B, Guo J. Parkinson's disease and gut microbiota: from clinical to mechanistic and therapeutic studies. *Transl Neurodegener* 2023; **12**: 59 [PMID: 38098067 DOI: 10.1186/s40035-023-00392-8]
40 **Silva DF**, Empadinhas N, Cardoso SM, Esteves AR. Neurodegenerative Microbially-Shaped Diseases: Oxidative Stress Meets Neuroinflammation. *Antioxidants (Basel)* 2022; **11**: 2141 [PMID: 36358513 DOI: 10.3390/antiox11112141]
41 **Li Y**, Chen Y, Jiang L, Zhang J, Tong X, Chen D, Le W. Intestinal Inflammation and Parkinson's Disease. *Aging Dis* 2021; **12**: 2052-2068 [PMID: 34881085 DOI: 10.14336/AD.2021.0418]
42 **Tansey MG**, Wallings RL, Houser MC, Herrick MK, Keating CE, Joers V. Inflammation and immune dysfunction in Parkinson disease. *Nat Rev Immunol* 2022; **22**: 657-673 [PMID: 35246670 DOI: 10.1038/s41577-022-00684-6]
43 **Morgenstern C**, Lastres-Becker I, Demirdöğen BC, Costa VM, Daiber A, Foresti R, Motterlini R, Kalyoncu S, Arioz BI, Genc S, Jakubowska M, Trougakos IP, Piechota-Polanczyk A, Mickael M, Santos M, Kensler TW, Cuadrado A, Copple IM. Biomarkers of NRF2 signalling: Current status and future challenges. *Redox Biol* 2024; **72**: 103134 [PMID: 38643749 DOI: 10.1016/j.redox.2024.103134]
44 **Seegert D**, Rosenstiel P, Pfahler H, Pfefferkorn P, Nikolaus S, Schreiber S. Increased expression of IL-16 in inflammatory bowel disease. *Gut* 2001; **48**: 326-332 [PMID: 11171821 DOI: 10.1136/gut.48.3.326]
45 **Sivandzade F**, Prasad S, Bhalerao A, Cucullo L. NRF2 and NF-κB interplay in cerebrovascular and neurodegenerative disorders: Molecular mechanisms and possible therapeutic approaches. *Redox Biol* 2019; **21**: 101059 [PMID: 30576920 DOI: 10.1016/j.redox.2018.11.017]
46 **Zhang C**, Zhao M, Wang B, Su Z, Guo B, Qin L, Zhang W, Zheng R. The Nrf2-NLRP3-caspase-1 axis mediates the neuroprotective effects of Celastrol in Parkinson's disease. *Redox Biol* 2021; **47**: 102134 [PMID: 34600334 DOI: 10.1016/j.redox.2021.102134]
47 **Tan AH**, Lim SY, Lang AE. The microbiome-gut-brain axis in Parkinson disease - from basic research to the clinic. *Nat Rev Neurol* 2022; **18**: 476-495 [PMID: 35750883 DOI: 10.1038/s41582-022-00681-2]
48 **York AG**, Skadow MH, Oh J, Qu R, Zhou QD, Hsieh WY, Mowel WK, Brewer JR, Kaffe E, Williams KJ, Kluger Y, Smale ST, Crawford JM, Bensinger SJ, Flavell RA. IL-10 constrains sphingolipid metabolism to limit inflammation. *Nature* 2024; **627**: 628-635 [PMID: 38383790 DOI: 10.1038/s41586-024-07098-5]
49 **Lee SY**, Jhun J, Woo JS, Lee KH, Hwang SH, Moon J, Park G, Choi SS, Kim SJ, Jung YJ, Song KY, Cho ML. Gut microbiome-derived

butyrate inhibits the immunosuppressive factors PD-L1 and IL-10 in tumor-associated macrophages in gastric cancer. *Gut Microbes* 2024; **16**: 2300846 [PMID: 38197259 DOI: 10.1080/19490976.2023.2300846]

50 **Bido S**, Nannoni M, Muggeo S, Gambarè D, Ruffini G, Bellini E, Passeri L, Iaia S, Luoni M, Provinciali M, Giannelli SG, Giannese F, Lazarevic D, Gregori S, Broccoli V. Microglia-specific IL-10 gene delivery inhibits neuroinflammation and neurodegeneration in a mouse model of Parkinson's disease. *Sci Transl Med* 2024; **16**: eadm8563 [PMID: 39167665 DOI: 10.1126/scitranslmed.adm8563]

51 **Espinosa-Oliva AM**, Ruiz R, Soto MS, Boza-Serrano A, Rodriguez-Perez AI, Roca-Ceballos MA, García-Revilla J, Santiago M, Serres S, Economopoulus V, Carvajal AE, Vázquez-Carretero MD, García-Miranda P, Klementieva O, Oliva-Martín MJ, Deierborg T, Rivas E, Sibson NR, Labandeira-García JL, Machado A, Peral MJ, Herrera AJ, Venero JL, de Pablos RM. Inflammatory bowel disease induces pathological α-synuclein aggregation in the human gut and brain. *Neuropathol Appl Neurobiol* 2024; **50**: e12962 [PMID: 38343067 DOI: 10.1111/nan.12962]

52 **Munoz-Pinto MF**, Candeias E, Melo-Marques I, Esteves AR, Maranha A, Magalhães JD, Carneiro DR, Sant'Anna M, Pereira-Santos AR, Abreu AE, Nunes-Costa D, Alarico S, Tiago I, Morgadinho A, Lemos J, Figueiredo PN, Januário C, Empadinhas N, Cardoso SM. Gut-first Parkinson's disease is encoded by gut dysbiome. *Mol Neurodegener* 2024; **19**: 78 [PMID: 39449004 DOI: 10.1186/s13024-024-00766-0]

53 **Mok SW**, Wong VK, Lo HH, de Seabra Rodrigues Dias IR, Leung EL, Law BY, Liu L. Natural products-based polypharmacological modulation of the peripheral immune system for the treatment of neuropsychiatric disorders. *Pharmacol Ther* 2020; **208**: 107480 [PMID: 31972182 DOI: 10.1016/j.pharmthera.2020.107480]

World Journal of Gastroenterology

Submit a Manuscript: https://www.f6publishing.com

World J Gastroenterol 2025 April 21; 31(15): 104996

DOI: 10.3748/wjg.v31.i15.104996

ISSN 1007-9327 (print) ISSN 2219-2840 (online)

ORIGINAL ARTICLE

Basic Study

Multi-omics reveals the associations among the fecal metabolome, intestinal bacteria, and serum indicators in patients with hepatocellular carcinoma

Jing Feng, Jun-Ping Wang, Jian-Ran Hu, Ping Li, Pin Lv, Hu-Cheng He, Xiao-Wei Cheng, Zheng Cao, Jia-Jing Han, Qiang Wang, Qian Su, Li-Xin Liu

Specialty type: Gastroenterology and hepatology

Provenance and peer review: Unsolicited article; Externally peer reviewed.

Peer-review model: Single blind

Peer-review report's classification

Scientific Quality: Grade A, Grade B

Novelty: Grade A, Grade B

Creativity or Innovation: Grade B, Grade B

Scientific Significance: Grade A, Grade B

P-Reviewer: Qian XK; Wang C

Received: January 9, 2025

Revised: February 18, 2025

Accepted: March 24, 2025

Published online: April 21, 2025

Processing time: 100 Days and 3.3 Hours

Jing Feng, Li-Xin Liu, Department of Gastroenterology, The First Hospital of Shanxi Medical University, Taiyuan 030001, Shanxi Province, China

Jing Feng, Qiang Wang, Qian Su, Department of Infectious Diseases and Hepatology, Shanxi Provincial People's Hospital, Affiliated to Shanxi Medical University, Taiyuan 030012, Shanxi Province, China

Jun-Ping Wang, Pin Lv, Hu-Cheng He, Zheng Cao, Jia-Jing Han, Department of Gastroenterology, Shanxi Provincial People's Hospital, Affiliated to Shanxi Medical University, Taiyuan 030012, Shanxi Province, China

Jian-Ran Hu, Ping Li, Department of Biological Science and Technology, Jinzhong University, Jinzhong 030619, Shanxi Province, China

Xiao-Wei Cheng, Department of Interventional Therapy, Shanxi Provincial People's Hospital, Affiliated to Shanxi Medical University, Taiyuan 030012, Shanxi Province, China

Corresponding author: Li-Xin Liu, Department of Gastroenterology, The First Hospital of Shanxi Medical University, No. 85 Jiefang South Road, Yingze District, Taiyuan 030001, Shanxi Province, China. lixinliu6@hotmail.com

Abstract

BACKGROUND

Hepatocellular carcinoma (HCC), the predominant form of primary liver cancer, is a key contributor to cancer-related deaths globally. However, HCC diagnosis solely based on blood biochemical markers lacks both sensitivity and specificity.

AIM

To investigate alterations of the fecal metabolome and intestinal bacteria and reveal the correlations among differential metabolites, distinct bacteria, and serum indicators.

METHODS

To uncover potentially effective therapeutic targets for HCC, we utilized non-targeted liquid chromatography-mass spectrometry and high-throughput DNA

sequencing targeting the 16S rRNA gene. This comprehensive approach allowed us to investigate the metabolome and microbial community structure of feces samples obtained from patients with HCC. Furthermore, we conducted an analysis to assess the interplay between the fecal metabolome and intestinal bacterial population.

RESULTS

In comparison to healthy controls, a notable overlap of 161 differential metabolites and 3 enriched Kyoto Encyclopedia of Genes and Genomes pathways was observed in the HCC12 (comprising patients with stage I and II HCC) and HCC34 groups (comprising patients with stage III and IV HCC). *Lachnospira*, *Streptococcus*, and *Veillonella* had significant differences in abundance in patients with HCC. Notably, *Streptococcus* and *Veillonella* exhibited significant correlations with serum indicators such as alpha-fetoprotein (AFP). Meanwhile, several differential metabolites [*e.g.*, 4-keto-2-undecylpyrroline, dihydrojasmonic acid, 1,8-heptadecadiene-4,6-diyne-3,10-diol, 9(S)-HOTrE] also exhibited significant correlations with serum indicators such as γ-glutamyl transferase, total bilirubin, AFP, aspartate aminotransferase, and albumin. Additionally, these two genera also had significant associations with differential metabolites such as 1,2-Dipentadecanoyl-rac-glycerol (15:0/20:0/0:0), arachidoyl ethanolamide, and 4-keto-2-undecylpyrroline.

CONCLUSION

Our results suggest that the metabolome of fecal samples and the composition of intestinal bacteria hold promise as potential biomarkers for HCC diagnosis.

Key Words: Hepatocellular carcinoma; Fecal metabolomics; Intestinal bacteria; Correlation analysis; Non-targeted liquid chromatography-mass spectrometry

Core Tip: This study investigated the alterations in the fecal metabolome and intestinal bacteria, and elucidated the correlations among differential metabolites, distinct bacterial taxa, and serum indicators. By employing non-targeted liquid chromatography-mass spectrometry and high-throughput DNA sequencing technologies, the researchers discovered that three Kyoto Encyclopedia of Genes and Genomes pathways, namely retinol metabolism, steroid hormone biosynthesis, and ascorbate and aldarate metabolism, were significantly enriched by differential metabolites, along with three representative bacterial genera: *Streptococcus*, *Veillonella*, and *Lachnospira*. Notably, *Streptococcus* and *Veillonella* exhibited evident correlations with serum indicators and differential metabolites. The findings suggest that the fecal metabolome and the composition of intestinal bacteria hold considerable potential as biomarkers for the diagnosis of hepatocellular carcinoma.

Citation: Feng J, Wang JP, Hu JR, Li P, Lv P, He HC, Cheng XW, Cao Z, Han JJ, Wang Q, Su Q, Liu LX. Multi-omics reveals the associations among the fecal metabolome, intestinal bacteria, and serum indicators in patients with hepatocellular carcinoma. *World J Gastroenterol* 2025; 31(15): 104996
URL: https://www.wjgnet.com/1007-9327/full/v31/i15/104996.htm
DOI: https://dx.doi.org/10.3748/wjg.v31.i15.104996

INTRODUCTION

Primary liver cancer ranked as the third most common cause of cancer-related mortality globally in 2020. Hepatocellular carcinoma (HCC) is the major form of liver cancer, accounting for 75%-85% of liver cancer cases, and it carries a 5-year survival rate lower than 7%[1,2]. To date, early diagnosis is a prerequisite for the effectiveness of various therapies (*e.g.*, surgical resection, and radiation). To improve the prognosis of HCC, it will be important to decode the effects of key clinical and biochemical features on disease duration and treatment response. Consequently, predictive biomarkers are essential for clinical diagnosis and therapy strategy selection in HCC.

Several indicators in blood have been used clinically. For example, high levels of serum alpha-fetoprotein (AFP) are closely associated with elevated mortality, and they have been used to evaluate the risk of tumor relapse after surgical removal and liver transplantation. High levels of vascular endothelial growth factor-A and angiopoietin-2 are associated with an adverse prognosis in HCC, but neither can predict treatment response. Cytokines, such as interleukin-6, interferon alpha, and transforming growth factor-β, have garnered attention as potential predictive biomarkers of the treatment response in HCC. However, definitive conclusions regarding their efficacy, clinical relevance, and specificity in prognosticating treatment outcomes necessitate additional research endeavors and larger-scale prospective studies[3].

The exploration of potential biomarkers for early diagnosis, accurate prognosis, and precision stratification purposes is vital to reducing the disease burden of HCC. Mass spectrometry (MS) is a powerful metabolomics analysis technique that has been applied to different experimental methods and instrument platforms at different stages of biomarker discovery. Currently, MS-based metabolomics analysis has been applied to different samples (such as blood), and it has revealed a

large number of HCC biomarkers[4]. In a study of the sera of 68 patients with HCC, 33 patients with liver cirrhosis, and 34 healthy controls (HCs), Li *et al*[5] identified five metabolites with significant alterations in abundance in HCC: Taurochenodeoxycholic acid, glycochenodeoxycholate, ouabain, theophylline, and xanthine. Based on an analysis of 52 patients with HCC and 59 HCs by liquid chromatography–MS, Liu *et al*[6] reported that the levels of DL-3-phenyllactic acid, L-tryptophan, glycocholic acid, and 1-methylnicotinamide were increased in tissue and portal vein serum samples in HCC, whereas the levels of linoleic acid and phenol were decreased in portal vein and stool samples. Zhang *et al*[7] found that the levels of 15 short-chain fatty acids such as propionate, butyrate, isobutyrate, and 2-methylbutyrate were extremely altered in the feces of patients with HCC. However, the research on the differential metabolites in feces of patients with HCC is insufficient.

The link between the gut microbiota and HCC was recently depicted by numerous researchers. High serum levels of lipopolysaccharide have been observed in patients with chronic liver disease (*e.g.*, HCC, cirrhosis, alcoholic hepatitis)[8], suggesting potential alterations in the ecological structure of the gut microbiota. For example, probiotics can regulate gut microbiota and T-cell differentiation and then interfere with the progression of HCC[9]. Ma *et al*[10] reported that *Bacteroides thetaiotaomicron* and its metabolite acetic acid effectively disturbed the recurrence of HCC and improved clinical outcomes. Therefore, compared with HCs, there are differences in the gut microbiota structure of patients with HCC, but current research has not revealed a consistent pattern. In this study, we investigated the alterations and correlations of the fecal metabolome and gut microbiota in individuals with different stages of HCC to provide novel predictive biotargets for the selection of treatment strategies.

MATERIALS AND METHODS

Patient specimens

Stool and blood samples were gathered from patients with HCC undergoing treatment and subsequent follow-ups at Shanxi Provincial People's Hospital (Taiyuan, Shanxi Province, China) from 2021 to 2022. The study protocol was approved by the medical ethics committee of Shanxi Provincial People's Hospital affiliated to Shanxi Medical University (No. 2021-45). Written informed consent was obtained from all participants in this study. For the HC cohort, the specimens were procured from individuals who were deemed medically fit and who had abstained from antibiotic consumption for at least 1 month preceding their enrollment in the study. Table 1 provides an overview of the demographic details and clinical characteristics of the study participants.

Serum indicator analysis

All patients and HCs underwent assessment of the following blood indicators after 12 hours of fasting: Alanine aminotransferase (ALT), aspartate aminotransferase (AST), total bilirubin (TBIL), γ-glutamyl transferase (GGT), and AFP.

Untargeted metabolomic analysis

Fecal samples were analyzed using an ACQUITY UPLC I-Class PLUS System (Waters, Milford, MA, United States) by Biomarker Technologies (Beijing, China). The column used in this study was the Waters Acquity UPLC HSS T3 column (1.8 μm × 2.1 mm × 100 mm). Mobile phase A consisted of 0.1% formic acid aqueous solution, and 0.1% formic acid acetonitrile was used as mobile phase B. Primary and secondary MS data were collected in the MSe mode using a Xevo G2-XS QTof high-resolution mass spectrometer (Waters) under the control of acquisition software (MassLynx V4.2, Waters).

Following normalization of the original peak area data relative to the total peak area, subsequent analyses were performed. To assess the reproducibility within a group of samples and the performance of quality control samples, both principal component analysis (PCoA) and Spearman's correlation analysis were employed. The classified compounds were queried for their pathway associations and categorization details within the Kyoto Encyclopedia of Genes and Genomes (KEGG), Human Metabolome Database, and Lipid Maps repositories. Utilizing the grouping information, the fold changes (FCs) were computed and compared, and a *t*-test was employed to assess the statistical significance (*P* value) of the differences observed for each compound. R software facilitated orthogonal partial least squares discriminant analysis (OPLS-DA) modeling and validated model reliability *via* 200 permutation tests. Employing multiple cross-validation techniques, we computed the variable importance in projection (VIP) score for the model. Differential metabolites were screened using a combined approach incorporating FCs, *P* values, and VIP scores from the OPLS-DA model. KEGG pathway enrichment significance for differential metabolites was assessed *via* a hypergeometric distribution test.

Fecal microbiota analysis

DNA was extracted from fecal samples. The V3-V4 region of 16S rRNA gene was amplified using the following primers: F, 5'-ACTCCTACGGGAGGCAGCA-3'; and R, 5'-GGACTACHVGGGTWTCTAAT-3'. Following polymerase chain reaction amplification with sequencing adapters, the products underwent purification, quantification, and homogenization to create a sequencing library. This library, once verified, was subjected to sequencing on the Illumina Novaseq 6000 platform by Biomarker Technologies. The raw data were analyzed using the base-calling method, transformed into the original sequenced reads, and stored in the FASTQ file format. Clean reads were obtained after filtration of the raw reads by Trimmomatic v0.33 and the removal of primer sequences by cutadapt 1.9.1. To obtain non-chimeric reads, the clean reads were concatenated using Usearch v10 and denoised, and chimeric sequences were removed using the dada2

Table 1 Demographic profiles and clinical features of the participants in the study, mean ± SD/*n* (%)

Characteristic	HC (*n* = 19)	HCC	
		HCC12 (*n* = 18)	HCC34 (*n* = 20)
Gender			
Female	6	3	3
Male	13 (68.42)	15 (83.33)	17 (85.00)
Age (years)	51.42 ± 7.27	65.83 ± 8.49[b,1]	57.60 ± 8.32[a,b,2]
BMI (kg/m^2)	24.73 ± 2.73	22.40 ± 3.70[a,1]	22.49 ± 3.36[a,b,2]
Stage			
I		7	
II		11	
III			11
IV			9
Complicated with HBV infection		12 (66.67)	18 (90)
Complicated with cirrhosis		18 (100)	19 (95)
ALT (IU/L)	31.34 ± 13.28	24.68 ± 13.70	43.69 ± 34.80[a,2]
AST (IU/L)	20.07 ± 7.09	47.84 ± 30.10[b,1]	73.54 ± 48.00[b,1]
ALB (g/L)	47.39 ± 4.24	34.41 ± 5.49[b,1]	31.37 ± 3.97[b,1]
ALP (IU/L)	79.29 ± 27.75	142.92 ± 183.94	177.34 ± 125.17[b,1]
GGT (mmol/L)	17.41 ± 8.24	111.30 ± 111.34[b,1]	85.48 ± 59.86[b,1]
TBIL (mmol/L)	12.06 ± 4.86	30.33 ± 18.98[b,1]	50.29 ± 52.58[b,1]
AFP (ng/mL)	1.21 ± 1.23	177.50 ± 370.07[b,1]	553.16 ± 548.05[b,1,2]

[a]$P < 0.05$.
[b]$P < 0.01$.
[1]P calculated hepatocellular carcinoma *vs* healthy control.
[2]P calculated comprising patients with stage III and IV hepatocellular carcinoma *vs* comprising patients with stage I and II hepatocellular carcinoma.
HC: Healthy control; HCC: Hepatocellular carcinoma; HCC12: Comprising patients with stage I and II hepatocellular carcinoma; HCC34: Comprising patients with stage III and IV hepatocellular carcinoma; BMI: Body mass index; HBV: Hepatitis B virus; ALT: Alanine aminotransferase; AST: Aspartate aminotransferase; ALB: Albumin; ALP: Alkaline phosphatase; GGT: γ-glutamyl transferase; TBIL: Total bilirubin; AFP: Alpha-fetoprotein.

method in QIIME2 2020.6. Utilizing species annotation and abundance analysis, deeper exploration was conducted into the microbial community's composition, α- and β-diversity indices, dominant bacterial taxa, and functional prediction capabilities. The raw 16S rDNA gene sequencing data have been submitted to the NCBI Sequence Read Archive for access and further analysis (https://www.ncbi.nlm.nih.gov/sra/PRJNA1127013).

Correlation analysis

Correlation analysis between fecal differential metabolites and dominant bacterial taxa or serum indicators was performed using Spearman's correlation analysis. Visualized correlations are denoted by red (positive) and blue (negative) hues, with an ellipse shape indicating the strength of the absolute correlation.

Statistical analysis

Statistical evaluations were conducted in R software (The R Foundation for Statistical Computing, Vienna, Austria) and GraphPad Prism 5 (GraphPad Software, Boston, MA, United States). To discern differential bacterial taxa across groups, permutational multivariate analysis of variance was applied. For multiple comparisons, false discovery rate-adjusted P values were used, with $P < 0.05$ denoting statistical significance and $P < 0.01$ indicating high significance.

RESULTS

Clinical characteristics of the study population

Our cohort of 38 patients included 32 men (84.21%). Twenty-three patients (60.53%) were older than 60 years of age, and

37 patients (97.37%) had cirrhosis. The primary risk factor was hepatitis B virus infection in 30 patients (78.95%). According to the tumor node metastasis staging criteria, 7 (18.42%), 11 (28.95%), 11 (28.95%), and 9 patients (23.68%) had stage I, II, III, and IV HCC, respectively. The mean serum levels of ALT, AST, albumin (ALB), alkaline phosphatase (ALP), GGT, TBIL, and AFP are listed in Table 1, and the detailed values of each sample are presented in Supplementary Table 1. In contrast to the HC group, patients with HCC exhibited markedly elevated serum concentrations of AST, ALB, GGT, TBIL, and AFP. Notably, the mean ALP level in patients with stage I-II HCC was higher than that in HCs, but the difference was not significant. However, substantial differences in ALP levels were noted among patients with HCC. In addition, the serum level of AFP in patients with HCC was remarkably increased ($P < 0.05$), and its levels were significantly higher in advanced HCC stages (III and IV) than in earlier stages (I and II, $P < 0.05$). Receiver operating characteristic (ROC) curve analysis indicated that body mass index, ALT, ALB, ALP, GGT, TBIL, and AFP were significantly associated with the occurrence of HCC. However, ALT [HC *vs* HCC12 (comprising patients with stage I and II HCC), area under the curve (AUC) = 0.6550, $P = 0.1074$; HC *vs* HCC34 (comprising patients with stage III and IV HCC), AUC = 0.5684, $P = 0.4651$] were not associated with HCC (Figure 1A and B, Table 2). Furthermore, only 13 patients with HCC (34.21%) had AFP levels exceeding 400 ng/mL (Supplementary Table 1). Therefore, the sensitivity and specialty of serum indicators in the diagnosis of HCC appeared limited.

Differential metabolites and correlations with serum indicators

The overall differences in the three comparisons are displayed in Figure 1C. R2Y (HC *vs* HCC12, 0.943; HC *vs* HCC34, 0.937; HCC12 *vs* HCC34, 0.995) and Q2Y (HC *vs* HCC12, 0.596; HC *vs* HCC34, 0.42; HCC12 *vs* HCC34, 0.32) suggested that the models were reliable.

The screening criteria for differentially accumulated metabolites comprised $P \leq 0.05$ and VIP ≥ 1. The levels of the metabolites in each sample were displayed as a heatmap in Figure 1D and as volcano plots in Figure 2A-C. As presented in Table 2, 3351 metabolites were detected. In comparison with HCs, the levels of 209 and 118 metabolites were increased in HCC12 and HCC34, respectively, whereas 177 and 297, respectively, were lower (Figure 1E and Table 3). In total, 161 differential metabolites were shared in the two comparisons (HC *vs* HCC12 and HC *vs* HCC34), and seven of them were also significantly altered in the comparison of HCC12 *vs* HCC34 (Figure 1E), including cholylglutamic acid, beta-D-gentiobiosyl crocetin, tryptophyl-proline, pisumionoside, PS [16:0/20:5 (6E,8Z,11Z,14Z,17Z)-OH (5)], 5-hydroxyindoleacetic acid, and lithocholate 3-O-glucuronide. Additionally, ROC analysis was conducted, with Supplementary Figure 1 (HC *vs* HCC12) and Supplementary Figure 2 (HC *vs* HCC34) depicting the ROC curves of the top 10 metabolites by AUC.

To further evaluate the biological significance of differentially accumulated metabolites, we investigated their correlations with serum indicators by Spearman's correlation analysis. The serum indicators and differential metabolites with the strongest correlation are listed in Table 4. AST and ALB were significantly correlated with the differential metabolites in HCC34. The AST level was positively correlated with those of 25-acetyl-6,7-didehydrofevicordin F 3-glucoside and coumatetralyl, whereas the ALB level was positively correlated with those of cholylglutamic acid, propamocarb, and 3b-hydroxy-6b-angeloyloxy-7 (11)-eremophilen-12,8b-olide and negatively correlated with those of 25-acetyl-6,7-didehydrofevicordin F 3-glucoside and 5-ribosylparomamine. Interestingly, we found that AFP was negatively correlated with six differential metabolites [(1S)-1-hydroxy-23,24-didehydro-25,26,27-trinorcalciol, dihydrojasmonic acid, 3-nor-3-oxopanasinsan-6-ol, (6R,7S)-6,7-epoxy-1,3-tetradecadiyne, and 1,8-heptadecadiene-4,6-diyne-3,10-diol] in HCC12 and positively correlated with vamorolone. However, in HCC34, no differential metabolites were significantly correlated with the AFP level. GGT and TBIL were correlated with different metabolites in the HCC12 and HCC34 groups. Concerning other blood indicators, we did not identify differential metabolites significantly correlated with their levels. Notably, six metabolites [(1S)-1-hydroxy-23,24-didehydro-25,26,27-trinorcalciol, dihydrojasmonic acid, vamorolone, 3-nor-3-oxopanasinsan-6-ol, (6R,7S)-6,7-epoxy-1,3-tetradecadiyne, and 1,8-heptadecadiene-4,6-diyne-3,10-diol] were significantly correlated with both TBIL and AFP levels in HCC12 compared with HCs, and 25-acetyl-6,7-didehydrofevicordin F 3-glucoside was related to both AST and ALB in HCC34.

KEGG pathway enrichment analysis

To investigate the critical metabolic pathways altered in patients with HCC, the differentially accumulated metabolites were mapped to the KEEG database. According to the *P* values, number of metabolites involved, and pathway impact, the two most significant KEGG pathways in the HC *vs* HCC12 comparison were retinol metabolism ($P < 0.01$, impact value = 0.47938) and steroid hormone biosynthesis ($P < 0.05$, impact value = 0.15113), followed by terpenoid backbone biosynthesis ($P = 0.24036$, impact value = 0.18571) and glycerophospholipid metabolism ($P = 0.10058$, impact value = 0.15634; Figure 2D and Supplementary Table 2). Retinol metabolism ($P < 0.05$, impact value = 0.26289) and steroid hormone biosynthesis ($P < 0.01$, impact value = 0.17926) were also significantly enriched in the HC *vs* HCC34 comparison. Meanwhile, ascorbate and aldarate metabolism ($P < 0.01$, impact value = 0) was observed (Figure 2E and Supplementary Table 2). These results implied that retinol metabolism, steroid hormone biosynthesis, and ascorbate and aldarate metabolism might be critical to the pathogenesis and development of HCC.

Alterations of the gut microbiota in patients with HCC

To explore the potential function of the gut microbiota in HCC, we investigated the alterations of the ecological structure of the intestinal bacteria. α-diversity was evaluated using four indices, namely abundance-based coverage estimator, Chao1, Simpson, and Shannon (Figure 3A), and the results revealed no significant changes in richness and evenness. However, PCoA identified significant differences among the HC, HCC12, and HCC34 groups, as only a portion of the samples in the three groups overlapped (Figure 3B). Furthermore, the results of OPLS-DA also suggested that these three

Table 2 Receiver operating characteristic analysis of serum indicators

Characteristic	HC *vs* HCC12		HC *vs* HCC34	
	AUC	*P* value	AUC	*P* value
BMI	0.7047	0.0335	0.7000	0.0328
ALT	0.6550	0.1074	0.5684	0.4651
AST	0.8816	< 0.0001	0.9842	< 0.0001
ALB	0.9737	< 0.0001	1	< 0.0001
ALP	0.6170	0.2242	0.8132	0.0008
GGT	0.9064	< 0.0001	0.9289	< 0.0001
TBIL	0.8553	0.0002	0.9263	< 0.0001
AFP	0.9474	< 0.0001	0.9763	< 0.0001

HC: Healthy control; HCC12: Comprising patients with stage I and II hepatocellular carcinoma; HCC34: Comprising patients with stage III and IV hepatocellular carcinoma; BMI: Body mass index; ALT: Alanine aminotransferase; AST: Aspartate aminotransferase; ALB: Albumin; ALP: Alkaline phosphatase; GGT: γ-glutamyl transferase; TBIL: Total bilirubin; AFP: Alpha-fetoprotein.

Table 3 Numbers of differentially accumulated metabolites

Group	Total	Differential metabolites	Up	Down
HC *vs* HCC34	3351	386	209	177
HC *vs* HCC12	3351	415	118	297

HC: Healthy control; HCC12: Comprising patients with stage I and II hepatocellular carcinoma; HCC34: Comprising patients with stage III and IV hepatocellular carcinoma.

groups were separated from each other (Figure 3C), indicating that the community compositions of intestinal bacteria were extremely changed in patients with HCC compared with those in healthy individuals. As illustrated in Figure 3B and C, unweighted pair-group method with arithmetic means revealed a clear separation of the HC group from the HCC12 or HCC34 group (Figure 3D).

The dominant distinct bacterial taxa and their correlations with serum indicators

To identify the primary differential bacterial taxa in patients with HCC, an evaluation of the relative abundance of all bacterial phyla was conducted, with the top 10 most abundant phyla presented in Figure 4A. Of them, *Firmicutes* and *Bacteroidetes* were the two most abundant bacterial phyla. We further compared the relative abundance of various bacterial phyla among the three groups (HC, HCC12, and HCC34), and no distinct phyla were found (Figure 4B).

Then, the relative abundance of bacterial genera was analyzed in each sample, and the top 10 genera are presented in Figure 5A. The proportions of these 10 bacterial genera varied among the samples. Therefore, the dominant taxa in each group were analyzed using linear discriminant analysis (LDA) effect size. The hierarchical relationship of the main communities in each group is displayed in a cladogram in Figure 5B. Three bacterial communities, namely *Lachnospira*, unclassified *Lachnospira* species, and *Selenomonadaceae*, were enriched in the HC group. Four taxa, including *Proteobacteria*, *Gammaproteobacteria*, *Enterobacterales*, and *Enterobacteriaceae*, were dominant in the HCC12 group. The communities enriched in the HCC34 group were unclassified *Rothia* species, *Micrococcales*, *Rothia*, *Micrococcaceae*, unclassified *Veillonella* species, *Veillonella*, unclassified *Streptococcus* species, *Streptococcaceae*, *Streptococcus*, *Lactobacillales*, and *Bacilli*. The LDA score was also utilized to depict the results as a bar chart, as presented in Figure 5C. Notably, three representative bacterial genera were observed, of which the relative abundance of *Lachnospira* was extremely lower in the HCC12 and HCC34 groups, whereas that of *Streptococcus* and *Veillonella* was remarkably increased in these groups (Figure 5D).

Furthermore, the correlations between intestinal bacteria and serum indicators were investigated. Spearman's correlation analysis was used to analyze the correlations between the top 20 differentially abundant bacterial genera and serum indicators in each comparison (Figure 6). In the HC *vs* HCC12 comparison, seven bacterial genera, namely *Streptococcus*, *Veillonella*, *Parabacteroides*, *Lachnoclostridium*, *Lachnospira*, *Roseburia*, and *Subdoligranulum*, were significantly correlated with at least one serum indicator. In the HC *vs* HCC34 comparison, six genera were identified, specifically *Lachnoclostridium, Lachnospira*, *Streptococcus*, *Rothia*, *Veillonella*, and *Haemophilus*. The common genera were *Streptococcus*, *Veillonella*, *Lachnoclostridium*, and *Lachnospira*. Of these, the abundance of *Streptococcus* was positively correlated with the levels of five serum indicators, including GGT, AST, ALP, TBIL, and AFP, in both comparisons and negatively correlated with the serum level of ALB in the HC *vs* HCC34 comparison. *Veillonella* had significant positive correlations with TBIL (HC *vs* HCC12 and HC *vs* HCC34), AFP (HC *vs* HCC12 and HC *vs* HCC34), GGT (HC *vs* HCC34), and AST levels (HC *vs*

Table 4 Correlations between differential metabolites and serum indicators

Serum indicator	HC *vs* HCC12			HC *vs* HCC34		
	Metabolite	Coefficient	*P* value	Metabolite	Coefficient	*P* value
AST				25-Acetyl-6,7-didehydrofevicordin F 3-glucoside	6.92E-01	5.27E-03
				Coumatetralyl	6.42E-01	4.87E-02
ALB				25-Acetyl-6,7-didehydrofevicordin F 3-glucoside	-6.99E-01	3.68E-03
				Cholylglutamic acid	6.82E-01	8.41E-03
				Propamocarb	6.62E-01	2.07E-02
				3b-Hydroxy-6b-angeloyloxy-7(11)-eremophilen-12,8b-olide	6.55E-01	2.81E-02
				5-Ribosylparomamine	-6.50E-01	3.46E-02
GGT	4-Keto-2-undecylpyrroline	-7.01E-01	7.23E-03	Flurandrenolide	6.86E-01	6.99E-03
				Alanine amine	6.79E-01	9.67E-03
				Trans-Oct-2-enoyl-CoA	6.59E-01	2.34E-02
				1′-Hydroxyversicolorone	6.57E-01	2.62E-02
TBIL	(1S)-1-hydroxy-23,24-didehydro-25,26,27-trinorcalciol	-4.29E-01	6.47E-06	2-(Ethylamino)ethanol	6.83E-01	8.12E-03
	Dihydrojasmonic acid	-3.17E-01	1.15E-02	Vitamin A	-6.70E-01	1.49E-02
	Vamorolone	5.05E-01	1.33E-02	9-cis-Retinoic acid	-6.69E-01	1.52E-02
	3-NOR-3-OXOPANASINSAN-6-OL	-3.54E-01	2.85E-02	3,4-Dimethyl-5-pentyl-2-furanpropanoic acid	-6.57E-01	2.60E-02
	(6R,7S)-6,7-Epoxy-1,3-tetradecadiyne	-4.55E-01	3.34E-02			
	1,8-Heptadecadiene-4,6-diyne-3,10-diol	-3.73E-01	3.39E-02			
	9(S)-HOTrE	-2.56E-01	3.56E-02			
AFP	(1S)-1-hydroxy-23,24-didehydro-25,26,27-trinorcalciol	-7.02E-01	6.95E-03			
	Dihydrojasmonic acid	-6.97E-01	8.88E-03			
	Vamorolone	6.95E-01	9.67E-03			
	3-NOR-3-OXOPANASINSAN-6-OL	-6.85E-01	1.52E-02			
	(6R,7S)-6,7-Epoxy-1,3-tetradecadiyne	-6.66E-01	3.51E-02			
	1,8-Heptadecadiene-4,6-diyne-3,10-diol	-6.60E-01	4.35E-02			

HC: Healthy control; HCC12: Comprising patients with stage I and II hepatocellular carcinoma; HCC34: Comprising patients with stage III and IV hepatocellular carcinoma; AST: Aspartate aminotransferase; ALB: Albumin; GGT: γ-glutamyl transferase; TBIL: Total bilirubin; AFP: Alpha-fetoprotein.

HCC34) and a negative correlation with ALB levels (HC *vs* HCC34). *Lachnoclostridium* exhibited negative correlations with AST and AFP levels in both comparisons. *Lachnospira* was negatively associated with TBIL, AFP, and GGT levels in the HC *vs* HCC12 comparison. Meanwhile, in the HC *vs* HCC34 comparison, the genus was and negatively correlated with ALP, AST, AFP, GGT, and TBIL levels and positively correlated with ALB levels.

Correlation analysis of the metabolome and intestinal bacteria in patients with HCC

The correlation between the fecal metabolome and intestinal bacteria was analyzed using Spearman's rank correlation coefficient. The top 10 bacteria in terms of the absolute value of Log_2FC were selected. Differential bacterial phyla (genera) were screened using analysis of variance with the criterion of $P < 0.05$. In the HC *vs* HCC12 comparison, four differentially abundant bacterial phyla, namely *Firmicutes*, *Proteobacteria*, *Fusobacteriota*, and *Desulfobacterota*, were associated with metabolites including 4-keto-2-undecylpyrroline, retinoic acid, and flurandrenolide (Figure 7A, upper panel). Five genera

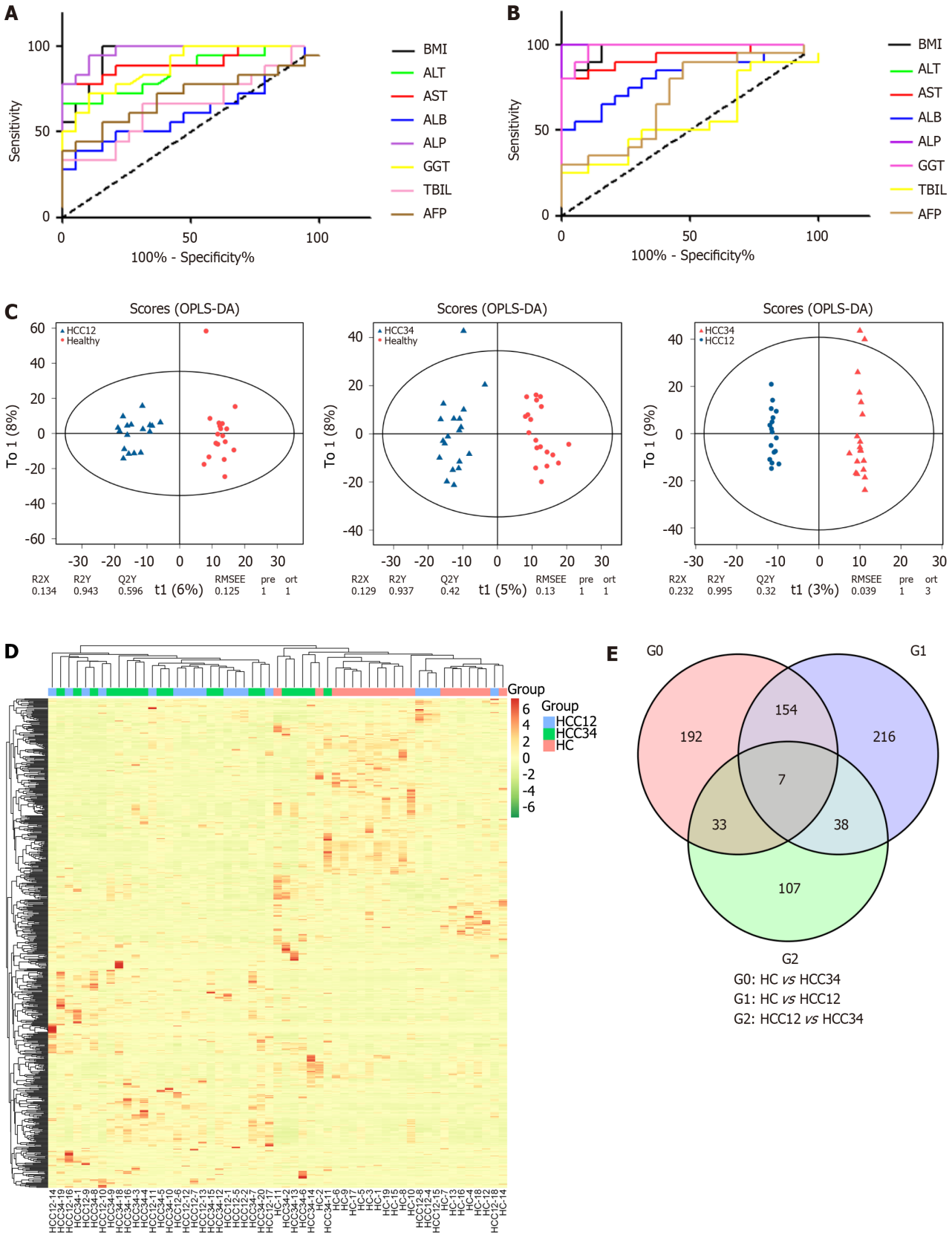

Figure 1 Receiver operating characteristic analysis of serum indicators and alteration analysis of fecal metabolic profiling. A and B: Receiver operating characteristic curves of healthy control (HC) *vs* comprising patients with stage I and II hepatocellular carcinoma (HCC12) (A) and HC *vs* comprising patients with stage III and IV hepatocellular carcinoma (HCC34) (B); C: Orthogonal partial least squares discriminant analysis score plots of HC *vs* HCC12, HC *vs* HCC34, and HCC12 *vs* HCC34; D: Clustered heatmap of the differential metabolites in each group; E: Venn diagram of the differential metabolites in each comparison. BMI: Body mass index; ALT: Alanine aminotransferase; AST: Aspartate aminotransferase; ALB: Albumin; ALP: Alkaline phosphatase; GGT: γ-glutamyl transferase; TBIL: Total bilirubin; AFP: Alpha-fetoprotein; OPLS-DA: Orthogonal partial least squares discriminant analysis; HC: Healthy control; HCC: Hepatocellular carcinoma; HCC12: Comprising patients with stage I and II hepatocellular carcinoma; HCC34: Comprising patients with stage III and IV hepatocellular

carcinoma.

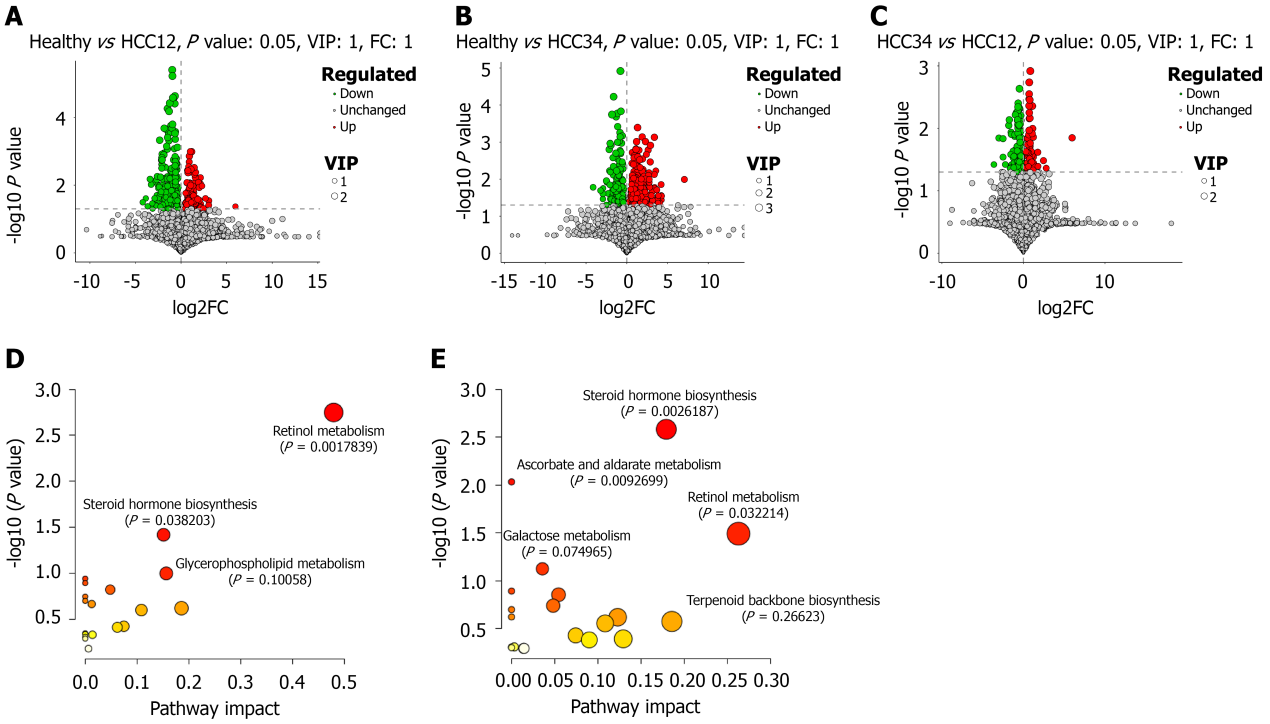

Figure 2 Volcano plots of the differential metabolites and bubble plots of the Kyoto Encyclopedia of Genes and Genomes pathways. A-C: The differential metabolites of healthy control (HC) *vs* comprising patients with stage I and II hepatocellular carcinoma (HCC12) (A), HC *vs* comprising patients with stage III and IV hepatocellular carcinoma (HCC34) (B), and HCC12 *vs* HCC34 (C) were displayed as volcano plots; D and E: Kyoto Encyclopedia of Genes and Genomes enrichment analysis was separately performed on the MetaboAnalyst website (https://www.metaboanalyst.ca/) for the differential metabolites in the two comparisons, namely HC *vs* HCC12 (D) and HC *vs* HCC34 (E). HCC: Hepatocellular carcinoma; HCC12: Comprising patients with stage I and II hepatocellular carcinoma; HCC34: Comprising patients with stage III and IV hepatocellular carcinoma; VIP: Variable importance in projection; FC: Fold change.

(*Klebsiella*, *Agathobacter*, *Escherichia Shigella*, *Roseburia*, and *Veillonella*) were significantly correlated with 4-keto-2-undecyl-pyrroline (*Klebsiella* and *Agathobacter*, $P < 0.05$; *Veillonella*, $P < 0.01$), allo-hydroxycitric acid lactone ($P < 0.05$), and flurandrenolide levels ($P < 0.05$, Figure 7A, lower panel). Of these, *Klebsiella* and *Escherichia Shigella* belong to *Proteobacteria*, and *Agathobacter*, *Roseburia*, and *Veillonella* all belong to *Firmicutes*. In the HC *vs* HCC34 comparison, three genera were associated with the metabolites flurbiprofen glucuronide and DG (15:0/20:0/0:0) (Figure 7B, upper panel), and five genera had significant correlations with eight metabolites (Figure 7B, lower panel). Notably, *Streptococcus* and *Megamonas* both belong to *Firmicutes*. *Streptococcus* exhibited positive association with the levels of DG (15:0/20:0/0:0) ($P < 0.05$), and *Megamonas* was positively correlated with PZ-peptide ($P < 0.05$) and glycyrrhizic acid levels ($P < 0.01$). In the HCC12 *vs* HCC34 comparison, three phyla displayed significant correlations with four metabolites (Figure 7C, upper panel). Interestingly, arachidoyl ethanolamide had a significant correlation with *Streptococcus* ($P < 0.01$, Figure 7C, lower panel). Meanwhile, *Bacteroides* was associated with 5-hydroxyferulate ($P < 0.05$) and carteolol levels ($P < 0.01$). Combined with the correlation analysis with serum indicators (Figure 6), *Streptococcus* and *Veillonella* appeared to be most important in the onset and development of HCC.

DISCUSSION

Blood-based biomarkers are commonly used indicators for diagnosing liver diseases. AFP is the conventional blood diagnostic marker for HCC. The normal AFP concentration ranges from 0 to 40 ng/mL, and it is significantly elevated in the blood of 60%-70% of patients with HCC. Meanwhile, approximately 30% of patients with HCC exhibit negative AFP levels clinically[11]. Additionally, AFP levels can be changed in response to liver injury and some other liver diseases (such as steatohepatitis, fatty liver, and chronic or active hepatitis)[12], resulting in false-positive diagnostic results. Thus, the specificity and sensitivity of AFP as a diagnostic indicator for HCC are limited. To reduce misdiagnosis, additional blood indicators need to be comprehensively evaluated clinically, such as ALT and AST. However, alterations in the levels of these indicators are usually related to various factors. For example, in addition to HCC, ALT is also associated with long-term alcohol consumption, fatty liver disease, and the use of certain liver-damaging drugs (such as isoniazid tablets and rifampicin tablets)[13]. AST is one of the biomarkers of myocardial injury, and its abnormal elevation is also

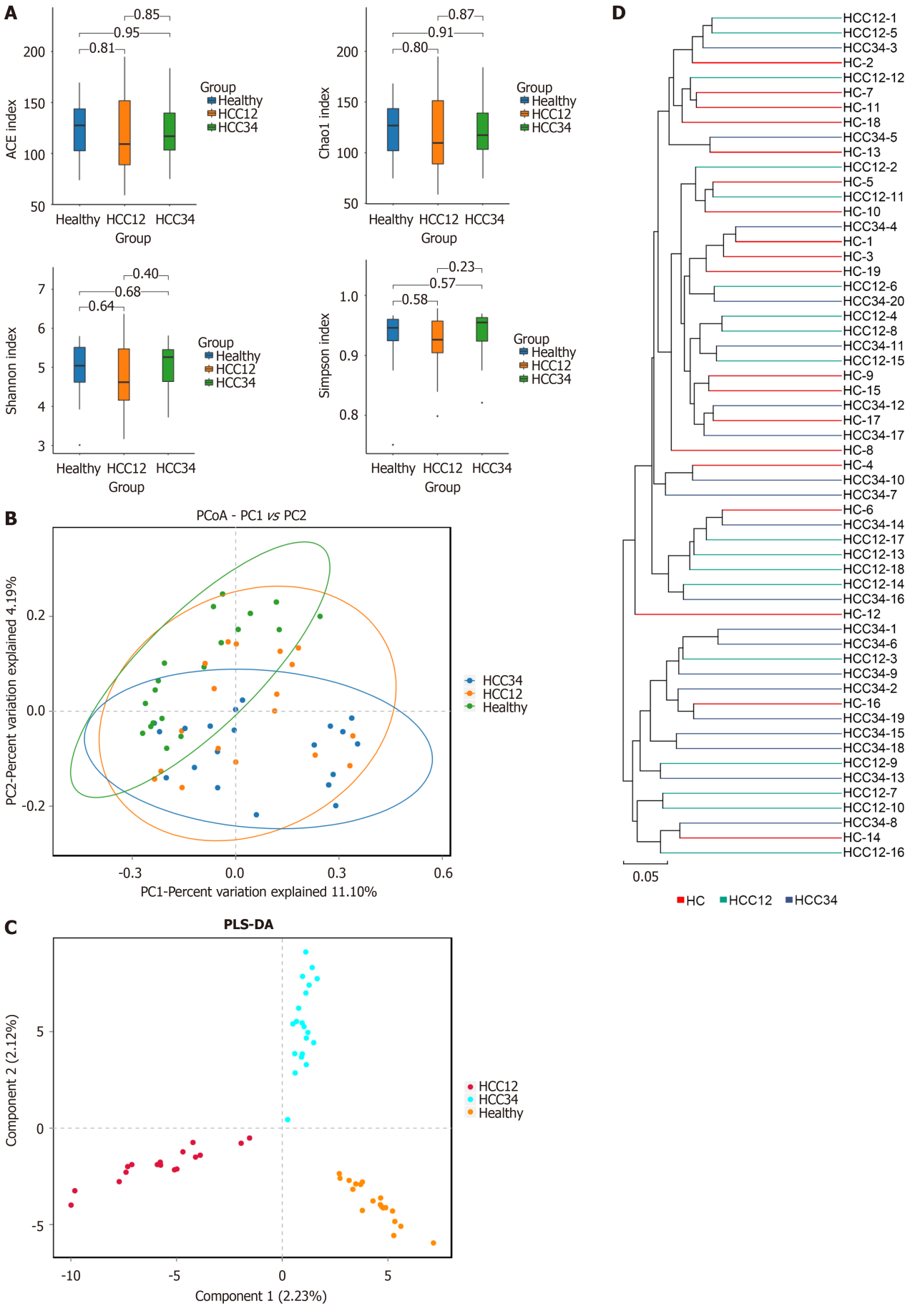

Figure 3 Alterations of the ecological structure of the intestinal bacteria in patients with hepatocellular carcinoma. A: Assessment of α-

diversity within fecal samples sourced from patients with hepatocellular carcinoma; B: Visualization of unweighted UniFrac principal component analysis scores through a scatter plot; C: Scatter plot of orthogonal partial least squares discriminant analysis of the metabolic profiling of each group; D: Construction of a hierarchical clustering dendrogram utilizing the unweighted pair group method with arithmetic mean. PCoA: Principal component analysis; HCC12: Comprising patients with stage I and II hepatocellular carcinoma; HCC34: Comprising patients with stage III and IV hepatocellular carcinoma; ACE: Abundance-based coverage estimator; PLS-DA: Partial least squares discriminant analysis; HC: Healthy control.

closely related to glucose and lipid metabolism disorders[14]. ALB is associated with kidney disease and decreased immune function[15]. Elevated ALP might be caused by jaundice, rickets, leukemia, and other diseases[16]. The significant increase in GGT levels in serum might be related to pancreatic head cancer, cirrhosis, and other diseases[17]. Abnormally elevated TBIL levels can be suggestive of conditions including hemolysis and gallstones[18]. We analyzed blood indicators in 38 patients with HCC, with 13 patients (3 in the HCC12 group and 10 in the HCC34 group) having AFP levels exceeding 400 ng/mL. Interestingly, among patients with AFP levels lower than 40 ng/mL, 19 had normal serum levels, including 13 and 6 in the HCC12 and HCC34 groups, respectively (Tables 1 and Supplementary Table 1). Although six other blood indicators were also measured in this study, their diagnostic value for HCC was limited. In addition to blood indicators, liver ultrasonography is also used clinically to screen patients with HCC. However, because of the limited specificity and sensitivity of ultrasonography, early liver cancer lesions might not be detected promptly, and false-negative results cannot be avoided. Therefore, new and more effective biomarkers urgently need to be developed.

Metabolomics studies of feces, biofluids, and tissues have been considered powerful methods for describing metabolic features during the onset of HCC. A study involving 262 patients with HCC identified three metabolites (taurocholic acid, lysophosphoethanolamine, and lysophosphatidylcholine) with significantly increased levels in the sera of patients with HCC[19]. Jee *et al*[20] found five serum metabolites (leucine, phenylalanine, tyrosine, arachidonic acid, and 5-hydroxyhexanoic acid) were highly correlated with the occurrence of HCC among 37 significantly differential metabolites using an ultra-performance liquid chromatography-MS method. Compared with body fluid samples, the metabolites enriched in feces are partly sourced from the gut microbiota, potentially reflecting the pathogenesis and progression of HCC and the interplay between the gut microbiota and disease progression[21]. Of note, the fecal metabolome largely reflects the community structure of the gut microbiota, and it is considered a functional indicator of the gut microbiota[22]. Research by Liu *et al*[6] uncovered that the concentrations of linoleic acid and phenol in feces and hepatic portal vein blood samples from patients with HCC were notably diminished in comparison to those found in HCs. Furthermore, linoleic acid and phenol exhibit suppressive effects on the viability and colony formation of HCC cells, specifically Hep3B and Huh7 cells, while inducing apoptosis in these cells. However, these compounds did not exert similar effects on normal hepatocyte cells, such as MIHA cells[6]. In this study, we identified seven low-abundance metabolites in the HCC12 group, including three (retinol, retinoate, and 9-cis-retinoic acid) involved in retinol metabolism and four (dehydroepiandrosterone, dehydroepiandrosterone sulfate, androstenediol, and androstenedione) involved in steroid hormone biosynthesis (Figure 2D). Two differential metabolites with reduced levels in the HCC34 group, (retinol and 9-cis-retinoic acid) are involved in retinol metabolism, other six metabolites with decreased levels (dehydroepiandrosterone, dehydroepiandrosterone sulfate, androstenediol, 17-alpha-hydroxyprogesterone, estrone, and 16-glucuronide-estriol) are involved in steroid hormone biosynthesis, and two metabolites (myo-inositol and beta-D-glucuronoside) are involved in ascorbate and aldarate metabolism (Figure 2E). Retinol metabolism has been observed to be inhibited in patients with metabolic dysfunction-associated fatty liver disease[23,24], and they have critical roles in the regulation of metabolic disorders attributable to carbon tetrachloride-induced liver fibrosis[25]. Furthermore, retinaldehyde storage was extremely reduced in patients with HCC, and retinol metabolism might be a potential diagnostic and prognostic marker in HCC[26]. Steroid hormones play crucial roles in multiple metabolic pathways, and the liver is responsible for maintaining their homeostasis[27]. Steroid hormone imbalance has been linked to multiple liver disorders. For instance, hypoestrogenism can trigger the onset and progression of non-alcoholic fatty liver disease in post-menopausal females[28]. Deficiency of testosterone, the primary androgen, might contribute to the development of sarcopenia in male patients with liver cirrhosis[29]. Therefore, inhibition of steroid hormone biosynthesis might lead to HCC. Ascorbate was demonstrated to affect the proliferation and viability of tumor cells[30]. It has been reported that ascorbate and aldarate metabolism is associated with the development of metabolic-associated steatotic liver disease (MASLD)[31]. Notably, several studies also reported associations of retinol metabolism or steroid hormone biosynthesis with the gut microbiota. Han *et al*[32] found that the interaction between the gut microbiota and retinol metabolism could modulate white adipose tissue accumulation and obesity. A recent study demonstrated that during liver regeneration, the gut microbiota and systemic metabolism undergo extensive alterations and exhibit a strong correlation. Among the gut microbes, *Escherichia Shigella*, *Lactobacillus*, *Akkermansia*, and *Muribaculaceae* emerged as the representative differential bacterial taxa. Meanwhile, steroid hormone biosynthesis was the most prominent metabolic pathway[33]. However, few reports examined the relationship between ascorbate and aldarate metabolism and the gut microbiota. In the present study, we observed that both retinol metabolism and steroid hormone biosynthesis were suppressed in patients with stage I-IV HCC (the HCC12 and HCC34 groups). Additionally, ascorbate and aldarate metabolism was dysregulated in patients with stage III-IV HCC (the HCC34 group). Meanwhile, we also identified several gut bacterial genera, including *Streptococcus*, *Veillonella*, and *Lachnospira*, with significant alterations. These findings imply potential associations of the gut microbiota with the aforementioned metabolic pathways.

Differential metabolites have emerged as potential biomarkers in a variety of diseases. For example, 2-methyl-1-propylamine and estrone display excellent diagnostic capabilities in the early stage of cervical intraepithelial neoplasia [34]. Palmitoylcarnitine and sphingosine might be potential biomarkers of colorectal cancer[35]. Nineteen serum

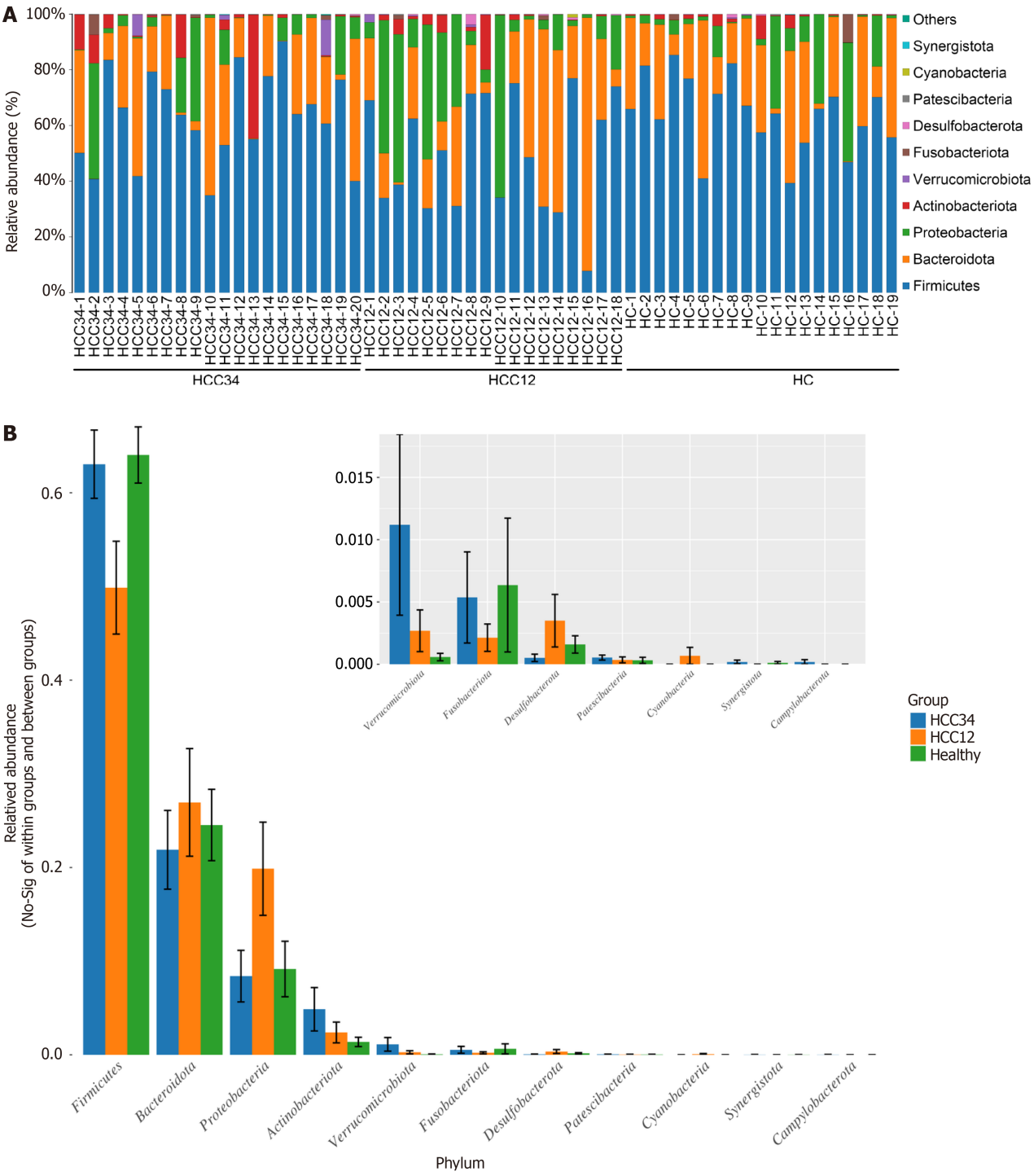

Figure 4 The phylum-level composition of the gut microbiota in patients with hepatocellular carcinoma. A: The 10 phyla with the highest abundance in each sample; B: Variance analysis of the 10 most abundant bacterial phyla among the groups. HC: Healthy control; HCC: Hepatocellular carcinoma; HCC12: Comprising patients with stage I and II hepatocellular carcinoma; HCC34: Comprising patients with stage III and IV hepatocellular carcinoma.

metabolites related to energy metabolism, lipid metabolism, amino acid metabolism, and citric acid metabolism were considered potential biomarkers of pancreatic ductal adenocarcinoma[36]. Eight differential metabolites were identified as alternative markers for predicting the formation of gastroesophageal cancer[37]. In combination with AUC analysis (Supplementary Figure 1 and 2), the correlations of differential metabolites with serum indicators (Table 4) demonstrated that several metabolites were likely biomarkers for different stages of HCC. We further investigated the associations between these metabolites and liver physiological activities by reviewing the literature and searching relevant databases. For example, 25-acetyl-6,7-didehydrofevicordin F 3-glucoside is an intermediate metabolite mainly generated from saponin, and it is usually associated with lipid peroxidation, fatty acid metabolism, cell signaling, and lipid metabolism. Cholylglutamic acid is a conjugate that mainly consists of an amino acid and a primary bile acid such as cholic acid, deoxycholic acid, and chenodeoxycholic acid[38]. Quinn *et al*[39] reported that these bile acid-amino acid conjugates are produced by gut microbes such as *Clostridia* species, and they were frequently found in patients with inflammatory bowel

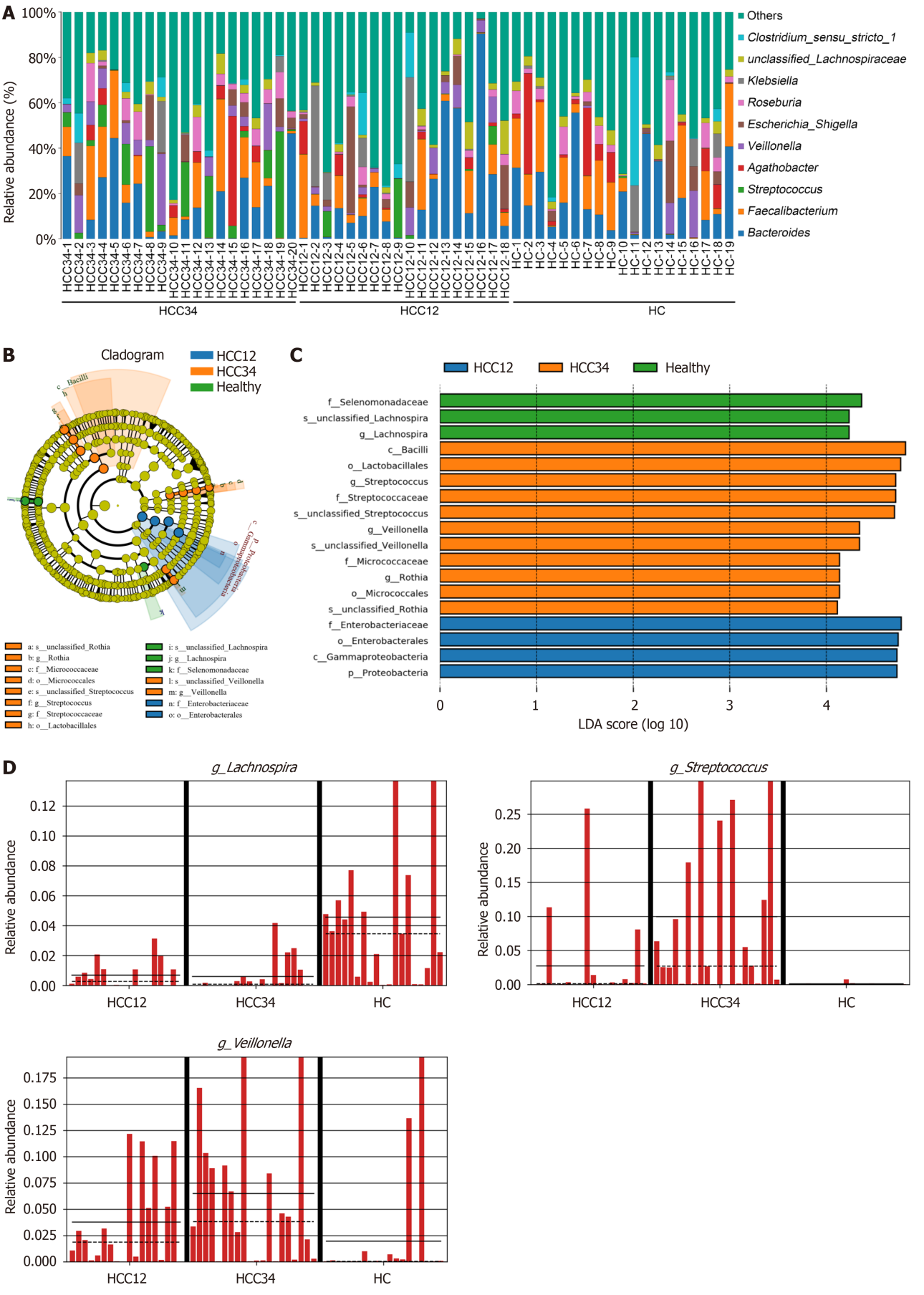

Figure 5 Screening of the dominant differential bacterial communities in patients with hepatocellular carcinoma. A: The top 10 most dominant bacterial genera and their proportional presence in the three groups; B: Linear discriminant analysis effect size; C: Linear discriminant analysis score; D: Three

representative bacterial genera with significant intergroup differences. The median is indicated by the dashed line, whereas the solid line denotes the mean. HCC: Hepatocellular carcinoma; HC: Healthy control; HCC12: Comprising patients with stage I and II hepatocellular carcinoma; HCC34: Comprising patients with stage III and IV hepatocellular carcinoma; LDA: Linear discriminant analysis.

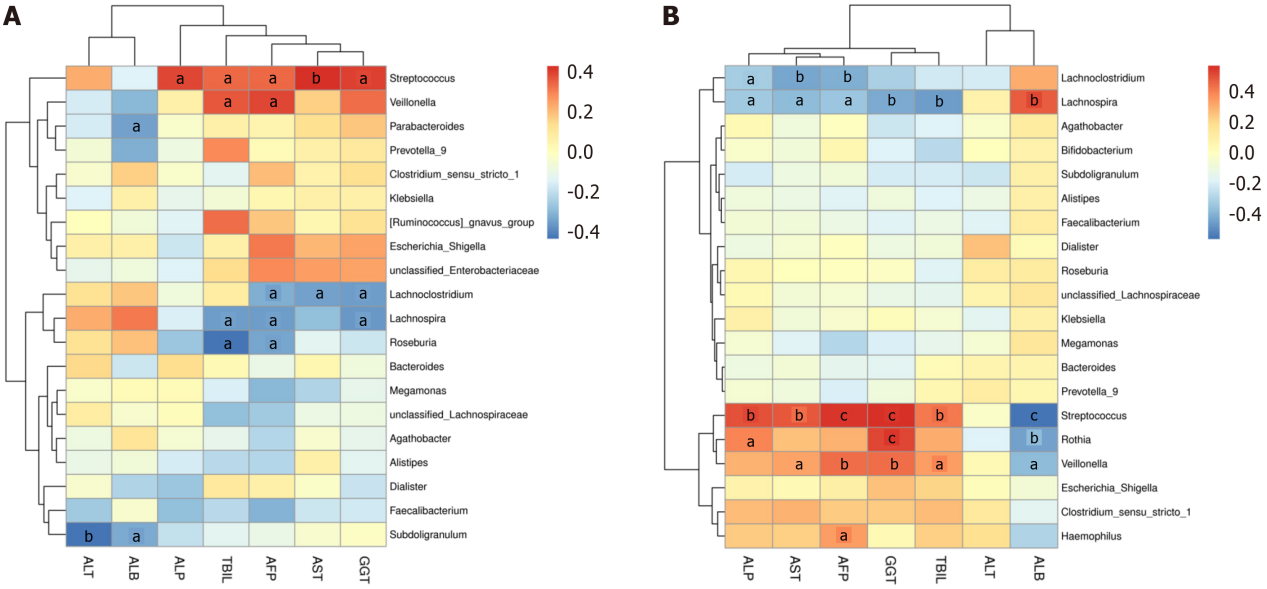

Figure 6 Correlation analysis of intestinal microbiota and serum indicators. The heatmap presents the correlations between the top 20 differentially abundant bacterial genera and serum indicators. A: In the comparisons healthy control (HC) *vs* comprising patients with stage I and II hepatocellular carcinoma (HCC12); B: HC *vs* comprising patients with stage III and IV hepatocellular carcinoma (HCC34). $^{a}P < 0.05$. $^{b}P < 0.01$. $^{c}P < 0.001$. ALT: Alanine aminotransferase; AST: Aspartate aminotransferase; ALB: Albumin; ALP: Alkaline phosphatase; GGT: γ-glutamyl transferase; TBIL: Total bilirubin; AFP: Alpha-fetoprotein.

disease and cystic fibrosis and in infants. They appeared to activate the farnesoid X receptor and inhibit the expression of bile acid synthesis genes[39]. Trans-2-enoyl-CoA was found to be involved in the sphingosine-to-glycerolipid metabolic pathway in mammals[40], and it also participates in the fatty acid elongation cycle[41]. Vitamin A (retinol), a yellow, fat-soluble antioxidant, is vital for embryogenesis, vision, cell function, immune regulation, and metabolism. Liver diseases causing fibrosis and cirrhosis disrupt vitamin A homeostasis, often leading to deficiency. Upon liver injury, hepatic stellate cells (HSCs) are transformed into myofibroblasts. These cells overproduce extracellular matrix, causing fibrosis. As HSCs deplete retinyl ester stores during this change, vitamin A deficiency ensues. Non-alcoholic fatty liver disease, a liver-related aspect of metabolic syndrome, spans from mild steatosis to steatohepatitis, and it can progress to cirrhosis and liver cancer[42]. 9-Cis-retinoic acid is the main active form of vitamin A, and it can bind to nuclear retinoic acid receptors and retinoid X receptors. 9-Cis-retinoic acid is typically used in the combinational treatment of breast, liver, and gastric cancers[43]. 3,4-Dimethyl-5-pentyl-2-furanpropanoic acid is a furan fatty acid that might be produced by gut microbes, and it is considered a healthy biomarker[44]. 4-keto-2-undecylpyrroline is a pyrroline which was mainly produced by genus *Streptococcus*[45]. 3-Nor-3-oxopanasinsan-6-ol is considered a potential biomarker for the progression of intestinal pathology in mice infected with *Schistosoma*[46]. Interestingly, hydroxyversicolorone, a natural product newly isolated from a blocked mutant of *Aspergillus parasiticus*, has been synthesized in labeled form and incorporated intact into aflatoxin B1 by mycelial suspensions of wild-type *Aspergillus parasiticus*[47]. 2-(Ethylamino) ethanol is not a naturally occurring metabolite, and it is only found in individuals exposed to this compound or its derivatives. This compound has been identified in human blood[48]. However, the biological functions of some of the differential metabolites listed in Table 4 have not been reported.

The total number of bacterial cells residing in the human body is approximately 3.9×10^{13}, and most of them survive in the gastrointestinal tract[49]. During the evolutionary process, the gut microbiota and host have co-evolved, establishing a mutually beneficial relationship[50]. The profound connection between the gut microbiota (*e.g.*, intestinal bacteria) and liver function affects the onset and progression of HCC. Investigations revealed that the gut microbiota of individuals with HCC undergoes alterations in its composition, with the abundance of more than 30 distinct types of intestinal microorganisms potentially changing during the early stages of the disease. This underscores the pivotal role of the gut microbiota in the initiation and progression of HCC across various stages starting from a benign liver condition[51]. Metabolites generated by the gut microbiota, along with pro-inflammatory molecules secreted by intestinal epithelial cells, have the capacity to traverse the portal vein and enter the liver. Once there, they can contribute to the development and progression of liver cancer[52]. A plethora of evidence indicates that the gut–liver axis affects the progression of liver diseases, namely fibrosis, cirrhosis, and cancer. For example, *Klebsiella pneumoniae* is related to MASLD in humans, and it can also cause MASLD in mice. The abundance of *Bacteroides* species and *Ruminococcaceae* was much higher in patients with HCC than in healthy individuals, whereas the opposite trend was noted for the abundance of *Bifidobacterium*[53]. A study revealed that some intestinal microorganisms (*e.g.*, *Clostridium*) transformed primary bile acids into deoxycholic

A **HC *vs* HCC12**

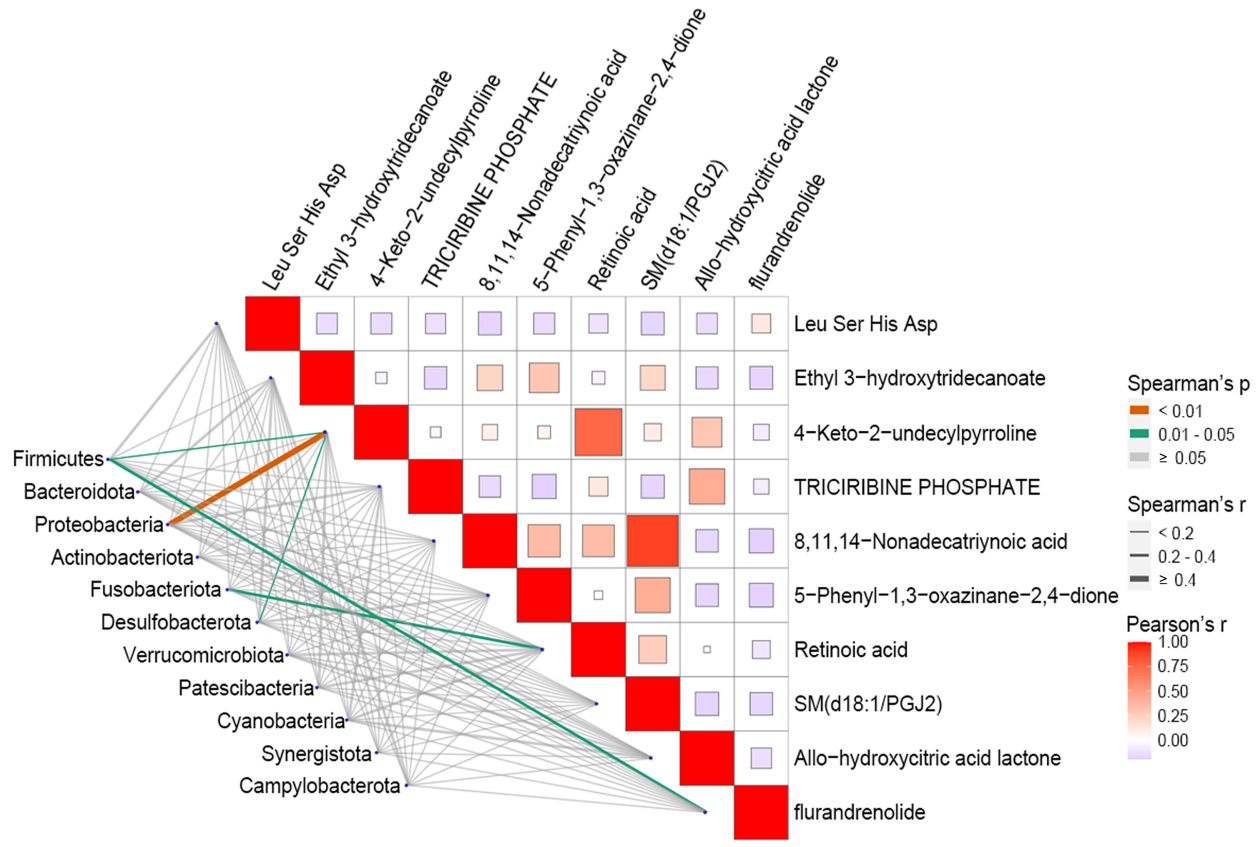
Leu Ser His Asp
Ethyl 3−hydroxytridecanoate
4−Keto−2−undecylpyrroline
TRICIRIBINE PHOSPHATE
8,11,14−Nonadecatriynoic acid
5−Phenyl−1,3−oxazinane−2,4−dione
Retinoic acid
SM(d18:1/PGJ2)
Allo−hydroxycitric acid lactone
flurandrenolide
Firmicutes
Bacteroidota
Proteobacteria
Actinobacteriota
Fusobacteriota
Desulfobacterota
Verrucomicrobiota
Patescibacteria
Cyanobacteria
Synergistota
Campylobacterota
Spearman's p
< 0.01
0.01 - 0.05
≥ 0.05
Spearman's r
< 0.2
0.2 - 0.4
≥ 0.4
Pearson's r
1.00
0.75
0.50
0.25
0.00

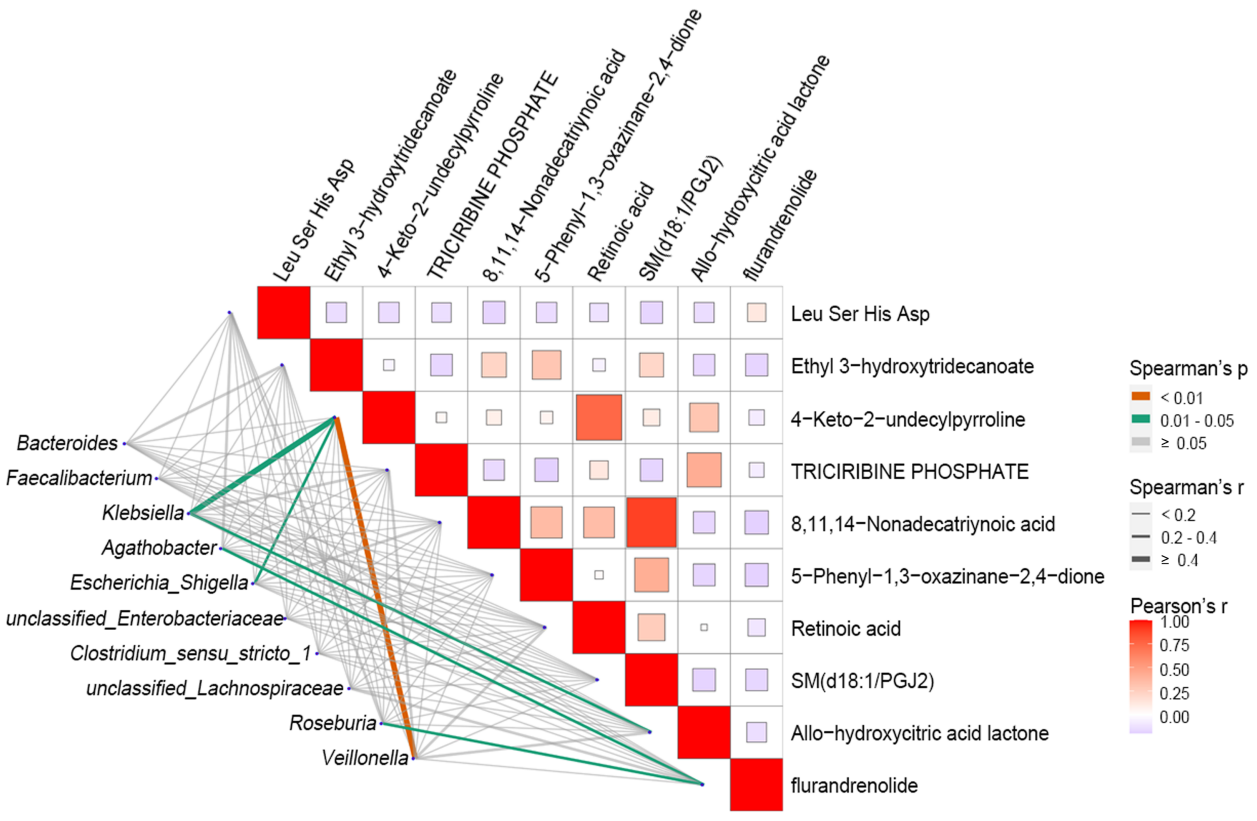
Leu Ser His Asp
Ethyl 3−hydroxytridecanoate
4−Keto−2−undecylpyrroline
TRICIRIBINE PHOSPHATE
8,11,14−Nonadecatriynoic acid
5−Phenyl−1,3−oxazinane−2,4−dione
Retinoic acid
SM(d18:1/PGJ2)
Allo−hydroxycitric acid lactone
flurandrenolide
Bacteroides
Faecalibacterium
Klebsiella
Agathobacter
Escherichia_Shigella
unclassified_Enterobacteriaceae
Clostridium_sensu_stricto_1
unclassified_Lachnospiraceae
Roseburia
Veillonella
Spearman's p
< 0.01
0.01 - 0.05
≥ 0.05
Spearman's r
< 0.2
0.2 - 0.4
≥ 0.4
Pearson's r
1.00
0.75
0.50
0.25
0.00

B

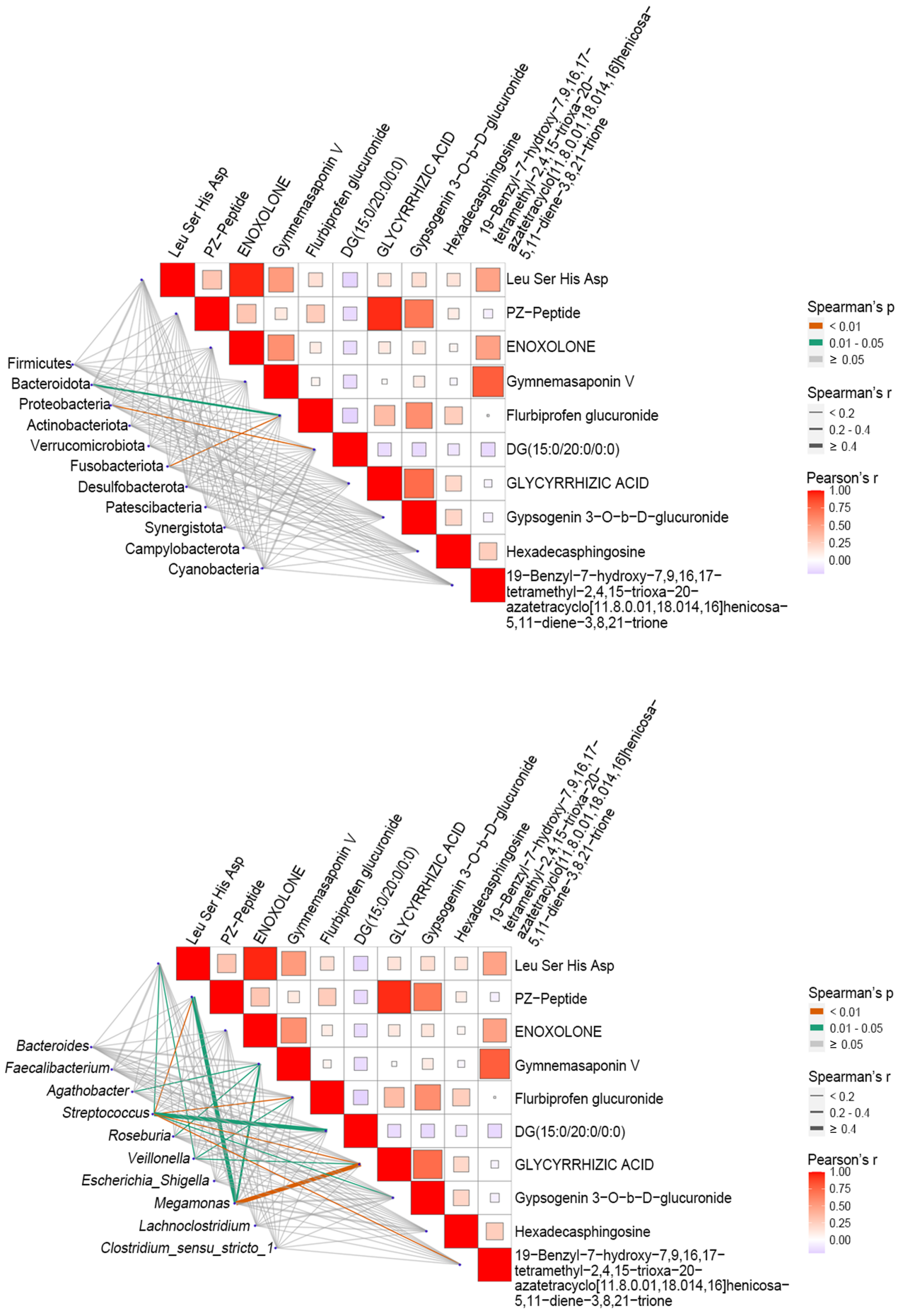
HC *vs* HCC34
Leu Ser His Asp
PZ-Peptide
ENOXOLONE
Gymnemasaponin V
Flurbiprofen glucuronide
DG(15:0/20:0/0:0)
GLYCYRRHIZIC ACID
Gypsogenin 3-O-b-D-glucuronide
Hexadecasphingosine
19-Benzyl-7-hydroxy-7,9,16,17-tetramethyl-2,4,15-trioxa-20-azatetracyclo[11.8.0.01,18.014,16]henicosa-5,11-diene-3,8,21-trione
Firmicutes
Bacteroidota
Proteobacteria
Actinobacteriota
Verrucomicrobiota
Fusobacteriota
Desulfobacterota
Patescibacteria
Synergistota
Campylobacterota
Cyanobacteria
Spearman's p
< 0.01
0.01 - 0.05
≥ 0.05
Spearman's r
< 0.2
0.2 - 0.4
≥ 0.4
Pearson's r
1.00
0.75
0.50
0.25
0.00
Bacteroides
Faecalibacterium
Agathobacter
Streptococcus
Roseburia
Veillonella
Escherichia_Shigella
Megamonas
Lachnoclostridium
Clostridium_sensu_stricto_1

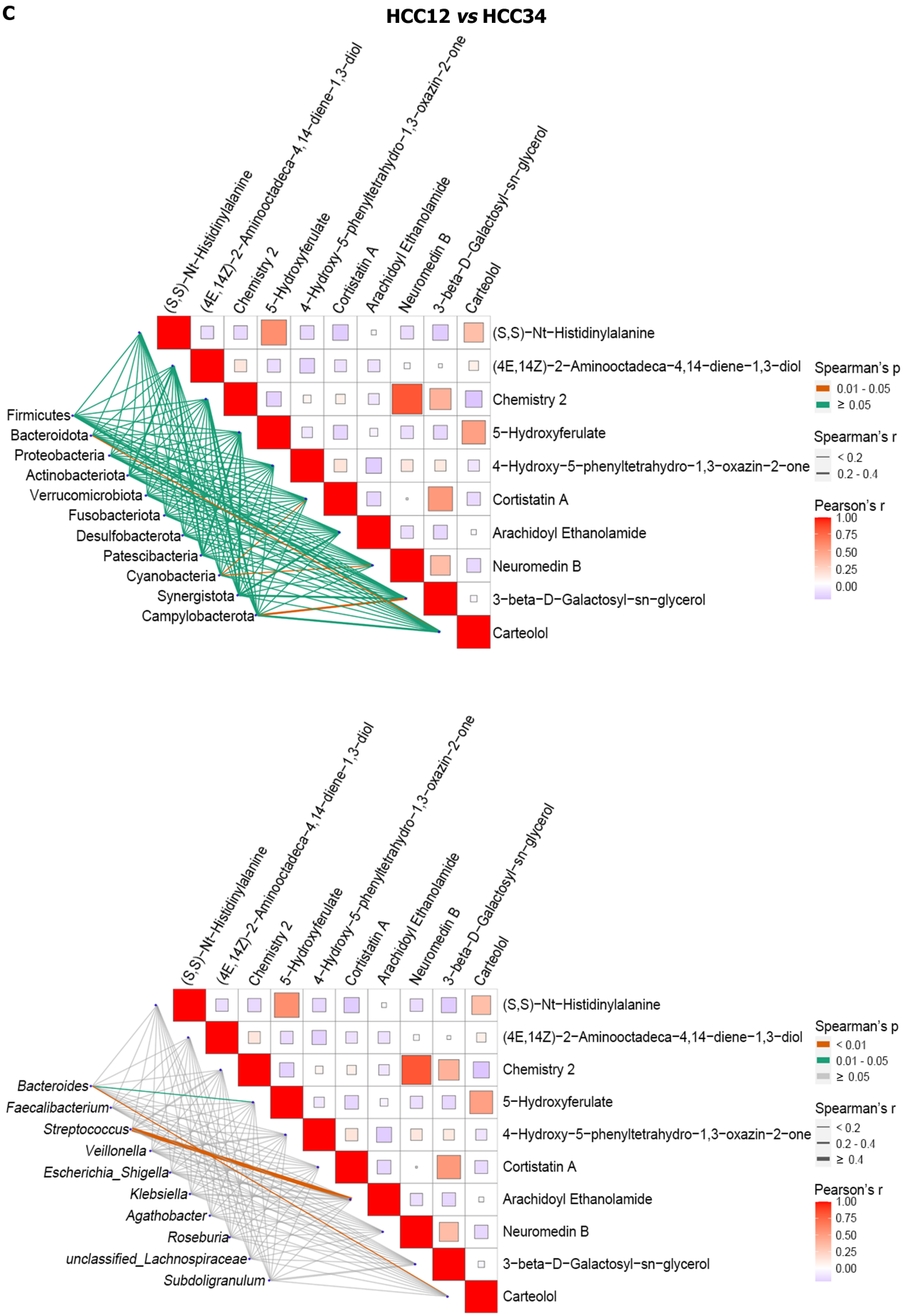

Figure 7 Heatmap of the correlations between differential metabolites and bacterial genera in fecal samples. A-C: Correlation analysis of the

differential metabolites and bacterial genera based on comparisons including healthy control (HC) *vs* comprising patients with stage I and II hepatocellular carcinoma (HCC12) (A), HC *vs* comprising patients with stage III and IV hepatocellular carcinoma (HCC34) (B), and HCC12 *vs* HCC34 (C). Correlation analysis was conducted between differential metabolites and bacteria at the phylum (upper panel) and genus level (lower panel).

acid, which stimulate liver cells to release inflammatory factors and tumor-promoting factors through enterohepatic circulation. HCC occurred once the host was exposed to chemical carcinogens [*e.g.*, 7, 12-dimethylbenz(a)anthracene]. Inhibition of deoxycholic acid-producing intestinal bacteria by antibiotic therapy effectively reduced the risk of HCC in carcinogen-induced obese mice[54]. Therefore, the community structure of intestinal bacteria affects the pathogenesis of HCC. In this study, three representative differential bacterial genera, namely *Lachnospira*, *Streptococcus*, and *Veillonella*, were identified in the HCC12 and HCC34 groups. *Lachnospira* was reported to exhibit similar temporal patterns and causative relationships with *Akkermansia* and *Bifidobacterium* in HCC[55], and we found that the abundance of *Lachnospira* was extremely decreased in the HCC12 and HCC34 groups (Figure 5D). The relative abundance of *Streptococcus* was positively associated with AFP levels in the sera of older patients with HCC[56]. Our findings also confirmed these results (Figure 6). *Streptococcus* is an anaerobic bacterium, and it has been considered a diagnostic marker for gastrointestinal cancer. For example, a significant increase in the abundance of *Streptococcus* might lead to gastric[57] or colon cancer[58, 59]. *Streptococcus* also appeared to serve as a potential biomarker of liver metastasis in gastric cancer[60]. Wu *et al*[61] believed that gut microbiota-driven metabolic alterations might affect cachexia in gastric cancer, and *Streptococcus* was one of the main genera with an increase in abundance. In the patients with HCC, *Streptococcus* and *Veillonella* both exhibited constant increases in abundance in fecal samples during disease progression[62]. They were identified as two cirrhosis-related genera, and they were significantly correlated with the metabolic profile[63]. Zheng *et al*[64] revealed that *Streptococcus* and *Veillonella* also contributed to the early recurrence of HCC, and the potential mechanism was that gut microbe-derived acetic acid could provide the energy for tumor cell proliferation. A study conducted in Thailand reported that the abundance of *Veillonella* was significantly higher in patients with intrahepatic cholangiocarcinoma than in those with HCC[65]. Our findings indicated that *Streptococcus* was positively correlated with DG (15:0/20:0/0:0) levels and negatively correlated with enoxolone and leucine-serine-histidine-asparticacid levels (HCC12 group, Figure 6). Enoxolone exerts cytotoxic effects on human gingival fibroblasts and strong inhibitory effects on bacterial growth[66], and the combination of enoxolone and silibinin can prevent prostate cancer cell growth in mice[67]. In the HCC12 *vs* HCC34 comparison, *Streptococcus* had a positive correlation with arachidoyl ethanolamide, which displayed cannabinoid-like effects in mice[68] and a clear decrease in content in plasma from an Alzheimer's disease mouse model[69] but no association with HCC. Additionally, *Lachnospira* was positively associated with the levels of flurandrenolide (HC *vs* HCC12) and five other metabolites, including leucine-serine-histidine-asparticacid, glycyrrhizic acid, PZ-peptide, hexadecasphingosine, and flurbiprofen glucuronide (Figure 7). Based on existing research reports, glycyrrhizic acid exerts hepatoprotective effects[70] by inhibiting high-mobility group box 1[71]. PZ-peptide was reported to trigger the opening of tight junctions and enhance the transport of paracellular solutes by stimulating transepithelial sodium ion flux across the colonic segments, resulting in uptake by hepatocytes[72]. Therefore, these three bacterial genera, along with their associated metabolites, have the potential to serve as distinctive biomarkers for screening and diagnosing alterations in the gut microbiota of patients with HCC. In the context of HCC onset and progression, the fluctuations in patients' gut bacterial community architecture and fecal metabolomic landscapes are exceedingly intricate. Diverse bacterial communities yield a rich spectrum of secondary metabolites. These metabolites engage in a web of complex interactions and impose disparate effects on the host. Furthermore, patients' dietary patterns and pharmaceutical regimens can significantly disrupt their liver metabolic processes and reshape the composition of their gut microbiota. In light of these complexities centered around HCC, more thorough and meticulous research endeavors are imperative to elucidate the precise role of the gut microbiota in the development and advancement of HCC.

CONCLUSION

In summary, this study revealed that the sensitivity and specificity of serum indicators were insufficient in the diagnosis of HCC. Compared with the findings in the HC group, 161 overlapped differential metabolites and 3 identical enriched KEGG metabolic pathways were identified in the HCC12 and HCC34 groups. *Lachnospira*, *Streptococcus*, and *Veillonella* were the representative differential bacterial genera in the feces of patients with HCC. *Streptococcus* and *Veillonella* were both significantly correlated with serum indicators. Several differential metabolites [*e.g.*, 4-keto-2-undecylpyrroline, dihydrojasmonic acid, 1,8-heptadecadiene-4,6-diyne-3,10-diol, 9(S)-HOTrE], which displayed significant correlations with serum indicators such as GGT, TBIL, AFP, AST, and ALB, might be potential biomarkers of HCC. Furthermore, *Streptococcus* and *Veillonella* also had significant associations with differential metabolites such as DG (15:0/20:0/0:0), arachidoyl ethanolamide, and 4-keto-2-undecylpyrroline. Our findings suggested that the fecal metabolome and gut microbiota might be potential targets for the diagnosis of HCC.

ACKNOWLEDGEMENTS

We sincerely thank all patients and individuals for their participation.

FOOTNOTES

Author contributions: Feng J conceived and designed the experiments, performed the experiments, and analyzed the data; Wang JP performed the experiments, and analyzed the data; Hu JR and Li P analyzed the data and prepared figures and/or tables; Lv P, He HC, Cheng XW, Cao Z, Han JJ, Wang Q, and Su Q performed the experiments; Liu LX conceived and designed the experiments and authored or reviewed drafts of the article; All authors read and approved the final manuscript.

Supported by the Department of Science and Technology of Shanxi Province, No. 20210302124369; the Health Commission of Shanxi Province, No. 2021116; and Shanxi Administration of Traditional Chinese Medicine, No. 2024ZYY2C054.

Institutional review board statement: The study protocol was approved by the medical ethics committee of Shanxi Provincial People's Hospital (No. 2021-45).

Institutional animal care and use committee statement: This study does not involve any animal-related experiments.

Conflict-of-interest statement: The authors declare that they have no conflict of interest.

Data sharing statement: Raw 16S rDNA gene sequencing data were deposited at NCBI Sequence Read Archive (SRA) (https://www.ncbi.nlm.nih.gov/sra/PRJNA1127013). The data are available as of the date of publication.

Country of origin: China

ORCID number: Jing Feng 0000-0001-8415-6296; Li-Xin Liu 0000-0002-0246-6838.

S-Editor: Fan M
L-Editor: A
P-Editor: Zhao S

REFERENCES

1 **Sung H**, Ferlay J, Siegel RL, Laversanne M, Soerjomataram I, Jemal A, Bray F. Global Cancer Statistics 2020: GLOBOCAN Estimates of Incidence and Mortality Worldwide for 36 Cancers in 185 Countries. *CA Cancer J Clin* 2021; **71**: 209-249 [PMID: 33538338 DOI: 10.3322/caac.21660]
2 **Vogel A**, Meyer T, Sapisochin G, Salem R, Saborowski A. Hepatocellular carcinoma. *Lancet* 2022; **400**: 1345-1362 [PMID: 36084663 DOI: 10.1016/S0140-6736(22)01200-4]
3 **Qin R**, Jin T, Xu F. Biomarkers predicting the efficacy of immune checkpoint inhibitors in hepatocellular carcinoma. *Front Immunol* 2023; **14**: 1326097 [PMID: 38187399 DOI: 10.3389/fimmu.2023.1326097]
4 **Shen EY**, U MRA, Cox IJ, Taylor-Robinson SD. The Role of Mass Spectrometry in Hepatocellular Carcinoma Biomarker Discovery. *Metabolites* 2023; **13** [PMID: 37887384 DOI: 10.3390/metabo13101059]
5 **Li X**, Yi Y, Wu T, Chen N, Gu X, Xiang L, Jiang Z, Li J, Jin H. Integrated microbiome and metabolome analysis reveals the interaction between intestinal flora and serum metabolites as potential biomarkers in hepatocellular carcinoma patients. *Front Cell Infect Microbiol* 2023; **13**: 1170748 [PMID: 37260707 DOI: 10.3389/fcimb.2023.1170748]
6 **Liu J**, Geng W, Sun H, Liu C, Huang F, Cao J, Xia L, Zhao H, Zhai J, Li Q, Zhang X, Kuang M, Shen S, Xia Q, Wong VW, Yu J. Integrative metabolomic characterisation identifies altered portal vein serum metabolome contributing to human hepatocellular carcinoma. *Gut* 2022; **71**: 1203-1213 [PMID: 34344785 DOI: 10.1136/gutjnl-2021-325189]
7 **Zhang J**, Yang S, Wang J, Xu Y, Zhao H, Lei J, Zhou Y, Chen Y, Wu L, Zhou M, Li Y, Li Y. Integrated LC-MS metabolomics with dual derivatization for quantification of FFAs in fecal samples of hepatocellular carcinoma patients. *J Lipid Res* 2021; **62**: 100143 [PMID: 34710433 DOI: 10.1016/j.jlr.2021.100143]
8 **Lin RS**, Lee FY, Lee SD, Tsai YT, Lin HC, Lu RH, Hsu WC, Huang CC, Wang SS, Lo KJ. Endotoxemia in patients with chronic liver diseases: relationship to severity of liver diseases, presence of esophageal varices, and hyperdynamic circulation. *J Hepatol* 1995; **22**: 165-172 [PMID: 7790704 DOI: 10.1016/0168-8278(95)80424-2]
9 **Li J**, Sung CY, Lee N, Ni Y, Pihlajamäki J, Panagiotou G, El-Nezami H. Probiotics modulated gut microbiota suppresses hepatocellular carcinoma growth in mice. *Proc Natl Acad Sci U S A* 2016; **113**: E1306-E1315 [PMID: 26884164 DOI: 10.1073/pnas.1518189113]
10 **Ma H**, Yang L, Liang Y, Liu F, Hu J, Zhang R, Li Y, Yuan L, Feng F. B. thetaiotaomicron-derived acetic acid modulate immune microenvironment and tumor growth in hepatocellular carcinoma. *Gut Microbes* 2024; **16**: 2297846 [PMID: 38270111 DOI: 10.1080/19490976.2023.2297846]
11 **Gil-Rojas S**, Suárez M, Martínez-Blanco P, Torres AM, Martínez-García N, Blasco P, Torralba M, Mateo J. Application of Machine Learning Techniques to Assess Alpha-Fetoprotein at Diagnosis of Hepatocellular Carcinoma. *Int J Mol Sci* 2024; **25**: 1996 [PMID: 38396674 DOI: 10.3390/ijms25041996]
12 **Suresh D**, Srinivas AN, Kumar DP. Etiology of Hepatocellular Carcinoma: Special Focus on Fatty Liver Disease. *Front Oncol* 2020; **10**: 601710 [PMID: 33330100 DOI: 10.3389/fonc.2020.601710]
13 **Ghany MG**, Feld JJ, Chang KM, Chan HLY, Lok ASF, Visvanathan K, Janssen HLA. Serum alanine aminotransferase flares in chronic

hepatitis B infection: the good and the bad. *Lancet Gastroenterol Hepatol* 2020; **5**: 406-417 [PMID: 32057301 DOI: 10.1016/S2468-1253(19)30344-9]

14 **Xiao G**, Yang J, Yan L. Comparison of diagnostic accuracy of aspartate aminotransferase to platelet ratio index and fibrosis-4 index for detecting liver fibrosis in adult patients with chronic hepatitis B virus infection: a systemic review and meta-analysis. *Hepatology* 2015; **61**: 292-302 [PMID: 25132233 DOI: 10.1002/hep.27382]

15 **Ghosh T**, Bhadra K. A mini review on human serum albumin - natural alkaloids interaction and its role as drug carrier. *J Biomol Struct Dyn* 2024; 1-18 [PMID: 38345005 DOI: 10.1080/07391102.2024.2314254]

16 **Jiang C**, Hu F, Li J, Gao G, Guo X. Diagnostic value of alkaline phosphatase and bone-specific alkaline phosphatase for metastases in breast cancer: a systematic review and meta-analysis. *Breast Cancer Res Treat* 2023; **202**: 233-244 [PMID: 37522998 DOI: 10.1007/s10549-023-07066-z]

17 **Zhang Y**, Zhang Z, Wu M, Zhang R. Advances and Perspectives of Responsive Probes for Measuring γ-Glutamyl Transpeptidase. *ACS Meas Sci Au* 2024; **4**: 54-75 [PMID: 38404494 DOI: 10.1021/acsmeasuresciau.3c00045]

18 **Nano J**, Muka T, Cepeda M, Voortman T, Dhana K, Brahimaj A, Dehghan A, Franco OH. Association of circulating total bilirubin with the metabolic syndrome and type 2 diabetes: A systematic review and meta-analysis of observational evidence. *Diabetes Metab* 2016; **42**: 389-397 [PMID: 27396752 DOI: 10.1016/j.diabet.2016.06.002]

19 **Tan Y**, Yin P, Tang L, Xing W, Huang Q, Cao D, Zhao X, Wang W, Lu X, Xu Z, Wang H, Xu G. Metabolomics study of stepwise hepatocarcinogenesis from the model rats to patients: potential biomarkers effective for small hepatocellular carcinoma diagnosis. *Mol Cell Proteomics* 2012; **11**: M111.010694 [PMID: 22084000 DOI: 10.1074/mcp.M111.010694]

20 **Jee SH**, Kim M, Kim M, Yoo HJ, Kim H, Jung KJ, Hong S, Lee JH. Metabolomics Profiles of Hepatocellular Carcinoma in a Korean Prospective Cohort: The Korean Cancer Prevention Study-II. *Cancer Prev Res (Phila)* 2018; **11**: 303-312 [PMID: 29500188 DOI: 10.1158/1940-6207.CAPR-17-0249]

21 **Zhao L**, Ni Y, Su M, Li H, Dong F, Chen W, Wei R, Zhang L, Guiraud SP, Martin FP, Rajani C, Xie G, Jia W. High Throughput and Quantitative Measurement of Microbial Metabolome by Gas Chromatography/Mass Spectrometry Using Automated Alkyl Chloroformate Derivatization. *Anal Chem* 2017; **89**: 5565-5577 [PMID: 28437060 DOI: 10.1021/acs.analchem.7b00660]

22 **Zierer J**, Jackson MA, Kastenmüller G, Mangino M, Long T, Telenti A, Mohney RP, Small KS, Bell JT, Steves CJ, Valdes AM, Spector TD, Menni C. The fecal metabolome as a functional readout of the gut microbiome. *Nat Genet* 2018; **50**: 790-795 [PMID: 29808030 DOI: 10.1038/s41588-018-0135-7]

23 **Ashla AA**, Hoshikawa Y, Tsuchiya H, Hashiguchi K, Enjoji M, Nakamuta M, Taketomi A, Maehara Y, Shomori K, Kurimasa A, Hisatome I, Ito H, Shiota G. Genetic analysis of expression profile involved in retinoid metabolism in non-alcoholic fatty liver disease. *Hepatol Res* 2010; **40**: 594-604 [PMID: 20618457 DOI: 10.1111/j.1872-034X.2010.00646.x]

24 **Saeed A**, Bartuzi P, Heegsma J, Dekker D, Kloosterhuis N, de Bruin A, Jonker JW, van de Sluis B, Faber KN. Impaired Hepatic Vitamin A Metabolism in NAFLD Mice Leading to Vitamin A Accumulation in Hepatocytes. *Cell Mol Gastroenterol Hepatol* 2021; **11**: 309-325.e3 [PMID: 32698042 DOI: 10.1016/j.jcmgh.2020.07.006]

25 **Dong S**, Chen QL, Song YN, Sun Y, Wei B, Li XY, Hu YY, Liu P, Su SB. Mechanisms of CCl4-induced liver fibrosis with combined transcriptomic and proteomic analysis. *J Toxicol Sci* 2016; **41**: 561-572 [PMID: 27452039 DOI: 10.2131/jts.41.561]

26 **Han J**, Han ML, Xing H, Li ZL, Yuan DY, Wu H, Zhang H, Wang MD, Li C, Liang L, Song YY, Xu AJ, Wu MC, Shen F, Xie Y, Yang T. Tissue and serum metabolomic phenotyping for diagnosis and prognosis of hepatocellular carcinoma. *Int J Cancer* 2020; **146**: 1741-1753 [PMID: 31361910 DOI: 10.1002/ijc.32599]

27 **Charni-Natan M**, Aloni-Grinstein R, Osher E, Rotter V. Liver and Steroid Hormones-Can a Touch of p53 Make a Difference? *Front Endocrinol (Lausanne)* 2019; **10**: 374 [PMID: 31244779 DOI: 10.3389/fendo.2019.00374]

28 **Robeva R**, Mladenović D, Vesković M, Hrnčić D, Bjekić-Macut J, Stanojlović O, Livadas S, Yildiz BO, Macut D. The interplay between metabolic dysregulations and non-alcoholic fatty liver disease in women after menopause. *Maturitas* 2021; **151**: 22-30 [PMID: 34446275 DOI: 10.1016/j.maturitas.2021.06.012]

29 **Moctezuma-Velázquez C**, Low G, Mourtzakis M, Ma M, Burak KW, Tandon P, Montano-Loza AJ. Association between Low Testosterone Levels and Sarcopenia in Cirrhosis: A Cross-sectional Study. *Ann Hepatol* 2018; **17**: 615-623 [PMID: 29893704 DOI: 10.5604/01.3001.0012.0930]

30 **Sanookpan K**, Chantaravisoot N, Kalpongnukul N, Chuenjit C, Wattanathamsan O, Shoaib S, Chanvorachote P, Buranasudja V. Pharmacological Ascorbate Elicits Anti-Cancer Activities against Non-Small Cell Lung Cancer through Hydrogen-Peroxide-Induced-DNA-Damage. *Antioxidants (Basel)* 2023; **12** [PMID: 37760080 DOI: 10.3390/antiox12091775]

31 **Mindikoglu AL**, Opekun AR, Putluri N, Devaraj S, Sheikh-Hamad D, Vierling JM, Goss JA, Rana A, Sood GK, Jalal PK, Inker LA, Mohney RP, Tighiouart H, Christenson RH, Dowling TC, Weir MR, Seliger SL, Hutson WR, Howell CD, Raufman JP, Magder LS, Coarfa C. Unique metabolomic signature associated with hepatorenal dysfunction and mortality in cirrhosis. *Transl Res* 2018; **195**: 25-47 [PMID: 29291380 DOI: 10.1016/j.trsl.2017.12.002]

32 **Han H**, Zhang S, Wang M, Yi B, Zhao Y, Schroyen M, Zhang H. Retinol metabolism signaling participates in microbiota-regulated fat deposition in obese mice. *J Nutr Biochem* 2025; **136**: 109787 [PMID: 39461600 DOI: 10.1016/j.jnutbio.2024.109787]

33 **Sun R**, Fei F, Jin D, Yang H, Xu Z, Cao B, Li J. The integrated analysis of gut microbiota and metabolome revealed steroid hormone biosynthesis is a critical pathway in liver regeneration after 2/3 partial hepatectomy. *Front Pharmacol* 2024; **15**: 1407401 [PMID: 39188944 DOI: 10.3389/fphar.2024.1407401]

34 **Nuer-Allornuvor GF**, Alolga RN, Liang S, Ling Z, Jingjing W, Xu BQ, Jiangli Z, Ennin VK, Zhou Z, Ying X. GC-MS-based untargeted plasma metabolomics identifies a 2-biomarker panel for possible diagnosis of precancerous cervical intraepithelial neoplasia stages from cervical cancer. *Sci Rep* 2024; **14**: 17649 [PMID: 39085248 DOI: 10.1038/s41598-024-64574-8]

35 **Wang X**, Guan X, Tong Y, Liang Y, Huang Z, Wen M, Luo J, Chen H, Yang S, She Z, Wei Z, Zhou Y, Qi Y, Zhu P, Nong Y, Zhang Q. UHPLC-HRMS-based Multiomics to Explore the Potential Mechanisms and Biomarkers for Colorectal Cancer. *BMC Cancer* 2024; **24**: 644 [PMID: 38802800 DOI: 10.1186/s12885-024-12321-7]

36 **Teng T**, Shi H, Fan Y, Guo P, Zhang J, Qiu X, Feng J, Huang H. Metabolic responses to the occurrence and chemotherapy of pancreatic cancer: biomarker identification and prognosis prediction. *Sci Rep* 2024; **14**: 6938 [PMID: 38521793 DOI: 10.1038/s41598-024-56737-4]

37 **Che J**, Zhao Y, Gu B, Li S, Li Y, Pan K, Sun T, Han X, Lv J, Zhang S, Fan B, Li C, Wang C, Wang J, Zhang T. Untargeted serum metabolomics reveals potential biomarkers and metabolic pathways associated with the progression of gastroesophageal cancer. *BMC Cancer* 2023; **23**: 1238 [PMID: 38102546 DOI: 10.1186/s12885-023-11744-y]

38 **Guzior DV**, Quinn RA. Review: microbial transformations of human bile acids. *Microbiome* 2021; **9**: 140 [PMID: 34127070 DOI: 10.1186/s40168-021-01101-1]

39 **Quinn RA**, Melnik AV, Vrbanac A, Fu T, Patras KA, Christy MP, Bodai Z, Belda-Ferre P, Tripathi A, Chung LK, Downes M, Welch RD, Quinn M, Humphrey G, Panitchpakdi M, Weldon KC, Aksenov A, da Silva R, Avila-Pacheco J, Clish C, Bae S, Mallick H, Franzosa EA, Lloyd-Price J, Bussell R, Thron T, Nelson AT, Wang M, Leszczynski E, Vargas F, Gauglitz JM, Meehan MJ, Gentry E, Arthur TD, Komor AC, Poulsen O, Boland BS, Chang JT, Sandborn WJ, Lim M, Garg N, Lumeng JC, Xavier RJ, Kazmierczak BI, Jain R, Egan M, Rhee KE, Ferguson D, Raffatellu M, Vlamakis H, Haddad GG, Siegel D, Huttenhower C, Mazmanian SK, Evans RM, Nizet V, Knight R, Dorrestein PC. Global chemical effects of the microbiome include new bile-acid conjugations. *Nature* 2020; **579**: 123-129 [PMID: 32103176 DOI: 10.1038/s41586-020-2047-9]

40 **Wakashima T**, Abe K, Kihara A. Dual functions of the trans-2-enoyl-CoA reductase TER in the sphingosine 1-phosphate metabolic pathway and in fatty acid elongation. *J Biol Chem* 2014; **289**: 24736-24748 [PMID: 25049234 DOI: 10.1074/jbc.M114.571869]

41 **Kato R**, Takenaka Y, Ohno Y, Kihara A. Catalytic mechanism of trans-2-enoyl-CoA reductases in the fatty acid elongation cycle and its cooperative action with fatty acid elongases. *J Biol Chem* 2024; **300**: 105656 [PMID: 38224948 DOI: 10.1016/j.jbc.2024.105656]

42 **Saeed A**, Dullaart RPF, Schreuder TCMA, Blokzijl H, Faber KN. Disturbed Vitamin A Metabolism in Non-Alcoholic Fatty Liver Disease (NAFLD). *Nutrients* 2017; **10**: 29 [PMID: 29286303 DOI: 10.3390/nu10010029]

43 **Costantini L**, Molinari R, Farinon B, Merendino N. Retinoic Acids in the Treatment of Most Lethal Solid Cancers. *J Clin Med* 2020; **9**: 360 [PMID: 32012980 DOI: 10.3390/jcm9020360]

44 **Xu L**, Sinclair AJ, Faiza M, Li D, Han X, Yin H, Wang Y. Furan fatty acids - Beneficial or harmful to health? *Prog Lipid Res* 2017; **68**: 119-137 [PMID: 29051014 DOI: 10.1016/j.plipres.2017.10.002]

45 **Lu Y**, Liu D, Jiang R, Li Z, Gao X. Prodigiosin: unveiling the crimson wonder - a comprehensive journey from diverse bioactivity to synthesis and yield enhancement. *Front Microbiol* 2024; **15**: 1412776 [PMID: 38903802 DOI: 10.3389/fmicb.2024.1412776]

46 **Chienwichai P**, Tipthara P, Tarning J, Limpanont Y, Chusongsang P, Chusongsang Y, Kiangkoo N, Adisakwattana P, Reamtong O. Identification of trans-genus biomarkers for early diagnosis of intestinal schistosomiasis and progression of gut pathology in a mouse model using metabolomics. *PLoS Negl Trop Dis* 2024; **18**: e0011966 [PMID: 38381759 DOI: 10.1371/journal.pntd.0011966]

47 **Wen Y**, Hatabayashi H, Arai H, Kitamoto HK, Yabe K. Function of the cypX and moxY genes in aflatoxin biosynthesis in Aspergillus parasiticus. *Appl Environ Microbiol* 2005; **71**: 3192-3198 [PMID: 15933021 DOI: 10.1128/AEM.71.6.3192-3198.2005]

48 **Barupal DK**, Fiehn O. Generating the Blood Exposome Database Using a Comprehensive Text Mining and Database Fusion Approach. *Environ Health Perspect* 2019; **127**: 97008 [PMID: 31557052 DOI: 10.1289/EHP4713]

49 **Sender R**, Fuchs S, Milo R. Are We Really Vastly Outnumbered? Revisiting the Ratio of Bacterial to Host Cells in Humans. *Cell* 2016; **164**: 337-340 [PMID: 26824647 DOI: 10.1016/j.cell.2016.01.013]

50 **Bäckhed F**, Ley RE, Sonnenburg JL, Peterson DA, Gordon JI. Host-bacterial mutualism in the human intestine. *Science* 2005; **307**: 1915-1920 [PMID: 15790844 DOI: 10.1126/science.1104816]

51 **Kang Y**, Cai Y, Yang Y. The Gut Microbiome and Hepatocellular Carcinoma: Implications for Early Diagnostic Biomarkers and Novel Therapies. *Liver Cancer* 2022; **11**: 113-125 [PMID: 35634424 DOI: 10.1159/000521358]

52 **Tripathi A**, Debelius J, Brenner DA, Karin M, Loomba R, Schnabl B, Knight R. The gut-liver axis and the intersection with the microbiome. *Nat Rev Gastroenterol Hepatol* 2018; **15**: 397-411 [PMID: 29748586 DOI: 10.1038/s41575-018-0011-z]

53 **Yuan J**, Chen C, Cui J, Lu J, Yan C, Wei X, Zhao X, Li N, Li S, Xue G, Cheng W, Li B, Li H, Lin W, Tian C, Zhao J, Han J, An D, Zhang Q, Wei H, Zheng M, Ma X, Li W, Chen X, Zhang Z, Zeng H, Ying S, Wu J, Yang R, Liu D. Fatty Liver Disease Caused by High-Alcohol-Producing Klebsiella pneumoniae. *Cell Metab* 2019; **30**: 1172 [PMID: 31801057 DOI: 10.1016/j.cmet.2019.11.006]

54 **Yoshimoto S**, Loo TM, Atarashi K, Kanda H, Sato S, Oyadomari S, Iwakura Y, Oshima K, Morita H, Hattori M, Honda K, Ishikawa Y, Hara E, Ohtani N. Obesity-induced gut microbial metabolite promotes liver cancer through senescence secretome. *Nature* 2013; **499**: 97-101 [PMID: 23803760 DOI: 10.1038/nature12347]

55 **Ponziani FR**, De Luca A, Picca A, Marzetti E, Petito V, Del Chierico F, Reddel S, Paroni Sterbini F, Sanguinetti M, Putignani L, Gasbarrini A, Pompili M. Gut Dysbiosis and Fecal Calprotectin Predict Response to Immune Checkpoint Inhibitors in Patients With Hepatocellular Carcinoma. *Hepatol Commun* 2022; **6**: 1492-1501 [PMID: 35261212 DOI: 10.1002/hep4.1905]

56 **Zhang W**, Xu X, Cai L, Cai X. Dysbiosis of the gut microbiome in elderly patients with hepatocellular carcinoma. *Sci Rep* 2023; **13**: 7797 [PMID: 37179446 DOI: 10.1038/s41598-023-34765-w]

57 **Zhou CB**, Pan SY, Jin P, Deng JW, Xue JH, Ma XY, Xie YH, Cao H, Liu Q, Xie WF, Zou XP, Sheng JQ, Wang BM, Wang H, Ren JL, Liu SD, Sun YW, Meng XJ, Zhao G, Chen JX, Cui Y, Wang PQ, Guo HM, Yang L, Chen X, Ding J, Yang XN, Wang XK, Qian AH, Hou LD, Wang Z, Chen YX, Fang JY. Fecal Signatures of Streptococcus anginosus and Streptococcus constellatus for Noninvasive Screening and Early Warning of Gastric Cancer. *Gastroenterology* 2022; **162**: 1933-1947.e18 [PMID: 35167866 DOI: 10.1053/j.gastro.2022.02.015]

58 **Flemer B**, Warren RD, Barrett MP, Cisek K, Das A, Jeffery IB, Hurley E, O'Riordain M, Shanahan F, O'Toole PW. The oral microbiota in colorectal cancer is distinctive and predictive. *Gut* 2018; **67**: 1454-1463 [PMID: 28988196 DOI: 10.1136/gutjnl-2017-314814]

59 **Dinakaran V**, Mandape SN, Shuba K, Pratap S, Sakhare SS, Tabatabai MA, Smoot DT, Farmer-Dixon CM, Kesavalu LN, Adunyah SE, Southerland JH, Gangula PR. Identification of Specific Oral and Gut Pathogens in Full Thickness Colon of Colitis Patients: Implications for Colon Motility. *Front Microbiol* 2018; **9**: 3220 [PMID: 30666239 DOI: 10.3389/fmicb.2018.03220]

60 **Yu D**, Yang J, Jin M, Zhou B, Shi L, Zhao L, Zhang J, Lin Z, Ren J, Liu L, Zhang T, Liu H. Fecal Streptococcus Alteration Is Associated with Gastric Cancer Occurrence and Liver Metastasis. *mBio* 2021; **12**: e0299421 [PMID: 34872346 DOI: 10.1128/mBio.02994-21]

61 **Wu J**, Zhang R, Yin Z, Chen X, Mao R, Zheng X, Yuan M, Li H, Lu Y, Liu S, Gao X, Sun Q. Gut microbiota-driven metabolic alterations reveal the distinct pathogenicity of chemotherapy-induced cachexia in gastric cancer. *Pharmacol Res* 2024; **209**: 107476 [PMID: 39490563 DOI: 10.1016/j.phrs.2024.107476]

62 **Yang J**, He Q, Lu F, Chen K, Ni Z, Wang H, Zhou C, Zhang Y, Chen B, Bo Z, Li J, Yu H, Wang Y, Chen G. A distinct microbiota signature precedes the clinical diagnosis of hepatocellular carcinoma. *Gut Microbes* 2023; **15**: 2201159 [PMID: 37089022 DOI: 10.1080/19490976.2023.2201159]

63 **Sharma SP**, Gupta H, Kwon GH, Lee SY, Song SH, Kim JS, Park JH, Kim MJ, Yang DH, Park H, Won SM, Jeong JJ, Oh KK, Eom JA, Lee KJ, Yoon SJ, Ham YL, Baik GH, Kim DJ, Suk KT. Gut microbiome and metabolome signatures in liver cirrhosis-related complications. *Clin Mol Hepatol* 2024; **30**: 845-862 [PMID: 39048520 DOI: 10.3350/cmh.2024.0349]

64 **Zheng C**, Lu F, Chen B, Yang J, Yu H, Wang D, Xie H, Chen K, Xie Y, Li J, Bo Z, Wang Y, Chen G, Deng T. Gut microbiome as a

biomarker for predicting early recurrence of HBV-related hepatocellular carcinoma. *Cancer Sci* 2023; **114**: 4717-4731 [PMID: 37778742 DOI: 10.1111/cas.15983]

65 **Pomyen Y**, Chaisaingmongkol J, Rabibhadana S, Pupacdi B, Sripan D, Chornkrathok C, Budhu A, Budhisawasdi V, Lertprasertsuke N, Chotirosniramit A, Pairojkul C, Auewarakul CU, Ungtrakul T, Sricharunrat T, Phornphutkul K, Sangrajang S, Loffredo CA, Harris CC, Mahidol C, Wang XW, Ruchirawat M; TIGER-LC Consortium. Gut dysbiosis in Thai intrahepatic cholangiocarcinoma and hepatocellular carcinoma. *Sci Rep* 2023; **13**: 11406 [PMID: 37452065 DOI: 10.1038/s41598-023-38307-2]

66 **Munar-Bestard M**, Llopis-Grimalt MA, Ramis JM, Monjo M. Comparative In Vitro Evaluation of Commercial Periodontal Gels on Antibacterial, Biocompatibility and Wound Healing Ability. *Pharmaceutics* 2021; **13** [PMID: 34575578 DOI: 10.3390/pharmaceutics13091502]

67 **Friedman CA**, Saha A, Lavender Hackman G, Lu X, Lodi A, Tiziani S, DiGiovanni J. Novel two-tiered screening approach identifies synergistic combinations of natural compounds for prostate cancer prevention and treatment. *Mol Carcinog* 2024; **63**: 589-600 [PMID: 38197430 DOI: 10.1002/mc.23674]

68 **Watanabe K**, Matsunaga T, Nakamura S, Kimura T, Ho IK, Yoshimura H, Yamamoto I. Pharmacological effects in mice of anandamide and its related fatty acid ethanolamides, and enhancement of cataleptogenic effect of anandamide by phenylmethylsulfonyl fluoride. *Biol Pharm Bull* 1999; **22**: 366-370 [PMID: 10328555 DOI: 10.1248/bpb.22.366]

69 **Gong Y**, Liu Y, Zhou L, Di X, Li W, Li Q, Bi K. A UHPLC-TOF/MS method based metabonomic study of total ginsenosides effects on Alzheimer disease mouse model. *J Pharm Biomed Anal* 2015; **115**: 174-182 [PMID: 26210744 DOI: 10.1016/j.jpba.2015.07.007]

70 **Zhou L**, Chen S, Wei Y, Sun Y, Yang Y, Lin B, Li Y, Wang C. Glycyrrhizic acid restores the downregulated hepatic ACE2 signaling in the attenuation of mouse steatohepatitis. *Eur J Pharmacol* 2024; **967**: 176365 [PMID: 38316247 DOI: 10.1016/j.ejphar.2024.176365]

71 **Wang C**, Leng M, Ding C, Zhu X, Zhang Y, Sun C, Lou P. Ferritinophagy-mediated ferroptosis facilitates methotrexate-induced hepatotoxicity by high-mobility group box 1 (HMGB1). *Liver Int* 2024; **44**: 691-705 [PMID: 38082504 DOI: 10.1111/liv.15811]

72 **Shin TH**, Lee PS, Kwon OS, Chung YB. Extensive hepatic uptake of Pz-peptide, a hydrophilic proline-containing pentapeptide, into isolated hepatocytes compared with colonocytes and Caco-2 cells. *Arch Pharm Res* 2003; **26**: 70-75 [PMID: 12568362 DOI: 10.1007/BF03179935]

World Journal of Gastroenterology

Submit a Manuscript: https://www.f6publishing.com

World J Gastroenterol 2025 April 21; 31(15): 102752

DOI: 10.3748/wjg.v31.i15.102752

ISSN 1007-9327 (print) ISSN 2219-2840 (online)

LETTER TO THE EDITOR

Arachidonate 15-lipoxygenase: A promising therapeutic target for alleviating inflammation in acute pancreatitis

Duygu Kirkik, Sevgi Kalkanli Tas

Specialty type: Gastroenterology and hepatology

Provenance and peer review: Invited article; Externally peer reviewed.

Peer-review model: Single blind

Peer-review report's classification

Scientific Quality: Grade A, Grade A, Grade B, Grade C

Novelty: Grade A, Grade A, Grade A, Grade B

Creativity or Innovation: Grade A, Grade B, Grade B, Grade B

Scientific Significance: Grade A, Grade A, Grade B, Grade C

P-Reviewer: Elgendy AA; Ko CY; Kumar A

Received: October 28, 2024

Revised: February 21, 2025

Accepted: March 7, 2025

Published online: April 21, 2025

Processing time: 172 Days and 14.5 Hours

Duygu Kirkik, Sevgi Kalkanli Tas, Department of Immunology, Hamidiye Medicine Faculty, University of Health Sciences, Istanbul 34668, Türkiye

Duygu Kirkik, Department of Medical Biology, Hamidiye Medicine Faculty, University of Health Sciences, Istanbul 34668, Türkiye

Corresponding author: Duygu Kirkik, PhD, Assistant Professor, Department of Immunology, Hamidiye Medicine Faculty, University of Health Sciences, Mekteb-i Tıbbiyye-i Şâhane (Haydarpaşa) Külliyesi Selimiye Mah Tıbbiye Cad No. 38, Istanbul 34668, Türkiye. dygkirkik@gmail.com

Abstract

This article discusses the significant findings from the study on the transfection of arachidonate 15-lipoxygenase (ALOX15) and its therapeutic potential in managing acute pancreatitis (AP). The research highlights the role of ALOX15 in attenuating inflammatory responses, apoptosis, and autophagy in a cerulein-induced AP murine model. By using a recombinant lentiviral vector for efficient gene delivery, the study provides compelling evidence for the protective effects of ALOX15 transfection on pancreatic tissue. The authors demonstrate that ALOX15 reduces the expression of key inflammatory markers like interleukin-β and tumor necrosis factor α while promoting apoptosis through caspase-3 activation. Furthermore, the modulation of autophagy and structural preservation of pancreatic acinar cells suggest that ALOX15 could be a promising therapeutic target for AP. The implications of these findings are discussed, emphasizing the potential for future clinical translation and further research to explore the molecular mechanisms and therapeutic applications of ALOX15 in inflammatory diseases.

Key Words: Acute pancreatitis; Arachidonate 15-lipoxygenase; Inflammation; Apoptosis; Autophagy

Core Tip: This article highlights the therapeutic potential of arachidonate 15-lipoxygenase (ALOX15) in acute pancreatitis (AP). By modulating inflammatory responses, promoting apoptosis, and facilitating autophagy, ALOX15 plays a critical role in cellular homeostasis and tissue recovery in AP. The enzyme's dual action on pro- and anti-inflammatory pathways offers promising avenues for targeted therapies that go beyond symptomatic relief. Understanding ALOX15's mechanisms could pave the way for innovative treatment approaches in AP, potentially reducing complications and improving patient outcomes.

Citation: Kirkik D, Kalkanli Tas S. Arachidonate 15-lipoxygenase: A promising therapeutic target for alleviating inflammation in acute pancreatitis. *World J Gastroenterol* 2025; 31(15): 102752
URL: https://www.wjgnet.com/1007-9327/full/v31/i15/102752.htm
DOI: https://dx.doi.org/10.3748/wjg.v31.i15.102752

TO THE EDITOR

Acute pancreatitis (AP) is a sudden and severe inflammatory response in the pancreas, an organ essential for digestive enzyme production and blood sugar regulation. This condition can present with symptoms ranging from abdominal pain and nausea to systemic complications, and its mortality rate varies significantly, from 3% in mild cases to as high as 17% in severe cases[1,2]. AP has a global incidence ranging from 13 to 45 cases per 100000 people annually, with increasing trends reported in recent years. The incidence varies across regions, with higher rates observed in Western countries compared to Asia[3]. Hospitalization rates for AP have risen significantly, posing a substantial burden on healthcare systems. According to recent data, AP accounts for approximately 275000 hospital admissions annually in the United States alone, with similar trends reported in Europe[4]. The likelihood of mortality depends on the disease's intensity, the patient's overall health, and the presence of complications such as infection, tissue necrosis, or organ failure[1,2]. In modern clinical practice, gallstones and alcohol consumption are recognized as the leading triggers of AP. However, regional and cultural factors cause variations in AP's prevalence across different countries. Gallstones are responsible for around 40%-60% of AP cases. When they obstruct the bile or pancreatic ducts, they create a backup of bile and digestive enzymes, leading to intense inflammation in the pancreas. Alcohol consumption, on the other hand, is implicated in 10%-20% of AP cases[5,6]. Although the condition typically requires more than 50 g of daily alcohol consumption to develop, only less than 5% of chronic drinkers develop AP, suggesting that other less-understood mechanisms might be at play[7]. Hypertriglyceridemia, an elevated level of triglycerides in the blood, accounts for another 5%-10% of AP cases. This form of AP is suspected when serum triglyceride levels surpass 1000 mg/dL in individuals without gallstones or a notable history of alcohol use. When triglycerides are excessively high, they can break down into free fatty acids, which then damage pancreatic cells and prompt inflammation[6]. In addition to these primary causes, a variety of medications and agents have been identified as contributors to AP. The drugs most commonly associated with AP include immunosuppressants like 6-mercaptopurine and azathioprine, as well as certain antibiotics and antiviral drugs, such as isoniazid and didanosine. Loop diuretics, often prescribed for heart failure, are also known to potentially induce AP. Each of these medications may cause AP through direct cellular toxicity or by triggering immune responses that lead to inflammation [8,9].

The lipoxygenase pathway, specifically arachidonate 15-lipoxygenase (ALOX15), has been identified as a key mediator in inflammatory and immune responses in AP. ALOX15 catalyzes the oxygenation of polyunsaturated fatty acids like arachidonic acid, resulting in metabolites such as 15-hydroxyeicosatetraenoic acid (15-HETE), which play essential roles in both promoting and resolving inflammation[10,11]. This dual functionality makes ALOX15 a unique and potentially valuable therapeutic target. To investigate the role of ALOX15 in AP, a cerulein-induced murine model was used in this study. A recombinant lentiviral vector encoding ALOX15 was transfected into pancreatic tissues, allowing for a direct assessment of its effects on inflammatory responses, apoptosis, and autophagy[12].

The aim of this article is to discuss the therapeutic potential of ALOX15 as a dual modulator of pro- and anti-inflammatory pathways and to examine how targeting ALOX15 could offer a novel approach to treating AP. Additionally, the article underscores the need for further research into ALOX15's molecular interactions and its potential in personalized AP treatment strategies.

ALOX15 AND THE INFLAMMATORY CASCADE IN AP

In AP, the inflammatory response is a double-edged sword: While it helps to combat tissue injury, an excessive or prolonged inflammatory response exacerbates tissue damage and contributes to disease progression. ALOX15 plays a crucial role in this inflammatory cascade, modulating both pro-inflammatory and anti-inflammatory mediators. ALOX15-derived metabolites such as 15-HETE are known to influence immune cell behavior, including the recruitment and activation of macrophages and neutrophils, which are essential in early inflammation but can worsen tissue damage if unchecked[12,13].

Sun *et al*[12] investigated the effects of ALOX15 transfection on inflammation, apoptosis, and autophagy by modulating tumor necrosis factor α (TNF-α), interleukin (IL)-1β, and IL-6 levels. Their study utilized multiple assays to assess these effects in experimental AP models. ELISA analysis confirmed that ALOX15 significantly reduced MCP-1 levels, a key chemokine involved in AP pathogenesis. Western blot analysis demonstrated a marked reduction in NF-κB activation in pancreatic tissue, correlating with a suppressed inflammatory response. Furthermore, cleaved caspase-3 levels were significantly increased in ALOX15-transfected models, indicating enhanced apoptotic activity. Histopathological analysis using hematoxylin & eosin staining revealed reduced pancreatic edema and inflammatory infiltration, while TUNEL assay results confirmed an increase in apoptotic cell numbers. Additionally, transmission electron microscopy analysis showed a decrease in autophagic vacuoles in ALOX15-transfected pancreatic cells, suggesting improved cellular homeostasis. These findings collectively highlight the role of ALOX15 in controlling AP progression by reducing inflammation, inducing apoptosis, and modulating autophagy[12].

Research on experimental AP models has shown that ALOX15 impacts cytokine levels, specifically reducing pro-inflammatory cytokines like TNF-α, IL-1β, and IL-6, which are key drivers of the inflammatory response in AP. In animal models transfected with ALOX15, reductions in serum amylase levels, pancreatic tissue water content, and cytokine expression were observed, indicating that ALOX15 mitigates inflammation by balancing cytokine production and cellular oxidative stress[10,14]. These findings suggest that ALOX15 has the potential to stabilize inflammatory processes in AP, a vital component in preventing the progression to more severe disease states.

ROLE OF ALOX15 IN APOPTOSIS AND AUTOPHAGY: PROMOTING CELLULAR HOMEOSTASIS IN AP

Apoptosis, or programmed cell death, is essential for eliminating damaged cells and limiting inflammatory cascades in AP. Autophagy, a parallel process, enables cells to degrade and recycle damaged cellular components, aiding in cell survival under stress. Together, these processes are pivotal in maintaining cellular homeostasis, especially in diseases like AP where cell turnover and tissue repair are critical[15].

ALOX15 influences apoptosis by regulating caspase-3, an enzyme essential in the apoptotic pathway. To assess caspase-3 activation, a colorimetric caspase-3 activity assay was performed, revealing a significant increase in enzyme activity in ALOX15-transfected AP models compared to control groups (2.4-fold increase, $P < 0.05$). Additionally, Western blot analysis demonstrated that cleaved caspase-3 expression was upregulated by 1.9-fold ($P < 0.01$) in ALOX15-overexpressing pancreatic tissue. Enhanced caspase-3 activation in ALOX15-transfected AP models suggests that ALOX15 facilitates the removal of damaged pancreatic cells, thereby reducing the buildup of necrotic tissue and alleviating inflammation[12].

ALOX15 AS A THERAPEUTIC TARGET IN AP: A DUAL MECHANISM OF ACTION

Currently, there is no FDA-approved pharmacological treatment specifically for AP, and management is primarily supportive. Fluid resuscitation, pain control (using opioids such as fentanyl and hydromorphone), and nutritional support remain the cornerstone of AP management. Some investigational therapies targeting inflammation, such as IL-1 receptor antagonists (anakinra) and phosphodiesterase inhibitors, have shown promise but lack regulatory approval. Additionally, drugs like gabexate mesylate (a protease inhibitor) and ulinastatin (a serine protease inhibitor) have been explored in clinical studies, particularly in Asia, but are not widely adopted globally[16-19].

In addition to these investigational drugs, other molecular targets have been explored to mitigate pancreatic inflammation and injury. NF-κB inhibitors, such as sulfasalazine, aim to suppress the pro-inflammatory cytokine cascade in AP. Meanwhile, antioxidants like N-acetylcysteine have been tested to counteract oxidative stress-induced pancreatic injury [20]. Recent studies have also investigated trypsin inhibitors to reduce premature enzyme activation and tissue damage in AP.

The therapeutic potential of ALOX15 in AP lies in its ability to balance pro- and anti-inflammatory responses. Specifically, ALOX15 modulates key pro-inflammatory mediators, including TNF-α, IL-1β, IL-6, and MCP-1, which drive pancreatic inflammation and contribute to systemic inflammatory responses in AP. On the other hand, ALOX15 promotes the production of anti-inflammatory lipid mediators such as 15-HETE and lipoxin A4, which are crucial in resolving inflammation, reducing leukocyte infiltration, and restoring pancreatic homeostasis. By orchestrating this balance, ALOX15 not only suppresses excessive inflammation but also facilitates tissue repair and resolution of AP[12]. Targeting ALOX15 pathways could lead to treatments that either enhance the enzyme's anti-inflammatory effects or inhibit its role in pro-inflammatory processes, depending on the disease stage. For instance, ALOX15 inhibitors or activators could be used to modulate lipid mediator production, reducing cytokine storm-like effects in severe AP cases and promoting resolution of inflammation in mild to moderate cases.

Developing agents that modulate ALOX15 activity could provide a targeted approach for AP therapy, focusing on the enzyme's roles in apoptosis, autophagy, and inflammation. This would be particularly useful in cases where current treatments, which focus on symptom relief and supportive care, are insufficient for controlling inflammation and preventing organ failure[13,15].

FUTURE DIRECTIONS AND RESEARCH CONSIDERATIONS

While ALOX15 presents a promising therapeutic target in AP, several challenges need to be addressed before its clinical application. One major concern is the potential for off-target effects where modulating ALOX15 activity could inadvertently impact other inflammatory pathways or lipid metabolism. Furthermore, patient responses to ALOX15-targeted therapies may vary due to genetic polymorphisms and differences in baseline enzyme expression, necessitating further research into personalized treatment approaches. Additionally, achieving precise control over ALOX15 activity remains a key challenge in clinical settings, as excessive inhibition or activation could disrupt homeostatic immune functions. Future studies should focus on developing selective ALOX15 modulators with optimized pharmacokinetics and minimal side effects to enhance its therapeutic potential in AP.

Clinical trials testing ALOX15 modulators in AP patients would provide invaluable insights into its therapeutic viability. Current studies suggest that manipulating ALOX15 may help reduce inflammation, enhance cellular recovery, and prevent chronic complications in AP patients[12,14,15].

CONCLUSION

ALOX15 is a promising target for AP treatment, offering a unique approach to controlling inflammation, promoting apoptosis, and enhancing autophagy. By modulating key aspects of cellular response, ALOX15 may help reduce the severity of AP and improve patient outcomes. Future research into ALOX15-targeted therapies has the potential to revolutionize the management of AP, moving beyond symptomatic treatment toward addressing the disease's underlying cellular mechanisms. Further investigations should focus on the development of ALOX15 modulators that can be clinically tested in AP patients. Understanding its interactions with other inflammatory pathways, genetic variations influencing its activity, and potential combination therapies could enhance its therapeutic application. Given its role in regulating both inflammation and tissue repair, ALOX15 represents a promising candidate for personalized AP treatment strategies, potentially improving patient outcomes and reducing the burden of this disease.

FOOTNOTES

Author contributions: Kirkik D and Kalkanli Tas S contributed to this paper; Kirkik D designed the overall concept and outline of the manuscript; Kalkanli Tas S contributed to the discussion and design of the manuscript; Kirkik D and Kalkanli Tas S contributed to the writing and editing of the manuscript, illustrations, and literature review.

Conflict-of-interest statement: The authors report no relevant conflicts of interest for this article.

Country of origin: Türkiye

ORCID number: Duygu Kirkik 0000-0003-1417-6915; Sevgi Kalkanli Tas 0000-0001-5288-6040.

S-Editor: Li L
L-Editor: Filipodia
P-Editor: Zhao S

REFERENCES

1 **Singh VK**, Bollen TL, Wu BU, Repas K, Maurer R, Yu S, Mortele KJ, Conwell DL, Banks PA. An assessment of the severity of interstitial pancreatitis. *Clin Gastroenterol Hepatol* 2011; **9**: 1098-1103 [PMID: 21893128 DOI: 10.1016/j.cgh.2011.08.026]

2 **van Brunschot S**, van Grinsven J, van Santvoort HC, Bakker OJ, Besselink MG, Boermeester MA, Bollen TL, Bosscha K, Bouwense SA, Bruno MJ, Cappendijk VC, Consten EC, Dejong CH, van Eijck CH, Erkelens WG, van Goor H, van Grevenstein WMU, Haveman JW, Hofker SH, Jansen JM, Laméris JS, van Lienden KP, Meijssen MA, Mulder CJ, Nieuwenhuijs VB, Poley JW, Quispel R, de Ridder RJ, Römkens TE, Scheepers JJ, Schepers NJ, Schwartz MP, Seerden T, Spanier BWM, Straathof JWA, Strijker M, Timmer R, Venneman NG, Vleggaar FP, Voermans RP, Witteman BJ, Gooszen HG, Dijkgraaf MG, Fockens P; Dutch Pancreatitis Study Group. Endoscopic or surgical step-up approach for infected necrotising pancreatitis: a multicentre randomised trial. *Lancet* 2018; **391**: 51-58 [PMID: 29108721 DOI: 10.1016/S0140-6736(17)32404-2]

3 **Ouyang G**, Pan G, Liu Q, Wu Y, Liu Z, Lu W, Li S, Zhou Z, Wen Y. The global, regional, and national burden of pancreatitis in 195 countries and territories, 1990-2017: a systematic analysis for the Global Burden of Disease Study 2017. *BMC Med* 2020; **18**: 388 [PMID: 33298026 DOI: 10.1186/s12916-020-01859-5]

4 **Li CL**, Jiang M, Pan CQ, Li J, Xu LG. The global, regional, and national burden of acute pancreatitis in 204 countries and territories, 1990-

2019. *BMC Gastroenterol* 2021; **21**: 332 [PMID: 34433418 DOI: 10.1186/s12876-021-01906-2]

5 **Roberts SE**, Morrison-Rees S, John A, Williams JG, Brown TH, Samuel DG. The incidence and aetiology of acute pancreatitis across Europe. *Pancreatology* 2017; **17**: 155-165 [PMID: 28159463 DOI: 10.1016/j.pan.2017.01.005]

6 **Tenner S**, Baillie J, DeWitt J, Vege SS; American College of Gastroenterology. American College of Gastroenterology guideline: management of acute pancreatitis. *Am J Gastroenterol* 2013; **108**: 1400-15; 1416 [PMID: 23896955 DOI: 10.1038/ajg.2013.218]

7 **Lankisch PG**, Lowenfels AB, Maisonneuve P. What is the risk of alcoholic pancreatitis in heavy drinkers? *Pancreas* 2002; **25**: 411-412 [PMID: 12409838 DOI: 10.1097/00006676-200211000-00015]

8 **Yadav D**, Pitchumoni CS. Issues in hyperlipidemic pancreatitis. *J Clin Gastroenterol* 2003; **36**: 54-62 [PMID: 12488710 DOI: 10.1097/00004836-200301000-00016]

9 **He K**, Zhou X, Du H, Zhao J, Deng R, Wang J. A review on the relationship between Arachidonic acid 15-Lipoxygenase (ALOX15) and diabetes mellitus. *PeerJ* 2023; **11**: e16239 [PMID: 37849828 DOI: 10.7717/peerj.16239]

10 **Singh NK**, Rao GN. Emerging role of 12/15-Lipoxygenase (ALOX15) in human pathologies. *Prog Lipid Res* 2019; **73**: 28-45 [PMID: 30472260 DOI: 10.1016/j.plipres.2018.11.001]

11 **Heydeck D**, Ufer C, Kakularam KR, Rothe M, Liehr T, Poulain P, Kuhn H. Functional Characterization of Transgenic Mice Overexpressing Human 15-Lipoxygenase-1 (ALOX15) under the Control of the aP2 Promoter. *Int J Mol Sci* 2023; **24**: 4815 [PMID: 36902243 DOI: 10.3390/ijms24054815]

12 **Sun HW**, Bai YY, Qin ZL, Li RZ, Madzikatire TB, Akuetteh PDP, Li Q, Kong HR, Jin YP. Transfection of 12/15-lipoxygenase effectively alleviates inflammatory responses during experimental acute pancreatitis. *World J Gastroenterol* 2024; **30**: 4544-4556 [PMID: 39563743 DOI: 10.3748/wjg.v30.i42.4544]

13 **Snodgrass RG**, Brüne B. Regulation and Functions of 15-Lipoxygenases in Human Macrophages. *Front Pharmacol* 2019; **10**: 719 [PMID: 31333453 DOI: 10.3389/fphar.2019.00719]

14 **Xu X**, Li J, Zhang Y, Zhang L. Arachidonic Acid 15-Lipoxygenase: Effects of Its Expression, Metabolites, and Genetic and Epigenetic Variations on Airway Inflammation. *Allergy Asthma Immunol Res* 2021; **13**: 684-696 [PMID: 34486255 DOI: 10.4168/aair.2021.13.5.684]

15 **Ivanov I**, Kuhn H, Heydeck D. Structural and functional biology of arachidonic acid 15-lipoxygenase-1 (ALOX15). *Gene* 2015; **573**: 1-32 [PMID: 26216303 DOI: 10.1016/j.gene.2015.07.073]

16 **Seta T**, Noguchi Y, Shikata S, Nakayama T. Treatment of acute pancreatitis with protease inhibitors administered through intravenous infusion: an updated systematic review and meta-analysis. *BMC Gastroenterol* 2014; **14**: 102 [PMID: 24886242 DOI: 10.1186/1471-230X-14-102]

17 **Pezzilli R**, Morselli-Labate AM, Corinaldesi R. NSAIDs and Acute Pancreatitis: A Systematic Review. *Pharmaceuticals (Basel)* 2010; **3**: 558-571 [PMID: 27713268 DOI: 10.3390/ph3030558]

18 **Ceppa EP**, Lyo V, Grady EF, Knecht W, Grahn S, Peterson A, Bunnett NW, Kirkwood KS, Cattaruzza F. Serine proteases mediate inflammatory pain in acute pancreatitis. *Am J Physiol Gastrointest Liver Physiol* 2011; **300**: G1033-G1042 [PMID: 21436316 DOI: 10.1152/ajpgi.00305.2010]

19 **Ramudo L**, Manso MA. N-acetylcysteine in acute pancreatitis. *World J Gastrointest Pharmacol Ther* 2010; **1**: 21-26 [PMID: 21577291 DOI: 10.4292/wjgpt.v1.i1.21]

20 **Pădureanu V**, Florescu DN, Pădureanu R, Ghenea AE, Gheonea DI, Oancea CN. Role of antioxidants and oxidative stress in the evolution of acute pancreatitis (Review). *Exp Ther Med* 2022; **23**: 197 [PMID: 35126700 DOI: 10.3892/etm.2022.11120]

World Journal of Gastroenterology

Submit a Manuscript: https://www.f6publishing.com

World J Gastroenterol 2025 April 21; 31(15): 104528

DOI: 10.3748/wjg.v31.i15.104528

ISSN 1007-9327 (print) ISSN 2219-2840 (online)

LETTER TO THE EDITOR

Rethinking carnitine palmitoyltransferase II and liver stem cells in metabolic dysfunction-associated fatty liver disease-related hepatocellular carcinoma

Hong Cai, Chun-Hui Yang, Peng Gao

Specialty type: Gastroenterology and hepatology

Provenance and peer review: Invited article; Externally peer reviewed.

Peer-review model: Single blind

Peer-review report's classification

Scientific Quality: Grade A, Grade C, Grade C

Novelty: Grade A, Grade B, Grade C

Creativity or Innovation: Grade A, Grade B, Grade C

Scientific Significance: Grade A, Grade C, Grade C

P-Reviewer: Cheng HW; Singh Y

Received: December 28, 2024

Revised: February 27, 2025

Accepted: March 13, 2025

Published online: April 21, 2025

Processing time: 113 Days and 3.9 Hours

Hong Cai, Chun-Hui Yang, Peng Gao, Department of Clinical Laboratory, The Second Hospital of Dalian Medical University, Dalian 116023, Liaoning Province, China

Co-first authors: Hong Cai and Chun-Hui Yang.

Corresponding author: Peng Gao, PhD, Professor, Department of Clinical Laboratory, The Second Hospital of Dalian Medical University, No. 467 Zhongshan Road, Dalian 116023, Liaoning Province, China. gaop@dmu.edu.cn

Abstract

This article discusses a recent study by Wang *et al* that sheds light on the metabolic and immunological mechanisms driving the progression of metabolic dysfunction-associated fatty liver disease (MAFLD) to hepatocellular carcinoma (HCC). The study highlights the role of mitochondrial carnitine palmitoyltransferase II (CPT II) inactivity, which activates liver cancer stem cells marked by cluster of differentiation 44 (CD44) and CD24 expression, promoting HCC development. Using dynamic mouse models and clinical samples, Wang *et al* identified CPT II downregulation, mitochondrial membrane potential alterations, and reduced intrahepatic $CD4^+$ T cell as key drivers of disease progression. The findings link these changes to steroid biosynthesis and p53 signaling, contributing to T-cell dysfunction and immunosuppression. This article emphasizes the relevance of these results in understanding MAFLD pathogenesis and discusses potential therapeutic strategies targeting CPT II activity, mitochondrial function, and immune surveillance to prevent or mitigate HCC development in advanced MAFLD.

Key Words: Metabolic dysfunction-associated fatty liver disease; Carnitine palmitoyltransferase II; Hepatocellular carcinoma; Liver cancer stem cells; Mitochondrial dysfunction; Metabolic dysfunction

Core Tip: This article reviews a recent study by Wang *et al* investigating how carnitine palmitoyltransferase II (CPT II) inactivity drives malignant progression in metabolic dysfunction-associated fatty liver disease (MAFLD) through aberrant lipid metabolism, T-cell dysfunction, and liver cancer stem cell activation. Their work revealed that mitochondrial damage and reduced CPT II activity under lipid-rich conditions may be early indicators of liver cancer risk, influencing immune cell profiles and the stem cell-like properties of hepatocytes. Understanding these processes could pave the way for novel preventative and therapeutic interventions targeting the metabolic and immunological underpinnings of MAFLD-related hepatocarcinogenesis.

Citation: Cai H, Yang CH, Gao P. Rethinking carnitine palmitoyltransferase II and liver stem cells in metabolic dysfunction-associated fatty liver disease-related hepatocellular carcinoma. *World J Gastroenterol* 2025; 31(15): 104528
URL: https://www.wjgnet.com/1007-9327/full/v31/i15/104528.htm
DOI: https://dx.doi.org/10.3748/wjg.v31.i15.104528

TO THE EDITOR

Metabolic dysfunction-associated fatty liver disease (MAFLD) is increasingly recognized as a global health concern. It encompasses a spectrum of hepatic pathologies ranging from simple steatosis to inflammatory stages (metabolic dysfunction-associated steatohepatitis). Uncontrolled metabolic dysfunction-associated steatohepatitis is prone to progressing to cirrhosis, and eventually, to hepatocellular carcinoma (HCC)[1]. While the precise molecular drivers of this progression have yet to be fully elucidated, there is growing evidence that mitochondrial dysfunction, immunosuppression, and the activation of liver cancer stem cells (LCSCs) act in concert to spur malignant changes. The recent article by Wang *et al*[2] offers a compelling look at how mitochondrial CPT II inactivity and LCSC activation synergize to drive MAFLD progression to HCC (Figure 1). These findings mark a critical step in delineating the metabolic and immunologic cues that facilitate malignant transformation in MAFLD.

Understanding CPT II inactivity in MAFLD progression

Mitochondria serve as central hubs of energy production and lipid metabolism[3]. In the normal liver, efficient mitochondrial fatty acid β-oxidation ensures metabolic homeostasis. However, in MAFLD, particularly under conditions of chronic caloric surplus and lipid accumulation, mitochondrial pathways become dysregulated[4]. A variety of metabolic alterations occur in MAFLD, including increased fatty acid synthesis, reduced fatty acid oxidation, and altered glucose metabolism. These changes lead to an accumulation of lipids within hepatocytes, which can cause lipotoxicity, oxidative stress, and mitochondrial dysfunction. CPT II, an enzyme located on the inner mitochondrial membrane, is essential for the transport of long-chain fatty acids into mitochondria for β-oxidation[5]. In the context of MAFLD, research has shown that CPT II activity significantly decreases as the disease progresses. This decrease in CPT II function leads to impaired mitochondrial fatty acid oxidation, excessive lipid accumulation, and alterations in the mitochondrial membrane potential, collectively creating a metabolically compromised and oxidative stress-rich environment. These metabolic alterations not only disrupt normal liver function but also create conditions that favor the survival and expansion of LCSC, thereby linking metabolic dysfunction directly to oncogenic processes. In MAFLD, these mitochondrial disturbances are correlated with decreased numbers of intrahepatic $CD4^+$ T cells, weakened immune surveillance, and aberrant activation of LCSC, as indicated by increased cluster of differentiation (CD44) and CD24 expression. As LCSC gain a foothold, they contribute to the malignant transformation of hepatocytes and the progression from simple steatosis to advanced HCC.

Elucidating the molecular mechanisms: CPT II inactivity and oncogenic pathways

While recent studies highlight the critical role of CPT II in the pathogenesis and malignancy of MAFLD, the precise molecular mechanisms linking CPT II inactivity to specific oncogenic pathways remain underexplored. Wang *et al*[2] have begun to bridge this gap by associating CPT II inactivity with alterations in key signaling pathways such as p53 and Wnt/β-catenin. The p53 pathway, known for its role in tumor suppression, is often dysregulated in cancerous transformations. CPT II inactivity may exacerbate oxidative stress, leading to p53 mutations or inactivation, thereby undermining genomic stability and promoting tumorigenesis[6]. Additionally, the Wnt/β-catenin pathway, crucial for cell proliferation and differentiation, may be aberrantly activated in the context of impaired fatty acid oxidation. The metabolic stress induced by CPT II inactivity could lead to the stabilization and nuclear translocation of β-catenin, driving the expression of genes that promote cellular proliferation and stemness[7]. Hypotheses for these interactions include the possibility that accumulated lipids and resultant metabolic byproducts directly modify components of these pathways, or that secondary effects of mitochondrial dysfunction, such as altered energy status and redox balance, indirectly influence these oncogenic signaling cascades. Future research should aim to delineate these connections through targeted experiments, such as assessing the impact of CPT II restoration on p53 and Wnt/β-catenin pathway activity, or exploring the use of pathway inhibitors in models of CPT II inactivity.

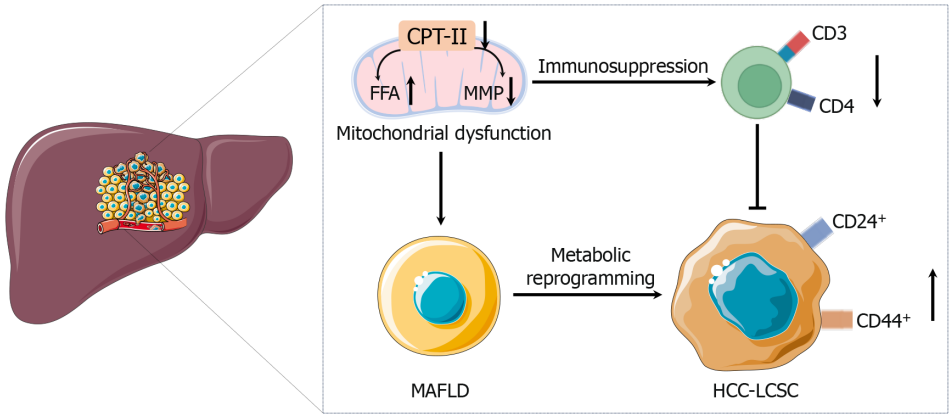

Figure 1 Schematic representation of the role of mitochondrial dysfunction in the progression of metabolic dysfunction-associated fatty liver disease to hepatocellular carcinoma. CPT II: Carnitine palmitoyltransferase II; FFA: Free fatty acid; HCC: Hepatocellular carcinoma; LCSC: Liver cancer stem cell; MAFLD: Metabolic dysfunction-associated fatty liver disease; MMP: Mitochondrial membrane potential.

Comparative metabolic and immunological characteristics: MAFLD vs other liver diseases

While mitochondrial dysfunction and CPT II alterations may contribute to carcinogenesis in various liver diseases, the specific metabolic and immunological landscape of MAFLD appears uniquely conducive to HCC development. A more in-depth comparison with other liver diseases, such as alcoholic liver disease (ALD), highlights these distinctions. In ALD, mitochondrial dysfunction is also a prominent feature; however, the primary drivers include ethanol metabolism, acetaldehyde toxicity, and oxidative stress from reactive oxygen species. Unlike MAFLD, where chronic lipid accumulation is central, ALD is characterized by inflammation driven by different mechanisms, such as acetaldehyde adducts and gut-derived endotoxins[8].

Immunologically, MAFLD is associated with a distinct profile of immune cell infiltration and cytokine production compared to ALD. For instance, MAFLD-related HCC often exhibits a unique immunosuppressive microenvironment marked by reduced $CD4^+$ T-cell populations and increased regulatory T cells, whereas ALD may show more pronounced neutrophilic infiltration and different cytokine profiles[9]. These differences suggest that CPT II inactivity's role in MAFLD-related HCC is intertwined with specific immunometabolic alterations that are not as prominent or differently manifested in other liver diseases. Therefore, the downregulation of CPT II in MAFLD might represent a unique metabolic vulnerability that, when combined with MAFLD-specific immune dysregulation, particularly fosters an environment conducive to HCC development.

Linking immunosuppression and mitochondrial dysfunction

The immune landscape of the liver is complex, integrating innate and adaptive responses. In a healthy liver, T cells maintain a vigilant watch, clearing early neoplastic lesions and preventing malignant outgrowth[10]. However, chronic lipid accumulation and mitochondrial dysfunction appear to erode this immune vigilance. Wang *et al*[2] reported a reduction in intrahepatic $CD3^+$ and $CD4^+$ T cells as the disease progressed. Losing these T cells means a breakdown in adaptive immunity, providing a permissive niche for cancer initiation and progression[11]. This T-cell depletion may be rooted in altered metabolism at the cellular level. Like hepatocytes, T cells rely heavily on mitochondrial function for energy generation[12]. Mitochondrial damage and reduced CPT II function can impair T-cell fitness, rendering them less capable of mounting an effective antitumor response[13]. Mitochondrial dysfunction can also lead to increased oxidative stress and an environment conducive to tumor-promoting inflammation rather than tumor-destructive immunity[14]. Such a shift would promote the survival and proliferation of LCSC and transformed hepatocytes.

LCSC activation: A new frontier in MAFLD-related HCC progression

Identifying LCSCs offers crucial insight into how MAFLD progresses to HCC[15]. LCSCs are characterized by markers such as CD44 and CD24, which are indicative of cells possessing heightened self-renewal capacity, resistance to conventional therapies, and the ability to initiate tumors[16]. Wang *et al*[2] reported that CPT II inactivity is strongly correlated with LCSC activation. These findings extend beyond a simple correlation, indicating that CPT II inactivity is a pivotal initiating factor in metabolic reprogramming within hepatocytes. As CPT II activity decreases, long-chain fatty acid β-oxidation becomes inefficient, leading to the accumulation of lipids, diminished mitochondrial membrane potential, and increased oxidative stress. Within this lipid-rich, mitochondrion-compromised environment, certain hepatocytes may gain selective advantages, adopting characteristics commonly associated with stem-like cells. These LCSCs, characterized by markers such as CD44 and CD24, exhibit enhanced self-renewal capacity, therapeutic resistance, and tumor-initiating potential. Moreover, the study's insights into immunological alterations, particularly decreased intrahepatic $CD3^+$ and $CD4^+$ T-cell populations, suggest that CPT II inactivity indirectly fosters an immunosuppressive microenvironment. The loss of adaptive immune surveillance creates a niche where LCSCs can thrive, escape immune-mediated destruction, and drive malignant transformation.

As CPT II activity wanes, an environment rich in lipids and prone to oxidative stress emerges. This environment likely provides selective pressure for a subset of hepatocytes, enabling them to acquire stem cell-like properties and evade normal growth control[17]. The inactivity or reduction of CPT II contributes to a lipid-rich, metabolically stressed milieu that, in turn, influences the cellular signaling pathways integral to maintaining a stem-like phenotype. With impaired CPT II activity, cells accumulate lipids and reduce their reliance on mitochondrial β-oxidation. This shift can favor glycolysis and other metabolic pathways associated with rapid proliferation and stress resistance, which are hallmarks of stem-like cells[18]. The imbalance created by lipid accumulation and diminished mitochondrial function elevates oxidative stress. Increased reactive oxygen species and altered mitochondrial membrane potential can activate or repress key transcription factors and signaling pathways (*e.g.*, p53, peroxisome proliferator-activated receptor, and steroid biosynthesis pathways). These specific alterations in p53 signaling can lead to impaired apoptosis and increased cell survival, while changes in steroid biosynthesis may modulate immune responses by altering cytokine profiles and T-cell receptor signaling, thereby contributing to the suppression of intrahepatic $CD4^+$ T cells. These pathways influence the cell cycle, apoptosis, and differentiation states, driving cells toward a more stem-like, undifferentiated phenotype[19]. Reduced CPT II activity is correlated with diminished intrahepatic $CD4^+$ T cells and compromised immune surveillance. This weakened immunological ability allows LCSC to persist, evade immune-mediated destruction, and sustain their "stemness" without the selective pressure normally exerted by a healthy immune system. By linking mitochondrial CPT II inactivity with LCSC activation, this study reveals a key mechanistic nexus bridging metabolic dysfunction, immune evasion, and oncogenic transformation.

Mechanistic insights and bioinformatic clues

In addition to their experimental findings, Wang *et al*[2] employed transcriptomic analyses to clarify the underlying pathways and gene networks associated with MAFLD progression and the emergence of HCC. Differentially expressed genes in intrahepatic T cells were enriched in lipid biosynthesis-related pathways, steroid biosynthesis, the peroxisome proliferator-activated receptor pathway, and p53 signaling. Steroid biosynthesis and lipid metabolism pathways, in particular, reinforce the notion that metabolic reprogramming can foster a tumor-friendly microenvironment[20]. The genes involved in the p53 and cell cycle pathways highlight how critical tumor suppressor networks become dysregulated during this process. p53, a vital guardian of genomic stability, often becomes subverted in cancerous transformations[21]. Thus, the links among CPT II inactivity, lipid metabolic shifts, and changes in p53 signaling suggest that metabolic dysfunction could undermine one of the cell's primary tumor suppression mechanisms[22]. Moreover, these findings align with a body of literature indicating that MAFLD pathogenesis involves not only passive lipid accumulation but also active metabolic reprogramming. This reprogramming might be a preamble to oncogenic signaling cascades that culminate in cellular dedifferentiation, stemness, and ultimately malignancy.

Given the growing interest in the role of the tumor microenvironment (TME) in cancer progression, it is essential to consider how metabolic dysfunction and immune dysregulation within the TME contribute to the activation of LCSC. Metabolic alterations such as CPT II inactivity create a hypoxic and nutrient-deprived environment, which can induce stress responses in hepatocytes. These stress responses may lead to the secretion of factors that promote stemness and support the maintenance of LCSCs. Additionally, immunosuppressive cytokines and altered immune cell populations within the TME can further facilitate the survival and expansion of LCSCs, thereby driving HCC development from MAFLD.

Comparisons with other research and nomenclature shifts

The evolving nomenclature shifting from nonalcoholic fatty liver disease to MAFLD emphasizes the metabolic underpinnings of this liver disease spectrum[23]. Wang *et al*[2] contributed meaningfully to this reframed understanding by pinpointing metabolic enzymes, such as CPT II, as both biomarkers and facilitators of malignant progression. Their work parallels the concerns of other recent publications focusing on immune and metabolic alterations in advanced liver diseases. Notably, previous studies have emphasized the roles of inflammation, insulin resistance, and simple steatosis in MAFLD progression[24]. While these remain critical aspects, Wang *et al*[2] broke new ground by centering on a key mitochondrial enzyme and linking its inactivity to impaired immunity and stem cell activation. This approach provides a more nuanced molecular narrative, helping us better understand why some patients with steatosis progress to HCC while others do not.

Clinical implications and potential interventions

Understanding the role of CPT II inactivity in LCSC activation and T-cell dysfunction has several potential clinical applications. First, therapies aimed at restoring CPT II activity or enhancing mitochondrial β-oxidation could help prevent the malignant progression of MAFLD. Nutritional interventions, pharmacological agents targeting mitochondrial function, or gene therapy approaches to restore CPT II expression may represent avenues for slowing or halting disease progression. However, the feasibility of these strategies faces several challenges. Restoring CPT II activity *in vivo* requires precise delivery mechanisms to effectively target hepatocytes without off-target effects. Pharmacological agents must be both potent and specific to avoid disrupting other aspects of mitochondrial function. Additionally, gene therapy approaches, while promising, are still in their infancy for liver diseases and must overcome hurdles related to safety, delivery vectors, and long-term expression. Second, monitoring CPT II levels and LCSC markers (CD44 and CD24) could improve risk stratification for MAFLD patients. Identifying those at high risk of malignant progression before overt HCC emerges would allow earlier interventions and possibly improve outcomes. Integration of the CPT II status with imaging and other noninvasive biomarkers could form a composite index that physicians might use to predict HCC risk in MAFLD patients. However, establishing standardized assays for CPT II and LCSC markers, along with validating their predictive

power in large, diverse cohorts, remains a significant task. Third, the interplay between mitochondrial dysfunction and the immune system revealed by Wang *et al*[2] suggests that immunotherapies or interventions to restore T-cell function might be more effective if combined with metabolic reprogramming strategies. As checkpoint inhibitors and chimeric antigen receptor T-cell therapies have advanced in the field of HCC, understanding how best to restore a metabolically favorable and immunostimulatory environment in the liver could increase the success of these treatments. However, combining metabolic therapies with immunotherapies introduces complexity in treatment regimens and necessitates careful evaluation of potential interactions and cumulative toxicities.

Limitations and future directions

Wang *et al*[2] presented an insightful link between CPT II inactivity, LCSC activation, and immunosuppression in MAFLD progression toward HCC. However, several key aspects warrant further investigation. First, while their findings highlight a connection between mitochondrial dysfunction and tumorigenesis, the direct influence of CPT II inactivity on specific oncogenic mutations or tumor suppressor genes remains unclear. Transcriptomic data revealed the enrichment of genes involved in p53 signaling and other pathways commonly disrupted in HCC, such as the Wnt/β-catenin pathway. Future studies should dissect whether CPT II inactivity predisposes hepatocytes to genetic mutations or if it merely enhances the tumorigenic potential of cells already harboring these alterations.

A more granular analysis of transcriptomic and metabolomic data could clarify how CPT II inactivity interacts with well-known oncogenic networks. Investigations that track p53 target gene dysregulation in CPT II-inactive contexts or that identify downstream effectors of Wnt signaling sensitive to metabolic stress may help establish a causal model. In addition, examining the roles of other carnitine palmitoyltransferases, such as CPT I isoforms, could reveal complementary or compensatory mechanisms influencing fatty acid flux and disease progression. Addressing whether other metabolic enzymes, such as CPT I isoforms, may compensate for CPT II inactivity in certain contexts could provide insights into potential redundancy and resilience within metabolic pathways. Pinpointing how these mitochondrial transporters integrate with diverse signaling pathways may provide a more comprehensive view of metabolic reprogramming in HCC.

Importantly, not all HCCs are driven by CPT II inactivity. Some tumors rely heavily on alternative pathways, such as glycolysis, glutamine metabolism, or aberrant cholesterol synthesis. Identifying distinct metabolic subtypes of HCC and determining where CPT II fits into this landscape could refine risk stratification, guide therapeutic choices, and enhance prognostic models. Furthermore, discussing potential resistance mechanisms that might emerge during therapeutic interventions targeting CPT II or LCSCs is crucial for developing robust treatment strategies. Ultimately, a multipronged research approach encompassing genetic, metabolic, and immunological dimensions is needed to validate the significance of CPT II and to translate these insights into effective targeted interventions for MAFLD-related HCC.

Relevance to current clinical practice

Currently, liver biopsy remains the gold standard for diagnosing advanced liver disease states, but it is invasive and not suitable for routine population-level screening. Noninvasive markers are needed, and Wang *et al*'s work[2] on CPT II and LCSC markers will potentially contribute to the development of blood-based or imaging-correlated tests. Additionally, the immunological context provided by their study may guide the use of adjunctive therapies designed to restore healthy immune function in the liver microenvironment. Given the increasing global prevalence of metabolic disorders and their hepatic manifestations, the study by Wang *et al*[2] is timely. As the number of patients with MAFLD continues to increase, the burden of HCC is linked to metabolic dysregulation. By teasing apart the complex relationships among lipid overload, mitochondrial dysfunction, immune dysregulation, and cancer stem cell activation, this research helps establish a path toward more effective prevention and intervention strategies.

Based on the above, we wondered whether it is possible to integrate research on ketogenic diets with the understanding that CPT II activity in the context of tumor metabolism is largely indirect and remains an area ripe for further investigation. A ketogenic diet shifts the body's energy utilization from carbohydrates to fats, increasing the reliance on fatty acid oxidation and ketone body production. Normal cells can often adapt to this metabolic shift by efficiently using fatty acids and ketones as alternative energy substrates. On the other hand, tumor cells frequently display a rigid dependency on glucose and may have reduced flexibility in adjusting to low-glucose, high-fat conditions. Wang *et al*[2] suggested that CPT II inactivity plays a pivotal role in promoting LCSC activation and mitochondrial dysfunction in MAFLD-related HCC. If a tumor cell population is compromised in its ability to oxidize long-chain fatty acids due to impaired CPT II function, it may struggle to thrive under the metabolic constraints imposed by a ketogenic diet. Such an inability to properly engage in fatty acid β-oxidation could render tumor cells more vulnerable and less capable of sustaining growth in a low-glucose environment.

Conversely, if interventions were developed to increase CPT II activity or improve mitochondrial fatty acid oxidation, normal cells might better adapt to the high-fat, low-carbohydrate conditions of a ketogenic diet. Moreover, tumor cells potentially harboring genetic mutations or other metabolic inefficiencies might fail to achieve similar metabolic flexibility, thereby revealing a metabolic vulnerability that could be therapeutically exploited. While direct experimental data linking CPT II function, ketogenic diets, and cancer progression are still scarce, the theoretical groundwork suggests that the interplay between these factors could be significant. Future studies are needed to clarify the molecular mechanisms underlying this relationship and to determine whether targeting CPT II-mediated fatty acid oxidation can enhance the tumor-suppressive effects of a ketogenic diet.

Implications for future diagnostic and therapeutic strategies

From a diagnostic perspective, integrating CPT II levels with imaging modalities such as magnetic resonance imaging-

proton density fat fraction or transient elastography could yield a more refined noninvasive assessment of disease progression[25,26]. Although Wang *et al*[2] did not focus on imaging technologies, one can envision a combined approach where patients at risk of malignant progression are identified early by a signature involving metabolic enzymes, LCSC markers, and imaging-based quantification of steatosis or fibrosis. Several potential strategies have emerged for this purpose. Pharmacological restoration of CPT II activity or mitochondrial function may normalize β-oxidation and reduce lipotoxicity. Agents that enhance T-cell metabolism or block the deleterious effects of a lipid-rich environment on immune function might help maintain surveillance against neoplastic clones[17]. Similarly, targeted therapies against $CD44^+$ or $CD24^+$ LCSCs, either by blocking their survival pathways or by resensitizing them to conventional chemotherapy, could be combined with metabolic therapies to halt malignant progression. A multipronged approach that corrects mitochondrial dysfunction, restores immune competence, and targets stem-like tumor cells may offer the best chance for long-term disease control. However, each of these strategies comes with its own set of challenges, including ensuring specificity, minimizing off-target effects, and overcoming the heterogeneity of tumor cell populations.

Positioning CPT II in the broader landscape of HCC research

HCC is a notoriously heterogeneous disease with numerous etiological underpinnings, from chronic viral hepatitis to alcohol, induced cirrhosis and metabolic disorders[24]. The rise of MAFLD as a principal driver of HCC, however, necessitates a pivot toward understanding metabolic alterations at the core of tumorigenesis. While significant strides have been made in understanding the roles of inflammation, fibrosis, and oncogenic signaling pathways, relatively less attention has been given to early metabolic disruptions such as CPT II inactivity[13]. Wang *et al*[2] position CPT II not only as a marker but also potentially as a linchpin in a cascade leading from benign lipid accumulation to malignant transformation. This perspective encourages the research community to explore other mitochondrial enzymes and transporters and their roles in shaping the TME. By doing so, we might uncover a network of metabolic vulnerabilities in HCC that could be therapeutically exploited.

CONCLUSION

MAFLD-related HCC exemplifies the challenges of a disease deeply rooted in metabolic imbalance and immunological compromise. As global rates of obesity, insulin resistance, and related metabolic disorders continue to increase, we can expect MAFLD- and consequently MAFLD-associated HCC to grow as a public health concern. Identifying early biomarkers and unraveling the molecular mediators of this progression are pressing priorities. CPT II emerges from this study as a critical piece of that puzzle. When viewed alongside LCSC markers and immune cell profiles, CPT II inactivity may serve as both a harbinger and a driver of malignant changes. With further validation and deeper exploration, these insights could pave the way for novel biomarkers and targeted therapeutics aimed at restoring mitochondrial function, supporting effective immune responses, and mitigating LCSC-driven oncogenesis. The study by Wang *et al*[2] advances our knowledge of how metabolic dysfunction, immune dysregulation, and cancer stem cell biology intersect in the progression of MAFLD to HCC. By demonstrating that CPT II inactivity promotes malignant progression through LCSC activation and impaired T-cell function, the authors provide a valuable framework for future research and clinical strategies.

FOOTNOTES

Author contributions: Cai H and Yang CH contributed equally as co-first authors; Cai H contributed to the discussion, writing, and editing of the manuscript, as well as the review of the literature; Yang CH designed the overall concept and outline of the manuscript; Gao P reviewed and revised the manuscript for important intellectual content; All authors read and approved the final version of the manuscript to be published.

Conflict-of-interest statement: The authors have no conflicts of interest to declare.

Country of origin: China

ORCID number: Peng Gao 0000-0001-6932-5370.

S-Editor: Wei YF
L-Editor: Filipodia
P-Editor: Zhao S

REFERENCES

1 **Nguyen VH**, Le MH, Cheung RC, Nguyen MH. Differential Clinical Characteristics and Mortality Outcomes in Persons With NAFLD and/or MAFLD. *Clin Gastroenterol Hepatol* 2021; **19**: 2172-2181.e6 [PMID: 34033923 DOI: 10.1016/j.cgh.2021.05.029]

2 **Wang LL**, Lu YM, Wang YH, Wang YF, Fang RF, Sai WL, Yao DF, Yao M. Carnitine palmitoyltransferase-II inactivity promotes malignant progression of metabolic dysfunction-associated fatty liver disease *via* liver cancer stem cell activation. *World J Gastroenterol* 2024; **30**: 5055-5069 [PMID: 39713165 DOI: 10.3748/wjg.v30.i47.5055]

3 **Borcherding N**, Brestoff JR. The power and potential of mitochondria transfer. *Nature* 2023; **623**: 283-291 [PMID: 37938702 DOI: 10.1038/s41586-023-06537-z]

4 **Badmus OO**, Hillhouse SA, Anderson CD, Hinds TD, Stec DE. Molecular mechanisms of metabolic associated fatty liver disease (MAFLD): functional analysis of lipid metabolism pathways. *Clin Sci (Lond)* 2022; **136**: 1347-1366 [PMID: 36148775 DOI: 10.1042/CS20220572]

5 **Fujiwara N**, Nakagawa H, Enooku K, Kudo Y, Hayata Y, Nakatsuka T, Tanaka Y, Tateishi R, Hikiba Y, Misumi K, Tanaka M, Hayashi A, Shibahara J, Fukayama M, Arita J, Hasegawa K, Hirschfield H, Hoshida Y, Hirata Y, Otsuka M, Tateishi K, Koike K. CPT2 downregulation adapts HCC to lipid-rich environment and promotes carcinogenesis *via* acylcarnitine accumulation in obesity. *Gut* 2018; **67**: 1493-1504 [PMID: 29437870 DOI: 10.1136/gutjnl-2017-315193]

6 **Wang S**, El-Deiry WS. Requirement of p53 targets in chemosensitization of colonic carcinoma to death ligand therapy. *Proc Natl Acad Sci U S A* 2003; **100**: 15095-15100 [PMID: 14645705 DOI: 10.1073/pnas.2435285100]

7 **Li H**, Chen J, Liu J, Lai Y, Huang S, Zheng L, Fan N. CPT2 downregulation triggers stemness and oxaliplatin resistance in colorectal cancer *via* activating the ROS/Wnt/β-catenin-induced glycolytic metabolism. *Exp Cell Res* 2021; **409**: 112892 [PMID: 34688609 DOI: 10.1016/j.yexcr.2021.112892]

8 **Dubinkina VB**, Tyakht AV, Odintsova VY, Yarygin KS, Kovarsky BA, Pavlenko AV, Ischenko DS, Popenko AS, Alexeev DG, Taraskina AY, Nasyrova RF, Krupitsky EM, Shalikiani NV, Bakulin IG, Shcherbakov PL, Skorodumova LO, Larin AK, Kostryukova ES, Abdulkhakov RA, Abdulkhakov SR, Malanin SY, Ismagilova RK, Grigoryeva TV, Ilina EN, Govorun VM. Links of gut microbiota composition with alcohol dependence syndrome and alcoholic liver disease. *Microbiome* 2017; **5**: 141 [PMID: 29041989 DOI: 10.1186/s40168-017-0359-2]

9 **Soysouvanh F**, Rousseau D, Bonnafous S, Bourinet M, Strazzulla A, Patouraux S, Machowiak J, Farrugia MA, Iannelli A, Tran A, Anty R, Luci C, Gual P. Osteopontin-driven T-cell accumulation and function in adipose tissue and liver promoted insulin resistance and MAFLD. *Obesity (Silver Spring)* 2023; **31**: 2568-2582 [PMID: 37724058 DOI: 10.1002/oby.23868]

10 **Jett KA**, Baker ZN, Hossain A, Boulet A, Cobine PA, Ghosh S, Ng P, Yilmaz O, Barreto K, DeCoteau J, Mochoruk K, Ioannou GN, Savard C, Yuan S, Abdalla OH, Lowden C, Kim BE, Cheng HM, Battersby BJ, Gohil VM, Leary SC. Mitochondrial dysfunction reactivates α-fetoprotein expression that drives copper-dependent immunosuppression in mitochondrial disease models. *J Clin Invest* 2023; **133**: e154684 [PMID: 36301669 DOI: 10.1172/JCI154684]

11 **Sun H**, Zhang L, Wang Z, Gu D, Zhu M, Cai Y, Li L, Tang J, Huang B, Bosco B, Li N, Wu L, Wu W, Li L, Liang Y, Luo L, Liu Q, Zhu Y, Sun J, Shi L, Xia T, Yang C, Xu Q, Han X, Zhang W, Liu J, Meng D, Shao H, Zheng X, Li S, Pan H, Ke J, Jiang W, Zhang X, Han X, Chu J, An H, Ge J, Pan C, Wang X, Li K, Wang Q, Ding Q. Single-cell transcriptome analysis indicates fatty acid metabolism-mediated metastasis and immunosuppression in male breast cancer. *Nat Commun* 2023; **14**: 5590 [PMID: 37696831 DOI: 10.1038/s41467-023-41318-2]

12 **Han S**, Georgiev P, Ringel AE, Sharpe AH, Haigis MC. Age-associated remodeling of T cell immunity and metabolism. *Cell Metab* 2023; **35**: 36-55 [PMID: 36473467 DOI: 10.1016/j.cmet.2022.11.005]

13 **Brown ZJ**, Fu Q, Ma C, Kruhlak M, Zhang H, Luo J, Heinrich B, Yu SJ, Zhang Q, Wilson A, Shi ZD, Swenson R, Greten TF. Carnitine palmitoyltransferase gene upregulation by linoleic acid induces CD4(+) T cell apoptosis promoting HCC development. *Cell Death Dis* 2018; **9**: 620 [PMID: 29795111 DOI: 10.1038/s41419-018-0687-6]

14 **Mansouri A**, Gattolliat CH, Asselah T. Mitochondrial Dysfunction and Signaling in Chronic Liver Diseases. *Gastroenterology* 2018; **155**: 629-647 [PMID: 30012333 DOI: 10.1053/j.gastro.2018.06.083]

15 **Hernaez R**, Peck-Radosavljevic M. MAFLD, HCC and the dilemma of (changing) terminology in liver diseases. *Gut* 2023; **72**: 9-11 [PMID: 35169004 DOI: 10.1136/gutjnl-2022-326992]

16 **Lee D**, Na J, Ryu J, Kim HJ, Nam SH, Kang M, Jung JW, Lee MS, Song HE, Choi J, Lee GH, Kim TY, Chung JK, Park KH, Kim SH, Kim H, Seo H, Kim P, Youn H, Lee JW. Interaction of tetraspan(in) TM4SF5 with CD44 promotes self-renewal and circulating capacities of hepatocarcinoma cells. *Hepatology* 2015; **61**: 1978-1997 [PMID: 25627085 DOI: 10.1002/hep.27721]

17 **González-Romero F**, Mestre D, Aurrekoetxea I, O'Rourke CJ, Andersen JB, Woodhoo A, Tamayo-Caro M, Varela-Rey M, Palomo-Irigoyen M, Gómez-Santos B, de Urturi DS, Núñez-García M, García-Rodríguez JL, Fernández-Ares L, Buqué X, Iglesias-Ara A, Bernales I, De Juan VG, Delgado TC, Goikoetxea-Usandizaga N, Lee R, Bhanot S, Delgado I, Perugorria MJ, Errazti G, Mosteiro L, Gaztambide S, Martinez de la Piscina I, Iruzubieta P, Crespo J, Banales JM, Martínez-Chantar ML, Castaño L, Zubiaga AM, Aspichueta P. E2F1 and E2F2-Mediated Repression of CPT2 Establishes a Lipid-Rich Tumor-Promoting Environment. *Cancer Res* 2021; **81**: 2874-2887 [PMID: 33771899 DOI: 10.1158/0008-5472.CAN-20-2052]

18 **Che L**, Chi W, Qiao Y, Zhang J, Song X, Liu Y, Li L, Jia J, Pilo MG, Wang J, Cigliano A, Ma Z, Kuang W, Tang Z, Zhang Z, Shui G, Ribback S, Dombrowski F, Evert M, Pascale RM, Cossu C, Pes GM, Osborne TF, Calvisi DF, Chen X, Chen L. Cholesterol biosynthesis supports the growth of hepatocarcinoma lesions depleted of fatty acid synthase in mice and humans. *Gut* 2020; **69**: 177-186 [PMID: 30954949 DOI: 10.1136/gutjnl-2018-317581]

19 **Zhu Y**, Gu L, Lin X, Zhou X, Lu B, Liu C, Li Y, Prochownik EV, Karin M, Wang F, Li Y. P53 deficiency affects cholesterol esterification to exacerbate hepatocarcinogenesis. *Hepatology* 2023; **77**: 1499-1511 [PMID: 35398929 DOI: 10.1002/hep.32518]

20 **Di Leo L**, Vegliante R, Ciccarone F, Salvatori I, Scimeca M, Bonanno E, Sagnotta A, Grazi GL, Aquilano K, Ciriolo MR. Forcing ATGL expression in hepatocarcinoma cells imposes glycolytic rewiring through PPAR-α/p300-mediated acetylation of p53. *Oncogene* 2019; **38**: 1860-1875 [PMID: 30367149 DOI: 10.1038/s41388-018-0545-0]

21 **Eslam M**, Sanyal AJ, George J; International Consensus Panel. MAFLD: A Consensus-Driven Proposed Nomenclature for Metabolic Associated Fatty Liver Disease. *Gastroenterology* 2020; **158**: 1999-2014.e1 [PMID: 32044314 DOI: 10.1053/j.gastro.2019.11.312]

22 **Sakurai Y**, Kubota N, Yamauchi T, Kadowaki T. Role of Insulin Resistance in MAFLD. *Int J Mol Sci* 2021; **22**: 4156 [PMID: 33923817 DOI: 10.3390/ijms22084156]

23 **Xia T**, Du M, Li H, Wang Y, Zha J, Wu T, Ju S. Association between Liver MRI Proton Density Fat Fraction and Liver Disease Risk. *Radiology* 2023; **309**: e231007 [PMID: 37874242 DOI: 10.1148/radiol.231007]

24 **van Katwyk S**, Coyle D, Cooper C, Pussegoda K, Cameron C, Skidmore B, Brener S, Moher D, Thavorn K. Transient elastography for the diagnosis of liver fibrosis: a systematic review of economic evaluations. *Liver Int* 2017; **37**: 851-861 [PMID: 27699993 DOI: 10.1111/liv.13260]

25 **Barsch M**, Salié H, Schlaak AE, Zhang Z, Hess M, Mayer LS, Tauber C, Otto-Mora P, Ohtani T, Nilsson T, Wischer L, Winkler F, Manne S, Rech A, Schmitt-Graeff A, Bronsert P, Hofmann M, Neumann-Haefelin C, Boettler T, Fichtner-Feigl S, van Boemmel F, Berg T, Rimassa L, Di Tommaso L, Saeed A, D'Alessio A, Pinato DJ, Bettinger D, Binder H, John Wherry E, Schultheiss M, Thimme R, Bengsch B. T-cell exhaustion and residency dynamics inform clinical outcomes in hepatocellular carcinoma. *J Hepatol* 2022; **77**: 397-409 [PMID: 35367533 DOI: 10.1016/j.jhep.2022.02.032]

26 **Mossmann D**, Müller C, Park S, Ryback B, Colombi M, Ritter N, Weißenberger D, Dazert E, Coto-Llerena M, Nuciforo S, Blukacz L, Ercan C, Jimenez V, Piscuoglio S, Bosch F, Terracciano LM, Sauer U, Heim MH, Hall MN. Arginine reprograms metabolism in liver cancer *via* RBM39. *Cell* 2023; **186**: 5068-5083.e23 [PMID: 37804830 DOI: 10.1016/j.cell.2023.09.011]

World Journal of Gastroenterology

Submit a Manuscript: https://www.f6publishing.com

World J Gastroenterol 2025 April 21; 31(15): 104574

DOI: 10.3748/wjg.v31.i15.104574

ISSN 1007-9327 (print) ISSN 2219-2840 (online)

LETTER TO THE EDITOR

Prognostic value of the triglyceride-glucose index in advanced gastric cancer: A call for further exploration

Hong-Jie Meng, Yi Mao, De-Qing Zhao, Sheng-Guang Shi

Specialty type: Gastroenterology and hepatology

Provenance and peer review: Unsolicited article; Externally peer reviewed.

Peer-review model: Single blind

Peer-review report's classification

Scientific Quality: Grade A, Grade B, Grade B, Grade B, Grade B

Novelty: Grade A, Grade B, Grade B, Grade B, Grade B

Creativity or Innovation: Grade A, Grade B, Grade B, Grade B, Grade B

Scientific Significance: Grade A, Grade A, Grade B, Grade B, Grade B

P-Reviewer: Govindarajan KK; Li ZP; Wang SB

Received: December 25, 2024

Revised: March 9, 2025

Accepted: March 17, 2025

Published online: April 21, 2025

Processing time: 114 Days and 20.9 Hours

Hong-Jie Meng, Yi Mao, De-Qing Zhao, Sheng-Guang Shi, Department of Gastrointestinal Surgery Ward, Zhuji People's Hospital, Zhuji 311800, Zhejiang Province, China

Corresponding author: Hong-Jie Meng, MD, Associate Chief Physician, Senior Researcher, Department of Gastrointestinal Surgery Ward, Zhuji People's Hospital, No. 9 Jianmin Road, Taozhu Street, Zhuji 311800, Zhejiang Province, China. mhj7768@163.com

Abstract

Gastric cancer (GC) remains a leading cause of cancer-related mortality worldwide, necessitating the identification of reliable prognostic indicators to enhance treatment outcomes. Recent research has highlighted the triglyceride-glucose (TyG) index as a potential surrogate marker for insulin resistance, which may significantly influence the prognosis of patients undergoing immunotherapy combined with chemotherapy. In this context, the study by Yao *et al* demonstrates that a high TyG index correlates with improved overall survival and progression-free survival in advanced GC patients receiving sintilimab and chemotherapy. Specifically, patients in the high TyG group had a significantly longer median progression-free survival of 9.8 months [95% confidence interval (CI): 9.2-10.9] compared to 8.0 months (95%CI: 7.5-8.5) in the low TyG group (hazard ratio = 0.58, 95%CI: 0.43-0.79, $P < 0.001$). Similarly, the median overall survival was significantly longer in the high TyG group at 23.1 months (95%CI: 21.2-NA) *vs* 16.5 months (95%CI: 13.9-18.3) in the low TyG group (hazard ratio = 0.30, 95%CI: 0.21-0.42, $P < 0.001$). These findings underscore the strong prognostic potential of the TyG index in guiding treatment strategies for advanced GC. These findings underscore the need for further investigation into the TyG index's role as a prognostic tool and its underlying mechanisms in influencing treatment efficacy. We advocate for additional multicenter studies to validate these results and explore the TyG index's applicability across diverse patient populations, ultimately aiming to refine treatment strategies and improve patient outcomes in advanced GC.

Key Words: Advanced gastric cancer; Chemotherapy; Insulin resistance; Prognostic marker; Triglyceride-glucose index; Tumor microenvironment

Core Tip: The triglyceride-glucose (TyG) index, a surrogate marker for insulin resistance, has emerged as a potential prognostic factor in advanced gastric cancer. Recent findings suggest that a high TyG index correlates with improved overall survival and progression-free survival in patients undergoing immunotherapy combined with chemotherapy. This highlights the clinical relevance of insulin sensitivity in modulating treatment efficacy. Further multicenter studies are essential to validate its prognostic value across diverse populations and to explore underlying mechanisms. Integrating the TyG index into comprehensive prognostic models may optimize treatment strategies and improve patient outcomes in advanced gastric cancer.

Citation: Meng HJ, Mao Y, Zhao DQ, Shi SG. Prognostic value of the triglyceride-glucose index in advanced gastric cancer: A call for further exploration. *World J Gastroenterol* 2025; 31(15): 104574
URL: https://www.wjgnet.com/1007-9327/full/v31/i15/104574.htm
DOI: https://dx.doi.org/10.3748/wjg.v31.i15.104574

TO THE EDITOR

We are writing to discuss the insightful article by Yao *et al*[1], recently published. This study presents a significant advancement in our understanding of prognostic factors in advanced gastric cancer (GC), particularly in the context of emerging immunotherapeutic strategies.

SIGNIFICANCE OF THE TYG INDEX

The triglyceride-glucose (TyG) index is calculated using fasting triglyceride and fasting glucose levels, following the formula: TyG = ln [fasting triglycerides (mg/dL) × fasting glucose (mg/dL)/2], serves as a surrogate marker for insulin resistance[2]. Insulin resistance has been implicated in various malignancies, including GC, where it may promote tumorigenesis through several mechanisms such as enhanced cellular proliferation, increased angiogenesis, and immune evasion[3]. The findings from Yao *et al*[1] indicating that a high TyG index correlates with improved overall survival (OS) and progression-free survival in patients undergoing treatment with sintilimab and chemotherapy are particularly noteworthy. Specifically, their study reported that patients with a high TyG index (≥ 1.79) had a significantly longer median progression-free survival of 9.8 months [95% confidence interval (CI): 9.2-10.9] compared to 8.0 months (95%CI: 7.5-8.5) in the low TyG index group (< 1.79) [hazard ratio (HR) = 0.58, 95%CI: 0.43-0.79, $P < 0.001$]. The median OS was also significantly extended in the high TyG index group, reaching 23.1 months (95%CI: 21.2-NA) compared to 16.5 months (95%CI: 13.9-18.3) in the low TyG index group (HR = 0.30, 95%CI: 0.21-0.42, $P < 0.001$). In multivariate analysis, the TyG index was identified as an independent prognostic factor for OS (HR = 0.36, 95%CI: 0.24-0.55, $P < 0.001$), further reinforcing its predictive value. These results suggest that metabolic status, as reflected by the TyG index, plays a crucial role in shaping treatment outcomes in advanced GC. This relationship suggests that insulin sensitivity may play a role in modulating the efficacy of immunotherapy, potentially influencing treatment outcomes[1,3].

CLINICAL IMPLICATIONS

The TyG index has shown significant prognostic value in advanced GC, with Yao *et al*[1] reporting a notable survival benefit in patients with a high TyG index (median OS: 23.1 months *vs* 16.5 months, HR = 0.30, $P < 0.001$)[2]. These findings suggest that metabolic profiling could serve as an additional stratification tool in clinical decision-making, allowing for more tailored treatment strategies. Integrating the TyG index into prognostic models alongside established biomarkers, such as programmed death-ligand 1 (PD-L1) expression and electrocorticography performance status, may refine patient selection for intensive therapeutic regimens, particularly in combination with immunotherapy[4,5].

Given the mechanistic links between insulin resistance and immunotherapy response, the TyG index may also help predict immune checkpoint inhibitor efficacy. Insulin resistance, through the phosphatidylinositol 3-kinase (PI3K)/protein kinase B (Akt)/mammalian target of rapamycin (mTOR) signaling pathway, promotes tumor growth and alters the tumor microenvironment, contributing to immune suppression and metabolic competition. Patients with a high TyG index, indicative of metabolic dysregulation, may benefit from adjunctive metabolic interventions (*e.g.*, metformin or mTOR inhibitors) to enhance their responsiveness to immunotherapy[1]. Additionally, the predictive role of the TyG index in identifying patients at risk of immune exhaustion due to metabolic competition warrants further investigation[6,7].

Future research should explore whether metabolic modulation strategies could synergize with immune checkpoint blockade to improve patient outcomes. For example, patients with a high TyG index could be prioritized for intensive therapeutic regimens or innovative treatment approaches, while those with lower indices might benefit from closer monitoring or alternative therapeutic options. Such stratification could ultimately contribute to enhanced survival outcomes and improved quality of life for affected patients[1,8,9].

Table 1 The Role of the triglyceride-glucose index in metabolic dysfunction and gastric cancer progression

Metabolic factor	Associated changes	Impact on gastric cancer
Insulin resistance	↑ PI3K/Akt/mTOR activation, ↑ growth signals, ↓ apoptosis	Promotes tumor proliferation and therapy resistance
Lipotoxicity	↑ Free fatty acids, ↑ IL-6/TNF-α, ↑ inflammation	Enhances pro-tumor immune suppression
Glucotoxicity	↑ Oxidative stress, ↑ DNA damage, ↑ chronic inflammation	Facilitates tumor progression and metastasis
Altered TME	↑ Metabolic competition (glucose depletion), ↓ T-cell function	Reduces efficacy of immunotherapy
Hyperlipidemia and obesity	↑ Systemic inflammation, ↑ lipid metabolism dysfunction	Alters immune response, may influence prognosis

PI3K: Phosphatidylinositol 3-kinase; Akt: Protein kinase B; mTOR: Mammalian target of rapamycin; TME: Tumor microenvironment; IL: Interleukin; TNF: Tumor necrosis factor.

MECHANISTIC INSIGHTS

This study paves the way for deeper investigation into the biological mechanisms connecting insulin resistance with cancer progression and treatment response[10,11]. Insulin resistance is known to activate multiple oncogenic signaling pathways, notably the PI3K/Akt/mTOR pathway[12]. This pathway regulates cellular metabolism, proliferation, and survival, and its dysregulation is implicated in cancer progression and therapeutic resistance. Persistent insulin resistance leads to chronic activation of PI3K/Akt signaling, promoting tumor growth and impairing the efficacy of immune checkpoint inhibitors by fostering an immunosuppressive environment[13]. Hyperactivation of mTOR can also reduce T-cell function, limiting the anti-tumor immune response[14,15]. Given the intricate interplay between metabolic dysfunction and GC progression, we summarize the key metabolic factors associated with the TyG index and their respective effects in Table 1.

Additionally, insulin resistance influences the tumor microenvironment through multiple mechanisms. First, it enhances systemic and local inflammation *via* upregulation of pro-inflammatory cytokines (*e.g.*, interleukin-6, tumor necrosis factor-α), which can create an immunosuppressive niche[10,16,17]. Second, the altered metabolic landscape associated with insulin resistance leads to increased competition for glucose between tumor cells and immune cells, particularly T cells. Since effector T cells rely heavily on glycolysis for energy, metabolic competition in an insulin-resistant state may result in T-cell exhaustion and impaired anti-tumor immunity. Finally, increased circulating insulin levels can stimulate the expression of PD-L1 on tumor and immune cells, potentially affecting the response to programmed death 1/PD-L1 blockade therapies[18,19]. Future research should focus on unraveling these intricate pathways and exploring their interactions with immunotherapeutic agents, such as sintilimab, to enhance our understanding and improve therapeutic outcomes.

NEED FOR MULTICENTER STUDIES

While the study by Yao *et al*[1] presents compelling evidence, the importance of multicenter studies cannot be overstated [20]. Such investigations are crucial for improving the generalizability of the findings across diverse populations and clinical settings[21]. Differences in genetic backgrounds, lifestyle factors, and comorbidities can profoundly impact both insulin resistance and cancer biology. Consequently, validating the TyG index as a prognostic tool in heterogeneous cohorts will be indispensable for confirming its applicability and reliability in routine clinical practice.

FUTURE DIRECTIONS

Future investigations should aim to integrate the TyG index with other biomarkers and clinical parameters to construct a more comprehensive prognostic model. Such models could include factors such as tumor staging, histological subtypes, and molecular characteristics, offering a more nuanced and holistic perspective on patient prognosis.

CONCLUSION

In conclusion, I commend Yao *et al*[1] for their valuable contribution to advancing our understanding of prognostic markers in advanced GC. The TyG index emerges as a promising tool for improving patient stratification and optimizing treatment strategies in this challenging clinical domain. Further research into the utility of this biomarker and its potential incorporation into routine clinical practice is essential to enhance outcomes for patients with advanced GC.

FOOTNOTES

Author contributions: Meng HJ conceptualization, writing, reviewing and editing; Mao Y methodology and formal analysis; Zhao DQ and Shi SG supervision and writing of the original draft; Meng HJ, Mao Y, Zhao DQ, and Shi SG participated in drafting the manuscript and have read it, and all authors thoroughly reviewed and endorsed the final manuscript.

Conflict-of-interest statement: All the authors report no relevant conflicts of interest for this article.

Country of origin: China

ORCID number: Hong-Jie Meng 0009-0003-8794-6893.

S-Editor: Bai Y
L-Editor: A
P-Editor: Zhao S

REFERENCES

1 **Yao ZY**, Ma X, Cui YZ, Liu J, Han ZX, Song J. Impact of triglyceride-glucose index on the long-term prognosis of advanced gastric cancer patients receiving immunotherapy combined with chemotherapy. *World J Gastroenterol* 2025; **31**: 102249 [PMID: 39926212 DOI: 10.3748/wjg.v31.i5.102249]
2 **Cai C**, Chen C, Lin X, Zhang H, Shi M, Chen X, Chen W, Chen D. An analysis of the relationship of triglyceride glucose index with gastric cancer prognosis: A retrospective study. *Cancer Med* 2024; **13**: e6837 [PMID: 38204361 DOI: 10.1002/cam4.6837]
3 **Okamura T**, Hashimoto Y, Hamaguchi M, Obora A, Kojima T, Fukui M. Triglyceride-glucose index (TyG index) is a predictor of incident colorectal cancer: a population-based longitudinal study. *BMC Endocr Disord* 2020; **20**: 113 [PMID: 32709256 DOI: 10.1186/s12902-020-00581-w]
4 **Tao S**, Yu L, Li J, Xie Z, Huang L, Yang D, Tan Y, Zhang W, Huang X, Xue T. Prognostic value of triglyceride-glucose index in patients with chronic coronary syndrome undergoing percutaneous coronary intervention. *Cardiovasc Diabetol* 2023; **22**: 322 [PMID: 38017540 DOI: 10.1186/s12933-023-02060-7]
5 **Xu J**, Xu W, Chen G, Hu Q, Jiang J. Association of TyG index with prehypertension or hypertension: a retrospective study in Japanese normoglycemia subjects. *Front Endocrinol (Lausanne)* 2023; **14**: 1288693 [PMID: 37964964 DOI: 10.3389/fendo.2023.1288693]
6 **Liu W**, Wang Y, Luo J, Liu M, Luo Z. Pleiotropic Effects of Metformin on the Antitumor Efficiency of Immune Checkpoint Inhibitors. *Front Immunol* 2020; **11**: 586760 [PMID: 33603734 DOI: 10.3389/fimmu.2020.586760]
7 **Eikawa S**, Nishida M, Mizukami S, Yamazaki C, Nakayama E, Udono H. Immune-mediated antitumor effect by type 2 diabetes drug, metformin. *Proc Natl Acad Sci U S A* 2015; **112**: 1809-1814 [PMID: 25624476 DOI: 10.1073/pnas.1417636112]
8 **Leone RD**, Powell JD. Fueling the Revolution: Targeting Metabolism to Enhance Immunotherapy. *Cancer Immunol Res* 2021; **9**: 255-260 [PMID: 33648947 DOI: 10.1158/2326-6066.CIR-20-0791]
9 **Li Y**, Tang J, Jiang J, Chen Z. Metabolic checkpoints and novel approaches for immunotherapy against cancer. *Int J Cancer* 2022; **150**: 195-207 [PMID: 34460110 DOI: 10.1002/ijc.33781]
10 **Zhan S**, Wang L, Wang W, Li R. Insulin resistance in NSCLC: unraveling the link between development, diagnosis, and treatment. *Front Endocrinol (Lausanne)* 2024; **15**: 1328960 [PMID: 38449844 DOI: 10.3389/fendo.2024.1328960]
11 **Leitner BP**, Siebel S, Akingbesote ND, Zhang X, Perry RJ. Insulin and cancer: a tangled web. *Biochem J* 2022; **479**: 583-607 [PMID: 35244142 DOI: 10.1042/BCJ20210134]
12 **Zhang YY**, Li YJ, Xue CD, Li S, Gao ZN, Qin KR. Effects of T2DM on cancer progression: pivotal precipitating factors and underlying mechanisms. *Front Endocrinol (Lausanne)* 2024; **15**: 1396022 [PMID: 39290325 DOI: 10.3389/fendo.2024.1396022]
13 **Nepstad I**, Hatfield KJ, Grønningsæter IS, Aasebø E, Hernandez-Valladares M, Hagen KM, Rye KP, Berven FS, Selheim F, Reikvam H, Bruserud Ø. Effects of insulin and pathway inhibitors on the PI3K-Akt-mTOR phosphorylation profile in acute myeloid leukemia cells. *Signal Transduct Target Ther* 2019; **4**: 20 [PMID: 31240133 DOI: 10.1038/s41392-019-0050-0]
14 **Rascio F**, Spadaccino F, Rocchetti MT, Castellano G, Stallone G, Netti GS, Ranieri E. The Pathogenic Role of PI3K/AKT Pathway in Cancer Onset and Drug Resistance: An Updated Review. *Cancers (Basel)* 2021; **13**: 3949 [PMID: 34439105 DOI: 10.3390/cancers13163949]
15 **He Y**, Sun MM, Zhang GG, Yang J, Chen KS, Xu WW, Li B. Targeting PI3K/Akt signal transduction for cancer therapy. *Signal Transduct Target Ther* 2021; **6**: 425 [PMID: 34916492 DOI: 10.1038/s41392-021-00828-5]
16 **Mani N**, Andrews D, Obeng RC. Modulation of T cell function and survival by the tumor microenvironment. *Front Cell Dev Biol* 2023; **11**: 1191774 [PMID: 37274739 DOI: 10.3389/fcell.2023.1191774]
17 **Liu X**, Hoft DF, Peng G. Tumor microenvironment metabolites directing T cell differentiation and function. *Trends Immunol* 2022; **43**: 132-147 [PMID: 34973923 DOI: 10.1016/j.it.2021.12.004]
18 **Pellegrino M**, Secli V, D'Amico S, Petrilli LL, Caforio M, Folgiero V, Tumino N, Vacca P, Vinci M, Fruci D, de Billy E. Manipulating the tumor immune microenvironment to improve cancer immunotherapy: IGF1R, a promising target. *Front Immunol* 2024; **15**: 1356321 [PMID: 38420122 DOI: 10.3389/fimmu.2024.1356321]
19 **Nojima I**, Eikawa S, Tomonobu N, Hada Y, Kajitani N, Teshigawara S, Miyamoto S, Tone A, Uchida HA, Nakatsuka A, Eguchi J, Shikata K, Udono H, Wada J. Dysfunction of CD8 + PD-1 + T cells in type 2 diabetes caused by the impairment of metabolism-immune axis. *Sci Rep*

2020; **10**: 14928 [PMID: 32913271 DOI: 10.1038/s41598-020-71946-3]

20 **Pan K**, Nelson RA, Wactawski-Wende J, Lee DJ, Manson JE, Aragaki AK, Mortimer JE, Phillips LS, Rohan T, Ho GYF, Saquib N, Shadyab AH, Nassir R, Rhee JJ, Hurria A, Chlebowski RT. Insulin Resistance and Cancer-Specific and All-Cause Mortality in Postmenopausal Women: The Women's Health Initiative. *J Natl Cancer Inst* 2020; **112**: 170-178 [PMID: 31184362 DOI: 10.1093/jnci/djz069]

21 **Seifirad S**, Alquran L. The bigger, the better? When multicenter clinical trials and meta-analyses do not work. *Curr Med Res Opin* 2021; **37**: 321-326 [PMID: 33287578 DOI: 10.1080/03007995.2020.1860922]

Published by **Baishideng Publishing Group Inc**
7041 Koll Center Parkway, Suite 160, Pleasanton, CA 94566, USA
Telephone: +1-925-3991568
E-mail: office@baishideng.com
Help Desk: https://www.f6publishing.com/helpdesk
https://www.wjgnet.com